DEVELOPMENTS IN CAMPYLOBACTER, HELICOBACTER & RELATED ORGANISMS RESEARCH – CHRO 2019

EDITED BY: Ozan Gundogdu, Nicolae Corcionivoschi and Stuart A. Thompson
PUBLISHED IN: Frontiers in Microbiology, Frontiers in Public Health and Frontiers in Veterinary Science

frontiers Research Topics

frontiers

ISSN 1664-8714
ISBN 978-2-88966-480-1
DOI 10.3389/978-2-88966-480-1

About Frontiers

Frontiers is more than just an open-access publisher of scholarly articles: it is a pioneering approach to the world of academia, radically improving the way scholarly research is managed. The grand vision of Frontiers is a world where all people have an equal opportunity to seek, share and generate knowledge. Frontiers provides immediate and permanent online open access to all its publications, but this alone is not enough to realize our grand goals.

Frontiers Journal Series

The Frontiers Journal Series is a multi-tier and interdisciplinary set of open-access, online journals, promising a paradigm shift from the current review, selection and dissemination processes in academic publishing. All Frontiers journals are driven by researchers for researchers; therefore, they constitute a service to the scholarly community. At the same time, the Frontiers Journal Series operates on a revolutionary invention, the tiered publishing system, initially addressing specific communities of scholars, and gradually climbing up to broader public understanding, thus serving the interests of the lay society, too.

Dedication to Quality

Each Frontiers article is a landmark of the highest quality, thanks to genuinely collaborative interactions between authors and review editors, who include some of the world's best academicians. Research must be certified by peers before entering a stream of knowledge that may eventually reach the public - and shape society; therefore, Frontiers only applies the most rigorous and unbiased reviews.
Frontiers revolutionizes research publishing by freely delivering the most outstanding research, evaluated with no bias from both the academic and social point of view. By applying the most advanced information technologies, Frontiers is catapulting scholarly publishing into a new generation.

What are Frontiers Research Topics?

Frontiers Research Topics are very popular trademarks of the Frontiers Journals Series: they are collections of at least ten articles, all centered on a particular subject. With their unique mix of varied contributions from Original Research to Review Articles, Frontiers Research Topics unify the most influential researchers, the latest key findings and historical advances in a hot research area! Find out more on how to host your own Frontiers Research Topic or contribute to one as an author by contacting the Frontiers Editorial Office: frontiersin.org/about/contact

DEVELOPMENTS IN CAMPYLOBACTER, HELICOBACTER & RELATED ORGANISMS RESEARCH – CHRO 2019

Topic Editors:
Ozan Gundogdu, University of London, United Kingdom
Nicolae Corcionivoschi, Agri-Food and Biosciences Institute (AFBI), United Kingdom
Stuart A. Thompson, Augusta University, United States

Citation: Gundogdu, O., Corcionivoschi, N., Thompson, S. A., eds. (2021). Developments in Campylobacter, Helicobacter & Related Organisms Research – CHRO 2019. Lausanne: Frontiers Media SA.
doi: 10.3389/978-2-88966-480-1

Table of Contents

frontiers in Microbiology

EDITORIAL
published: 08 January 2021
doi: 10.3389/fmicb.2020.622582

Editorial: Developments in Campylobacter, Helicobacter & Related Organisms Research – CHRO 2019

Nicolae Corcionivoschi[1], *Stuart A. Thompson*[2] *and Ozan Gundogdu*[3]*

[1] Bacteriology Branch, Veterinary Sciences Division, Agri-Food and Biosciences Institute (AFBI), Belfast, United Kingdom, [2] Medical College of Georgia, Augusta University, Augusta, GA, United States, [3] Department of Infection Biology, Faculty of Infectious and Tropical Diseases, London School of Hygiene and Tropical Medicine, London, United Kingdom

Keywords: ***Campylobacter***, ***Helicobacter***, **CHRO 2019, gastrointestinal pathogen,** ***Campylobacter Helicobacter*** **and Related Organisms**

Editorial on the Research Topic

Developments in Campylobacter, Helicobacter & Related Organisms Research – CHRO 2019

Campylobacter spp. and *Helicobacter* spp. are important gastrointestinal pathogens that are major causes of acute gastroenteritis and gastric disease, respectively (Polk and Peek, 2010; Gundogdu and Wren, 2020). *Campylobacter* spp. are considered the leading bacterial cause of human gastroenteritis. In low-resource settings, *Campylobacter* infections are common in young children and correlate with stunted growth and life-long physical and cognitive deficiencies (Amour et al., 2016). In high-resource regions, an estimated 1 in every 100 individuals develop a *Campylobacter*-related illness each year. *Helicobacter* spp. can colonize the human stomach and increase the risk of ulcers and stomach cancer (Salama et al., 2013). *Helicobacter pylori* is the most common species with some reports indicating up to 50% of the population are infected (Brown, 2000). Both *Campylobacter* spp. and *Helicobacter* spp. possess a plethora of survival and virulence factors that have allowed them to survive and persist successfully (Gundogdu et al., 2016; Hathroubi et al., 2018; Capurro et al., 2019; El Abbar et al., 2019; Liaw et al., 2019). For both *Campylobacter* spp. and *Helicobacter* spp., contaminated foods play an important role in the transmission of the microorganism to humans (Tegtmeyer et al., 2017; Ijaz et al., 2018; Quaglia and Dambrosio, 2018; Sibanda et al., 2018; McKenna et al., 2020).

The 20th International workshop on *Campylobacter*, *Helicobacter,* and Related Organisms (CHRO) was held in Belfast, Northern Ireland from September 8–11th, 2019. This biennial conference provided researchers with an opportunity to display the most recent findings in our understanding of *Campylobacter*, *Helicobacter,* and related organisms. The conference showcased the research from different topics ranging from pathogenicity and virulence factors; poultry and non-poultry epidemiology and ecology; emerging and related species; control strategies; outbreak/epidemiology and public health; detection methods and characterization; antibiotics and antimicrobials; bioinformatics, and genomics and evolution; immunology and host response. This Frontiers Research Topic provides a framework to showcase a selection of this current research.

A number of manuscripts focussed on the association between *Campylobacter* and poultry, indicating the growing importance of this research field. Quyen et al. described an optimized Loop Mediated Isothermal Amplification (LAMP) method for rapid detection of *Campylobacter* spp. in broilers, with increased specificity and sensitivity. Lafontaine et al. investigated the prebiotic galacto-oligosaccharide (GOS) on broiler chickens colonized with *C. jejuni*. The authors identified

OPEN ACCESS

Edited and reviewed by:
Giovanna Suzzi,
University of Teramo, Italy

Reviewed by:
Rosanna Tofalo,
University of Teramo, Italy

***Correspondence:**
Ozan Gundogdu
ozan.gundogdu@lshtm.ac.uk

Specialty section:
This article was submitted to Food Microbiology, a section of the journal Frontiers in Microbiology

Received: *28 October 2020*
Accepted: *14 December 2020*
Published: *08 January 2021*

Citation:
Corcionivoschi N, Thompson SA and Gundogdu O (2021) Editorial: Developments in Campylobacter, Helicobacter & Related Organisms Research – CHRO 2019. Front. Microbiol. 11:622582. doi: 10.3389/fmicb.2020.622582

that GOS-fed birds had increased growth performance, however an increased IL-17A did not prevent colonization with *C. jejuni*. Chinivasagam et al. investigated the use of bacteriophages to control *Campylobacter* in commercially farmed broiler chickens in Australia. Muhandiramlage et al. investigated the physiological and morphological changes on *Campylobacter* isolates from chicken meat that were induced with chlorine.

Studies also continued to investigate the genomics and epidemiology of strains from different sources around the globe. Abd El-Hamid et al. described the genetic diversity of *C. jejuni* strains isolated from avian and human sources from Egypt. Terefe et al. investigated the co-occurrence of *Campylobacter* spp. in children from eastern Ethiopia and their association with environmental enteric dysfunction, diarrhea, and host microbiome. The authors highlighted the association between specific microbiome composition and gut permeability, gut inflammation, enteric dysfunction severity, and diarrhea. Mutschall et al. investigated *C. jejuni* strain dynamics in a raccoon population in southern Ontario, Canada. The authors noted that due to a high prevalence and rapid subtype turnover, racoons may act as vectors in the transmission of clinically relevant *C. jejuni* subtypes at the interface of rural, urban, and more natural environments. Hetman et al. described recovery bias of common *C. jejuni* subtypes in mixed cultures. The authors emphasized the importance of selecting multiple colonies per sample, using both enrichment and non-enrichment isolation procedures to maximize the probability of recovering multiple subtypes present in a sample. Phung et al. discussed the routes of infection of *C. hepaticus* which causes spotty liver disease in chickens. The authors highlighted that environmental sources are a likely transmission source of *C. hepaticus*.

In relation to survival, Riedel et al. analyzed the transcriptomic differences in *C. jejuni* and *C. coli* when exposed to elevated temperatures of 46°C, identifying several chaperones with increased gene expression indicative of a general involvement within heat stress response. Lv et al. described methods to detect and quantify *C. jejuni* from the viable but non-culturable (VBNC) state. The authors discuss the use of PMA-qPCR as a rapid, specific and sensitive method for the detection and quantification of VBNC *C. jejuni*.

Research focussing on immunology and host response was presented by Butkevych et al. who discussed the impact of epithelial apoptosis and subepithelial immune responses in *C. jejuni*-induced barrier disruption. The authors highlighted that *C. jejuni* infection and the consequent subepithelial immune activation leads to intestinal barrier dysfunction predominantly through caspase-3-dependent epithelial apoptosis. Pathogenicity and virulence factors were investigated by Li et al. who describe a putative novel role for FlhF in terms of directly regulating flagellar genes and further our understanding of FlhF in relation to *Campylobacter* flagellar biosynthesis and flagellation. Konkel et al. provided a comprehensive review of *Campylobacter* adherence and invasion, specifically focussing on fibronectin and binding from CadF and FlpA adhesins. Guérin et al. investigated the membrane proteocomplexome of *C. jejuni* using 2-D blue native/SDS-PAGE in conjunction with bioinformatic analysis. The authors identified a range of membrane protein complexes (MCPs) in *C. jejuni* 81–176 where these MCPs are involved in protein folding, molecules trafficking, oxidative phosphorylation, membrane structuration, peptidoglycan biosynthesis, motility and chemotaxis, stress signaling, efflux pumps, and virulence. Duma et al. discussed the influence of protein glycosylation on *C. fetus* physiology. The authors used label-free quantitative (LFQ) proteomics, identifying more than 100 proteins significantly altered in expression in two *C. fetus* subsp. *fetus* protein glycosylation (*pgl*) mutants (*pglX* and *pglJ*) compared to the wild-type strain. The authors provided a study which gives insight into the unique protein N-glycosylation pathway of *C. fetus*, but also expands our knowledge on the influence of protein N-glycosylation on *Campylobacter* cell physiology. Tejera et al. performed a genome-scale metabolic model driven design of a medium for *C. jejuni* M1cam strain. The authors showed that with a well-curated metabolic model, it is possible to design media to grow *Campylobacter* and that this has implications for the study of new *Campylobacter* species defined through metagenomics.

This Research Topic will increase the knowledge base and understanding of the processes of survival of *Campylobacter* spp. and *Helicobacter* spp. within the environment, in particular, relating to food safety, and to host-pathogen interactions.

AUTHOR CONTRIBUTIONS

All authors contributed to the drafting of the editorial.

REFERENCES

Amour, C., Gratz, J., Mduma, E., Svensen, E., Rogawski, E. T., Mcgrath, M., et al. (2016). Epidemiology and impact of *Campylobacter* infection in children in 8 low-resource settings: results from the MAL-ED study. *Clin. Infect. Dis.* 63, 1171–1179. doi: 10.1093/cid/ciw542

Brown, L. M. (2000). *Helicobacter pylori*: epidemiology and routes of transmission. *Epidemiol. Rev.* 22, 283–297. doi: 10.1093/oxfordjournals.epirev.a018040

Capurro, M. I., Greenfield, L. K., Prashar, A., Xia, S., Abdullah, M., Wong, H., et al. (2019). VacA generates a protective intracellular reservoir for *Helicobacter pylori* that is eliminated by activation of the lysosomal calcium channel TRPML1. *Nat. Microbiol.* 4, 1411–1423. doi: 10.1038/s41564-019-0441-6

El Abbar, F. M., Li, J., Owen, H. C., Daugherty, C. L., Fulmer, C. A., Bogacz, M., et al. (2019). RNA Binding by the *Campylobacter jejuni* post-transcriptional regulator CsrA. *Front. Microbiol.* 10:1776. doi: 10.3389/fmicb.2019.01776

Gundogdu, O., Da Silva, D. T., Mohammad, B., Elmi, A., Wren, B. W., Van Vliet, A. H., et al. (2016). The *Campylobacter jejuni* oxidative stress regulator RrpB is associated with a genomic hypervariable region and altered oxidative stress resistance. *Front. Microbiol.* 7:2117. doi: 10.3389/fmicb.2016.02117

Gundogdu, O., and Wren, B. W. (2020). Microbe profile: *Campylobacter jejuni*–survival instincts. *Microbiology* 166, 230–232. doi: 10.1099/mic.0.000906

Hathroubi, S., Zerebinski, J., and Ottemann, K. M. (2018). *Helicobacter pylori* biofilm involves a multigene stress-biased response, including a structural role for flagella. *mBio* 9:e01973-18. doi: 10.1128/mBio.01973-18

Ijaz, U. Z., Sivaloganathan, L., McKenna, A., Richmond, A., Kelly, C., Linton, M., et al. (2018). Comprehensive longitudinal microbiome analysis of the

chicken cecum reveals a shift from competitive to environmental drivers and a window of opportunity for *Campylobacter*. *Front. Microbiol.* 9:2452. doi: 10.3389/fmicb.2018.02452

Liaw, J., Hong, G., Davies, C., Elmi, A., Sima, F., Stratakos, A., et al. (2019). The *Campylobacter jejuni* type VI secretion system enhances the oxidative stress response and host colonization. *Front. Microbiol.* 10:2864. doi: 10.3389/fmicb.2019.02864

McKenna, A., Ijaz, U. Z., Kelly, C., Linton, M., Sloan, W. T., Green, B. D., et al. (2020). Impact of industrial production system parameters on chicken microbiomes: mechanisms to improve performance and reduce *Campylobacter*. *Microbiome* 8:128. doi: 10.1186/s40168-020-00908-8

Polk, D. B., and Peek, R. M. Jr. (2010). *Helicobacter pylori*: gastric cancer and beyond. *Nat. Rev. Cancer* 10, 403–414. doi: 10.1038/nrc2857

Quaglia, N. C., and Dambrosio, A. (2018). *Helicobacter pylori*: a foodborne pathogen? *World J. Gastroenterol.* 24, 3472–3487. doi: 10.3748/wjg.v24.i31.3472

Salama, N. R., Hartung, M. L., and Muller, A. (2013). Life in the human stomach: persistence strategies of the bacterial pathogen *Helicobacter pylori*. *Nat. Rev. Microbiol.* 11, 385–399. doi: 10.1038/nrmicro3016

Sibanda, N., McKenna, A., Richmond, A., Ricke, S. C., Callaway, T., Stratakos, A. C., et al. (2018). A review of the effect of management practices on *Campylobacter* prevalence in poultry farms. *Front. Microbiol.* 9:2002. doi: 10.3389/fmicb.2018.02002

Tegtmeyer, N., Wessler, S., Necchi, V., Rohde, M., Harrer, A., Rau, T. T., et al. (2017). *Helicobacter pylori* employs a unique basolateral type IV secretion mechanism for CagA delivery. *Cell Host Microbe* 22, 552.e5–560.e5. doi: 10.1016/j.chom.2017.09.005

Conflict of Interest: The authors declare that the research was conducted in the absence of any commercial or financial relationships that could be construed as a potential conflict of interest.

frontiers in Microbiology

ORIGINAL RESEARCH
published: 18 October 2019
doi: 10.3389/fmicb.2019.02353

Genetic Diversity of *Campylobacter jejuni* Isolated From Avian and Human Sources in Egypt

Marwa I. Abd El-Hamid[1†‡], Norhan K. Abd El-Aziz[1†‡], Mohamed Samir[2‡], El-sayed Y. El-Naenaeey[1], Etab M. Abo Remela[3,4], Rasha A. Mosbah[5] and Mahmoud M. Bendary[6‡]*

[1] Department of Microbiology, Faculty of Veterinary Medicine, Zagazig University, Zagazig, Egypt, [2] Department of Zoonoses, Faculty of Veterinary Medicine, Zagazig University, Zagazig, Egypt, [3] Department of Bacteriology, Mycology and Immunology, Faculty of Veterinary Medicine, Kafrelsheikh University, Kafrelsheikh, Egypt, [4] Department of Biology, College of Science, Taibah University, Medina, Saudi Arabia, [5] Fellow Pharmacist at Zagazig University Hospital, Zagazig, Egypt, [6] Department of Microbiology and Immunology, Faculty of Pharmacy, Port Said University, Port Said, Egypt

OPEN ACCESS

Edited by:
Stuart A. Thompson, Augusta University, United States

Reviewed by:
Mohamed K. Fakhr, The University of Tulsa, United States
Heriberto Fernandez, Austral University of Chile, Chile

***Correspondence:**
Norhan K. Abd El-Aziz
norhan_vet@hotmail.com; nourhan_vet@zu.edu.eg

† These authors have contributed equally to this work as first authors

‡ORCID:
Marwa I. Abd El-Hamid
orcid.org/0000-0002-1560-6158
Norhan K. Abd El-Aziz
orcid.org/0000-0001-8309-9058
Mohamed Samir
orcid.org/0000-0002-1166-0480
Mahmoud M. Bendary
orcid.org/0000-0002-1788-0038

Specialty section:
This article was submitted to Food Microbiology, a section of the journal Frontiers in Microbiology

Received: *26 June 2019*
Accepted: *27 September 2019*
Published: *18 October 2019*

Citation:
Abd El-Hamid MI, Abd El-Aziz NK, Samir M, El-Naenaeey EY, Abo Remela EM, Mosbah RA and Bendary MM (2019) Genetic Diversity of Campylobacter jejuni Isolated From Avian and Human Sources in Egypt. Front. Microbiol. 10:2353. doi: 10.3389/fmicb.2019.02353

Campylobacter jejuni (*C. jejuni*) are able to colonise and infect domestic poultry and also pose a risk for humans. The aim of this study was to determine the extent of genotypic diversity among *C. jejuni* isolates recovered from avian and human sources in Egypt. Furthermore, the short variable region (SVR) of flagellin A (*flaA*) gene was analysed for the presence of allelic variants. Our results showed that *C. jejuni* isolates differ in their capacity to harbour each of the virulence genes alone or when present in various combinations. The *flaA* gene was detected in all *C. jejuni* strains and none of the strains had all the studied virulence genes together. When considering *C. jejuni* strains from the investigated sources, the *cdtC* gene was the most similar, while the *cdtB* and *iam* genes were the most dissimilar. We could identify 13 novel alleles in the analysed strains. The analyses of virulence gene patterns, *flaA* gene sequences and allelic variants showed that *C. jejuni* strains from different sources overlapped largely suggesting potential involvement of poultry in transmitting *C. jejuni* to humans. We also found that the strains isolated from the same host were highly heterogeneous, with chicken strains exhibiting the highest diversity. Moreover, the human strains were clustered closer to chicken ones than to those from pigeon. The results of this study should be taken into consideration when assessing the epidemiology and risk potential of Egyptian *C. jejuni* not only in poultry, but also in humans.

Keywords: alleles, *C. jejuni*, *flaA* typing, humans, poultry, virulence

INTRODUCTION

Campylobacter jejuni (*C. jejuni*) is one of the most frequent bacterial causes of foodborne gastroenteritis worldwide (European Food Safety Authority, 2014). It has been isolated from chickens, turkeys, pigeons and quails (Vazquez et al., 2010; Kovacic et al., 2013; Ramees et al., 2015), where they colonise the intestinal tract and could contaminate the carcasses during processing (e.g., defeathering and evisceration) (Hermans et al., 2011). Human infection occurs commonly through consumption of contaminated poultry meat (Humphrey et al., 2007).

Many studies addressed the virulence characteristics of *C. jejuni* (Frazão et al., 2017; Maansi et al., 2018). In Egypt, limited studies have focussed on the genotypic diversity (Ahmed et al., 2015) and the antimicrobial resistance of *C. jejuni* (Abd El-Tawab et al., 2018), yet none of these studies explored the virulence patterns of *C. jejuni* among different sources, particularly pigeons.

It is well established that *C. jejuni* exhibits high diversity with regard to the presence of virulence and/or pathogenicity traits including adherence (Coote et al., 2007), invasion (Zheng et al., 2006), toxicity (Abuoun et al., 2005), and molecular mimicry (Datta et al., 2003). Determining the extent of genetic heterogeneity of *C. jejuni* will tell about the disease burden in certain populations and will aid in predicting the potential source of infection (McCarthy et al., 2007); all are valuable information that can be delivered to surveillance and control programmes with an overarching goal of reducing the disease in poultry and its transmission to humans.

The genomic instability of the flagellin gene, due to frequent occurrence of genomic recombination (Harrington et al., 1997), makes it a good candidate for studying the genetic diversity of *C. jejuni*. Therefore, molecular typing of *flaA* gene, and in particular its short variable region (SVR; ∼150 base pairs), has been widely used in studying the genotypic diversity of such bacteria (Meinersmann et al., 1997, 2005; Wardak and Jagielski, 2009). *flaA* typing represents a convenient and cost-effective typing-scheme, which suits the situation in developing countries, particularly when quick characterisation of the strains is needed. Previous studies have demonstrated that direct sequencing of PCR-amplified *flaA*-SVRs is useful for *Campylobacter* genotyping, particularly in short-term and localised epidemiological investigations, allowing similar or higher discriminatory power than multilocus sequence typing (MLST). Furthermore, MLST is unable to distinguish closely related strains in small-scale outbreak investigations and additional methods like *flaA* typing may be required in order to obtain sufficient resolution (Meinersmann et al., 1997; Sails et al., 2003).

Campylobacter jejuni isolated from humans and poultry are known to be genetically diverse (Ramonaite et al., 2017). Although *C. jejuni* in Egypt is widely distributed in avian hosts (Rahimi and Ameri, 2011; Abd El-Tawab et al., 2018) and humans (Sainato et al., 2018), there are limited studies that addressed the genetic heterogeneity among Egyptian *C. jejuni*.

To unravel the extent of genetic diversity of Egyptian *C. jejuni*, we analysed both virulence gene profiles and *flaA* allelic variants in *C. jejuni* isolated from chickens, pigeons and humans. The knowledge gained from this study is highly relevant to the epidemiology and control efforts geared toward reducing *C. jejuni* infection in Egypt.

MATERIALS AND METHODS

Samples

The study was conducted during the period from 2015–2018. A total of 270 samples were collected from individual broiler chickens (n = 90) [chicken meat (n = 65) and cloacal swabs (n = 25)] and fresh pigeon droplets (n = 180) of different ages from 10 retail outlets in Zagazig city, Sharkia Governorate, Egypt. Moreover, 270 human stool samples were collected from gastroenteritis patients attending Zagazig University hospital located in the same city, Zagazig. The collected samples were transported in an ice box within 3 h to the laboratory for bacteriological analysis. The animal study was approved by the committee of Animal Welfare and Research Ethics, Faculty of Veterinary Medicine, Zagazig University. Regarding the human study, it was approved by the research ethical committee of Faculty of Medicine, Zagazig University and the work was carried out in accordance with the Code of Ethics of the World Medical Association (Declaration of Helsinki) for studies involving humans. Written informed consents were obtained from the patients participating in the research study after a full description of the study purpose.

Isolation and Identification of *C. jejuni*

For the isolation of *Campylobacter* species, samples were enriched in Preston *Campylobacter* selective enrichment broth (Oxoid, United Kingdom) at 42°C for 48 h. The enrichment cultures were first streaked onto modified charcoal cefoperazone deoxycholate agar (mCCDA; Oxoid, United Kingdom), then transferred onto Columbia agar (Oxoid, United Kingdom) plates supplemented with 5% sterile defibrinated horse blood. The plates were incubated at 42°C in darkness for 48 h under microaerobic conditions (Vandepitte et al., 2003). The presumptive isolates were confirmed as *C. jejuni* by biochemical tests including catalase, oxidase, hippurate and indoxyl acetate hydrolyses, and susceptibility to cephalothin and nalidixic acid (30 μg/disc, each) (Quinn et al., 1994). Genomic DNA was extracted from fresh *C. jejuni* cultures using the QIAamp DNA Mini kit (Qiagen, Germany) according to the manufacturer's instructions. Polymerase chain reaction (PCR)-based amplification of 23S rRNA and *hipO* genes was done to confirm the identification of *C. jejuni* isolates (Wang et al., 2002).

PCR-Based Detection of Virulence Genes

Campylobacter jejuni isolates were screened for the presence of 7 virulence genes namely *flaA*, *virB11*, *wlaN*, *iam*, *cdtA*, *cdtB* and *cdtC*. All PCR assays were performed in a 25 μL reaction mixture containing 12.5 μL of EmeraldAmp Max PCR Master Mix (Takara, Japan), 1 μL of each primer (20 pM; Metabion, Germany), 6 μL of purified *C. jejuni* DNA and 4.5 μL of nuclease-free water. Primers used for PCR assays are listed in **Table 1**.

FlaA-SVR Sequencing and Allelic Typing

Sequencing of internal 402 bp fragments of the *flaA*-SVR amplicons was performed using the previously described primer pair Fla242FU and Fla625RU (Meinersmann et al., 1997). The *flaA* amplicons were purified using the QIAquick PCR purification kit (Qiagen, United States) and sequenced in an ABI 3130 automated DNA Sequencer (Applied Biosystems, United States) using the BigDye® Terminator v3.1 Cycle

TABLE 1 | Oligonucleotide primers used for the amplification of genus, species and virulence genes of *C. jejuni* isolates.

Target gene	Primer name	Oligonucleotide sequence (5′→3′)	Amplicon size (bp)	Reference
23S rRNA	23SF	TATACCGGTAAGGAGTGCTGGAG	650	Wang et al., 2002
	23SR	ATCAATTAACCTTCGAGCACCG		
hipO	CJF	ACTTCTTTATTGCTTGCTGC	323	Wang et al., 2002
	CJR	GCCACAACAAGTAAAGAAGC		
cdtA	GNW	GGAAATTGGATTTGGGGCTATACT	165	Wieczorek et al., 2012
	IVH	ATCACAAGGATAATGGACAAT		
cdtB	VAT2	GTTAAAATCCCCTGCTATCAACCA	495	Wieczorek et al., 2012
	WMI-R	GTTGGCACTTGGAATTTGCAAGGC		
cdtC	WMI-F	TGGATGATAGCAGGGGATTTTAAC	555	Wieczorek et al., 2012
	LPF-X	TTGCACATAACCAAAAGGAAG		
flaA	FLA242FU	CTATGGATGAGCAATT(AT)AAAAT	402	Meinersmann et al., 1997
	FLA625RU	CAAG(AT)CCTGTTCC(AT)ACTGAAG		
virB11	virB-232	TCTTGTGAGTTGCCTTACCCCTTTT	494	Datta et al., 2003
	virB-701	CCTGCGTGTCCTGTGTTATTTACCC		
wlaN	wlaN DL-39	TTAAGAGCAAGATATGAAGGTG	672	Kordinas et al., 2005
	wlaN DL-41	CCATTTGAATTGATATTTTTG		
iam	IAMF	GCGCAAATATTATCACCC	518	Wieczorek et al., 2012
	IAMR	TTCACGACTACTACTATGCGG		

Sequencing Kit (Applied Biosystems, United States). *flaA*-SVR sequences were compared with those previously published at GenBank using Basic Local Alignment Search Tool (BLAST) available at the National Center for Biotechnology Information (NCBI)[1]. To investigate the genetic relatedness of *C. jejuni* isolates, a phylogenetic tree was built based on *flaA*-SVR sequences using neighbour-joining method (Saitou and Nei, 1987) and the Kimura's two-parameter method (Kimura, 1980) as an estimator for the evolutionary distance among strains. The topology of the tree was evaluated by 1,000 iterations of a bootstrap analysis. This analysis was done using MEGA software (v. 5) (Tamura et al., 2011). A quantitative assessment of the similarity among the analysed sequences was done by running a Clustal W multiple alignment (Thompson et al., 1994) of all sequences. This enabled the generation of percent identity among pairs of *flaA*-SVR gene sequences without accounting for phylogenetic relationships. This analysis was done using the MegAlign software in the Lasergene (v. 7.1.0) package (DNASTAR, Madison, WI, United States).

To retrieve the allelic variants of *C. jejuni* strains, all nucleotide and peptide sequences of *flaA*-SVRs, using their accession numbers as queries, were used as inputs in *Campylobacter* pubMLST *flaA* Oxford database[2]; these were then compared against reference *C. jejuni* strains deposited in this database. The allelic variants of *flaA*-SVR nucleotides and peptides of *C. jejuni* strains were assigned accordingly.

Bioinformatics and Data Analyses

PC-ORD Software (v. 5, Oregon, United States), the web-based tools MetaboAnalyst (Chong and Xia, 2018), heatmapper (Babicki et al., 2016) and SPSS software (v. 25, IBM, United States) were used for bioinformatics and statistical analyses of the data. To analyse the overall clustering pattern of *C. jejuni* strains, the frequency of each virulence gene, scored as binary data (present = 1, absent = 0), was used as input in a non-metric multidimensional scaling (nMDS) analysis based on the Euclidean distance. To visualise the association between the studied virulence genes and thus their contribution to strain clustering pattern, we performed a hierarchical clustering using the virulence genes scored as binary data. To determine the relationship between the strain sources, a hierarchical clustering, based on Euclidean distances, was generated using the frequency of the presence of each virulence gene in each source as inputs. The estimated Euclidean distances were used to assess the degree of convergence among strain sources. To visualise the association between the strain sources and the virulence genes, a 2-D correspondence analysis was done, which explained 96% of the variance in the data. A third dimension was not used as its contribution was very low (proportion of inertia = 0.4). To determine the degree of similarity of each virulence gene among strains isolated from various hosts, we applied a random forest non-parametric classification method as described previously (Babicki et al., 2016). The degree of similarity of each gene among *C. jejuni* strains was determined considering the following isolation sources: human, chicken meat, chicken cloacal swabs and pigeon; chicken (meat and cloacal swabs together), human and pigeon; chicken (meat and cloacal swabs together) and human; human and pigeon; human and birds (chicken and pigeon). In this approach, the frequency of each virulence gene was firstly used to build up random forest classification model (the model prediction is based on the majority vote of an ensemble of 500 tree trial; out of bag error, OOB error = 0.6) in the respective source comparison. The degree of similarity of each gene was then evaluated by measuring the increase

[1] www.ncbi.nlm.nih.gov/BLAST/

[2] http://pubmlst.org/campylobacter/

of the OOB error when the respective gene is permuted. To quantify the discriminatory power of each gene, a classic univariate receiver operating characteristic (ROC) curve was created using inputs similar to that described for the random forest classification. This enabled estimating the area under the curve (AUC) for each gene, which ranges from 0 to 1 (0 = least discriminatory power; 1 = highest discriminatory power). It was only technically possible to run the ROC analysis on the virulence genes comparing human and bird isolates.

Genotypic Diversity of *C. jejuni* Strains

Both Simpson's (D_1) (Simpson, 1949) and Shannon's (H) (Shannon, 1948) diversity indices were used to assess the diversity of *C. jejuni* strains among various sources and within each source using the virulence genes profile as input data. Simpson's diversity index was calculated based on the equation: 1-D. In this equation, $D = \Sigma \frac{n(n-1)}{N(N-1)} =$, where Σ = summation, n = total number of bacterial strains showing a particular gene profile and N = total number of bacterial strains in the respective source (e.g., in human strains). Simpson's index has a range of 0–1, with 0 indicates identical bacterial strains and 1 indicates the highest diverse bacterial strains. Shannon's diversity index (H) was calculated using the following equation: $H = -\sum_{i=1}^{s} Pi\ lnpi$, where pi is the proportion of bacterial strains expressing a particular gene profile divided by the total number of bacterial strains in the respective source, In is the natural log of the pi, Σ is the summation, and s is the number of species. The concordance of the two indices was determined by calculating the Pearson correlation (r). This analysis was done using the Past3 software (v. 3.23), Oslo (Hammer et al., 2001).

Statistical Analysis

Statistical analysis of the frequencies of virulence genes within *C. jejuni* strains isolated from different hosts was assessed by Fisher's exact test considering P-value < 0.05 as a cut off level. Data was analysed using Stata statistical software version 12 (TX, United States).

Nucleotide Sequence Accession Numbers

The *flaA*-SVR nucleotide sequences generated in this study have been deposited into the GenBank database with accession numbers KX066127-KX066135, MG677923-MG677934 and MK281494-MK281513.

RESULTS

Prevalence of *C. jejuni* in Chickens, Pigeons and Humans

The overall prevalence of *C. jejuni* in avian samples (i.e., chicken and pigeon samples) was 11.11% (30/270). Fourteen out of 90 (15.56%) chicken samples were positive for *C. jejuni*; 10 from 65 chicken meat (15.38%) and 4 from 25 cloacal swabs (16%), while the isolation rate of *C. jejuni* in pigeon droplets was 8.89% (16/180). Moreover, 11 *C. jejuni* were isolated from 270 human stool samples (4.07%). Typical *C. jejuni* colonies were small, shiny, round, and grey on mCCDA agar medium. No haemolysis on Columbia blood agar and positive reactions for catalase, oxidase and hippurate and indoxyl acetate hydrolyses presumptively identified *C. jejuni* isolates. Besides, the analysed isolates were typically sensitive to nalidixic acid and resistant to cephalothin as measured by the inhibition zones around the relevant antibiotic discs. The genus and species identification of the isolates were further confirmed by PCR detection of 23S rRNA and *hipO* genes, respectively.

Frequency of Virulence Genes in *C. jejuni* Isolates

As depicted in **Table 2**, the *flaA* gene was present in all analysed *C. jejuni* strains (n = 41). The *cdtA, cdtB,* and *cdtC* toxin genes were similarly detected in *C. jejuni* strains (80.49%, each), whereas the three CDT toxin genes were simultaneously found in 58.54% of the analysed strains. Only two subunits of the CDT toxin gene (e.g., *cdtBC*, *cdtAC,* and *cdtAB*) were detected in 3 (7.32%), 3 (7.32%) and 6 (14.63%) of the strains, respectively. Moreover, 3 *C. jejuni* strains (7.32%) harboured the *cdtC* gene only and 2 strains (4.88%) had no CDT toxin genes at all (**Supplementary Table S1**). Besides, *iam*, *wlaN* and *virB11* genes were found in 34.15, 12.20, and 9.76% of *C. jejuni* strains, respectively.

The presence of the *cdtB* gene in human and pigeon strains was significantly (P = 0.0001) higher (100%, each) than in chicken ones (42.86%). Additionally, *iam* gene was significantly

TABLE 2 | Occurrence of virulence genes in *C. jejuni* strains under study.

Source	No. of *C. jejuni* strains	Frequency of virulence genes, no. (%)						
		cdtA	*cdtB*	*cdtC*	*flaA*	*virB11*	*wlaN*	*iam*
Pigeon	16	14 (87.50)	16 (100.00)	14 (87.50)	16 (100.00)	1 (6.25)	0 (0.00)	8 (50.00)
Chicken	14	9 (64.29)	6 (42.86)	10 (71.43)	14 (100.00)	2 (14.29)	3 (21.43)	6 (42.86)
Human	11	10 (90.91)	11 (100.00)	9 (81.82)	11 (100.00)	1 (9.09)	2 (18.18)	0 (0.00)
Total	41	33 (80.49)	33 (80.49)	33 (80.49)	41 (100.00)	4 (9.76)	5 (12.20)	14 (34.15)
*P-value**		0.173	0.000*	0.545	1.000	0.763	0.164	0.021*

**Statistical significance was calculated using Fisher's exact test (P-value < 0.05).*

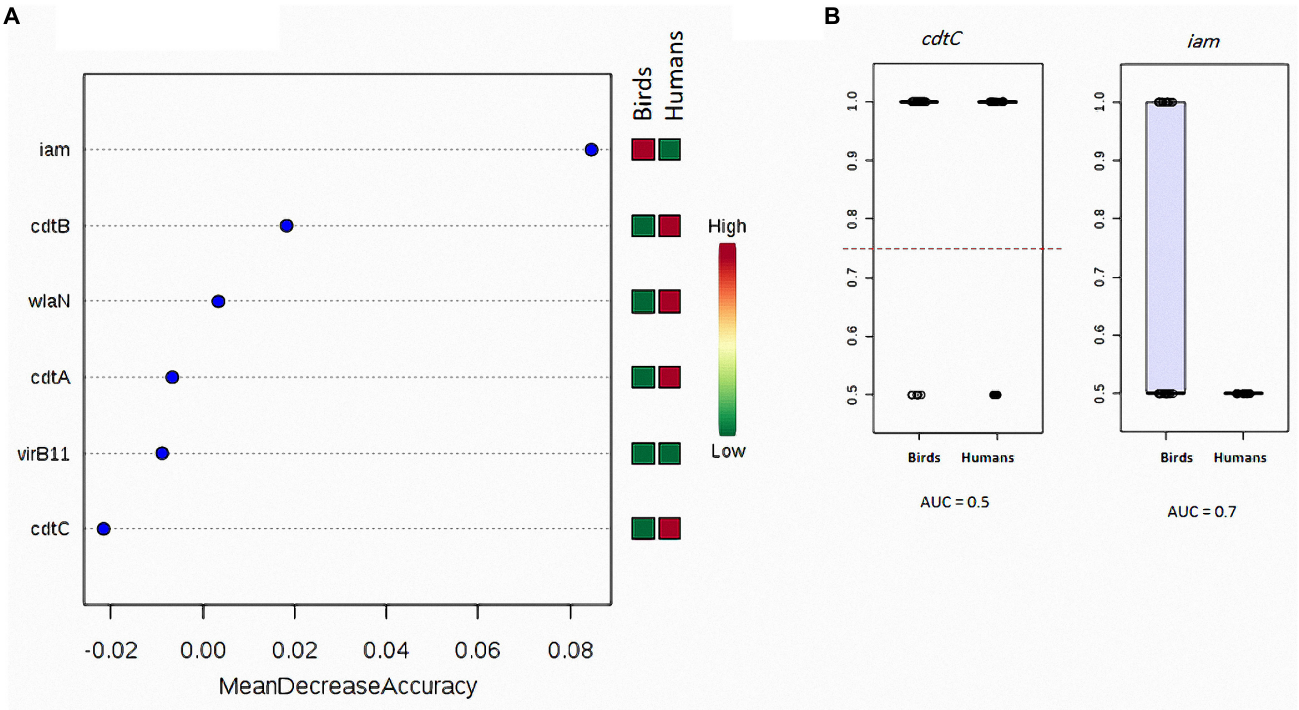

FIGURE 1 | Degree of similarity and discriminatory power of analysed virulence genes in *C. jejuni* strains among various sources. **(A)** Random forest classification showing the predictive accuracy of the studied genes (*X*-axis). The mini heat map shows the frequency distribution of each gene in the respective strain sources. Each dot refers to one gene with the respective mean decrease accuracy. **(B)** Box-plot showing the differences in the distribution of *cdtC* and *iam* genes between birds and human sources of *C. jejuni*. The horizontal dotted line refers to the optimal cutoff value. The AUC data were generated by running the ROC curves as described in the "Materials and Methods" section.

(P = 0.021) more frequently detected in pigeon strains (50%) when compared to chicken (42.86%) and human ones (0%).

The random forest classification analysis showed that *cdtC* gene exhibited the highest similarity (the least mean decrease accuracy) when considering *C. jejuni* isolated from human and birds (chicken meat, chicken cloacal swabs and pigeon together) (**Figure 1A**). This gene was also the most similar when considering the following strain sources: (i) human, chicken meat, chicken cloacal swabs and pigeon, (ii) human and chicken (meat and cloacal swabs together), (iii) human and pigeon and (iv) human, chicken and pigeon (**Supplementary Figure S1**). On contrary, *iam* was the most dissimilar gene when considering *C. jejuni* strains from (i) human and birds (chicken meat, chicken cloacal swabs and pigeon together) and (ii) human and pigeon. The *cdtB* gene was the most dissimilar one when considering *C. jejuni* strains from (i) human, chicken meat, chicken cloacal swabs and pigeon, (ii) human, chicken (meat and cloacal swabs together) and pigeon and (iii) chicken (meat and cloacal swabs together) and humans. ROC-curve analysis (**Figure 1B**) on the human and bird strains revealed that the *cdtC* gene had lower AUC value (0.5) than that of the *iam* gene (0.7).

The results showed that none of the *C. jejuni* strains harboured all the seven virulence genes together. More than half of the strains (87.80%) possessed three or more virulence genes (**Table 3**). Irrespective of the strain source, *cdtABC, flaA* combination dominated the overall gene profiles, being encoded by 10 strains (24.39%), followed by *cdtABC, flaA, iam* pattern (7/41, 17.07%) (**Supplementary Table S1** and **Table 4**).

The strains from pigeon and human sources (n = 27) harbored at least 3–6 virulence genes. In contrast, 50% of the chicken strains were positive for up to 3 virulence genes (**Table 3**). As shown in **Supplementary Table S1** and **Table 5**, *cdtABC, flaA* dominated the gene profiles in human strains (5/11, 45.45%), was not detected at all in chicken strains and was the second frequent pattern in pigeon strains (5/16, 31.25%). While, *cdtABC, flaA, iam* pattern was the most frequent in pigeon (6/16, 37.50%), it was not detected in any of human strains and was found in only one chicken strain (1/14, 7.14%). The *cdtC, flaA* was the dominant pattern in chicken strains (3/14, 21.43%), but none of human or pigeon strains possessed this pattern.

Clustering Pattern of the Virulence Genes and Their Association With *C. jejuni* Strains

Considering the 41 *C. jejuni* strains separately (**Figure 2B**) and when grouped by their sources (**Figure 3A**), the virulence genes formed two separate clusters. The first cluster contained *cdtA*, *cdtB,* and *cdtC* genes and the second one included *iam, virB11* and *wlaN* genes. The *flaA* gene was not included in this analysis as it was detected in 100% of the strains. By running a corresponding

TABLE 3 | Frequency of *C. jejuni* strains isolated from avian and human sources carrying virulence genes.

No. of identified virulence genes	Human (*n* = 11)	Chicken* (*n* = 14)	Pigeon (*n* = 16)	Human and pigeon (*n* = 27)	Human and chicken* (*n* = 25)	Chicken* and pigeon (*n* = 30)	Human and chicken* and pigeon (*n* = 41)
1	0 (0.00)	2 (14.29)	0 (0.00)	0 (0.00)	2 (8.00)	2 (6.67)	2 (4.88)
2	0 (0.00)	3 (21.43)	0 (0.00)	0 (0.00)	3 (12.00)	3 (10.00)	3 (7.32)
3	3 (27.27)	2 (14.29)	3 (18.75)	6 (22.22)	5 (20.00)	5 (16.67)	8 (19.51)
4	5 (45.45)	2 (14.29)	6 (37.50)	11 (40.74)	7 (28.00)	8 (26.67)	13 (31.71)
5	3 (27.27)	2 (14.29)	6 (37.50)	9 (33.33)	5 (20.00)	8 (26.67)	11 (26.83)
6	0 (0.00)	3 (21.43)	1 (6.25)	1 (3.70)	3 (12.00)	4 (13.33)	4 (9.76)
7	0 (0.00)	0 (0.00)	0 (0.00)	0 (0.00)	0 (0.00)	0 (0.00)	0 (0.00)
Simpson diversity	0.64	0.82	0.67	0.6722	0.80	0.82	0.77
Shannon diversity	1.06	1.77	1.223	1.18	1.71	1.7	1.60

*Numbers of strains and percentages in parentheses indicate the proportion of those carrying the respective virulence genes. *Chicken strains refer to those isolated from chicken meat + chicken cloacal swabs.*

analysis (**Figure 3B**), it was evident that *cdtA, cdtB, cdtC,* and *flaA* genes were more associated with *C. jejuni* strains from humans, chicken meat and pigeons. The remaining genes (i.e., *iam, virB11* and *wlaN*) showed a scattered pattern, being more associated with the chicken swab strains.

Genetic Diversity of *C. jejuni* Strains Based on Their Virulence Genes Profiles

The nMDS and the dendogram analyses (**Figures 2**, **3A**) of *C. jejuni* strains (n = 41) showed a non-consistent clustering pattern and high diversity among the analysed strains. The human and bird strains overlapped largely. A similar overlap was observed when analysing the 41 strains grouped by their sources (**Figure 3A**). The dendogram analysis showed that the human strains were genetically closer to those from chickens (Euclidean distance = 0.19) than to those from pigeons (Euclidean distance = 0.26) (**Figure 3A**). As shown in **Table 3**, irrespective of the strain source, the overall Simpson's and Shannon's diversity indices of all strains were 0.77 and 1.60, respectively. The highest diversity was observed in *C. jejuni* strains isolated from chickens, followed by those from pigeons and humans. Overall, the results of both diversity indices were highly positively correlated in a significant manner (Pearson correlation, r = 0.9; P = 0.001).

Genetic Diversity of *C. jejuni* Based on *flaA*-SVR Gene Sequences

Using the BLAST tool, it was found that our *flaA*-SVR sequences and the flanking regions had 92–99% similarity with those of the previously published *C. jejuni* strains.

The phylogenetic analysis (**Figure 4**) and the proximity matrix (**Supplementary Table S2**) revealed sequence heterogeneity among our *C. jejuni* strains. While pigeon strains were phylogenetically related, some of them were clustered close to (e.g., strain No. 13) or shared the same lineage with (e.g., strain No. 12) chicken or human strains. The proximity matrix (**Supplementary Table S2**) indicated that the bacterial population within chickens and pigeons had less similarity on average (average similarity, each = 86.9%) than those within humans (average similarity = 93.4%).

Allelic Diversity of *C. jejuni*

We identified 17 and 12 allele variants at nucleotide and peptide levels, respectively (**Table 4** and **Supplementary Table S1**) with 13 novel alleles at the nucleotide level (Bold numbers in **Supplementary Table S1** and **Table 4**). Irrespective of the strain source, allele 177 was the most frequently identified nucleotide variant (13/41, 31.71%), followed by allele 288 (n = 4, 9.76%). The *flaA*-SVR nucleotide allele 177 was the dominant one in human (6/11, 54.55%) and chicken (6/14, 42.86%) strains, whereas alleles 718, 38 and 1118 were the most frequent in pigeon strains (2/16, 12.5%, each). Certain allele variants were not identified in human and chicken strains, yet were detected in pigeon strains (**Supplementary Table S1**). At the peptide level, allele 74 was the most frequently identified variant (13/41, 31.71%), followed by allele 92 (7/41, 17.07%) and allele 239 (4/41, 9.76%). The *flaA*-SVR peptide allele 74 was the most prevalent in human (6/11, 54.55%) and chicken (6/14, 42.86%) strains, whereas allele 239 predominated in pigeon strains (4/16, 25%). The nMDS plots that was built based on all identified alleles (**Supplementary Figures S2A,B**) indicated that *C. jejuni* strains isolated from humans and birds were highly diverse and overlapped largely. Considering all identified alleles (at both the nucleotide and peptide levels), human strains were clustered with chicken strains and were positioned apart from pigeon ones (**Supplementary Figures S2C,D**).

DISCUSSION

Campylobacter jejuni can colonise and infect domestic poultry and pose a risk for humans. In the current study, we analysed the genetic heterogeneity of Egyptian *C. jejuni* isolates recovered from avian and human sources. Characterisation of *C. jejuni* isolates from different sources is vital for a better understanding of the impact of multiple sources on the disease burden. The current study revealed low overall prevalence rates of *C. jejuni* in chicken and human samples (15.56 and 4.07%, respectively). Similar prevalence rates have been reported in a recent study conducted in Egypt (18.12 and 4.1%, respectively) (Ahmed et al., 2015). Moreover, the carriage rate of *C. jejuni*

TABLE 4 | Virulence gene patterns, allelic variants and mutations in *flaA*-SVR of *C. jejuni* isolated from avian and human sources.

Isolate code no.	Source	Virulence genes pattern	*flaA*-SVR nucleotide allele (No. of variations)	*flaA*-SVR peptide allele (No. of variations)	**Translation variation reference → clone	Accession no.
1	Pigeon droplets	*cdtABC*, *flaA*, *virB11*, *iam*	**781** (30)	191 (16)	^{49}I → ^{26}T, ^{60}N → ^{37}K, ^{63}V → ^{40}E, ^{64}K → ^{41}I, ^{72}S → ^{49}T, ^{74}K → ^{51}R, ^{76}G → ^{53}I, ^{77}L → ^{54}F, ^{84}E → ^{61}R, ^{85}R → ^{62}I, ^{86}I → ^{63}T, ^{90}G → ^{67}E, ^{93}Q → ^{70}P, ^{94}F → ^{71}L, ^{95}T → ^{72}P, ^{96}L → ^{73}F	KX066127.1
2	Pigeon droplets	*cdtABC*, *flaA*, *iam*	**731** (32)	191 (16)	^{49}I → ^{27}T, ^{57}A → ^{35}E, ^{60}N → ^{38}K, ^{63}V → ^{41}E, ^{64}K → ^{42}I, ^{66}T → ^{44}I, ^{67}I → ^{45}M, ^{72}S → ^{50}T, ^{74}K → ^{52}R, ^{84}E → ^{62}R, ^{85}R → ^{63}I, ^{86}I → ^{64}T, ^{93}Q → ^{71}P, ^{94}F → ^{72}L, ^{96}L → ^{74}F, ^{101}G → ^{79}H	KX066128.1
3	Pigeon droplets	*cdtABC*, *flaA*, *iam*	**940***	58 (10)	^{49}I → ^{26}T, ^{77}L → ^{54}V, ^{84}G → ^{61}A, ^{86}I → ^{63}S, ^{89}S → ^{66}R, ^{93}Q → ^{70}A, ^{94}F → ^{71}V, ^{96}L → ^{73}V, ^{99}Y → ^{76}F, ^{101}G → ^{78}A	KX066129.1
4	Pigeon droplets	*cdtABC*, *flaA*, *iam*	38 (17)	5 (7)	^{49}I → ^{27}T, ^{71}Q → ^{49}H, ^{74}K → ^{52}N, ^{79}R → ^{57}C, ^{89}S → ^{67}F, ^{96}L → ^{74}F, ^{106}K → ^{84}P	KX066130.1
5	Pigeon droplets	*cdtABC*, *flaA*, *iam*	**1118** (18)	239 (13)	^{56}G → ^{32}C, ^{57}A → ^{33}S, ^{59}S → ^{35}L, ^{62}T → ^{38}I, ^{71}Q → ^{47}I, ^{76}G → ^{52}A, ^{78}T → ^{54}K, ^{79}R → ^{55}C, ^{90}G → ^{66}T, ^{92}V → ^{68}E, ^{99}Y → ^{75}S, ^{101}A → ^{77}C, ^{104}D → ^{80}V	KX066131.1
6	Pigeon droplets	*cdtABC*, *flaA*, *iam*	**1275** (19)	209 (13)	^{57}A → ^{35}S, ^{62}T → ^{40}I, ^{64}K → ^{42}I, ^{68}G → ^{46}A, ^{70}T → ^{48}S, ^{71}Q → ^{49}H, ^{72}S → ^{50}T, ^{75}I → ^{53}M, ^{94}L → ^{72}V, ^{96}L → ^{74}F, ^{99}Y → ^{77}D, ^{102}I → ^{80}K, ^{104}D → ^{82}V	KX066132.1
7	Pigeon droplets	*cdtABC*, *flaA*	**186** (25)	356 (17)	^{62}T → ^{37}A, ^{63}I → ^{38}V, ^{64}K → ^{39}I, ^{65}A → ^{40}V, ^{72}S → ^{47}P, ^{73}S → ^{48}F, ^{74}K → ^{49}Q, ^{78}T → ^{53}S, ^{85}R → ^{60}S, ^{86}I → ^{61}V, ^{88}S → ^{63}T, ^{93}Q → ^{68}S, ^{96}L → ^{71}P, ^{99}Y → ^{74}D, ^{101}G → ^{76}S, ^{103}D → ^{78}H, ^{104}D → ^{79}G	KX066134.1
8	Pigeon droplets	*cdtABC*, *flaA*	9 (26)	60 (15)	^{33}A → ^{8}T, ^{49}I → ^{24}V, ^{52}E → ^{27}K, ^{57}A → ^{32}E, ^{66}T → ^{41}I, ^{67}I → ^{42}T, ^{72}S → ^{47}T, ^{77}L → ^{52}F, ^{82}T → ^{57}R, ^{83}G → ^{58}V, ^{90}G → ^{65}S, ^{94}F → ^{69}A, ^{96}L → ^{71}H, ^{102}L → ^{77}R, ^{106}Q → ^{81}L	KX066135.1
9	Pigeon droplets	*cdtAB*, *flaA*	**781** (31)	191 (14)	^{49}I → ^{26}T, ^{57}A → ^{34}E, ^{60}N → ^{37}K, ^{63}V → ^{40}E, ^{64}K → ^{41}I, ^{72}S → ^{49}T, ^{74}K → ^{51}R, ^{76}G → ^{53}I, ^{84}E → ^{61}R, ^{85}R → ^{62}I, ^{86}I → ^{63}T, ^{93}Q → ^{70}P, ^{94}F → ^{71}L, ^{96}L → ^{73}F	MK281505
10	Pigeon droplets	*cdtAB*, *flaA, iam*	**1118** (17)	239 (13)	^{56}G → ^{33}C, ^{57}A → ^{34}S, ^{59}S → ^{36}L, ^{62}T → ^{39}I, ^{68}G → ^{45}A, ^{71}Q → ^{48}N, ^{76}G → ^{53}A, ^{78}T → ^{55}K, ^{79}R → ^{56}C, ^{90}G → ^{67}T, ^{92}V → ^{69}E, ^{101}A → ^{78}C, ^{104}D → ^{81}V	MK281506
11	Pigeon droplets	*cdtBC*, *flaA*	**938** (19)	209 (12)	^{57}A → ^{34}S, ^{62}T → ^{39}I, ^{64}K → ^{41}I, ^{68}G → ^{45}A, ^{70}T → ^{47}S, ^{71}Q → ^{48}N, ^{72}S → ^{49}T, ^{75}I → ^{52}M, ^{94}L → ^{71}V, ^{96}L → ^{73}F, ^{102}I → ^{79}K, ^{104}D → ^{81}V	MK281507
12	Pigeon droplets	*cdtABC*, *flaA*	177 (10)	74 (5)	^{32}I → ^{38}T, ^{36}T → ^{42}A, ^{58}S → ^{64}G, ^{71}Q → ^{77}L, ^{102}I → ^{108}L	MK281508

(Continued)

TABLE 4 | Continued

Isolate code no.	Source	Virulence genes pattern	*flaA*-SVR nucleotide allele (No. of variations)	*flaA*-SVR peptide allele (No. of variations)	**Translation variation reference → clone	Accession no.
13	Pigeon droplets	*cdtABC*, *flaA*, *iam*	**1486** (11)	92 (8)	^{19}Q → ^{11}L, ^{26}M → ^{18}I, ^{29}L → ^{21}I, ^{63}V → ^{55}M, ^{77}V → ^{69}F, ^{96}I → ^{88}V, ^{97}K → ^{89}Q, ^{99}Y → ^{91}F	MK281509
14	Pigeon droplets	*cdtABC*, *flaA*	**756** (26)	58 (9)	^{49}I → ^{26}T, ^{74}K → ^{51}N, ^{86}I → ^{63}S, ^{89}S → ^{66}R, ^{94}F → ^{71}V, ^{96}L → ^{73}V, ^{99}Y → ^{76}F, ^{101}G → ^{78}A, ^{106}K → ^{83}P	MK281510
15	Pigeon droplets	*cdtBC*, *flaA*	38 (18)	239 (5)	^{49}I → ^{27}T, ^{74}K → ^{52}N, ^{89}S → ^{67}R, ^{96}L → ^{74}F, ^{106}Q → ^{84}P	MK281511
16	Pigeon droplets	*cdtABC*, *flaA*	**1183***	239 (15)	^{57}A → ^{32}S, ^{59}S → ^{34}L, ^{62}T → ^{37}I, ^{64}K → ^{39}I, ^{70}T → ^{45}S, ^{71}Q → ^{46}I, ^{72}S → ^{47}T, ^{75}I → ^{50}M, ^{90}G → ^{65}T, ^{94}F → ^{69}V, ^{96}L → ^{71}F, ^{99}Y → ^{74}S, ^{101}A → ^{76}C, ^{102}I → ^{77}K, ^{104}D → ^{79}V	MK281512
17	Chicken meat	*cdtABC*, *flaA*, *wlaN*, *iam*	177 (8)	74 (5)	^{32}I → ^{38}T, ^{36}T → ^{42}A, ^{58}S → ^{64}G, ^{71}Q → ^{77}L, ^{102}I → ^{108}L	MG677923.1
18	Chicken meat	*cdtABC*, *flaA*, *virB11*, *iam*	177 (9)	74 (5)	^{10}Q → ^{10}E, ^{23}N → ^{23}Y, ^{39}N → ^{39}D, ^{76}G → ^{76}D, ^{89}S → ^{89}L	MG677924.1
19	Chicken meat	*cdtABC*, *flaA*, *iam*	**1486** (11)	92 (7)	^{19}Q → ^{13}L, ^{26}M → ^{20}I, ^{63}V → ^{57}M, ^{80}F → ^{74}I, ^{87}F → ^{81}L, ^{97}K → ^{91}Q, ^{104}D → ^{98}E	MG677925.1
20	Chicken meat	*cdtAB*, *flaA*, *iam*	177 (12)	74 (8)	^{5}A → ^{11}V, ^{32}I → ^{38}T, ^{36}T → ^{42}A, ^{45}S → ^{51}N, ^{58}S → ^{64}G, ^{71}Q → ^{77}L, ^{81}E → ^{87}A, ^{102}I → ^{108}L	MG677926.1
21	Chicken cl. swab	*cdtAB*, *flaA*	**526***	211 (13)	^{62}T → ^{38}I, ^{67}I → ^{43}L, ^{71}Q → ^{47}H, ^{72}S → ^{48}T, ^{74}K → ^{50}I, ^{80}F → ^{56}V, ^{85}K → ^{61}S, ^{86}I → ^{62}V, ^{94}F → ^{70}A, ^{95}T → ^{71}A, ^{99}Y → ^{75}A, ^{102}I → ^{78}V, ^{103}D → ^{79}G	KX066133.1
22	Chicken cl. swab	*cdtABC*, *flaA*, *virB11*, *wlaN*	177 (9)	74 (6)	^{5}A → ^{11}V, ^{32}I → ^{38}T, ^{36}T → ^{42}A, ^{58}S → ^{64}G, ^{71}Q → ^{77}L, ^{102}I ^{108}L	MK281494
23	Chicken cl. swab	*cdtAC*, *flaA*, *wlaN*, *iam*	177 (12)	74 (8)	^{5}A → ^{11}V, ^{32}I → ^{38}T, ^{36}T → ^{42}A, ^{45}S → ^{51}N, ^{58}S → ^{64}G, ^{71}Q → ^{77}L, ^{81}E → ^{87}A, ^{102}I → ^{108}L	MK281513
24	Chicken cl. swab	*flaA*	**288***	92 (9)	^{10}Q → ^{8}E, ^{23}N → ^{21}Y, ^{26}M → ^{24}I, ^{39}N → ^{37}D, ^{63}V → ^{61}S, ^{76}G → ^{74}D, ^{80}F → ^{78}I, ^{87}F → ^{85}L, ^{89}S → ^{87}L	MK281495
25	Chicken meat	*cdtC*, *flaA*	**1486** (12)	92 (7)	^{19}Q → ^{15}L, ^{26}M → ^{22}I, ^{29}L → ^{25}I, ^{39}N → ^{35}D, ^{63}V → ^{59}M, ^{97}K → ^{93}Q, ^{104}D → ^{100}E	MK281496
26	Chicken meat	*flaA*	177 (5)	74 (2)	^{39}N → ^{15}D, ^{80}F → ^{56}I	MK281497
27	Chicken meat	*cdtC*, *flaA*	**288** (8)	92 (4)	^{26}M → ^{21}I, ^{63}V → ^{58}M, ^{87}F → ^{82}L, ^{104}D → ^{99}E	MK281498
28	Chicken meat	*cdtAC*, *flaA*, *iam*	9 (27)	211 (15)	^{33}A → ^{8}T, ^{62}T → ^{37}I, ^{67}I → ^{42}L, ^{72}S → ^{47}T, ^{74}K → ^{49}I, ^{80}F → ^{55}V, ^{82}T → ^{57}R, ^{85}K → ^{60}S, ^{86}I → ^{61}V, ^{94}F → ^{69}A, ^{95}T → ^{70}A, ^{96}L → ^{71}H, ^{99}Y → ^{74}A, ^{102}I → ^{77}V, ^{103}D → ^{78}G	MK281499
29	Chicken meat	*cdtC*, *flaA*	**526** (23)	211 (13)	^{49}I → ^{24}V, ^{67}I → ^{42}L, ^{71}Q → ^{46}H, ^{72}S → ^{47}T, ^{74}K → ^{49}I, ^{80}F → ^{55}V, ^{83}G → ^{58}V, ^{85}K → ^{60}S, ^{86}I → ^{61}V, ^{94}F → ^{69}A, ^{95}T → ^{70}A, ^{102}I → ^{77}V, ^{103}D → ^{78}G	MK281500

(Continued)

TABLE 4 | Continued

Isolate code no.	Source	Virulence genes pattern	*flaA*-SVR nucleotide allele (No. of variations)	*flaA*-SVR peptide allele (No. of variations)	**Translation variation reference → clone	Accession no.
30	Chicken meat	*cdtAC*, *flaA*	**526***	60 (14)	^{52}E → ^{28}K, ^{62}T → ^{38}I, ^{66}T → ^{42}I, ^{67}I → ^{43}T, ^{71}Q → ^{47}H, ^{72}S → ^{48}T, ^{74}K → ^{50}I, ^{80}F → ^{56}L, ^{90}G → ^{66}S, ^{94}F → ^{70}A, ^{95}T → ^{71}A, ^{99}Y → ^{75}A, ^{102}L → ^{78}R, ^{103}D → ^{79}G	MK281501
31	Human stool	*cdtABC*, *flaA*, *virB11*	177 (8)	74 (5)	^{32}I → ^{38}T, ^{36}T → ^{42}A, ^{58}S → ^{64}G, ^{71}Q → ^{77}L, ^{102}I → ^{108}L	MG677927.1
32	Human stool	*cdtABC*, *flaA*	239 (10)	9 (8)	^{1}K → ^{7}R, ^{12}L → ^{18}S, ^{27}E → ^{33}D, ^{36}T → ^{42}S, ^{42}Q → ^{48}H, ^{73}S → ^{79}A, ^{92}V → ^{98}D, ^{98}N → ^{104}S	MG677928.1
33	Human stool	*cdtABC*, *flaA*, *wlaN*	**288** (11)	92 (7)	^{8}D → ^{14}A, ^{26}M → ^{32}I, ^{29}L → ^{35}V, ^{63}V → ^{69}M, ^{71}Q → ^{77}L, ^{87}F → ^{93}L, ^{104}D → ^{110}E	MG677929.1
34	Human stool	*cdtABC*, *flaA*	177 (15)	74 (7)	^{10}Q → ^{10}E, ^{23}N → ^{23}Y, ^{52}E → ^{52}Q, ^{65}A → ^{65}G, ^{76}G → ^{76}D, ^{88}T → ^{88}A, ^{89}S → ^{89}L	MG677930.1
35	Human stool	*cdtABC*, *flaA*, *wlaN*	**1064** (10)	267 (10)	^{4}Q → ^{10}P, ^{17}M → ^{23}L, ^{31}N → ^{37}T, ^{38}F → ^{44}I, ^{50}N → ^{56}Y, ^{66}T → ^{72}I, ^{79}R → ^{85}I, ^{91}V → ^{97}A, ^{102}I → ^{108}L, ^{107}Y → ^{113}L	MG677931.1
36	Human stool	*cdtABC*, *flaA*	239 (9)	9 (8)	^{8}D → ^{14}E, ^{10}Q → ^{16}H, ^{19}Q → ^{25}K, ^{39}N → ^{45}Y, ^{46}G → ^{52}R, ^{62}T → ^{68}P, ^{74}K → ^{80}Q, ^{106}K → ^{112}Q	MG677932.1
37	Human stool	*cdtABC*, *flaA*	177 (14)	74 (9)	^{3}T → ^{3}I, ^{19}Q → ^{19}E, ^{34}N → ^{34}Y, ^{52}E → ^{52}D, ^{70}T → ^{70}S, ^{77}V → ^{77}A, ^{96}I → ^{96}V, ^{101}G → ^{101}S, ^{106}K → ^{106}E	MG677933.1
38	Human stool	*cdtABC*, *flaA*	**288** (7)	92 (5)	^{9}G → ^{2}V, ^{34}N → ^{27}S, ^{58}S → ^{51}T, ^{63}V → ^{56}M, ^{106}K → ^{99}R	MG677934.1
39	Human stool	*cdtAB*, *flaA*	177 (8)	74 (5)	^{32}I → ^{38}T, ^{36}T → ^{42}A, ^{58}S → ^{64}G, ^{71}Q → ^{77}L, ^{102}I → ^{108}L	MK281502
40	Human stool	*cdtBC*, *flaA*	177 (8)	74 (4)	^{32}I → ^{38}T, ^{36}T → ^{42}A, ^{58}S → ^{64}G, ^{71}Q → ^{77}L	MK281503
41	Human stool	*cdtAB*, *flaA*	177 (13)	74 (8)	^{19}Q → ^{12}E, ^{34}N → ^{27}Y, ^{52}E → ^{45}D, ^{70}T → ^{63}S, ^{77}V → ^{70}A, ^{96}I → ^{89}V, ^{101}G → ^{94}S, ^{106}K → ^{99}E	MK281504

*SVR, short variable region; cl. swab, cloacal swabs; A, alanine; R, arginine; N, asparagine; D, aspartic acid; C, cysteine; E, glutamic acid; Q, glutamine; G, glycine; H, histidine; I, isoleucine; L, leucine; K, lysine; M, methionine; F, phenylalanine; P, proline; S, serine; T, threonine; Y, tyrosine; V, valine. * Nucleotide alleles with asterisks have frameshift rather than point mutations. Novel allelic variants identified in this study are shown in bold. **The information to the left of the arrow refer to the identity and the position on the reference strains (deposited on http://pubmlst.org/campylobacter/) and the information to the right of the arrow show the corresponding identity and position on the query strains.*

in pigeon droplets (8.89%) was found to be much lower than that in chickens. A previous Canadian study reported also a low infection rate of *C. jejuni* in pigeons (9.1%) (Gabriele-Rivet et al., 2016).

The observation that the *flaA* gene was encoded by all analysed strains suggests the importance of this gene as a virulence marker in our Egyptian *C. jejuni* strains and possibly other *C. jejuni*. Our results corporate previous reports (e.g., Datta et al., 2003; Talukder et al., 2008; Rizal et al., 2010; Wieczorek et al., 2012; Shyaka et al., 2015), which also identified *flaA* gene in 100% of *C. jejuni* strains. However, a lower prevalence of *flaA* gene (75.5%) was reported in *C. jejuni* isolated from chicken meat in Brazil (Melo et al., 2013). This difference may be attributed to the isolate source, sample type and geographical location (Corcoran et al., 2006).

The *cdtA*, *cdtB*, and *cdtC* were detected in the analysed strains by the same percentage (80.49%), and more than half (58.54%) of the strains possessed the three CDT toxin genes together. Previous studies (Datta et al., 2003; Rozynek et al., 2005) reported that the prevalence of each of *cdtA*, *cdtB*, or *cdtC* genes in *C. jejuni* isolated from poultry and humans exceeded 80%. The high frequency of the co-existence of these subunits and their close genotypic association (**Figures 2B**, **3A**) was previously reported in Poland (70.8%) (Wieczorek and Osek, 2011) indicating that they are highly likely to co-express during an infection event. This is supported by the knowledge that these three subunits are required for full CDT toxin activity (Martinez et al., 2006).

The random forest classification and ROC analyses applied herein showed that the *cdtC* gene exhibited the highest similarity and thus the least discriminatory power (low AUC values) among

TABLE 5 | Distribution of virulence associated genes and identified allele numbers (at both nucleotide and peptide levels) among the entire collection of *C. jejuni* strains.

Isolate source	Virulence gene pattern*	*flaA*-SVR types (alleles)	
		Nucleotide	Peptide
Human (*n* = 11)	*cdtABC*, *flaA* (5); *cdtAB*, *flaA* (2); *cdtABC*, *flaA*, *wlaN* (2); *cdtBC*, *flaA* (1); *cdtABC*, *flaA*, *virB11* (1)	177 (6); 288 (2); 239 (2); 1064 (1)	74 (6); 92 (2); 9 (2); 267 (1)
Chicken (*n* = 14)	*cdtC*, *flaA* (3); *flaA* (2); *cdtABC*, *flaA*, *iam* (1); *cdtABC*, *flaA*, *virB11*, *iam* (1); *cdtAB*, *flaA* (1); *cdtAB*, *flaA, iam* (1); *cdtABC*, *flaA*, *wlaN*, *iam* (1); *cdtABC*, *flaA*, *virB11*, *wlaN* (1); *cdtAC*, *flaA*, *wlaN*, *iam* (1); *cdtAC*, *flaA*, *iam* (1); *cdtAC*, *flaA* (1)	177 (6); 526 (3); 288 (2); 1486 (2); 9 (1)	74 (6); 92 (4); 211 (3); 60 (1)
Pigeon (*n* = 16)	*cdtABC*, *flaA*, *iam* (6); *cdtABC*, *flaA* (5); *cdtBC*, *flaA* (2); *cdtABC*, *flaA*, *virB11*, *iam* (1); *cdtAB*, *flaA* (1); *cdtAB*, *flaA, iam* (1)	781 (2); 38 (2); 1118 (2); 731 (1); 940 (1); 1275 (1); 186 (1); 9 (1); 938 (1); 177 (1); 1486 (1); 756 (1); 1183 (1)	239 (4); 191 (3); 58 (2); 209 (2); 5 (1); 356 (1); 60 (1); 74 (1); 92 (1)

*SVR, short variable region. *Numbers in parentheses indicate the number of strains containing the respective virulence genes combination.*

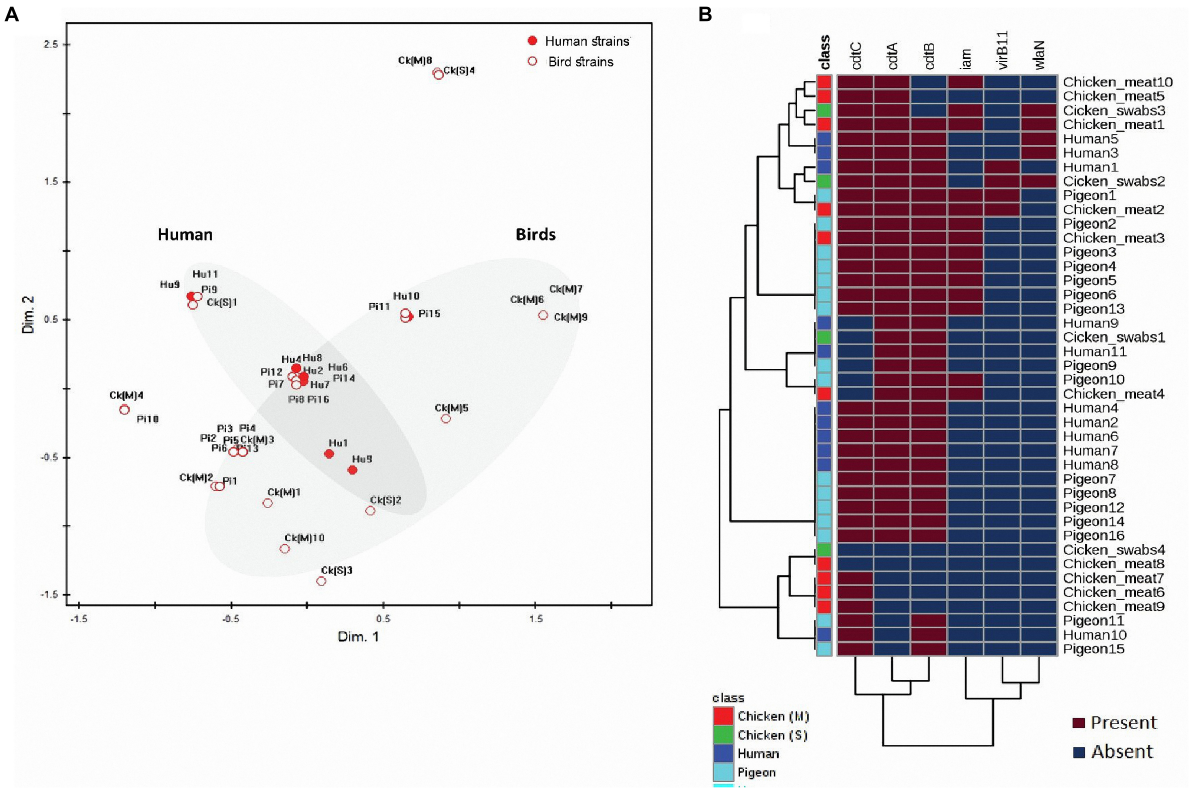

FIGURE 2 | Distribution and clustering of *C. jejuni* strains and the encoded virulence genes. **(A)** Non-metric multidimensional scaling (nMDS) showing the overlap between the bacterial strains (*n* = 41) represented by their sources. **(B)** Hierarchical clustering analyses showing the clustering pattern of both bacterial strains (*n* = 41) and the associated virulence genes (*n* = 6). *FlaA* gene was excluded from this analysis as it was expressed in all strains. The nMDS and the heat map were generated based on the expression profile of the studied virulence genes (*cdtC, cdtA, cdtB, iam, virB11,* and *wlaN*) in all strains (*n* = 41). Hu, human; pi, pigeon; ck (M), chicken meat and ck (S), chicken swabs. Bird strains refer to all strains from chicken and pigeon.

C. jejuni strains from all examined sources, whereas *iam* and *cdtB* were the highest dissimilar genes among strains from different sources and that *iam* gene has relatively high discriminatory power (high AUC value) than *cdtC* gene. It is plausible to assume that the genes (e.g., *cdtC*), which have similar frequency and low discriminatory power among strains isolated from different hosts could infer about the potential sources of infection if their expression potential was tracked back after an outbreak. However, the genes (e.g., *iam* and *cdtB*), which tend to have dissimilar frequencies and have high discriminatory power could differentiate among infection sources. While this result was based on a small data set, it suggests the potential importance of certain

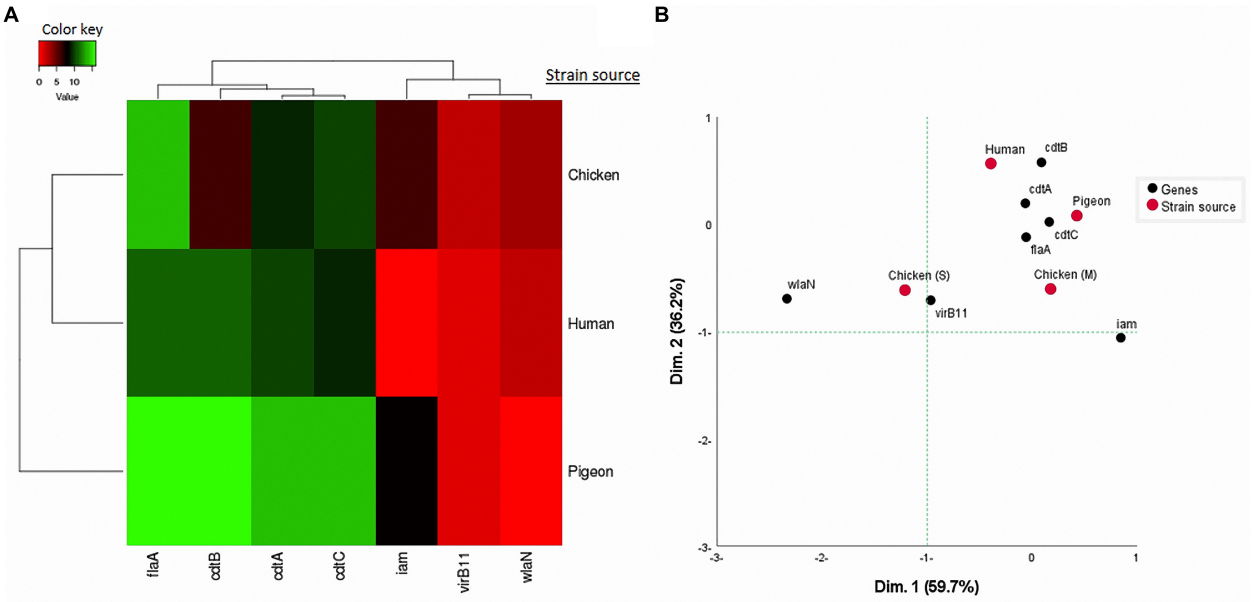

FIGURE 3 | (A) Hierarchical clustering of *C. jejuni* strain sources (human, pigeon, and chicken) and the associated virulence genes based on Euclidian distance. **(B)** Two-dimensional correspondence analysis (CA) showing the association between the sources of *C. jejuni* strains [human, pigeon, chicken meat (M) and cloacal swabs (S)] and the studied virulence genes.

genes in tracking and differentiating the sources of *C. jejuni* infection in human in small outbreaks. An additional wide scale profiling that includes more virulence genes in a large number of strains is needed to generalise these data.

In the current study, we analysed both virulence gene patterns and *flaA*-SVR sequences and alleles to better understand the extent of genetic diversity of *C. jejuni* strains among and within each host. Irrespective of the strain sources, we found a clear overlap among human and bird strains. In support of this, the overall Simpson's and Shannon's diversity indices were relatively high (**Table 3**). There was also a random distribution of the virulence gene patterns across the strains. Similar variabilities in the prevalence of virulence genes among *C. jejuni* have been reported previously (Abu-Madi et al., 2016). Taken together, these data reflect the high genetic diversity of our Egyptian *C. jejuni* strains.

Sequence-based *flaA*-SVR typing has been reported as a reliable genotyping method yielding reproducible results (Acke et al., 2010; El-Adawy et al., 2013). In the current study, the distribution of *flaA*-SVR alleles highlighted the diversity of the studied Egyptian *C. jejuni* strains when compared to those described previously in the PubMLST database. The variability in *flaA*-SVR gene sequences and alleles (**Supplementary Figure S2**) supported the impression from the virulence gene heterogeneity and further indicated the genotypic diversity of *C. jejuni*. The observed variation in the alleles/peptides might be due to the occurrence of distinct mutations (e.g., transition, transversion, additions or deletions). These genetic alterations could afford a survival advantage of the bacteria, which in turn might lead to evasion of the host immune response (Jerome et al., 2011). A similar heterogeneity was also obtained by Corcoran et al. who studied 41 *C. jejuni* strains from humans and poultry (Corcoran et al., 2006). Moreover, Ramees et al. (2015) reported a diversity of 65% among 32 analysed *C. jejuni* strains irrespective of their sources.

The current analysis showed that *C. jejuni* strains isolated from the same host did not reveal a similar frequency or distribution of both virulence genes and the *flaA* allelic variants (**Supplementary Table S1**), suggesting that *C. jejuni* strains studied here are not host-specific. Similar diversity was also shown previously (Corcoran et al., 2006) after analysing *flaA* gene of *C. jejuni* isolated from humans and poultry. Moreover, Vidal et al. (2016) reported a high genotypic diversity of *C. jejuni* isolated from a chicken broiler flock. The particular distribution of certain strains in certain niche could be attributed to differential response to environmental factors and/or management practices. This, in turn, will modulate the bacterial phenotypic properties (e.g., infectivity, survival and pathogenicity) and ultimately the colonisation in the host (Ahmed et al., 2002; Vidal et al., 2016). Taken together, these results indicate the existence of *C. jejuni* as quasi-species colonising the same host, which demonstrates the low host adaptability and the weak clonality of these *C. jejuni* strains as was suggested previously (Corcoran et al., 2006).

As evidenced by the measurement of diversity indices, virulence gene patterns and the average similarity of *flaA*-SVR sequences, chicken strains were found to be highly diverse relative to those from human or pigeon. The rationale behind the high diversity of *C. jejuni* in this particular host is not yet clear. However, the uniqueness of the chicken as a host for such bacteria (Awad et al., 2018) and the high load of *C. jejuni* (10^6 – 10^8 colony forming units/g) (Beery et al., 1988) in chicken gut might

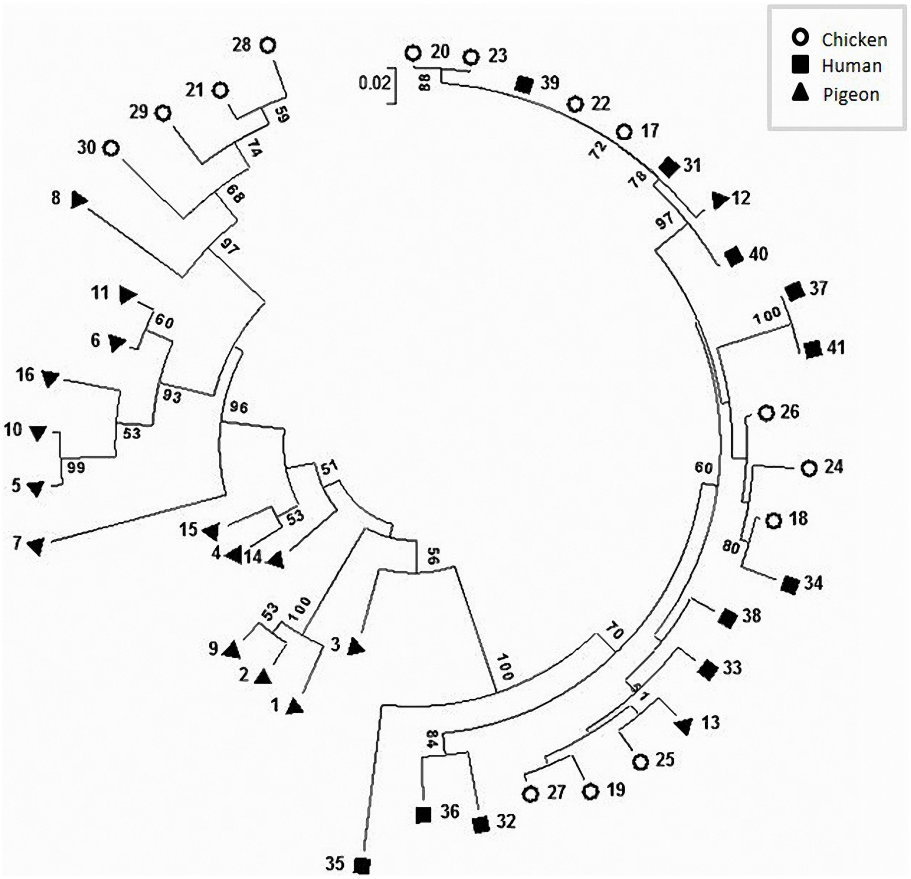

FIGURE 4 | Circular phylogenetic tree of the *flaA*-SVR sequences generated using the neighbour-joining method. The numbers on each branch indicate the calculated bootstrap values. The scale-bar indicates a branch length equivalent to a 2% difference in the nucleotide sequence.

account for this heterogeneity, which usually stems from frequent recombination and plasmid transfer among strains in the same niche. These data demonstrate the importance of chickens in the epidemiology and infection dynamics of *C. jejuni* in Egypt.

Applying a hierarchical clustering on the frequency of the presence of each virulence gene (**Figure 3A**) and allelic/peptide variants (**Supplementary Figures S2C,D**) in *C. jejuni* strains revealed that human strains were genotypically clustered close to chicken strains rather than to pigeon ones. While this needs to be interpreted using large studies, it suggests the importance of chicken as a source of human infection with *C. jejuni* as was stated previously (Oh et al., 2017).

A shortcoming of this study is due to the limited funding resources. Therefore, we described the diversity of *C. jejuni* depending on sequence-based typing of *flaA*-SVR gene, which is less costly and thus fits more the situation in developing countries, notably Egypt. While this approach is convenient for small-scale investigations, using advanced techniques such as pulsed-field gel electrophoresis (PFGE) and MLST would have added more sensitivity and accuracy to the results and would allow comparing different typing methods at once. Future studies are warranted in this direction. In conclusion, this is the first report in Egypt that describes the extent of genetic diversity of *C. jejuni* isolated from chickens, pigeons and humans. It suggests the possible role of poultry, particularly chickens, in the transmission of *C. jejuni* to humans. It is recommended to consider these observations in the future epidemiological evaluation and risk assessment of *C. jejuni* not only in poultry, but also in humans.

DATA AVAILABILITY STATEMENT

The datasets generated for this study can be found in the GenBank database with accession numbers KX066127–KX066135, MG677923–MG677934, and MK281494–MK281513.

ETHICS STATEMENT

The animal study was approved by the committee of Animal Welfare and Research Ethics of Faculty of Veterinary Medicine, Zagazig University. The study involving human participants was reviewed and approved by the research ethical committee of Faculty of Medicine, Zagazig University. The patients/participants provided their written informed consent to participate in this study.

AUTHOR CONTRIBUTIONS

MA, NA, and EA designed the study. MA and NA carried out the molecular analyses and participated in the data analysis. MS performed the bioinformatics and statistical analyses of the data. EE, MB, and RM conceived the study and participated in the design. MA, NA, and MS wrote the initial draft of the manuscript. All authors approved the final manuscript.

ACKNOWLEDGMENTS

The authors express their deep gratitude to Dr. Ahmed Hefny (Veterinary Hospital, Faculty of Veterinary Medicine, Zagazig University, Egypt) for his assistance during the collection of chicken samples and isolation of the bacteria. The authors are thankful to Dr. Hazem Ramadan (Hygiene and Zoonosis Department, Faculty of Veterinary Medicine, Mansoura University, Egypt) for his critical reading of the manuscript.

SUPPLEMENTARY MATERIAL

The Supplementary Material for this article can be found online at: https://www.frontiersin.org/articles/10.3389/fmicb.2019.02353/full#supplementary-material

FIGURE S1 | Degree of similarity of analysed virulence genes across the sources of *C. jejuni* strains. The figures show random forest classification with the predictive accuracy of each of the studied genes plotted on the *X*-axis against the respective gene name on the *Y*-axis. The mini heat maps show the frequency distribution of each gene in the respective strain sources.

FIGURE S2 | Clustering patterns and diversity of *C. jejuni* strains based on frequency of *flaA*-SVR alleles. **(A,B)** Show a non-metric multidimensional scaling of the 41 analysed strains based on the presence and absence of all alleles of the *flaA*-SVR nucleotides **(A)** and proteins **(B)**. **(C,D)** Show clustering pattern of *C. jejuni* strain sources (based on Euclidean distance) using the frequency of alleles at the nucleotide **(C)** and protein **(D)** levels as input data.

TABLE S1 | Frequency of virulence gene combinations, and nucleotide and peptide alleles among 41*C. jejuni* strains from different sources.

TABLE S2 | Distance matrix showing the percentage of similarity between each pair of the strains based on the alignment of *flaA*-SVR sequences. HU: humans, PI: pigeon, CK: chicken. *** indicates 100% similarity.

REFERENCES

Abd El-Tawab, A. A., Ammar, A. M., Ahmed, H. A., Ei Hofy, F. I., and Hefny, A. A. (2018). Fluoroquinolone resistance and *gyrA* mutations in *Campylobacter jejuni* and *Campylobacter coli* isolated from chicken in Egypt. *J. Glob. Antimicrob. Resist.* 13, 22–23. doi: 10.1016/j.jgar.2018.02.019

Abu-Madi, M., Behnke, J. M., Sharma, A., Bearden, R., and Al-Banna, N. (2016). Prevalence of virulence/stress genes in *Campylobacter jejuni* from chicken meat sold in Qatari retail outlets. *PLoS One* 11:e0156938. doi: 10.1371/journal.pone.0156938

Abuoun, M., Manning, G., Cawthraw, S. A., Ridley, A., Ahmed, I. H., Wassenaar, T. M., et al. (2005). Cytolethal distending toxin (CDT)-negative *Campylobacter jejuni* strains and anti-CDT neutralizing antibodies are induced during human infection but not during colonization in chickens. *Infect. Immun.* 73, 3053–3062. doi: 10.1128/IAI.73.5.3053-3062.2005

Acke, E., McGill, K., Lawlor, A., Jones, B. R., Fanning, S., and Whyte, P. (2010). Genetic diversity among *Campylobacter jejuni* isolates from pets in Ireland. *Vet. Rec.* 166, 102–106. doi: 10.1136/vr.c357

Ahmed, H. A., El Hofy, F. I., Ammar, A. M., Abd El Tawab, A. A., and Hefny, A. A. (2015). ERIC-PCR genotyping of some *Campylobacter jejuni* isolates of chicken and human origin in Egypt. *Vector Borne Zoonotic Dis.* 15, 713–717. doi: 10.1089/vbz.2015.1836

Ahmed, I. H., Manning, G., Wassenaar, T. M., Cawthraw, S., and Newell, D. G. (2002). Identification of genetic differences between two *Campylobacter jejuni* strains with different colonization potentials. *Microbiol.* 148, 1203–1212. doi: 10.1099/00221287-148-4-1203

Awad, W. A., Hess, C., and Hess, M. (2018). Re-thinking the chicken-*Campylobacter jejuni* interaction: a review. *Avian. Pathol.* 47, 352–363. doi: 10.1080/03079457.2018.1475724

Babicki, S., Arndt, D., Marcu, A., Liang, Y., Grant, J. R., Maciejewski, A., et al. (2016). Heatmapper: web-enabled heat mapping for all. *Nucleic Acids Res.* 44, W147–W153. doi: 10.1093/nar/gkw419

Beery, J. T., Hugdahl, M. B., and Doyle, M. P. (1988). Colonization of gastrointestinal tracts of chicks by *Campylobacter jejuni*. *Appl. Environ. Microbiol.* 54, 2365–2370.

Chong, J., and Xia, J. (2018). MetaboAnalystR: an R package for flexible and reproducible analysis of metabolomics data. *Bioinformatics* 34, 4313–4314. doi: 10.1093/bioinformatics/bty528

Coote, J. G., Stewart-Tull, D. E., Owen, R. J., Bolton, F. J., Siemer, B. L., Candlish, D., et al. (2007). Comparison of virulence-associated *in vitro* properties of typed strains of *Campylobacter jejuni* from different sources. *J. Med. Microbiol.* 56, 722–732. doi: 10.1099/jmm.0.47130-0

Corcoran, D., Quinn, T., Cotter, L., Whyte, P., and Fanning, S. (2006). Antimicrobial resistance profiling and *fla*-typing of Irish thermophillic *Campylobacter* spp. of human and poultry origin. *Lett. Appl. Microbiol.* 43, 560–565. doi: 10.1111/j.1472-765X.2006.01987.x

Datta, S., Niwa, H., and Itoh, K. (2003). Prevalence of 11 pathogenic genes of *Campylobacter jejuni* by PCR in strains isolated from humans, poultry meat and broiler and bovine faeces. *J. Med. Microbiol.* 52, 345–348. doi: 10.1099/jmm.0.05056-0

El-Adawy, H., Hotzel, H., Tomaso, H., Neubauer, H., Taboada, E. N., Ehricht, R., et al. (2013). Detection of genetic diversity in *Campylobacter jejuni* isolated from a commercial turkey flock using *flaA* typing, MLST analysis and microarray assay. *PLoS One* 8:e51582. doi: 10.1371/journal.pone.0051582

European Food Safety Authority. (2014). The European Union summary report on trends and sources of zoonoses, zoonotic agents and food-borne outbreaks in 2012. *EFSA J.* 12, 99–107. doi: 10.2903/j.efsa.2014.3547

Frazão, M. R., Medeiros, M. I., Duque, S. D., and Falcão, J. P. (2017). Pathogenic potential and genotypic diversity of *Campylobacter jejuni*: a neglected food-borne pathogen in Brazil. *J. Med. Microbiol.* 66, 350–359. doi: 10.1099/jmm.0.000424

Gabriele-Rivet, V., Fairbrother, J. H., Tremblay, D., Harel, J., Côté, N., and Arsenault, J. (2016). Prevalence and risk factors for *Campylobacter* spp., *Salmonella* spp., *Coxiella burnetii*, and Newcastle disease virus in feral pigeons (Columba livia) in public areas of Montreal, Canada. *Can. J. Vet. Res.* 80, 81–85.

Hammer, Ø, Harper, D. A. T., and Ryan, P. D. (2001). PAST: paleontological statistics software package for education and data analysis. *Palaeontol. Electronica* 4, 4–9.

Harrington, C. S., Thomson-Carter, F. M., and Carter, P. E. (1997). Evidence for recombination in the flagellin locus of *Campylobacter jejuni*: implications for the flagellin gene typing scheme. *J. Clin. Microbiol.* 35, 2386–2392.

Hermans, D., Van Deun, K., Martel, A., Van Immerseel, F., Messens, W., Heyndrickx, M., et al. (2011). Colonization factors of *Campylobacter jejuni* in the chicken gut. *Vet. Res.* 42:82. doi: 10.1186/1297-9716-42-82

Humphrey, T., O'Brien, S., and Madsen, M. (2007). *Campylobacters* as zoonotic pathogens: a food production perspective. *Int. J. Food Microbiol.* 117, 237–257. doi: 10.1016/j.ijfoodmicro.2007.01.006

Jerome, J. P., Bell, J. A., Plovanich-Jones, A. E., Barrick, J. E., Brown, C. T., and Mansfield, L. S. (2011). Standing genetic variation in contingency loci drives the rapid adaptation of *Campylobacter jejuni* to a novel host. *PLoS One* 6:e16399. doi: 10.1371/journal.pone.0016399

Kimura, M. (1980). A simple method for estimating evolutionary rates of base substitutions through comparative studies of nucleotide sequences. *J. Mol. Evol.* 16, 111–120. doi: 10.1007/bf01731581

Kordinas, V., Nicolaou, C., Ioannidis, A., Papavasileiou, E., John Legakis, N., and Chatzipanagiotou, S. (2005). Prevalence of four virulence genes in *Campylobacter jejuni* determined by PCR and sequence analysis. *Mol. Diagn.* 9, 211–215. doi: 10.1007/bf03260094

Kovacic, A., Listes, I., Vucica, C., Kozacinski, L., Tripkovic, I., and Sisko-Kraljevic, K. (2013). Distribution and genotypic characterization of *Campylobacter jejuni* isolated from poultry in Split and Dalmatia County. *Croatia. Zoonoses Public Health* 60, 269–276. doi: 10.1111/j.1863-2378.2012.01519.x

Maansi, N. R., Kumar, D., and Upadhyay, A. K. (2018). Virulence typing and antibiotic susceptibility profiling of thermophilic campylobacters isolated from poultry, animal, and human species. *Vet. World* 11, 1698–1705. doi: 10.14202/vetworld.2018.1698-1705

Martinez, I., Mateo, E., Churruca, E., Girbau, C., Alonso, R., and Fernandez-Astorga, A. (2006). Detection of *cdtA*, *cdtB*, and *cdtC* genes in *Campylobacter jejuni* by multiplex PCR. *Int. J. Med. Microbiol.* 296, 45–48. doi: 10.1016/j.ijmm.2005.08.003

McCarthy, N. D., Colles, F. M., Dingle, K. E., Bagnall, M. C., Manning, G., Maiden, M. C., et al. (2007). Host-associated genetic import in *Campylobacter jejuni*. *Emerg. Infect. Dis.* 13, 267–272. doi: 10.3201/eid1302.060620

Meinersmann, R. J., Helsel, L. O., Fields, P. I., and Hiett, K. L. (1997). Discrimination of *Campylobacter jejuni* isolates by *fla* gene sequencing. *J. Clin. Microbiol.* 35, 2810–2814.

Meinersmann, R. J., Phillips, R. W., Hiett, K. L., and Fedorka-Cray, P. (2005). Differentiation of *Campylobacter* populations as demonstrated by flagellin short variable region sequences. *Appl. Environ. Microbiol.* 71, 6368–6374. doi: 10.1128/AEM.71.10.6368-6374.2005

Melo, R. T., Nalevaiko, P. C., Mendonça, E. P., Borges, L. W., Fonseca, B. B., Beletti, M. E., et al. (2013). *Campylobacter jejuni* strains isolated from chicken meat harbor several virulence factors and represent a potential risk to humans. *Food Control* 33, 227–231. doi: 10.1016/j.foodcont.2013.02.032

Oh, J. Y., Kwon, Y. K., Wei, B., Jang, H. K., Lim, S. K., Kim, C. H., et al. (2017). Epidemiological relationships of *Campylobacter jejuni* strains isolated from humans and chickens in South Korea. *J. Microbiol.* 55, 13–20. doi: 10.1007/s12275-017-6308-8

Quinn, P. J., Carter, M. E., Markey, B. K., and Carter, G. R. (eds) (1994). "*Campylobacter* species," in *Clinical Veterinary Microbiology*, (London: Mosby-Year Book Europe Limited), 268–272.

Rahimi, E., and Ameri, M. (2011). Antimicrobial resistance patterns of *Campylobacter* spp. isolated from raw chicken, turkey, quail, partridge, and ostrich meat in Iran. *Food Control* 22, 1165–1170. doi: 10.1016/j.foodcont.2011.01.010

Ramees, T. P., Suman Kumar, M., Dubal, Z. B., Sivakumar, A. M., Gupta, S., Dhama, K., et al. (2015). Genotyping of *Campylobacter jejuni* and *C. coli* from different sources and human by ERIC-PCR. *J. Vet. Public Health* 13, 93–98.

Ramonaite, S., Tamuleviciene, E., Alter, T., Kasnauskyte, N., and Malakauskas, M. (2017). MLST genotypes of *Campylobacter jejuni* isolated from broiler products, dairy cattle and human campylobacteriosis cases in Lithuania. *BMC Infect. Dis.* 17:430. doi: 10.1186/s12879-017-2535-1

Rizal, A., Kumar, A., and Vidyarthi, A. S. (2010). Prevalence of pathogenic genes in *Campylobacter jejuni* isolated from poultry and human. *Internet J. Food Saf.* 12, 29–34.

Rozynek, E., Dzierzanowska-Fangrat, K., Jozwiak, P., Popowski, J., Korsak, D., and Dzierzanowska, D. (2005). Prevalence of potential virulence markers in Polish *Campylobacter jejuni* and *Campylobacter coli* isolates obtained from hospitalized children and from chicken carcasses. *J. Med. Microbiol.* 54, 615–619. doi: 10.1099/jmm.0.45988-0

Sails, A. D., Swaminathan, B., and Fields, P. I. (2003). Clonal complexes of *Campylobacter jejuni* identified by multilocus sequence typing correlate with strain associations identified by multilocus enzyme electrophoresis. *J. Clin. Microbiol.* 41, 4058–4067. doi: 10.1128/jcm.41.9.4058-4067.2003

Sainato, R., ElGendy, A., Poly, F., Kuroiwa, J., Guerry, P., Riddle, M. S., et al. (2018). Epidemiology of *Campylobacter* infections among children in Egypt. *Am. J. Trop. Med. Hyg.* 98, 581–585. doi: 10.4269/ajtmh.17-0469

Saitou, N., and Nei, M. (1987). The neighbor-joining method: a new method for reconstructing phylogenetic trees. *Mol. Biol. Evol.* 4, 406–425. doi: 10.1093/oxfordjournals.molbev.a040454

Shannon, C. A. (1948). Mathematical theory of communication. *Bell Syst. Tech. J.* 27, 379–423. doi: 10.1002/j.1538-7305.1948.tb01338.x

Shyaka, A., Kusumoto, A., Chaisowwong, W., Okouchi, Y., Fukumoto, S., Yoshimura, A., et al. (2015). Virulence characterization of *Campylobacter jejuni* isolated from resident wild birds in Tokachi area, Japan. *J. Vet. Med. Sci.* 77, 967–972. doi: 10.1292/jvms.15-0090

Simpson, E. H. (1949). Measurement of diversity. *Nature* 163:688. doi: 10.1038/163688a0

Talukder, K. A., Aslam, M., Islam, Z., Azmi, I. J., Dutta, D. K., Hossain, S., et al. (2008). Prevalence of virulence genes and cytolethal distending toxin production in *Campylobacter jejuni* isolates from diarrheal patients in Bangladesh. *J. Clin. Microbiol.* 46, 1485–1488. doi: 10.1128/JCM.01912-07

Tamura, K., Peterson, D., Peterson, N., Stecher, G., Nei, M., and Kumar, S. (2011). MEGA5: molecular evolutionary genetics analysis using maximum likelihood, evolutionary distance, and maximum parsimony methods. *Mol. Biol. Evol.* 28, 2731–2739. doi: 10.1093/molbev/msr121

Thompson, J. D., Higgins, D. G., and Gibson, T. J. (1994). CLUSTAL W: improving the sensitivity of progressive multiple sequence alignment through sequence weighting, position-specific gap penalties and weight matrix choice. *Nucleic Acids Res.* 22, 4673–4680. doi: 10.1093/nar/22.22.4673

Vandepitte, J., Verhaegen, J., Engbaek, K., Rohner, P., Piot, P., and Heuck, C. (2003). *Basic Laboratory Procedures in Clinical Bacteriology*, 2nd Edn. Geneva: World Health Organization.

Vazquez, B., Esperon, F., Neves, E., Lopez, J., Ballesteros, C., and Munoz, M. J. (2010). Screening for several potential pathogens in feral pigeons (*Columba livia*) in Madrid. *Acta Vet. Scand.* 52:45. doi: 10.1186/1751-0147-52-45

Vidal, A. B., Colles, F. M., Rodgers, J. D., McCarthy, N. D., Davies, R. H., Maiden, M. C. J., et al. (2016). Genetic diversity of *Campylobacter jejuni* and *Campylobacter coli* isolates from conventional broiler flocks and the impacts of sampling strategy and laboratory method. *Appl. Environ. Microbiol.* 82, 2347–2355. doi: 10.1128/AEM.03693-15

Wang, G., Clark, C. G., Taylor, T. M., Pucknell, C., Barton, C., Price, L., et al. (2002). Colony multiplex PCR assay for identification and differentiation of *C. jejuni*, *C. coli*, *C. lari*, *C. upsaliensis* and *C. fetus* subsp. fetus. *J. Clin. Microbiol.* 40, 4744–4747.

Wardak, S., and Jagielski, M. (2009). Evaluation of genotypic and phenotypic methods for the differentiation of *Campylobacter jejuni* and *Campylobacter coli* clinical isolates from Poland. II. PFGE, ERIC-PCR, PCR-*fla*A-RFLP and MLST. *Med. Dośw. Mikrobiol.* 61, 63–77.

Wieczorek, K., and Osek, J. (2011). Molecular characterization of *Campylobacter* spp. isolated from poultry faeces and carcasses in Poland. *Acta Vet. Brno* 80, 19–27. doi: 10.2754/avb201180010019

Wieczorek, K., Szewczyk, R., and Osek, J. (2012). Prevalence, antimicrobial resistance, and molecular characterization of *Campylobacter jejuni* and *C. coli* isolated from retail raw meat in Poland. *Vet. Med.* 57, 293–299. doi: 10.17221/6016-vetmed

Zheng, J., Meng, J., Zhao, S., Singh, R., and Song, W. (2006). Adherence to and invasion of human intestinal epithelial cells by *Campylobacter jejuni* and *Campylobacter coli* isolates from retail meat products. *J. Food Prot.* 69, 768–774. doi: 10.4315/0362-028x-69.4.768

Conflict of Interest: The authors declare that the research was conducted in the absence of any commercial or financial relationships that could be construed as a potential conflict of interest.

frontiers in Microbiology

ORIGINAL RESEARCH
published: 24 October 2019
doi: 10.3389/fmicb.2019.02443

A Sensitive, Specific and Simple Loop Mediated Isothermal Amplification Method for Rapid Detection of *Campylobacter* spp. in Broiler Production

Than Linh Quyen[1], Steen Nordentoft[2†], Aaydha Chidambara Vinayaka[2], Tien Anh Ngo[2†], Pia Engelsmenn[2], Yi Sun[3], Mogens Madsen[1], Dang Duong Bang[2] and Anders Wolff[1]**

[1] Department of Biotechnology and Biomedicine, Technical University of Denmark (DTU-Bioengineering), Lyngby, Denmark, [2] National Food Institute, Technical University of Denmark (DTU-Food), Lyngby, Denmark, [3] Department of Health Technology, Technical University of Denmark (DTU-Health Tech), Lyngby, Denmark

OPEN ACCESS

Edited by:
Nicolae Corcionivoschi,
Agri-Food and Biosciences Institute (AFBI), United Kingdom

Reviewed by:
Xiaonan Lu,
University of British Columbia, Canada
Robert J. Moore,
RMIT University, Australia

***Correspondence:**
Dang Duong Bang
ddba@food.dtu.dk
Anders Wolff
awol@dtu.dk

†Present address:
Steen Nordentoft,
Novo Nordisk A/S, Bagsværd, Denmark
Tien Anh Ngo,
Vinmec Biobank, Vinmec HealthCare System, Hanoi, Vietnam

Specialty section:
This article was submitted to Food Microbiology, a section of the journal Frontiers in Microbiology

Received: 20 June 2019
Accepted: 10 October 2019
Published: 24 October 2019

Citation:
Quyen TL, Nordentoft S, Vinayaka AC, Ngo TA, Engelsmenn P, Sun Y, Madsen M, Bang DD and Wolff A (2019) A Sensitive, Specific and Simple Loop Mediated Isothermal Amplification Method for Rapid Detection of Campylobacter spp. in Broiler Production. Front. Microbiol. 10:2443. doi: 10.3389/fmicb.2019.02443

Campylobacteriosis is one of the most common foodborne diseases worldwide. Two *Campylobacter* species – *C. jejuni* and *C. coli* in poultry and poultry products are considered to be the main source of human campylobacteriosis. Therefore, studying *Campylobacter* status in poultry flocks is needed to prevent transmission of disease and reduce human risk, health cost, and economic losses. In this study, we adapted and used a Loop-Mediated Isothermal Amplification (LAMP) assay for specific, sensitive, simple and cost-effective rapid detection of *C. jejuni* and *C. coli* in the poultry production chain. Amplified LAMP products were detected using a small, low-cost portable commercial blue LED transilluminator and a direct visual detection strategy was demonstrated. By using optimized conditions for amplification a limit of detection (LOD) of 50 CFU/ml was achieved for testing of *C. jejuni* and *C. coli* in spiked chicken feces without enrichment. The method took 60–70 min from receiving the samples to the final results (including 30 min for amplification). The optimized LAMP showed a relative accuracy of 98.4%, a specificity of 97.9%, and a sensitivity of 100% in comparison to real-time PCR method. Cohen's kappa index also showed an excellent agreement (0.94) between the two methods. The results showed that the method is specific, sensitive and is suitable to develop for rapid detection of *Campylobacter* spp. at poultry production.

Keywords: campylobacteriosis, *Campylobacter* spp., loop mediated isothermal amplification, broiler fecal sample, broiler chicken production, rapid detection

INTRODUCTION

Campylobacteriosis is one of the leading causes of bacterial diarrhea worldwide (CDC, 2017; Helwigh et al., 2017). Two *Campylobacter* species, *C. jejuni* and *C. coli* account for the majority of human campylobacteriosis (Lawson et al., 1999; Tresse et al., 2017). Poultry and poultry products are considered to be the main sources for disease transmission (Wingstrand et al., 2006; Powell et al., 2012). The prevalence of *Campylobacter* in broiler flocks remains high (Sibanda et al., 2018). Data obtained from an electronically distributed survey in Denmark reported that 63% of the broiler farms tested positive for *Campylobacter* (Sandberg et al., 2015). Thus, there is an urgent need for a fast and simple method suitable for the detection of *Campylobacter* within poultry production chains.

Identification of *C. jejuni* and *C. coli* using conventional bacterial cultures in combination with biochemical-based assay are time-consuming (requiring more than 4 days) and laborious (Biesta-Peters et al., 2019). Therefore, several alternate methods have been developed and reported for the detection of *Campylobacter* spp. (**Supplementary Table S1**). Although ELISA (enzyme-linked immunosorbent assay) (RIDASCREEN® Campylobacter, R-Biopharm AG, Darmstadt, Germany) and real-time polymerase chain reaction (real-time PCR) (Alves et al., 2016) could detect *Campylobacter* in much shorter time (within 2 h) from fecal materials, the limit of detection remains high (**Supplementary Table S1**). Moreover, real-time PCR require sophisticated and expensive equipment to amplify and detect the presence of *Campylobacter*. Therefore, both PCR and real-time PCR are not suitable for rapid detection of the pathogens in the production chains. LAMP has been used to overcome the drawbacks of the PCR. LAMP is faster than PCR (de Paz et al., 2014; Sabike and Yamazaki, 2019) and can be performed under constant temperature in a range of 60–65°C, thus eliminating the need for sophisticated thermal control as in PCR (Mori et al., 2013; Sun et al., 2015). LAMP has several advantages such as fast reaction, simple operation, low cost, high sensitivity and specificity (Njiru, 2012; Velders et al., 2018). Moreover, the LAMP reaction is more tolerant to inhibitors in comparison to PCR and real-time PCR assays (Stedtfeld et al., 2014; Kosti et al., 2015). The LAMP reaction produces large amounts of amplified products (dsDNA). It can therefore even be detected by naked eyes when using appropriate DNA staining techniques (Xie et al., 2014). With these advantages, the LAMP may be suitable for rapid detection of pathogens in the poultry production chains.

LAMP was developed for the detection of *Campylobacter* spp. in poultry samples such as meat, carcass swabs, and fecal samples (Yamazaki et al., 2008, 2009b; Sabike et al., 2016; Romero and Cook, 2018; Sabike and Yamazaki, 2019). To study the epidemiology of *Campylobacter* spp. and to prevent transmission in the production chain, the time taken for detection of *Campylobacter* is crucial. However, to detect the presence of the *Campylobacter* spp. in cloacal swabs, ceca, meat and environmental cleaning samples, an enrichment step of 22 to 24 h is needed (Yamazaki et al., 2009b; Sabike et al., 2016; Sabike and Yamazaki, 2019). Consequently, it takes a total of at least 24–26 h for sample enrichment, preparation, amplification, and detection. Moreover, *Campylobacter* grows slowly and requires specific microaerobic conditions to grow, which makes it difficult to apply this method for the detection of *Campylobacter* spp. in the production chains. In contrast, stool specimens may not require an enrichment step since *Campylobacter* infected chicken feces may contain up to 10^9 *Campylobacter* per gram (Corry and Atabay, 2001; Hermans et al., 2010; Addis and Sisay, 2015). However, the content of inhibitors in feces is frequently high, which could inhibit the LAMP reaction (Schrader et al., 2012). In one study, to detect *Campylobacter* spp. directly from poultry feces with a limit of detection (LOD) of 1.2–1.4 CFU per test, the stool samples had to be diluted 1:4000 to reduce the inhibition effects (Yamazaki et al., 2008). Therefore, the method could not detect the fecal samples containing less than 1.2×10^6 CFU of *C. coli* or 1.4×10^6 CFU of *C. jejuni* per gram of stool specimen.

In this study, to provide a simple, rapid, cost-effective and sensitive method suitable for rapid detection of *Campylobacter* spp. within poultry production chains, we have developed an optimized LAMP assay with smaller reaction volume, a shorter reaction time, and higher sensitivity using a commercial LAMP kit. We also evaluated the use of a commercial mini UV transilluminator, which is small, simple, low cost and portable for LAMP detection. Moreover, for evaluation of the performance of the optimized LAMP method, a conventional real-time PCR was used in parallel to study the epidemiology of *Campylobacter* infection in a broiler farm.

MATERIALS AND METHODS

DNA Preparation

Chromosomal DNA from all bacteria strains used in this study (listed in **Table 1**) was isolated using DNeasy Blood and Tissue kit (Qiagen, Germany). The DNA concentration was determined by NanoDrop (Thermo Scientific, United States).

Preparation of DNA from fecal sock samples: Each pair of boot socks was placed in a stomacher bag containing 200 ml of saline (0.9% NaCl). Fecal materials were released by gentle manipulation of the socks for 2 min. 1 ml of the suspension was collected and centrifuged at 5000 × *g* for 5 min. After discarding the supernatant, the pellet was used for DNA extraction by

TABLE 1 | Bacterial strains used in this study.

No.	Bacterial strains	Source
1.	*C. jejuni*	NTCC 11284
2.	*C. coli*	CCUG 11283
3.	*C. lari*	CCUG 18267 and CUUG 860115
4.	*C. larilio 56*	CCUG 19512 and CUUG 920306
5.	*C. larilio 34*	CCUG 20575 and CUUG 870508
6.	*C. mucosalis*	CCUG 6822
7.	*C. sputorums* subsp. *spo*	CCUG 9728
8.	*C. upsaliensis*	CCUG 14913
9.	*C. upsaliensis*	CCUG 23626
10.	*C. fetus* subsq. *fetus*	CCUG 6823A and CCUG 940118
11.	*C. concisus*	CCUG 13144 and CUUG 950201
12.	*C. hyointestinalis*	CCUG 19512 and CUUG 920306
13.	*S.* Typhimurium	DVI Jeo 3979 Jgt.110
14.	*S.* Enteritidis	92243/nybol 3L
15.	*S.* Dublin	H64004
16.	*S. derby*	DVI SD1
17.	*E. faecalis*	ATCC 29212
18.	*E. faecium*	CCUG 47860
19.	*E. coli*	CCUG 17620
20.	*S. pneumoniae*	ATCC 49619
21.	*P. hauseri*	CCUG 36761
22.	*C. freundii*	CCUG 418
23.	*A. skirrowii*	CCUG 10374 and CCUG 910801
24.	*A. cryaerophilus*	CCUG 17801
25.	*A. butlezi*	CCUG30485
26.	*Y. ruckerii*	ATCC 29473

an automate KingFisher™ Purification system (Thermo Fisher, Copenhagen, Denmark) or stored at minus 20°C for later use. Further, the pellet was treated with 200 μl of lysis buffer consisting of 190 μl of magnetic lysis buffer and 10 μl of Proteinase K (20 mg/ml) followed by incubation for 10 min at room temperature. 100 μl of the treated sample was used to purify DNA by an automate KingFisher™ Purification system using the Magnesil KF Genomic DNA kit (Promega, Denmark) described previously (Lund et al., 2003). Finally, the supernatant was used as the template for real-time PCR and the LAMP assay.

Real-Time PCR

A real-time PCR targeting the 16S rRNA gene of thermophilic *Campylobacter* species (*C. jejuni*, *C. coli*) was used as a reference method to evaluate the performance of the LAMP (Josefsen et al., 2010). Primer sequences used for real-time PCR were listed in **Supplementary Table S2**. Each reaction contained 25 μl of master mixture consisting of 1X buffer, 2.5 mM of $MgCl_2$, 2.5 U of Tth enzyme (Roche, Denmark), 6.96% Glycerol (Merck, Germany), 0.6 mM of dNTPs, 0.01 mg/ml of BSA, 0.5 μM of forward primer OT-1559, 0.5 μM of reverse primer 18-1, 0.076 μM of *Campylobacter* LNA probe, 0.06 μM of IAC probe, 0.24×10^{-9} μM of IAC (primers used for construction of the internal amplification control) (**Supplementary Table S2**) (Life Technology Europe, Roskilde, Denmark), 10 μl of DNA template and 2.22 μl of PCR grade water (Sigma-Aldrich, Denmark). The real-time PCR conditions were 95°C for 3 min, followed by 40 cycles of 95°C for 15 s, 60°C for 60 s and 72°C for 30 s. The real-time PCR was performed on a MxPro-Mx3005P (Agilent Technologies ApS Glostrup, Denmark).

LAMP Assay

The LAMP assay was carried out using a Loopamp *Campylobacter* detection kit (Eiken Chemical Co., Ltd., Tokyo, Japan). The kit consists of a set of specific primers to recognize the oxidoreductase gene from *C. jejuni* and aspartate kinase gene from *C. coli*. The kit does not specifically identify *C. jejuni* or *C. coli* but can detect both species. LAMP reaction contained 12.5 μl of the master mixture consisting of 6.25 μl of the reaction mixture, 1.25 μl of primer mixture *Campylobacter*, 0.5 μl of *Bst* DNA polymerase, 2.5 μl of distilled water and 2 μl of the template. In the LAMP reactions, PCR grade water was used as negative control, and purified genomic DNA was used as positive control. The LAMP reaction was performed on a Dri-Block® DB-2TC (TECHNE, Staffordshire, United Kingdom) at a constant temperature of 65°C for 30 or 60 min. The reactions were terminated by heating up to 80°C for 2 min.

Preparation of *Campylobacter*-Spiked Fecal Samples for Testing the Sensitivity of LAMP

Initially, fecal sock samples were pre-confirmed for the absence of *C. jejuni* and *C. coli* by both conventional culture and real-time PCR. Different dilutions of *Campylobacter* cells for spiking in the fecal sock samples were prepared from serial 10-fold dilutions in saline water from stock cultures (OD_{600} = 0.3, spectrophotometer UV-1600PC) of a *C. jejuni* CCUG 11284 and a *C. coli* CCUG 11283 separately. 100 μl of each dilution was used to spike in 1 ml suspension of the *Campylobacter* negative fecal sock samples. The mixtures were centrifuged at 5000g for 5 min and the pellets were then used for DNA extraction as described above. The samples were analyzed by both LAMP and real-time PCR methods. Further, 100 μl of each dilution from 10^{-1} to 10^{-8} were spread on blood agar plates for determining colony forming unit (CFU) and the plates were incubated at 41.5°C in the microaerobic atmosphere. The CFU was determined by colonies counting after 48 h of incubation.

Data Analysis

Evaluation of assays precision between real-time PCR and LAMP was calculated based on relative accuracy, relative specificity, relative sensitivity and Cohen's kappa index as described previously (Chin et al., 2016; Vinayaka et al., 2019) using following formulas:

$$\textit{Relative accuracy } AC\,(\%) = \frac{(\mathrm{PA} + \mathrm{NA})}{\mathrm{N}} \times 100$$

$$\textit{Relative specificity } SP\,(\%) = \frac{\mathrm{NA}}{\mathrm{N}-} \times 100$$

$$\textit{Relative sensitivity } SE\,(\%) = \frac{\mathrm{PA}}{\mathrm{N}+} \times 100$$

$$\textit{Cohen's Kappa index} = \frac{\mathrm{P\,(o)} - \mathrm{P(e)}}{1 - \mathrm{P(e)}}$$

Where:

PA: the positive agreement between the real-time PCR and LAMP methods;

NA: the negative agreement between the real-time PCR and LAMP methods;

N: total number of samples (NA + PA + PD + ND);

PD: false positives in the LAMP method;

ND: false negatives in the LAMP method;

N−: total number of negative results (NA + PD);

N+: total number of positive results (PA + PD);

P(o): (PA + NA)/N; and

P(e): {(positive recovery in real-time PCR/total number of tested samples (N)) × (negative recovery in real-time PCR/total number of tested samples (N))} + {(negative recovery in LAMP/total number of tested samples (N)) × (negative recovery in real-time PCR/total number of tested samples (N))}.

Visual Detection of LAMP Products

LAMP products were visually detected by two different methods: direct visual detection under UV light by staining DNA using SYBR® Safe DNA intercalating dye and agarose gel electrophoresis.

Direct visual detection using SYBR® Safe staining DNA: The SYBR® Safe (10 000X concentrate in DMSO, Life Technology, Denmark) was diluted 1:10, and 1 μl of diluted dye was added to each tube after LAMP reaction. The tubes were

observed under UV light from a portable DR22 blue LED transilluminator (**Supplementary Figure S1**) (Clare Chemical Research, Inc., United States).

Gel electrophoresis detection: After LAMP reactions, 5 μl of each amplified LAMP product were loaded on 2% agarose gel containing 1X of SYBR® Safe DNA Gel Stain (Invitrogen, Life Technologies, United States). Gel electrophoresis was carried out at 100 volts for 60 min and the gel electrophoresis patterns were observed under Bio-Rad Gel Doc 2000 UV transilluminator (Bio-Rad Life Science, Denmark).

Study Design and Selection of Poultry Farm

To evaluate the ability of the method for rapid detection of *Campylobacter*, an evaluation trial was conducted in a large broiler farm located in Jutland, Denmark. The farm comprises 16 houses that are placed in blocks of four. All the four blocks have the same design with an entrance in the middle leading to a corridor from where there are doors to access to the 4 houses (**Figure 1**). During the poultry production period, fecal samples were collected from 16 houses, separately. Sampling was done on a weekly basis for four weeks by the boot sock sampling method as described previously (Food Standard Agency annual report, 2004/05). Briefly, elastic textile bands (Qualicum Scientific Ltd./Solar Biological Inc, United Kingdom) moistured with tryptone buffer (SteriSox, SODIBOX Nevez, France) were placed on clean boots. Fecal samples were collected from the floor of each poultry house by a farmer walking around the house. The socks were then placed in zipper bags and sent to the laboratory. The samples were processed in the lab as described above.

RESULTS AND DISCUSSION

Optimization of LAMP Assay Conditions

Different volumes of the LAMP reaction ranging from 3 to 25 μl were selected and tested using 2 ng of *C. jejuni* DNA as a template. It is estimated that 2 ng DNA *C. jejuli* corresponds to 1.13×10^6 genome equivalents (Chin et al., 2017). We observed LAMP products in all the reaction volumes tested such as 25, 12.5, and 6 μl (**Figure 2A**). Even small reaction volumes of 3 and 5 μL were sufficient enough to generate good LAMP signals (result not shown). The results indicated that the reaction volume had no influence on the LAMP efficiency and assay principle.

Different reaction times of 5, 10, 15, 30, 45, and 60 min using 2 ng of *Campylobacter* DNA as a template were also tested to define a suitable reaction time for the LAMP assay. There were no visible LAMP amplifications for 5 and 10 min reactions, but LAMP products were visible after 15 min (**Figure 2B**). More amplified LAMP products were obtained after 30 min, whereas the intensity remained the same as the reaction went on for 45 and 60 min (**Figure 2B**). Hence, 30 min of incubation has been selected for further experiments.

It is intended to adopt this technique into the poultry production chains wherein, the cost of each test is a primary concern. Many studies of LAMP assay were reported using different volumes (12.5 μl, 25 μl, even 50 μl) for LAMP reactions (Kato et al., 2005; Wang et al., 2008; Yamazaki et al., 2008, 2009b; Peng et al., 2011; Zhang et al., 2013). However, until now, no study has addressed appropriate reaction volume for LAMP assay. The cost of one *Campylobacter* Detection Kit with 48 reactions (25 μl per reaction as recommended by manufacture) from Eiken Ltd., Japan was 4456,50 DKK. As a consequence, each reaction (25 μl as recommended by the manufacturer) cost ∼93 DKK which was a rather high cost for screening pathogens at farms. Therefore, the result of this study showing reaction volume did not influence the efficiency of the assay will help reduction of the cost when using LAMP for the detection of pathogens at farms. Further, KingFisher™ Purification system used in this study concentrates the samples and provides a good quality of DNA template. The cost of DNA extraction and purification is ∼23 DKK per sample and it is possible to process 24 samples at once in approximately 20 min.

Diagnosis time of foodborne disease screening is considered to be vital for preventing transmission and decreasing economic losses in broiler production. Rapid detection strategies with high specificity and sensitivity are of much relevance for broiler production. In this study, after 30 min of the LAMP reaction we were able to detect the presence of *C. coli*/*C. jejuni* in fecal samples as low as 50 CFU/mL without enrichment. The reaction time in this study was shorter in comparison to previous reports (35–60 min) (Iwamoto et al., 2003; Kato et al., 2005; Wang et al., 2008; Yamazaki et al., 2009a; Yang et al., 2010; Zhang et al., 2012, 2013). Zhuang et al. (2014) reported a LAMP reaction that can detect *Salmonella* in chicken feces within 25 min with a detection limit of 200 CFU per reaction that was 200 times higher than this study. Total time from sample preparation to the final result in this study was 60–70 min, and it is much shorter than previous reports (Kato et al., 2005; Okamura et al., 2008; Yamazaki et al., 2008, 2009b; Techathuvanan et al., 2010).

Comparison of the Sensitivity of Optimized LAMP Assay at Different Reaction Times

To compare the sensitivity of the optimized LAMP assay, reaction time of 30 min was compared with 60 min of amplification. A serial dilution of *C. jejuni* DNA ranging from 0.1 pg to 2 ng was prepared and used as a template for the LAMP reaction. **Figure 3** shows that there were no LAMP amplified products when 0.1 pg of DNA template was used in both reaction times. In contrast, LAMP amplified products were observed with all other template concentrations tested. This result confirmed that, the optimized LAMP has similar sensitivity at 30 and 60 min of amplification.

Sensitivity of Optimized LAMP Assay in *C. jejuni*/*C. coli* Cells Spiked Fecal Samples

The optimized LAMP assay was also tested with the whole cell of *C. jejuni* and *C. coli* spiked into chicken fecal samples as described above. LODs of 1 CFU/reaction (corresponding to 50 CFU/ml) were observed for both *C. jejuni* and *C. coli* within 30 min of amplification (**Figure 4**). The optimized LAMP assay, in this study, showed better performance with lower LOD and

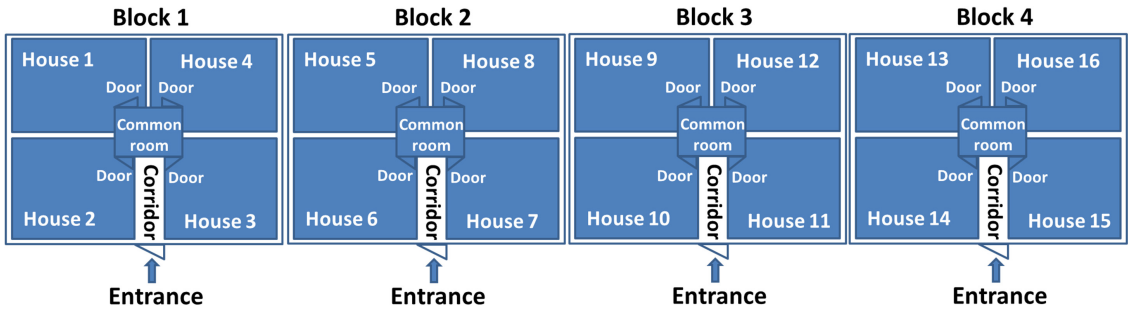

FIGURE 1 | The design of the broiler houses.

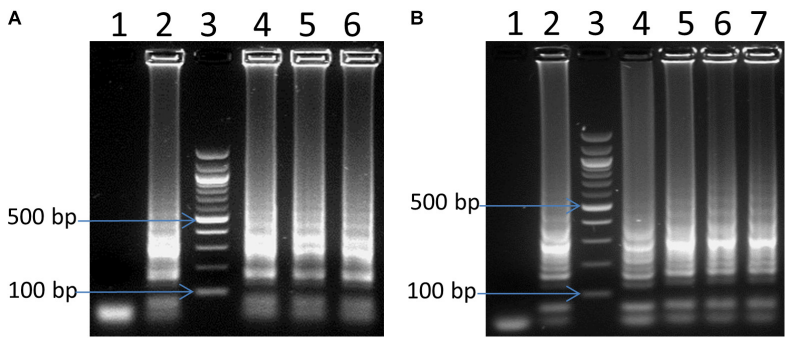

FIGURE 2 | Optimization of LAMP for reaction volume **(A)** and amplification time **(B)**. In panel **(A)**, lane 4, 5 and 6: 6, 12.5, and 25 μL reaction volume, respectively. In panel **(B)**, lane 4, 5, 6 and 7: 15 min, 30 min, 45 and 60 min, respectively. In both panels **(A,B)**: lane 1: negative control, lane 2: positive control, and lane 3: 100 bp ladder.

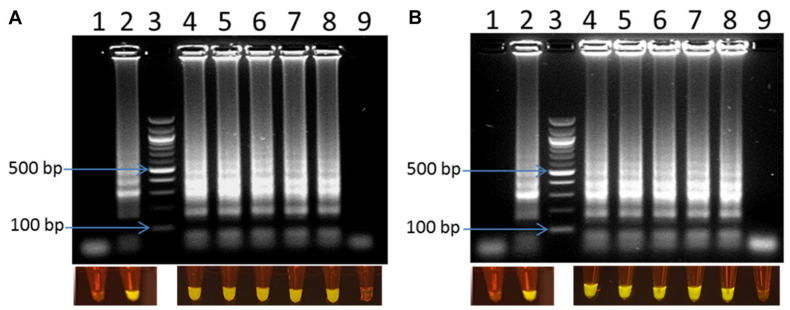

FIGURE 3 | Visual detection of LAMP products on 2% agarose gel electrophoresis and using SYBR® Safe staining DNA for sensitivity of the LAMP using pure DNA of *C. jejuni* in 30 min **(A)** and 60 min **(B)**. In both panels: lane 1: negative control, lane 2: positive control, lane 3: 100 bp ladder, and lane 4–9: 2 ng, 0.2 ng, 20 pg, 2 pg, 1 pg, 0.1 pg DNA of *C. jejuni*, respectively.

shorter reaction time than previous reports (1.2–1.4 CFU and 5 CFU per reaction within 60 min) (Yamazaki et al., 2008; Romero and Cook, 2018).

Application of the Optimized LAMP Assay to Detect *Campylobacter* in Poultry Farm

Efficiency of the optimized LAMP assay was also tested with real poultry fecal samples. A total of 64 boot-sock samples were collected and tested for the presence of C. *jejuni* and *C. coli*. Results showed that out of 64 samples tested, 17 samples were positive and 47 samples were negative for *C. jejuni* and *C. coli* (**Table 2**). There was 100% coincidence between the gel electrophoresis-based detection method and the visual observation using blue LED transilluminator (**Figure 5**). On the other hand, in the real-time PCR method, 18 samples were found positive and 46 samples were found negative with *C. jejuni*/*C. coli*. Comparing the results of the two methods showed a relative accuracy, specificity, and sensitivity of 98.43, 97.87, and 100%, respectively for the LAMP method. Cohen's kappa index showed an excellent agreement between the real-time PCR and the LAMP

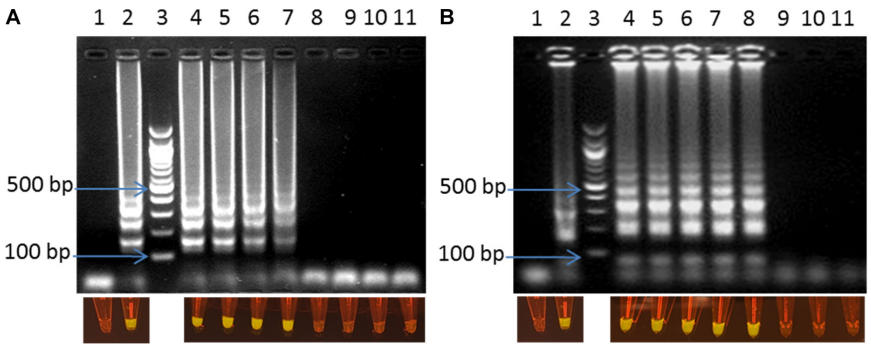

FIGURE 4 | Visual detection of LAMP products on 2% agarose gel electrophoresis and using SYBR® Safe staining DNA for the sensitivity of the fecal spiked sample with *C. jejuni* **(A)** and *C. coli* **(B)**. In both panels: lane 1: negative control, lane 2: positive control, lane 3: 100bp ladder, and lane 4–11: 10^{-1}–10^{-8} dilution.

(Cohen's kappa = 0.94) (**Table 2**). One sample tested positive with the real-time PCR but negative with LAMP assay was further confirmed by conventional PCR using a different primer set developed in our lab. Out of four tests performed with this sample, the results were negative for *C. jejuni*/*C. coli* in 2 attempts and positive only for *C. jejuni* in another 2 attempts (data not shown). This difference in the results between the two methods may be attributed to a low number of target concentration in the tested sample.

Visual Detection of LAMP Products Using Commercial Portable DR22 Blue LED Transilluminator

LAMP products could be detected by gel electrophoresis after amplification. **Figure 3** showed that positive amplification was observed in positive control and with DNA target from 1 pg to 2 ng. On the other hand, the products could also be observed directly by adding 1 µl of 1:10 SYBR® Safe. Under a commercial portable DR22 blue LED transilluminator, both positive control and the reactions with DNA target concentrations ranging from 1 pg to 2 ng of DNA changed from transparent to yellow, while no color change was observed in the negative control and with 0.1 pg of DNA template (**Figure 3**). This result showed that there was no difference in the detection limit between the gel electrophoresis and color-change observation by the low cost commercial DR22 blue LED transilluminator. The coincidence of results of gel electrophoresis and direct visual detection were also observed in **Figures 4**, **5**.

TABLE 2 | Comparison of real-time PCR and LAMP assay for detection of chicken feces from sock samples.

Samples	Real-time PCR	LAMP
Positive	18	17
Negative	46	47
Total	64	64
Comparison of real-time and LAMP		
Relative accuracy (AC%)	98.43	
Relative specificity (SP%)	97.87	
Relative sensitivity (SE%)	100	
Cohen's kappa index	0.94	

Determination of Specificity of the LAMP Assay

Twenty six bacterial strains as listed in **Table 1** were tested for the specificity of the assay. As one can see in **Supplementary Figure S2**, LAMP positive reactions were observed only with *C. jejuni* and *C. coli* DNA templates, while no LAMP amplification was detected from the reactions using DNA from the other 24 bacterial reference strains that included 10 other *Campylobacter* species. The results showed that the LAMP assay was highly specific for *C. jejuni* and *C. coli*.

Epidemiology of *Campylobacter* in Broilers Farm

For this study, we have collected fecal samples weekly from sixteen broiler houses for testing *Campylobacter* through three rotations of poultry production (**Table 3**). After each rotation, the houses were cleaned and disinfected before starting a new rotation. The first rotation lasted 4 weeks. In the first and second week, *Campylobacter* was not detected in any of the sixteen houses. In the third week, *Campylobacter* was found in house number 2 in block 1 and house 16 in block 4. Only a week later, *Campylobacter* was detected in all the houses of block 1 and block 4. The second rotation lasted only 2 weeks. In the first week, *Campylobacter* was detected in house number 14 and 16 of block 4. One week later, *Campylobacter* was found in all the houses in block 4 and also house number 12 in block 3. The third rotation in this study lasted four weeks and no *Campylobacter* was found in the first and second week. In the third week, *Campylobacter* was found in house number 12 in block 3. In the fourth week, all houses in block 3 were positive for *Campylobacter*. The results showed clearly that, once *Campylobacter* was introduced into the broiler houses, it was transmitted easily and quickly to other broilers houses and other broilers blocks.

Campylobacter is abundant in cloaca, cecum and large intestine of poultry, up to 10^9 CFU/g of feces (Corry and Atabay, 2001; Hermans et al., 2010). After excretion, *Campylobacter*

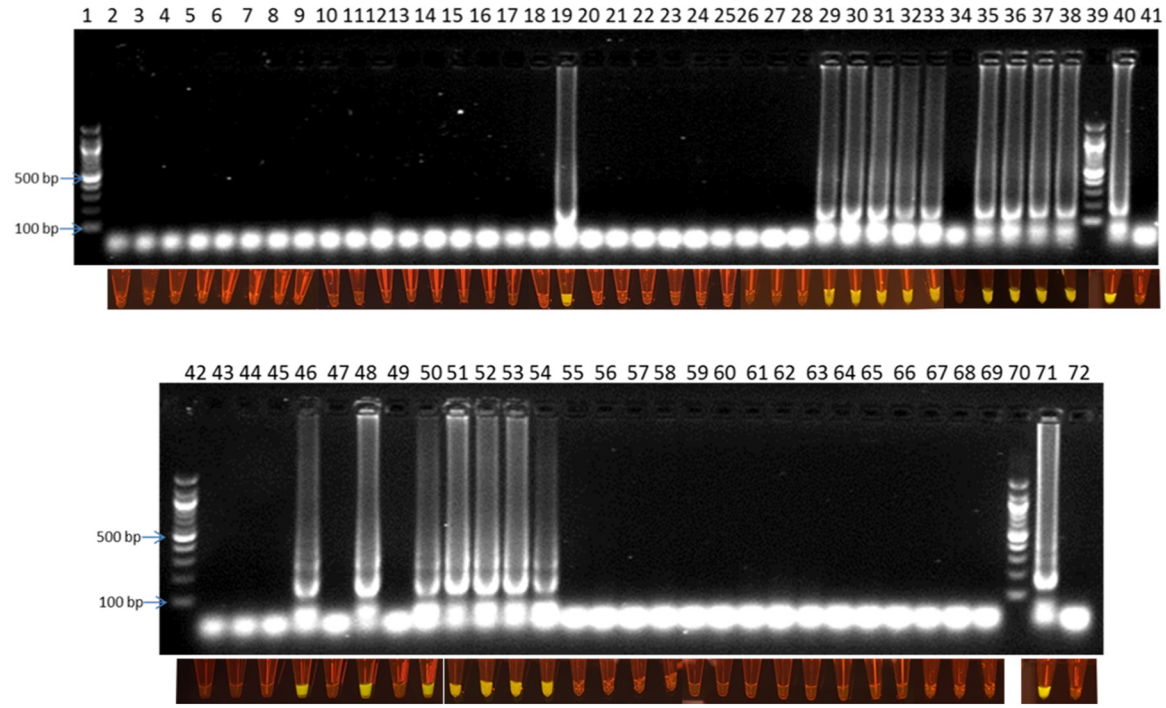

FIGURE 5 | Visual detection of LAMP products on 2% agarose gel electrophoresis and using SYBR® Safe staining DNA for chicken fecal samples: lane 1, 39, 42, and 70: 100 bp ladder, lane 40 and 71: positive control, lane 41 and 72: negative control, and lane 2–38 and 43–69: samples from rotation 1, 2 and 3.

survives from a minimum of 2 days up to 14 days in the feces (Smith et al., 2016). Therefore, the feces may play a key role in the transmission of *Campylobacter*. Wild animals such as crawling insects, arthropods and flies have been shown to be vectors that can transfer *Campylobacter* from outside into broiler houses as well as from fecal materials inside broiler houses to other broiler houses (Sheppard, 2014). A study carried out in Denmark showed that there were 8.2 and 70.2% of flies caught

TABLE 3 | Screening of *Campylobacter* from rotations.

	House	Rotation 1				Rotation 2*		Rotation 3			
		Week 1	Week 2	Week 3	Week 4	Week 1	Week 2	Week 1	Week 2	Week 3	Week 4
Block 1	1	–	–	–	+	–	–	–	–	–	–
	2	–	–	+	+	–	–	–	–	–	–
	3	–	–	–	+	–	–	–	–	–	–
	4	–	–	–	+	–	–	–	–	–	–
Block 2	5	–	–	–	–	–	–	–	–	–	–
	6	–	–	–	–	–	–	–	–	–	–
	7	–	–	–	–	–	–	–	–	–	–
	8	–	–	–	–	–	–	–	–	–	–
Block 3	9	–	–	–	–	–	–	–	–	–	+
	10	–	–	–	–	–	–	–	–	–	+
	11	–	–	–	–	–	–	–	–	–	+
	12	–	–	–	–	–	+	–	–	+	+
Block 4	13	–	–	–	+	–	+	–	–	–	–
	14	–	–	–	+	+	+	–	–	–	–
	15	–	–	–	+	–	+	–	–	–	–
	16	–	–	+	+	+	+	–	–	–	–

*–: negative; +: positive. *Rotation 2 last only 2 weeks since once Campylobacter was introduced to the broiler houses; it is transmitted easily and quickly to other broiler houses. So producer decided to stop the production in order to reduce economic loss.*

outside a broiler house positive with *Campylobacter* as confirmed with conventional culture and PCR method, respectively (Hald et al., 2004). This study suggests that flies may play an important role in *Campylobacter* infection of broiler flocks during summer. Besides, air and dust are also considered as a source of the transmission (Berrang et al., 2004; Wilson, 2004). Bull et al. (2006) reported that approximately 6% of air samples were positive for *Campylobacter* once the broiler flocks were positive with *Campylobacter* (Bull et al., 2006). Furthermore, in the early stage of the colonization, *Campylobacter* can spread into the air of the broiler house (Olsen et al., 2009).

In addition, water may also contribute as a source of *Campylobacter* transmission in broilers houses. Bull et al. (2006) reported that approximately 31% of water samples from drinkers were positive with *Campylobacter* once flocks were positive with *Campylobacter* (Bull et al., 2006). Moreover, *Campylobacter* can persist for long periods in well-water and can also survive under various conditions for days (Buswell et al., 1998), weeks (Korhonen and Martikalnon, 1991), and even months (Rollins and Colwell, 1986; Thomas et al., 2002) in different aqueous environment (Schallenberg et al., 2005).

Although humidity in the broiler house is not a direct source of the transmission, it can influence the transmission of *Campylobacter*. Line (2006) showed that, at low relative humidity (30% ± 10%), the colonization of *Campylobacter* was delayed compared with high relative humidity (80% ± 10%) since it has been shown that water can enhance the survival of *Campylobacter* in broiler flocks (Trigui et al., 2015).

CONCLUSION

In summary, the present study describes a simple and rapid LAMP assay for the detection of *C. jejuni* and *C. coli* in chicken feces. The assay conditions were optimized for low reaction volume and shorter time of reaction. With the optimized conditions, it was possible to detect *C. jejuni* and *C. coli* in spiked chicken feces as low as 50 CFU/ml within 60–70 min in total. The LAMP assay was compared with an in house real-time PCR. Cohen's kappa index showed excellent agreement between the two methods. The optimized LAMP method was used to study the transmission of *Campylobacter* at a Danish poultry farm. The results confirmed the capability of the LAMP technique as a rapid screening method for the detection of *Campylobacter* spp. at poultry production.

DATA AVAILABILITY STATEMENT

All datasets generated for this study are included in the manuscript/**Supplementary Files**.

AUTHOR CONTRIBUTIONS

DB, AW, AV, SN, MM, and YS designed the work. TQ and PE performed the experiments. DB, TQ, AW, AV, SN, TN, and YS wrote the manuscript.

FUNDING

This study was supported by the Department of Biotechnology and Biomedicine, Technical University of Denmark, Denmark; a national GUDP-funded project through the ISOAMKIT Project No. 34009-15-1038 (www.isoamkit.com/en/); two EU H2020-funded projects, SMARTDIAGNOS, grant no. 687697 (www.smartdiagnos.eu), and VIVALDI, grant no. 773422 (www.vivaldi-ia.eu); and the EMIDA project, grant no. 3405-11-0433.

ACKNOWLEDGMENTS

We thank Kirsten Michaëlis from DTU Food for technical assistant.

SUPPLEMENTARY MATERIAL

The Supplementary Material for this article can be found online at: https://www.frontiersin.org/articles/10.3389/fmicb.2019.02443/full#supplementary-material

REFERENCES

Addis, M., and Sisay, D. (2015). A review on major food-borne bacterial illnesses. *J. Trop. Dis.* 3:176. doi: 10.4176/2329-891X.1000176

Alves, J., Hirooka, E. Y., and de Oliveira, T. C. R. M. (2016). Development of a multiplex real-time PCR assay with an internal amplification control for the detection of *Campylobacter* spp. and *Salmonella* spp. in chicken meat. *LWT Food Sci. Technol.* 72, 175–181. doi: 10.1016/j.lwt.2016.04.051

Berrang, M. E., Northcutt, J. K., and Dickens, J. A. (2004). The contribution of airborne contamination to *Campylobacter* counts on defeathered broiler carcasses. *J. Appl. Poult. Res.* 13, 1–4. doi: 10.1093/japr/13.1.1

Biesta-Peters, E. G., Jongenburger, I., de Boer, E., and Jacobs-Reitsma, W. F. (2019). Validation by interlaboratory trials of EN ISO 10272 - microbiology of the food chain - Horizontal method for detection and enumeration of *Campylobacter* spp. - part 1: detection method. *Int. J. Food Microbiol.* 288, 39–46. doi: 10.1016/j.ijfoodmicro.2018.05.007

Bull, S. A., Allen, V. M., Domingue, G., Jørgensen, F., Frost, J. A., Ure, R., et al. (2006). Sources of *Campylobacter* spp. colonizing housed broiler flocks during rearing. *Appl. Environ. Microbiol.* 72, 645–652. doi: 10.1128/AEM.72.1.645

Buswell, C. M., Herlihy, Y. M., Lawrence, L. M., McGuiggan, J. T. M., Marsh, P. D., Keevil, C. W., et al. (1998). Extended survival and persistence of *Campylobacter* spp. water and aquatic biofilms and their detection by immunofluorescent-antibody and -rRNA staining. *Appl. Environ. Microbiol.* 64, 733–741.

CDC (2017). *Foodborne Diseases Active Surveillance Network (FoodNet): FoodNet 2015 Surveillance Report (Final Data)*. Atlanta: U.S. Department of Health and Human Services.

Chin, W. H., Sun, Y., Høgberg, J., Hung, T. Q., Wolff, A., and Bang, D. D. (2017). Solid-phase PCR for rapid multiplex detection of *Salmonella* spp. at the subspecies level, with amplification efficiency comparable to conventional PCR. *Anal. Bioanal. Chem.* 409, 2715–2726. doi: 10.1007/s00216-017-0216-y

Chin, W. H., Sun, Y., Høgberg, J., Quyen, T. L., Engelsmann, P., Wolff, A., et al. (2016). Direct PCR – A rapid method for multiplexed detection of different

serotypes of *Salmonella* in enriched pork meat samples. *Mol. Cell. Probes* 32, 24–32. doi: 10.1016/j.mcp.2016.11.004

Corry, J. E. L., and Atabay, H. I. (2001). Poultry as a source of *Campylobacter* and related organisms. *J. Appl. Microbiol.* 90, 96S–114S. doi: 10.1046/j.1365-2672.2001.01358.x

de Paz, H. D., Brotons, P., and Muñoz-Almagro, C. (2014). Molecular isothermal techniques for combating infectious diseases: towards low-cost point-of-care diagnostics. *Expert Rev. Mol. Diagn.* 14, 827–843. doi: 10.1586/14737159.2014.940319

Hald, B., Bang, D. D., Pedersen, K., Dybdahl, J., Madsen, M., and Study, T. (2004). Flies and *Campylobacter* broiler flocks. *Emerg. Infect. Dis.* 10, 1490–1492.

Helwigh, B., Julia, C., and Luise, M. (2017). *Anonymous, 2016. Annual Report on Zoonoses in Denmark 2017*. Søborg: National Food Institute.

Hermans, D., Martel, A., van Deun, K., Verlinden, M., van Immerseel, F., Garmyn, A., et al. (2010). Intestinal mucus protects *Campylobacter jejuni* in the ceca of colonized broiler chickens against the bactericidal effects of medium-chain fatty acids. *Poult. Sci.* 89, 1144–1155. doi: 10.3382/ps.2010-00717

Iwamoto, T., Sonobe, T., and Hayashi, K. (2003). Loop-mediated isothermal amplification for direct detection of *Mycobacterium tuberculosis* complex, *M. avium*, and *M. intracellulare* in sputum samples. *J. Clin. Microbiol.* 41, 2616–2622. doi: 10.1128/JCM.41.6.2616-2622.2003

Josefsen, M. H., Lofstrom, C., Hansen, T. B., Christensen, L. S., Olsen, J. E., and Hoorfar, J. (2010). Rapid quantification of viable *Campylobacter* bacteria on chicken carcasses, using real-time PCR and propidium monoazide treatment, as a tool for quantitative risk assessment. *Appl. Environ. Microbiol.* 76, 5097–5104. doi: 10.1128/AEM.00411-10

Kato, H., Yokoyama, T., Kato, H., and Arakawa, Y. (2005). Rapid and simple method for detecting the toxin B gene of *Clostridium difficile* in stool specimens by loop-mediated isothermal amplification. *J. Clin. Microbiol.* 43, 6108–6112. doi: 10.1128/JCM.43.12.6108-6112.2005

Korhonen, L. K., and Martikalnon, P. J. (1991). Survival of *Escherichia coli* and *Campylobacter jejuni* in untreated and filtered lake water. *J. Appl. Bacteriol.* 71, 379–382. doi: 10.1111/j.1365-2672.1991.tb03804.x

Kosti, T., Ellis, M., Williams, M. R., Stedtfeld, T. M., Kaneene, J. B., Stedtfeld, R. D., et al. (2015). Thirty-minute screening of antibiotic resistance genes in bacterial isolates with minimal sample preparation in static self-dispensing 64 and 384 assay cards. *Appl. Microbiol. Biotechnol.* 99, 7711–7722. doi: 10.1007/s00253-015-6774-z

Lawson, A. J., Logan, J. M., O'neill, G. L., Desai, M., and Stanley, J. (1999). Large-scale survey of *Campylobacter* species in human gastroenteritis by PCR and PCR-enzyme-linked immunosorbent assay. *J. Clin. Microbiol.* 37, 3860–3864.

Line, J. E. (2006). Influence of relative humidity on transmission of *Campylobacter jejuni* in broiler chickens. *Poult. Sci.* 85, 1145–1150. doi: 10.1093/ps/85.7.1145

Lund, M., Wedderkopp, A., Waino, M., Nordentoft, S., Bang, D. D., Pedersen, K., et al. (2003). Evaluation of PCR for detection of *Campylobacter* in a national broiler surveillance programme in Denmark. *J. Appl. Microbiol.* 94, 929–935. doi: 10.1046/j.1365-2672.2003.01934.x

Mori, Y., Kanda, H., and Notomi, T. (2013). Loop-mediated isothermal amplification (LAMP): recent progress in research and development. *J. Infect. Chemother.* 19, 404–411. doi: 10.1007/s10156-013-0590-0

Njiru, Z. K. (2012). Loop-mediated isothermal amplification technology: towards point of care diagnostics. *PLoS Negl. Trop. Dis.* 6:e1572. doi: 10.1371/journal.pntd.0001572

Okamura, M., Ohba, Y., Kikuchi, S., Suzuki, A., Tachizaki, H., Takehara, K., et al. (2008). Loop-mediated isothermal amplification for the rapid, sensitive, and specific detection of the O9 group of *Salmonella* in chickens. *Vet. Microbiol.* 132, 197–204. doi: 10.1016/j.vetmic.2008.04.029

Olsen, K. N., Lund, M., Skov, J., Christensen, L. S., and Hoorfar, J. (2009). Detection of *Campylobacter* bacteria in air samples for continuous real-time monitoring of *Campylobacter* colonization in broiler flocks. *Appl. Environ. Microbiol.* 75, 2074–2078. doi: 10.1128/AEM.02182-08

Peng, Y., Xie, Z., Liu, J., Pang, Y., Deng, X., Xie, Z., et al. (2011). Visual detection of H3 subtype avian influenza viruses by reverse transcription loop-mediated isothermal amplification assay. *Virol. J.* 8:337. doi: 10.1186/1743-422X-8-337

Powell, L. F., Lawes, J. R., Clifton-Hadley, F. A., Rodgers, J., Harris, K., Evans, S. J., et al. (2012). The prevalence of *Campylobacter* spp. in broiler flocks and on broiler carcases, and the risks associated with highly contaminated carcases. *Epidemiol. Infect.* 140, 2233–2246. doi: 10.1017/S0950268812000040

Rollins, D. M., and Colwell, R. R. (1986). Viable but nonculturable stage of *Campylobacter jejuni* and its role in survival in the natural aquatic environment. *Appl. Environ. Microbiol.* 52, 531–538.

Romero, M. R., and Cook, N. (2018). A rapid LAMP-based method for screening poultry samples for *Campylobacter* without enrichment. *Front. Microbiol.* 9:2401. doi: 10.3389/fmicb.2018.02401

Sabike, I. I., Uemura, R., Kirino, Y., Mekata, H., Sekiguchi, S., Okabayashi, T., et al. (2016). Use of direct LAMP screening of broiler fecal samples for *Campylobacter jejuni* and *Campylobacter coli* in the positive flock identification strategy. *Front. Microbiol.* 7:1582. doi: 10.3389/fmicb.2016.01582

Sabike, I. I., and Yamazaki, W. (2019). Improving the detection accuracy and time for *Campylobacter jejuni* and *Campylobacter coli* in naturally infected live and slaughtered chicken broilers using a real-time fluorescent loop-mediated isothermal amplification approach. *J. Food Prot.* 82, 189–193. doi: 10.4315/0362-028X.JFP-18-179

Sandberg, M., Sørensen, L. L., Steenberg, B., Chowdhury, S., Ersbøll, A. K., and Alban, L. (2015). Risk factors for *Campylobacter* colonization in Danish broiler flocks, 2010 to 2011. *Poult. Sci.* 94, 447–453. doi: 10.3382/ps/peu065

Schallenberg, M., Bremer, P. J., Henkel, S., Launhardt, A., and Burns, C. W. (2005). Survival of *Campylobacter jejuni* in water: effect of grazing by the freshwater crustacean Daphnia cannata (Cladocera). *Appl. Environ. Microbiol.* 71, 5085–5088. doi: 10.1128/AEM.71.9.5085-5088.2005

Schrader, C., Schielke, A., Ellerbroek, L., and Johne, R. (2012). PCR inhibitors - occurrence, properties and removal. *J. Appl. Microbiol.* 113, 1014–1026. doi: 10.1111/j.1365-2672.2012.05384.x

Sheppard, S. K. (2014). *Campylobacter Ecology and Evolution | Book*. Norfolk: Caister Academic Press.

Sibanda, N., McKenna, A., Richmond, A., Ricke, S. C., Callaway, T., Stratakos, A. C., et al. (2018). A review of the effect of management practices on *Campylobacter* prevalence in poultry farms. *Front. Microbiol.* 9:2002. doi: 10.3389/fmicb.2018.02002

Smith, S., Meade, J., Gibbons, J., McGill, K., Bolton, D., and Whyte, P. (2016). The impact of environmental conditions on *Campylobacter jejuni* survival in broiler faeces and litter. *Infect. Ecol. Epidemiol.* 6:31685. doi: 10.3402/iee.v6.31685

Stedtfeld, R. D., Stedtfeld, M., Kronlein, M., Seyrig, G., Ste, R. J., Cupples, A. M., et al. (2014). DNA extraction-free quantification of *Dehalococcoides* spp. in groundwater using a hand-held device. *Environ. Sci. Technol.* 48, 13855–13863. doi: 10.1021/es503472h

Sun, Y., Linh, Q. T., Hung, T. Q., Chin, W. H., Wolff, A., and Dang Duong, B. (2015). A lab-on-a-chip system with integrated sample preparation and loop-mediated isothermal amplification for rapid and quantitative detection of *Salmonella* spp. in food samples. *Lab Chip* 15, 1898–1904. doi: 10.1039/C4LC01459F

Techathuvanan, C., Draughon, F. A., and D'Souza, D. H. (2010). Loop-mediated isothermal amplification (LAMP) for the rapid and sensitive detection of *Salmonella* Typhimurium from pork. *J. Food Sci.* 75, M165–M172. doi: 10.1111/j.1750-3841.2010.01554.x

Thomas, C., Hill, D., and Mabey, M. (2002). Culturability, injury and morphological dynamics of thermophilic *Campylobacter* spp. within a laboratory-based aquatic model system. *J. Appl. Microbiol.* 92, 433–442. doi: 10.1046/j.1365-2672.2002.01550.x

Tresse, O., Alvarez-Ordóñez, A., and Connerton, I. F. (2017). Editorial: about the foodborne pathogen *Campylobacter*. *Front. Microbiol.* 8:1908. doi: 10.3389/fmicb.2017.01908

Trigui, H., Thibodeau, A., Fravalo, P., Letellier, A. P., and Faucher, S. (2015). Survival in water of *Campylobacter jejuni* strains isolated from the slaughterhouse. *Springerplus* 4:799. doi: 10.1186/s40064-015-1595-1

Velders, A. H., Schoen, C., and Saggiomo, V. (2018). Loop-mediated isothermal amplification (LAMP) shield for Arduino DNA detection. *BMC Res. Notes* 11:93. doi: 10.1186/s13104-018-3197-9

Vinayaka, A. C., Ngo, T. A., Kant, K., Engelsmann, P., Dave, V. P., Shahbazi, M.-A., et al. (2019). Rapid detection of *Salmonella enterica* in food samples by a novel approach with combination of sample concentration and direct PCR. *Biosens. Bioelectron.* 129, 224–230. doi: 10.1016/j.bios.2018.09.078

Wang, L., Shi, L., Alam, M. J., Geng, Y., and Li, L. (2008). Specific and rapid detection of foodborne *Salmonella* by loop-mediated isothermal amplification method. *Food Res. Int.* 41, 69–74. doi: 10.1016/j.foodres.2007.09.005

Wilson, I. G. (2004). Airborne *Campylobacter* infection in a poultry worker: case report and review of the literature. *Commun. Dis. Public Health* 7, 349–353.

Wingstrand, A., Neimann, J., Engberg, J., Nielsen, E. M., Gerner-Smidt, P., Wegener, H. C., et al. (2006). Fresh chicken as main risk factor for campylobacteriosis. Denmark. *Emerg. Infect. Dis.* 12, 280–284. doi: 10.3201/eid1202.050936

Xie, L., Xie, Z. Z. Z., Zhao, G., Liu, J., Pang, Y., Deng, X., et al. (2014). A loop-mediated isothermal amplification assay for the visual detection of duck circovirus. *Virol. J.* 11, 76. doi: 10.1186/1743-422X-11-76

Yamazaki, W., Taguchi, M., Ishibashi, M., Kitazato, M., Nukina, M., Misawa, N., et al. (2008). Development and evaluation of a loop-mediated isothermal amplification assay for rapid and simple detection of *Campylobacter jejuni* and *Campylobacter coli*. *J. Med. Microbiol.* 57, 444–451. doi: 10.1099/jmm.0.47688-0

Yamazaki, W., Taguchi, M., Ishibashi, M., Nukina, M., Misawa, N., and Inoue, K. (2009a). Development of a loop-mediated isothermal amplification assay for sensitive and rapid detection of *Campylobacter fetus*. *Vet. Microbiol.* 136, 393–396. doi: 10.1016/j.vetmic.2008.11.018

Yamazaki, W., Taguchi, M., Kawai, T., Kawatsu, K., Sakata, J., Inoue, K., et al. (2009b). Comparison of loop-mediated isothermal amplification assay and conventional culture methods for detection of *Campylobacter jejuni* and *Campylobacter coli* in naturally contaminated chicken meat samples. *Appl. Environ. Microbiol.* 75, 1597–1603. doi: 10.1128/AEM.02004-08

Yang, J., Yang, R., Cheng, A., Wang, M., Fu, L., Yang, S., et al. (2010). A simple and rapid method for detection of Goose Parvovirus in the field by loop-mediated isothermal amplification. *Virol. J.* 7, 14. doi: 10.1186/1743-422X-7-14

Zhang, J., Zhu, J., Ren, H., Zhu, S., Zhao, P., Zhang, F., et al. (2013). Rapid visual detection of highly pathogenic *Streptococcus suis* serotype 2 isolates by use of loop-mediated isothermal amplification. *J. Clin. Microbiol.* 51, 3250–3256. doi: 10.1128/JCM.01183-13

Zhang, Y., Shan, X., Shi, L., Lu, X., Tang, S., Wang, Y., et al. (2012). Development of a fimY-based loop-mediated isothermal amplification assay for detection of *Salmonella* in food. *Food Res. Int.* 45, 1011–1015. doi: 10.1016/j.foodres.2011.02.015

Zhuang, L., Gong, J., Li, Q., Zhu, C., Yu, Y., Dou, X., et al. (2014). Detection of *Salmonella* spp. by a loop-mediated isothermal amplification (LAMP) method targeting *bcfD* gene. *Lett. Appl. Microbiol.* 59, 658–664. doi: 10.1111/lam.12328

Conflict of Interest: SN is currently employed by the company Novo Nordisk A/S, Bagsværd, Denmark. TN is currently employed by Vinmec HealthCare System, Hanoi, Vietnam.

The remaining authors declare that the research was conducted in the absence of any commercial or financial relationships that could be construed as a potential conflict of interest.

frontiers in Microbiology

ORIGINAL RESEARCH
published: 10 January 2020
doi: 10.3389/fmicb.2019.02920

Detection and Quantification of Viable but Non-culturable *Campylobacter jejuni*

*Ruiling Lv[1,2], Kaidi Wang[1], Jinsong Feng[1], Dustin D. Heeney[1], Donghong Liu[2] and Xiaonan Lu[1]**

[1] Food, Nutrition, and Health Program, Faculty of Land and Food Systems, The University of British Columbia, Vancouver, BC, Canada, [2] College of Biosystems Engineering and Food Science, Zhejiang University, Hangzhou, China

Campylobacter can enter a viable but non-culturable (VBNC) state to evade various stresses, and this state is undetectable using traditional microbiological culturing techniques. These VBNC bacterial cells retain metabolism and demonstrate pathogenic potential due to their ability to resuscitate under favorable conditions. Rapid and accurate determination of VBNC *Campylobacter* is critical to further understand the induction and resuscitation of the dormancy state of this microbe in the agri-food system. Here, we integrated propidium monoazide (PMA) with real-time polymerase chain reaction (qPCR) targeting the *rpoB* gene to detect and quantify *Campylobacter jejuni* in the VBNC state. First, we optimized the concentration of PMA (20 μM) that could significantly inhibit the amplification of dead cells by qPCR with no significant interference on the amplification of viable cell DNA. PMA-qPCR was highly specific to *C. jejuni* with a limit of detection (LOD) of 2.43 log CFU/ml in pure bacterial culture. A standard curve for *C. jejuni* cell concentrations was established with the correlation coefficient of 0.9999 at the linear range of 3.43 to 8.43 log CFU/ml. Induction of *C. jejuni* into the VBNC state by osmotic stress (i.e., 7% NaCl) was rapid (<48 h) and effective (>10% population). The LOD of PMA-qPCR for VBNC *C. jejuni* exogenously applied to chicken breasts was 3.12 log CFU/g. In conclusion, PMA-qPCR is a rapid, specific, and sensitive method for the detection and quantification of VBNC *C. jejuni* in poultry products. This technique can give insight into the prevalence of VBNC *Campylobacter* in the environment and agri-food production system.

Keywords: *Campylobacter*, food safety, viable but non-culturable, quantitative PCR, intercalating agent

OPEN ACCESS

Edited by:
Nicolae Corcionivoschi, Agri-Food and Biosciences Institute (AFBI), United Kingdom

Reviewed by:
Hengyi Xu, Nanchang University, China
Abdi Elmi, University of London, United Kingdom

****Correspondence:***
Xiaonan Lu
xiaonan.lu@ubc.ca

Specialty section:
This article was submitted to Food Microbiology, a section of the journal Frontiers in Microbiology

Received: *16 October 2019*
Accepted: *04 December 2019*
Published: *10 January 2020*

Citation:
Lv R, Wang K, Feng J, Heeney DD, Liu D and Lu X (2020) Detection and Quantification of Viable but Non-culturable Campylobacter jejuni. Front. Microbiol. 10:2920. doi: 10.3389/fmicb.2019.02920

INTRODUCTION

Campylobacter is responsible for the most frequently reported foodborne gastrointestinal infection in the world (Silva et al., 2011). It is a microaerobic bacterium but highly prevalent in the aerobic food processing environment, such as poultry farms and slaughter facilities. The Centers for Disease Control indicates that *Campylobacter* spp. caused a total of 472 foodborne outbreaks, 4,209 illnesses, and 315 hospitalizations from 2011 to 2017 in the United States (CDC, 2018). Among them, *Campylobacter jejuni* is the major species that represent 95% of the total contaminations.

Typical transmission routes include contaminated dairy, water, and poultry products, with poultry products associated with 25% of the cases (Silva et al., 2011).

Campylobacter jejuni can enter a viable but non-culturable (VBNC) state upon exposure to various stress, including low temperature, oxygen, acid treatment, and salt treatment (Silva et al., 2011). VBNC cells are unable to divide in the conventional culture media while they retain membrane integrity and metabolic activity (Ramamurthy et al., 2014). The VBNC state is considered by some researchers to be related to other stress-induced phenotypes, such as antibiotic-tolerant persister cells, and is hypothesized to be a terminal stage in the dormancy continuum (Oliver, 2005). To date, 85 bacterial species have been described to form VBNC cells under stress conditions, including *Escherichia*, *Vibrio*, *Listeria*, and *Campylobacter* (Pinto et al., 2015). Bacterial cells in the VBNC stage can remain dormant for several months before resuscitation under favorable conditions (Baffone et al., 2006). For example, VBNC *C. jejuni* cells have been reported to resuscitate *in vivo* with mouse infections (Baffone et al., 2006), in microaerobic conditions (Bovill and Mackey, 1997), and in embryonated chicken eggs (Cappelier et al., 1999). VBNC cells are thought to be avirulent due to a reduced rate of gene expression and protein translation required for pathogenesis. However, VBNC cells that become resuscitated can regain full infective phenotypes (Baffone et al., 2006; Pinto et al., 2015), representing a real threat to the public health.

Current methods for the detection of *C. jejuni* are widely culture dependent, which severely underestimate the presence of VBNC cells (Baffone et al., 2006). Several assays have been applied to the detection of VBNC cells, such as the direct fluorescent antibody–direct viable count (DFA–DVC) method, substrate responsiveness combined with fluorescent *in situ* hybridization (DVC–FISH assay), and LIVE/DEAD BacLight bacteria viability kit combined with flow cytometry. However, most of these methods are costly, unspecific, technically challenging, or unable to conduct quantification. Therefore, it is imperative that we develop novel methods for the detection and quantification of VBNC *C. jejuni* in the agri-food system. To this point, molecular techniques have been developed to detect and identify *C. jejuni* in the environment, especially with DNA amplification methods, including polymerase chain reaction (PCR) and variations thereof (Magajna and Schraft, 2015; Castro et al., 2018). Critically, PCR and quantitative PCR (qPCR) methods are not able to differentiate between viable and non-viable (dead) bacterial cells. One promising method for the detection of viable cells in a mixture of live and dead cells is the use of propidium monoazide (PMA) coupled to qPCR (Magajna and Schraft, 2015; Castro et al., 2018). PMA creates strong covalent bonds to double-stranded DNA after photoactivation, but the bulky structure of this molecule and the positive charges prevent itself from entering bacterial cells with intact membranes (Nocker et al., 2006). PMA-bound DNA inhibits DNA polymerases and therefore is not amplified during reactions, enabling the differentiation between viable and dead cells. Thus, VBNC cell count can be estimated by subtracting the number of culturable cells from the total viable cell count determined using PMA-qPCR. This technique has been used for the detection of different VBNC bacterial cells, such as *Escherichia coli* and *Vibrio parahaemolyticus* (Afari and Hung, 2018; Chang and Lin, 2018; Zhong and Zhao, 2018; Telli and Dogruer, 2019).

In the current study, we implemented and optimized the PMA-qPCR method to quantify viable cells in pure cultures of *C. jejuni* in the background of dead cells. VBNC cells of *C. jejuni* were then induced by osmotic stress and artificially contaminated onto commercial chicken breasts to validate the performance of PMA-qPCR coupled with the plating assay.

MATERIALS AND METHODS

Bacterial Strains and Growth Conditions

Bacterial strains are listed in **Table 1**. *C. jejuni* was routinely cultivated under microaerobic conditions (85% N_2, 10% CO_2, and 5% O_2) on Mueller–Hinton (MH) agar (BD Difco, Thermo Fisher Scientific, Waltham, United States) supplemented with 5% defibrinated sheep blood (Alere Inc., Stittsville, ON, Canada) at 37°C. *C. jejuni* broth cultures were prepared by picking a single bacterial colony into the MH broth (BD Difco, Thermo Fisher Scientific, Waltham, United States) with constant shaking at 175 rpm for 16–18 h at the same aforementioned conditions.

PMA Treatment and DNA Extraction

Propidium monoazide (Biotium, Fremont, United States) was diluted and added to 450 μl of unwashed bacterial cell culture

TABLE 1 | Bacterial strains used for the specificity test of qPCR.

Bacterial species	Strain	Source	PMA-qPCR result
Campylobacter jejuni	ATCC 33560	Bovine feces	+
	F38011	Human clinical isolate	+
	1658	Human clinical isolate	+
	NCTC 11168	Human clinical isolate	+
	81–116	Human clinical isolate	+
Campylobacter coli	RM 1875	Human clinical isolate	
	RM 2228	Human clinical isolate	-
	RM 5611	Human clinical isolate	-
Escherichia coli	O103:H2	Bovine feces	-
	O118:H16	Bovine feces	-
Salmonella enteritis	0EA2699	Human clinical isolate	-
	3512H	Human clinical isolate	-
Listeria monocytogenes	SEA 15B88	Human clinical isolate	-
Listeria monocytogenes	15B98	Human clinical isolate	-
Pseudomonas aeruginosa	H288	Human clinical isolate	-

at various concentrations into 1.7-ml graduated micro-centrifuge tubes manufactured from resin (LifeGene, Modiín, Israel). A bacterial cell–PMA mixture was kept in the dark on ice with constant shaking at 150 rpm for 10 min. Then, DNA crosslinking was performed by exposing the tubes horizontally to a 300-W halogen light (120 V; GE Lighting, General Electric Co., Cleveland, United States) at a distance of 20 cm for 10 min. The mixture was centrifuged at 15,000 × *g* and washed one time with sterile distilled deionized water (ddH_2O) to remove the residual PMA before DNA extraction. Genomic DNA of pure bacterial cultures was extracted by thermal treatment at 100°C for 10 min, followed by incubation on ice for 10 min. To compare the extraction efficiency, DNA extraction of both pure bacterial cultures and spiked chicken carcasses was also performed using the Presto Mini gDNA Bacteria Kit (Geneaid, Taiwan, China) as specified by the manufacturer. The quality and concentration of DNA were determined using a NanoDrop UV-Vis spectrophotometer (Thermo Fisher Scientific, Waltham, United States). DNA was stored at -20°C until qPCR analysis. The optimal concentration of PMA required for further qPCR experiments was determined using live and heat-inactivated *C. jejuni* cells. Live cells at different concentrations were collected by diluting the exponential phase culture, and dead cells were prepared by heating 1 ml of 6 log CFU/ml *C. jejuni* culture at 90°C for 5 min in 1.7-ml micro-centrifuge tubes as aforementioned using a heat block (VWR International, Pennsylvania, United States) (Pacholewicz et al., 2013). The death rate was confirmed by the plating assay (data not shown). Separate samples containing 6 log CFU/ml of live and heat-inactivated *C. jejuni* cells were treated with PMA at concentrations of 0, 10, 15, 20, 50, and 100 μM, respectively, prior to DNA extraction as previously described.

PMA-qPCR

The primers targeting the DNA-directed RNA polymerase *rpoB* were used for *C. jejuni* detection as previously described (Silvestri et al., 2017). The sequences of the primers were *rpoB* 1 (5′-GAGTAAGCTTGCTAAGATTAAAG-3′) and *rpoB* 2 (5′-AAGAAGTTTTAGAGTTTCTCC-3′), and the amplicon length was 121 bp. Each qPCR reaction (total 20 μl) contained 1 × SensiFAST SYBR Mix (Bioline, Taunton, United States), 2 μl of DNA temple, 100 nM of each primer, and sterile ddH_2O. The qPCRs were performed in an Applied Biosystems 7500 Real Time PCR system (Thermo Fisher Scientific, Waltham, MA, United States) with an initial denaturation at 50°C for 2 min and 95°C for 10 min, followed by 40 cycles of 95°C for 15 s and 60°C for 1 min. A negative control (ddH_2O) was included in each qPCR run, and each sample was tested in triplicate. The specificity of the *rpoB* primer set was evaluated using 15 different bacterial strains as listed in **Table 1** in the optimized PMA-qPCR assay. The sensitivity of the PMA-qPCR assay was determined with 10-fold serial dilutions of viable *C. jejuni* F38011 cells ranging from 1 to 8 log CFU/ml in a background of 6 log CFU/ml dead cells (inactivated at 90°C). The lowest CFU/ml of *C. jejuni* that generated Ct values < 35 was considered as the limit of detection (LOD) of this assay. A standard curve correlating Ct value and known concentration of *C. jejuni* cells was established and used to estimate the amplification efficiency and quantification capability. The amplification efficiency (*E*) was calculated using the slope of the standard curve $E = [10^{(-1/slope)} - 1] * 100\%$.

Induction of VBNC *C. jejuni*

Overnight *C. jejuni* culture was adjusted to OD_{600} = 0.3 (∼9 log CFU/ml) and washed with phosphate-buffered saline (PBS). Bacterial cells were then suspended in 7% (w/v) NaCl solution to a final concentration of 8 log CFU/ml and incubated for 48 h at 37°C. The culturable cell population and viable cell population were separately monitored by the plating assay and PMA-qPCR at 3, 6, 9, 12, 24, and 48 h. VBNC cell concentrations were estimated as the difference between culturable cells and viable cells. The LOD of the plating assay was determined to be 1 CFU/ml based on the presence of one colony on the MH blood agar with 1 ml of bacterial sample (Silvestri et al., 2017). When the culturable cell concentration was less than 1 CFU/ml, it was considered that all of the viable cells quantified by PMA-qPCR were VBNC cells. As validation, 100 μl of the putative VBNC cell suspensions was transferred into the fresh MH broth and incubated under the optimum microaerobic conditions for 72 h to confirm that no cells could be resuscitated.

Detection of VBNC *C. jejuni* in Chicken Samples

The reliability of PMA-qPCR was investigated by the detection of VBNC *C. jejuni* in chicken samples. Boneless and skinless chicken breasts were purchased from a local supermarket in Vancouver and stored at −20°C. Chicken was cut to ∼25 g per piece and exposed to 250 ml of 1% (w/v) chlorine for 10 min, followed by three times of washing with ddH_2O before drying for 1 h at 22°C. The chicken sample was contaminated with 100 μl of VBNC cells induced by osmotic stress for 48 h at the final concentrations ranging from 1.12 to 7.12 log CFU/ml and left to air-dry at 22°C for 1 h.

To recover the VBNC cells for determination, inoculated chicken samples were separately placed in the sterile sample bags and rinsed with 10 ml of peptone water. After manually massaging the bag for 3 min at 22°C, 1 ml of liquid was collected for DNA extraction and PMA-qPCR. A standard curve was generated by comparing Ct values to the known concentrations of VBNC cells applied to the chicken samples. Spiking of ddH_2O onto chicken samples was regarded as the negative control. Recovery of non-treated culturable *Campylobacter* with the aforementioned rinsing procedure was assessed by the plating assay.

Statistical Analysis

All the trials were conducted with at least three replicates in each experiment. Means and standard deviations of Ct values were calculated using the Microsoft Excel program (Seattle, United States). Figures were generated using the Origin software (Version 9.2, Origin Corp., Boston, MA, United States). One-way analysis of variance (ANOVA), followed by Duncan's test for

multiple comparisons with a confidence level of 95% ($P < 0.05$), was performed using the SPSS Statistics software (Version 20, IBM, United States).

RESULTS AND DISCUSSION

Campylobacter is the leading cause of bacterial diarrheal disease worldwide (Burnham and Hendrixson, 2018). Due to the wide consumption and high prevalence of *C. jejuni* in poultry, this food source is considered as the major transmission route for *C. jejuni* infections (Silva et al., 2011). Unfavorable environmental conditions, such as desiccation, aerobic stress, and starvation, can induce *C. jejuni* to enter the VBNC state and evade detection using the culture-based methods (Baffone et al., 2006). These VBNC cells can remain viable for an extended time period, resuscitate under favorable conditions, recover metabolism and virulence (Ramamurthy et al., 2014; Pinto et al., 2015), and subsequently pose an important concern to the public health. Few research has been performed on the detection and quantification of VBNC *C. jejuni* yet.

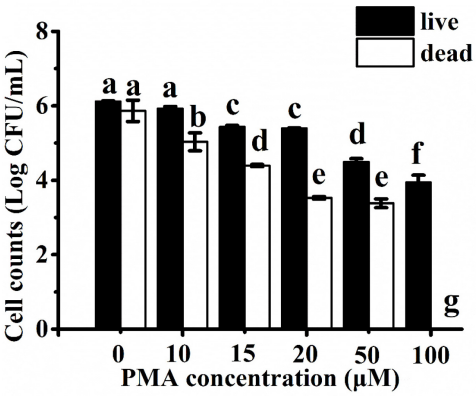

FIGURE 1 | *Campylobacter jejuni* cell counts estimated using Ct values from the propidium monoazide (PMA) with real-time polymerase chain reaction (qPCR) assay after treatment with different concentrations of PMA. Live and heat-inactivated cells at 6 log CFU/ml were treated and tested separately. Different letters indicated significant differences among different groups ($P < 0.05$).

Optimization of PMA Concentration

VBNC cells are now recognized to coexist with culturable and dead cells in bacterial cultures grown in the standardized laboratory condition (Kassem et al., 2013; Bronowski et al., 2014; Ayrapetyan et al., 2018). Therefore, we used a DNA-intercalating dye (i.e., PMA) to inhibit the amplification of DNA present in the dead cells. Previous studies identified 2–100 μM of PMA to be the optimal concentration range that was specific and compatible to determine the viability of each bacterial species in different matrices (Magajna and Schraft, 2015; Castro et al., 2018; Salas-Masso et al., 2019). PMA treatment with a higher concentration could inhibit DNA amplification of viable cells and lead to underestimation of viable cell count or even false-negative results. On the contrary, a lower concentration of PMA may not be fully effective to inhibit the signal from the dead cells and may cause overevaluation. Thus, it is crucial to determine the optimal concentration of PMA as the pretreatment for assay performance.

To compare the ability of PMA to differentiate between viable and heat-inactivated *C. jejuni* cells, each culture was separately treated with increasing concentrations of PMA (i.e., 0–100 μM) before DNA extraction and qPCR. DNA amplification curves from 6 log CFU/ml of viable cells treated with PMA at concentrations of <20 μM were similar to the non-PMA-treated samples (<1 log CFU/ml reduction). DNA amplification of live cells was significantly inhibited (>2 log CFU/ml reduction) when treated with concentrations of PMA above 20 μM (**Figure 1**). In contrast, the amplification of DNA from 6 log CFU/ml of dead cells decreased in a PMA dose-dependent manner up to 20 μM (**Figure 1**). There was no significant difference ($P > 0.05$) in the amplification when the dead cells were treated with 20 or 50 μM of PMA, while no amplification from the dead cells was observed at 100 μM of PMA. Therefore, 20 μM of PMA was used in the following study as it could effectively inhibit DNA amplification of the dead *C. jejuni* cells without significant influence on quantifying viable bacterial cells.

Previous studies indicated that PMA-qPCR was an effective approach to quantify viable *Campylobacter* cells in different sample matrices (Josefsen et al., 2010; Melero et al., 2011; Seinige et al., 2014). However, the optimal concentration of PMA varied among different studies. For example, Josefsen et al. (2010) reported that PMA treatment of 10 μg/ml (23.81 μM) achieved complete inhibition of the qPCR signal from the dead *Campylobacter* cells at a concentration of 6 log CFU/ml, but Pacholewicz et al. (2013) failed to completely inhibit the signal of dead cells >4 log CFU/ml by using a similar PMA-qPCR approach. In other studies, 47 and 50 μM of PMA were separately used to enumerate viable *Campylobacter* in chicken meat (Seinige et al., 2014; Castro et al., 2018). The variations in the concentration of PMA applied in the aforementioned studies might be due to the diverse sensitivity of the cell membrane of different *Campylobacter* strains as well as the penetration power of PMA to the corresponding viable and dead cells (Fittipaldi et al., 2012). Other variables were also introduced into these studies, including the amplicon size, sample matrices, the power and type of light, incubation time, and photoactivation time (Pacholewicz et al., 2013). In addition, other DNA-intercalating dyes, such as ethidium monoazide (EMA), have been used to couple with qPCR for the quantification of viable *Campylobacter* cells (Webb et al., 2016). PMA was selected in the current study because it has a lower cytotoxicity and a wider range of application for both Gram-negative and Gram-positive cells than EMA (Nocker and Camper, 2009; Fittipaldi et al., 2012).

Specificity and Sensitivity of PMA-qPCR Assay for *C. jejuni* Pure Culture

The specificity of the *rpoB* primer set was determined by testing DNA from a total of 15 strains from six different bacterial species (**Table 1**). The application of DNA from six *C. jejuni* strains all resulted in positive amplification

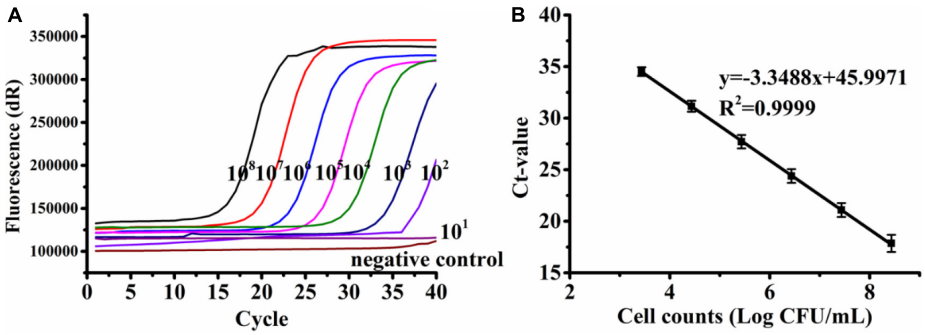

FIGURE 2 | Representative amplification curves **(A)** and standard curve **(B)** generated from 10-fold serial dilutions of viable *Campylobacter jejuni* F38011 cells ranging from 2.43 to 8.43 log CFU/ml in the background of 6 log CFU/ml of dead cells. Bacterial genomic DNA was extracted using the boiling method. Standard deviations were calculated based upon three replicates.

(Ct value ranging from 20.614 to 24.926). In comparison, no amplification was observed from the genomic DNA extracted from other bacterial species. We therefore validated 100% specificity for the detection of *C. jejuni*. The *rpoB* gene was also targeted in a previous study of using qPCR for the detection of viable *C. jejuni* due to its high sensitivity, heterogeneity, and suitable size of the amplification product (Silvestri et al., 2017).

A standard curve was established from the serially diluted viable *C. jejuni* F38011 cells in the background of 6 log CFU/ml of dead cells in relation to the Ct values. The linear regression slope was determined to be −3.3379 with a correlation coefficient (R^2) of 0.9999 (**Figure 2**), and PCR amplification efficiency was calculated to be 99.34%. The standard curve was linear over a range of 3.43 to 8.43 log CFU/ml, and the LOD of PMA-qPCR was determined to be 2.43 log CFU/ml. Other qPCR assays developed in the previous studies reported LODs for *Campylobacter* to be 1 log CFU/ml (Melero et al., 2011), 1.5 log CFU/ml (Tsiouris et al., 2019), and 2 log CFU/ml (Josefsen et al., 2010). Several variables including the quantification of total cells (dead and viable) versus viable cells, the use of different intercalating dyes (e.g., EMA), bacterial strains, designed primers, DNA extraction protocol, and qPCR procedure could contribute to the difference of the reported LODs.

Various DNA extraction methods may influence the sensitivity and effectiveness of qPCR due to differences in quantity and/or quality of the extracted nucleic acids (Demeke et al., 2009). Here, similar standard curves were developed when genomic DNA was extracted from *C. jejuni* F38011 using either a cheaper boiling method (**Figure 2B**) or a more expensive commercial extraction kit (**Supplementary Figure S1**), demonstrating that the amplification efficiency of qPCR was consistent between the two extraction methods. PMA-qPCR was applied to separately amplify the DNA extracted from the pure culture of four *C. jejuni* strains and establish the corresponding standard curves. The correlation coefficients (R^2) of all the four standard curves ranged from 0.9993 to 1 (**Supplementary Figure S1**), indicating that the developed PMA-qPCR assay was accurate and capable of quantifying various *C. jejuni* strains with a dynamic concentration range of 3 to 8 log CFU/ml.

Induction of VBNC *C. jejuni* by Osmotic Stress

Osmotic stress is an effective and rapid approach to induce bacteria into the VBNC state (Magajna and Schraft, 2015). NaCl is a potent antimicrobial that has been commonly used in food preservation (Csonka, 1989). Thus, 7% (w/v) NaCl solution was used to provide osmotic stress and induce *C. jejuni* into the VBNC state. The number of culturable and viable cells under osmotic stress was separately monitored using the plating assay and PMA-qPCR (**Figure 3**). For *C. jejuni* F38011, culturable cell counts decreased rapidly at the beginning of the osmotic treatment (3.76 log CFU/ml reduction at 37°C after 9 h) and continued over time, but the reduction of viable cell counts was negligible (<1 log CFU/ml) up to 48 h (**Figure 3A**). The difference between viable and culturable cell counts increased over time, indicating the accumulation of VBNC *C. jejuni* cells upon prolonged exposure to the osmotic stress. After osmotic treatment for 48 h, no culturable *C. jejuni* cells were detected by the plating assay (<1 CFU/ml), and no bacterial growth was observed after enrichment in MH broth for 72 h in a microaerobic condition at 37°C. *C. jejuni* F38011 had an estimated VBNC cell count of 7.84 log CFU/ml after 48 h of incubation with the osmotic stress.

When other *C. jejuni* strains were treated with the osmotic stress (**Figures 3B–D**), there was complete loss of culturability after an average of 24 h. In comparison, the viable cell counts were stagnant (average 7.98 log CFU/ml) over 48 h. The resistance to osmotic stress and progression into the VBNC state varied among different *C. jejuni* strains. In comparison, *E. coli* O157:H7 required 72 h of incubation in a 13% (w/v) NaCl solution to transit all viable cells into the VBNC state (Makino et al., 2000). The same transition was observed to require 5 days in *Salmonella enterica* in a 7% (w/v) NaCl solution (Kusumoto et al., 2012). Thus, *C. jejuni* demonstrated less tolerance to the osmotic stress than other enteric pathogens and exhibited a swifter progression into the VBNC state.

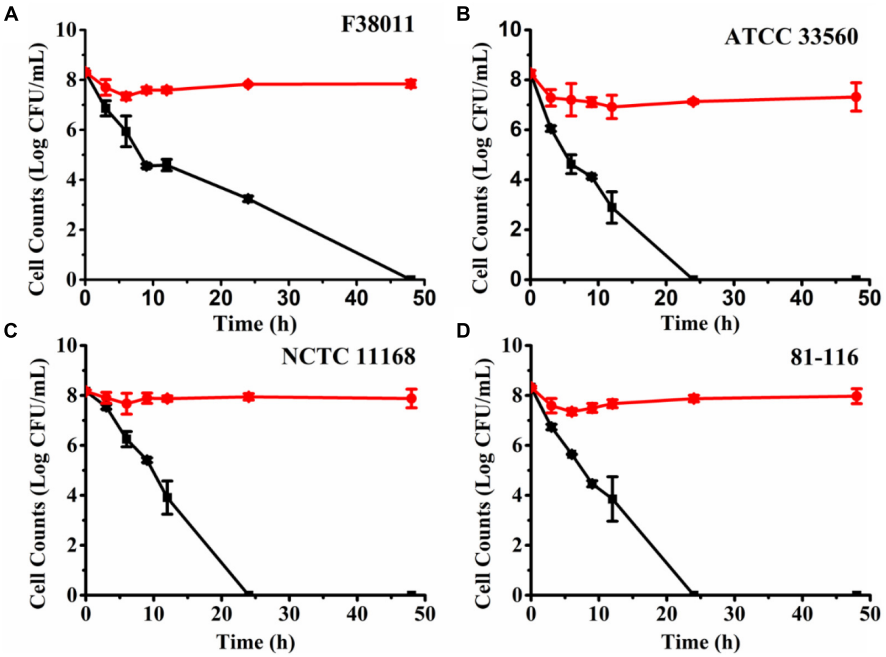

FIGURE 3 | Induction of viable but non-culturable (VBNC) *Campylobacter jejuni* F38011 **(A)**, ATCC 33560 **(B)**, NCTC 11168 **(C)** and 81-116 **(D)** under osmotic pressure in 7% (w/v) NaCl solution. Red circles (●) represent the viable cell counts quantified using PMA with real-time polymerase chain reaction (qPCR), while black squares (■) represent culturable cell counts determined using the plating assay. The difference between viable cells and culturable cells was considered as VBNC bacterial cells. The error bar was calculated based upon three replicates.

It is known that bacteria constantly sense and adapt to osmotic stress by the accumulation of intracellular ions (e.g., K^+) and synthesis or import of compatible solutes so as to continue normal metabolism and cellular functions (McLaggan et al., 1994; Kempf and Bremer, 1998). For example, *E. coli* contains the Bet system and ProP/ProU transporter system to synthesize and transport glycine betaine in a high-osmolality environment (Jackson et al., 2009). However, *C. jejuni* lacks these typical osmotic protective systems that are common in other Gram-negative bacteria (Garenaux et al., 2008; Cameron et al., 2012). Instead, several genes have been implicated in responding to hyperosmotic conditions in *C. jejuni*, including *htrB* (encoding high-temperature response protein B), *ppk* (encoding polyphosphate kinase), a sensor histidine kinase (CJM1_1208) (Bronowski et al., 2017), and *gltD* and *glnA* that encode proteins for glutamate and glutamine synthesis, respectively (Cameron et al., 2012). Further study is required to determine if these genes are actively transcribed and play potential roles in the progression of *C. jejuni* into the VBNC state under osmotic stress or not.

Quantification of VBNC *C. jejuni* in Poultry Products Using PMA-qPCR

Since poultry is one of the major sources of *C. jejuni* contamination and a common vehicle for foodborne transmission of *Campylobacteriosis* (Young et al., 2007), we further evaluated the performance of PMA-qPCR to quantify the model contamination of chicken meat with VBNC *C. jejuni* cells. A VBNC bacterial cocktail of four *C. jejuni* strains induced by 7% (w/v) NaCl solution was spiked to chicken samples at known concentrations and subsequently determined using PMA-qPCR. The correlation coefficient (R^2) between Ct values and the spiked concentration of VBNC *C. jejuni* cells was determined to be 0.9825, with a quantification range of 3.12 to 7.12 log CFU/g. There was no amplification observed in chicken samples that were not artificially contaminated, indicating that 1% (w/v) chlorine was an effective decontamination method used in

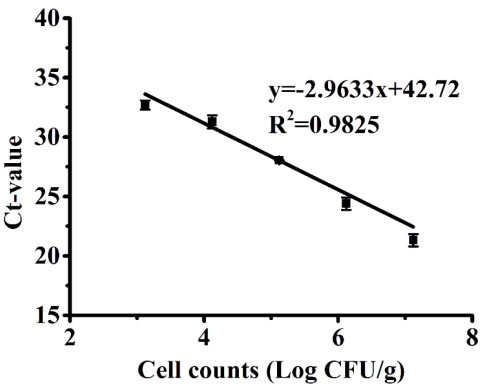

FIGURE 4 | Standard curves produced from 10-fold serial dilutions of the VBNC cocktail of *Campylobacter jejuni* cells ranging from 3.12 to 7.12 log CFU/g recovered from chicken samples. The error bar was calculated based upon three replicates.

the poultry industry to remove endogenous *C. jejuni* cells. In addition, the standard curve used for the chicken experiments (**Figure 4**) was established by first isolating VBNC cells and diluting them to known concentrations prior to application on the chicken samples. Considering that the efficiency of cell recovery and DNA extraction may vary among different initial concentrations of cells added to the chicken samples, it could explain why the amplification efficiency for this assay was relatively high (slope = −2.96, efficiency = 117%). The LOD of the PMA-qPCR assay for VBNC *C. jejuni* in chicken products was 3.12 log CFU/g (equivalent to 3.52 log CFU/ml of chicken rinse solution), which was higher than that determined in the pure bacterial culture (2.43 log CFU/ml), which was likely due to polymerase-inhibitory compounds in the chicken rinse solution, such as the background of dead bacterial cells and endogenous chicken molecules (Bae and Wuertz, 2012). It is also possible that the rinsing procedure could not fully recover all the VBNC cells spiked onto the chicken samples. In the preliminary spiking experiment, the recovery rate of culturable *C. jejuni* cells on chicken samples was 84.14%. The LOD of PMA-qPCR in the current study was improved in comparison to a previous study, in which qPCR exhibited a LOD of 1.2×10^4 CFU/g for the quantification of viable *C. jejuni* in poultry neck-skin samples (Papic et al., 2017). Others employing PMA-qPCR to quantify *Campylobacter* in chicken carcasses reported LOD values as low as 10 CFU/g (Rantsiou et al., 2010) and 2 log CFU/ml (Josefsen et al., 2010). In other studies, PMA-qPCR was applied to detect VBNC *E. coli* O157:H7 in different agri-food products, with a LOD of 4.51 log CFU/ml in meatballs (Zhong and Zhao, 2018) and 3 log CFU/g in leaf (Dinu and Bach, 2013). The LODs derived from these studies were comparable to that in the current study. Variations in the gene/species targeted for amplification, primer design, PMA concentration, and DNA extraction method could account for some of these variations.

CONCLUSION

A rapid, specific, and sensitive PMA-qPCR combined with the plating assay was developed for the detection and quantification VBNC *C. jejuni* in pure culture and poultry products. This method could be used to quantify the endogenous contamination of poultry and other food products by VBNC *C. jejuni* cells, which may evade detection by conventional culturing methods. The developed PMA-qPCR assay can assist in identifying sources of contamination and eventually reduce the prevalence of *C. jejuni* in the environment and agri-food system.

DATA AVAILABILITY STATEMENT

All datasets generated for this study are included in the article/**Supplementary Material**.

AUTHOR CONTRIBUTIONS

RL contributed to conducting bench work and manuscript writing. KW, JF, and DH contributed to the experimental design, conducting part of the bench work, and manuscript editing. DL contributed to the experimental design. XL contributed to the experimental design, and manuscript writing and editing.

FUNDING

Financial support to XL in the form of a Discovery Grant from the Natural Sciences and Engineering Research Council of Canada (NSERC RGPIN-2019-03960) and a Discovery Accelerator Grant from the Natural Sciences and Engineering Research Council of Canada (PGPAS-2019-00024) is gratefully acknowledged.

SUPPLEMENTARY MATERIAL

The Supplementary Material for this article can be found online at: https://www.frontiersin.org/articles/10.3389/fmicb.2019.02920/full#supplementary-material

REFERENCES

Afari, G. K., and Hung, Y. C. (2018). Detection and verification of the viable but nonculturable (VBNC) state of *Escherichia coli* O157:H7 and *Listeria monocytogenes* using flow cytometry and standard plating. *J. Food Sci.* 83, 1913–1920. doi: 10.1111/1750-3841.14203

Ayrapetyan, M., Williams, T., and Oliver, J. D. (2018). Relationship between the viable but nonculturable state and antibiotic persister cells. *J. Bacteriol.* 200:e00249-18. doi: 10.1128/jb.00249-18

Bae, S., and Wuertz, S. (2012). Survival of host-associated bacteroidales cells and their relationship with *Enterococcus* spp., *Campylobacter jejuni*, *Salmonella enterica Serovar Typhimurium*, and adenovirus in freshwater microcosms as measured by propidium monoazide-quantitative PCR. *Appl. Environ. Microbiol.* 78, 922–932. doi: 10.1128/aem.05157-11

Baffone, W., Casaroli, A., Citterio, B., Pierfelici, L., Campana, R., Vittoria, E., et al. (2006). *Campylobacter jejuni* loss of culturability in aqueous microcosms and ability to resuscitate in a mouse model. *Int. J. Food Microbiol.* 107, 83–91. doi: 10.1016/j.ijfoodmicro.2005.08.015

Bovill, R. A., and Mackey, B. M. (1997). Resuscitation of 'non-culturable' cells from aged cultures of *Campylobacter jejuni*. *Microbiology* 143, 1575–1581. doi: 10.1099/00221287-143-5-1575

Bronowski, C., James, C. E., and Winstanley, C. (2014). Role of environmental survival in transmission of *Campylobacter jejuni*. *FEMS Microbiol. Lett.* 356, 8–19. doi: 10.1111/1574-6968.12488

Bronowski, C., Mustafa, K., Goodhead, I., James, C. E., Nelson, C., Lucaci, A., et al. (2017). *Campylobacter jejuni* transcriptome changes during loss of culturability in water. *PLoS One* 12:e0188936. doi: 10.1371/journal.pone.0188936

Burnham, P. M., and Hendrixson, D. R. (2018). *Campylobacter jejuni*: collective components promoting a successful enteric lifestyle. *Nat. Rev. Microbiol.* 16, 551–565. doi: 10.1038/s41579-018-0037-9

Cameron, A., Frirdich, E., Huynh, S., Parker, C. T., and Gaynor, E. C. (2012). Hyperosmotic stress response of *Campylobacter jejuni*. *J. Bacteriol.* 194, 6116–6130. doi: 10.1128/jb.01409-12

Cappelier, J. M., Minet, J., Magras, C., Colwell, R. R., and Federighi, M. (1999). Recovery in embryonated eggs of viable but nonculturable *Campylobacter jejuni*

cells and maintenance of ability to adhere to HeLa cells after resuscitation. *Appl. Environ. Microbiol.* 65, 5154–5157.

Castro, A., Dorneles, E. M. S., Santos, E. L. S., Alves, T. M., Silva, G. R., Figueiredo, T. C., et al. (2018). Viability of *Campylobacter* spp. in frozen and chilled broiler carcasses according to real-time PCR with propidium monoazide pretreatment. *Poult. Sci.* 97, 1706–1711. doi: 10.3382/ps/pey020

CDC, (2018). *National Outbreak Reporting System*. Atlanta, GA: CDC.

Chang, C. W., and Lin, M. H. (2018). Optimization of PMA-qPCR for *Staphylococcus aureus* and determination of viable bacteria in indoor air. *Indoor Air* 28, 64–72. doi: 10.1111/ina.12404

Csonka, L. N. (1989). Physiological and genetic responses of bacteria to osmotic stress. *Microbiol. Rev.* 53, 121–147.

Demeke, T., Ratnayaka, I., and Phan, A. (2009). Effects of DNA extraction and purification methods on real-time quantitative pcr analysis of roundup ready (R) soybean. *J. AOAC Int.* 92, 1136–1144.

Dinu, L.-D., and Bach, S. (2013). Detection of viable but non-culturable *Escherichia coli* O157:H7 from vegetable samples using quantitative PCR with propidium monoazide and immunological assays. *Food Control* 31, 268–273. doi: 10.1016/j.foodcont.2012.10.020

Fittipaldi, M., Nocker, A., and Codony, F. (2012). Progress in understanding preferential detection of live cells using viability dyes in combination with DNA amplification. *J. Microbiol. Methods* 91, 276–289. doi: 10.1016/j.mimet.2012.08.007

Garenaux, A., Jugiau, F., Rama, F., de Jonge, R., Denis, M., Federighi, M., et al. (2008). Survival of *Campylobacter jejuni* strains from different origins under oxidative stress conditions: effect of temperature. *Curr. Microbiol.* 56, 293–297. doi: 10.1007/s00284-007-9082-8

Jackson, D. N., Davis, B., Tirado, S. M., Duggal, M., van Frankenhuyzen, J. K., Deaville, D., et al. (2009). Survival mechanisms and culturability of *Campylobacter jejuni* under stress conditions. *Antonie Van Leeuwenhoek* 96, 377–394. doi: 10.1007/s10482-009-9378-8

Josefsen, M. H., Löfström, C., Hansen, T. B., Christensen, L. S., Olsen, J. E., and Hoorfar, J. (2010). Rapid quantification of viable *Campylobacter* bacteria on chicken carcasses, using real-time PCR and propidium monoazide treatment, as a tool for quantitative risk assessment. *Appl. Environ. Microbiol.* 76, 5097–5104. doi: 10.1128/AEM.00411-10

Kassem, I. I., Chandrashekar, K., and Rajashekara, G. (2013). Of energy and survival incognito: a relationship between viable but non-culturable cells formation and inorganic polyphosphate and fornate metabolism in *Campylobacter jejuni*. *Front. Microbiol.* 4:183. doi: 10.3389/fmicb.2013.00183

Kempf, B., and Bremer, E. (1998). Uptake and synthesis of compatible solutes as microbial stress responses to high-osmolality environments. *Arch. Microbiol.* 170, 319–330. doi: 10.1007/s002030050649

Kusumoto, A., Asakura, H., and Kawamoto, K. (2012). General stress sigma factor RpoS influences time required to enter the viable but non-culturable state in *Salmonella enterica*. *Microbiol. Immunol.* 56, 228–237. doi: 10.1111/j.1348-0421.2012.00428.x

Magajna, B., and Schraft, H. (2015). Evaluation of Propidium Monoazide and quantitative PCR to quantify viable *Campylobacter jejuni* biofilm and planktonic cells in log phase and in a viable but Nonculturable State. *J. Food Prot.* 78, 1303–1311. doi: 10.4315/0362-028x.jfp-14-583

Makino, S. I., Kii, T., Asakura, H., Shirahata, T., Ikeda, T., Takeshi, K., et al. (2000). Does enterohemorrhagic *Escherichia coli* O157 : H7 enter the viable but nonculturable state in salted salmon roe? *Appl. Environ. Microbiol.* 66, 5536–5539. doi: 10.1128/aem.66.12.5536-5539.2000

McLaggan, D., Naprstek, J., Buurman, E. T., and Epstein, W. (1994). Interdependence of K+ and glutamate accumulation during osmotic adaptation of *Escherichia coli*. *J. Biol. Chem.* 269, 1911–1917.

Melero, B., Cocolin, L., Rantsiou, K., Jaime, I., and Rovira, J. (2011). Comparison between conventional and qPCR methods for enumerating *Campylobacter jejuni* in a poultry processing plant. *Food Microbiol.* 28, 1353–1358. doi: 10.1016/j.fm.2011.06.006

Nocker, A., and Camper, A. K. (2009). Novel approaches toward preferential detection of viable cells using nucleic acid amplification techniques. *FEMS Microbiol. Lett.* 291, 137–142. doi: 10.1111/j.1574-6968.2008.01429.x

Nocker, A., Cheung, C.-Y., and Camper, A. K. (2006). Comparison of propidium monoazide with ethidium monoazide for differentiation of live vs. dead bacteria by selective removal of DNA from dead cells. *J. Microbiol. Methods* 67, 310–320. doi: 10.1016/j.mimet.2006.04.015

Oliver, J. D. (2005). The viable but nonculturable state in bacteria. *J. Microbiol.* 43, 93–100.

Pacholewicz, E., Swart, A., Lipman, L. J., Wagenaar, J. A., Havelaar, A. H., and Duim, B. (2013). Propidium monoazide does not fully inhibit the detection of dead *Campylobacter* on broiler chicken carcasses by qPCR. *J. Microbiol. Methods* 95, 32–38. doi: 10.1016/j.mimet.2013.06.003

Papic, B., Pate, M., Henigman, U., Zajc, U., Gruntar, I., Biasizzo, M., et al. (2017). New approaches on quantification of *Campylobacter jejuni* in poultry samples: the use of digital PCR and real-time PCR against the ISO standard plate count method. *Front. Microbiol.* 8:331. doi: 10.3389/fmicb.2017.00331

Pinto, D., Santos, M. A., and Chambel, L. (2015). Thirty years of viable but nonculturable state research: unsolved molecular mechanisms. *Crit. Rev. Microbiol.* 41, 61–76. doi: 10.3109/1040841X.2013.794127

Ramamurthy, T., Ghosh, A., Pazhani, G. P., and Shinoda, S. (2014). Current perspectives on viable but non-culturable (VBNC) pathogenic bacteria. *Front. Public Health* 2:103. doi: 10.3389/fpubh.2014.00103

Rantsiou, K., Lamberti, C., and Cocolin, L. (2010). Survey of *Campylobacter jejuni* in retail chicken meat products by application of a quantitative PCR protocol. *Int. J. Food Microbiol.* 141, S75–S79. doi: 10.1016/j.ijfoodmicro.2010.02.002

Salas-Masso, N., Linh, Q. T., Chin, W. H., Wolff, A., Andree, K. B., Furones, M. D., et al. (2019). The use of a DNA-intercalating dye for quantitative detection of viable *Arcobacter* spp. Cells (v-qPCR) in Shellfish. *Front. Microbiol.* 10:368. doi: 10.3389/fmicb.2019.00368

Seinige, D., Krischek, C., Klein, G., and Kehrenberg, C. (2014). Comparative analysis and limitations of ethidium monoazide and propidium monoazide treatments for the differentiation of viable and nonviable *Campylobacter* cells. *Appl. Environ. Microbiol.* 80, 2186–2192. doi: 10.1128/AEM.03962-13

Silva, J., Leite, D., Fernandes, M., Mena, C., Gibbs, P. A., and Teixeira, P. (2011). *Campylobacter* spp. as a foodborne pathogen: a review. *Front. Microbiol.* 2:200. doi: 10.3389/fmicb.2011.00200

Silvestri, E. E., Yund, C., Taft, S., Bowling, C. Y., Chappie, D., Garrahan, K., et al. (2017). Considerations estimating microbial environmental data concentrations collected from a field setting. *J. Exposure Sci. Environ. Epidemiol.* 27, 141–151. doi: 10.1038/jes.2016.3

Telli, A. E., and Dogruer, Y. (2019). Discrimination of viable and dead *Vibrio parahaemolyticus* subjected to low temperatures using propidium monoazide - quantitative loop mediated isothermal amplification (PMA-qLAMP) and PMA-qPCR. *Microb. Pathog.* 132, 109–116. doi: 10.1016/j.micpath.2019.04.029

Tsiouris, V., Economou, E., Lazou, T., Georgopoulou, I., and Sossidou, E. (2019). The role of whey on the performance and *Campylobacteriosis* in broiler chicks. *Poult. Sci.* 98, 236–243. doi: 10.3382/ps/pey388

Webb, A. L., Taboada, E. N., Selinger, L. B., Boras, V. F., and Inglis, G. D. (2016). Efficacy of wastewater treatment on *Arcobacter butzleri* density and strain diversity. *Water Res.* 105, 291–296. doi: 10.1016/j.watres.2016.09.003

Young, K. T., Davis, L. M., and Dirita, V. J. (2007). *Campylobacter jejuni*: molecular biology and pathogenesis. *Nat. Rev. Microbiol.* 5, 665–679. doi: 10.1038/nrmicro1718

Zhong, J., and Zhao, X. (2018). Detection of viable but non-culturable *Escherichia coli* O157:H7 by PCR in combination with propidium monoazide. *Biotech* 8:28. doi: 10.1007/s13205-017-1052-7

Conflict of Interest: The authors declare that the research was conducted in the absence of any commercial or financial relationships that could be construed as a potential conflict of interest.

frontiers in Microbiology

ORIGINAL RESEARCH
published: 14 January 2020
doi: 10.3389/fmicb.2019.03030

Prebiotic Driven Increases in IL-17A Do Not Prevent *Campylobacter jejuni* Colonization of Chickens

*Geraldine M. Flaujac Lafontaine[1], Philip J. Richards[1], Phillippa L. Connerton[1], Peter M. O'Kane[1], Nacheervan M. Ghaffar[1], Nicola J. Cummings[1], Neville M. Fish[2] and Ian F. Connerton[1]**

[1] Division of Microbiology, Brewing and Biotechnology, School of Biosciences, University of Nottingham, Loughborough, United Kingdom, [2] Saputo Dairy UK, Dairy Crest Innovation Centre, Harper Adams University, Newport, United Kingdom

Worldwide *Campylobacter jejuni* is a leading cause of foodborne disease. Contamination of chicken meat with digesta from *C. jejuni*-positive birds during slaughter and processing is a key route of transmission to humans through the food chain. Colonization of chickens with *C. jejuni* elicits host innate immune responses that may be modulated by dietary additives to provide a reduction in the number of campylobacters colonizing the gastrointestinal tract and thereby reduce the likelihood of human exposure to an infectious dose. Here we report the effects of prebiotic galacto-oligosaccharide (GOS) on broiler chickens colonized with *C. jejuni* when challenged at either an early stage in development at 6 days of age or 20 days old when campylobacters are frequently detected in commercial flocks. GOS-fed birds had increased growth performance, but the levels of *C. jejuni* colonizing the cecal pouches were unchanged irrespective of the age of challenge. Dietary GOS modulated the immune response to *C. jejuni* by increasing cytokine IL-17A expression at colonization. Correspondingly, reduced diversity of the cecal microbiota was associated with *Campylobacter* colonization in GOS-fed birds. In birds challenged at 6 days-old the reduction in microbial diversity was accompanied by an increase in the relative abundance of *Escherichia* spp. Whilst immuno-modulation of the Th17 pro-inflammatory response did not prevent *C. jejuni* colonization of the intestinal tract of broiler chickens, the study highlights the potential for combinations of prebiotics, and specific competitors (synbiotics) to engage with the host innate immunity to reduce pathogen burdens.

Keywords: *Campylobacter*, galacto-oligosaccharide, prebiotic, broiler chicken, innate immunity, microbiota, Th17, pro-inflammatory response

OPEN ACCESS

Edited by:
Nicolae Corcionivoschi, Agri-Food and Biosciences Institute (AFBI), United Kingdom

Reviewed by:
Paul Wigley, University of Liverpool, United Kingdom
Odile Tresse, INRA Centre Angers-Nantes Pays de la Loire, France

****Correspondence:***
Ian F. Connerton
ian.connerton@nottingham.ac.uk

Specialty section:
This article was submitted to Food Microbiology, a section of the journal Frontiers in Microbiology

Received: *23 September 2019*
Accepted: *17 December 2019*
Published: *14 January 2020*

Citation:
Flaujac Lafontaine GM, Richards PJ, Connerton PL, O'Kane PM, Ghaffar NM, Cummings NJ, Fish NM and Connerton IF (2020) Prebiotic Driven Increases in IL-17A Do Not Prevent Campylobacter jejuni Colonization of Chickens. Front. Microbiol. 10:3030. doi: 10.3389/fmicb.2019.03030

INTRODUCTION

Campylobacter spp. are recognized as the major contributor to bacterial foodborne illness worldwide (Kaakoush et al., 2015). Campylobacterosis was the most frequently reported human zoonotic disease in the European Union in 2017 with 246,158 confirmed cases of gastrointestinal illness (EFSA, 2018). The most common species associated with human disease is *C. jejuni* (84.4%), but *C. coli* also represent a significant disease burden (9.2%; EFSA, 2018). *C. jejuni* and

Abbreviations: *C. jejuni*, *Campylobacter jejuni*; CFU, colony forming unit; FCR, feed conversion ratio; GoI, gene of interest; GOS, galacto-oligosaccharide; GIT, gastro-intestinal tract; IL, interleukin.

C. coli are referred to as thermophilic species as they can grow at 42°C, making them suited to colonize the intestinal tracts of poultry species (reviewed by Sahin et al., 2015). Poultry are a major source of campylobacters with an estimated 80% of human illness arising from poultry sources (Andreoletti et al., 2010). Source attribution estimates referenced at the point of exposure indicate 65–69% of human cases are from exposure to chicken meat (Ravel et al., 2017). Poultry meat is frequently contaminated with intestinal content harboring high levels of *Campylobacter* cells during slaughter and carcass processing, which constitutes the main risk to public health (Osimani et al., 2017). This has prompted the EU to adopt a microbiological sampling plan for broiler chicken carcasses with a limit of 1,000 CFU/g (Commission Regulation (EU) 2017/1495). Strict on-farm biosecurity measures to prevent *Campylobacter* exposure and flock colonization of broiler chickens have been implemented in many countries, but these alone do not maintain *Campylobacter*-free flocks (Newell et al., 2011). Intervention strategies have been developed aimed at reducing levels of *Campylobacter* colonization, and thereby human exposure, if the reductions can be translated on to chicken meat (Rosenquist et al., 2003; Newell et al., 2011; Sahin et al., 2015). *Campylobacter* colonization has been associated with poor flock health and performance in commercial broiler chicken production (Bull et al., 2008), although performance issues are not manifest in all circumstances (Gormley et al., 2014). The impact of *Campylobacter* colonization on bird health has been reported to vary with the broiler breed/rate of growth, stocking density, intercurrent infectious or immunosuppressive challenges and the colonizing organism (Humphrey et al., 2015; Li L. et al., 2018). It is, however, clear that *Campylobacter* colonization elicits a Th17 pro-inflammatory response in broiler chickens (Reid et al., 2016; Connerton et al., 2018). Intestinal intraepithelial lymphocytes characterized as either $CD3^{+}CD25^{+}$ cells or γδ T cells have been reported to express intracellular IL-17A in the lower intestine of chickens (Walliser and Göbel, 2018). Not all inflammatory responses lead to negative outcomes for the host. It has been questioned whether dietary anti-inflammatory additives aimed at the detrimental consequences of intestinal inflammation may actually impair necessary responses of young animals that are required to overcome the challenges present in commercial production to achieve favorable performance outcomes (Broom and Kogut, 2018). Zootechnical performance remains a key driver in the poultry industry, at the same time public and regulatory concerns are mounting regarding welfare and antibiotic use in poultry production. Although progress has been made toward reducing antibiotic use in poultry production in several countries has been reported more remains to be achieved (Speksnijder et al., 2015). It has been proposed that the rational manipulation of poultry feed formulation can improve pathogen resistance, improve production, and reduce the threat posed by zoonotic pathogens through the food chain (Kogut, 2009; Swaggerty et al., 2019). Intestinal innate immune responses to feed and pathogen challenges are strongly influenced by the gut microbiota (Kogut et al., 2018). The addition of probiotic microorganisms, prebiotics and phytobiotics in feed are approaches by which the gut microbiota of broiler chickens may be influenced (reviewed by Pedroso et al., 2013; Pourabedin and Zhao, 2015; Van Immerseel et al., 2017; Clavijo and Flórez, 2018). It is proposed that these approaches will be most effective when introduced early in life to establish a robust microbiota that benefits production (Rubio, 2019). We have recently reported that the inclusion of the prebiotic GOS in juvenile broiler feed enhances the growth and feed conversion rates of broiler chickens, increases ileal and cecal IL-17A gene expression and brings about changes in the cecal populations of key *Lactobacillus* spp. (Richards et al., 2019b). GOS represent host-indigestible carbohydrates that have been identified as promoting beneficial bacteria in humans and animals, which include *Bifidobacteria*, *Bacteroides*, and *Lactobacillaceae* (Jung et al., 2008; Hughes et al., 2017; Van Bueren et al., 2017; Tian et al., 2019).

In the present study, we have examined whether the impact of a GOS diet on host fitness, immune response and changes in the gut microbiota would support the clearance of *Campylobacter jejuni* in broiler chickens. For this purpose, we fed isocaloric GOS or control diets from hatch to 20 days of age to modulate the intestinal innate immune status and gut microbiota of broiler chickens. Two approaches were taken to determine the role of development on host response. In one experiment birds were challenged at an early stage of development at 6 days old to determine the persistence of *C. jejuni* in the modified gut environment and assess corresponding intestinal chemokine and cytokine gene expression, and the prevailing intestinal microbiota throughout the typical broiler chicken lifespan of 35 days. In a separate experiment birds were challenged at 20 days old, when campylobacters are frequently first detected in commercial flocks, with similar observations made until the trial ended when birds reached 35 days old.

MATERIALS AND METHODS

Trial Design

Two independently performed trials monitored the effect of dietary GOS on development of the gut innate immune responses and the cecal microbiota of broiler chickens challenged with *C. jejuni* HPC5 at either an early stage of development (6 days old) or late stage (20 days old), the age at which birds often become *Campylobacter* positive in commercial production. Birds were randomly assigned to either a group fed a control diet (referred to as *Campylobacter*) or to a group fed a GOS-supplemented diet (referred to as GOS + *Campylobacter*) for the duration of the experiment. In the early 6-day old challenge experiment (referred to as 6-dc), two groups of 35 birds were kept in pens from day of hatch until day 6 when all birds were administered *C. jejuni*, and subsequently independently caged until the end of the study on day 35. Birds were randomly selected (n = 7) from each diet group and euthanized prior to sampling intestinal tissues and contents at 8, 15, 22, 28, and 35 days of age (da). For the late 20-day challenge trial (referred to as 20-dc), two groups of 21 birds were similarly housed in pens until 20 days when the birds were administered *C. jejuni* and independently caged until the end of the study at 35 days. Again, randomly selected birds (n = 7) from each diet group were euthanized

for intestinal sampling at 22, 28, and 35 days. All experimental birds post challenge were maintained in independent housing to prevent the birds sharing intestinal microbiota through coprophagy, which would otherwise confound the experimental design by reducing the number of replicates.

Experimental Animals

Day-of-hatch male Ross 308 broiler chicks purchased from a local hatchery were randomly assigned on the basis of weight to control or GOS diet groups. Birds were brooded in floor pens on wood shavings until the day of *Campylobacter* challenge. Birds were housed in a controlled environment under strict conditions of biosecurity and kept under controlled light (L:D 12:12) with *ad libitum* access to food and water throughout the study. Temperatures conformed to the Code of Practice for the Housing and Care of Animals Bred, Supplied or Used for Scientific Purposes 2014. Welfare monitoring of the chickens was undertaken two or three times every 24 h post *Campylobacter* challenge. Birds in the control group were sustained on a wheat-based diet provided as starter crumb for 0–10 days, grower pellets for 11–24 days and finisher pellets for 25–35 days. The starter diet contained wheat (59.9% w/w), soya meal (32.5% w/w), soybean oil (3.65% w/w), limestone (0.6% (w/w), calcium phosphate (1.59% w/w), sodium bicarbonate (0.27% w/w), the enzymes phytase and xylanase (dosed according to the manufacturer's instructions; DSM Nutritional Products Ltd., PO Box 2676 CH-4002 Basel, CH) and a vitamin mix containing NaCl salt, lysine HCl, DL-methionine and threonine. The grower and finisher diets increased the wheat content at the expense of soya meal by 2 and 5% w/w, respectively. The 6-dc prebiotic GOS + *Campylobacter* treatment group had the starter feed supplemented with GOS from 1 to 10 days at 3.37% w/w and then 11–35 days at 1.695% w/w, whilst the 20-dc birds were fed 3.37% w/w GOS throughout the experiment. The GOS was provided as Nutrabiotic® GOS that contains 74% GOS w/w dry matter (Dairy Crest Ltd., Davidstow, Cornwall, United Kingdom). GOS preparations contain a mixture of monosaccharides (glucose and galactose) and oligosaccharides (DP2 – DP8) with the exception of lactose that is a residual component of the production process. The enzymatic synthesis of GOS produces β-(1–3) or β-(1–4) or β-(1–6)-linked galactose residues (1 to 7) with a terminal β-(1–3) or β-(1–4) or β-(1–6)-linked glucose. Isocaloric content adjustments for GOS inclusion were for the starter feed (wheat 54.0% w/w) soya meal (33.9% w/w) and soybean oil (4.88% w/w); for the grower feed (wheat 54.7% w/w) soya meal (32.2% w/w) and soybean oil (6.76% w/w); for the finisher feed (wheat 60.33% w/w) soya meal (26.7% w/w) and soybean oil (6.84% w/w). The feed and paper liners on which the chicks were delivered were found negative for *Salmonella* using standard enrichment procedures. At the time of challenge all birds were administered by oral gavage a dose of 1×10^7 CFU *C. jejuni* HPC5, a well-characterized broiler chicken isolate, suspended in MRD (Oxoid, Thermo Fisher Scientific, Altrincham, United Kingdom) in volumes of 0.1 ml for the 6-dc birds or in 1 ml for the 20-dc birds. For sample collection, birds were euthanized by either exposure to rising CO_2 gas or parenteral barbiturate overdose followed by cervical dislocation depending on bird mass in accordance with Schedule 1 of the United Kingdom Animals (Scientific Procedures) Act 1986. Ileal tissues were collected from approximately 3 cm distal to Meckel's diverticulum and cecal tissues isolated from the distal tips of the cecal pouches. Samples of intestinal tissue were immediately frozen in liquid nitrogen for subsequent RNA isolation or preserved in 10% (w/v) neutral buffered formalin (Thermo Fisher Scientific) for histological assessment. Cecal contents were collected and used either to enumerate *Campylobacter* or for isolation of total genomic DNA extraction.

Performance and Growth Rate

Live weights and all feed consumed were recorded for all birds at regular intervals from the start of the experiment until the end at 35 days. FCR were calculated as a ratio of feed consumed to the live weight of the birds. Bird growth rates were compared for each of the birds that remained at the end of the 35 days rearing period that collectively represent all the birds for which repeated measurements of the mass were recorded throughout the broiler chicken lifespan.

Bacterial Enumeration

Approximately 1 g of digesta was aseptically collected from both ceca and combined in pre-weighed universal containers before a 10% w/v suspension was prepared in MRD. *Campylobacter* were enumerated in triplicate from decimal dilutions prepared in MRD using a modification of the Miles and Misra technique (Miles et al., 1938). For each triplicate dilution set, five aliquots were dispensed onto CCDA agar (PO0119; Oxoid) prepared with the addition of agar to 2% (to prevent swarming) and with addition of CCDA Selective Supplement SR0155 (Oxoid). Plates were incubated at 42°C in a microaerobic atmosphere (2% H_2, 5% CO_2, 5% O_2, and 88% N_2 v/v) for 48 h (Don Whitley Scientific modified atmospheric cabinet, Shipley, United Kingdom).

Histology

Tissue samples fixed in a 10% formalin solution were dehydrated through a series of alcohol solutions, cleared in xylene, and embedded in paraffin wax (Microtechnical Services Ltd., Exeter, United Kingdom). Sections (3 to 5 μm thick) were prepared and stained with modified hematoxylin and eosin (H&E). After staining, the slides were scanned by NanoZoomer Digital Pathology System (Hamamatsu, Welwyn Garden City, United Kingdom). Villus height and crypt depth were recorded from operator blinded measurements collected using the NanoZoomer Digital Pathology Image Program (Hamamatsu) from histology stained slides scanned at 40× resolution for each tissue sample. Villus height was determined from the tip of the villus to the crypt opening and the associated crypt depth was measured from the base of the crypt to the level of the crypt opening. The ratios of villus height to relative crypt depth (v/c ratio) were calculated from these measurements. Dimensions for 10 well-oriented villi per tissue sample of 3 or 4 birds per diet group at each sampling time were analyzed.

RNA Isolation and RT-qPCR of the Cytokines and Chemokines

Total RNAs were isolated from ceca and ileum tissue biopsies using NucleoSpin RNA purification kit (Macherey-Nagel, GmbH & co. KG, Düren; DE) according to the manufacturer's protocol with the following modifications. Tissue samples were homogenized with the kit Lysis buffer and 2.8 mm ceramic beads (MO BIO Laboratories Inc., Carlsbad, United States) using TissueLyser II (Qiagen, Hilden, Germany). Subsequently total RNAs were extracted as described in the protocol with a DNaseI treatment step as per the manufacturer's instructions. Purified RNAs were eluted in nuclease free water, validated for quality and quantity using UV spectrophotometry (Nanodrop ND-1000, Labtech International Ltd., Uckfield, United Kingdom), and stored long term at −80°C. RNAs with OD260/280 ratio between 1.9 and 2.1 were deemed high quality, the ratios were found with a mean of 2.12 ± 0.01. Reverse Transcription was performed with 1 μg of RNA, SuperScript II (Invitrogen Life Technologies, Carlsbad, CA, United States) and random hexamers as described previously (Connerton et al., 2018). Quantitative PCR reaction was performed with cDNA template derived from 4 ng of total RNA in triplicate using SYBR Green Master mix (Applied Biosystems, Thermo Fisher Scientific). The RNA level of expression was determined by qPCR using the Roche Diagnostics LightCycler 480 (Hoffmann La Roche AG, CH). The primers sequence for GAPDH, INF-γ, IL-1β, IL-6, IL-10, IL-17A, IL-17F, ChCXCLi1, and ChCXCLi2 (**Table 1**) were previously described (Kaiser et al., 2003; Nang et al., 2011; Rasoli et al., 2015; Reid et al., 2016). Cytokines and chemokines transcripts fold change (FC) were calculated according to the manufacturer using the $2^{-\Delta\Delta Cp}$ method (Livak and Schmittgen, 2001). Averages of the triplicate Ct values were analyzed with the target genes of interest (GOI) values normalized to those of the housekeeping gene Glyceraldehyde 3-phosphate dehydrogenase (GAPDH).

Microbiota Analysis

DNA was isolated from cecal content using the MoBio PowerSoil kit (now QIAGEN Ltd., Manchester, United Kingdom) according to the manufacturer's instructions. The V4 regions of the bacterial 16S rRNA genes were PCR amplified using the primers 515f (5′ GTGCCAGCMGCCGCGGTAA 3′) and 806r (5′ GGACTACHVGGGTWTCTAAT 3′) (Caporaso et al., 2011). Amplicons were then sequenced on the Illumina MiSeq platform (Illumina Inc., San Diego, United States) using 2 × 250 bp cycles (reagent kit V2). The 16S rRNA gene sequences were quality filtered and clustered into OTUs in Mothur (Schloss et al., 2009) using the Schloss lab. MiSeq SOP[1], accessed 2018-10-05; Kozich et al., 2013). Batch files of Mothur commands used in this study are available at https://github.com/PJRichards/lafontaine_campy_gos. Raw sequences for 16S rDNA data originally reported in this article are deposited in the NCBI database within BioProject PRJNA380214 under SRA study SRP133552. Comparative 16S rDNA data from mock-challenged birds reproduced in this study was downloaded from NCBI PRJNA380214 (the FTP code is available from GitHub repository as described below). Post-processing rarefaction curves were plotted to assess sampling effort (**Supplementary Figure S1**).

Data and Statistical Analysis

All figures were drawn and unless otherwise stated all tests for statistical significance were performed using R 3.6.1 (R Core Team, 2019) in RStudio 1.2.1 (RStudio Team, 2015). All R scripts have been made available here: https://github.com/PJRichards/lafontaine_campy_gos. Histology measurements for each diet regimen of age-matched birds were compared using ANOVA.

Zootechnical Data

Bird growth rates were compared by determining rate of growth from 15 days for each of the birds that remained at the end of the trial at 35 days, i.e., birds for which repeated measurements of the mass were recorded throughout the growing period (*Campylobacter* treatment group, $n = 7$; GOS + *Campylobacter* treatment, $n = 8$). Growth rate was determined for individual birds for the period of linear growth post-challenge (6-dc birds between 15 and 35 days; 20-dc birds between 22 and 35 days). Growth rates (g/day) were compared between cohorts using Student's *t* test. Further comparison was made between the mass of age-matched birds using Student's *t* test. *C. jejuni* viable counts were $\log_{10}$-transformed and tested for significance using Student's *t* test.

Microbiota – 16S rRNA Gene Sequence Data

Comparisons were made of α-diversity metrics (Shannon diversity and inverse Simpson's indices) generated in mothur. For the four treatment groups in 6-dc birds at 8 days (2 dpi) differences in α-diversity were tested for using ANOVA with Tukey multiple comparison of means test (*p* was adjusted for multiple comparisons). For subsequent comparisons of α-diversity at 15, 22, 28 and 35 days between two treatment groups only (*Campylobacter* and GOS + *Campylobacter*) Student's *t* test was used to test for significance. Correspondingly, comparisons of Chao richness between the four treatment groups in 6-dc birds at 8 days (2 dpi) were made using a Kruskal-Wallis test with Benjamini-Hochberg FDR correction as were subsequent comparisons at 15, 22, 28, and 35 days. Note that a randomly selected community was deleted from the GOS + *Campylobacter* treatment group at 15 days and 35 (birds 2 and 6, respectively) to even group size and allow unbiased comparisons. For 20-dc birds, comparisons of α-diversity were made using Student's *t* test and comparisons of Chao richness were made using a Kruskal-Wallis test. Differences in bacterial composition were tested for by modeling compositional population data in terms of a Dirichlet distribution and using a likelihood ratio test in DirtyGenes (Shaw et al., 2019). Differential OTUs were identified with LEfSE in mothur (Schloss et al., 2009; Segata et al., 2011).

[1]https://github.com/mothur/mothur

TABLE 1 | Primer sequences for the gene expression determined by qPCR.

Target gene	Primer sequence (5′-3′)	Product size (bp)	NCBI Accession number	References
GAPDH	F: GACGTGCAGCAGGAACACTA R: TCTCCATGGTGGTGA AGACA	343	NM_204305.1	Nang et al. (2011)
INF-γ	F: TGAGCCAGATTGTTTCGATG R: CTTGGCCAGGTCCATGATA	152	NM_205149.1	Nang et al. (2011)
IL-1β	F: GGATTCTGAGCACACCACAGT R: TCTGGTTGATGTCGAAGATGTC	272	NM_204524.1	Nang et al. (2011)
IL-10	F: GCTGCGCTTCTACACAGATG R: TCCCGTTCTCATCCATCTTC	203	NM_001004414.2	Nang et al. (2011)
IL-6	F: GCTCGCCGGCTTCGA R: GGTAGGTCTGAAAGGCGAACAG	71	NM_204628.1	Kaiser et al. (2003)
IL-17A	F: CATGGGATTACAGGATCGATGA R: GCGGCACTGGGCATCA	68	NM_204460.1	Reid et al. (2016)
IL-17F	F: TGACCCTGCCTCTAGGATGATC R: GGGTCCTCATCGAGCCTGTA	78	XM_426223.5	Reid et al. (2016)
ChCXCLi-1	F: CCGATGCCAGTGCATAGAG R: CCTTGTCCAGAATTGCCTTG	191	NM_205018.1	Rasoli et al. (2015)
ChCXCLi-2	F: CCTGGTTTCAGCTGCTCTGT R: GCGTCAGCTTCACATCTTGA	128	NM_205498.1	Rasoli et al. (2015)

Intestinal Cytokine and Chemokine Transcription

Host cytokine and chemokine transcript levels were assessed by RT-qPCR of transcribed RNA isolated from ileal and cecal tissue sections. Cytokine and chemokine normalized expression was determined for each sample as $2^{-\Delta\ Cp}$ with ΔCp = Cp of GoI – Cp of housekeeping gene (GAPDH). The relative gene expression between birds fed a control (*Campylobacter*) or a GOS diet (GOS + *Campylobacter*), results were determined as a group mean FC, which was calculated from $2^{-\Delta\ \Delta\ Cp}$ with ΔΔCp = ΔCp (GOS diet) - ΔCp (average ΔCp of control). Differences between treatment groups were assessed using Wilcoxon rank sum tests with Benjamini-Hochberg FDR correction.

RESULTS

Dietary Galacto-Oligosaccharide Improved the Growth Performance of *Campylobacter jejuni*-Colonized Broiler Chickens

The aim of this research was to determine whether GOS could still act as a prebiotic and confer a growth performance advantages to broiler chickens colonized when colonized by *C. jejuni*. Chickens fed a GOS diet performed better than those fed the calorie-matched control diet (**Figures 1A,B**). Differences in the body weights were evident from 22 days for the 6-dc birds ($p \leq 0.029$) until slaughter at 35 days (mean body weights *Campylobacter* treatment = 2276 g, GOS + *Campylobacter* treatment = 2722; $p = 0.029$) (**Figure 1A**). Differences in the weights of the 20-da challenged birds were observed at 35 days (mean body weights *Campylobacter* = 2055 g, GOS + *Campylobacter* = 2341; $p = 0.004$) (**Figure 1B**). The growth rates of the 6-da challenged birds fed GOS increased in the period 15–35 days compared to the challenged chickens fed a control diet (control = mean 83.6 g/day, GOS = mean 105.1 g/day; $p = 0.0233$), and similarly for the 20-da challenged birds for the period 22–35 days (control = mean 85.3 g/day, GOS = mean 97.6 g/day; $p = 0.007$).

The cumulative FCR up to 35 days for 6-dc birds fed control diet ($n = 7$) was 1.45 and for the GOS diet ($n = 8$) was 1.42 while the FCR for 20-dc birds fed control diet ($n = 7$) was 1.56 and for GOS diet ($n = 7$) was 1.58 (data not shown). The contemporary breed performance objectives for male Ross 308 were body weight 2,283 g and FCR of 1.54 at 35 days (Aviagen Performance Objectives, 2014).

Dietary Galacto-Oligosaccharide Inclusion Did Not Prevent *Campylobacter jejuni* Colonization of Broiler Chickens

To assess the impact of dietary GOS on *C. jejuni* colonization we sacrificed birds over the rearing period to determine the cecal viable *Campylobacter* counts ($n = 7$). All birds were culture-negative for *Campylobacter* spp. until oral gavage with *C. jejuni* HPC5 at 6 days for the early-challenge cohort (6-dc) or 20 days for the late-challenge birds (20-dc). Birds challenged at 6 days (**Figure 1C**) showed incomplete colonization at 2 dpi (2/7 and 3/7 for the control and GOS cohorts, respectively), but the treatment groups all showed complete colonization with *C. jejuni* at 9 dpi. Mean colonization levels of 6.4 $\log_{10}$ CFU/g for the control diet and 5.9 $\log_{10}$ CFU/g for the GOS diet were recorded (15 days). The birds then remained colonized thereafter to the end of the 35 days rearing period with no significant differences between the colonization levels of the dietary groups at any time (**Figure 1C**). The 20-dc birds (**Figure 1D**) were all found colonized at 8 dpi with mean colonization levels of 6.8 $\log_{10}$ CFU/g for the control and 7.2 $\log_{10}$ CFU/g for the GOS diet (28 days). Viable counts of *Campylobacter* in cecal content remained high at the end of the

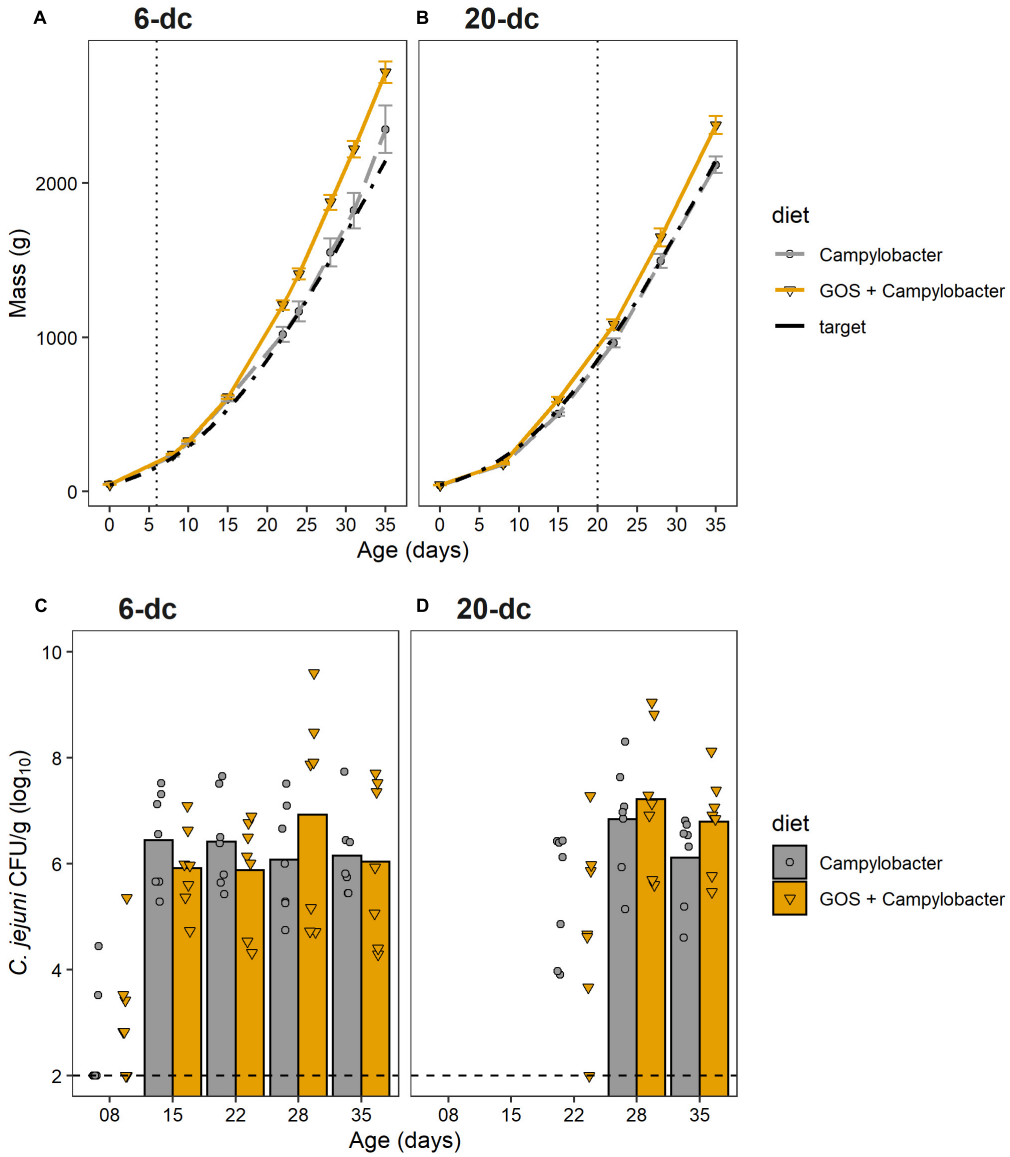

FIGURE 1 | GOS improves growth performance of broiler chickens, but does not affect *C. jejuni* colonization of the ceca. **(A,B)** Chicken live total mass from day of hatch to 35 days for 6-dc birds **(A)** and 20-dc birds **(B)**. The plots show the performances of the experimental treatments GOS + *Campylobacter* (GOS diet) *Campylobacter* (control diet) and the Ross 308 performance objective as the Target (Aviagen Performance Objectives, 2014). The dashed line indicates age at challenge. **(C,D)** Viable counts of *Campylobacter* recovered from the cecal content of 6-dc birds **(C)** and 20-dc birds **(D)**. Data markers indicate *Campylobacter* CFU isolated from individual birds. Bars indicate mean *Campylobacter* CFU, excluding cohorts where *Campylobacter* levels were below the limit of detection. There are no significant differences in the *Campylobacter* counts for the GOS diet compared to control diet post colonization ($p > 0.05$). The dashed line indicates minimum level of detection.

rearing period with no significant differences between the diets at any time, independent of the age of challenge.

Intestinal Villus and Crypt Metrics Were Affected by Dietary Galacto-Oligosaccharide Post-infection With *Campylobacter jejuni*

Villus and crypt metrics were determined from 10 well-oriented villi for 3 to 4 birds from each group in a blind assessment of formalin-fixed H&E-stained ileum sections. Measurement comparisons of the GOS and control diet groups for 6-dc birds showed greater villus length at 8 (2 dpi; $p = 0.04$) and 15 days (9 dpi; $p = 0.002$) for the *C. jejuni* colonized GOS-fed chickens compared to the *C. jejuni* colonized birds on control feed (**Table 2**). By 22 days the villus lengths of the 6-dc treatment groups were not significantly different and remained so until the end of the trial at 35 days. Comparison of the crypt depth measurements demonstrated that the GOS-fed birds at 15 days ($p = 0.005$) had significantly deeper crypts than the birds on the

TABLE 2 | Ileal histomorphometry.

	Histology measurements									
	8 days	**SD**	**15 days**	**SD**	**22 days**	**SD**	**28 days**	**SD**	**35 days**	**SD**
Villus length (μm)										
Campy (6-dc)	550	74	560	64	803	33	940	71	934	32
Campy + GOS (6-dc)	671	15	796	58	824	61	814	63	888	40
Campy (20-dc)	–		–		636	56	746	88	954	98
Campy + GOS (20-dc)	–		–		766	82	922	114	1092	124
p-value (6-dc)	0.04		0.002		0.56		0.09		0.31	
p-value (20-dc)	–		–		0.04		0.05		0.13	
Crypt depth (μm)										
Campy (6-dc)	117	12	111	7	125	8	128	5	121	8
Campy + GOS (6-dc)	110	8	133	4	128	5	132	8	122	11
Campy (20-dc)	–		–		82	16	92	24	104	22
Campy + GOS (20-dc)	–		–		106	12	102	38	128	44
p-value (6-dc)	0.32		0.005		0.65		0.49		0.69	
p-value (20-dc)	–		–		0.05		0.67		0.37	
Villus length/Crypt depth ratio (v/c)										
Campy (6-dc)	4.70	0.84	5.05	0.60	6.42	0.17	7.34	0.63	7.72	0.82
Campy + GOS (6-dc)	6.10	0.38	5.98	0.39	6.44	0.31	6.17	0.59	7.28	0.27
Campy (20-dc)	–	–	–	–	7.76	0.80	8.11	0.74	9.17	0.91
Campy + GOS (20-dc)	–	–	–	–	7.23	0.91	9.04	0.82	8.53	0.72
p-value (6-dc)	0.02		0.04		0.83		0.08		0.35	
p-value (20-dc)	–		–		0.42		0.14		0.31	

Villus length, crypt depth and ratio villus length/crypt ratios presented as mean values (±standard deviation) of the measurement of 10 well-orientated villi for 3 to 4 birds per group. Corresponding probabilities (p) were calculated using ANOVA tests, differences were considered significant at $p < 0.05$.

control diet. Differences in the villus and crypt measurements affected differences in the villus to crypt ratios at 8 days ($p = 0.02$) and 15 days ($p = 0.04$) with the GOS-fed birds exhibiting greater ratios. For the 20-dc cohorts the GOS-fed birds also exhibited significant increases in villus height compared to the control diet after *C. jejuni* colonization at 22 days (2 dpi; $p = 0.04$) and 28 days (8 dpi; $p = 0.05$). A significant increase in the crypt depth for the GOS-fed birds over the birds on the control diet was also recorded at 22 days ($p = 0.05$), but not thereafter. These differences did not result in significant differences in the villus to crypt ratios for the 20-dc experiment.

Dietary Galacto-Oligosaccharide Modulates IL-17 Transcription Post *Campylobacter* Colonization

Immuno-modulatory effects of dietary GOS on the innate immune responses of intestinal tissues from *C. jejuni*-colonized broilers were assessed. RNAs were extracted from biopsies collected from ileal and cecal tissues to enable RT-PCR quantification of cytokine and chemokine gene transcripts representing the major inflammatory pathways of chickens. Cytokines IL-17A, IL-17F, IL-6, IL-1β and chemokines ChCXCLi-1, ChCXCLi-2 (also known as ChIL-8) have previously been described as markers of the Th17 pathway (Reid et al., 2016). IFN-γ is related to the Th1 pathway and the anti-inflammatory cytokine IL-10 is largely expressed from regulatory T cells (Treg) in chickens to control the inflammatory effects of the Th cell responses.

The innate immune response of ileal tissues for the early challenged birds (6-dc) was characterized by modulation in the expression of IL-17A in *C. jejuni*-colonized birds on control feed compared to *C. jejuni*-colonized GOS-fed birds (**Figure 2A**). Following *Campylobacter* challenge IL-17A transcript levels were far greater in the GOS-fed birds (884-fold difference) than those on the control diet at 8 days (2 dpi; *p-adj* = 0.005). By 15 days the difference had declined to 12-fold due to an increase in IL-17A in the *C. jejuni*-colonized birds on the control diet (9 dpi; *p-adj* = 0.02). The rise in IL-17A continued in the birds on the control diet until 35 days such that a significant difference was recorded in favor of the control diet birds from 22 days (16 dpi; *p-adj* = 0.02), whilst the IL-17A levels were maintained in the GOS-fed birds throughout the time course. The pro-inflammatory cytokine IL-17F exhibited a significant increase in expression at 22 days (16 dpi; *p-adj* = 0.03) and 28 days (22 dpi; *p-adj* = 0.005) in the control birds. Over the transition period, the regulatory cytokine IL-10 expression was significantly greater at 15 days (9 dpi; *p-adj* = 0.05) and 22 days (16 dpi; *p-adj* = 0.03) in the *C. jejuni*-colonized birds on control diet compared to the GOS diet (GOS + *Campylobacter* treatment). For the late challenged birds (20-dc; **Figure 2B**), IL-6 was recorded as significantly greater for the *C. jejuni*-colonized birds on the control diet at 35 days (29 dpi; *p-adj* = 0.005), largely owing to a fall in the IL-6 levels of the birds on the GOS diet (GOS + *Campylobacter* treatment).

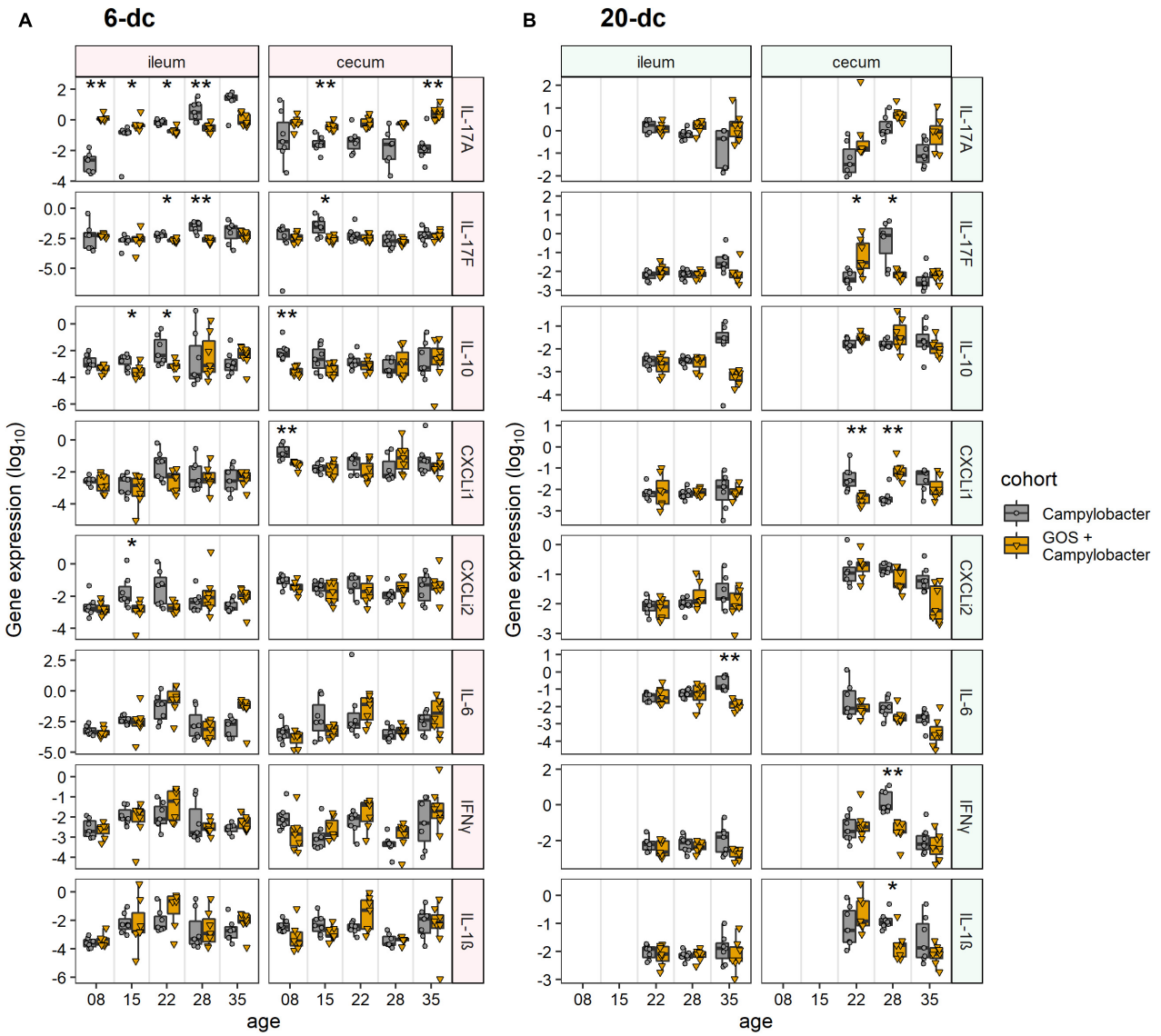

FIGURE 2 | Modulation of cecal and ileal innate immune responses to dietary GOS in *Campylobacter*-challenged broiler chickens. The figures report cytokine and chemokine normalized gene expression for 6-dc birds **(A)** and 20-dc birds **(B)** fed a control diet (*Campylobacter* treatment) or a GOS diet (GOS + *Campylobacter* treatment) recorded as $\log_{10}$ of the ratio for gene of interest/GAPDH from qPCR data of individual birds. Corresponding probabilities (*p-adj*) were calculated using non-parametric Wilcoxon rank sum tests with Benjamini-Hochberg FDR correction, where differences at *p-adj* < 0.05 were considered significant and are summarized in the plot using asterisks (**p-adj* ≤ 0.05; ***p-adj* ≤ 0.01).

In cecal tissues IL-17A expression was also maintained in the GOS-fed birds post *C. jejuni* colonization. In the early challenge experiment (6-dc) IL-17A expression levels declined in the birds fed the control diet throughout the time course with significant differences recorded at 15 days (9 dpi; *p-adj* = 0.005) and 35 days (288-fold at 29 dpi; *p-adj* = 0.01) compared to the birds on the GOS containing diet (**Figure 2A**). Pro-inflammatory IL-17F exhibited a significant increase at 15 days in the *C. jejuni*-colonized birds fed the control diet compared to the birds on the GOS diet (9 dpi; *p-adj* = 0.04). This was preceded by differential increases at 8 days in IL-10 (2 dpi; *p-adj* = 0.002) and ChCXCLi-1 (2 dpi; *p-adj* = 0.002). The late challenged birds (20-dc) featured a significant switch in the expression of IL-17F from low to high for the *C. jejuni*-colonized birds on the control diet between 22da (2 dpi; *p-adj* = 0.04) and 28 days (8 dpi; *p-adj* = 0.02), and conversely the birds on the GOS diet exhibited a high to low change in gene expression over the period (treatment GOS + *Campylobacter*). Increases in IL-17F were accompanied by significant increases in IFN-γ (8 dpi; *p-adj* = 0.005) and IL-1β (8 dpi; *p-adj* = 0.02) at 22da for the *C. jejuni*-colonized birds on the control diet. Transcription of the chemokine ChCXCLi-1 was observed to exhibit the opposite trend to IL-17F over the 22 days (2 dpi; *p-adj* = 0.005) to 28 days (8 dpi; *p-adj* = 0.005) transition, with a fall in the mean expression value for the

C. jejuni-colonized birds on the control diet compared to an increase in the *C. jejuni*-colonized GOS-fed birds (treatment GOS + *Campylobacter* in **Figure 2B**).

Galacto-Oligosaccharide -Induced Microbiota Diversity Shifts in *Campylobacter*-Challenged Birds

At 2 dpi (8 days) the α-diversity of the cecal microbiota of 6-dc birds was lower in GOS + *Campylobacter* treated birds than the *C. jejuni*-colonized birds on the control diet (treatment *Campylobacter*), as indicated by lower Shannon entropy (p = 0.046) and inverse Simpson index (p = 0.022; **Figure 3A**). This may be attributed to the dietary GOS as the inverse Simpson's index of mock-challenged birds on a GOS diet was also lower than that of the *Campylobacter* treatment birds on the control diet (p = 0.032), with the difference observed in the corresponding Shannon entropy values approaching the significance threshold (p = 0.058). Shannon entropy was also lower in GOS + *Campylobacter* treatment birds at 28 days (22 dpi; p = 0.009) and 35 days (29 dpi; p = 0.038) as presented in **Figure 3A**. There were no other observed differences in α-diversity or species richness (Chao) in 6-dc birds. In the 20-dc experiment at 22 days (2 dpi) the inverse Simpson index of the cecal microbiota of the GOS + *Campylobacter* treatment birds was significantly greater than *Campylobacter* treatment birds (p = 0.0469; **Figure 3B**). The responses recorded for the inverse Simpson index at 2 dpi for the 6-dc and 20-dc experiments show opposite trends, however, a similar trend can be noted in the higher α-diversity of 6-dc GOS + *Campylobacter* treatment birds at the same age (22 days), although these changes did not reach significance. The modulation in α-diversity at this age could be attributable to changes in host development or changes in diet formulation of grower to finisher related to husbandry.

Comparison of the phylum composition of 6-dc birds at 8 days (2 dpi) indicates that the cecal microbiota of *Campylobacter* treatment birds was significantly different from the microbiota of the GOS + *Campylobacter* treatment birds (p = 0.0003) (**Figure 3C**). Comparison of the microbiota of GOS + *Campylobacter* treatment birds with the cecal microbiota of age-matched mock-challenged birds on the GOS diet alone at 8 days (2 dpi) did not reveal any phyla-level differences (p = 0.1613), whilst mock-challenged birds on either control or GOS diets also had different phyla compositions (p = 0.0096). These data suggest that the differences in microbiota ecology are linked to dietary GOS and not *Campylobacter*-colonization *per se*. No difference in phylum-composition was determined in 6-dc birds at 15 days (9 dpi; p = 0.301), 22 days (16 dpi; p = 0.69) or 35 days (p = 0.055). However, the composition of the cecal microbiota of birds from the GOS + *Campylobacter* and the *Campylobacter* treatment groups were different at 28 days (22 dpi; p = 0.0004), which likely corresponds with the reverse in α-diversity first observed at this age. No differences were determined in the phylum-composition of 20-dc birds at 2 dpi (p = 0.742) (**Figure 3D**).

At OTU level 16S rRNA gene sequencing reads were clustered at 97% similarity, which serves as a proxy for species-level distinction. The 6-dc birds at 8 days (2 dpi) show a key differential OTU between *Campylobacter*-colonized birds on the control diet (*Campylobacter* treatment) versus *C. jejuni*-colonized birds on the GOS diet (GOS + *Campylobacter* treatment) had strong sequence similarity to *Escherichia coli* (OTU0001; 99.21%, **Supplementary Figure S2A**). OTU0001 did not discriminate the microbiota of the *Campylobacter*-challenged birds on the control diet (*Campylobacter* treatment) from the microbiota of mock-challenged birds on the GOS diet (**Supplementary Figure S2C**). In addition, previous analysis of the mock-challenged controls by our laboratory indicated that *Lactobacillus johnsonii* outcompetes *L. crispatus* in GOS-fed birds (Richards et al., 2019b). In the analysis presented here OTU0002 has strong sequence similarity with the *L. crispatus* strain (97.21%) and OTU0017 has a strong sequence similarity with *L. johnsoniii* (98.03%). In 6-dc birds at 8 days (2 dpi) both OTU0002 (*L. crispatus*) and OTU0017 (*L. johnsoniii*) are associated with dietary GOS (**Supplementary Figure S2B**). However, *L. johnsoniii* (OTU0017) continues to be associated with dietary GOS at: 15 days (9 dpi), 22 days (16 dpi) and 28 days (22 dpi). Whereas, *L. crispatus* (OTU0002) is later associated with the control diet at 15 days (9 dpi) and 35 days (29 dpi).

DISCUSSION

Concerns are growing regarding the over use of antimicrobials in animal production, and any concomitant increase in risk of antimicrobial resistance transferring to humans (Landers et al., 2012). These concerns have brought about calls for restricting antibiotic use in food producing animals (Tang et al., 2017). Although the European Union banned antimicrobial growth promoters since 2006, the practice continues in many countries and has prompted calls for a worldwide ban, particularly in the poultry and pig industries. It is becoming increasingly evident that improved on farm-performance at the expense of intestinal health and the zoonotic dissemination of antimicrobial resistance cannot continue (Awad et al., 2015, 2017; Smith et al., 2016). Under increasing economic pressure, the poultry industry is pursuing effective alternative methods to promote bird growth whilst controlling farm sources of antimicrobial resistance and zoonotic disease. Prebiotic feed additives such as GOS, a by-product of the dairy industry, have revealed potential growth-promoting effects in piglets (Alizadeh et al., 2016) and chickens (Richards et al., 2019b), whilst fructo-ologosaccharide (FOS) have been reported to reduce *Salmonella* colonization of chicks (Fukata et al., 1999). Here, we assess the impact of a GOS prebiotic on chickens colonized by *C. jejuni* at either 6 or 20 days with respect to their zootechnical performance, gut architecture and differences in intestinal cytokine and chemokine transcription (the experimental designs and corresponding data are summarized in **Figure 4**).

Two independent trials show significant differences in live bodyweights of *C. jejuni*-challenged birds, the birds fed GOS additive were significantly heavier at the typical market age of 35 days compared to a calorie-match control diet. GOS

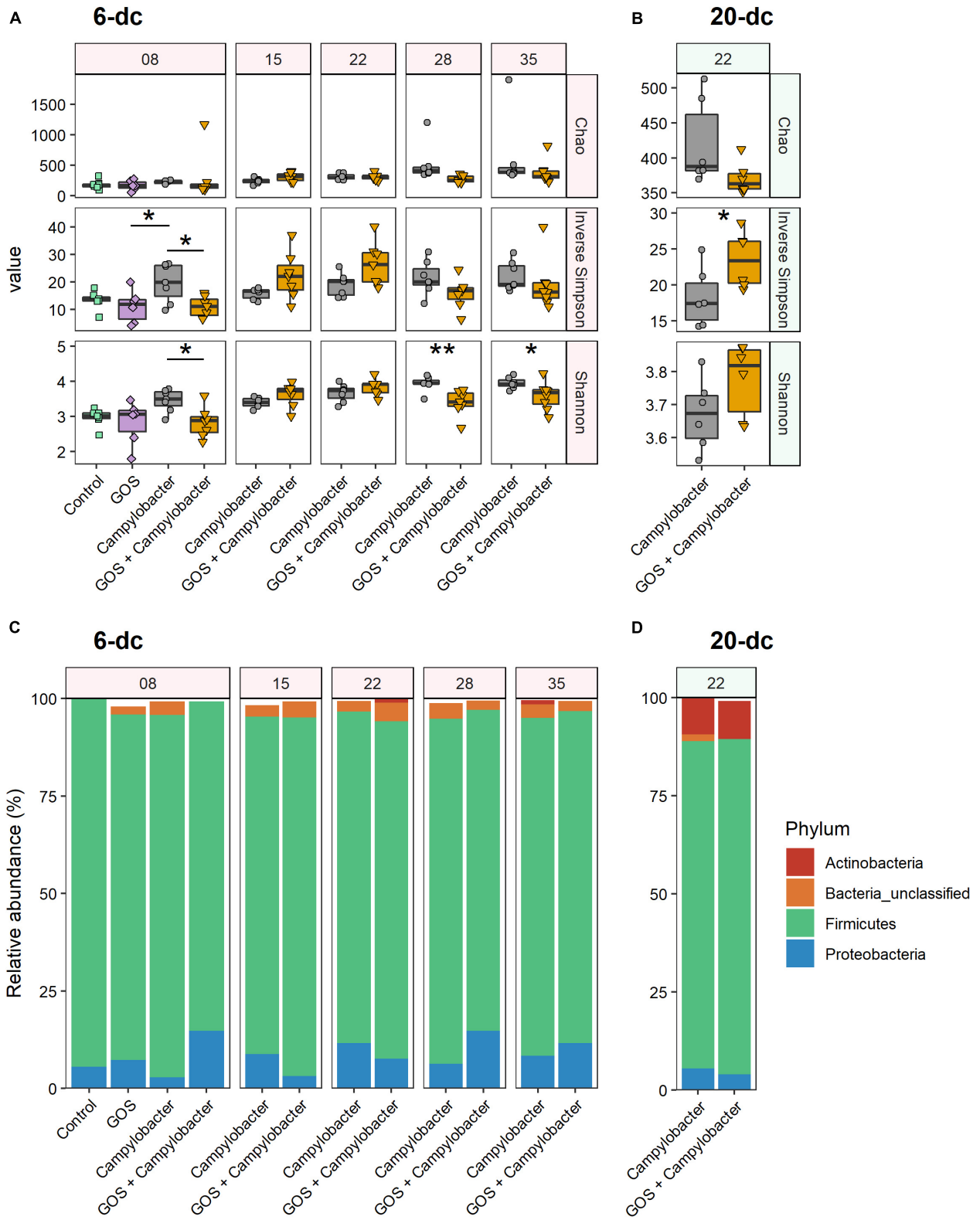

FIGURE 3 | Dietary GOS promotes differential shifts in the cecal microbiota post *Campylobacter* challenge. **(A,B)** Cecal α-diversity for 6-dc birds **(A)** and 20-dc birds **(B)** described as Chao richness, Inverse Simpson diversity and Shannon diversity (as indicated by panels on right hand side of the figure). The age of the birds are in days as indicated by the numerals in the strip at the top of the figure. Significant differences between groups are indicated by asterisks (*$p \leq 0.05$; **$p \leq 0.01$). **(C,D)** OTU relative abundance for 6-dc birds **(C)** and 20-dc birds **(D)** summarized at Phyla level.

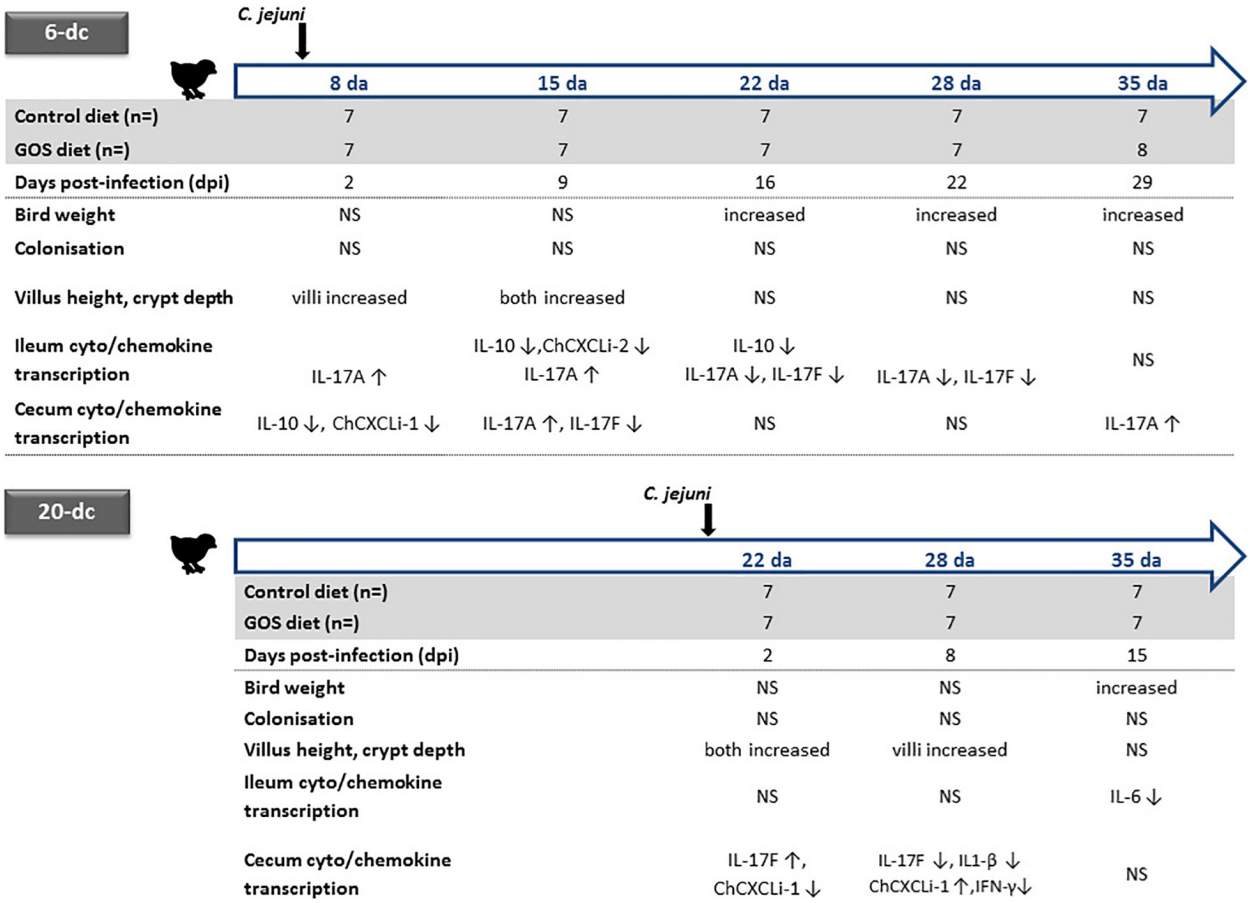

FIGURE 4 | Summary of age dependent differences for dietary GOS in *C. jejuni* colonized broiler chickens. Significant changes in the live weight, cecal *C. jejuni* colonization levels, ileal villus and crypt metrics are indicated for the GOS-fed birds compared to the birds on the control diet colonized at either 6 or 20 days of age (da) with *C. jejuni*. Relative changes in the transcription of ileal and cecal cytokines and chemokines for GOS-fed bird compared to controls are indicated for age matched birds by up arrows (↑) for increases and down arrows for decreases in cytokine/chemokine expression (↓). NS indicates no significant differences between the birds on the GOS or control diet.

supplementation improved the growth rate performance of *Campylobacter*-colonized broiler chickens irrespective of the timing of the challenge with *C. jejuni* at either 6 days or 20 days of age. However, dietary GOS inclusion did not prevent or reduce *C. jejuni* HPC5 colonization of broiler chickens GIT within the 35 days lifespan of the birds. *C. jejuni* HPC5 is a broiler chicken isolate that has been used routinely and reliably to colonize the intestinal tract of broiler chickens (Loc Carrillo et al., 2005; Scott et al., 2007; Connerton et al., 2018). In recent years several studies have employed 16S rRNA gene sequences to comprehensively document changes in the cecal microbiota that accompany *Campylobacter*-colonization of broilers. These studies have noted differences in the relative abundance of Bifidobacterium, Lactobacillaceae, Clostridium cluster XIVa and Mollicutes, with transient age related shifts in specific members of the Lachnospiraceae and Ruminococcaceae (Thibodeau et al., 2015, 2017; Connerton et al., 2018; Richards et al., 2019a). As an extension of the outputs from these studies it was recognized that transitions in the cecal microbiota were evident between 14 and 18 days that coincide with the reduced availability of maternal antibodies, and represent a window of opportunity for the entry for bacteria to bloom and new intestinal microbes to become established that can affect changes in gut health (Awad et al., 2016; Connerton et al., 2018; Ijaz et al., 2018). Early prebiotic diets offer the prospect of achieving a stable microbiota that can resist opportunist expansion or colonists. Prebiotic oligosaccharides have previously been reported to reduce the cecal *C. jejuni* colonization loads of broiler chickens, for example the use of a chicory fructan additive for 42 days in male Ross 308 birds (Yusrizal and Chen, 2003), or as the use of mannan-oligosaccharide (MOS) with male Cobb 500 birds at 34 days (Baurhoo et al., 2009). It is conceivable that improved broiler breeding programs and optimized diets will produce heavier birds faster, which will require fast-resolving methods that reduce or displace unwelcome gut bacteria.

Intestinal histomorphometric parameters are considered indicators of gut health whereby a healthy ileal mucosa should display long villi with high villus/crypt ratios. A transient increase

in villus length and crypt depth was observed over the first 2 weeks post-challenge for birds sustained on the GOS diet irrespective of the timing of *Campylobacter* challenge. Increases in the absorption surface provide a favorable environment for nutrient uptake leading to efficient feed utilization. Several studies have shown the beneficial effects of dietary additives on Ross 308 broiler chicken villus architecture and body weight gain during heat stress challenges such as prebiotic supplements (Silva et al., 2010), alpha-lipoic acid additive (Yoo et al., 2016), or probiotic mixtures (Song et al., 2014). Similarly, the data presented here suggests that nutrient absorption competence associated with the development of villi in the small intestine of birds fed the GOS diet, leads to an increase in body weight despite gut colonization by *C. jejuni*.

Intestinal mucosa constitutes a physical and immunological protective barrier for the integrity of the intestinal tract to prevent infection by pathogens and maintain an environment that can sustain a healthy and productive microbiota. However, the composition of the gut microbiota is under surveillance of the mucosal innate and adaptive immune systems (Kraehenbuhl and Neutra, 1992). Numerous immune cell populations such as regulatory T-cells (Treg), Th17 cells, IgA-secreting plasma cells, natural killer cells (NK), macrophages, dentritic cells (DCs), innate lymphoid cells (ILCs) contribute to host defense against infection with pathogenic microbes (Honda and Littman, 2012). Members of the IL-17 family of cytokines, IL-17A and IL-17F are produced by a subset of CD4 + T cells named Th17, and have more recently been associated in the gut with dendritic cells and group 3 innate lymphoid cells (ILC3) (Li S. et al., 2018). While they beneficially mediate resistance to extracellular bacterial and fungal infection via enhanced mucosal production of mucus and antimicrobial peptides, IL-17A and IL-17F are also involved in several autoimmune disorders (Bettelli et al., 2007; Yang et al., 2008; Ishigame et al., 2009).

Here, we demonstrate dietary GOS inclusion can maintain transcript levels of IL-17A and suppress IL-17F post colonization with *C. jejuni*. Previously we have shown *C. jejuni* challenge at 6 days triggered a transient increases in IL-17A and IL-17F in broiler chickens at 15 days (9 dpi) compared with non-colonized birds (Connerton et al., 2018), and more recently that dietary GOS increases the expression of IL-17A in juvenile birds up to 15 days (Richards et al., 2019b). In mice IL-17A expression has been proposed to benefit intestinal barrier function and IL-17F to weaken intestinal integrity, since IL-17A inhibition exacerbates induced colitis (Maxwell et al., 2015) and IL-17F suppression is protective (Tang et al., 2018). Evidence suggests the modulation of IL-17A is associated with the regulation of the tight junction formation and regulation of the mucosal barrier via activation of the ERK MAPK pathway (Awane et al., 1999; Cario et al., 2000; Kinugasa et al., 2000). *C. jejuni* colonization of the chicken intestine appears to result in the expression of both the IL-17 subtypes with opposing effects mediated at different times. The dominant response may in part explain why there are differences in the impact of *C. jejuni* colonization reported for different bacterial types on various broiler chicken breeds (Humphrey et al., 2014, 2015). An increase of IL-17A in response to dietary GOS in the presence or absence of *C. jejuni* colonization may well benefit intestinal health and contribute to the increased growth rate observed for GOS-fed birds. GOS does not prevent *C. jejuni* colonization but may also lead to performance improvements by suppression of IL-17F under circumstances when *C. jejuni* colonization has been reported to be associated with bird health and productivity (Bull et al., 2008). These current studies were conducted in clean controlled biosecure facilities such that the birds would not be subject to exposure to endemic viral, bacterial and protozoal pathogens that are frequently encountered by commercial broiler chickens. Under these circumstances the impact of prebiotic priming of intestinal innate immunity may be of greater importance in field applications.

Consistent with previous reports we observed GOS-driven changes in the cecal microbiota of chickens featuring specific operational taxonomic units identifiable as lactobacilli (Hughes et al., 2017; Azcarate-Peril et al., 2018). Colonization by *C. jejuni* did not prevent the differential increase in abundance of Otu0017 (*L. johnsoniii*) associated previously with dietary GOS (Richards et al., 2019b). At 2dpi for the 6-dc birds Otu0002 (*L. crispatus*) and Otu0017 (*L. johnsoniii*) showed increases in abundance in association with the GOS-diet. However, Otu0017 (*L. johnsoniii*) remained an abundant member of the GOS + *Campylobacter* treatment group over the course of the experiment, and in contrast the relative abundance of Otu0002 (*L. crispatus*) fell such that it exhibited significantly greater abundance at 9 and 29 dpi in the *Campylobacter* treatment group fed the control diet. These data are consistent with *L. johnsonii* outcompeting *L. crispatus* in GOS-fed birds, and consistent with the hypothesis that *L. johnsonii* contributes to the stability of the innate immune response observed in GOS-fed birds. *L. johnsonii* is an established probiotic species that has been reported to improve growth performance, intestinal development, and act as competitive exclusion agent against bacterial pathogens in broiler chickens (La Ragione et al., 2004; Wang et al., 2017).

IL-17A responses to probiotics have been reported for *ex vivo* Peyer's patch stimulated T cells derived from mice orally administered with lactic acid bacteria (*L. bulgaricus* or *Streptococcus thermophilus*). Over 7 days the stimulated T cells exhibited increases in the levels of IL-17 whilst IL-10 and Th2 IL-4 remained unchanged (Kamiya et al., 2016). In chickens transient IL-17 induction has been observed during the natural development the intestinal microbiota (Crhanova et al., 2011). In the absence of IL-22, pro-inflammatory Th17 induction did not result in intestinal damage but upon *Salmonella* Enteritidis challenge tissue damage was observed as a result of a Th17 response that features the cytokines IL-17 and IL-22.

CONCLUSION

In conclusion the data support the contention that GOS diet-induced microbiota shifts can: (1) Improve the growth rate

of broiler chickens independent of *C. jejuni* colonization. (2) Maintain ileal and cecal IL-17A transcription that can positively influence gut health in the presence of *C. jejuni*. (3) Suppress IL-17F expression arising as a consequence *C. jejuni* colonization that has the potential to impair gut integrity and health.

DATA AVAILABILITY STATEMENT

All 16S rDNA sequence data originally reported here is available at under accessions SRR10059315 to SRR10059356 in NCBI SRA study SRP133552. All other 16S rDNA sequences reported in this study are also available from NCBI SRA study SRP133552. Raw zootechnical and qPCR gene expression data is available from https://github.com/PJRichards/lafontaine_campy_gos.

ETHICS STATEMENT

Experiments involving the use of birds were subjected to approval process under National Guidelines by the United Kingdom Home Office. Work on this project was approved under United Kingdom Government Home Office Project Licensing ASPA 86. The project license has been reviewed and approved by the University Ethics Committee prior to submission to the Home Office, which includes the scrutiny of animal welfare, ethics and handling.

AUTHOR CONTRIBUTIONS

NF contributed to the study design. NF and IC conceived and designed the experiments. GF, PR, PC, PO'K, NG, NC, and IC performed the experiments. GF, PR, PC, and IC analyzed the data and wrote the manuscript. All authors approved the final manuscript for publication.

FUNDING

The authors acknowledge the support from Saputo Dairy UK.

ACKNOWLEDGMENTS

The authors thank Darren L. Smith at University of Northumbria, Newcastle upon Tyne, for NGS sequencing.

SUPPLEMENTARY MATERIAL

The Supplementary Material for this article can be found online at: https://www.frontiersin.org/articles/10.3389/fmicb.2019.03030/full#supplementary-material

FIGURE S1 | Rarefaction curves indicating sampling efficiency of cecal bacterial communities. Collectors curved were constructed for 16S rDNA sequences curated using mothur pipeline. Communities are presented by cohort as indicated by text in strip at the top of each panel. The colors indicate the rarefaction curves for individual bird in each cohort (key inset).

FIGURE S2 | GOS responsive OTUs in age-matched broilers. Discriminative OTUs were identified using LEfSE between 6-dc challenged birds: Treatments *Campylobacter* and GOS + *Campylobacter* **(A)**, 20-dc challenged birds: Treatments *Campylobacter* and GOS + *Campylobacter* **(B)**, and 6-dc *Campylobacter*-challenged and GOS mock-challenged control birds: Treatments *Campylobacter* and GOS **(C)**. Comparisons of OTU relative abundance were made between age-matched cohorts that were rarefied to include only OTU $\geq$ 10 reads. For clarity only OTU with $p < 0.05$ for the embedded Kruskal Wallis ANOVA test and LDA ($\log_{10}$) > 2 are reported (Mothur defaults).

REFERENCES

Alizadeh, A., Akbari, P., Difilippo, E., Schols, H. A., Ulfman, L. H., Schoterman, M. H. C., et al. (2016). The piglet as a model for studying dietary components in infant diets: effects of galacto-oligosaccharides on intestinal functions. *Br. J. Nutr.* 115, 605–618. doi: 10.1017/S0007114515004997

Andreoletti, O., Budka, H., Buncic, S., Collins, J. D., Griffin, J., Hald, T., et al. (2010). Scientific opinion on quantification of the risk posed by broiler meat to human campylobacteriosis in the EU. *EFSA J.* 8:1437. doi: 10.2903/j.efsa.2010.1437

Aviagen Performance Objectives (2014). *Ross 308 Broiler Performance Objectives.* Scotland, UK: Aviagen Limited Newbridge, Midlothian EH28 8SZ.

Awad, W. A., Hess, C., and Hess, M. (2017). Enteric pathogens and their toxin-induced disruption of the intestinal barrier through alteration of tight junctions in chickens. *Toxins* 9:E60. doi: 10.3390/toxins9020060

Awad, W. A., Mann, E., Dzieciol, M., Hess, C., Schmitz-Esser, S., Wagner, M., et al. (2016). Age-related differences in the luminal and mucosa-associated gut microbiome of broiler chickens and shifts associated with *Campylobacter jejuni* infection. *Front. Cell. Infect. Microbiol.* 6:154. doi: 10.3389/fcimb.2016.00154

Awad, W. A., Smorodchenko, A., Hess, C., Aschenbach, J. R., Molnár, A., Dublecz, K., et al. (2015). Increased intracellular calcium level and impaired nutrient absorption are important pathogenicity traits in the chicken intestinal epithelium during *Campylobacter jejuni* colonization. *Appl. Microbiol. Biotechnol.* 99, 6431–6441. doi: 10.1007/s00253-015-6543-z

Awane, M., Andres, P. G., Li, D. J., and Reinecker, H. C. (1999). NF-κB-inducing kinase is a common mediator of IL- 17-, TNF-α-, and IL- 1β-induced chemokine promoter activation in intestinal epithelial cells. *J. Immunol.* 162, 5337–5344.

Azcarate-Peril, M. A., Butz, N., Cadenas, M. B., Koci, M., Ballou, A., Mendoza, M., et al. (2018). An attenuated *Salmonella enterica* serovar Typhimurium strain and galactooligosaccharides accelerate clearance of *Salmonella* infections in poultry through modifications to the gut microbiome. *Appl. Environ. Microbiol.* 84, 2526–2543. doi: 10.1128/AEM.02526-17

Baurhoo, B., Ferket, P. R., and Zhao, X. (2009). Effects of diets containing different concentrations of mannanoligosaccharide or antibiotics on growth performance, intestinal development, cecal and litter microbial populations, and carcass parameters of broilers. *Poult. Sci.* 88, 2262–2272. doi: 10.3382/ps.2008-00562

Bettelli, E., Oukka, M., and Kuchroo, V. K. (2007). TH-17 cells in the circle of immunity and autoimmunity. *Nat. Immunol.* 8, 345–350. doi: 10.1038/ni0407-345

Broom, L. J., and Kogut, M. H. (2018). Inflammation: friend or foe for animal production? *Poult. Sci.* 97, 510–514. doi: 10.3382/ps/pex314

Bull, S. A., Thomas, A., Humphrey, T., Ellis-Iversen, J., Cook, A. J., Lovell, R., et al. (2008). Flock health indicators and *Campylobacter* spp. in commercial housed broilers reared in Great Britain. *Appl. Environ. Microbiol.* 74, 5408–5413. doi: 10.1128/AEM.00462-08

Caporaso, J. G., Lauber, C. L., Walters, W. A., Berg-Lyons, D., Lozupone, C. A., Turnbaugh, P. J., et al. (2011). Global patterns of 16S rRNA diversity at a depth of millions of sequences per sample. *Proc. Natl. Acad. Sci. U.S.A.* 108, 4516–4522. doi: 10.1073/pnas.1000080107

Cario, E., Rosenberg, I. M., Brandwein, S. L., Beck, P. L., Reinecker, H. C., and Podolsky, D. K. (2000). Lipopolysaccharide activates distinct signaling pathways in intestinal epithelial cell lines expressing Toll-like receptors. *J. Immunol.* 164, 966–972. doi: 10.4049/jimmunol.164.2.966

Clavijo, V., and Flórez, M. J. V. (2018). The gastrointestinal microbiome and its association with the control of pathogens in broiler chicken production: a review. *Poult. Sci.* 97, 1006–1021. doi: 10.3382/ps/pex359

Connerton, P. L., Richards, P. J., Lafontaine, G. M., O'Kane, P. M., Ghaffar, N., Cummings, N. J., et al. (2018). The effect of the timing of exposure to *Campylobacter jejuni* on the gut microbiome and inflammatory responses of broiler chickens. *Microbiome* 6:88. doi: 10.1186/s40168-018-0477-5

Crhanova, M., Hradecka, H., Faldynova, M., Matulova, M., Havlickova, H., Sisak, F., et al. (2011). Immune response of chicken gut to natural colonization by gut microflora and to *Salmonella enterica* serovar enteritidis infection. *Infect. Immun.* 79, 2755–2763. doi: 10.1128/IAI.01375-10

EFSA (2018). The European Union summary report on trends and sources of zoonoses, zoonotic agents and food-borne outbreaks in 2017. *EFSA J.* 16:5500. doi: 10.2903/j.efsa.2018.5500

Fukata, T., Sasai, K., Miyamoto, T., and Baba, E. (1999). Inhibitory effects of competitive exclusion and fructooligosaccharide, singly and in combination, on *Salmonella* colonization of chicks. *J. Food Prot.* 62, 229–233. doi: 10.4315/0362-028x-62.3.229

Gormley, F. J., Bailey, R. A., Watson, K. A., McAdam, J., Avendaño, S., Stanley, W. A., et al. (2014). *Campylobacter* colonization and proliferation in the broiler chicken upon natural field challenge is not affected by the bird growth rate or breed. *Appl. Environ. Microbiol.* 80, 6733–6738. doi: 10.1128/AEM.02162-14

Honda, K., and Littman, D. R. (2012). The microbiome in infectious disease and inflammation. *Annu. Rev. Immunol.* 30, 759–795. doi: 10.1146/annurev-immunol-020711-074937

Hughes, R. A., Ali, R. A., Mendoza, M. A., Hassan, H. M., and Koci, M. D. (2017). Impact of dietary galacto-oligosaccharide (GOS) on chicken's gut microbiota, mucosal gene expression, and *Salmonella* colonization. *Front. Vet. Sci.* 4:192. doi: 10.3389/fvets.2017.00192

Humphrey, S., Chaloner, G., Kemmett, K., Davidson, N., Williams, N., Kipar, A., et al. (2014). *Campylobacter jejuni* is not merely a commensal in commercial broiler chickens and affects bird welfare. *mBio* 5:e01364-14. doi: 10.1128/mBio.01364-14

Humphrey, S., Lacharme-Lora, L., Chaloner, G., Gibbs, K., Humphrey, T., Williams, N., et al. (2015). Heterogeneity in the infection biology of *Campylobacter jejuni* isolates in three infection models reveals an invasive and virulent phenotype in a ST21 isolate from poultry. *PLoS One* 10:e0141182. doi: 10.1371/journal.pone.0141182

Ijaz, U. Z., Sivaloganathan, L., McKenna, A., Richmond, A., Kelly, C., Linton, M., et al. (2018). Comprehensive longitudinal microbiome analysis of the chicken cecum reveals a shift from competitive to environmental drivers and a window of opportunity for *Campylobacter*. *Front. Microbiol.* 9:2452. doi: 10.3389/fmicb.2018.02452

Ishigame, H., Kakuta, S., Nagai, T., Kadoki, M., Nambu, A., Komiyama, Y., et al. (2009). Differential roles of interleukin-17A and -17F in host defense against mucoepithelial bacterial infection and allergic responses. *Immunity* 30, 108–119. doi: 10.1016/j.immuni.2008.11.009

Jung, S. J., Houde, R., Baurhoo, B., Zhao, X., and Lee, B. H. (2008). Effects of galacto-oligosaccharides and a *Bifidobacteria lactis*-based probiotic strain on the growth performance and fecal microflora of broiler chickens. *Poult. Sci.* 87, 1694–1699. doi: 10.3382/ps.2007-00489

Kaakoush, N. O., Castaño-Rodríguez, N., Mitchell, H. M., and Man, S. M. (2015). Global epidemiology of *Campylobacter* infection. *Clin. Microbiol. Rev.* 28, 687–720. doi: 10.1128/CMR.00006-15

Kaiser, P., Underwood, G., and Davison, F. (2003). Differential cytokine responses following Marek's disease virus infection of chickens differing in resistance to Marek's disease. *J. Virol.* 77, 762–768. doi: 10.1128/jvi.77.1.762-768.2003

Kamiya, T., Watanabe, Y., Makino, S., Kano, H., and Tsuji, N. (2016). Improvement of intestinal immune cell function by lactic acid bacteria for dairy products. *Microorganisms* 5:E1. doi: 10.3390/microorganisms5010001

Kinugasa, T., Sakaguchi, T., Gu, X., and Reinecker, H. (2000). Claudins regulate the intestinal barrier in response to immune mediators. *Gastroenterology* 118, 1001–1011. doi: 10.1016/S0016-5085(00)70351-9

Kogut, M. H. (2009). Impact of nutrition on the innate immune response to infection in poultry. *J. Appl. Poult. Res.* 18, 111–124. doi: 10.3382/japr.2008-00081

Kogut, M. H., Genovese, K. J., Swaggerty, C. L., He, H., and Broom, L. (2018). Inflammatory phenotypes in the intestine of poultry: not all inflammation is created equal. *Poult. Sci.* 97, 2339–2346. doi: 10.3382/ps/pey087

Kozich, J. J., Westcott, S. L., Baxter, N. T., Highlander, S. K., and Schloss, P. D. (2013). Development of a dual-index sequencing strategy and curation pipeline for analyzing amplicon sequence data on the MiSeq Illumina sequencing platform. *Appl. Environ. Microbiol.* 79, 5112–5120. doi: 10.1128/AEM.01043-13

Kraehenbuhl, J.-P., and Neutra, M. R. (1992). Molecular and cellular basis of immune protection of mucosal surfaces. *Physiol. Rev.* 72, 853–879. doi: 10.1152/physrev.1992.72.4.853

La Ragione, R. M., Narbad, A., Gasson, M. J., and Woodward, M. J. (2004). *In vivo* characterization of *Lactobacillus johnsonii* FI9785 for use as a defined competitive exclusion agent against bacterial pathogens in poultry. *Lett. Appl. Microbiol.* 38, 197–205. doi: 10.1111/j.1472-765X.2004.01474.x

Landers, T. F., Cohen, B., Wittum, T. E., and Larson, E. L. (2012). A review of antibiotic use in food animals: perspective, policy, and potential. *Public Health Rep.* 127, 4–22. doi: 10.1177/003335491212700103

Li, L., Pielsticker, C., Han, Z., Kubasová, T., Rychlik, I., Kaspers, B., et al. (2018). Infectious bursal disease virus inoculation infection modifies *Campylobacter jejuni*-host interaction in broilers. *Gut Pathog.* 10:13. doi: 10.1186/s13099-018-0241-1

Li, S., Bostick, J. W., and Zhou, L. (2018). Regulation of innate lymphoid cells by aryl hydrocarbon receptor. *Front. Immunol.* 8:1909. doi: 10.3389/fimmu.2017.01909

Livak, K. J., and Schmittgen, T. D. (2001). Analysis of relative gene expression data using real-time quantitative PCR and the 2-ΔΔCT method. *Methods* 25, 402–408. doi: 10.1006/meth.2001.1262

Loc Carrillo, C., Atterbury, R. J., El-Shibiny, A., Connerton, P. L., Dillon, E., Scott, A., et al. (2005). Bacteriophage therapy to reduce *Campylobacter jejuni* colonization of broiler chickens. *Appl. Environ. Microbiol.* 71, 6554–6563. doi: 10.1128/AEM.71.11.6554-6563.2005

Maxwell, J. R., Zhang, Y., Brown, W. A., Smith, C. L., Byrne, F. R., Fiorino, M., et al. (2015). Differential roles for interleukin-23 and interleukin-17 in intestinal immunoregulation. *Immunity* 43, 739–750. doi: 10.1016/j.immuni.2015.08.019

Miles, A. A., Misra, S. S., and Irwin, J. O. (1938). The estimation of the bactericidal power of the blood. *J. Hyg.* 38, 732–749. doi: 10.1017/S002217240001158X

Nang, N., Lee, J., Song, B., Kang, Y., Kim, H., and Seo, S. (2011). Induction of inflammatory cytokines and toll-like receptors in chickens infected with avian H9N2 influenza virus. *Vet. Res.* 42:64. doi: 10.1186/1297-9716-42-64

Newell, D. G., Elvers, K. T., Dopfer, D., Hansson, I., Jones, P., James, S., et al. (2011). Biosecurity-based interventions and strategies to reduce *Campylobacter* spp. on poultry farms. *Appl. Environ. Microbiol.* 77, 8605–8614. doi: 10.1128/AEM.01090-10

Osimani, A., Aquilanti, L., Pasquini, M., and Clementi, F. (2017). Prevalence and risk factors for thermotolerant species of *Campylobacter* in poultry meat at retail in Europe. *Poult. Sci.* 96, 3382–3391. doi: 10.3382/ps/pex143

Pedroso, A. A., Hurley-Bacon, A. L., Zedek, A. S., Kwan, T. W., Jordan, A. P. O., Avellaneda, G., et al. (2013). Can probiotics improve the environmental microbiome and resistome of commercial poultry production? *Int. J. Environ. Res. Public Health* 10, 4534–4559. doi: 10.3390/ijerph10104534

Pourabedin, M., and Zhao, X. (2015). Prebiotics and gut microbiota in chickens. *FEMS Microbiol. Lett.* 362:fnv122. doi: 10.1093/femsle/fnv122

R Core Team (2019). *R: a Language and Environment for Statistical Computing*. Available at: https://www.r-project.org (accessed July 5, 2019).

Rasoli, M., Yeap, S. K., Tan, S. W., Roohani, K., Kristeen-Teo, Y. W., Alitheen, N. B., et al. (2015). Differential modulation of immune response and cytokine profiles in the bursae and spleen of chickens infected with very virulent infectious bursal disease virus. *BMC Vet. Res.* 11:75. doi: 10.1186/s12917-015-0377-x

Ravel, A., Hurst, M., Petrica, N., David, J., Mutschall, S. K., Pintar, K., et al. (2017). Source attribution of human campylobacteriosis at the point of exposure by combining comparative exposure assessment and subtype comparison based on comparative genomic fingerprinting. *PLoS One* 12:e0183790. doi: 10.1371/journal.pone.0183790

Reid, W. D. K., Close, A. J., Humphrey, S., Chaloner, G., Lacharme-Lora, L., Rothwell, L., et al. (2016). Cytokine responses in birds challenged with the

human food-borne pathogen *Campylobacter jejuni* implies a Th17 response. *R. Soc. Open Sci.* 3:150541. doi: 10.1098/rsos.150541

Richards, P. J., Connerton, P. L., and Connerton, I. F. (2019a). Phage biocontrol of *Campylobacter jejuni* in chickens does not produce collateral effects on the gut microbiota. *Front. Microbiol.* 10:476. doi: 10.3389/fmicb.2019.00476

Richards, P. J., Flaujac Lafontaine, G. M., Connerton, P. L., Liang, L., Asiani, K., Fish, N. M., et al. (2019b). Galacto-oligosaccharides modulate the juvenile gut microbiome and innate immunity to improve broiler chicken performance. *bioRxiv[Preprint]* doi: 10.1101/631259

Rosenquist, H., Nielsen, N. L., Sommer, H. M., Nørrung, B., and Christensen, B. B. (2003). Quantitative risk assessment of human campylobacteriosis associated with thermophilic *Campylobacter* species in chickens. *Int. J. Food Microbiol.* 83, 87–103. doi: 10.1016/S0168-1605(02)00317-3

RStudio Team (2015). *RStudio: Integrated Development for R*. Boston, MA: RStudio, Inc.

Rubio, L. A. (2019). Possibilities of early life programming in broiler chickens via intestinal microbiota modulation. *Poult. Sci.* 98, 695–706. doi: 10.3382/ps/pey416

Sahin, O., Kassem, I. I., Shen, Z., Lin, J., Rajashekara, G., and Zhang, Q. (2015). *Campylobacter* in poultry: ecology and potential interventions. *Avian Dis.* 59, 185–200. doi: 10.1637/11072-032315-review

Schloss, P. D., Westcott, S. L., Ryabin, T., Hall, J. R., Hartmann, M., Hollister, E. B., et al. (2009). Introducing mothur: open-source, platform-independent, community-supported software for describing and comparing microbial communities. *Appl. Environ. Microbiol.* 75, 7537–7541. doi: 10.1128/AEM.01541-09

Scott, A. E., Timms, A. R., Connerton, P. L., Carrillo, C. L., Radzum, K. A., and Connerton, I. F. (2007). Genome dynamics of *Campylobacter jejuni* in response to bacteriophage predation. *PLoS Pathog.* 3:e119. doi: 10.1371/journal.ppat.0030119

Segata, N., Izard, J., Waldron, L., Gevers, D., Miropolsky, L., Garrett, W. S., et al. (2011). Metagenomic biomarker discovery and explanation. *Genome Biol.* 12:R60. doi: 10.1186/gb-2011-12-6-r60

Shaw, L. M., Blanchard, A., Chen, Q., An, X., Davies, P., Tötemeyer, S., et al. (2019). DirtyGenes: testing for significant changes in gene or bacterial population compositions from a small number of samples. *Sci. Rep.* 9:2373. doi: 10.1038/s41598-019-38873-4

Silva, V. K., da Silva, J. D. T., Gravena, R. A., Marques, R. H., Hada, F. H., and de Moraes, V. M. B. (2010). Yeast extract and prebiotic in pre-initial phase diet for broiler chickens raised under different temperatures. *Rev. Bras. Zootec.* 39, 165–174. doi: 10.1590/S1516-35982010000100022

Smith, S., Messam, L. L. M., Meade, J., Gibbons, J., McGill, K., Bolton, D., et al. (2016). The impact of biosecurity and partial depopulation on *Campylobacter* prevalence in Irish broiler flocks with differing levels of hygiene and economic performance. *Infect. Ecol. Epidemiol.* 6:31454. doi: 10.3402/iee.v6.31454

Song, J., Xiao, K., Ke, Y. L., Jiao, L. F., Hu, C. H., Diao, Q. Y., et al. (2014). Effect of a probiotic mixture on intestinal microflora, morphology, and barrier integrity of broilers subjected to heat stress. *Poult. Sci.* 93, 581–588. doi: 10.3382/ps.2013-03455

Speksnijder, D. C., Mevius, D. J., Bruschke, C. J., and Wagenaar, J. A. (2015). Reduction of veterinary antimicrobial use in the Netherlands. The Dutch Success Model. *Zoonoses Public Health* 62, 79–87. doi: 10.1111/zph.12167

Swaggerty, C., Callaway, T., Kogut, M., Piva, A., and Grilli, E. (2019). Modulation of the immune response to improve health and reduce foodborne pathogens in poultry. *Microorganisms* 7:65. doi: 10.3390/microorganisms7030065

Tang, C., Kakuta, S., Shimizu, K., Kadoki, M., Kamiya, T., Shimazu, T., et al. (2018). Suppression of IL-17F, but not of IL-17A, provides protection against colitis by inducing Treg cells through modification of the intestinal microbiota. *Nat. Immunol.* 19, 755–765. doi: 10.1038/s41590-018-0134-y

Tang, K. L., Caffrey, N. P., Nóbrega, D. B., Cork, S. C., Ronksley, P. E., Barkema, H. W., et al. (2017). Restricting the use of antibiotics in food-producing animals and its associations with antibiotic resistance in food-producing animals and human beings: a systematic review and meta-analysis. *Lancet Planet. Health* 1, e316–e327. doi: 10.1016/S2542-5196(17)30141-9

Thibodeau, A., Fravalo, P., Yergeau, É, Arsenault, J., Lahaye, L., and Letellier, A. (2015). Chicken caecal microbiome modifications induced by *Campylobacter jejuni* colonization and by a non-antibiotic feed additive. *PLoS One* 10:e0131978. doi: 10.1371/journal.pone.0131978

Thibodeau, A., Letellier, A., Yergeau, É, Larrivière-Gauthier, G., and Fravalo, P. (2017). Lack of evidence that selenium-yeast improves chicken health and modulates the caecal microbiota in the context of colonization by *Campylobacter jejuni*. *Front. Microbiol.* 8:451. doi: 10.3389/fmicb.2017.00451

Tian, S., Wang, J., Yu, H., Wang, J., and Zhu, W. (2019). Changes in ileal microbial composition and microbial metabolism by an early-life galacto-oligosaccharides intervention in a neonatal porcine model. *Nutrients* 11:1753. doi: 10.3390/nu11081753

Van Bueren, A. L., Mulder, M., Van Leeuwen, S., and Dijkhuizen, L. (2017). Prebiotic galactooligosaccharides activate mucin and pectic galactan utilization pathways in the human gut symbiont *Bacteroides thetaiotaomicron*. *Sci. Rep.* 7:40478. doi: 10.1038/srep40478

Van Immerseel, F., Eeckhaut, V., Moore, R. J., Choct, M., and Ducatelle, R. (2017). Beneficial microbial signals from alternative feed ingredients: a way to improve sustainability of broiler production? *Microb. sBiotechnol.* 10, 1008–1011. doi: 10.1111/1751-7915.12794

Walliser, I., and Göbel, T. W. (2018). Chicken IL-17A is expressed in αβ and γδ T cell subsets and binds to a receptor present on macrophages, and T cells. *Dev. Comp. Immunol.* 81, 44–53. doi: 10.1016/j.dci.2017.11.004

Wang, H., Ni, X., Qing, X., Zeng, D., Luo, M., Liu, L., et al. (2017). Live probiotic *Lactobacillus johnsonii* BS15 promotes growth performance and lowers fat deposition by improving lipid metabolism, intestinal development, and gut microflora in broilers. *Front. Microbiol.* 8:1073. doi: 10.3389/fmicb.2017.01073

Yang, X. O., Chang, S. H., Park, H., Nurieva, R., Shah, B., Acero, L., et al. (2008). Regulation of inflammatory responses by IL-17F. *J. Exp. Med.* 205, 1063–1075. doi: 10.1084/jem.20071978

Yoo, J., Yi, Y. J., Koo, B., Jung, S., Yoon, J. U., Kang, H. B., et al. (2016). Growth performance, intestinal morphology, and meat quality in relation to alpha-lipoic acid associated with vitamin C and E in broiler chickens under tropical conditions. *Rev. Bras. Zootec.* 45, 113–120. doi: 10.1590/S1806-92902016000300005

Yusrizal, and Chen, T. C. (2003). Effect of adding chicory fructans in feed on fecal and intestinal microflora and excreta volatile ammonia. *Int. J. Poult. Sci.* 2, 188–194. doi: 10.3923/ijps.2003.188.194

Conflict of Interest: NF is employed by Dairy Crest Ltd.

The remaining authors declare that the research was conducted in the absence of any conflict of interest.

The authors declare that this study received funding from Saputo Dairy UK. The funder had the following involvement with the study: NF contributed to the study design.

frontiers in Veterinary Science

ORIGINAL RESEARCH
published: 15 January 2020
doi: 10.3389/fvets.2019.00505

Campylobacter hepaticus, the Cause of Spotty Liver Disease in Chickens: Transmission and Routes of Infection

Canh Phung[1], Ben Vezina[1], Arif Anwar[2], Timothy Wilson[2], Peter C. Scott[2], Robert J. Moore[1] and Thi Thu Hao Van[1]*

[1] School of Science, RMIT University, Bundoora West Campus, Bundoora, VIC, Australia, [2] Scolexia Pty Ltd., Moonee Ponds, VIC, Australia

The epidemiology of Spotty Liver Disease (SLD) was investigated by assaying 1,840 samples collected from layer chickens and the environment in poultry farms across Australia for the presence of *Campylobacter hepaticus*, the agent responsible SLD in chickens. A *C. hepaticus* specific PCR and bacterial culture were used. Results showed that birds could be infected with *C. hepaticus* up to 8 weeks before clinical SLD was manifested. In addition, birds could be infected long before laying starts, as young as 12 weeks old, but the peak period for SLD outbreaks was when the birds were 26–27 weeks old. *Campylobacter hepaticus* DNA was detected in motile organisms such as wild birds and rats and so these organisms may be vectors for *C. hepaticus* dissemination. Moreover, water, soil, mites, flies, and dust samples from SLD infected farms were also found to be PCR-positive for *C. hepaticus* DNA. However, it still remains to be determined whether these environmental sources carry any viable *C. hepaticus*. The indications from this study are that environmental sources are a likely transmission source of *C. hepaticus*. Therefore, biosecurity practices need to be strictly followed to prevent the spread of SLD amongst and between flocks. Also, a rapid, molecular detection method such as PCR should be used as to monitor for *C. hepaticus* presence in flocks before clinical disease is apparent, and therefore inform the use of biosecurity and therapeutic measures to help prevent SLD outbreaks.

Keywords: *Campylobacter hepaticus*, chicken, environment, epidemiology, spotty liver disease, transmission

OPEN ACCESS

Edited by:
Ozan Gundogdu, University of London, United Kingdom

Reviewed by:
Shaun Cawthraw, Animal and Plant Health Agency, United Kingdom
Abdi Elmi, University of London, United Kingdom

****Correspondence:***
Robert J. Moore
rob.moore@rmit.edu.au

Specialty section:
This article was submitted to Veterinary Infectious Diseases, a section of the journal Frontiers in Veterinary Science

Received: *01 November 2019*
Accepted: *20 December 2019*
Published: *15 January 2020*

Citation:
Phung C, Vezina B, Anwar A, Wilson T, Scott PC, Moore RJ and Van TTH (2020) Campylobacter hepaticus, the Cause of Spotty Liver Disease in Chickens: Transmission and Routes of Infection. Front. Vet. Sci. 6:505. doi: 10.3389/fvets.2019.00505

INTRODUCTION

Spotty Liver Disease (SLD) has been a persistent problem in the Australian and UK poultry industries for several decades and its presence in North America has recently been confirmed (1–3). In Australia, SLD was first noted in the 1980s (4, 5) and now the disease is regarded as one of the most important disease challenges for the Australian egg industry (6). Affected flocks can have an acute reduction in egg production of up to 25%, and an increase in mortality of up to 10% (1, 2). SLD outbreaks most commonly occur when the birds are reaching the peak of lay and the outbreaks can happen all year round (1, 4). The disease is particularly prevalent in free-ranging flocks but sporadically occurs in other housing systems such as conventional cages, controlled environmental cages, and barn systems (4).

Although SLD has been recognized for many years, perhaps as early as 1954 in the USA (7), the etiology of the disease was only determined recently, when a novel *Campylobacter* was isolated

from infected birds in 2015 in England (8). Then, the same species was independently isolated in Australia from SLD affected birds and it was characterized and formally named as *Campylobacter hepaticus* in 2016 (9). SLD was induced by experimental exposure of egg-laying chickens to *C. hepaticus* and the bacteria was recovered from the birds; thus addressing Koch's postulates to formally demonstrate its role in the pathogenicity of SLD (10).

Campylobacter hepaticus is a Gram-negative, S-shaped bacterium, grows under microaerobic conditions at 37° and 42°C, and has single bipolar flagella. *Campylobacter hepaticus* ranges in size from 0.3 to 0.4 μm wide and 1.0–1.2 μm long (3, 8, 9). *Campylobacter hepaticus* has a reduced genome size (1.48–1.51 Mb) and a lower G+C content (27.9–28.5%) than most *Campylobacter* species (11, 12). *Campylobacter hepaticus* grows slowly *in vitro*; requiring at least 3 days for visible colonies to form on blood agar (3, 8). Isolation of *C. hepaticus* from primary sources is difficult because of the faster growth of other microorganisms and the absence of a fully selective media (3, 9). To date, all *C. hepaticus* isolates reported in the literature have been recovered from bile or liver samples, in which *C. hepaticus* is often present as a monoculture. Although *C. hepaticus* is present throughout the gastrointestinal tract of infected birds (13), no isolates have been recovered from such microbiological complex samples.

As *C. hepaticus* has only recently been identified, vaccines are yet to be developed to help to reduce the impact of SLD. Furthermore, laboratory studies attempting to control SLD using feed additives showed no reduction in disease. However, in field studies, both the incidence and the severity of SLD outbreaks can be reduced by the inclusion of some feed additives, particularly a combination of oregano and sanguinarine feed additives (14). There have been no published studies regarding the epidemiology of the bacterium and how it is transmitted between and within chicken flocks. Studies on closely related species commonly isolated from poultry, *Campylobacter jejuni* and *Campylobacter coli*, have shown the presence of these bacteria in multiple sources besides poultry (15–17), including, wild birds (18, 19), cattle (20), pigs (21), dogs (22), flies (23, 24), darkling beetles (25), water (26), and soils (27).

This study aimed to determine possible transmission routes of *C. hepaticus* in layer farms by investigating the presence of the bacterium in the birds and environmental samples, and by investigating the spread of infection within flocks. By defining potential sources of *C. hepaticus* and understanding the dynamics of spread to and within a flock, appropriate biosecurity measures can be designed to minimize transmission to and within flocks.

A large collection of fecal swabs, caecum, and bile samples were collected from pullets during rearing and from hens in production. A variety of environmental samples were also collected on farms, including soil, water, dust, wild bird feces, rats, mice, and insects. A selection of *C. hepaticus* isolates recovered from bile samples were subjected to whole genome sequencing to examine the conservation or divergence of *C. hepaticus* genomes in different outbreaks.

MATERIALS AND METHODS

Study Design and Sample Collection

A total of 1,076 chicken and environmental samples were collected at 2–4 week intervals from three layer farms in Victoria and a further 764 chicken and environmental samples were collected from other chicken farms across Australia. For the three main study farms, the bird samples and environmental samples were collected when birds were transferred from rearing farm (16 weeks old) until peak laying period (26–30 weeks old). For samples from other farms across Australia, samples were collected from chickens across all ages, with or without clinical signs of SLD. All samples were transferred to the laboratory in insulated boxes with ice packs.

Samples were subjected to *C. hepaticus* specific PCR (SLD-PCR) and bacterial isolation to detect the presence of *C. hepaticus* in the samples. Genome sequencing and comparative genomic analysis were performed to examine the similarity of *C. hepaticus* isolates recovered from different farms.

DNA Extraction

DNA from all samples was prepared using the DNeasy PowerSoil Kit (Qiagen) according to the manufacturer's instructions. DNA from fecal swabs and bile samples were prepared by either boiling of sample resuspended in water and direct use of the supernatant or DNeasy PowerSoil Kit as described previously (28). For each batch of DNA extractions cultured *C. hepaticus* cells were used as a positive control and water as a negative control.

Polymerase Chain Reaction (PCR)

Isolated DNA was subjected to PCR amplification to detect the presence of *C. hepaticus* DNA. PCR primers specific to *C. hepaticus* were used as previously described by Van et al. (13). The PCR assay has been shown to be species-specific for *C. hepaticus,* with the limit of detection of the assay $10^{0.9}$ (7.9) CFU/reaction.

Isolation of *C. hepaticus*

To isolate *C. hepaticus*, bile samples were directly streaked onto horse blood agar (HBA) plates [Brucella broth (BBL) supplemented with 1.5% agar (BBL) and 5% defibrinated horse blood (Equicell)], as described previously (9). A combination of filter membrane and *Campylobacter* selective media approaches (called the motile-filter method in this paper) were used for the isolation of *C. hepaticus* from fecal, caecal, and soil samples. Fifty milligrams of samples were resuspended in 200 μl sterile Milli-Q water and 50 μl of the mix was spotted onto 0.65 μm cellulose acetate filter membranes (Sartorius Stedim Biotech) and placed on the surface of HBA plates supplemented with *Campylobacter* selective supplement (Skirrow, Oxoid) (HBAS) and left for 30 min. The filter was then removed and the plate incubated. Motile organisms, including *C. hepaticus*, can move through the membrane whereas non-motile organisms are trapped on top and removed with the filter. Isolation of *C. hepaticus* from environmental samples was attempted by suspension of samples in Brucella broth (10 times dilution) and direct plating onto HBAS plates as well as using the motile-filter method. All plates were incubated at 37°C for 3–5 days

under microaerobic conditions using CampyGen 3.5L (Oxoid, CN0035A) in an anaerobic jar.

MALDI-TOF MS to Identify Bacterial Species

The identity of *C. hepaticus*–like colonies was confirmed by matrix assisted laser desorption/ionization time of flight mass spectrometry (MALDI-TOF MS) using a Microflex LT mass spectrometer (Bruker MALDI Biotyper System, Bruker Daltonics) according to the manufacturer's instructions.

Whole-Genome Sequencing and Genomic Analysis

Campylobacter hepaticus isolates obtained from this study were subjected to whole-genome sequencing. DNA of *C. hepaticus* was extracted using an Isolate II Genomic DNA Kit (Bioline). The Nextera XT DNA Library Preparation Kit (Illumina) was used for genomic library construction and purified libraries were sequenced using Illumina MiSeq with 2 × 300 bp paired-end reads. Sequences were assembled using the A5 MiSeq pipeline (29) then annotated using RAST (http://rast.nmpdr.org/). Genome comparisons against the existing database of *C. hepaticus* sequences were performed using OrthoANI: https://www.ezbiocloud.net/tools/ani (ANI) and the Basic Local Alignment Search Tool (BLAST, https://blast.ncbi.nlm.nih.gov/Blast.cgi). Contigs with suspected plasmid elements and genes were Blasted against the NCBI database. Significant matches were identified with >98% coverage and identity to previously characterized plasmids from other *Campylobacter* species.

RESULTS

Prevalence of *C. hepaticus* in Three Farms Monitored Over Time

In the three study farms from which samples were collected over time, a total of 1,076 chicken and environmental samples were analyzed (**Table 1**).

On Farm 1, 432 chicken samples including fecal swabs, caecal content, bile, and 48 environmental samples were collected. No clinical signs of SLD and no *C. hepaticus* were detected during the 10-week period investigated in bird samples. However, one soil sample contained *C. hepaticus* DNA. Egg production and the mortality rate on this farm were normal. Egg production ranged between 92 and 94% from weeks 24 to 30.

On Farm 2, 335 chicken samples and 11 environmental samples were collected. No *C. hepaticus* was detected in samples taken at the time of transfer of the pullets from the rearing farm or in the first 4 weeks on the production farm (17, 19, and 22 weeks of age). However, at 26 weeks clinical signs of SLD were observed and confirmed on autopsy. Several samples from the layers began to register as *C. hepaticus* positive by PCR. At that time *C. hepaticus* was also detected by PCR in dust collected from the shed (2/2) and *C. hepaticus* was isolated from bile samples from birds with typical SLD lesions in their livers. However, the proportion of birds in which *C. hepaticus* could be detected in fecal swabs was low, with only 4 out of 53 samples *C. hepaticus*-PCR positive (**Table 1**). At the next collection times the proportion of PCR positive birds increased. At 27 weeks 12/50 and at 30 weeks 14/50 fecal swab samples were *C. hepaticus*-PCR positive. All environmental samples collected at 30 weeks on this farm, including wild bird feces, dust, rat feces and water were also PCR-positive for *C. hepaticus*. Egg production on this farm dropped from 93.4% at week 24 to 90.4% at week 26. After the low of egg production at week 26 it recovered to 93.7% by week 31. Mortalities peaked at week 26.

On farm 3, 240 chicken samples and 10 environmental samples were collected. All samples were PCR negative for *C. hepaticus* at 18 and 21 weeks old (the first two collection points). At the third collection point, when chickens were 24 weeks old, *C. hepaticus* was detected by PCR in 3/50 fecal swab samples, 1/3 bile samples and 1/1 dust samples, however, no clinical signs of SLD in chickens were observed. Two weeks later, when the birds were 26 weeks old, an SLD outbreak occurred on Farm 3 and *C. hepaticus* was detected by PCR in 23/50 cloacal swab samples, 2/2 bile samples, 1/1 rat fecal sample and 1/1 dust sample. Collected beetles and flies were negative for *C. hepaticus* in all three study farms (0/15). Egg production on this farm fell from 92.1% at week 24 to 87% at week 27 and unlike in Farm 2 egg production did not recover to 90% or above from week 30 onwards. Mortalities peaked at week 25.

Campylobacter hepaticus was isolated by culture from most of the bile samples from the birds with clear clinical signs of SLD. Failure to isolate was usually due to growth of other fast growing bacterial contaminants present in samples, which out-grew the slow-growing *C. hepaticus*. No *C. hepaticus* was cultured from any of the environmental samples.

Prevalence of *C. hepaticus* in Various Farms Across Australia

In addition to the temporal study of *C. hepaticus* occurrence on three farms, samples were also taken on an *ad hoc* basis from other farms in Australia over a period of 1 year, collected by collaborating veterinarians during their routine farm visits. Samples were collected from birds in farms with and without SLD outbreaks.

A total of 710 chicken samples and 54 environmental samples were collected. *C. hepaticus* was detected in chicken samples and environmental samples (**Table 2**). No *C. hepaticus* was found in 1- or 2-week-old chickens but the bacterium was present in some pullets at 12, 17, and 18 weeks-old without any clinical signs of SLD. In one farm where *C. hepaticus* was detected in cloacal swabs by PCR at 18 weeks old, *C. hepaticus* was also found not only in cloacal swab samples but also in environmental samples including water, flies and rat feces. Eight weeks later, at 26 weeks old, an SLD outbreak occurred on this farm and *C. hepaticus* was again detected in environmental samples (mites and flies). *C. hepaticus* was found in some wild bird feces, rat feces and soil samples from these *ad hoc* samples. These types of environmental sources were also found to be positive for *C. hepaticus* in the main study farms in Victoria (**Table 1**). SLD outbreaks were mostly observed in laying hen when they were in peak production.

TABLE 1 | The presence of *Campylobacter hepaticus* in three farms monitored over time.

Sample type	No. samples	*Campylobacter hepaticus* positive							SLD status
		PCR (positive/total)						Culture	
FARM 1									
Age (weeks)		18	20	22	24	26	28		No *Campylobacter hepaticus* found during 10 weeks of study on Farm 1
Fecal swabs	348	0/95	0/47	0/57	0/50	0/50	0/49	Nd	
Bile	25		0/4	0/8	0/4	0/9		Nd	
Caecum	59	0/9	0/10	0/10	0/10	0/10	0/10	Nd	
Beetles	5	0/3	0/2					Nd	
Flies	4	0/1	0/3					Nd	
Rat feces	4	0/4						Nd	
Soil	34	1/1	0/18			0/15		Nd	
Mouse caecum	1	0/1						Nd	
FARM 2									
Age (weeks)		17	19	22	26	27	30		SLD outbreaks started to occur when chickens were 26 weeks old on Farm 2
Fecal swab	303	0/50	0/50	0/50	4/53	12/50	14/50	Nd	
Bile	19	0/5			2/3	4/10	1/1	3	
Caecum	13	0/5				8/8		Neg	
Litter	1		0/1					Neg	
Wild bird feces	1						1/1	Neg	
Rat feces	1						1/1	Neg	
Dust	3				2/2		1/1	Neg	
Water	1						1/1	Neg	
Flies	1			0/1				Neg	
Butterflies	1					0/1		Neg	
Earwig	1					0/1		Neg	
Spider	1					0/1		Neg	
FARM 3									
Age (weeks)		18	21	24	26	28			*C. hepaticus* was detected when chickens were at 24 weeks old, no SLD clinical signs. SLD outbreak occurred when chickens were 26 weeks old on Farm 3
Fecal swabs	235	0/45	0/50	3/50	9/40	23/50		Nd	
Bile	5			1/3		2/2		1	
Litter	1	0/1						Neg	
Rat feces	1					1/1		Neg	
Dust	3			1/2		1/1		Neg	
Beetles	4	0/1			0/2	0/1		Neg	
Flies	1					0/1		Neg	
Total	1,076								

Nd, not done; Neg, negative; blank cell, samples not collected.

However, one SLD outbreak was observed in chicken at 60–62 weeks-old, and *C. hepaticus* was isolated from these birds.

Sixteen isolates from diverse locations (6 from Queensland, 6 from Victoria, 2 from Western Australia, 1 from South Australia and 5 from New South Wales) isolated during this study were subjected to whole genome sequencing.

Isolation of *C. hepaticus* From Microbially Complex Samples

Campylobacter hepaticus has previously been isolated from bile or liver samples. Direct plating of such samples is usually successful because bile and liver samples from SLD affected birds often carry monocultures of *C. hepaticus* and are therefore not subjected to contaminant growth. However, environmental samples and samples from the gastrointestinal tract of chickens usually carry complex microbiotas, meaning the direct plating method or enrichment methods are ineffective. The motile-filter method was implemented and tested on fresh fecal samples from SLD affected birds, and *C. hepaticus* was recovered, thus demonstrating for the first time the successful isolation of *C. hepaticus* from microbiologically complex samples. The fecal samples used to demonstrate isolation from complex microbiota were from birds that were experimentally infected with *C. hepaticus,* as part of previously reported research (10). Once

TABLE 2 | The presence of *C. hepaticus* in *ad hoc* samples collected around Australia.

Sample types/number of collections	Number of samples	*C. hepaticus* PCR positive	*C. hepaticus* culture positive*
FECAL SWAB			
<17 week/7	146	11	Nd
17–29 week/15	396	116	Nd
29–40 week/2	45	11	Nd
>40 week	0	0	0
BILE			
<17 week/1	4	0	0
17–29/27	100	40	14
29–40/3	3	2	2
>40/3	16	8	5
Rat feces/3	4	1	Neg
Wild Bird feces/2	5	1	Neg
Mites/3	3	2	Nd
Flies/4	6	3	Nd
Water /1	1	1	Neg
Soil/5	25	1	Neg
Beetles/1	2	0	Nd
Ants/2	4	Neg	Nd
Slatter bugs/1	1	Neg	Nd
Black flies/2	1	Neg	Nd
Beetles/1	1	Neg	Nd
Earwigs/1	1	Neg	Nd

*Nd, not done; Neg, negative.

the motile-filter method was successfully tested it was applied to environmental samples, but no viable *C. hepaticus* could be recovered from any of the samples.

Genome Sequencing of 16 *C. hepaticus* Isolates Showed That They Are Closely Related

Sixteen new isolates were sequenced and their genomes were compared to the reference genome sequence of *C. hepaticus* HV10 (GenBank: NZ_CP031611.1). As shown in **Table 3**, genome size ranged from 1,478,686 to 1,534,365 bp and the average G+C content ranged from 27.91 to 28.16%. The average nucleotide identity of the genome sequence of these isolates against *C. hepaticus* HV10 showed a high similarity of 99.95% amongst all isolates. The ANI values and MALDI TOF results identified the cultured isolates as *C. hepaticus*. Two isolates from Queensland (QLD) contain a plasmid with 99% identity to *Campylobacter jejuni* subsp. *jejuni* 81-176 plasmid, pTet, containing a tetracycline resistant gene, *tet(O)*. Phenotypic resistance to tetracycline was experimentally confirmed. The whole genome sequence data has been deposited in the NCBI database under BioProject PRJNA485661, the accession numbers of the individual genomes are detailed in **Supplementary Information**.

TABLE 3 | The similarity of new *C. hepaticus* isolates compared to *C. hepaticus* type strain, HV10.

Isolates/ Location	Number of contigs	Genome size (bp)	% GC	OrthoANIu (%)	Plasmid
C. hepaticus HV10/VIC	1	1,520,669	28.03	100	
VIC_1/VIC	43	1,481,639	27.91	100	
VIC_2/VIC	46	1,482,274	27.92	99.98	
VIC_3/VIC	44	1,484,585	27.91	99.98	
VIC_4/VIC	44	1,484,170	27.91	99.97	
VIC_5/VIC	42	1,482,790	27.91	99.99	
VIC_6/VIC	86	1,479,165	27.98	99.98	
QLD_1/QLD	46	1,517,443	28.00	99.96	Yes
QLD_2/QLD	45	1,521,414	28.00	99.95	Yes
QLD_3/QLD	47	1,522,162	27.97	99.96	
QLD-4/QLD	51	1,482,233	27.92	99.97	
QLD_5/QLD	49	1,478,686	27.93	99.96	
QLD_6/QLD	45	1,479,394	27.92	99.95	
WA_1/WA	49	1,534,365	27.94	99.97	
WA_2/WA	49	1,532,307	27.94	99.98	
SA_1/SA	32	1,524,262	27.97	99.98	
NSW_1/NSW	90	1,515,141	28.16	99.96	

DISCUSSION

Clinical SLD outbreaks were observed in two of the three farms that were monitored over 10 weeks. In both farms, SLD occurred during peak-laying age at 26 and 28 weeks of age; this timing agrees with previous reporting of the most common age at which disease is seen (4). Both outbreaks in the monitored farms occurred during winter. Outbreaks from other unmonitored farms occurred throughout the year. In previous decades the disease had also been referred to as "Summer Hepatitis" because of an apparent tendency to most commonly occur in summer. However, based on our findings from this epidemiological study and other experience over the last 5 years, it is clear that the disease can occur all year round. Although the first outbreaks of SLD in a flock generally occur as the birds enter peak lay, further outbreaks, within the same flock, can occur at later ages (4). In one of the *ad hoc* sampled flocks, an SLD outbreak occurred in birds of 60–62 weeks of age. *Campylobacter hepaticus* was successfully isolated from an SLD affected bird from this flock.

The identification of *C. hepaticus* as the etiological agent of SLD, and the development of sensitive PCR detection methods, has enabled us to move beyond the simple cataloging of clinical signs to now study the underlying dynamics of pathogen infection and spread. It is clear that birds can be infected with *C. hepaticus* many weeks before overt clinical disease becomes obvious. The *ad hoc* sampling showed birds as young as 12 weeks of age were infected, and this is of pivotal importance as it means rear pullets can be a source of contamination to a previously clean site. Furthermore, in the detailed temporal study, *C. hepaticus* was detected in Farm 3 two weeks before disease was seen. This has several implications. First, it indicates that infection with *C. hepaticus* may not be sufficient to induce disease; some

other predisposing factors are also required. The hypothesized predisposing factor(s) may influence SLD outcomes by increasing the abundance of *C. hepaticus* or by altering the susceptibility of the host. Second, it shows that rapid molecular detection methods such as PCR can be used for early detection and identification of flocks at risk of an SLD outbreak. Forewarned of infection status, concerted efforts can be made to reduce the possibility of other predisposing events (e.g., changes in feed, problems with water supply) occurring, that could precipitate an SLD outbreak. Clinical observations have shown that birds are most likely to suffer the first occurrence of SLD when they enter peak lay (4). It has been hypothesized that the physiological changes that occur because of a rapid increase in egg production, such as negative nutrient balance, may affect liver metabolism and act as a predisposing factor for disease progression (6, 30). We hypothesis that factors affecting gastrointestinal tract microbiota during peak lay period, such as changes in feeding patterns, may play an important role in SLD development. These predisposing factors may act by increasing the population levels of the pathogen and/or by making the bird more susceptible to the as yet unknown virulence factors expressed by *C. hepaticus*.

In SLD affected farms, only 10–50% of birds had detectable levels of *C. hepaticus* in fecal swab samples. This demonstrated that some birds within a flock do not acquire the pathogen or are able to quickly overcome it during an SLD outbreak. It is not currently known if these birds have acquired immunity from previous exposure to *C. hepaticus* or whether they have just not been exposed to a sufficient infective dose. Based on this and other field observations and reliable induction by oral administration of large doses (10^8 and more) of *C. hepaticus*, it has been surmised that infection is likely to spread within a flock via the fecal-oral route (6, 10). It has also been shown that birds manifesting clinical SLD have large numbers of *C. hepaticus* in their gastrointestinal tracts, (13), and in the current study it has been shown that viable bacteria can be cultured from the feces of infected birds. It, therefore, appears that all birds in a flock undergoing an SLD outbreak would be exposed to *C. hepaticus* via the fecal-oral route. However, the finding that not all birds in an infected flock have detectable levels of *C. hepaticus* may indicate that the infective dose of *C. hepaticus* is very high.

Campylobacter hepaticus DNA was detected in a variety of environmental samples including wild bird feces, flies, and rat feces from SLD-positive farms. These motile organisms might be vectors for *C. hepaticus* dissemination. A recent study that investigated biosecurity practices on Australian commercial layer farms showed that wild birds were commonly reported to be present in free-range farms (73%) and it was noted that they are potential sources of diseases that can be transmitted to laying hens (31). Flies have previously been implicated in the transmission of other *Campylobacter* species to chickens (32). Some water, soil, mite, and dust samples were also PCR-positive for *C. hepaticus* DNA. Water, soil, dust and mites could be intermediate sources for the transmission of *C. hepaticus* to and/or from the potential animal vectors and transfer to chickens and between chickens within a flock. Positive samples were mainly obtained from farms in which clinical SLD was occurring, but a few positive samples were from farms which had no apparent clinical SLD at the time of sample collection, indicating a potential route of transmission for *C. hepaticus* due to environmental factors described above. This may also explain the higher propensity of SLD in free-range layers, who have more frequent interactions with diverse environmental sources.

Although *C. hepaticus* DNA was detected in environmental samples by PCR (wild bird feces, rat feces, mouse caecum, soil, water, dust, mites, and flies), no viable *C. hepaticus* were recovered from these samples, even though the motile-filter method was used successfully for *C. hepaticus* isolation from chicken feces of experimentally infected birds. However, the fecal samples from the experimentally infected birds were qualitatively different to the environmental samples as they were collected immediately after birds defecated and were quickly (< 2 h) transferred to the laboratory, on ice, whereas the environmental samples were usually of unknown age and took considerable time (sometimes several days at ambient temperatures) to transport to the laboratory for analysis. *Campylobacter* spp. are usually considered to be sensitive to environmental exposure, so it is unsurprising that viable *C. hepaticus* could not be recovered. Given that PCR indicated many environmental samples were positive, these sources cannot be ruled out as initial transmission reservoirs. Another consideration is that various *Campylobacter* species are known to enter a viable but non-culturable (VBNC) state under stress, and therefore cannot be routinely recovered using conventional culture methods (33), which may also account for the discrepancies between the PCR positive and culture negative samples. It is possible that *C. hepaticus* VBNC cells could be present in environmental samples. VBNC cells can be resuscitated under specific conditions, such as ingestion (34), and so there may be bacteria present, that could cause infection in chickens, even though we haven't been able to detect them by conventional isolation methods. The available evidence indicates that *C. jejuni* VBNCs can be resuscitated by inoculation of chicken embryos but not by direct oral inoculation of chickens (35, 36), but *C. hepaticus* may be different. Further research is required to investigate this possibility and understand whether such organisms could play a role in disease transmission.

Genome sequencing and bioinformatics analysis of 16 isolates from different farms in VIC/QLD/WA/SA/NSW indicated that they are all highly similar to the *C. hepaticus* type strain, HV10. The genome sequences of all isolates were examined for plasmid content as plasmids may play an important role in dissemination of antibiotic resistance genes. Two isolates contained plasmids with very high sequence similarity to *C. jejuni* pTet-like plasmids. *C. hepaticus* isolates from Australia and UK have previously been reported to contain tetracycline-resistant plasmids, but they contained different *C. jejuni* and *C. coli* plasmids (11, 12). Currently, chlortetracycline is the main treatment option available for the control of SLD in Australia. With plasmid borne resistance arising in *C. hepaticus* the use of this treatment becomes ineffective in some flocks.

In conclusion, this study found that birds can be infected with *C. hepaticus* during rear and prior to the onset of lay, without any clinical SLD. SLD outbreaks occurred mainly at peak lay but could also occur earlier or later in the production cycle. Clean production sites may lose their negative

C. hepaticus through the transfer of positive pullets. Therefore, it is of epidemiological significance to collect samples from birds from several weeks of age until the peak lay period to investigate when the birds become infected with *C. hepaticus*. Once birds are infected with *C. hepaticus*, measures, such as antibiotic treatment, have been used to recover from clinical SLD but the emergence of tetracycline resistance encoding plasmids foreshadows the need for alternative treatments and management practices. As environmental sources are a likely transmission source of *C. hepaticus*, biosecurity methods need to be strictly followed to prevent the spread of this bacteria, such as avoiding standing water on the range, as we found *C. hepaticus* can survive for several days in water (unpublished data). It appears that control of rodents and birds should also be emphasized as an important biosecurity measure to help reduce the probability of SLD outbreaks.

DATA AVAILABILITY STATEMENT

All datasets generated for this study are included in the article/**Supplementary Material**.

AUTHOR CONTRIBUTIONS

TV and RM conceived the study. CP, BV, and TV carried out the laboratory work. AA, TW, and PS collected samples and arranged for sample collection by other veterinarians. CP and TV drafted the manuscript and all authors edited the manuscript.

FUNDING

We acknowledge the financial support from Poultry Hub Australia that enabled us to carry out this research (PHA Project No. 2018-432).

ACKNOWLEDGMENTS

We thank veterinarians from various farms around Australia who provided samples for the study.

SUPPLEMENTARY MATERIAL

The Supplementary Material for this article can be found online at: https://www.frontiersin.org/articles/10.3389/fvets.2019.00505/full#supplementary-material

REFERENCES

1. Grimes T, Reece R. Spotty liver disease – an emerging disease in free-range egg layers in Australia. In: *Proceedings of the Sixtieth Western Poultry Disease Conference*. Sacremento, CA (2011). p. 53–6.
2. Crawshaw TR, Young SC. Increased mortality on a free-range layer site. *Vet Rec*. (2003) 153:664.
3. Gregory M, Klein B, Sahin O, Girgis G. Isolation and characterization of *Campylobacter hepaticus* from layer chickens with spotty liver disease in the United States. *Avian Dis*. (2018) 62:79–85. doi: 10.1637/11752-092017-Reg.1
4. Scott PC, Moore RJ, Wilson G. *Determining the Cause and Methods of Control for Spotty Liver Disease*. Australia Egg Corporation Limited Publication No. 1SX091A (2016).
5. Crawshaw T. A review of the novel thermophilic *Campylobacter, Campylobacter hepaticus,* a pathogen of poultry. *Transbound Emerg Dis*. (2019) 66: 1481–92. doi: 10.1111/tbed.13229
6. Moore RJ, Scott PC, Van TTH. Spotlight on avian pathology: *Campylobacter hepaticus*, the cause of spotty liver disease in layers. *Avian Pathol*. (2019) 48:285–7. doi: 10.1080/03079457.2019.1602247
7. Tudor DC. A liver degeneration of unknown origin in chickens. *J Am Vet Med Assoc*. (1954) 125:219–20.
8. Crawshaw TR, Chanter JI, Young SC, Cawthraw S, Whatmore AM, Koylass MS, et al. Isolation of a novel thermophilic *Campylobacter* from cases of spotty liver disease in laying hens and experimental reproduction of infection and microscopic pathology. *Vet Microbiol*. (2015) 179:315–21. doi: 10.1016/j.vetmic.2015.06.008
9. Van TTH, Elshagmani E, Gor MC, Scott PC, Moore RJ. *Campylobacter hepaticus* sp. nov., isolated from chickens with spotty liver disease. *Int J Syst Evol Microbiol*. (2016) 66:4518–24. doi: 10.1099/ijsem.0.001383
10. Van TTH, Elshagmani E, Gor MC, Anwar A, Scott PC, Moore RJ. Induction of spotty liver disease in layer hens by infection with *Campylobacter hepaticus*. *Vet Microbiol*. (2017) 199:85–90. doi: 10.1016/j.vetmic.2016.12.033
11. Petrovska L, Tang Y, Jansen van Rensburg MJ, Cawthraw S, Nunez J, Sheppard SK, et al. Genome reduction for niche association in *Campylobacter hepaticus*, a cause of spotty liver disease in poultry. *Front Cell Infect Microbiol*. (2017) 7:354. doi: 10.3389/fcimb.2017.00354
12. Van TTH, Lacey JA, Vezina B, Phung C, Anwar A, Scott PC, et al. Survival mechanisms of *Campylobacter hepaticus* identified by genomic analysis and comparative transcriptomic analysis of *in vivo* and *in vitro* derived bacteria. *Front Microbiol*. (2019) 10:107. doi: 10.3389/fmicb.2019.00107
13. Van TTH, Gor MC, Anwar A, Scott PC, Moore RJ. *Campylobacter hepaticus,* the cause of spotty liver disease in chickens, is present throughout the small intestine and caeca of infected birds. *Vet Microbiol*. (2017) 207:226–30. doi: 10.1016/j.vetmic.2017.06.022
14. Scott PC, Moore R, Wilson T, Anwar A, Van TTH. *Final Report on the AE funded Project to Examine the Effect of Feed Additives on Spotty Liver Disease*. Australian Eggs Limited Publication No. 1BS804a (2018).
15. Hermans D, Pasmans F, Messens W, Martel A, Van Immerseel F, Rasschaert G, et al. Poultry as a host for the zoonotic pathogen *Campylobacter jejuni*. *Vector Borne Zoonotic Dis*. (2012) 12:89–98. doi: 10.1089/vbz.2011.0676
16. Ahmed MFM, Schulz J, Hartung J. Survival of *Campylobacter jejuni* in naturally and artificially contaminated laying hen feces. *Poult Sci*. (2013) 92:364–9. doi: 10.3382/ps.2012-02496
17. Vaz CSL, Voss-Rech D, Pozza JS, Coldebella A, Silva VS. Isolation of *Campylobacter* from Brazilian broiler flocks using different culturing procedures. *Poult Sci*. (2014) 93:2887–92. doi: 10.3382/ps.2014-03943
18. Cody AJ, McCarthy ND, Bray JE, Wimalarathna HML, Colles FM, Jansen van Rensburg MJ, et al. Wild bird-associated *Campylobacter jejuni* isolates are a consistent source of human disease, in Oxfordshire, United Kingdom. *Environ Microbiol Rep*. (2015) 7:782–8. doi: 10.1111/1758-2229.12314
19. Hald, B., Skov, M. N., Nielsen, E. M., Rahbek, C., Madsen, J. J., Wainø, M., et al. *Campylobacter jejuni* and *Campylobacter coli* in wild birds on Danish livestock farms. *Acta Vet. Scand*. (2016) 58:11. doi: 10.1186/s13028-016-0192-9
20. Humphrey T, Mason M, Martin K. The isolation of *Campylobacter jejuni* from contaminated surfaces and its survival in diluents. *Int J Food Microbiol*. (1995) 26:295–303.
21. Varela NP, Friendship RM, Dewey CE. Prevalence of *Campylobacter* spp. isolated from grower-finisher pigs in Ontario. *Can Vet J*. (2007) 48:515–7.
22. Damborg P, Olsen KE, Møller Nielsen E, Guardabassi L. Occurrence of *Campylobacter jejuni* in pets living with human patients infected with *C jejuni*. *J Clin Microbiol*. (2004) 42:1363–4. doi: 10.1128/jcm.42.3.1363-1364.2004
23. Hald B, Skovgård H, Bang DD, Pedersen K, Dybdahl J, Jespersen JB, et al. Flies and *Campylobacter* infection of broiler flocks. *Emerging Infect Dis*. (2004) 10:1490–2. doi: 10.3201/eid1008.040129

24. Nichols GL. Fly transmission of *Campylobacter*. *Emerging Infect Dis*. (2005) 11:361–4. doi: 10.3201/eid1103.040460
25. Bates C, Hiett KL, Stern NJ. Relationship of *Campylobacter* isolated from poultry and from darkling beetles in New Zealand. *Avian Dis*. (2004) 48:138–47. doi: 10.1637/7082
26. Kim J, Oh E, Banting GS, Braithwaite S, Chui L, Ashbolt NJ, et al. An improved culture method for selective isolation of *Campylobacter jejuni* from wastewater. *Front Microbiol*. (2016) 7:1345. doi: 10.3389/fmicb.2016.01345
27. Ross CM, Donnison AM. *Campylobacter jejuni* inactivation in New Zealand soils. *J Appl Microbiol*. (2006) 101:1188–97. doi: 10.1111/j.1365-2672.2006.02984.x
28. Van TTH, Anwar A, Scott PC, Moore RJ. Rapid and specific methods to differentiate foodborne pathogens, *Campylobacter jejuni, Campylobacter coli*, and the new species causing Spotty Liver Disease in chickens, *Campylobacter hepaticus*. *Foodborne Pathog Dis*. (2018) 15:526–30. doi: 10.1089/fpd.2017.2367
29. Coil D, Jospin G, Darling AE. A5-miseq: an updated pipeline to assemble microbial genomes from Illumina MiSeq data. *Bioinformatics*. (2014) 31:587–9. doi: 10.1093/bioinformatics/btu661
30. Courtice JM, Mahdi LK, Groves PJ, Kotiw M. Spotty Liver Disease: a review of an ongoing challenge in commercial free-range egg production. *Vet Microbiol*. (2018) 227:112–8. doi: 10.1016/j.vetmic.2018.08.004
31. Scott AB, Singh M, Groves P, Hernandez-Jover M, Barnes B, Glass K, et al. Biosecurity practices on Australian commercial layer and meat chicken farms: Performance and perceptions of farmers. *PLoS ONE*. (2018) 13:e0195582. doi: 10.1371/journal.pone.0195582
32. Royden A, Wedley A, Merga JY, Rushton S, Hald B, Humphrey T, et al. A role for flies (*Diptera*) in the transmission of *Campylobacter* to broilers? *Epidemiol Infect*. (2016) 144:3326–34. doi: 10.1017/s0950268816001539
33. Zhao X, Zhong J, Wei C, Lin CW, Ding T. Current perspectives on viable but non-culturable state in foodborne pathogens. *Front Microbiol*. (2017) 8:580. doi: 10.3389/fmicb.2017.00580
34. Colwell RR, Brayton P, Herrington D, Tall B, Huq A, Levine MM. Viable but non-culturable *Vibrio cholerae* O1 revert to cultivable state in the human intestine. *World J Microbiol Biotechnol*. (1996) 12:28–31. doi: 10.1007/BF00327795
35. Chaveerach P, ter Huurne AA, Lipman LJ, van Knapen F. Survival and resuscitation of ten strains of *Campylobacter jejuni* and *Campylobatcer coli* under acid conditions. *Appl Environ Microbiol*. (2003) 69:711–4. doi: 10.1128/AEM.69.1.711-714.2003
36. Ziprin RL, Droleskey RE, Hume ME, Harvey RB. Failure of viable but nonculturable *Campylobacter jejuni* to colonize the cecum of newly hatched leghorn chicks. *Avian Dis*. (2003) 47:753–8. doi: 10.1637/7015

Conflict of Interest: AA, TW, and PS are employed by the company Scolexia Pty Ltd.

The remaining authors declare that the research was conducted in the absence of any commercial or financial relationships that could be construed as a potential conflict of interest.

frontiers in Veterinary Science

ORIGINAL RESEARCH
published: 11 February 2020
doi: 10.3389/fvets.2020.00027

Campylobacter jejuni Strain Dynamics in a Raccoon (*Procyon lotor*) Population in Southern Ontario, Canada: High Prevalence and Rapid Subtype Turnover

Steven K. Mutschall[1], Benjamin M. Hetman[2†], Kristin J. Bondo[3†], Victor P. J. Gannon[4], Claire M. Jardine[3,5] and Eduardo N. Taboada[6]*

[1] National Centre for Animal Diseases, Canadian Food Inspection Agency, Lethbridge, AB, Canada, [2] Department of Population Medicine, Ontario Veterinary College, University of Guelph, Guelph, ON, Canada, [3] Department of Pathobiology, Ontario Veterinary College, University of Guelph, Guelph, ON, Canada, [4] National Microbiology Laboratory at Lethbridge, Public Health Agency of Canada, Lethbridge, AB, Canada, [5] Canadian Wildlife Health Cooperative, Ontario Veterinary College, University of Guelph, Guelph, ON, Canada, [6] National Microbiology Laboratory, Public Health Agency of Canada, Winnipeg, MB, Canada

Free-ranging wildlife are increasingly recognized as potential reservoirs of disease-causing *Campylobacter* species such as *C. jejuni* and *C. coli.* Raccoons (*Procyon lotor*), which live at the interface of rural, urban, and more natural environments, are ideal subjects for exploring the potential role that wildlife play in the epidemiology of campylobacteriosis. We studied the prevalence and genetic diversity of *Campylobacter* from live-captured raccoons on five swine farms and five conservation areas in southwest Ontario. From 2011 to 2013, we collected fecal swabs ($n = 1,096$) from raccoons, and ($n = 50$) manure pit samples from the swine farm environment. We subtyped the resulting *Campylobacter* isolates ($n = 581$) using Comparative Genomic Fingerprinting (CGF) and 114 distinct subtypes were observed, including 96 and 18 subtypes among raccoon and manure pit isolates, respectively. *Campylobacter* prevalence in raccoons was 46.3%, with 98.7% of isolates recovered identified as *C. jejuni*. Novel raccoon-specific CGF subtypes ($n = 40/96$) accounted for 24.6% ($n = 143/581$) of *Campylobacter* isolates collected in this study. Our results also show that *C. jejuni* is readily acquired and lost in this wild raccoon population and that a high *Campylobacter* prevalence is observed despite transient carriage typically lasting 30 days or fewer. Moreover, although raccoons appeared to be colonized by species-adapted subtypes, they also harbored agriculture-associated genotypes that accounted for the majority of isolates observed (66.4%) and that are strongly associated with human infections. This suggests that raccoons may act as vectors in the transmission of clinically-relevant *C. jejuni* subtypes at the interface of rural, urban, and more natural environments.

Keywords: *Campylobacter*, longitudinal surveillance, molecular subtyping, *Procyon lotor*, raccoon, zoonoses

OPEN ACCESS

Edited by:
Ozan Gundogdu, University of London, United Kingdom

Reviewed by:
Friederike Hilbert, University of Veterinary Medicine Vienna, Austria
Frances Colles, University of Oxford, United Kingdom
Marja-Liisa Hänninen, University of Helsinki, Finland
Philip Edward Carter, Institute of Environmental Science and Research (ESR), New Zealand

***Correspondence:**
Eduardo N. Taboada
eduardo.taboada@canada.ca

†Present address:
Benjamin M. Hetman, Canadian Field Epidemiology Program, Center for Emergency Preparedness and Response, Public Health Agency of Canada, Ottawa, ON, Canada
Kristin J. Bondo, Department of Natural Resources Management, Texas Tech University, Lubbock, TX, United States

Specialty section:
This article was submitted to Veterinary Infectious Diseases, a section of the journal Frontiers in Veterinary Science

Received: *25 November 2019*
Accepted: *14 January 2020*
Published: *11 February 2020*

INTRODUCTION

Campylobacter species are the second most reported bacterial foodborne pathogen in Canada (1), and campylobacteriosis remains one of the most common enteric illnesses worldwide (2). Although human infections are primarily caused by two thermophilic species, *C. jejuni* and *C. coli*, several additional species have been reported to cause illness (3). It is generally accepted that the majority of *Campylobacter* infections are acquired through the handling and ingestion of contaminated poultry products (4–6). While *Campylobacter* is highly prevalent in poultry and poultry meat (7), it is also commonly found in a wide range of animal hosts that not only include livestock such as cattle and swine, but also household pets and wildlife (6, 8). Given that *Campylobacter* is actively shed in animal feces, environmental sources such as surface waters may also become contaminated through use by animals or due to surface run-off (9). This may lead to increased environmental transmission and dissemination of *Campylobacter* across different ecological niches, thereby creating additional routes of exposure to humans or other potential hosts (10).

Campylobacter have been isolated from a diverse array of free-ranging wildlife, including birds such as waterfowl and songbirds and mammals, including rodents, wild boars, and ungulates (8, 11–14). Although the presence of *C. jejuni* in free-ranging wildlife is not necessarily indicative of a role in the epidemiology of campylobacteriosis, an increasing number of studies is consistent with this possibility. For example, *Campylobacter* subtypes commonly associated with human illness have been detected in wildlife species (15, 16), and human clinical cases have been linked to wildlife via direct transmission (17–20) or source attribution (21). Furthermore, an increased occurrence of zoonotic pathogens, including *Campylobacter* and *Salmonella*, has been observed in free-ranging wildlife living in close proximity to livestock and or human populations (22, 23).

A recent scoping review on bacterial zoonotic pathogens in wild animals reported that the most frequently investigated wildlife groups were birds (47.3%), cervids (15.4%), and rodents (10.5%) (24). Similarly, much *Campylobacter* research on wildlife has focused on avian species, in large part due to *Campylobacter*'s affinity for avian hosts, but also due to host ecological factors such as increased anthropogenic contact and large habitat ranges. The importance of wild mammals in *Campylobacter* ecology and epidemiology is less clear. By comparison to avian species, there is a paucity of literature exploring the role of non-avian wildlife on transmission of *Campylobacter*. There is even less focus on synanthropic species, which live in habitats in close association with humans. In this regard, raccoons (*Procyon lotor*) represent ideal study subjects because they use a wide variety of habitats (25) and have the potential to move between urban, rural, and forested habitats.

Raccoons are known to carry a number of zoonotic agents (26–29) and they also display distinct social features such as the use of communal latrines (30), which may enhance mechanical transmission of certain microorganisms present in their feces (31). Previous studies have reported *Campylobacter* prevalence in raccoons ranging from 1% (32) to 41% (33). To our knowledge, there have been few, if any, longitudinal studies examining *Campylobacter* in a raccoon population over multiple years. The objectives of this study were to: (1) determine the prevalence of *Campylobacter* in raccoons captured on swine farms and conservation areas; (2) assess the genetic diversity, population structure, and ecology of *Campylobacter* subtypes observed in raccoons; (3) assess the dynamics of *Campylobacter* acquisition/loss in individual animals; and finally, (4) compare the subtypes observed in raccoons and human clinical cases to assess the potential role of raccoons in the epidemiology of campylobacteriosis.

MATERIALS AND METHODS

Animal Trapping and Sample Collection

Procedures for trapping and handling raccoons were approved by the Animal Care Committee at the University of Guelph following the guidelines of the Canadian Committee on Animal Care. For a detailed description and map of the study area as well as trapping and sampling procedures, please refer to Bondo et al. (27) and (29). From May 2011 to November 2013, raccoons were live-trapped on swine farms and conservation areas near the cities of Guelph and Cambridge in southern Ontario, Canada. Individual animals were identified by ear and transponder tags and were sampled only once per monthly trapping week; however, additional samples were collected from the same individual if they were caught in subsequent months. Rectal fecal swabs were collected using Cary-Blair swab applicators [BBL CultureSwab, (BD) Becton, Dickinson and Company, Annapolis, MD, USA]. At each swine farm, one lagoon (i.e., manure pit) sample was collected on the first day of each trapping week as previously described (29). Briefly, to collect lagoon samples, a 24′ Nasco Swing Sampler (Conbar, Monroeville, NJ, USA) was used to collect three sub-samples from three locations around the pit, and up to two depths (i.e., the top 1/3, and mid depth of the storage), for a total of six sub-samples. The samples were then pooled into one sample for analysis. All samples were kept refrigerated or on ice until processing. The median and average number of days between collection and processing was three; the maximum number of days for raccoon swabs was eight whereas for manure pit samples it was 11.

Campylobacter Isolation

Isolation of thermophilic *Campylobacter* species was performed as previously described (34). For samples collected prior to October 2011, the "conventional method" (enrichment followed by direct plating onto selective media) was used; the "membrane method" (enrichment followed by passive membrane filtration onto selective media) was used thereafter. Briefly, fecal swabs were immersed in 20 mL of Bolton broth (BB) containing BB selective supplement (SR0183, Oxoid), (20 mg/L cefoperazone, 20 mg/L vancomycin, 20 mg/L trimethoprim, and 50 mg/L cyclohexamine) and 5% laked horse blood (SR0048) and mixed rapidly for 20 s. Lagoon samples were mixed prior to adding 1 mL of sample to BB with supplement. Bolton broth cultures were incubated at

42°C in microaerobic conditions (10% CO_2, 5% O_2, 85% N_2) for 24 h and subsequently streaked onto modified blood-free charcoal cefoperazone deoxycholate agar supplemented with 32 mg/L cefoperazone and 10 mg/L amphotericin B (mCCDA) or passively filtered for 15 min through 0.65 μM cellulose acetate membrane filters onto the surface of mCCDA. All mCCDA plates were incubated for 48 h under the same microaerobic conditions. Three to five *Campylobacter*-like colonies were subcultured to blood agar and incubated for 24–48 h. Presumptive *Campylobacter* spp. colonies were identified on the basis of growth on mCCDA media, colony morphology, and oxidase tests. DNA was extracted from purified cultures using the EZ1 DNA tissue kit (Qiagen) according to the manufacturer's instructions for subsequent PCR speciation of presumptive *Campylobacter* isolates and subtyping of confirmed *Campylobacter* isolates.

PCR Confirmation of *Campylobacter* spp.

Presumptive *Campylobacter* isolates were confirmed by multiplex PCR targeting a *Campylobacter* genus-specific region of the 16S *rRNA* gene, and *mapA* and *ceuE* genes for *C. jejuni* and *C. coli* identification, respectively (35). Amplicons were visualized using a QIAxcel capillary electrophoresis instrument with the DNA Screening kit. The AM320 separation method was used along with a 15–3,000 bp alignment marker and the QX 100–2.5 kb DNA size marker. Data were analyzed and visualized using the BioCalculator v. 3.0 software.

Comparative Genomic Fingerprinting

Campylobacter spp. isolates were subtyped by Comparative Genomic Fingerprinting (CGF) as previously described (36). Briefly, CGF consists of 8 multiplex PCR reactions that together assess the presence or absence of a set of 40 accessory gene targets found to have variable carriage in the *Campylobacter* population and that are used to generate a highly discriminatory binary fingerprint. Products from the CGF PCRs were visualized on the QIAxcel as previously described (36) and were scored positive (1) or negative (0) based on presence or absence of each target amplicon using a combination of the BioCalculator software's binary peak calling and confirmed with visual curation. The resulting binary fingerprints were assigned a three-digit CGF subtype (e.g., 0923.002.001) derived from cluster membership in the Canadian *Campylobacter* CGF database (C3GFdb). Fingerprints identical to those already existing in the database were assigned the appropriate CGF subtype, while novel fingerprints were assigned a CGF subtype based on their similarity to existing fingerprints in the database. Isolates from the same sample with identical subtypes were assumed to be derived from a single clone and only one representative isolate was included in further analyses.

Association of CGF Type With Host Species

At the time of this analysis, the C3GFdb consisted of 4,847 distinct CGF profiles obtained from 19,141 *Campylobacter* isolates collected from across Canada, primarily from the last decade. These included 23.3% isolates derived from human clinical origin, 32.0% from poultry sources, 20.9% from cattle sources and 14.6% from environmental surface water samples. To compare epidemiologic attributes of subtypes observed among study isolates, we compiled summary statistics based on the composition of host-sources observed in the C3GFdb for each subtype in this study. We classified CGF subtypes observed in this study ($n = 114$) into four ecological range categories (ERC) based on the composition of sources from which they have been historically observed in the C3GFdb. Subtypes from the present study included: (I) Raccoon Exclusive (RE; $n = 44$); (II) Raccoon and Environmental Water (REW; $n = 16$); (III) Swine/Swine Lagoon (SSL; $n = 10$); and (IV) Mixed Host (MH; $n = 44$). Phylogenetic and source association analysis was performed using the R language for statistical computing (v.3.13) (37) and the following packages: *tidyverse* (38) and *ggtree* (39). A dendrogram was constructed from the 40-gene CGF profile using the "hamming" distance and "average linkage" clustering from the *dist* and *hclust* functions, respectively, and visualized using "ggtree." Clade designations were made based on a tree height "$h = 10$," which produced stable, genetically distinct groupings. For each of the CGF subtypes observed in the present study we identified the associated host-sources from the C3GFdb. For associations between CGF subtypes and MLST Clonal Complexes, we used an in-house database created from *in silico* CGF and MLST predictions generated from publicly available WGS data analyzed using the program Microbial *in silico* Typer (40); a table of associations is provided as **Supplementary Table S1**.

Analysis of Strain Dynamics

Forty-three percent ($n = 272/628$) of the raccoons in this study were captured on multiple occasions, with 18.5% ($n = 116/628$) captured three or more times, up to maximum of eight captures. These data were analyzed to examine strain dynamics at the level of individual animals as described below.

Statistical Analysis

CGF subtype diversity was assessed using the Simpson's Diversity Index (41) with a 95% confidence interval (42). A chi-square test statistic was used to explore the hypothesis that there was no significant difference in the distribution of isolates from prevalent *Campylobacter* clades (isolate count n > 9) between each of the location types (e.g., swine farm sites and conservation sites). Chi-square test statistics and *post-hoc* follow-up calculations for computing adjusted standardized residuals and z-scores for each clade were performed as described by Sharpe (43).

RESULTS

A High Prevalence of *Campylobacter* Was Found in the Raccoon Population Under Study

From May 2011 to November 2013, we collected 1,096 fecal swabs from 628 raccoons trapped on conservation areas ($n = 687$) and swine farms ($n = 409$), and 50 manure pit samples from the environment of the swine farm sites. The prevalence of *Campylobacter* spp. in raccoon fecal samples was 46.3% (508/1,096) (**Table 1**). There were no significant differences in

TABLE 1 | Frequency, prevalence and species of *Campylobacter* in fecal samples obtained from raccoons and swine farm manure pits.

Sample source	Sample size	*Campylobacter* positive samples		(95% confidence interval)	*C. jejuni*		*C. coli*		*C.* spp.	
	n	*n*	%		*n*	%	*n*	%	*n*	%
Raccoon	1,096	508	46.4	(0.434, 0.493)	502	98.8	1	0.2	6	1.2
Manure pit	50	17	34.0	(0.224, 0.478)	0	0.0	16	94.1	1	5.9

Campylobacter prevalence from raccoon fecal swabs with a sample-to-test interval of 1–2 days (46.7%, $n = 467$) vs. a 3–4 days (46.0%, $n = 363$), 5–6 days (48.5%, $n = 227$), or 7–8 days interval (33.3%, $n = 39$). Similarly, for swine manure pit samples, there were no significant differences in Campylobacter prevalence between sample-to-test intervals of 1–2 days (40.0%, $n = 10$) vs. 3–4 (38.1%, $n = 21$), 5–6 (33.3%, $n = 9$), or 7–11 days (22.2%, $n = 9$). Among the *Campylobacter* positive raccoon samples, 502 (98.8%) were positive for *C. jejuni*, six (1.2%) for *Campylobacter* spp. (unidentified *Campylobacter* species), and one for *C. coli* (**Table 1**). A single sample was found to harbor mixed *Campylobacter* species, testing positive for both *C. jejuni* and an undefined *Campylobacter* spp. Among swine manure pit samples 34.0% (17/50) were positive for *Campylobacter*, of which 94.1% (16/17) were positive for *C. coli* (**Table 1**). One sample tested positive for *Campylobacter* spp.

Campylobacter Circulating in the Raccoon Population Represent a Genetically Diverse Population

A total of 1,555 confirmed *Campylobacter* isolates derived from *Campylobacter*-positive raccoon fecal swabs were subtyped by CGF. A further 58 isolates were recovered from swine manure pit samples. After accounting for potentially clonal isolates (i.e., isolates from the same sample sharing the same CGF subtype), 610 isolates remained; this included 581 raccoon isolates and 29 manure pit sample isolates. Among the *Campylobacter* positive raccoon samples ($n = 508$), a single CGF subtype was recovered for the majority of the samples (443/508; 87.2%), two CGF types were recovered in 11.2% of samples (57/508), and three subtypes in 1.6% of samples (8/508). We observed a broad genetic diversity in the *Campylobacter* population, with a total of 114 distinct CGF subtypes identified among study isolates. Subtype clusters ranged in size from 1 to 36 isolates, with 13 subtypes comprising over 50% of isolates in the dataset ($n = 329/628$) and 51 subtypes detected in single instances. Forty-six subtypes, representing 21.3% of study isolates ($n = 130/610$), were novel and had not been previously observed in the C3GFdb. There were 96 subtypes observed among raccoon isolates (*C. jejuni* = 91; *Campylobacter* spp. = 4; *C. coli* = 1) and 18 subtypes observed among lagoon isolates (*C. coli* = 17; *Campylobacter* spp. = 1); no subtypes were shared between raccoons and manure pit samples. Clustering of the 114 CGF binary profiles revealed 8 major lineages, designated clades A–H (**Figure 1**). The clades segregated by *Campylobacter* species: clades A–C, G, and H comprised *C. jejuni* isolates; clade F comprised *C. coli* isolates; and clade D comprised non-*jejuni*/*coli* *Campylobacter* species isolates (i.e., undetermined). The majority of raccoon isolates were observed in clade A (52.0%; $n = 302$), followed by clades B and C, with 30.5% ($n = 177$) and 14.5% ($n = 84$) of isolates, respectively. A small number of raccoon isolates (3.1%; $n = 18$) were found distributed among clades D ($n = 5$), E ($n = 1$), F ($n = 1$), G ($n = 2$), and H ($n = 9$). Among swine lagoon isolates, the majority were found in clade F (89.7%; $n = 26$), with the remaining isolates (10.3%; $n = 3$) in clade D. Similar levels of diversity were observed between swine farms and conservation areas at the subtype level (Simpson's Index of 0.9648 and 0.9628, respectively). Although overall genotypic richness was similar between swine farms and conservation areas, there was a significant relationship between clade and location type. For clade A, more isolates were identified from swine farm sites compared to conservation sites ($p < 0.001$). In contrast, for clades B and C, fewer isolates were identified from swine farm sites compared to conservation sites ($p < 0.01$).

Campylobacter Subtypes in the Raccoon Population Display Different Types of Host Range Specificity

Among the four ecological range categories that we defined for the subtypes in this study (Raccoon Exclusive or RE; Raccoon and Environmental Water or REW; Swine/Swine Lagoon or SSL; and Mixed Host or MH), raccoon isolates were evenly distributed among RE, REW and MH subtypes (RE: 31.3%, $n = 182$; REW: 34.1%, $n = 198$; MH: 34.6%, $n = 201$). Swine lagoon isolates were similarly distributed among SSL and MH subtypes (SSL: 51.7%, $n = 15$; MH: 48.3%, $n = 14$). The distribution of ERC subtypes suggests a strong raccoon association for certain clades observed in our analysis (**Figure 1**). Clade C, which included 14.5% of raccoon isolates in the study, was strictly composed of RE subtypes, and these were novel to the C3GFdb. Clade A, which included the majority of raccoon isolates in the study (52.0%), comprised largely RE and REW subtypes ($n = 33/38$). Source frequencies from the C3GFdb (**Table 2**) indicate that a majority of isolates from clade A subtypes ($n = 461$) include raccoon isolates from this study (65.5%; $n = 302$) along with historical isolates from environmental water sources (26.2%; $n = 121$). A small number of isolates (6.9%; $n = 32$) comprised the remaining isolates in the clade and were derived from cattle, poultry, and human clinical sources (**Table 2**). Conversely, clades B and H, which included 30.5 and 1.6% of raccoon isolates, respectively, were of MH subtype composition ($n = 23/29$ and $n = 6/7$, respectively). Based on C3GFdb source association data, isolates from subtypes in clades B ($n = 2,118$) and H ($n = 1,329$) were primarily chicken-associated (clade B = 54.9%; clade H = 55.0%). Importantly, these clades included a large proportion of isolates from human clinical cases (14.4 and 33.3%, respectively), which is in contrast to clades A and C (1.7 and 0.0%, respectively). Unsurprisingly, the *C. coli* specific-clade F included 26/29 swine manure pit isolates and consisted of 9 SSL subtypes and 9 MH subtypes.

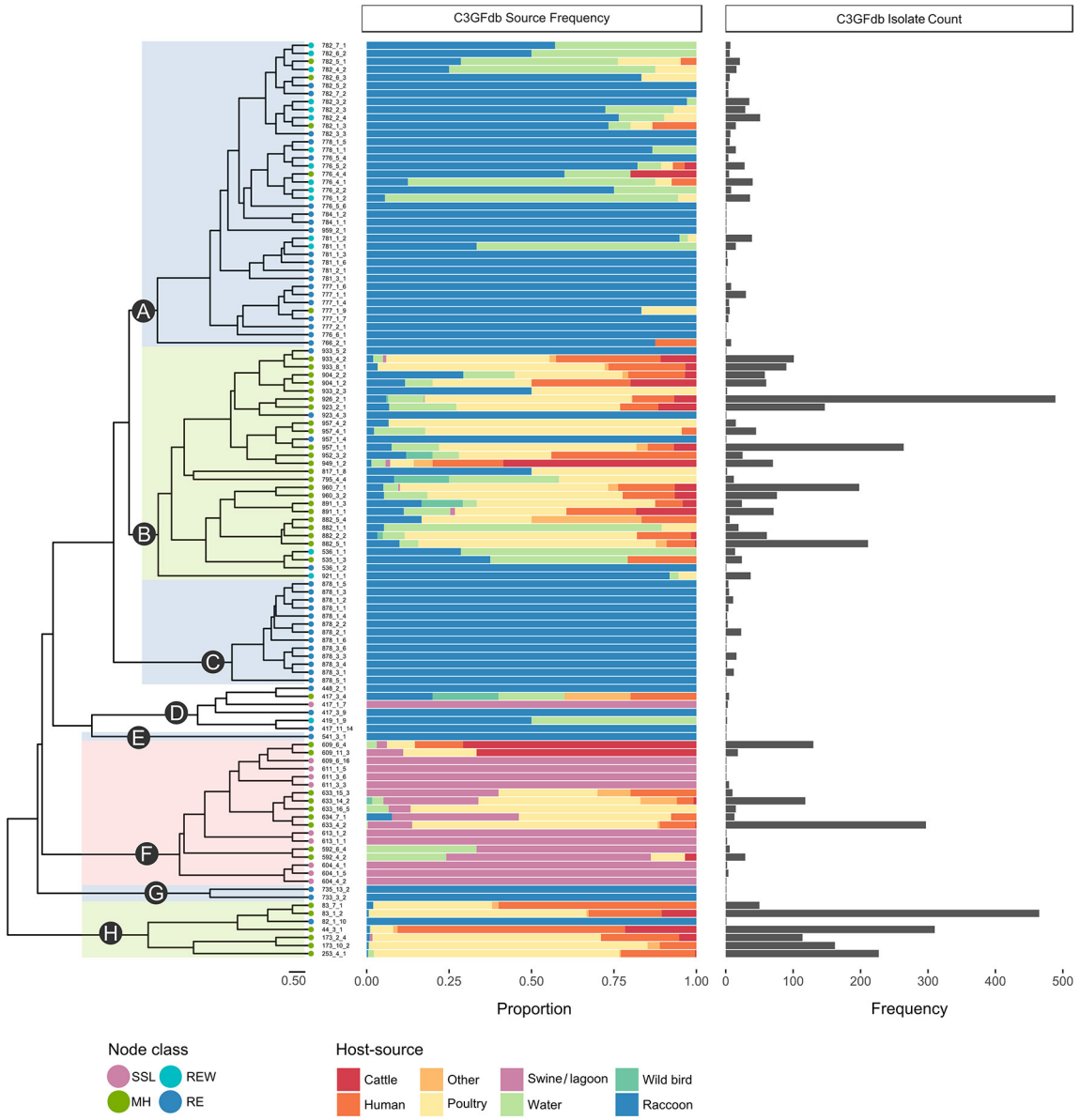

FIGURE 1 | Host-range specificity of *Campylobacter* subtypes observed in a raccoon population on conservation and swine farm sites in southwest Ontario, Canada. For each of the 114 CGF types in the dendrogram, host-source data from the C3GFdb is used to illustrate relative host-source associations. Terminal nodes of the tree were classified based on source composition of the CGF subtype (MH, mixed host; RE, raccoon exclusive; REW, raccoon and environmental water; SSL, swine and swine lagoon). A large proportion (~97%) of Raccoon isolates from this study are found in clades A, B, and C. Both clade A, which is largely composed of RE and REW subtypes, and clade C, which consists entirely of RE subtypes, appear to be raccoon-associated niche or host-adapted lineages. Clade B is primarily composed of MH subtypes with a large contribution from agriculture and human clinical sources.

Campylobacter Strain Dynamics in Raccoons Include Both Transient and Longer-Term Carriage Within Individual Animals

A total of 468 samplings (43%; n = 468/1,096) involved consecutive recapture events involving the same animal (**Figure 2**), with a majority (77%; n = 361/468) occurring within the same sampling year. The positive rate for *Campylobacter* was 67% (n = 242/361) and 69% (n = 74/107) among recaptures in the same and different sampling years, respectively (**Figure 2**). Among recaptures within the same sampling year, 58% (n = 209/361) reflected a *Campylobacter* status change, with either animals that acquired or lost *Campylobacter* (n = 139), and animals that acquired a different subtype (n = 70) between recaptures. This rate was 67% among recapture events in different sampling years (n = 72/107), including 52 cases of animals acquiring or losing *Campylobacter* between recaptures

TABLE 2 | Host-source distributions from the C3CGFb for each of the clades observed in raccoon and swine manure pit isolates.

Clade	CGF subtypes	C3CGFdb source distribution								This study		Total isolates
		Human clinical	Cattle	Poultry	Other	Swine	Wild bird	Wild mammals	Water	Raccoon	Manure pit	
A	38	8	2	22	0	0	0	6	121	302	0	461
B	29	306	171	1,163	33	5	11	15	237	177	0	2,118
C	13	0	0	0	0	0	0	1	0	84	0	85
D	6	1	0	0	1	0	1	0	2	5	3	13
E	1	0	0	0	0	0	0	0	0	1	0	1
F	18	60	107	319	16	104	2	0	19	1	26	654
G	2	0	0	0	0	0	0	0	0	2	0	2
H	7	443	123	731	15	1	0	2	5	9	0	1,329

Clade C was exclusively composed of raccoon isolates, while clade A was largely of raccoon and environmental water origin. Clades B and H showed broad source distributions and have been associated with "generalist" lineages. Clade G, a C. coli group, also showed a broad source distribution and included all C. coli swine lagoon isolates.

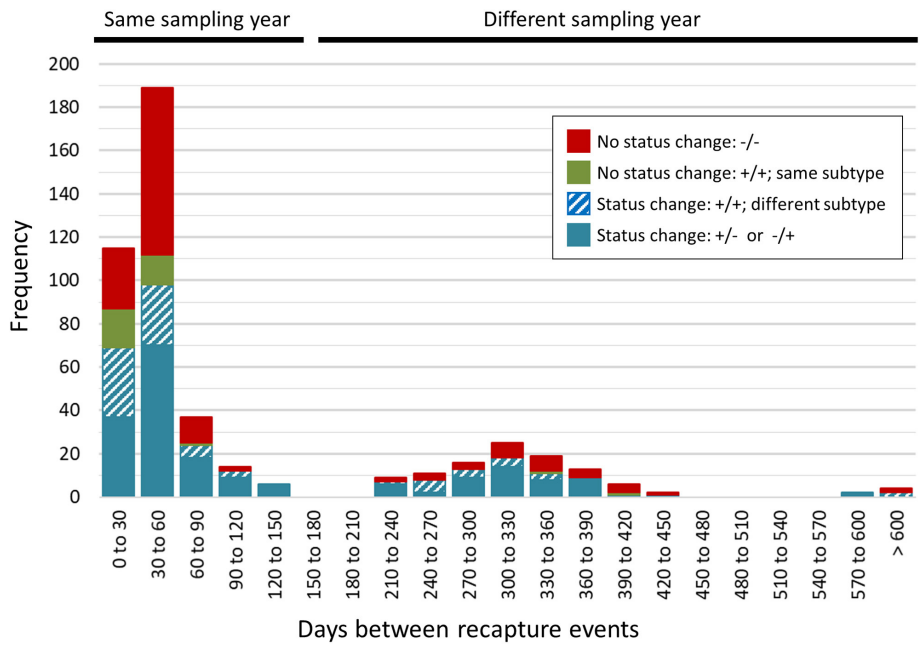

FIGURE 2 | Rapid changes in *Campylobacter* status in a raccoon population on conservation and swine farm sites in southwest Ontario, Canada. *Campylobacter* culture status was examined for consecutive recapture events involving the same animal ($n = 468$). A majority of consecutive recapture events (77%; $n = 361$) occurred within the same sampling year and 67% ($n = 242/361$) yielded a *Campylobacter* positive result. The positive rate among recapture events in different sampling years was 69% ($n = 74/107$). Overall, 89% of recapture events that involved a *Campylobacter* positive result ($n = 281/316$) reflected a *Campylobacter* status change, with either animals that tested positive after previously testing negative or vice-versa ($n = 191$), and animals testing positive in both cases but that shed a different subtype ($n = 90$). These strain dynamics are consistent with the rapid turnover of strains in this raccoon population.

and 20 cases of animals acquiring a different subtype. Overall, 60% ($n = 281/468$) of recapture events reflected a change in *Campylobacter* status, although the rate rises to 89% ($n = 281/316$) when excluding recaptures in which the animal tested negative on both occasions ($n = 152$). There were 125 instances of consecutive positive results, with a median of 35 days between recaptures (minimum = 25 days, maximum = 617 days). Of these, 40.0% ($n = 50/125$) occurred within a window of 0–30 days (i.e., short), an additional 33.6% ($n = 42/125$) occurred in a window of 31–60 days (i.e., intermediate), and 26.4% ($n = 33/125$) occurred in a window of >60 days (i.e., long), which included 22 recaptures that occurred on different sampling years. Overall, 72.0% of consecutive recaptures that were positive on both occasions ($n = 90/125$) yielded a different subtype on consecutive samplings. Among the 28% of consecutive recaptures yielding the same subtype ($n = 35/125$), we observed a decreasing proportion of matching subtypes as the time between sampling events increased (**Figure 3**). Furthermore, when examined in the context of ecological range, we observed that a larger proportion of recaptures in which the same subtype was consecutively isolated involved raccoon-associated subtypes (i.e., categories RE and REW) compared to MH subtypes

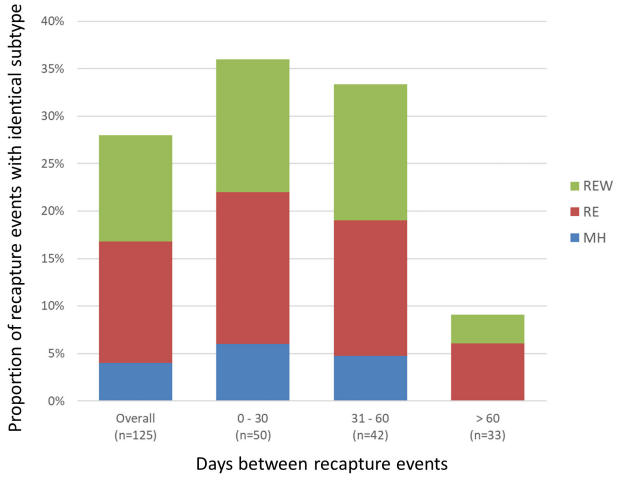

FIGURE 3 | Short- vs. long-term colonization with *Campylobacter* in a raccoon population on conservation and swine farm sites in southwest Ontario, Canada. Analysis of consecutive *Campylobacter* positive recapture events yielding an identical subtype indicates that as the duration between captures increased beyond 60 days, there is a large decrease in the number of cases where the same subtype was observed, suggesting that most animals are only transiently colonized. Among the small proportion of recapture events consistent with prolonged colonization (i.e., consecutive and temporally separated *Campylobacter*-positive recapture events yielding the same subtype), results indicate that these are more likely to involve raccoon-adapted subtypes from RE and REW categories.

(Overall: 30/35; 0–30 days: 15/18; 31–60 days: 12/14; and >60 days: 3/3). Among recapture events yielding changes in *Campylobacter* status on consecutive observations, the ratio of instances of strain acquisition to strain loss was similar across the three major raccoon-containing clades (A: 126/90; B: 66/46; C: 41/24 and across the various ERCs (MH: 73/57; RE: 80/53; REW: 87/56), all of which were similar to the overall ratio of acquisition-to-loss ($n = 240/166$).

DISCUSSION

The prevalence of *Campylobacter* spp. in raccoon fecal samples in this study was 46%, which is consistent with what was observed in a previous study from the same region of southwestern Ontario (41%) (33). Indeed, given the practical limitations imposed by potential delays in sample processing (3–11 days) due to shipping of fecal swabs from the study site (Guelph, Ontario) to the laboratory where microbiological work was carried out (Lethbridge, Alberta), it is very likely that our prevalence estimates underestimate true prevalence rates in this raccoon population. By contrast, studies from Japan and New York found only 1.3 and 6% of raccoons carried *Campylobacter*, respectively (32, 44). There are a limited number of studies systematically examining *Campylobacter* in raccoons or other medium sized mammals. Many studies instead rely on convenience-based sampling methodology, for example, intakes into a wildlife rehabilitation center (20, 45). The Grand River watershed in southern Ontario is heavily impacted by mixed agricultural activities, with farms making up ∼75% of the watershed (46).

In this study, we examined raccoons circulating in a range that included several swine farms and more natural environments in order to investigate *Campylobacter* prevalence, genetic diversity, and strain dynamics in this wild animal population. Significant genetic diversity was observed among raccoon isolates collected in this study, with 96 distinct CGF subtypes and at least eight major lineages observed in this population. Interestingly, there was a distinct lack of overlap in CGF subtypes observed in raccoons trapped at swine farm sites and samples obtained at those farms (i.e., manure pit samples) despite the high rates of *Campylobacter* recovery in these animals. Swine are known to preferentially harbor *C. coli*, which was recovered from nearly all manure pit samples analyzed. The near absence of *C. coli* in raccoons from this study was unexpected, as some level of *C. coli* exposure would be expected to take place in the swine-farm environment. Nonetheless, our findings are consistent with overall trends in the C3GFdb, in that of nearly 300 subtypes that have been observed in either raccoons or swine, only seven minor subtypes have included isolates recovered from both species. Other studies investigating interactions between wildlife and swine farms have shown little evidence of shared *Campylobacter* subtypes between farm fecal/manure isolates and small and medium sized wild mammals (such as mice, rats, badger, fox) (11, 47, 48). The swine in this study were housed indoors, which likely prevented raccoons from coming into direct contact with the animals or fresh swine feces. Furthermore, swine fecal wastes are generally managed in a more confined manner (e.g., manure pits) compared to other livestock such as cattle. Lastly, because raccoons have wide-ranging habitats, it is possible that raccoons trapped at swine farm sites may not have routinely used these areas to forage, thereby decreasing their exposure. Thus, there exist possible barriers (i.e., biological, physical, behavioral) that may limit the transmission of *C. coli* between swine and raccoons.

During the course of this longitudinal study, a significant proportion of samples represented cases in which the same animal was recaptured and these data were used to examine *Campylobacter* strain dynamics within individual animals, including patterns of short-, intermediate-, and long-term *Campylobacter* carriage and their shedding. A majority of recapture events (60%) yielded differences in *Campylobacter*-status, including cases in which the animal appeared to have acquired or lost *Campylobacter* between recaptures (40%), and cases in which the animal tested positive in both occasions but where we observed a difference in subtype (19%). Overall shifts in *Campylobacter* status increased to 89% if excluding recaptures in which the animal tested negative in both occasions. Moreover, we observed instances of *Campylobacter*-positive animals that appeared to revert to negative status on subsequent recaptures in as few as 25 days, with 18 instances occurring within 30 days. This would suggest that although *Campylobacter* prevalence in this raccoon population is high, carriage and shedding is likely transient, with the majority of raccoons harboring *C. jejuni* for only short periods of time (≤1 month). We also observed significant strain displacement among animals that tested positive for *Campylobacter* on consecutive recaptures,

with a different subtype observed in 72% of cases. Moreover, although we selected 1,555 isolates for subtyping from among the 508 fecal swabs that tested positive for *Campylobacter*, a majority of samples (87.2%) yielded a single subtype. Taken together, these data suggest that raccoons readily acquire and lose *Campylobacter*, with rapid turnover of strains among animals that remained *Campylobacter*-positive on consecutive samplings. Nonetheless, it is important to note possible confounding factors that could yield data consistent with transient carriage. These include limitations with microbiological and molecular subtyping methods (i.e., limit of detection/recovery of isolates leading to culture-negative samples or limiting the isolation of multiple strains from a single sample).

Our data yielded a small proportion of instances in which consecutive recaptures were *Campylobacter* positive and yielded the same subtype. Although these tended to be recapture events on consecutive months, a small number of cases included recaptures with significant temporal separation, up to a length of 394 days. It is unclear whether these represent ongoing colonization or re-infection with the same subtype; whole-genome sequence (WGS) analysis of these isolates is likely to shed light on this issue since the much higher discriminatory power of WGS-based subtyping approaches could help differentiate between these two types of events.

Our analysis of host source metadata from the Canadian *Campylobacter* CGF database (C3GFdb) revealed that the *C. jejuni* population found in raccoons consisted primarily of subtypes with a strong raccoon association and subtypes with a mixed-host association. These were primarily distributed among three major clades that included the majority of raccoon isolates in this study. Nearly one-third of raccoon isolates had subtypes that were novel to the C3GFdb, with many of these forming a clade that appears to be exclusive to raccoons. Most remaining isolates from raccoon-exclusive subtypes could be found in a clade that was otherwise composed primarily of subtypes that had previously been observed only among isolates from surface water samples. Host-adapted subtypes in wild animals and surface water have been described in previous studies (49–51). Although Stabler et al. (8) have previously described an apparent water and wildlife *C. jejuni* clade, this is the first report of *Campylobacter* subtypes that appear to be uniquely host-adapted to raccoons. It is noteworthy that the majority of events in which animals were positive for the same CGF subtype on consecutive recaptures (i.e., consistent with longer-term colonization) involved raccoon-adapted subtypes.

In contrast to raccoon-adapted clades, 78% of isolates in clade B, which contained approximately 30% of raccoon isolates in this study, were from subtypes with mixed-host association. Mixed-source genotypes have been well-described and typically include representatives from Clonal Complexes (CCs) described as 'generalists' including ST-45, ST-21, and ST-48 (52–55). These CCs are highly prevalent worldwide, known for their broad host distribution, including livestock, and high burden of human illness. During the course of validating CGF (36), we established correlations between specific CGF subtypes and corresponding CCs and have subsequently been able to refine these based on *in silico* subtyping predictions from WGS data (40, 56). Notably, many CGF subtypes within clade B have been characterized as belonging to CC ST-45, including CGF subtype 0926.002.001, which is the third most prevalent genotype in the C3GFdb and ranks sixth in terms of number of human clinical cases associated with it. Although clade H only comprised a small proportion of raccoon isolates in this study (1.6%), it is noteworthy because CGF subtypes from within clade H have been shown to belong to CCs ST-21 and ST-48 (57). Moreover, it includes CGF subtypes 0044.003.001 and 0083.001.002, which are among the most prevalent in Canada and rank second and third in terms of number of associated human clinical cases, respectively. Because of their synanthropic behavior, the potential for acquisition of clinically relevant *Campylobacter* subtypes by raccoons via the same routes of exposure as humans cannot be ruled out. Our data suggest that the high *Campylobacter* rates observed in this wild raccoon population are likely due to environmental and ecological factors, including high rates of mixed agriculture activities, which allow for sustained and consistent *Campylobacter* exposure to agriculture-associated genotypes strongly implicated in human cases of campylobacteriosis.

CONCLUSIONS

Prevalence of *Campylobacter* in the raccoon population under study, which is native to the Grand River Watershed in southwestern Ontario, Canada, was found to be much higher than what has been previously reported for other populations of small to medium-sized wild mammals. This high prevalence was observed despite evidence suggesting that individual animals were only transiently colonized, with a majority of raccoons harboring *C. jejuni* for only short periods of time (i.e., $\leq$1 month). Our data show significant genotypic flux within individual animals, which is consistent with the constant acquisition, loss, and replacement of strains, and suggest that this raccoon population is constantly exposed to a wide range of circulating but endemic strains. This may be due to ecological factors within the Grand River Watershed, where agriculture and human activities may give rise to a wide variety of *Campylobacter* sources. Although raccoons appear to be poor hosts for *C. coli* strains typically observed in swine, many of the *C. jejuni* subtypes observed in this raccoon population have been previously associated with agricultural sources (e.g., chickens, cattle) and human illness. Interestingly, raccoons were also found to carry *C. jejuni* subtypes within two clades that appear to be genetically distinct from genotypes recovered from humans and food animals and that appear to represent raccoon-associated niche- or host-adapted strains; the potential risk to human health from these strains remains unknown. Nevertheless, the high proportion of clinically-relevant generalist *Campylobacter* subtypes found in raccoon fecal samples suggests that raccoons likely act as transient vectors of *Campylobacter* and may play a role in the transmission of strains at the interface of rural, urban, and more natural environments.

DATA AVAILABILITY STATEMENT

The raw data supporting the conclusions of this article will be made available by the authors, without undue reservation, to any qualified researcher.

ETHICS STATEMENT

The animal study was reviewed and approved by Animal Care Committee at the University of Guelph.

AUTHOR CONTRIBUTIONS

SM led all aspects of laboratory and downstream analyses and drafted the manuscript. BH participated in laboratory and downstream analyses and assisted with manuscript preparation. KB participated in study design and fieldwork and assisted with manuscript preparation. VG contributed to study design and manuscript preparation. CJ conceived of the study, participated in its design and coordination, and assisted with manuscript preparation. ET participated in study design and coordination, contributed to downstream analyses, and manuscript preparation.

FUNDING

Financial support for this work was provided through the Public Health Agency of Canada and the Government of Canada's Genomics Research and Development Initiative (ET), the National Science and Engineering Research Council (CJ). KB received support through the United States Department of Agriculture and an Ontario Graduate Scholarship. The funders had no role in study design, data collection and analysis, decision to publish, or preparation of the manuscript.

ACKNOWLEDGMENTS

The authors would like to thank Erin Harkness, Samantha Allen, Samantha Kagan, and Mary Thompson for assisting with field data collection; Bryan Bloomfield for collecting manure pit samples and maintaining relations with landowners; Tami Harvey and Barbara Jefferson for submitting lab samples, and Quentin Papach for assisting with the development of a Microsoft Access database. The authors would also like to thank Morgan Chow, Madeline Tsoi, and Emily Che for technical assistance in microbiological work and the many contributors to the Canadian *Campylobacter* Comparative Genomic Fingerprinting Database (C3GFdb), without whom this work would not have been possible.

SUPPLEMENTARY MATERIAL

The Supplementary Material for this article can be found online at: https://www.frontiersin.org/articles/10.3389/fvets.2020.00027/full#supplementary-material

REFERENCES

1. Thomas MK, Murray R, Flockhart L, Pintar K, Pollari F, Fazil A, et al. Estimates of the burden of foodborne illness in Canada for 30 specified pathogens and unspecified agents, circa 2006. *Foodborne Pathog Dis.* (2013) 10:639–48. doi: 10.1089/fpd.2012.1389
2. Kaakoush NO, Castaño-Rodríguez N, Mitchell HM, Man SM. Global epidemiology of *Campylobacter* infection. *Clin Microbiol Rev.* (2015) 28:687–720. doi: 10.1128/CMR.00006-15
3. Lastovica AJ. Emerging *Campylobacter* spp.: the tip of the iceberg. *Clin Microbiol Newsl.* (2006) 28:49–56. doi: 10.1016/j.clinmicnews.2006.03.004
4. Nauta M, Hill A, Rosenquist H, Brynestad S, Fetsch A, van der Logt P, et al. A comparison of risk assessments on *Campylobacter* in broiler meat. *Int J Food Microbiol.* (2009) 129:107–23. doi: 10.1016/j.ijfoodmicro.2008.12.001
5. Skarp CPA, Hänninen ML, Rautelin HIK. Campylobacteriosis: the role of poultry meat. *Clin Microbiol Infect.* (2016) 22:103–9. doi: 10.1016/j.cmi.2015.11.019
6. Pintar KDM, Thomas KM, Christidis T, Otten A, Nesbitt A, Marshall B, et al. A comparative exposure assessment of *Campylobacter* in Ontario, Canada. *Risk Anal.* (2017) 37:677–715. doi: 10.1111/risa.12653
7. Suzuki H, Yamamoto S. *Campylobacter* contamination in retail poultry meats and by-products in the world: a literature survey. *J Vet Med Sci.* (2009) 71:255–61. doi: 10.1292/jvms.71.255
8. Stabler RA, Larsson JT, Al-Jaberi S, Nielsen EM, Kay E, Tam CC, et al. Characterization of water and wildlife strains as a subgroup of *Campylobacter jejuni* using DNA microarrays. *Environ Microbiol.* (2013) 15:2371–83. doi: 10.1111/1462-2920.12111
9. Jokinen C, Edge TA, Ho S, Koning W, Laing C, Mauro W, et al. Molecular subtypes of *Campylobacter* spp., *Salmonella enterica*, and *Escherichia coli* O157:H7 isolated from faecal and surface water samples in the Oldman River watershed, Alberta, Canada. *Water Res.* (2011) 45:1247–57. doi: 10.1016/j.watres.2010.10.001
10. Ravel A, Pintar K, Nesbitt A, Pollari F. Non food-related risk factors of campylobacteriosis in Canada: a matched case-control study. *BMC Public Health.* (2016) 16:1016. doi: 10.1186/s12889-016-3679-4
11. Petersen L, Nielsen EM, Engberg J, On SL, Dietz HH. Comparison of genotypes and serotypes of *Campylobacter jejuni* isolated from Danish wild mammals and birds and from broiler flocks and humans. *Appl Environ Microbiol.* (2001) 67:3115–21. doi: 10.1128/AEM.67.7.3115-3121.2001
12. Sippy R, Sandoval-Green CMJ, Sahin O, Plummer P, Fairbanks WS, Zhang Q, et al. Occurrence and molecular analysis of *Campylobacter* in wildlife on livestock farms. *Vet Microbiol.* (2012) 157:369–75. doi: 10.1016/j.vetmic.2011.12.026
13. Sasaki Y, Goshima T, Mori T, Murakami M, Haruna M, Ito K, et al. Prevalence and antimicrobial susceptibility of foodborne bacteria in wild boars (*Sus scrofa*) and wild deer (*Cervus nippon*) in Japan. *Foodborne Pathog Dis.* (2013) 10:985–91. doi: 10.1089/fpd.2013.1548
14. Carbonero A, Paniagua J, Torralbo A, Arenas-Montes A, Borge C, García-Bocanegra I. *Campylobacter* infection in wild artiodactyl species from southern Spain: Occurrence, risk factors and antimicrobial susceptibility. *Comp Immunol Microbiol Infect Dis.* (2014) 37:115–21. doi: 10.1016/j.cimid.2014.01.001
15. Kwan PSL, Barrigas M, Bolton FJ, French NP, Gowland P, Kemp R, et al. Molecular epidemiology of *Campylobacter jejuni* populations in dairy cattle, wildlife, and the environment in a farmland area. *Appl Environ Microbiol.* (2008) 74:5130–8. doi: 10.1128/AEM.02198-07
16. French NP, Midwinter A, Holland B, Collins-Emerson J, Pattison R, Colles F, et al. Molecular epidemiology of *Campylobacter jejuni* isolates from wild-bird fecal material in children's playgrounds. *Appl Environ Microbiol.* (2009) 75:779–83. doi: 10.1128/AEM.01979-08

17. Hudson SJ, Lightfoot NF, Coulson JC, Russell K, Sisson PR, Sobo AO. Jackdaws and magpies as vectors of milkborne human *Campylobacter* infection. *Epidemiol Infect.* (1991) 107:363–72. doi: 10.1017/S0950268800049001
18. Riordan T, Humphrey TJ, Fowles A. A point source outbreak of *Campylobacter* infection related to bird-pecked milk. *Epidemiol Infect.* (1993) 110:261–5. doi: 10.1017/S0950268800068187
19. Gardner TJ, Fitzgerald C, Xavier C, Klein R, Pruckler J, Stroika S, et al. Outbreak of campylobacteriosis associated with consumption of raw peas. *Clin Infect Dis.* (2011) 53:26–32. doi: 10.1093/cid/cir249
20. Saunders S, Smith K, Schott R, Dobbins G, Scheftel J. Outbreak of campylobacteriosis associated with raccoon contact at a wildlife rehabilitation centre, Minnesota, 2013. *Zoonoses Public Health.* (2016) 64:222–7. doi: 10.1111/zph.12300
21. Cody AJ, McCarthy ND, Bray JE, Wimalarathna HML, Colles FM, Jansen van Rensburg MJ, et al. Wild bird-associated *Campylobacter jejuni* isolates are a consistent source of human disease, in Oxfordshire, United Kingdom. *Environ Microbiol Rep.* (2015) 7:782–8. doi: 10.1111/1758-2229.12314
22. Andrés S, Vico JP, Garrido V, Grilló MJ, Samper S, Gavín P, et al. Epidemiology of subclinical salmonellosis in wild birds from an area of high prevalence of pig salmonellosis: phenotypic and genetic profiles of *Salmonella* isolates. *Zoonoses and Public Health.* (2013) 60:355–65. doi: 10.1111/j.1863-2378.2012.01542.x
23. Hald B, Skov MN, Nielsen EM, Rahbek C, Madsen JJ, Wainø M, et al. *Campylobacter jejuni* and *Campylobacter coli* in wild birds on Danish livestock farms. *Acta Vet Scand.* (2016) 58:11. doi: 10.1186/s13028-016-0192-9
24. Greig J, Rajić A, Young I, Mascarenhas M, Waddell L, LeJeune J. A scoping review of the role of wildlife in the transmission of bacterial pathogens and antimicrobial resistance to the food chain. *Zoonoses Public Health.* (2015) 62:269–84. doi: 10.1111/zph.12147
25. Rosatte R, Ryckman M, Ing K, Proceviat S, Allan M, Bruce L, et al. Density, movements, and survival of raccoons in Ontario, Canada: implications for disease spread and management. *J Mammal.* (2010) 91:122–35. doi: 10.1644/08-MAMM-A-201R2.1
26. Jardine CM, Janecko N, Allan M, Boerlin P, Chalmers G, Kozak G, et al. Antimicrobial resistance in *Escherichia coli* isolates from raccoons (*Procyon lotor*) in southern Ontario, Canada. *Appl Environ Microbiol.* (2012) 78:3873–9. doi: 10.1128/AEM.00705-12
27. Bondo KJ, Weese JS, Rouseau J, Jardine CM. Longitudinal study of *Clostridium difficile* shedding in raccoons on swine farms and conservation areas in Ontario, Canada. *BMC Vet Res.* (2015) 11:254. doi: 10.1186/s12917-015-0563-x
28. Bondo KJ, Pearl DL, Janecko N, Boerlin P, Reid-Smith RJ, Parmley J, et al. Epidemiology of antimicrobial resistance in *Escherichia coli* isolates from raccoons (*Procyon lotor*) and the environment on swine farms and conservation areas in Southern Ontario. *PLoS ONE.* (2016) 11:e0165303. doi: 10.1371/journal.pone.0165303
29. Bondo KJ, Pearl DL, Janecko N, Boerlin P, Reid-Smith RJ, Parmley J, et al. Impact of season, demographic and environmental factors on *Salmonella* occurrence in raccoons (*Procyon lotor*) from swine farms and conservation areas in southern Ontario. *PLoS ONE.* (2016) 11:e0161497. doi: 10.1371/journal.pone.0161497
30. Hirsch BT, Prange S, Hauver SA, Gehrt SD. Patterns of latrine use by raccoons (*Procyon lotor*) and implication for *Baylisascaris procyonis* transmission. *J Wildl Dis.* (2014) 50:243–9. doi: 10.7589/2013-09-251
31. Bondo KJ, Pearl DL, Janecko N, Boerlin P, Reid-Smith RJ, Parmley J, et al. Epidemiology of *Salmonella* on the paws and in the faeces of free-ranging raccoons (*Procyon Lotor*) in southern Ontario, Canada. *Zoonoses Public Health.* (2016) 63:303–10. doi: 10.1111/zph.12232
32. Lee K, Iwata T, Nakadai A, Kato T, Hayama S, Taniguchi T, et al. Prevalence of *Salmonella*, *Yersinia* and *Campylobacter* spp. in feral raccoons (*Procyon lotor*) and masked palm civets (*Paguma larvata*) in Japan. *Zoonoses and Public Health.* (2011) 58:424–31. doi: 10.1111/j.1863-2378.2010.01384.x
33. Viswanathan M, Pearl DL, Taboada EN, Parmley EJ, Mutschall S, Jardine CM. Molecular and statistical analysis of *Campylobacter* spp. and antimicrobial-resistant *Campylobacter* carriage in wildlife and livestock from Ontario farms. *Zoonoses Public Health.* (2016) 64:194–203. doi: 10.1111/zph.12295
34. Jokinen CC, Koot JM, Carrillo CD, Gannon VPJ, Jardine CM, Mutschall SK, et al. An enhanced technique combining pre-enrichment and passive filtration increases the isolation efficiency of *Campylobacter jejuni* and *Campylobacter coli* from water and animal fecal samples. *J Microbiol Methods.* (2012) 91:506–13. doi: 10.1016/j.mimet.2012.09.005
35. Denis M, Soumet C, Rivoal K, Ermel G, Blivet D, Salvat G, et al. Development of a m-PCR assay for simultaneous identification of *Campylobacter jejuni* and *C. coli*. *Lett Appl Microbiol.* (1999) 29:406–10. doi: 10.1046/j.1472-765X.1999.00658.x
36. Taboada EN, Ross SL, Mutschall SK, MacKinnon JM, Roberts MJ, Buchanan CJ, et al. Development and validation of a comparative genomic fingerprinting method for high-resolution genotyping of *Campylobacter jejuni*. *J Clin Microbiol.* (2012) 50:788–97. doi: 10.1128/JCM.00669-11
37. R Core Team. *R: A Language and Environment for Statistical Computing*. (2012). Available online at: http://www.R-project.org (accessed April, 2019).
38. Wickham H. *tidyverse*. (2017). Available online at: https://cran.r-project.org/web/packages/tidyverse/index.html (accessed April, 2019).
39. Yu G, Smith DK, Zhu H, Guan Y, Lam TTY. ggtree: an r package for visualization and annotation of phylogenetic trees with their covariates and other associated data. *Methods Ecol Evol.* (2017) 8:28–36. doi: 10.1111/2041-210X.12628
40. Kruczkiewicz P, Mutschall S, Barker D, Thomas JE, Van Domselaar GH, Gannon VP, et al. MIST: a tool for rapid *in silico* generation of molecular data from bacterial genome sequences. In: *Proc 4th Int Conf Bioinforma Models Methods Algorithms*. Barcelona (2013). p. 316–23.
41. Simpson EH. Measurement of diversity. *Nature.* (1949) 163:688. doi: 10.1038/163688a0
42. Grundmann H, Hori S, Tanner G. Determining confidence intervals when measuring genetic diversity and the discriminatory abilities of typing methods for microorganisms. *J Clin Microbiol.* (2001) 39:4190–2. doi: 10.1128/JCM.39.11.4190-4192.2001
43. Sharpe D. Your Chi-square test is statistically significant: now what? *Res Eval.* (2015) 20:1–10. doi: 10.12968/prps.2015.Sup170.15
44. Rainwater KL, Marchese K, Slavinski S, Humberg LA, Dubovi EJ, Jarvis JA, et al. Health survey of free-ranging raccoons (*Procyon lotor*) in central park, New York, New York, USA: implications for human and domestic animal health. *J Wildl Dis.* (2017) 53:272–84. doi: 10.7589/2016-05-096
45. Hamir AN, Franklin S, Wesley IV, Sonn RJ. *Campylobacter jejuni* and *Arcobacter* species associated with intussusception in a raccoon (*Procyon lotor*). *Vet Rec.* (2004) 155:338–40. doi: 10.1136/vr.155.11.338
46. GRCA. *Grand River Watershed Characterization Report – Executive Summary*. (2008). Available online at: https://www.sourcewater.ca/en/source-protection-areas/resources/Documents/Grand/Grand_Reports_Characterization_ES.pdf (accessed November 9, 2019).
47. Jensen AN, Dalsgaard A, Baggesen DL, Nielsen EM. The occurrence and characterization of *Campylobacter jejuni* and *C. coli* in organic pigs and their outdoor environment. *Vet Microbiol.* (2006) 116:96–105. doi: 10.1016/j.vetmic.2006.03.006
48. Meerburg BG, Jacobs-Reitsma WF, Wagenaar JA, Kijlstra A. Presence of *Salmonella* and *Campylobacter* spp. in wild small mammals on organic farms. *Appl Environ Microbiol.* (2006) 72:960–2. doi: 10.1128/AEM.72.1.960-962.2006
49. Sheppard SK, Colles FM, McCarthy ND, Strachan NJC, Ogden ID, Forbes KJ, et al. Niche segregation and genetic structure of *Campylobacter jejuni* populations from wild and agricultural host species. *Mol Ecol.* (2011) 20:3484–90. doi: 10.1111/j.1365-294X.2011.05179.x
50. Griekspoor P, Colles FM, McCarthy ND, Hansbro PM, Ashhurst-Smith C, Olsen B, et al. Marked host specificity and lack of phylogeographic population structure of *Campylobacter jejuni* in wild birds. *Mol Ecol.* (2013) 22:1463–72. doi: 10.1111/mec.12144
51. Weis AM, Storey DB, Taff CC, Townsend AK, Huang BC, Kong NT, et al. Genomic comparisons and zoonotic potential of *Campylobacter* between birds, primates, and livestock. *Appl Environ Microbiol.* (2016) 82:7165–75. doi: 10.1128/AEM.01746-16
52. Gripp E, Hlahla D, Didelot X, Kops F, Maurischat S, Tedin K, et al. Closely related *Campylobacter jejuni* strains from different sources reveal a generalist rather than a specialist lifestyle. *BMC Genom.* (2011) 12:584. doi: 10.1186/1471-2164-12-584
53. Sheppard SK, Cheng L, Méric G, de Haan CPA, Llarena AK, Marttinen P, et al. Cryptic ecology among host generalist *Campylobacter jejuni* in domestic animals. *Mol Ecol.* (2014) 23:2442–51. doi: 10.1111/mec.12742
54. Dearlove BL, Cody AJ, Pascoe B, Meric G, Wilson DJ, Sheppard SK. Rapid host switching in generalist *Campylobacter* strains erodes the signal for

tracing human infections. *ISME J.* (2016) 10:721–9. doi: 10.1038/ismej.2015.149

55. Llarena AK, Zhang J, Vehkala M, Välimäki N, Hakkinen M, Hänninen ML, et al. Monomorphic genotypes within a generalist lineage of *Campylobacter jejuni* show signs of global dispersion. *Microb Genom.* (2016) 2:e000088. doi: 10.1099/mgen.0.000088
56. Carrillo CD, Kruczkiewicz P, Mutschall S, Tudor A, Clark C, Taboada EN. A framework for assessing the concordance of molecular typing methods and the true strain phylogeny of *Campylobacter jejuni* and *C. coli* using draft genome sequence data. *Front Cell Infect Microbiol.* (2012) 2:57. doi: 10.3389/fcimb.2012.00057
57. Clark CG, Taboada E, Grant CCR, Blakeston C, Pollari F, Marshall B, et al. Comparison of molecular typing methods useful for detecting clusters of *Campylobacter jejuni* and *C. coli* isolates through routine surveillance. *J Clin Microbiol.* (2012) 50:798–809. doi: 10.1128/JCM.05733-11

Conflict of Interest: The authors declare that the research was conducted in the absence of any commercial or financial relationships that could be construed as a potential conflict of interest.

Citation: Mutschall SK, Hetman BM, Bondo KJ, Gannon VPJ, Jardine CM and Taboada EN (2020) Campylobacter jejuni Strain Dynamics in a Raccoon (Procyon lotor) Population in Southern Ontario, Canada: High Prevalence and Rapid Subtype Turnover. Front. Vet. Sci. 7:27. doi: 10.3389/fvets.2020.00027

frontiers in Microbiology

ORIGINAL RESEARCH
published: 06 March 2020
doi: 10.3389/fmicb.2020.00344

Contribution of Epithelial Apoptosis and Subepithelial Immune Responses in *Campylobacter jejuni*-Induced Barrier Disruption

*Eduard Butkevych, Fábia Daniela Lobo de Sá, Praveen Kumar Nattramilarasu and Roland Bücker**

Institute of Clinical Physiology/Nutritional Medicine, Medical Department, Division of Gastroenterology, Infectiology and Rheumatology, Charité-Universitätsmedizin Berlin, Berlin, Germany

OPEN ACCESS

Edited by:
Ozan Gundogdu,
University of London, United Kingdom

Reviewed by:
Ximin Zeng,
The University of Tennessee, Knoxville, United States
Salah Amasheh,
Freie Universität Berlin, Germany
Abigail Betanzos,
National Polytechnic Institute, Mexico

***Correspondence:**
Roland Bücker
roland-felix.buecker@charite.de

Specialty section:
This article was submitted to Infectious Diseases, a section of the journal Frontiers in Microbiology

Received: *19 November 2019*
Accepted: *17 February 2020*
Published: *06 March 2020*

Citation:
Butkevych E, Lobo de Sá FD, Nattramilarasu PK and Bücker R (2020) Contribution of Epithelial Apoptosis and Subepithelial Immune Responses in Campylobacter jejuni-Induced Barrier Disruption. Front. Microbiol. 11:344. doi: 10.3389/fmicb.2020.00344

Campylobacter jejuni is a widespread zoonotic pathogen and the leading bacterial cause of foodborne gastroenteritis in humans. Previous infection studies showed disruption of intercellular contacts, induction of epithelial apoptosis, and immune activation, all three contributing to intestinal barrier dysfunction leading to diarrhea. The present study aims to determine the impact of subepithelial immune cells on intestinal barrier dysfunction during *Campylobacter jejuni* infection and the underlying pathological mechanisms. Infection was performed in a co-culture of confluent monolayers of the human colon cell line HT-29/B6-GR/MR and THP-1 immune cells. Twenty-two hours after infection, transepithelial electrical resistance (TER) was decreased by 58 ± 6% compared to controls. The infection resulted in an increase in permeability for fluorescein (332 Da; 4.5-fold) and for FITC-dextran (4 kDa; 3.5-fold), respectively. In contrast, incubation of the co-culture with the pan-caspase inhibitor Q-VD-OPh during the infection resulted in a complete recovery of the decrease in TER and a normalization of flux values. Fluorescence microscopy showed apoptotic fragmentation in infected cell monolayers resulting in a 5-fold increase of the apoptotic ratio, accompanied by an increased caspase-3 cleavage and caspase-3/7 activity, which both were not present after Q-VD-OPh treatment. Western blot analysis revealed increased claudin-1 and claudin-2 protein expression. Inhibition of apoptosis induction did not normalize these tight junction changes. TNFα concentration was increased during the infection in the co-culture. In conclusion, *Campylobacter jejuni* infection and the consequent subepithelial immune activation cause intestinal barrier dysfunction mainly through caspase-3-dependent epithelial apoptosis. Concomitant tight junction changes were caspase-independent. Anti-apoptotic and immune-modulatory substances appear to be promising agents for treatment of campylobacteriosis.

Keywords: apoptosis, caspase, epithelial barrier, tumor necrosis factor alpha, *Campylobacter*, epithelial cell, immune cell co-culture, tight junction

INTRODUCTION

Diarrheal disease is a major cause of morbidity and mortality worldwide. *Campylobacter jejuni* (*C. jejuni*) is a frequent commensal bacterium in poultry and wild birds and the leading cause of bacterial diarrhea in humans. As a zoonotic pathogen being highly contagious via the fecal-oral route, *C. jejuni* infection occurs by consumption of raw or undercooked meat, raw dairy products or contaminated water. The symptoms of the campylobacteriosis vary from fever, aches, and dizziness to severe manifestations with abdominal cramps and bloody diarrhea. The disease is self-limiting and antibiotic treatment is only recommended in chronic or severe cases. Nevertheless, *C. jejuni* infection result in very large health costs (Hoffmann et al., 2012; Tam and O'Brien, 2016) and can lead to complications such as post-infectious reactive arthritis and Guillain-Barré syndrome.

The pathogenesis of intestinal barrier dysfunction in the *C. jejuni* infection is not completely understood. During the infection, bacteria adhere to the mucus and transmigrate through the mucus layer and the epithelium (Backert et al., 2013) by invasion of enterocytes (Konkel et al., 1999; Song et al., 2004) or paracellularly with no changes in epithelial integrity (Boehm et al., 2012). Subsequent epithelial barrier impairment and activation of the innate inflammatory response was described *in vitro* in human cell cultures (Jones et al., 2003; Hu et al., 2006). These processes are also observed *in vivo* in *C. jejuni* patients (Spiller et al., 2000; Bücker et al., 2018) and in experimentally infected immune-deficient mice (Fox et al., 2004; Bereswill et al., 2011). In the pathogenesis of epithelial barrier dysfunction, apart from immune cell infiltration, tight junction changes, focal leaks and sodium malabsorption, the *C. jejuni*-induced epithelial cell death accompanies the pathological changes in the *C. jejuni*-infected mucosa.

In previous studies on the related bacteria *Arcobacter butzleri* or *Campylobacter concisus*, we were able to show that epithelial cell death and in particular apoptosis induction and not the compromised tight junction alone can lead to the epithelial barrier defect during infection (Bücker et al., 2009; Nielsen et al., 2011).

Two canonical pathways of apoptosis activation have been elucidated - the extrinsic pathway and the intrinsic pathway. Induction of these pathways results in activation of initiator caspases, leading to apoptosis commitment. The extrinsic pathway is triggered by ligand binding to the tumor necrosis factor (TNF) receptor superfamily members. The intrinsic pathway involves the release of caspase-activating factors by mitochondria in response to intracellular injuries such as DNA damage. Initiator caspases are then able to cleave pro−caspases and thus turn on downstream effector pro−caspases -3, -6, and -7, which in turn activate or inhibit target proteins, leading to apoptotic cell death (Delhalle et al., 2003). Apoptosis in the gut is associated with intestinal cell shedding – extrusion of enterocytes at the surface as a result of the migration from the base of the crypt to the top of the epithelium (Bullen et al., 2006). This process promotes a continuous turnover of the intestinal cells achieved without loss of intestinal barrier function.

Epithelial apoptosis is a physiological process, but if stimulated it can exceed the regenerative capacity of the mucosa and the epithelium cannot sustain a proper barrier function. Increased apoptosis causes (i) a reduction of the transepithelial resistance (TER), (ii) loss of water and electrolytes as well as (iii) increased permeability for macromolecules leaking into the lumen (leak-flux diarrhea) or (iv) increased antigen uptake from the lumen into the organism (leaky gut) (Bojarski et al., 2001). Enhanced antigen presentation to the submucosal immune cells, being part of the "leaky gut" phenomenon, reinforces the inflammation. This signifies that the disease enters a vicious circle, with the result that the intestinal tissue damage may rise to extremes.

We hypothesize induction of apoptosis as possible pathomechanism, induced indirectly by cytokines or together with direct *C. jejuni* effectors, affecting cellular viability and epithelial integrity. Although an increase of epithelial apoptosis in *C. jejuni*-infected tissue is evident, its mechanisms and impact on epithelial barrier function have not been elucidated yet and was not taken under consideration of the immune response in an *in vitro* model.

In the present study, we applied a recently described *C. jejuni* infection model in a co-culture of HT-29/B6-GR/MR epithelial and THP-1 immune cells to investigate the mechanisms leading to intestinal barrier disruption during the infection, such as epithelial cell death and tight junction changes, as well as the impact of subepithelial immune activation.

MATERIALS AND METHODS

Co-culture of Human Epithelial Cells and Macrophage-Like Immune Cells

We performed the infection experiments in a co-culture of HT-29/B6-GR/MR epithelial cells and THP-1 immune cells as recently described (Lobo de Sá et al., 2019) with the modification of the filter insert with larger pore size to allow bacterial translocation. Briefly, HT-29/B6-GR/MR cells (Bergann et al., 2011) were cultivated in 25 cm^2 culture flasks for 7 days in RPMI 1640 culture medium (Sigma Aldrich, St. Louis, MO, United States) supplemented with 10% fetal calf serum (FCS; Gibco, Carlsbad, CA, United States), 1% penicillin/streptomycin (Corning, Wiesbaden, Germany), G418 (300 μg/ml; Invitrogen, Carlsbad, CA., United States) and hygromycin B (200 μg/ml; Biochrom GmbH, Berlin, Germany). For experimental use, cells were grown on 3 μm pore size Millicell PCF filters membranes (Merck Millipore, Billerica, MA, United States) at a density of 10^6 cells cm^{-2} with a medium change every 2 days for 9 to 11 days till confluence. On the day of the experiment, the cells were washed three times and incubated for at least 1 h in antibiotic-free culture medium in the presence of 10% heat-inactivated FCS. THP-1 cells were incubated in 12-well plates with the antibiotic-free medium in the presence of 10% heat inactivated FCS and 100 nM phorbol 12-myristate 13-acetate (PMA; Sigma Aldrich, St. Louis, MO, United States; solved in DMSO). After 24 h the culture medium was removed, adhesion and differentiation state of THP-1 cells were controlled under a light microscope. The co-culture was started by placing the PCF filters with HT-29/B6-GR/MR cells

into 12-well plates with adherent THP-1 immune cells at the bottom of the plate (**Figure 1**).

Pharmacological Inhibitors

For the inhibition of apoptosis, we incubated the *C. jejuni* infected and not infected co-culture of HT-29/B6-GR/MR and THP-1 cells with 10 μM Q-VD-OPh hydrate ((3S)-5-(2,6-difluorophenoxy)-3-[[(2S)-3-methyl-1-oxo-2-[(2-quinolinylcarbonyl) amino]butyl]amino] -4-oxo-pentanoic acid hydrate, Calbiochem, San Diego, CA, United States) solved in DMSO (Sigma Aldrich, St. Louis, MO, United States). Staurosporine (Sigma Aldrich, St. Louis, MO, United States) was used for the induction of apoptosis at the concentration of 1 μM. The culture medium was supplemented with the given pharmacological inhibitors for at least 1 h before the infection and during the whole duration of the experiment.

C. jejuni Infection of the Co-culture and Bacterial Transmigration

Campylobacter jejuni 81-167 reference strain was cultivated for 2 days on blood agar plates (Columbia Agar with Sheep Blood; Oxoid, Wesel, Germany) in an impermeable plastic container at 37°C with Oxoid CampyGen gas packs (Thermo Scientific, Waltham, MA, United States) to establish microaerobic conditions. For infection, we harvested bacterial colonies using an inoculation loop and resuspended them in the antibiotic-free cell-culture medium. After at least 2.5 h of further incubation in microaerobic conditions, the bacteria were gently centrifuged at 5000 × *g*, 10°C for 2 min, in favor of bacterial viability. The bacteria pellet was resuspended in Dulbecco's phosphate buffered saline (DPBS; Sigma Aldrich, St. Louis, MO, United States) for quantification of the infection dose. The number of bacteria was estimated using optical density measurement and adjusted to OD_{600} = 2. The HT-29/B6-GR/MR cells in the co-culture setting were infected on the apical side with a multiplicity of infection (MOI) of 350 (**Figure 1**).

For quantification of bacterial transmigration, 25 μl of medium were removed from the basolateral compartment of the 12-well plates at the time points of 6, 12, and 24 h post-infection. Samples were diluted in 10-fold steps with antibiotic-free culture medium, sufficiently vortexed and incubated on the blood agar plates for 36 h. The number of colony-forming units (CFU) was counted and adjusted by the dilution coefficient to calculate the number of transmigrated bacteria.

Cytometric Bead Array and Flow Cytometry

At the timepoint of 22 h after infection we collected the medium from basal compartment of the 12 well plate to analyze the secretion of cytokines (IL-1β, IL-2, IL-4, IL-6, IL-10, IL-17A, IFN-γ, and TNF-α) during the infection using a human cytometric bead array kit and manufacturers protocol (CBA; BD Biosciences human Th1, Th2, Th17 Kit, Flex Set IL-1β, Franklin Lakes, NJ, United States). Flow cytometric measurement were performed with FACS CantoII (BD Biosciences; Franklin Lakes, NJ, United States) and analyzed with FACP Array software v3.0 (BD Biosciences, Franklin Lakes, NJ, United States).

Measurement of Transepithelial Electrical Resistance

The transepithelial electrical resistance (TER) was assessed before and 22 h after the infection. We performed the measurement with a chopstick electrode set (STX2, World Precision Instruments, Sarasota, FL, United States) and an epithelial volt-ohm meter (Institute of Clinical Physiology, Charité, Berlin). Electrodes were washed with 80% ethanol and phosphate buffered saline (PBS; Sigma Aldrich, St. Louis, MO, United States) in between the measurements. In pre-tests we have measured the TER of infected monolayers at multiple time points over the incubation

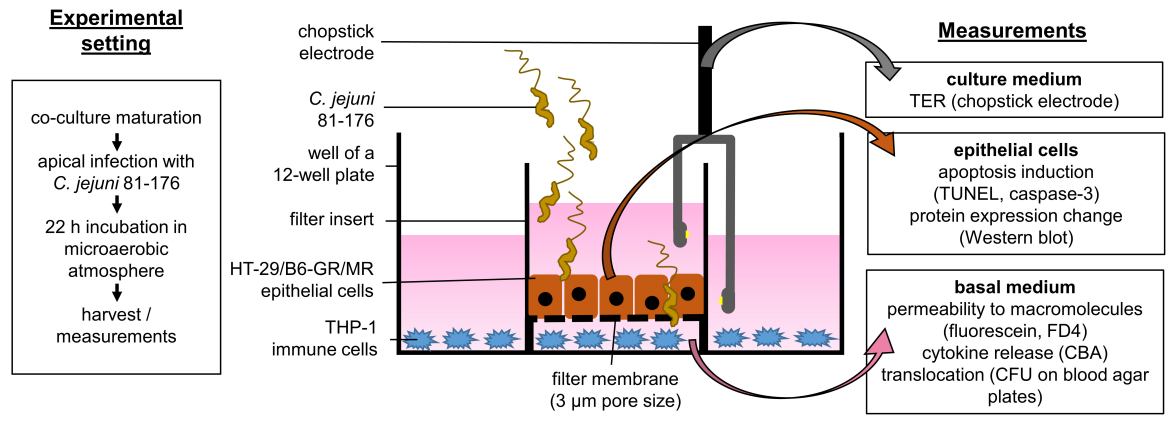

FIGURE 1 | Schematic sideview on the co-culture infection model. Epithelial cells HT-29/B6-GR/MR grown on filter supports were placed in a 12-well plate containing stimulated THP-1 immune cells. The co-culture was inoculated with *C. jejuni* 81-176 reference stain from the apical side. The infection experiments were performed under microaerobic conditions for 22 h with or without the apoptosis inhibitor Q-VD-OPh. After 22 h electrophysiological measurements were performed to assess the epithelial barrier integrity. Epithelial cells and basal medium were then harvested. The samples were further processed to evaluate the effects of the infection as well as the pathological mechanisms of epithelial barrier dysfunction caused by *C. jejuni*.

period to determine the earliest onset of the barrier effect (22 h post-infection). For the experiments, TER was measured in the epithelial monolayers before infection, then the co-cultures were placed in microaerobic atmosphere in favor of the bacteria. The monolayers were measured again after the incubation period of 22 h.

Transepithelial Permeability

For the measurement of the epithelial permeability 10 µl of fluorescein (332 Da, 100 mM, Fluorescein sodium salt, Sigma Aldrich, St. Louis, MO, United States) or fluorescein isothiocyanate-dextran solution (FITC-dextran, 4 kDa, 20 mM, Sigma Aldrich, St. Louis, MO, United States) dissolved in the culture medium was added to the apical side of the cell monolayer on PCF filter membranes placed in 12-well plates. The basal medium was removed at three subsequent time points every 15 (fluorescein) or 30 (FITC-dextran) minutes for the fluorescence measurement in a spectroflourometer (Infinite, Tecan GmbH, Mäennedorf, Switzerland). The standard for the fluorescent molecule concentration was determined in a dilution series. The permeability of the cell monolayer for the macromolecules was calculated from flux divided by concentration difference.

Apoptosis Staining and Tight Junction Immunofluorescence

We analyzed the epithelial apoptotic rate using the TUNEL protocol (*In situ* Cell Death Detection Kit, Roche, Mannheim, Germany). Cells grown on filter supports were fixed with 2% paraformaldehyde for 30 min at a time point of 22 h after *C. jejuni* infection, thereafter permeabilized with 0.5% Triton X-100. Cell monolayers were incubated with TUNEL reagent at 37°C, repeatedly washed with blocking solution containing 5% goat serum in DPBS. 4′,6-Diamidino-2-phenylindole (DAPI) was applied as a nuclear counterstain. Apoptosis-positive cells were visualized with confocal laser scanning microscopy (Zeiss LSM780, Jena, Germany) and counted per high-power field.

For immunostaining of tight junction proteins, the epithelial monolayers were washed with PBS, permeabilized with 0.5% Triton X-100 (Sigma Aldrich, St. Louis, MO, United States) for 7 min, and blocked for 10 min with 1% goat serum. Then the cells were incubated with the primary antibodies anti-occludin (1:100; Invitrogen, Carlsbad, CA, United States) and anti-ZO-1 (1:100; BD Biosciences, Franklin Lakes, NJ, United States) for 1 h at room temperature. Afterward, the cells were washed and incubated with the secondary antibodies; anti-rabbit-Alexa-Fluor-488 and anti-mouse-Alexa-Fluor-594 for 1 h (1:500; Invitrogen, Carlsbad, CA, United States). Finally, the cells were washed with water and ethanol, and embedded in ProTaq Mount Fluor (Biocyc, Luckenwalde, Germany). The subcellular distribution of the tight junctions was analyzed by confocal laser scanning microscopy (Zeiss LSM780, Jena, Germany).

Western Blot and Caspase Activity Analysis

Expression of tight junction proteins and caspase-3 cleavage during *C. jejuni* infection were investigated by Western blot analysis. Proteins were extracted from cell lysates 22 h post-infection. Cell-culture medium from the filter compartment containing extruded cells was centrifuged at 10000 × *g*, 4°C for 20 min. Supernatant was removed, the pellets were set aside on ice. Cell monolayers were treated with an ice-cold cell lysis buffer (10 mM Tris (pH 7.5), 150 mM NaCl, 0,5% Triton X-100, 1% SDS, complete protease inhibitor cocktail (Roche, Mannheim, Germany). Cells were scraped from filter supports carefully and added to the centrifuged cell pellet. Protein extraction and quantification, electrophoretic separation, western blotting and immunostaining were performed as previously described (Lobo de Sá et al., 2019). Nitrocellulose membranes were blocked with 1% PVP40 + 0.05% Tween20 for 2 h and incubated slewing in a box with primary antibodies anti-occludin, anti-claudin-2 (1:1000; Sigma Aldrich), anti-tricellulin, claudin-1, -4, -5, -8 (1:1000; Invitrogen, Carlsbad, CA, United States), and anti-caspase-3-cleaved (1:1000; Cell Signaling Technology, Denvers, MA, United States) overnight, and anti-β-actin (1:10000; Sigma Aldrich) over 4 h at 4°C. Afterward the membranes were washed with TBST buffer and incubated for 2 h at the room temperature with peroxidase conjugated secondary antibodies goat anti-rabbit IgG or goat anti-mouse IgG (Jackson ImmunoResearch, Ely, United Kingdom) prepared with 1% milk powder in TBST. Nitrocellulose membranes were then placed in the SuperSignal West Pico PLUS chemiluminescent peroxidase substrate (Thermo Scientific, Waltham, MA, United States) for 2 or 5 min for anti-β-actin and other antibodies, respectively. The chemiluminescence was measured using Fusion FX7 (Vilber Lourmat, Eberhardzell, Germany). ImageJ 1.52o quantification software was used for densitometric analysis. Signal intensity values were normalized by the loading control (β-actin) (Schneider et al., 2012). In parallel, the activity of caspase-3/7 was assessed using the Caspase-3/7 activity assay kit following manufacturer's protocol (SensoLyte; AnaSpec, Fremont, CA, United States). Cell lysates were incubated with caspase-substrate Ac-DEVD-AFC and the fluorescence intensity of the fluorogenic indicator product was measured at Ex/Em = 380 nm/500 nm (Tecan, Mäennedorf, Switzerland).

Statistical Analysis

All data are expressed as mean values ± standard error of the mean (SEM). Statistical analysis was performed using two-way unpaired Student's *t*-test with Bonferroni-Holm adjustment for multiple comparison. Significance level was set at $\alpha = 0.05$.

RESULTS

Subepithelial Immune Cells Caused Epithelial Barrier Dysfunction at an Early Time Point of *C. jejuni* Infection by Means of Apoptosis Induction

Campylobacter jejuni is known to cause epithelial barrier dysfunction. Transepithelial electrical resistance (TER) served as a functional parameter to measure the integrity of the epithelial cell monolayer. As in prior studies, we confirmed that a barrier

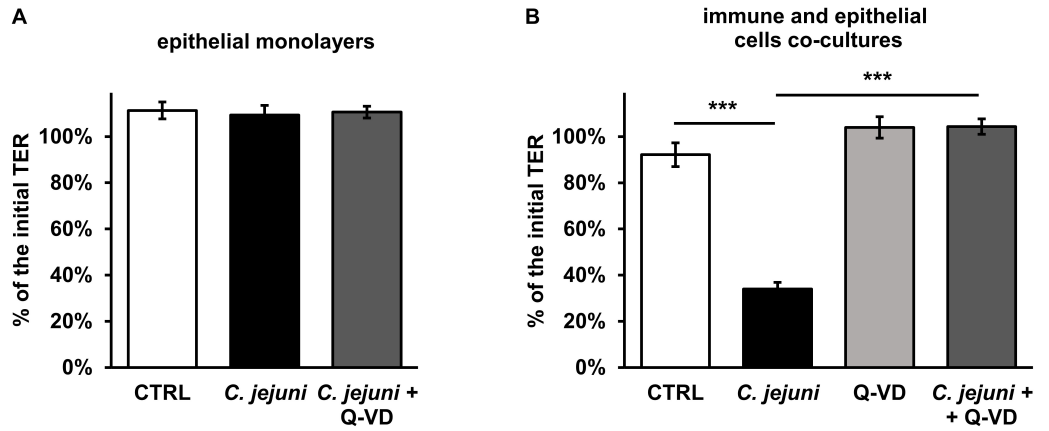

FIGURE 2 | Epithelial barrier function during the first day of Campylobacter jejuni infection in the epithelial mono-culture and co-culture. TER values were assessed 22 h after infection for **(A)** HT-29/B6-GR/MR intestinal epithelial cell mono-culture infected with *C. jejuni* (MOI 350) with or without a broad-spectrum caspase inhibitor Q-VD-OPh (10 μM). $n = 6$. **(B)** The co-culture of HT-29/B6-GR/MR and THP-1 cells was infected with *C. jejuni* with or without the apoptosis inhibitor Q-VD-OPh. The TER values are presented as mean values ± SEM. $n = 19$–21, $^{***}p < 0.001$, unpaired Student's *t*-test with Bonferroni-Holm correction for multiple comparisons.

defect of *C. jejuni*-infected HT-29/B6 cell monolayer occurred only after 40 to 48 h after exposure to the cell mono-culture (Bücker et al., 2018) with 41 ± 4% of initial TER ($p < 0.001$, $n = 7$–8, data not shown). In line with this, at an earlier incubation time point of 22 h after infection, the TER did not drop (**Figure 2A**). Also, the apoptosis inhibitor Q-VD-OPh did not result in any significant alteration of the TER in the HT-29/B6-GR/MR cell culture on the first day of incubation. Since the mucosal immune activation in campylobacteriosis is a key feature of the disease, a co-culture of HT-29/B6/GR-MR and activated THP-1 immune cells was used for the infection assay. The contribution to the TER effect by the subepithelial THP-1 cells in an early incubation period was shown here in comparison to the unaffected mono-culture (**Figures 2A,B**). 22 h after exposure of the co-culture with *C. jejuni*, the infection caused a reduction in TER of 58 ± 6% ($p < 0.001$) compared to the controls (**Figure 2B**). Whereas, the co-culture incubated with the pan-caspase inhibitor Q-VD-OPh showed no changes in TER during the infection with *C. jejuni*. Surprisingly, the developing decrease in TER was completely blocked by Q-VD-OPh. Thus, the inhibition of apoptosis led to a full recovery of the barrier defect.

Inhibition of Epithelial Apoptosis Normalized the Paracellular Permeability for Macromolecules in *C. jejuni* Infection

Besides TER measurements that rather reflect the ional permeability, we performed flux measurements of macromolecules in order to assess the barrier function for the paracellular leak pathway in our model. The permeability of the cell monolayer in the co-culture setting for small and mid-sized macromolecules changed during the *C. jejuni* infection. 22 h after infection, the fluorescein (332 Da) translocation from apical to the basal compartment increased 4.5-fold in infected samples compared to controls ($p < 0.001$), but remained steady under Q-VD-OPh treatment (**Figure 3A**). Similar to the fluorescein permeability, the FITC-dextran (4 kDa) translocation increased 3.5-fold during the infection ($p < 0.001$). Also, Q-VD-OPh incubation of the infected samples led to a full recovery of the FITC-dextran permeability (**Figure 3B**). The inhibition of apoptosis completely prevented the development of epithelial leaks and sufficiently sealed the epithelial barrier against the passage of macromolecules.

C. jejuni Infection Changed the Expression of Tight Junction Proteins

As molecular or cellular correlate to the barrier defect by *C. jejuni*, expression changes of tight junction proteins and/or epithelial cell damage (cell death) are thinkable. Therefore, we performed western blotting of treated epithelial cell monolayers. In the densitometric analysis of the Western blots, we discovered an almost 2-fold increase of an integral tight junction protein occludin ($p < 0.05$) and the barrier-forming claudin-1 protein ($p < 0.01$) expression. The claudin-1 effect was not diminished by apoptosis inhibition (**Figure 4A**). Cells incubated with Q-VD-OPh during the infection had similar increase in claudin-1 expression ($p < 0.01$) but only a change in occludin expression by trend. The channel-forming claudin-2 was also induced in HT-29/B6-GR/MR cells during the infection with ($p < 0.01$) and without ($p < 0.05$) concurrent apoptosis inhibition. Claudin-5 and claudin-8 show a reduction by trend that could develop an influence on the barrier integrity at a later time point of infection, whereas tricellulin and claudin-4 expression remained stable during the first hours of infection (**Figure 4A**). Tight junction expression changes were not prevented by apoptosis inhibition and presumably have a caspase-independent regulator. As the subcellular distribution of tight junction proteins can influence the epithelial barrier function, we analyzed immunofluorescent stainings of the treated monolayers. In confocal micrographs the intact co-localization of tight junction protein occludin together with zonula occludens protein-1 (ZO-1) was observed, without any re-distribution of tight junction protein signals

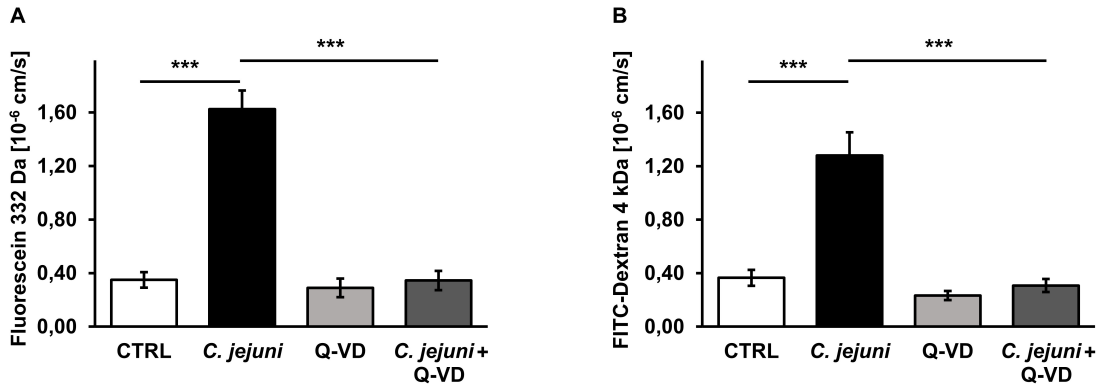

FIGURE 3 | Epithelial permeability toward macromolecules in *C. jejuni*-infected co-cultures 22 h post-infection. Co-cultures of HT-29/B6-GR/MR and THP-1- cells were infected with *C. jejuni* with or without apoptosis inhibitor Q-VD-OPh. **(A)** Fluorescein flux and **(B)** FITC-Dextran flux across the epithelial monolayer were measured after 22 h of *C. jejuni* infection. The flux measurements were performed in the cell monolayer filter supports and are presented as mean values ± SEM, $n = 6$, ***$p < 0.001$, unpaired Student's *t*-test with Bonferroni-Holm correction for multiple comparisons.

to intracellular compartments in treated or infected cells (**Figure 4B**). At most a zigzag pattern of the bicellular junction became visible in infected monolayers, which might indicate the beginning of the following impact of *C. jejuni* on tight junction protein redistribution at later stages of infection.

Epithelial Apoptosis in *C. jejuni* Infection Caused by Increased Caspase Activity

Although apoptosis can be initiated by different pathways, it ends up with a common final sequence of a few effector caspases. Therefore, we investigated the activation of caspase-3 in our infection model. The infection of the co-culture with *C. jejuni* resulted in an increased caspase-3 cleavage. In the densitometry analysis of Western blots, infected samples showed 9-fold increased band signal of the 19 kDa caspase-3 cleavage product ($p < 0.01$). This increase of the effector caspase was sufficiently blocked by the pan-caspase inhibitor Q-VD-OPh ($p < 0.01$) (**Figure 5A**). These changes correspond to the results of the caspase-3/7 activity assay. Here, a substantial rise of the effector caspase activity following the *C. jejuni* infection ($p < 0.001$) was measured with a completely inhibited activity, when incubated with Q-VD-OPh ($p < 0.001$) (**Figure 5B**). The effect of the changed number of apoptoses on the integrity of the cell monolayers was investigated after TUNEL staining by confocal laser scanning microscopy. *C. jejuni* infection led to 5-fold increase in the number of apoptotic cells in the cell culture. The increase in the apoptotic rate was prevented by incubation of the cell culture with the pan-caspase inhibitor Q-VD-OPh during the infection ($p < 0.001$) (**Figures 5C,D**). Thus, the predominant mechanism of the barrier defect in the early phase of infection was shown to be more caspase-dependent apoptosis induction than tight junction disruption.

Cytokine Secretion Was Induced in *C. jejuni*-Infected Co-culture

Increased apoptosis induction can develop from direct bacterial contact and/or subepithelial cytokine release. To understand the mechanism of epithelial cell apoptosis we further investigated the secretion of cytokines from THP-1 cells in the infected co-culture. *C. jejuni* infection resulted in a 2.5-fold caspase-independent increase of TNFα concentration ($p < 0.05$). Immune activation was not affected by apoptosis inhibition with Q-VD-OPh (**Figure 6A**). Other pro-inflammatory cytokines such as IFN-γ, IL-1β, IL-2, IL-6 or IL-17 were not induced by *C. jejuni* or influenced by apoptosis inhibition after 22 h in the used infection setting (**Figures 6B–F**). Production of TH2 cytokines IL-10 and IL-13 also remained unchanged (**Figures 6G,H**). Therefore, the cell death receptor pathway of TNFα might play the major role in our experimental setup.

C. jejuni Transmigration Across the Epithelium Was Not Limited by Apoptosis Inhibition

The translocation of *C. jejuni* and/or lipo-oligosaccharides (LOS) from the apical side through the epithelial monolayer, reaching the immune cells, is supposed as a pivotal step of the following aggravated outcome of the *C. jejuni* infection *in vivo*, leading to enhanced barrier disruption and again potentiated antigen influx into the subepithelium (leaky gut concept). In the transmigration experiment, we observed, that inhibition of apoptosis resulted not in a decrease, as expected, but in a 5.5-fold increase of bacterial translocation during the first 6 h of infection ($p < 0.05$, $n = 6$). After 12 h, the number of the bacteria, that reached basolateral compartment through the Q-VD-OPh incubated HT-29/B6-GR/MR cells, was only 3.5-times higher compared to the control infection in the co-culture ($p < 0.05$, $n = 6$) (**Figure 7**). At the time point of 24 h post-infection there was no significant difference between the two groups. Thus, the transmigration of *C. jejuni* was not limited by Q-VD-OPh, whereas the unrestricted passage of solutes and macromolecules could be diminished. Tight junction changes alone cannot explain the drop in resistance and increase in permeability for fluorescein and 4 kDa dextran. The increased apoptotic ratio in

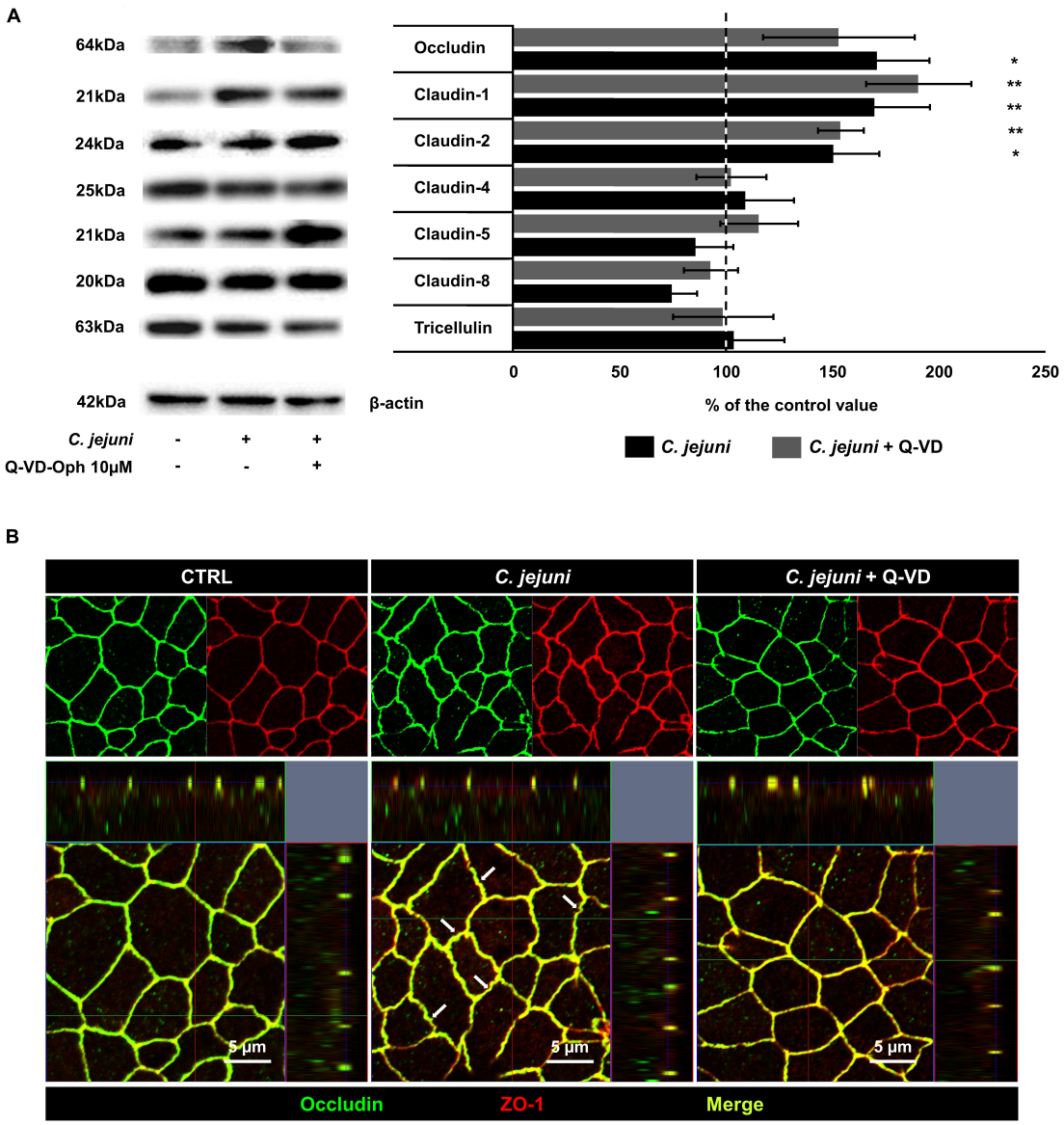

FIGURE 4 | Expression of tight junction proteins in *C. jejuni*-infected co-cultures 22 h post-infection. Co-cultures of HT-29/B6-GR/MR and THP-1- cells were infected with *C. jejuni* with or without apoptosis inhibitor Q-VD-OPh. **(A)** Western blot was performed on the cell lysates 22 h after infection. Expression level of tight junction proteins was normalized with β-actin. Immunoblots were subjected to densitometric analysis. The dashed line represents control value set to 100%. Q-VD-OPh control treatment did not change the expression level of the described tight junction proteins compared to untreated controls (data not shown). Data are presented as mean values in percent of the control values, ± SEM. $n = 7–9$, $^{*}p < 0.05$, $^{**}p < 0.01$, unpaired Student's *t*-test with Bonferroni-Holm adjustment for multiple comparisons. **(B)** The cell monolayers were analyzed by confocal microscopy after immunofluorescence staining. The micrographs show the localization of the tight junction proteins occludin (green) and zonula occludens protein-1; ZO-1 (red) at cell borders. The merge (yellow) image represents the co-localization of the tight junction proteins in a single plane of a *Z*-stack. White arrows indicate zigzag pattern of bicellular cell-cell contacts in *C. jejuni*-infected monolayers.

the monolayers seems to be the only barrier-relevant factor in the first phase of infection.

DISCUSSION

The perturbation of the intestinal barrier is considered to be a key mechanism for the development of *C. jejuni*-induced diarrhea. While apoptosis was hitherto insufficiently analyzed in the *C. jejuni*-infected epithelial cell culture, it is commonly referenced in *C. jejuni*-infected mice, apes and human tissues (Russell et al., 1993; Haag et al., 2012; Bücker et al., 2018). The role of apoptosis in epithelial barrier dysfunction was discussed but have never been investigated for the *C. jejuni* infection. Hence, we aimed on the effect of apoptosis induction on the barrier impairment caused by *C. jejuni* in an immune and epithelial cell co-culture approach to alleviate the diarrheal outcome of the disease. This novel method enabled us to study the interplay

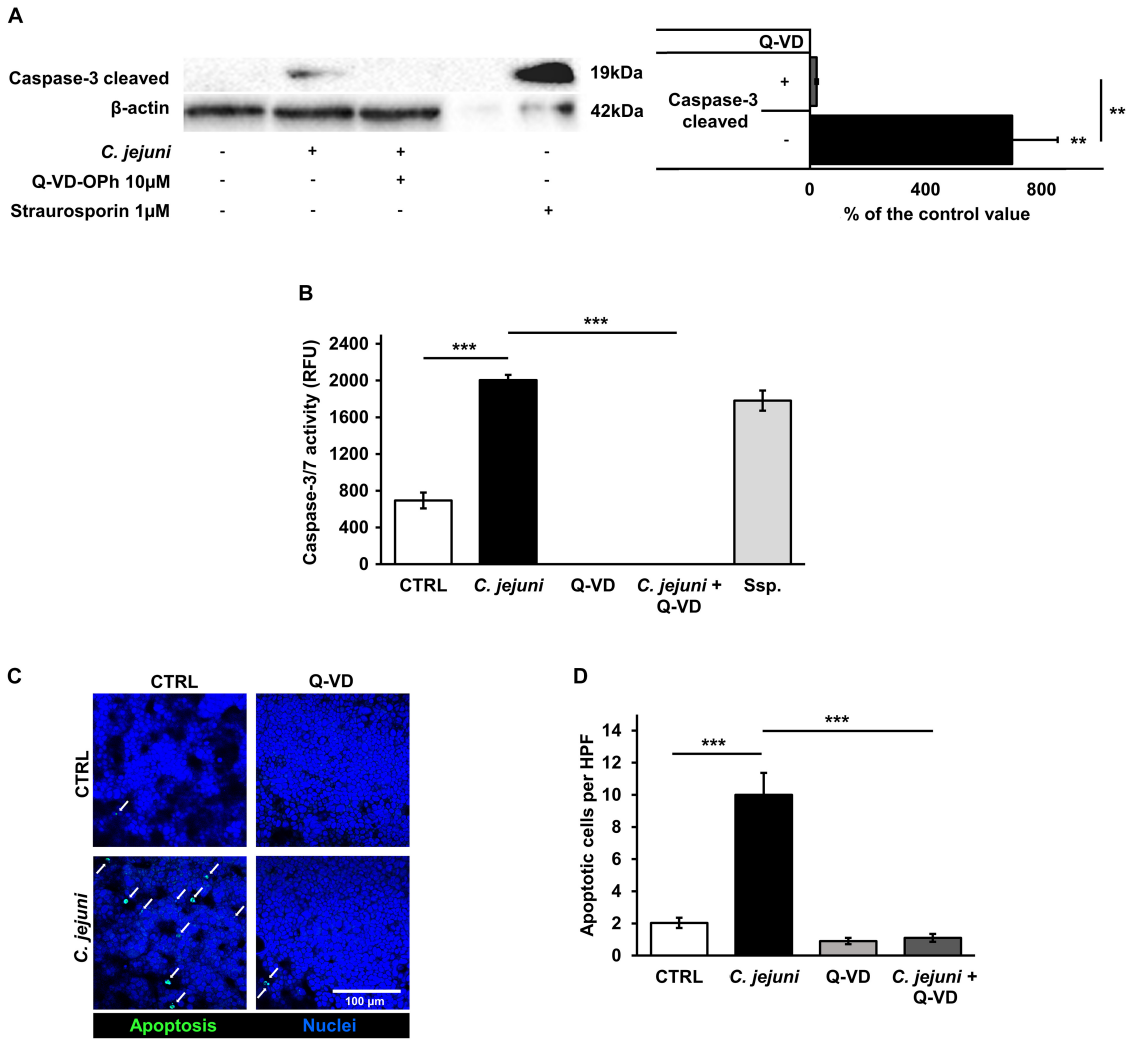

FIGURE 5 | Effects of the *C. jejuni* infection on caspase activity. Co-cultures of HT-29/B6-GR/MR and THP-1 cells were infected with *C. jejuni* with or without apoptosis inhibitor Q-VD-OPh. **(A)** Caspase-3 cleavage in western blot after *C. jejuni* infection. Immunoblotting was performed on the cell lysates 22 h after infection. Staurosporine was used for the induction of apoptosis at the concentration of 1 μM as a positive control. Western blot densitometry represented in percent of the mean value in control samples. Western Blot intensity was normalized with β-actin level, $n = 6$, $^{**}p < 0.01$. **(B)** Caspase-3/7 activity measured in a luminescense assay on cell lysates after 22 h of infection. Staurosporine (Ssp., 1 μM) incubated samples were used as positive controls. Data are represented in relative fluorescence units (RFU), $n = 6$, $^{***}p < 0.001$. **(C)** Apoptosis induction measured by TUNEL staining, showing DNA defragmentation in fluorescence microscopy. DAPI was applied as a nuclear counterstain. **(D)** Quantitative analysis of apoptotic cells in TUNEL staining (indicated by white arrows). Number of apoptosis positive cell nuclei was estimated in five high power fields per sample, containing approximately 1600 cells each. $n = 6$, $^{***}p < 0.001$, unpaired Student's *t*-test with Bonferroni-Holm adjustment for multiple comparisons.

of *C. jejuni* with the epithelial monolayer and immune cells, reflecting an infection model for the delineation of the diarrheal symptoms of the infection.

Q-VD-OPh as Inhibitor of *C. jejuni*-Triggered Barrier Dysfunction

For the first time we present a substance, the pan-caspase inhibitor Q-VD-OPh, which targets epithelial monolayers and completely inhibited the epithelial barrier dysfunction in *C. jejuni* infection. In the co-culture setting, it mitigated the decrease of the TER completely. No other compound was able to produce an outcome of this scale. In pre-tests, we targeted on the host cell signaling with the kinase inhibitors Y-27632 (PI3K) or ML-7 (MLCK) as well as blocking experiments on NF-κB activation (BAY 11-7082), but could not achieve any barrier-relevant protection effects (data not shown). In the literature, the improvement of barrier function was reported for use of vitamin D and PI3-kinase inhibitor LY294002 (Wine et al., 2008; Bücker et al., 2018). Their effects, ranging from mild to substantial, did not prevent from the loss of the barrier function, although *C. jejuni*-dependent activation of PI3K, ERK, p38, and NF-κB as well as impairment of actomyosin signaling were reported (Jin et al., 2003; Krause-Gruszczynska et al., 2007; Li et al., 2011).

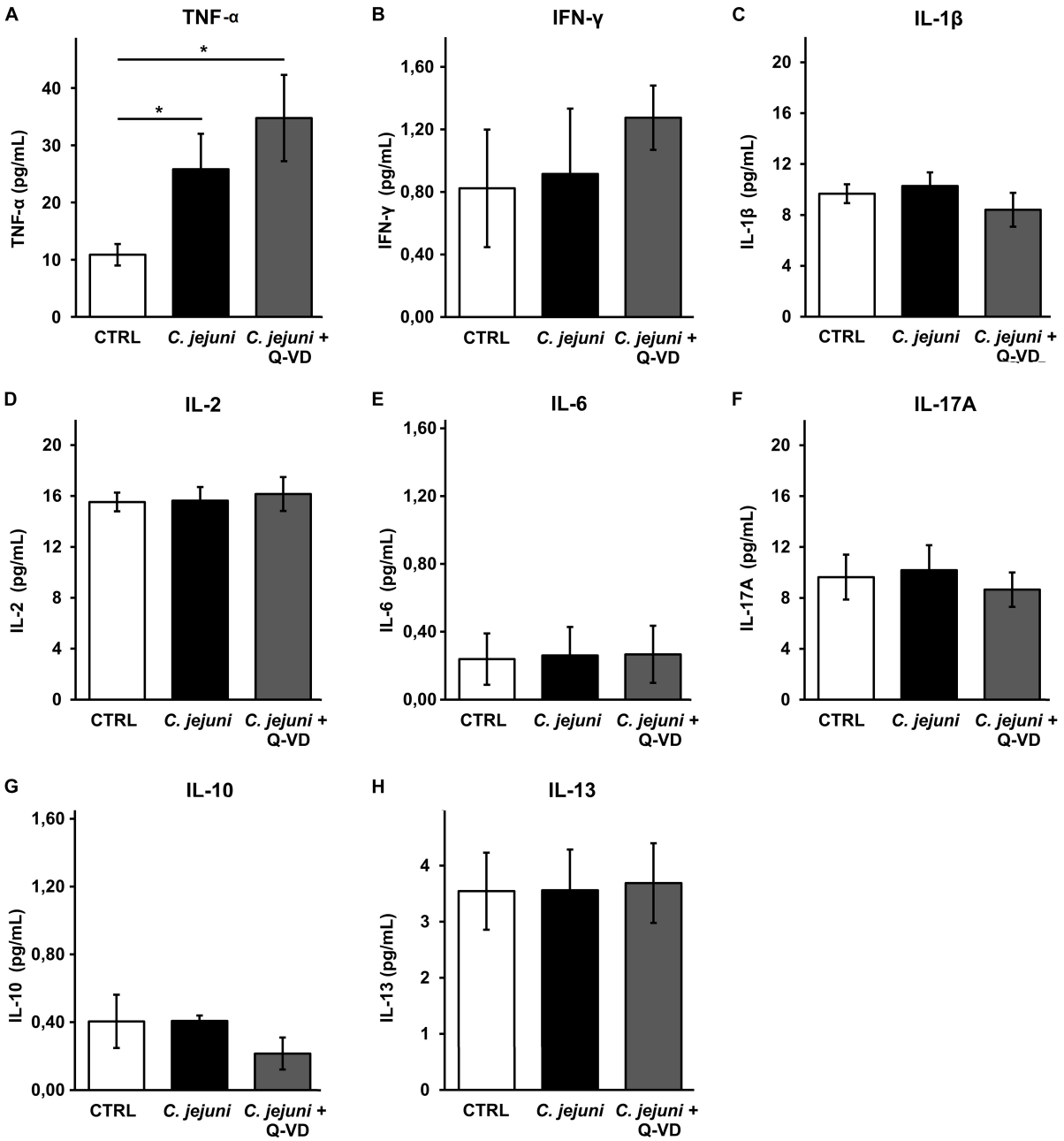

FIGURE 6 | Immune activation during *C. jejuni* infection. Co-cultures of HT-29/B6-GR/MR and THP-1 cells were infected with *C. jejuni* with or without apoptosis inhibitor Q-VD-OPh. The secretion of the barrier relevant cytokines such as TNF-α, INF-γ, and IL-1β **(A–C)** as well as further interleukins **(D–H)** were assessed in the infected co-culture after 22 h. Cytokine concentration was measured in the culture medium from basal compartment. The concentrations are presented as mean values ± SEM, $n = 6$, $^*p < 0.05$, unpaired Student's *t*-test with Bonferroni-Holm adjustment for multiple comparisons.

Recently published data on curcumin as a preventive drug against *C. jejuni*-induced barrier disruption showed a complete recovery of the barrier function of treated epithelial monolayers. Curcumin effects relied on immune regulation with a decreased level of cytokine production, protecting the enterocytes. In the same time frame, direct anti-apoptotic properties of curcumin were discussed (Lobo de Sá et al., 2019). Regarding the success of anti-apoptotic treatment with Q-VD-OPh, we consider apoptosis as a crucial pathomechanism for epithelial barrier dysfunction in the early stage of the *C. jejuni* infection.

Inhibition of Apoptosis as Mechanism for Reducing Macromolecule Passage

Inhibition of apoptosis resulted in the recovery of the increased epithelial permeability toward macromolecules after

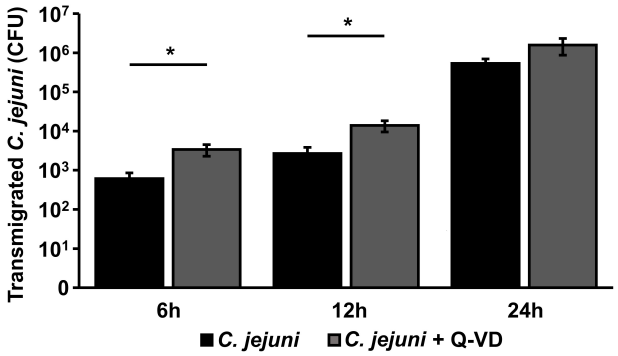

FIGURE 7 | Bacterial transmigration through an epithelial monolayer during *C. jejuni* infection. Co-cultures of HT-29/B6-GR/MR and THP-1 cells were infected with *C. jejuni* with or without apoptosis inhibitor Q-VD-OPh. Transmigration of *C. jejuni* through the epithelial monolayer was assessed 6, 12, and 24 h after infection of the co-culture. The numbers of colony forming units (CFU) are presented as mean values ± SEM on a logarithmic scale, $n = 12$, $^*p < 0.05$, unpaired Student's *t*-test.

infection to the level of control values. It is known that single-cell epithelial defects rapidly close by an actomyosin constriction "purse string" mechanism (Florian et al., 2002). As possible explanation for persistent barrier dysfunction, *C. jejuni* actively triggers signaling pathways to stimulate their own uptake by host cells using activation of the Rho GTPase, which in combination with induction of TNFα and INFγ pathways can lead to increased restitution time of single-cell lesions or increased numbers of cell extrusions (Günzel et al., 2006; Cróinín and Backert, 2012). Such mechanisms are also known for *Shigella*, *Salmonella*, and enterohaemorrhagic *Escherichia coli* during the initial stages of infection (Gudipaty and Rosenblatt, 2017). Increased epithelial permeability by single cell apoptosis facilitates unwanted loss of solutes and uptake of noxious agents (Gitter et al., 2000). One can conclude that apoptosis not only lead to barrier dysfunction in *C. jejuni* infection but can also be a part of the diarrheal mechanism and the cause of an excessive immune response, by increased antigen entry into the subepithelial compartment.

No Downregulation of Barrier-Relevant Tight Junction Proteins

Tight junction proteins are the main determinants for sealing the paracellular pathway. Their impairment causes the leak flux mechanism by increased paracellular permeability (Barmeyer et al., 2017). Considering the TER reduction and increased macromolecular leak flux caused by *C. jejuni*, we investigated the expression of tight junction proteins. Surprisingly, no downregulation of barrier-relevant tight junction proteins was observed. While the increased expression of claudin-2, a tight junction protein forming a channel for small cations and water, could partially explain the decrease in TER, but it could not be responsible for the translocation of larger molecules. The contribution of claudin-2 upregulation under inflammatory conditions is described *in vitro* and *in vivo* (Heller et al., 2005; Zeissig et al., 2007; Luettig et al., 2015).

In our co-culture model the reduced TER and increased paracellular flux could not be explained by the expression change of occludin. Increased expression of occludin was reported to strengthen the barrier (McCarthy et al., 1996), but without a sealing effect in TER by occludin *per se*, since occludin knockout mice did not develop a barrier impairment (Schulzke et al., 2005). Here, claudins with sealing properties maintain the paracellular barrier. However, it is a matter of debate whether in an occludin knockout animal or cell model, other tight junction proteins can functionally compensate a loss of occludin (Saitou et al., 2000; Schulzke et al., 2005). Also, in a Caco-2 occludin knockout cell monolayer, the integrity of the epithelial barrier was intact, likewise in the wildtype Caco-2 cells, as indicated by a stable TER. Interestingly, in the Caco-2 model the cleavage of occludin by the secreted *C. jejuni* protease HtrA was shown, that facilitated the paracellular movement of the bacteria between the host cells (Harrer et al., 2019). Occludin was described as a molecular target of *C. jejuni*, as well as other pathogens and bacteria or viruses, leading to a direct or indirect disruption of occludin. In our experiments, confocal micrographs of the *C. jejuni*-infected monolayers revealed no protein redistribution of occludin to intracellular compartments and the occludin signal was clearly present in the tight junction domain. In the same time a zigzag pattern of cell-cell contacts was visible that points to morphological changes or the pre-stage for the following tight junction changes (re-distribution or scattering) in the further course of infection.

In general, upregulation of claudin-1 increases the epithelial resistance and decreases paracellular permeability to macromolecules (Inai et al., 1999). We also observed a claudin-1 upregulation in *C. jejuni* infection, the claudin-1 paradox, claudin-1 increase while the TER is decreased, as also shown before for *C. fetus* and *C. jejuni in vivo*. (Bücker et al., 2017, 2018; Lobo de Sá et al., 2019). The overall increase of claudin-1 was associated with retraction of the protein from tight junction strands and localization in the basolateral membrane and intracellular compartments during the infection (Bücker et al., 2018). Both claudin-1 and claudin-2 upregulation is shown to be mediated by TNFα signaling (Amasheh et al., 2010). The TNFα level was increased in our *C. jejuni* infection model. Claudin-1 level is known to be strongly increased in apoptosis inductor-treated HT-29/B6 cells (Bojarski et al., 2004), but was caspase independent in our infection model. Although we could show a change in the expression of the measured tight junction proteins, similar expression change was observed in infected monolayers after Q-VD-OPh treatment that showed sufficient barrier function in TER measurement and no increase of paracellular permeability for macromolecules. Therefore, tight junction changes alone cannot explain the disturbed barrier function caused by *C. jejuni* infection and its recovery. As an example of the intact tight junction meshwork pattern we showed occludin in co-localization with ZO-1 in

controls, infected and Q-VD-OPh-treated monolayers in our co-culture setting. We propose that ongoing changes in tight junction protein expression and distribution, with impact on barrier function as reported (Bücker et al., 2018; Lobo de Sá et al., 2019) arise later on, with epithelial apoptosis being the main manifestation in the beginning of the infection, as shown here.

Impaired Barrier Function Results From Induction of Epithelial Apoptosis

The increased epithelial apoptosis was caspase-3-dependent, mediated by *C. jejuni* infection, and the subsequent increase in TNFα. While the related pathogens *Campylobacter concisus* and *Arcobacter butzleri* directly initiate epithelial cell death (necrosis and apoptosis) that were partially barrier relevant with significant effects on TER and molecule marker fluxes (Bücker et al., 2009; Nielsen et al., 2011), we did not find such evidence for *C. jejuni* in the literature. Hence, we could show for the first time that epithelial apoptosis has a main effect on epithelial barrier function in *C. jejuni* infection, and in the early phase (first day of infection) it is the predominant reason for barrier impairment.

Cytotoxic Mechanism Causing Epithelial Apoptosis

Regarding the inflammatory input, TNFα was the main cytokine increased during the infection. TNFα-induced barrier dysfunction was mostly caused by single−cell apoptotic events, increasing focal conductivity of the epithelium (Schulzke et al., 2006). Nevertheless, the immune response to the interaction with *C. jejuni* caused barrier impairment and induced overlapping effects of apoptosis and tight junction changes (Lobo de Sá et al., 2019). We proposed that *C. jejuni* possesses direct pro-apoptotic effectors. Previously, several bacterial proteins were associated with epithelial cell death. Cytolethal distending toxin prepared from *C. jejuni* was reported to cause cell cycle arrest and apoptosis in HeLa and epithelial Caco-2, or monocytic 28SC cells, while having no impact on T84 cells (Whitehouse et al., 1998; Kalischuk et al., 2007; Jain et al., 2009). The *Campylobacter* serine protease HtrA was shown as a virulence factor in mouse models with increased caspase-3 activity in both gnotobiotic IL-10-deficient mice and infant mice infected with *C. jejuni* wild type compared to *htrA*-deficient mutants (Heimesaat et al., 2014a,b; Schmidt et al., 2019). In both models, higher levels of pro-inflammatory cytokines such as TNFα, IL-6, and IFNγ in the colonic mucosa were measured in $HtrA^+$ *C. jejuni* infection. Thus, indirect effects on the epithelial cell death are conceivable. Cytokines secretion, e.g., IL-13, IL-1β, IFN-γ, IL-10, IL-6, IL-17A, and IL-2, did not differ from control values in our co-culture, with an exception of TNFα. Moreover, gamma-glutamyl transpeptidase was found to inhibit epithelial cells proliferation in Caco-2 and AGS cell lines but was not responsible for cellular apoptosis (Floch et al., 2014). Hence, although no bacterial factor produced by *C. jejuni* was reported to induce defined apoptosis in intestinal epithelial cells, defined cytotoxicity was shown before. Interestingly, cytokine cocktails composed of IFNγ, TNFα, IL-13, and IL-1β, found to be the main barrier relevant cytokines in *C. jejuni*-infected human biopsies, substantially aggravated the *C. jejuni*-mediated epithelial defects (Bücker et al., 2018). Treatment with TNFα, a combination of TNFα and IFNγ, as well as solely IL-13 was shown to cause barrier dysfunction not only by tight junction alterations but also by the means of epithelial apoptosis in HT-29/B6 cells and rat colon (Grotjohann et al., 2000; Gitter et al., 2006; Heller et al., 2008). Therefore, we consider synergistic effects of cytokines and pathogen-host interaction described in previous studies (Rees et al., 2008; Bücker et al., 2018) as the leading mechanism to epithelial apoptotic events. Thus, the co-culture setting as an infection model is particularly advantageous to further investigate these mechanisms.

Apoptosis as a Limiting Mechanism of *C. jejuni* Translocation

We assume that apoptosis inhibition not only tightens the barrier for solutes and macromolecules but also limits the translocation of *C. jejuni* via the paracellular route. The ability of *C. jejuni* to translocate across epithelial cell monolayer by paracellular and transcellular routes, is a crucial step of the infection. By reaching the subepithelial matrix, pathogen initiates the antigen presentation to the mucosal immune cells and reaches receptors located at the basolateral cell membrane of epithelial cells, like integrin receptors, which were shown to be necessary for cellular invasion (Backert et al., 2013). Surprisingly, transmigration of *C. jejuni* increased in Q-VD-OPh incubated samples. We suggest that the transcellular translocation capacity was increased with the higher number of viable epithelial cells. Additionally, the sealing of the focal leaks caused by apoptosis requires cytoskeletal transformation (Florian et al., 2002). Actin rearrangement and/or microtubule dynamics were also involved in the bacterial invasion process (Krause-Gruszczynska et al., 2007). Hence, this process might interfere after repair of apoptotic single cell lesions, resulting in impaired bacterial translocation.

The importance of epithelial cell death suggests the use of anti-apoptotic substances for prevention or treatment of the *C. jejuni* enteritis. Although medical use of caspase-inhibitors like Q-VD-OPh is unreasonable, substances with pronounced anti-apoptotic and immune-modulatory effect, e.g., vitamin D, curcumin and myrrh, have already been proven to their effectiveness in cell-culture or mouse models (Rosenthal et al., 2017; Bücker et al., 2018; Lobo de Sá et al., 2019; Mousavi et al., 2019). These compounds represent a potent alternative to the antibiotic treatment of *C. jejuni* infection.

CONCLUSION

Caspase-dependent epithelial apoptosis, caused either by TNFα or by direct bacterial cytotoxicity, are the main mechanisms of the *C. jejuni*-induced barrier dysfunction in the early state of infection. Epithelial apoptosis caused leakage of macromolecules

from apical to the subepithelial compartment but was not associated with tight junction changes or increased bacterial transmigration. Induction of apoptosis is a key mechanism for the development of leak flux diarrhea. These mechanisms provide further insight into new therapeutic approaches for the campylobacteriosis.

DATA AVAILABILITY STATEMENT

The raw data supporting the findings of this article will be made available by corresponding author, RB, or first author, EB, to any qualified researcher upon reasonable request.

AUTHOR CONTRIBUTIONS

EB and RB: conceptualization. EB, FL, and PN: data curation and Formal analysis. RB: funding acquisition, methodology, project administration, and supervision. EB: investigation and Writing the original draft. FL: resources. FL, PN, and RB: writing, review and editing.

FUNDING

The German Federal Ministries of Education and Research (BMBF) funded the study in connection with the zoonoses research consortium PAC-CAMPY to RB (IP8/01KI1725D). The funders had no influence in the study design, data collection, analysis, decision to publish, or preparation of the manuscript. We acknowledge support from the German Research Foundation (DFG) and the Open Access Publication Fund of the Charité–Universitätsmedizin Berlin.

ACKNOWLEDGMENTS

In-Fah Maria Lee and Anja Fromm are gratefully acknowledged for their excellent technical support.

REFERENCES

Amasheh, M., Fromm, A., Krug, S. M., Amasheh, S., Andres, S., Zeitz, M., et al. (2010). TNFα-induced and berberine-antagonized tight junction barrier impairment via tyrosine kinase, Akt and NFκB signaling. *J. Cell Sci.* 123, 4145–4155. doi: 10.1242/jcs.070896

Backert, S., Boehm, M., Wessler, S., and Tegtmeyer, N. (2013). Transmigration route of *Campylobacter jejuni* across polarized intestinal epithelial cells: Paracellular, transcellular or both? *Cell Commun. Signal.* 11:72. doi: 10.1186/1478-811X-11-72

Barmeyer, C., Fromm, M., and Schulzke, J. D. (2017). Active and passive involvement of claudins in the pathophysiology of intestinal inflammatory diseases. *Pflugers Arch. Eur. J. Physiol.* 469, 15–26. doi: 10.1007/s00424-016-1914-6

Bereswill, S., Fischer, A., Plickert, R., Haag, L. M., Otto, B., Kühl, A. A., et al. (2011). Novel murine infection models provide deep insights into the "Ménage à trois" of *Campylobacter jejuni*, microbiota and host innate immunity. *PLoS One* 6:e0020953. doi: 10.1371/journal.pone.0020953

Bergann, T., Fromm, A., Borden, S. A., Fromm, M., and Schulzke, J. D. (2011). Glucocorticoid receptor is indispensable for physiological responses to aldosterone in epithelial Na+ channel induction via the mineralocorticoid receptor in a human colonic cell line. *Eur. J. Cell Biol.* 90, 432–439. doi: 10.1016/j.ejcb.2011.01.001

Boehm, M., Hoy, B., Rohde, M., Tegtmeyer, N., Bæk, K. T., Oyarzabal, O. A., et al. (2012). Rapid paracellular transmigration of *Campylobacter jejuni* across polarized epithelial cells without affecting TER: role of proteolytic-active HtrA cleaving E-cadherin but not fibronectin. *Gut Pathog.* 4:3. doi: 10.1186/1757-4749-4-3

Bojarski, C., Gitter, A. H., Bendfeldt, K., Mankertz, J., Schmitz, H., Wagner, S., et al. (2001). Permeability of human HT-29/B6 colonic epithelium as a function of apoptosis. *J. Physiol.* 535, 541–552. doi: 10.1111/j.1469-7793.2001.00541.x

Bojarski, C., Weiske, J., Schöneberg, T., Schröder, W., Mankertz, J., Schulzke, J. D., et al. (2004). The specific fates of tight junction proteins in apoptopic epithelial cells. *J. Cell Sci.* 117, 2097–2107. doi: 10.1242/jcs.01071

Bücker, R., Krug, S. M., Fromm, A., Nielsen, H. L., Fromm, M., Nielsen, H., et al. (2017). *Campylobacter fetus* impairs barrier function in HT-29/B6 cells through focal tight junction alterations and leaks. *Ann. N. Y. Acad. Sci.* 1405, 189–201. doi: 10.1111/nyas.13406

Bücker, R., Krug, S. M., Moos, V., Bojarski, C., Schweiger, M. R., Kerick, M., et al. (2018). *Campylobacter jejuni* impairs sodium transport and epithelial barrier function via cytokine release in human colon. *Mucosal. Immunol.* 11, 474–485. doi: 10.1038/mi.2017.66

Bücker, R., Troeger, H., Kleer, J., Fromm, M., and Schulzke, J.-D. (2009). *Arcobacter butzleri* induces barrier dysfunction in intestinal HT-29/B6 cells. *J. Infect. Dis.* 200, 756–764. doi: 10.1086/600868

Bullen, T. F., Forrest, S., Campbell, F., Dodson, A. R., Hershman, M. J., Pritchard, D. M., et al. (2006). Characterization of epithelial cell shedding from human small intestine. *Lab. Investig.* 86, 1052–1063. doi: 10.1038/labinvest.3700464

Cróinín, T., and Backert, S. (2012). Host epithelial cell invasion by *Campylobacter jejuni*: trigger or zipper mechanism? *Front. Cell. Infect. Microbiol.* 2:25. doi: 10.3389/fcimb.2012.00025

Delhalle, S., Duvoix, A., Schnekenburger, M., Morceau, F., Dicato, M., and Diederich, M. (2003). "An introduction to the molecular mechanisms of *Apoptosis*," in *Annals of the New York Academy of Sciences*, ed. D. Braaten (New York, NY: New York Academy of Sciences), 1–8. doi: 10.1196/annals.1299.001

Floch, P., Pey, V., Castroviejo, M., Dupuy, J. W., Bonneu, M., de la Guardia, A. H., et al. (2014). Role of *Campylobacter jejuni* gamma-glutamyl transpeptidase on epithelial cell apoptosis and lymphocyte proliferation. *Gut Pathog.* 6:20. doi: 10.1186/1757-4749-6-20

Florian, P., Schöneberg, T., Schulzke, J. D., Fromm, M., and Gitter, A. H. (2002). Single-cell epithelial defects close rapidly by an actinomyosin purse string mechanism with functional tight junctions. *J. Physiol.* 545, 485–499. doi: 10.1113/jphysiol.2002.031161

Fox, J. G., Rogers, A. B., Whary, M. T., Ge, Z., Taylor, N. S., Xu, S., et al. (2004). Gastroenteritis in NF-kappaB-deficient mice is produced with wild-type *Camplyobacter jejuni* but not with *C. jejuni* lacking cytolethal distending toxin despite persistent colonization with both strains. *Infect. Immun.* 72, 1116–1125. doi: 10.1128/iai.72.2.1116-1125.2004

Gitter, A. H., Bendfeldt, K., Schmitz, H., Schulzke, J.-D., Bentzel, C. J., and Fromm, M. (2006). Epithelial barrier defects in HT-29/B6 colonic cell monolayers induced by tumor necrosis factor-α. *Ann. N. Y. Acad. Sci.* 915, 193–203. doi: 10.1111/j.1749-6632.2000.tb05242.x

Gitter, A. H., Bendfeldt, K., Schulzke, J. D., and Fromm, M. (2000). Leaks in the epithelial barrier caused by spontaneous and TNF-α-induced single-cell apoptosis. *FASEB J.* 14, 1749–1753. doi: 10.1096/fj.99-0898com

Grotjohann, I., Schmitz, H., Fromm, M., and Schulzke, J. D. (2000). Effect of TNF alpha and IFN gamma on epithelial barrier function in rat rectum in vitro. *Ann. N. Y. Acad. Sci.* 915, 282–286. doi: 10.1111/j.1749-6632.2000.tb05255.x

Gudipaty, S. A., and Rosenblatt, J. (2017). Epithelial cell extrusion: pathways and pathologies. *Semin. Cell Dev. Biol.* 67, 132–140. doi: 10.1016/j.semcdb.2016.05.010

Günzel, D., Florian, P., Richter, J. F., Troeger, H., Schulzke, J. D., Fromm, M., et al. (2006). Restitution of single-cell defects in the mouse colon epithelium differs from that of cultured cells. *Am. J. Physiol. Regul. Integr. Comp. Physiol.* 290, R1496–R1507. doi: 10.1152/ajpregu.00470.2005

Haag, L. M., Fischer, A., Otto, B., Plickert, R., Kühl, A. A., Göbel, U. B., et al. (2012). *Campylobacter jejuni* induces acute enterocolitis in gnotobiotic IL-10-/- mice via toll-like-receptor-2 and -4 signaling. *PLoS One* 7:e0040761. doi: 10.1371/journal.pone.0040761

Harrer, A., Bücker, R., Boehm, M., Zarzecka, U., Tegtmeyer, N., Sticht, H., et al. (2019). *Campylobacter jejuni* enters gut epithelial cells and impairs intestinal barrier function through cleavage of occludin by serine protease HtrA. *Gut Pathog.* 11:4. doi: 10.1186/s13099-019-0283-z

Heimesaat, M. M., Alutis, M., Grundmann, U., Fischer, A., Tegtmeyer, N., Böhm, M., et al. (2014a). The role of serine protease HtrA in acute ulcerative enterocolitis and extra-intestinal immune responses during *Campylobacter jejuni* infection of gnotobiotic IL-10 deficient mice. *Front. Cell. Infect. Microbiol.* 4:77. doi: 10.3389/fcimb.2014.00077

Heimesaat, M. M., Fischer, A., Alutis, M., Grundmann, U., Boehm, M., Tegtmeyer, N., et al. (2014b). The impact of serine protease HtrA in apoptosis, intestinal immune responses and extra-intestinal histopathology during *Campylobacter jejuni* infection of infant mice. *Gut Pathog.* 6:16. doi: 10.1186/1757-4749-6-16

Heller, F., Florian, P., Bojarski, C., Richter, J., Christ, M., Hillenbrand, B., et al. (2005). Interleukin-13 is the key effector Th2 cytokine in ulcerative colitis that affects epithelial tight junctions, apoptosis, and cell restitution. *Gastroenterology* 129, 550–564. doi: 10.1016/j.gastro.2005.05.002

Heller, F., Fromm, A., Gitter, A. H., Mankertz, J., and Schulzke, J.-D. (2008). Epithelial apoptosis is a prominent feature of the epithelial barrier disturbance in intestinal inflammation: effect of pro-inflammatory interleukin-13 on epithelial cell function. *Mucosal Immunol.* 1(Suppl. 1), S58–S61. doi: 10.1038/mi.2008.46

Hoffmann, S., Batz, M. B., and Morris, J. G. (2012). Annual cost of illness and quality-adjusted life year losses in the united states due to 14 foodborne pathogens. *J. Food Prot.* 75, 1292–1302. doi: 10.4315/0362-028X.JFP-11-417

Hu, L., Bray, M. D., Osorio, M., and Kopecko, D. J. (2006). *Campylobacter jejuni* induces maturation and cytokine production in human dendritic cells. *Infect. Immun.* 74, 2697–2705. doi: 10.1128/IAI.74.5.2697-2705.2006

Inai, T., Kobayashi, J., and Shibata, Y. (1999). Claudin-1 contributes to the epithelial barrier function in MDCK cells. *Eur. J. Cell Biol.* 78, 849–855. doi: 10.1016/S0171-9335(99)80086-7

Jain, D., Prasad, K. N., Sinha, S., and Vishwakarma, A. L. (2009). Cell cycle arrest & apoptosis of epithelial cell line by cytolethal distending toxin positive *Campylobacter jejuni*. *Indian J. Med. Res.* 129, 418–423.

Jin, S., Song, Y. C., Emili, A., Sherman, P. M., and Loong Chan, V. (2003). JIpA of *Campylobacter jejuni* interacts with surface-exposed heat shock protein 90α and triggers signalling pathways leading to the activation of NF-κB and p38 MAP kinase in epithelial cells. *Cell. Microbiol.* 5, 165–174. doi: 10.1046/j.1462-5822.2003.00265.x

Jones, M. A., Tötemeyer, S., Maskell, D. J., Bryant, C. E., and Barrow, P. A. (2003). Induction of proinflammatory responses in the human monocytic cell line THP-1 by *Campylobacter jejuni*. *Infect. Immun.* 71, 2626–2633. doi: 10.1128/iai.71.5.2626-2633.2003

Kalischuk, L. D., Inglis, G. D., and Buret, A. G. (2007). Strain-dependent induction of epithelial cell oncosis by *Campylobacter jejuni* is correlated with invasion ability and is independent of cytolethal distending toxin. *Microbiology* 153, 2952–2963. doi: 10.1099/mic.0.2006/003962-0

Konkel, M. E., Kim, B. J., Rivera-Amill, V., and Garvis, S. G. (1999). Bacterial secreted proteins are required for the internaliztion of *Campylobacter jejuni* into cultured mammalian cells. *Mol. Microbiol.* 32, 691–701. doi: 10.1046/j.1365-2958.1999.01376.x

Krause-Gruszczynska, M., Rohde, M., Hartig, R., Genth, H., Schmidt, G., Keo, T., et al. (2007). Role of the small Rho GTPases Rac1 and Cdc42 in host cell invasion of *Campylobacter jejuni*. *Cell. Microbiol.* 9, 2431–2444. doi: 10.1111/j.1462-5822.2007.00971.x

Li, Y. P., Vegge, C. S., Brøndsted, L., Madsen, M., Ingmer, H., and Bang, D. D. (2011). *Campylobacter jejuni* induces an anti-inflammatory response in human intestinal epithelial cells through activation of phosphatidylinositol 3-kinase/Akt pathway. *Vet. Microbiol.* 148, 75–83. doi: 10.1016/j.vetmic.2010.08.009

Lobo de Sá, F. D., Butkevych, E., Nattramilarasu, P. K., Fromm, A., Mousavi, S., Moos, V., et al. (2019). Curcumin mitigates immune-induced epithelial barrier dysfunction by *Campylobacter jejuni*. *Int. J. Mol. Sci.* 20:4830. doi: 10.3390/ijms20194830

Luettig, J., Rosenthal, R., Barmeyer, C., and Schulzke, J. D. (2015). Claudin-2 as a mediator of leaky gut barrier during intestinal inflammation. *Tissue Barriers* 3:e977176. doi: 10.4161/21688370.2014.977176

McCarthy, K. M., Skare, I. B., Stankewich, M. C., Furuse, M., Tsukita, S., Rogers, R. A., et al. (1996). Occludin is a functional component of the tight junction. *J. Cell Sci.* 109, 2287–2298.

Mousavi, S., Lobo de Sá, F. D., Schulzke, J.-D., Bücker, R., Bereswill, S., and Heimesaat, M. M. (2019). Vitamin D in acute campylobacteriosis-results from an intervention study applying a clinical *Campylobacter jejuni* induced Enterocolitis model. *Front. Immunol.* 10:2094. doi: 10.3389/fimmu.2019.02094

Nielsen, H. L., Nielsen, H., Ejlertsen, T., Engberg, J., Günzel, D., Zeitz, M., et al. (2011). Oral and fecal *Campylobacter* concisus strains perturb barrier function by apoptosis induction in HT-29/B6 intestinal epithelial cells. *PLoS One* 6:e0023858. doi: 10.1371/journal.pone.0023858

Rees, L. E. N., Cogan, T. A., Dodson, A. L., Birchall, M. A., Bailey, M., and Humphrey, T. J. (2008). *Campylobacter* and IFNγ interact to cause a rapid loss of epithelial barrier integrity. *Inflamm. Bowel Dis.* 14, 303–309. doi: 10.1002/ibd.20325

Rosenthal, R., Luettig, J., Hering, N. A., Krug, S. M., Albrecht, U., Fromm, M., et al. (2017). Myrrh exerts barrier-stabilising and -protective effects in HT-29/B6 and Caco-2 intestinal epithelial cells. *Int. J. Colorectal Dis.* 32, 623–634. doi: 10.1007/s00384-016-2736-x

Russell, R. G., O'Donnoghue, M., Blake, D. C., Zulty, J., and DeTolla, L. J. (1993). Early colonic damage and invasion of *Campylobacter jejuni* in experimentally challenged infant *Macaca mulatta*. *J. Infect. Dis.* 168, 210–215. doi: 10.1093/infdis/168.1.210

Saitou, M., Furuse, M., Sasaki, H., Schulzke, J. D., Fromm, M., Takano, H., et al. (2000). Complex phenotype of mice lacking occludin, a component of tight junction strands. *Mol. Biol. Cell* 11, 4131–4142. doi: 10.1091/mbc.11.12.4131

Schmidt, A. M., Escher, U., Mousavi, S., Boehm, M., Backert, S., Bereswill, S., et al. (2019). Protease activity of *Campylobacter jejuni* HtrA modulates distinct intestinal and systemic immune responses in infected secondary abiotic IL-10 deficient mice. *Front. Cell. Infect. Microbiol.* 9:79. doi: 10.3389/fcimb.2019.00079

Schneider, C. A., Rasband, W. S., and Eliceiri, K. W. (2012). NIH Image to ImageJ: 25 years of image analysis. *Nat. Methods* 9, 671–675. doi: 10.1038/nmeth.2089

Schulzke, J. D., Bojarski, C., Zeissig, S., Heller, F., Gitter, A. H., and Fromm, M. (2006). "Disrupted barrier function through epithelial cell apoptosis," in *Annals of the New York Academy of Sciences*, ed. D. Braaten (Malden, MA: Blackwell Publishing Inc), 288–299. doi: 10.1196/annals.1326.027

Schulzke, J. D., Gitter, A. H., Mankertz, J., Spiegel, S., Seidler, U., Amasheh, S., et al. (2005). Epithelial transport and barrier function in occludin-deficient mice. *Biochim. Biophys. Acta - Biomembr.* 1669, 34–42. doi: 10.1016/j.bbamem.2005.01.008

Song, Y. C., Jin, S., Louie, H., Ng, D., Lau, R., Zhang, Y., et al. (2004). FlaC, a protein of *Campylobacter jejuni* TGH9011 (ATCC43431) secreted through the flagellar apparatus, binds epithelial cells and influences cell invasion. *Mol. Microbiol.* 53, 541–553. doi: 10.1111/j.1365-2958.2004.04175.x

Spiller, R. C., Jenkins, D., Thornley, J. P., Hebden, J. M., Wright, T., Skinner, M., et al. (2000). Increased rectal mucosal enteroendocrine cells, T lymphocytes, and increased gut permeability following acute *Campylobacter enteritis* and in post-dysenteric irritable bowel syndrome. *Gut* 47, 804–811. doi: 10.1136/gut.47.6.804

Tam, C. C., and O'Brien, S. J. (2016). Economic cost of campylobacter, norovirus and rotavirus disease in the United Kingdom. *PLoS One* 11:e0138526. doi: 10.1371/journal.pone.0138526

Whitehouse, C. A., Balbo, P. B., Pesci, E. C., Cottle, D. L., Mirabito, P. M., and Pickett, C. L. (1998). *Campylobacter jejuni* cytolethal distending toxin causes a

G2-phase cell cycle block. *Infect. Immun.* 66, 1934–1940. doi: 10.1128/iai.66.5.1934-1940.1998

Wine, E., Chan, V. L., and Sherman, P. M. (2008). *Campylobacter jejuni* mediated disruption of polarized epithelial monolayers is cell-type specific, time dependent, and correlates with bacterial invasion. *Pediatr. Res.* 64, 599–604. doi: 10.1203/PDR.0b013e31818702b9

Zeissig, S., Bürgel, N., Günzel, D., Richter, J., Mankertz, J., Wahnschaffe, U., et al. (2007). Changes in expression and distribution of claudin 2, 5 and 8 lead to discontinuous tight junctions and barrier dysfunction in active Crohn's disease. *Gut* 56, 61–72. doi: 10.1136/gut.2006.094375

Conflict of Interest: The authors declare that the research was conducted in the absence of any commercial or financial relationships that could be construed as a potential conflict of interest.

frontiers in Microbiology

ORIGINAL RESEARCH
published: 24 March 2020
doi: 10.3389/fmicb.2020.00460

Investigating the Role of FlhF Identifies Novel Interactions With Genes Involved in Flagellar Synthesis in *Campylobacter jejuni*

*Xiaofei Li[1], Fangzhe Ren[1], Guoqiang Cai[2], Pingyu Huang[2], Qinwen Chai[2], Ozan Gundogdu[3], Xinan Jiao[4] and Jinlin Huang[4]**

[1] Jiangsu Key Laboratory of Zoonosis, Jiangsu Co-Innovation Center for Prevention and Control of Important Animal Infectious Diseases and Zoonoses, Yangzhou University, Yangzhou, China, [2] Key Laboratory of Prevention and Control of Biological Hazard Factors (Animal Origin) for Agrifood Safety and Quality, Ministry of Agriculture of China, Yangzhou, China, [3] Department of Infection Biology, Faculty of Infectious and Tropical Diseases, London School of Hygiene and Tropical Medicine, London, United Kingdom, [4] Joint International Research Laboratory of Agriculture and Agri-product Safety, Ministry of Education of China, Yangzhou, China

FlhF is a key protein required for complete flagellar synthesis, and its deletion results in the complete absence of a flagella and thus motility in *Campylobacter jejuni*. However, the specific mechanism still remains unknown. In this study, RNA-Seq, EMSAs, ChIP-qPCR and β-Galactosidase assays were performed to elucidate the novel interactions between FlhF and genes involved in flagellar synthesis. Results showed that FlhF has an overall influence on the transcription of flagellar genes with an *flhF* mutant displaying down-regulation of most flagellar related genes. FlhF can directly bind to the *flgI* promoter to regulate its expression, which has significant expression change in an *flhF* mutant. The possible binding site of FlhF to the *flgI* promoter was explored by continuously narrowing the *flgI* promoter region and performing further point mutations. Meanwhile, FlhF can directly bind to the promoters of *rpoD*, *flgS,* and *fliA* encoding early flagellin regulators, thereby directly or indirectly regulating the synthesis of class I, II, and III flagellar genes, respectively. Collectively, this study demonstrates that FlhF may directly regulate the transcription of flagellar genes by binding to their promoters as a transcriptional regulator, which will be helpful in understanding the mechanism of FlhF in flagellar biosynthetic and bacterial flagellation in general.

Keywords: ***Campylobacter jejuni*, FlhF, transcriptional regulator, flagellar biosynthesis, pathogenesis**

OPEN ACCESS

Edited by:
Paloma López, Center for Biological Research (CSIS), Spain

Reviewed by:
Ian F. Connerton, University of Nottingham, United Kingdom
Manuel Zúñiga Cabrera, Institute of Agrochemistry and Food Technology (IATA), Spain

****Correspondence:***
Jinlin Huang
jinlin@yzu.edu.cn

Specialty section:
This article was submitted to Food Microbiology, a section of the journal Frontiers in Microbiology

Received: *14 September 2019*
Accepted: *04 March 2020*
Published: *24 March 2020*

Citation:
Li X, Ren F, Cai G, Huang P, Chai Q, Gundogdu O, Jiao X and Huang J (2020) Investigating the Role of FlhF Identifies Novel Interactions With Genes Involved in Flagellar Synthesis in Campylobacter jejuni. Front. Microbiol. 11:460. doi: 10.3389/fmicb.2020.00460

INTRODUCTION

Campylobacter jejuni flagella are considered the main virulence factor playing a key role in many important biological activities, such as motility, chemotaxis, adhesion, secreting virulence and colonization factors (Beeby, 2015; Burnham and Hendrixson, 2018; Subramanian and Kearns, 2019). *C. jejuni* is a microaerophilic, Gram-negative bacterium, and is the leading cause of foodborne related gastroenteritis worldwide (Flint et al., 2016; Burnham and Hendrixson, 2018). It generates a single unsheathed flagellum at one or both poles of the cell (Hendrixson and Dirita, 2003; Matsunami et al., 2016; Liang and Connerton, 2018). Flagellar biosynthesis is complicated requiring expression of

more than 50 genes highly regulated by a complex regulatory network that ensures the coordinate expression to construct an intact flagella organelle (Balaban et al., 2009; Grinnage-Pulley et al., 2016; Liang and Connerton, 2018). Given the importance of flagella, a thorough understanding of its assembly is necessary.

In many bacteria, flagella genes are grouped together into operons and are controlled by global regulatory factors (Chilcott and Hughes, 2000; Prouty et al., 2001; Dasgupta et al., 2003; Liu and Ochman, 2007). In *C. jejuni* however, scattered flagellar genes lack a global regulatory factor, such as FlhDC in *E. coli*, creating a challenge for exploring the regulation mechanism on the flagellar synthesis. The formation of flagella is divided into three cascades (Balaban et al., 2009). In the early stage, σ70 factor-dependent class I genes are synthesized, including flagellar export apparatus (FEA, consisting of FlhA, FlhB, FliF, FliO, FliP, FliQ, and FliR), σ28, σ54 factors and FlgSR TCS. Then class II genes and class III genes are synthesized in sequence (Wösten et al., 2004; Joslin and Hendrixson, 2009; Lertsethtakarn et al., 2011). Although flagella have long been extensively studied, there remains a gap in our knowledge as to the regulation mechanisms of flagellar proteins synthesis (Gao et al., 2014).

One identified protein that primarily affects flagellar biosynthesis is FlhF. In other species, the disruption of *flhF* can lead to a range of different phenotypes, including reduced flagellar gene expression, decreased or absent motility, decreased virulence, abnormal flagella assembly and number, and even no flagellation (Kazmierczak and Hendrixson, 2013; Burnham and Hendrixson, 2018). In *C. jejuni*, an *flhF* mutant leads to a complete loss of motility and a non-flagellar phenotype. Despite FlhF having a crucial influence on the flagellar synthesis, the specific genetic regulatory mechanisms are unclear (Kim et al., 2012; Kazmierczak and Hendrixson, 2013; Schuhmacher et al., 2015). Thus far, many studies of FlhF have focused on its role in determining the position and number of flagella substructure. FlhF is a member of the signal recognition particle (SRP) associated GTPase family, however the exact function is not well defined (Kim et al., 2012; Guttenplan et al., 2013; Schniederberend et al., 2013; Schuhmacher et al., 2015; Gulbronson et al., 2016). Other studies have identified the influence on flagellar gene expression, nevertheless, the results reported have not always been in alignment (Niehus et al., 2004; Correa et al., 2005; Murray and Kazmierczak, 2006; Balaban et al., 2009; Kim et al., 2012). In *C. jejuni*, the specific mechanisms of FlhF still need to be explored in depth.

Transcriptional regulators are important for biological response and their adaptability to different conditions in the organism (Galán-Vásquez et al., 2016). Some organisms have many transcriptional regulators, for example *E. coli* has seven σ factors, *Bacillus subtilis* has 19, *Streptomyces coelicolor* over 60 and more than 100 in *Sorangium cellulosum* (Bervoets and Charlier, 2019). However, the *C. jejuni* genome carries only three sigma factors, RpoD, RpoN, and FliA (Hwang et al., 2011). Meanwhile, there are approximately 34 other transcription factors in *C. jejuni* (Wösten et al., 2004; Nachamkin et al., 2008; Grinnage-Pulley et al., 2016). Genome-wide analysis indicates that *C. jejuni* strains contain between approximately 1,650 and 1,800 genes (Parkhill et al., 2000; Hofreuter et al., 2006; Parker et al., 2006). So this indicates that all *C. jejuni* biological functions, including bacterial replication, adaptation to environments and bacterial pathogenicity are largely controlled by a limited number (∼2% of the total) of *C. jejuni* proteins (Nachamkin et al., 2008). Therefore, the discovery of new transcriptional factors and transcriptional regulation mechanisms is essential to better analyze *C. jejuni* biology.

Considering the crucial influence of FlhF on the flagellar synthesis, we speculate that FlhF may directly regulate flagellar genes expression like a transcription factor. We have applied EMSA and ChIP-qPCR to explore the transcriptional function of FlhF here. The overall influence of FlhF on flagellar gene expression was analyzed by RNA-Seq. We further explored whether FlhF directly regulates early flagellar regulatory factors including RpoD, RpoN, FliA, FlgSR two-component system (TCS) (Petersen et al., 2003; Wösten et al., 2004). Collectively, our results firstly reveal that FlhF may directly regulate flagellar genes transcription by binding the promoters of specific genes (Huffman and Brennan, 2002). Moreover, we proposed a pattern for the feasible transcriptional regulatory pathways of FlhF in flagellar synthesis which will be helpful in understanding the *C. jejuni* flagella biosynthetic pathway and bacterial flagellation in general.

MATERIALS AND METHODS

Bacterial Strains and Plasmids

All strains and plasmids used in this study are listed in **Supplementary Table S1**. Briefly, *C. jejuni* 81–176 strain and its derivatives were typically grown on *Campylobacter* blood-free selective agar containing charcoal cefoperazone deoxycholate (CCDA) (Oxoid, Basingstoke, United Kingdom) at 42°C under microaerobic conditions (85% N_2, 10% CO_2, and5% O_2). *Escherichia coli* DH5α and BL21 strains were grown at 37°C in Luria-Bertani (LB) broth or on LB agar (Ren et al., 2018). As required, antibiotics were added to the medium for *C. jejuni* or *E. coli* at the following concentrations: 100 μg ml^{-1} ampicillin, 50 μg ml^{-1} kanamycin, or 20 μg ml^{-1} chloramphenicol. The plasmid pMD-19T (simple) (TaKaRa, Dalian, China) was used as a suicide vector in cloning and strain construction. Plasmid pRK2013 (Biomedal, Seville, Spain) is a helper plasmid for triparental mating conjugation, while pUOA18 is a *C. jejuni* shuttle vector courtesy of Qijing Zhang (Iowa State University, Ames, United States).

Construction of *C. jejuni* Mutant and Complemented Strains

To inactivate *flhF*, its flanking regions and the Kan^R cassette were amplified from *C. jejuni* genome and pRY107, then, ligated into pMD-19T (simple) using T4 ligase to obtain a suicide plasmid. The primers used for strain construction are listed in **Supplementary Table S2**. The suicide plasmid was electroporated into *C. jejuni* competent cells, and the resulting transformants were selected on CCDA agar containing 50 μg ml^{-1} kanamycin. The *flhF* complement strain was constructed by the shuttle vector pUOA18 as previously described (Ren et al., 2018).

The target gene was amplified and ligated directly downstream of the promoter P*metk* in the shuttle vector. The recombinant plasmid was mobilized into the *flhF* mutant strain by triparental mating using *E. coli* DH5α transformant containing pUOA18-P*metk-flhF* plasmid as the donor strain and DH5α (pRK2013) as the helper strain, by the method described by Miller et al. (2000). The cultures of *flhF* mutant strain were removed and resuspended in PBS to an OD_{600} of 1.0. Overnight cultures of the donor and helper *E. coli* strains were subcultured into Luria-Bertani (LB) broth and grown to an OD_{600} of 1.2. Cells were mixed at a ratio of 1:1:10 (donor/helper/recipient), spotted onto the Mueller-Hinton (MH) agar plate (BD, United States), and incubated overnight at 42°C under microaerophilic conditions. The mating spot was then resuspended in Mueller-Hinton (MH) broth and plated onto CCDA plate amended with Polymyxin B (6.7 μg/ml), Rifampicin (10 μg/ml), Trimethoprim (5 μg/ml), and chloramphenicol (20 μg/ml). The plates were examined after 3–5 days for the appearance of *C. jejuni* colonies, and verified by polymerase chain reaction (PCR).

Expression and Purification of FlhF-His_6, CmeR-His_6

FlhF and CmeR proteins were expressed in *E. coli* DE3 system containing pET-30-FlhF and pCold I-CmeR, respectively. The *flhF*, *cmeR* genes were amplified from *C. jejuni* genome, then, ligated into pET-30a (between *Bam*HI and *Xho*I sites) and pCold I (between *Xho*I and *Sal*I sites), respectively, using the ClonExpress II one-step cloning kit (Vazyme, Nanjing, China) to generate the recombinant expressing plasmids used to transform *E. coli* DE3. Then they were cultured on a LB plate containing 50 μg/ml kanamycin and verified by PCR and nucleotide sequencing. The FlhF-His_6, CmeR-His_6 protein were expressed and purified from the soluble extract by affinity chromatography using a HiTrap Ni^{2+}-chelating column. The purification procedure followed the instructions of the manufacturer of the His Bind Purification Kit (Novagen, EMO Millipore corp, Billerica, MA, United States). Purified Protein were analyzed by SDS-PAGE (**Supplementary Figure S5**) and stored at −70°C.

Construction of Promoter-*lacZ* Transcriptional Fusions

The promoter regions of interest were amplified from *C. jejuni* genome and ligated into pMW10 to obtain promoter-*lacZ* transcriptional fusion plasmids (Wosten et al., 1998). With the aid of plasmid pRK2013, the transcriptional fusion plasmids were introduced into WT and the *flhF* mutant strain by amphiphilic mating conjugation, which was cultured on a CCDA agar containing 50 μg/ml kanamycin, and verified by PCR. The primers used for strain construction are listed in **Supplementary Table S2**.

RNA Isolation and Quantitative Real-Time PCR

Campylobacter jejuni 81-176, FlhF-kan mutant strain was grown on CCDA plates and suspended in Mueller-Hinton (MH) broth (BD, United States) with an initial OD_{540} of 0.07, cultured for 8 h with 42°C, 120 rpm, and total RNA was extracted by using an RNeasy plus mini kit (Qiagen, Hilden, Germany) obeying the instructions of manufacturer. cDNA was synthesized by a total of 500 ng of RNA using RT reagent kit (TaKaRa, Dalian, China), which was subjected to quantitative real-time PCR (qRT-PCR) or stored at −70°C until use. qRT-PCR was carried out in an ABI PRISM 7500 Real-Time PCR System (Applied Biosystems, Foster City, CA, United States) using a FastStart Universal SYBR Green Master (ROX) (Roche Diagnostics, Mannheim, Germany). Cycling conditions were as follows: 2 min at 50°C, then 40 cycles of 30 s at 95°C and 34 s at 60°C. As previously described, relative genes expression was calculated using the $2^{-\Delta\Delta CT}$ method (Livak and Schmittgen, 2001). All specific primers are listed in **Supplementary Table S2**, in which the *glyA* gene was used as an endogenous control. A series of 10-fold diluted cDNA were used as templates and the standard curves were generated for each candidate genes. The PCR efficiency (E) was calculated using the following formula (Pfaffl, 2001):

$$E = 10^{(-1/-\text{slope})}$$

RNA-Seq

To analyze the transcriptome, RNA-Seq libraries were generated for six bacterial samples [2 bacterial strains (WT, Δ*flhF*) × 3] from cDNA using instructions according to the TruSeq™ RNA sample preparation Kit (Illumina, San Diego, CA, United States). As previously described, the quality control of the total RNA samples was performed using a 2100 Bioanalyzer (Agilent) and the ND-2000 (NanoDrop Technologies). Only high-quality RNA samples (OD260/280 = 1.8∼2.2, OD260/230 ≥ 2.0, RIN ≥ 6.5) were used to construct sequencing library (Zhang et al., 2019). The cDNA was then synthesized according to the SuperScript double-strand cDNA synthesis kit (Invitrogen, Carlsbad, CA, United States). The RNA-Seq libraries were subjected to quality inspection using an Agilent 2100 Bioanalyzer (Agilent Technologies) and sequenced on an Illumina HiSeq4000 (Illumina Inc., San Diego, CA, United States), which was biologically replicated in a separate experiment by Majorbio (Shanghai, China). Sequence reads were processed and mapped as previously described (Garber et al., 2011). Gene expression (FPKM) and differential expression levels were analyzed using Rsem[1] and edgeR software[2]. For functional annotation of mRNA, we used Blastx with the NCBI-NR database, String, Swissprot and the Kyoto encyclopedia of genes and genomes (KEGG) database. Statistical analysis according to the method described in the previous period, P-value < 0.05 was considered to be statistically significant. All RNA-Seq data was uploaded to the EBI ENA databased (Accession number PRJEB34440).

Electrophoretic Mobility Shift Assay (EMSAs)

The EMSAs were performed as follows: PCR fragments encompassing the promoters of genes with FAM-labeled were

[1]http://deweylab.biostat.wisc.edu/rsem/

[2]http://www.bioconductor.org/packages/2.12/bioc/html/edgeR.html

amplified using genomic DNA of *C. jejuni* 81-176 as a template. The DNA fragments were gel-purified using MiniBEST Agarose Gel DNA Extraction Kit (Takara, Japan). Each PCR product (≈5 ng) was mixed with increasing concentrations of purified FlhF-His_6 in a final volume of 20 μl buffer containing 10 mM Tris-HCl (pH 8.0), 50 mM KCl, 1 mM DTT, 0.5 mM EDTA and 5% glycerol. The reactions were incubated for 30 min at 25°C and then loaded with 10×EMSA loading buffer on 6% polyacrylamide non-denaturing gels in 0.5 × Tris-borate-EDTA buffer. Each reaction was verified to be specific by adding 10-fold non-specific competitor [Poly(dI:dC)]. For a negative control, synthesized His-tag was incubated with *flgI* promoter, denoted as negative control (NC). For positive controls, cmeA promoter was incubated with the purified CmeR protein, and *cmeA* promoter alone, denoted as positive control (PC) (Cagliero et al., 2007).

ChIP-qPCR

The 3 × FLAG-tagged strain (WT *flhF*-FLAG) was grown under microaerobic conditions and then pelleted by centrifugation. As described previously (Blasco et al., 2012), however, with some variation, ChIP was performed based on established methods as follows. Formaldehyde was added to bacterial cells (1% final concentration) for cross-linking and then incubated at room temperature for 25 min. Reactions were quenched with 0.5 M glycine, and samples were pelleted and washed three times with PBS. The samples were then used for ChIP following the Chromatin Immunoprecipitation kit (Millipore, United States) protocol. The antibody used was the anti-FLAG mouse monoclonal antibody (Sigma). For ChIP-qPCR experiments, untreated chromatin was de-cross-linked by boiling for 10 min and purified for use as the "input" control. The relative enrichment of candidate gene promoters was performed with qRT-PCR and represents the value of the immunoprecipitated DNA divided by the input unprecipitated DNA. These values were normalized to the values obtained for each promoter precipitated using untagged wild-type in order to account for non-specific enrichment. The results represent the mean enrichment measured via qPCR in at least three biological replicate experiments.

β-Galactosidase Assay

Campylobacter jejuni cells carrying the transcriptional fusion plasmids were grown on CCDA plates and suspended in MH broth with the same OD_{600}. The cells with centrifugation were suspended thoroughly with 1 ml Z buffer (60 mM Na_2HPO_4, 40 mM NaH_2PO_4, 10 mM KCl, 1 mM $MgSO_4$, pH 7.0) and shaken vigorously to lyse the cells with adding 30 μl of chloroform and 0.1% SDS. The assays were performed at 37°C with 200 μl ONPG (*O*-nitrophenol-β-D-galactopyranoside, 4 mM, Sigma) and monitored at 420 nm (Cagliero et al., 2007). β-Galactosidase activities were calculated in Miller Units using the formula given below: β-Galactosidase activity = A420 × 1000 × min^{-1} × ml^{-1} × $A600^{-1}$. The results were reported as the mean of three biological replicates.

RESULTS

FlhF Has an Overall Impact on the Transcription of Flagella Components

To investigate which genes are regulated by FlhF on the transcriptional level, we performed high-throughput RNA sequencing based on the genetic background (*flhF* mutant vs. wild-type). RNA-Seq data (**Supplementary Table S3**) showed all the modulated flagellar related genes are down-regulated in the mutant, suggesting FlhF has a positive role in flagellar gene transcription. Among these down-regulated genes, 26 genes are involved in the process of flagellar biosynthesis. Grouping these genes according to their function and substructure affiliation showed a general trend of down-regulation from flagella export apparatus, motor/switch components, an unknown function (hypothetical genes with unknown function), flagellin glycosylation, transcription regulators, flagella basal body, the filament, to the most down-regulated which was the flagella hook

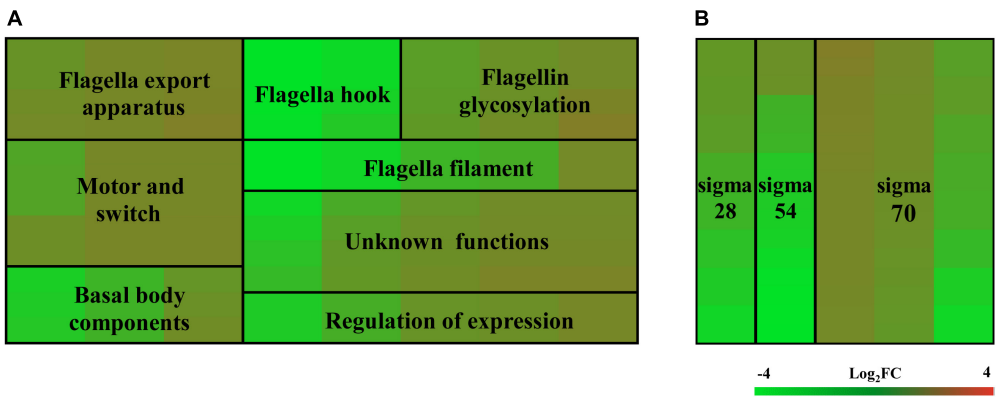

FIGURE 1 | Heat map of relative mRNA expression of *C. jejuni* flagella genes. The transcription of flagella genes in the RNA-Seq were analyzed according to their function and substructure affiliation **(A)**, as well as transcription cascade **(B)**. Flagella hook genes and class II genes were significantly affected according to the ANOVA analysis at $P < 0.05$. Green and red in the heat map represent down-regulation and up-regulation of genes in the *flhF* mutant relative to the wild-type strain, with more saturated colors representing a larger differential effect as listed in the bar.

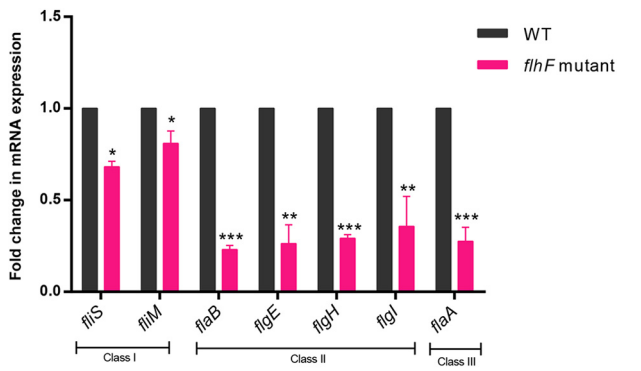

FIGURE 2 | qRT-PCR for verification of RNA-Seq data. qRT-PCR data demonstrated correlation with the RNA-Seq data when investigating the transcript fold-change difference between WT strain and the *flhF* mutant strain. Each sample was examined in three biological replicates and was repeated with three technical replicates. Data are presented as mean ± SD. Data were analyzed by using a one-sample *t*-test (*$P < 0.05$, **$P < 0.01$, ***$P < 0.001$).

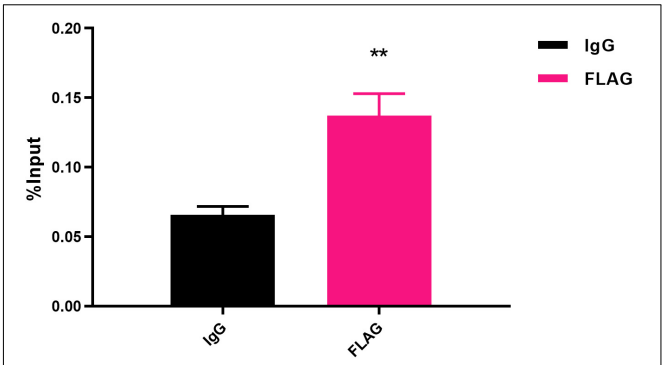

FIGURE 4 | Fold enrichment of the *flgI* promoter in ChIP samples measured via ChIP-qPCR. The results show the promoter of *flgI* was extremely enriched in FlhF-ChIP samples, and the relative quantity was significantly higher than in the IgG control samples. Genome fragments isolated from wild-type *flhF*-FLAG strain were immunoprecipitated with corresponding antibodies, and analyzed by real-time PCR using primer sets corresponding to transcriptional start site regions of the *flgI*. For ChIP-qPCR experiments, the sample was cross-linked and sonicated to generate small DNA fragments, and then divided into three parts. The first was used as an input control. The second was incubated with normal rabbit IgG that will not bind to nuclear proteins to generate immuno-precipitated DNA (IgG). The third was as ChIP-FLAG immunoprecipitated sample (FLAG) (O'Geen et al., 2010). Results represent mean enrichment as measured by qPCR in at least three biological replicate experiments. Data are presented as mean ± SD. Data were analyzed by one-sample *t*-test (**P values are < 0.01, but > 0.001) to estimate the significance of fold change between FlhF-ChIP samples and IgG control samples.

(**Figure 1A**). Flagellar genes are classified into three cascades, class I genes are σ70 dependent, while class II and class III genes require σ54 and σ28 factor, respectively (Ren et al., 2018). A one-way ANOVA analysis showed that class I, III, and II genes were significantly modified when comparing the *flhF* mutant to the respective wild-type strain (**Figure 1B**). qRT-PCR was performed to verify the results of the RNA-Seq data. Seven flagellar genes that belong to different cascades were randomly selected (**Figure 2**). The amplification efficiency of each pair of primers were close to 2 (**Supplementary Figure S1**) and the reference gene *glyA* was constantly expressed under this experimental condition due to the relatively stable CT values (**Supplementary Table S4**).

FlhF May Directly Regulate *flgI* Transcription by Binding Its Promoter

To determine the transcriptional function of FlhF, six genes with significantly different expression were randomly selected from the RNA-Seq results, including *fliK*, *flaB*, *flgE*, *flaA*, *flgL*, *flgI*, to explore whether FlhF binds their promoters by Electrophoretic

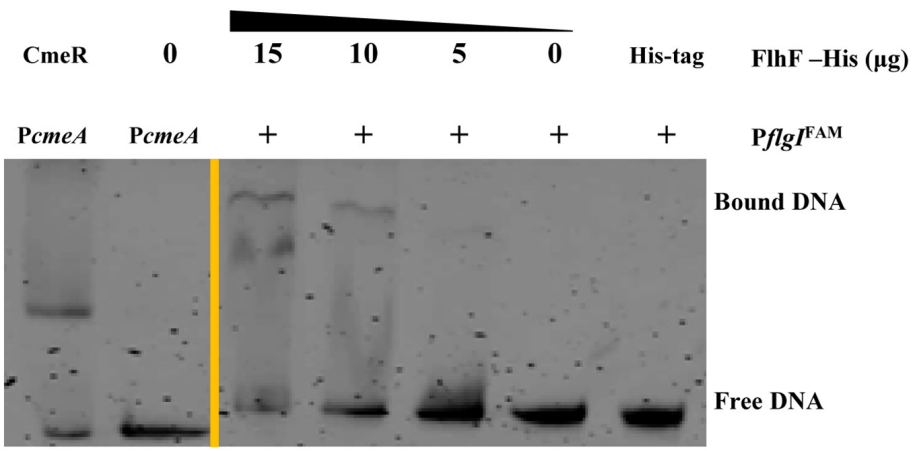

FIGURE 3 | FlhF directly interact with the *flgI* promoter. EMSA demonstrated that the fluorescently labeled DNA probes of the *flgI* promoter were incubated with purified FlhF-6His at different concentrations. Each reaction was verified to be specific by adding 10-fold non-specific competitor [Poly(dI:dC)]. For a negative control, synthesized His-tag was incubated with *flgI* promoter, denoted as negative control (NC). For positive controls, *cmeA* promoter was incubated with the purified CmeR protein, and *cmeA* promoter alone, denoted as positive control (PC). The "+" symbol indicates the presence of FlhF-6His.

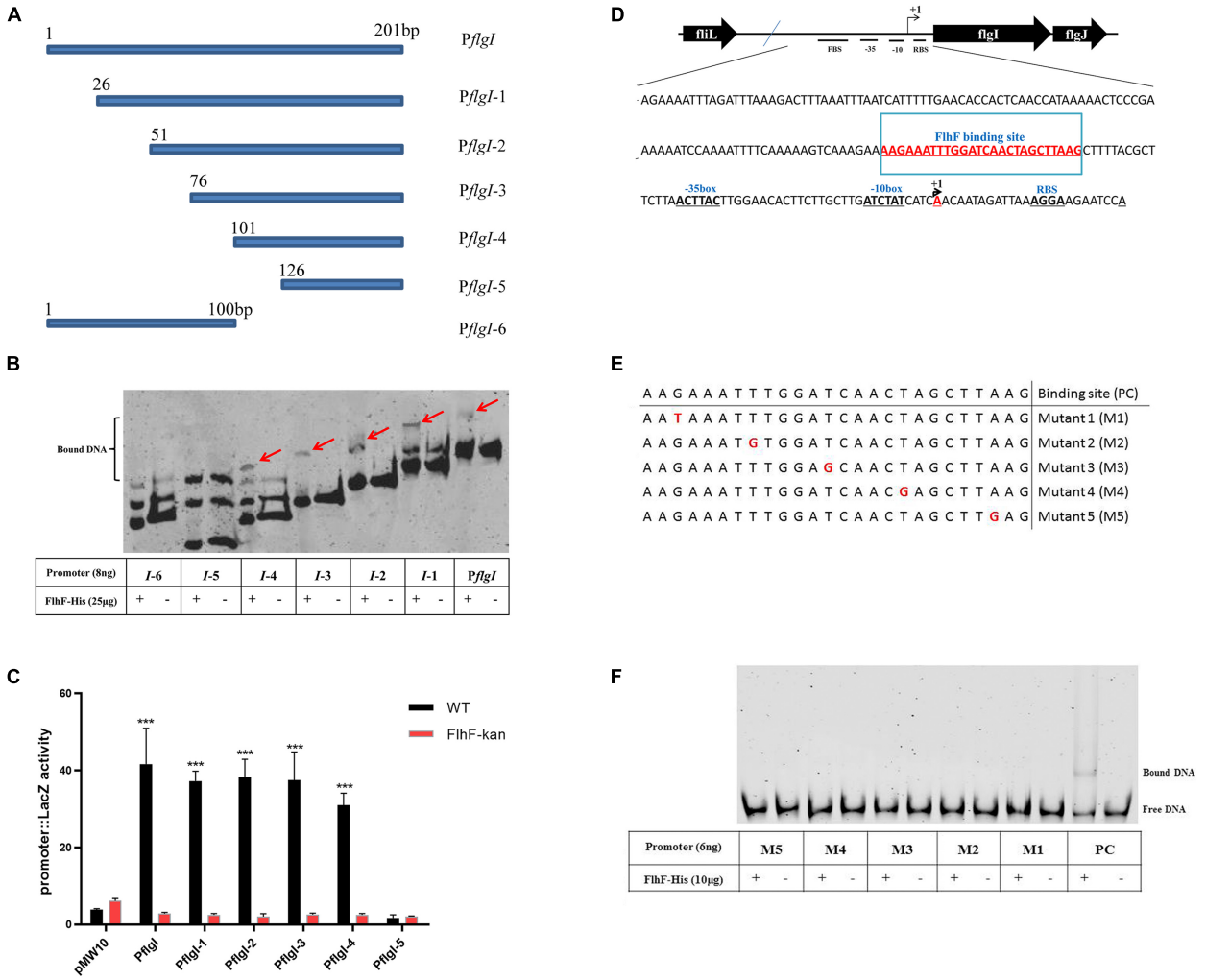

FIGURE 5 | FlhF- binding site in the *flgI* promoter. **(A)** A diagram of the *flgI* promoter (a 201 bp fragment of the promoter adjacent to the start codon "ATG") and the six regions carried on the DNA fragments used in this assay. Fragment names are displayed in figure. **(B)** EMSA analysis of FlhF specifically binding to the *flgI* promoter. All seven fragments (8 ng) with FAM labeled in **(A)** were incubated with purified FlhF-His_6 (25 μg). The "+" and "–" symbols indicate cultures incubated with FlhF-His_6 and without FlhF-His_6, respectively. The red arrows represent the bound DNA. Each reaction was verified to be specific by adding 10-fold non-specific competitor [Poly(dI:dC)]. **(C)** β-Galactosidase assay for verification of EMSA results. Expression of the β-Galactosidase activities in WT and *flhF* mutant strains containing different fragments. The activity is expressed as the mean ± SE from three biological experiments. The strains containing pMW10 served as negative control. Data were analyzed by *t*-test to estimate the significance of fold change between WT and FlhF-kan samples. The symbol "****" means $P < 0.001$. **(D)** Diagram showing the promoter region of the *flgI* gene. The ribosome-binding site (RBS) are underlined and the transcription start sites are labeled as +1 and marked in red. The −35/−10 motif were located directly upstream of the transcriptional start site +1A. We speculated that the FlhF-binding site was underlined and marked in red (−76 to −51). **(E)** A diagram of five different point mutations of possible FlhF-binding site on P*flgI* (a 26 bp fragment) and the six DNA fragments used in this assay. Fragment names are displayed in figure. PC signifies positive control. **(F)** EMSA analysis of the binding of FlhF to the five different point mutations. All six fragments (6 ng) with FAM labeled in **(E)** were incubated with purified FlhF-His_6 (10 μg). The "+" and "–" symbols indicate cultures incubated with FlhF-His_6 and without FlhF-His_6, respectively. Each reaction was verified to be specific by adding 10-fold non-specific competitor [Poly(dI:dC)].

mobility shift assay (EMSA). Our results demonstrated that the purified FlhF-His_6 bound to the promoter of *flgI* (**Figure 3**), the flagellar P-ring component, but did not bind to the promoters of other genes (**Supplementary Figures S2A–E**). The results were further verified by Chromatin Immunoprecipitation quantitative PCR (ChIP-qPCR) analysis (**Figure 4**). We selected *flgI* and *flaB* to perform ChIP-qPCR, which showed that the promoter of *flgI* was extremely enriched in FlhF-ChIP samples, and the relative quantity was significantly higher than in the IgG control samples (**Figure 4**), while the promoter of *flaB* was not enriched in the FlhF-ChIP samples (**Supplementary Figure S3**). In summary, all results demonstrated that FlhF may directly regulate *flgI* as a positive transcriptional regulator.

FlhF-Binding Site in the *flgI* Promoter

To delineate the contribution of portions of the *flgI* promoter for binding of FlhF, the *flgI* promoter was divided into six fragments (**Figure 5A**), which were amplified with FAM-labeling

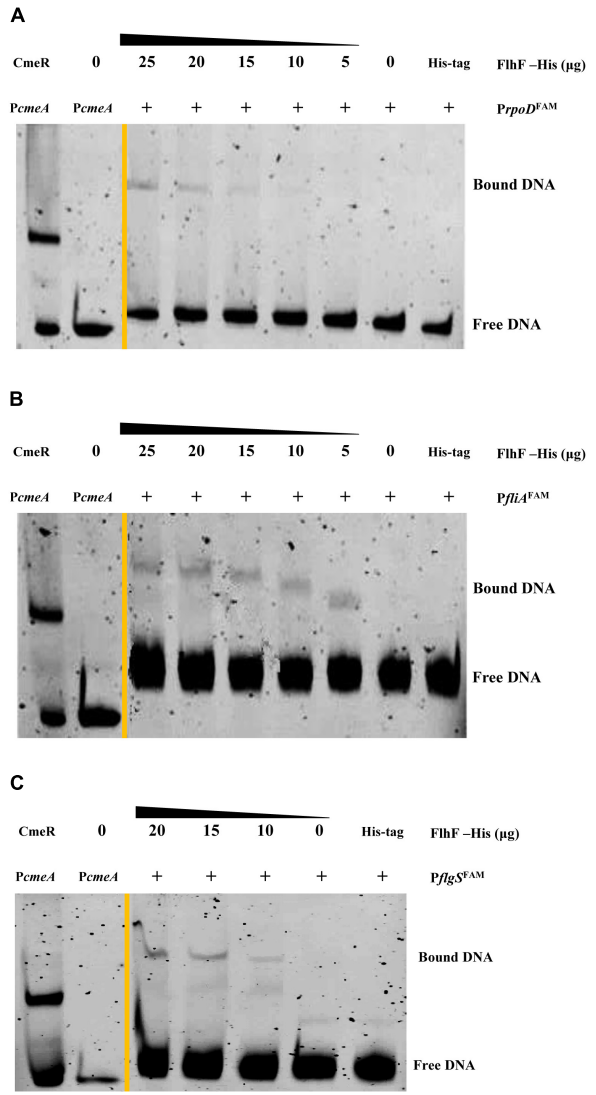

FIGURE 6 | FlhF directly interact with the promoter of *rpoD, fliA, flgS*. The fluorescently labeled DNA probes of the promoter were incubated with purified FlhF-HIS$_6$ at different concentrations and promoters **(A)** *rpoD*; **(B)** *fliA* and **(C)** *flgS* respectively. For a negative control, synthesized His-tag was incubated with *flgI* promoter, denoted as negative control (NC). Each reaction was verified to be specific by adding 10-fold non-specific competitor Poly(dI:dC)]. For positive controls, *cmeA* promoter was incubated with the purified CmeR protein, and *cmeA* promoter alone, denoted as positive control (PC). The "+" symbol indicates the presence of FlhF-6His.

TABLE 1 | Differentially expressed flagellar genes between the *flhF* mutant and wild-type strains.

Gene_ID	Log2FC	Class	Gene description
CJJ81176_RS00360	−7.721164828	I	Flagellar biosynthesis protein FlhF
CJJ81176_RS00345	−1.53294197	I	RNA polymerase sigma factor FliA
CJJ81176_RS02660	−1.489019921	I	Flagella export chaperone FliS
CJJ81176_RS00335	−1.108875525	I	Flagellar motor switch protein FliY
CJJ81176_RS00340	−1.055058784	I	Flagellar motor switch protein FliM
CJJ81176_RS00255	−4.034345574	II	Flagellar hook-length control protein FliK
CJJ81176_RS06435	−3.961478247	II	Flagellin B (FlaB)
CJJ81176_RS00265	−3.918053318	II	Flagellar hook protein FlgE
CJJ81176_RS00260	−3.83754024	II	Flagellar basal body rod modification protein
CJJ81176_RS08350	−3.541966567	II	Flagellar hook protein FlgE
CJJ81176_RS07025	−3.424321206	II	Flagellar protein FlgN
CJJ81176_RS07030	−3.19611075	II	Flagellar hook-associated protein FlgK
CJJ81176_RS03320	−3.036794005	II	Flagellar L-ring protein (FlgH)
CJJ81176_RS07020	−2.9346010678	II	Anti-σ factor (FlgM)
CJJ81176_RS07015	−2.87737963	II	Rod assembly protein (FlgJ)
CJJ81176_RS04235	−2.742932491	II	Flagellar hook-associated protein FlgL
CJJ81176_RS07010	−2.710980572	II	Flagellar P-ring protein (FlgI)
CJJ81176_RS00355	−2.073823244	II	MinD/ParA family protein (FlhG)
CJJ81176_RS02555	−1.831517369	II	Flagellar basal body rod protein FlgB
CJJ81176_RS03370	−1.76013941	II	Flagellar hook-basal body protein (FlgG2)
CJJ81176_RS03375	−1.678817425	II	Flagellar basal-body rod protein FlgG
CJJ81176_RS06440	−3.392189439	III	Flagellin A
CJJ81176_RS02655	−1.844789866	III	Flagellar filament capping protein FliD

Genes with log2 (fold change) > 1.0 or <1.0 with a p-value ≤ 0.05 were considered significant. Genes of unknown functions and those that encode hypothetical proteins were not included in this table.

and ligated into pMW10 to perform EMSA and β-Galactosidase assay here. EMSA results showed that the purified FlhF-His$_6$ bound to the fragments 1–4 of the *flgI* promoter, but did not bind to the fragments 5–6 (**Figure 5B**), which demonstrated that the putative binding site of FlhF in the *flgI* promoter was between 101–125 bp. β-Galactosidase assays performed to verify the results from 5B and showed that the fragments 1–4 of the *flgI* promoter had notable differences between the WT and *flhF* mutant strain, but fragment 5 has no difference with negligible activity, which was consistent with the EMSAs (**Figure 5C**). We used strains containing pMW10 served as a negative control. Therefore, we speculated the FlhF-binding site (FBS) in *flgI* promoter is the region "−76 to −51" (AAGAAATTTGGATCAACTAGCTTAAG) (**Figure 5D**). To further investigate the necessity of this motif for the binding of FlhF to the *flgI* promoter (P*flgI*), we selected a point mutation every 5 bp on the possible FlhF-binding site to generate five different point mutation fragments which were amplified with FAM-labeling (**Figure 5E**). EMSA results showed that the purified FlhF-His$_6$ bound to the 26 bp possible FlhF-binding site of the *flgI* promoter, but did not bind to the five different point mutation fragments (**Figure 5F**), which demonstrated that the five-point mutations abolish binding of FlhF to P*flgI*.

FlhF Directly Regulates Flagellar Gene Regulators *rpoD*, *fliA*, *flgS*

RNA-Seq results demonstrated that FlhF has an overall impact on the transcription of flagellar components. We hypothesize that FlhF may regulate flagellar gene expression by directly

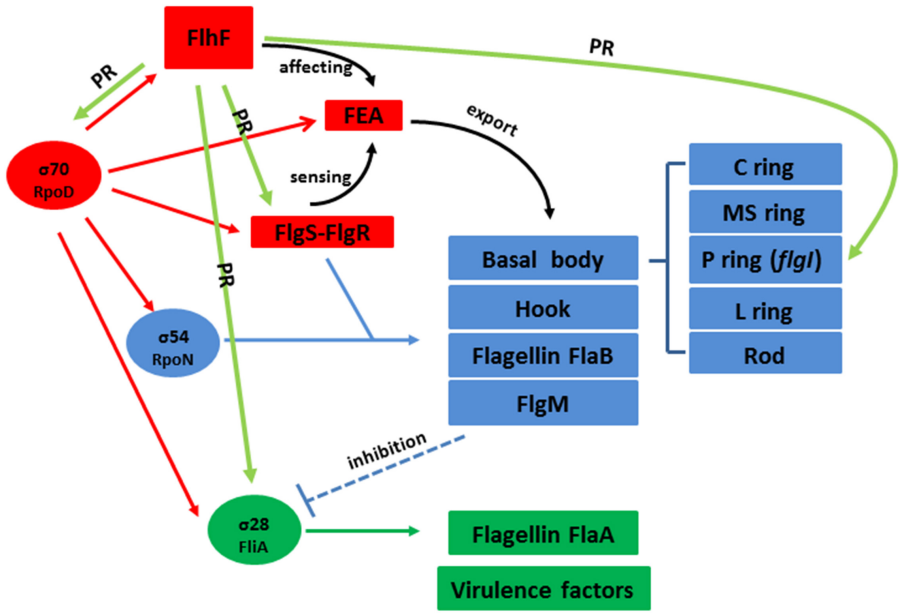

FIGURE 7 | Hypothetical model for the regulatory pathway of FlhF in the *C. jejuni* flagellar system. *C. jejuni* flagellar genes are classified into three cascades, class I genes (red) are σ70 (*rpoD*) dependent, while class II (blue) and class III (green) genes require σ54 (*rpoN*) and σ28 (*fliA*) factor, respectively. The σ70 factor-dependent class I genes are constitutively expressed. FlhF acts before the flagella export apparatus (FEA) formation. The FEA formation will also be detected by the FlgSR two-component system (TCS) and activates the σ54 factor-dependent class II genes. After FlgM is secreted from the cell, the inhibition of the σ28 factor-dependent class III genes is relieved and they are expressed. In our study, we speculate that FlhF may directly regulate the synthesis of class I and III flagellar genes by binding to the *rpoD* and *fliA* promoters, activating σ70 and σ28 factor respectively. For the class II flagellar genes, FlhF may bind P*flgS* to stimulate *flgS* phosphorylation of *flgR*, cooperating with σ54 factor, indirectly to initiate class II gene transcription synthesis. In addition FlhF may also directly regulate the specific class II gene *flgI* by binding to its promoter. "PR" signifies "positive regulating" and is presented with a green arrow. The black curved arrow represents the physiological function and the dotted arrow indicates inhibition.

regulating key regulatory factors *rpoD*, *rpoN*, *fliA*, *flgSR* TCS during flagellar synthesis. Hence, we explored whether FlhF regulates them directly by binding their promoters by EMSA. Results showed that the purified FlhF-His_6 bound to the promoters of *rpoD*, *fliA*, *flgS* (**Figures 6A–C**), but did not bind to the promoters of *rpoN* and *flgR* (**Supplementary Figures S4A,B**).

DISCUSSION

In *C. jejuni*, flagella is a major virulence factor with a complex synthesis process. FlhF is one of several key proteins that influence flagellar biosynthesis. Deletion of *flhF* results in a non-motile and non-flagellar phenotype. Despite FlhF having a crucial influence on flagellar synthesis, the specific mechanism of its role remains unclear (Kim et al., 2012; Kazmierczak and Hendrixson, 2013; Schuhmacher et al., 2015). In this study, RNA-Seq was performed to investigate the role of FlhF further. Previous studies involved in functionality of FlhF influencing the flagellar genes expression are varied depending on the bacteria of choice (Niehus et al., 2004; Correa et al., 2005; Murray and Kazmierczak, 2006; Lertsethtakarn et al., 2011; Kim et al., 2012). In *Helicobacter pylori*, FlhF was found to primarily affect class II and class III flagella genes expression. For *Pseudomonas aeruginosa*, a mutation of FlhF resulted in decreased transcription of the class IV gene *fliC*. In *Vibrio cholerae* and *Vibrio vulnificus*, FlhF positively affected the transcription of class III and class IV flagella genes. However, our results revealed that FlhF may act as an activator of flagellar genes and thus an overall influence on flagellar gene expression in *C. jejuni* (**Figure 2**).

In order to further explore how FlhF affects flagellar expression, in our study we investigated the putative function of FlhF directly influencing flagella synthesis by binding the promoter of flagellar genes. FlhF may positively control *flgI* expression by binding to promoter of *flgI* (**Figures 4–5**), which is the flagellar P-ring component (Boll and Hendrixson, 2013). The P-ring together with L-ring are thought to be required for smooth rotation, functioning as a sleeve in many motile bacteria (Hizukuri et al., 2006, 2008). We found *flgI* and *flgH* had 6.6-fold and 8-fold reduction in expression respectively after the deletion of *flhF* using RNA-Seq (**Supplementary Figure S3**), which indirectly supported our hypothesis that *flhF* has a potential regulatory role. Additionally, the protein-binding site and DNA binding site are important for transcriptional regulators. Our results have revealed that the possible binding site of FlhF in the *flgI* promoter is "AAGAAATTTGGATCAACTAGCTTAAG" (**Figure 5**). Five different point mutations were generated to further investigate that the complete promoter site may be necessary for binding

of FlhF to P*flgI*. Meanwhile, since FlhF mainly affects class II genes, we speculated that there may be other genes besides *flgI* that can be directly regulated by FlhF. ChIP-seq will be performed to identify further hits in the future.

In addition, we also found FlhF can directly bind to the promoters of *rpoD*, *flgS,* and *fliA* genes respectively (**Figure 6**). These genes are key regulatory factors during flagellar synthesis. Balaban proposed that FlhF may directly or indirectly influence the FEA-FlgSR pathway to initiate σ54-dependent genes expression in *C. jejuni* (Balaban et al., 2009). We propose FlhF may bind P*flgS* to stimulate *flgS* phosphorylation of *flgR*, cooperating with σ54 factor indirectly, to initiate class II gene transcription synthesis. Meanwhile, FlhF can also directly regulate specific class II gene *flgI*. In addition, FlhF may directly influence the synthesis of class I and III flagellar genes by binding to the *rpoD* and *fliA* promoters respectively. However, the expression of *fliA* is inhibited by FlgM, and interestingly both *fliA* and *flgM* were significantly downregulated in the absence of FlhF (**Table 1**). Thus, one possible hypothesis is that FlhF directly regulates *fliA* in an independent pathway to promote class III genes synthesis (FlgM being an anti-sigma factor that possibly does not affect *fliA* expression, but its activity). Finally, we proposed a hypothetical model for the regulatory pathway of FlhF in the flagellar system (**Figure 7**). In addition, in order to further investigate whether there are similar sites between the binding promoters, we compared the putative 26 bp binding sequence in P*flgI* with the P*rpoD*, P*fliA,* and P*flgS* promoters through the MEME website (Bailey, 2002). The MEME analysis identified a similar sequence, an AT-rich region (data not shown). We will explore the conservation of FlhF binding sequences in the future.

So far, a number of studies have reported that FlhF is a member of the signal recognition particle (SRP)-related GTPase family regulating the number and position of flagella (Green et al., 2009; Guttenplan et al., 2013). However, no FlhF homologs or functionally similar protein with DNA-binding activity has been reported. In our study, we hypothesis that in addition to being an SPR GTPase, FlhF can also directly influence flagella synthesis by binding to the promoters of flagellar genes in *C. jejuni*. In addition, the GTPase activity of FlhF is not required for flagellar gene transcription in *C. jejuni* (Gulbronson et al., 2016). Therefore, we speculate that the GTPase activity of FlhF may have little to do with the proposed regulation of FlhF here.

In summary, this study demonstrates that FlhF may directly regulate the transcription of flagellar genes by binding to their promoters as a transcriptional regulator. This will help in our attempts to understand the mechanistic role of FlhF in flagellar biosynthetic and bacterial flagellation. We hope this study will be used as foundation for future studies on FlhF function.

DATA AVAILABILITY STATEMENT

The data is on EBI ENA website with accession number PRJEB34440 (https://www.ebi.ac.uk/ena/data/search?query=PRJEB34440).

AUTHOR CONTRIBUTIONS

XL, FR, OG, JH, and XJ conceived and designed the experiments. XL, GC, PH, and QC performed the experiments. XL analyzed the data. XL, JH, and XJ contributed reagents, materials, and analysis tools. XL wrote the manuscript. OG and JH reviewed the manuscript.

FUNDING

This work was supported by the NSFC (31872493), National Key Research and Development Program of China (2018YFD0500500), Priority Academic Program Development of Jiangsu Higher Education Institutions, Yangzhou University High-end Talent Support Program and International Academic Exchange.

SUPPLEMENTARY MATERIAL

The Supplementary Material for this article can be found online at: https://www.frontiersin.org/articles/10.3389/fmicb.2020.00460/full#supplementary-material

REFERENCES

Bailey, T. L. (2002). Discovering novel sequence motifs with MEME. *Curr. Protoc. Bioinfor.* 00, 2.4.1–2.4.35. doi: 10.1002/0471250953.bi0204s00

Balaban, M., Joslin, S. N., and Hendrixson, D. R. (2009). FlhF and its GTPase activity are required for distinct processes in flagellar gene regulation and biosynthesis in *Campylobacter jejuni*. *J. Bacteriol.* 191, 6602–6611. doi: 10.1128/JB.00884-889

Beeby, M. (2015). Motility in the epsilon-*proteobacteria*. *Curr. Opin. Microbiol.* 28, 115–121. doi: 10.1016/j.mib.2015.09.005

Bervoets, I., and Charlier, D. (2019). Diversity, versatility and complexity of bacterial gene regulation mechanisms: opportunities and drawbacks for applications in synthetic biology. *FEMS Microbiol. Rev.* 43, 304–339. doi: 10.1093/femsre/fuz001

Blasco, B., Chen, J. M., Hartkoorn, R., Sala, C., Uplekar, S., Rougemont, J., et al. (2012). Virulence regulator EspR of mycobacterium tuberculosis is a nucleoid-associated protein. *PLoS Pathog.* 8:e1002621. doi: 10.1371/journal.ppat

Boll, J. M., and Hendrixson, D. R. (2013). A regulatory checkpoint during flagellar biogenesis in *Campylobacter jejuni* initiates signal transduction to activate transcription of flagellar genes. *mBio.* 4, e432–e413. doi: 10.1128/mBio.00432-413

Burnham, P. M., and Hendrixson, D. R. (2018). Campylobacter jejuni: collective components promoting a successful enteric lifestyle. *Nat. Rev. Microbiol.* 16, 551–565. doi: 10.1038/s41579-018-0037-39

Cagliero, C., Maurel, M.-C., Cloeckaert, A., and Payot, S. (2007). Regulation of the expression of the CmeABC efflux pump in *Campylobacter jejuni*: identification

of a point mutation abolishing the binding of the CmeR repressor in an in vitro-selected multidrug-resistant mutant. *FEMS Microbiol. Lett.* 267, 89–94. doi: 10.1111/j.1574-6968.2006.00558.x

Chilcott, G. S., and Hughes, K. T. (2000). Coupling of flagellar gene expression to flagellar assembly in *Salmonella enterica* serovar typhimurium and *Escherichia coli*. *Microbiol. Mol. Biol. Rev.* 64, 694–708. doi: 10.1128/mmbr.64.4.694-708.2000

Correa, N. E., Peng, F., and Klose, K. E. (2005). Roles of the regulatory proteins FlhF and FlhG in the *Vibrio cholerae* flagellar transcription hierarchy. *J Bacteriol.* 187, 6324–6332. doi: 10.1128/JB.187.18.6324

Dasgupta, N., Wolfgang, M. C., Goodman, A. L., Arora, S. K., Jyot, J., Lory, S., et al. (2003). A four-tiered transcriptional regulatory circuit controls flagellar biogenesis in *Pseudomonas aeruginosa*. *Mol. Microbiol.* 50, 809–824. doi: 10.1046/j.1365-2958.2003.03740.x

Flint, A., Stintzi, A., and Saraiva, L. M. (2016). Oxidative and nitrosative stress defences of *Helicobacter* and *Campylobacter* species that counteract mammalian immunity. *FEMS Microbiol. Rev.* 40, 938–960. doi: 10.1093/femsre/fuw025

Galán-Vásquez, E., Sánchez-Osorio, I., and Martínez-Antonio, A. (2016). Transcription factors exhibit differential conservation in bacteria with reduced genomes. *PLoS One* 11:e0146901. doi: 10.1371/journal.pone.0146901

Gao, B., Lara-Tejero, M., Lefebre, M., Goodman, A. L., and Galán, J. E. (2014). Novel components of the flagellar system in epsilon*proteobacteria*. *mBio* 5, 1–13. doi: 10.1128/mBio.01349-1314

Garber, M., Grabherr, M. G., Guttman, M., and Trapnell, C. (2011). Computational methods for transcriptome annotation and quantification using RNA-seq. *Nat. Methods* 8, 469–477. doi: 10.1038/nmeth.1613

Green, J. C. D., Kahramanoglou, C., Rahman, A., Pender, A. M. C., Charbonnel, N., and Fraser, G. M. (2009). Recruitment of the earliest component of the bacterial flagellum to the old cell division pole by a membrane-associated signal recognition particle family GTP-binding protein. *J. Mol. Biol.* 391, 679–690. doi: 10.1016/j.jmb.2009.05.075

Grinnage-Pulley, T., Mu, Y., Dai, L., and Zhang, Q. (2016). Dual repression of the multidrug efflux pump CmeABC by CosR and CmeR in *Campylobacter jejuni*. *Front. Microbiol.* 7:1097. doi: 10.3389/fmicb.2016.01097

Gulbronson, C. J., Ribardo, D. A., Balaban, M., Knauer, C., Bange, G., and Hendrixson, D. R. (2016). FlhG employs diverse intrinsic domains and influences FlhF GTPase activity to numerically regulate polar flagellar biogenesis in *Campylobacter jejuni*. *Mol. Microbiol.* 99, 291–306. doi: 10.1111/mmi.13231

Guttenplan, S. B., Shaw, S., and Kearns, D. B. (2013). The cell biology of peritrichous flagella in *Bacillus subtilis*. *Mol. Microbiol.* 87, 211–229. doi: 10.1111/mmi.12103

Hendrixson, D. R., and Dirita, V. J. (2003). Transcription of σ54 -dependent but not σ28 -dependent flagellar genes in *Campylobacter jejuni* is associated with formation of the flagellar secretory apparatus. *Mol. Microbiol.* 50, 687–702. doi: 10.1046/j.1365-2958.2003.3731.x

Hizukuri, Y., Kojima, S., Yakushi, T., Kawagishi, I., and Homma, M. (2008). Systematic Cys mutagenesis of FlgI, the flagellar P-ring component of *Escherichia coli*. *Microbiology* 154, 810–817. doi: 10.1099/mic.0.2007/013854-13850

Hizukuri, Y., Yakushi, T., Kawagishi, I., and Homma, M. (2006). Role of the intramolecular disulfide bond in FlgI, the flagellar P-ring component of *Escherichia coli*. *J. Bacteriol.* 188, 4190–4197. doi: 10.1128/JB.01896-1895

Hofreuter, D., Tsai, J., Watson, R. O., Novik, V., Altman, B., Benitez, M., et al. (2006). Unique features of a highly pathogenic *Campylobacter jejuni* strain. *Infect. Immun.* 74, 4694–4707. doi: 10.1128/IAI.00210-216

Huffman, J. L., and Brennan, R. G. (2002). Prokaryotic transcription regulators: more than just the helix-turn-helix motif. *Curr. Opin. Struct. Biol.* 12, 98–106. doi: 10.1016/S0959-440X(02)00295-296

Hwang, S., Jeon, B., Yun, J., and Ryu, S. (2011). Roles of RpoN in the resistance of *Campylobacter jejuni* under various stress conditions. *BMC Microbiol.* 11:207. doi: 10.1186/1471-2180-11-207

Joslin, S. N., and Hendrixson, D. R. (2009). Activation of the *Campylobacter jejuni* FlgSR two-component system is linked to the flagellar export apparatus. *J. Bacteriol.* 191, 2656–2667. doi: 10.1128/JB.01689-1688

Kazmierczak, B. I., and Hendrixson, D. R. (2013). Spatial and numerical regulation of flagellar biosynthesis in polarly flagellated bacteria. *Mol. Microbiol.* 88, 655–663. doi: 10.1111/mmi.12221

Kim, S. M., Lee, D. H., and Choi, S. H. (2012). Evidence that the *Vibrio vulnificus* flagellar regulator FlhF is regulated by a quorum sensing master regulator SmcR. *Microbiology* 158, 2017–2025. doi: 10.1099/mic.0.059071-59070

Lertsethtakarn, P., Ottemann, K. M., and Hendrixson, D. R. (2011). Motility and chemotaxis in *Campylobacter* and *Helicobacter*. *Annu. Rev. Microbiol.* 65, 389–410. doi: 10.1146/annurev-micro-090110-102908

Liang, L., and Connerton, I. F. (2018). FlhF(T368A) modulates motility in the bacteriophage carrier state of *Campylobacter jejuni*. *Mol. Microbiol.* 110, 616–633. doi: 10.1111/mmi.14120

Liu, R., and Ochman, H. (2007). Stepwise formation of the bacterial flagellar system. *Proc. Natl. Acad. Sci. U.S.A.* 104, 7116–7121. doi: 10.1073/pnas.0700266104

Livak, K. J., and Schmittgen, T. D. (2001). Analysis of relative gene expression data using real-time quantitative PCR and the 2(-delta delta C(T)) method. *Methods* 25, 402–408. doi: 10.1006/meth.2001.1262

Matsunami, H., Barker, C. S., Yoon, Y. H., Wolf, M., and Samatey, F. A. (2016). Complete structure of the bacterial flagellar hook reveals extensive set of stabilizing interactions. *Nat. Commun.* 7, 1–10. doi: 10.1038/ncomms13425

Miller, W. G., Bates, A. H., Horn, S. T., Brandl, M. T., Wachtel, M. R., and Mandrell, R. E. (2000). Detection on surfaces and in Caco-2 cells of *Campylobacter jejuni* cells transformed with new gfp, yfp, and cfp marker plasmids. *Appl. Environ. Microbiol.* 66, 5426–5436. doi: 10.1128/aem.66.12.5426-5436.2000

Murray, T. S., and Kazmierczak, B. I. (2006). FlhF Is required for swimming and swarming in *Pseudomonas aeruginosa*. *J. Bacteriol.* 188, 6995–7004. doi: 10.1128/JB.00790-796

Nachamkin, I., Szymanski, C. M., and Blaser, M. J. (eds) (2008). *Campylobacter*, 3rd Edn. Washington DC: ASM Press.

Niehus, E., Gressmann, H., Ye, F., Schlapbach, R., Dehio, M., Dehio, C., et al. (2004). Genome-wide analysis of transcriptional hierarchy and feedback regulation in the flagellar system of *Helicobacter* pylori. *Mol. Microbiol.* 52, 947–961. doi: 10.1111/j.1365-2958.2004.04006.x

O'Geen, H., Frietze, S., and Farnham, P. J. (2010). Using ChIP-seq technology to identify targets of zinc finger transcription factors. *Methods Mol. Biol.* 649, 437–455. doi: 10.1007/978-1-60761-753-2_27

Parker, C. T., Quinones, B., Miller, W. G., Horn, S. T., and Mandrell, R. E. (2006). Comparative genomic analysis of *Campylobacter jejuni* strains reveals diversity due to genomic elements similar to those present in *C. jejuni* strain RM1221. *J. Clin. Microbiol.* 44, 4125–4135. doi: 10.1128/JCM.01231-1236

Parkhill, J., Wren, B. W., Mungall, K., Ketley, J. M., Churcher, C., Basham, D., et al. (2000). The genome sequence of the food-borne pathogen *Campylobacter jejuni* reveals hypervariable sequences. *Nature* 403, 665–668. doi: 10.1038/35001088

Petersen, L., Larsen, T. S., Ussery, D. W., On, S. L. W., and Krogh, A. (2003). Rpo D promoters in *Campylobacter jejuni* exhibit a strong periodic signal instead of a - 35 box. *J. Mol. Biol.* 326, 1361–1372. doi: 10.1016/S0022-2836(03)00034-32

Pfaffl, M. W. (2001). A new mathematical model for relative quantification in real-time RT–PCR. *Nucleic Acids Res.* 29:e45. doi: 10.1093/nar/29.9.e45

Prouty, M. G., Correa, N. E., and Klose, K. E. (2001). The novel sigma54- and sigma28-dependent flagellar gene transcription hierarchy of *Vibrio cholerae*. *Mol. Microbiol.* 39, 1595–1609. doi: 10.1046/j.1365-2958.2001.02348.x

Ren, F., Lei, T., Song, Z., Yu, T., Li, Q., Huang, J., et al. (2018). Could FlhF be a key element that controls *Campylobacter jejuni* flagella biosynthesis in the initial assembly stage? *Microbiol. Res.* 207, 240–248. doi: 10.1016/j.micres.2017.12.006

Schniederberend, M., Abdurachim, K., Murray, T. S., and Kazmierczaka, B. I. (2013). The GTPase activity of FlhF is dispensable for flagellar localization, but not motility, in *Pseudomonas aeruginosa*. *J. Bacteriol.* 195, 1051–1060. doi: 10.1128/JB.02013-2012

Schuhmacher, J. S., Thormann, K. M., and Bange, G. (2015). How bacteria maintain location and number of flagella? *FEMS Microbiol. Rev.* 39, 812–822. doi: 10.1093/femsre/fuv034

Subramanian, S., and Kearns, D. B. (2019). Functional regulators of *Bacterial Flagella*. *Annu. Rev. Microbiol.* 73, 1–22. doi: 10.1146/annurev-micro-020518-115725

Wosten, M. M., Boeve, M., Koot, M. G., van Nuenen, A. C., and van der Zeijst, B. A. (1998). Identification of *Campylobacter jejuni* promoter sequences. *J. Bacteriol.* 180, 594–599.

Wösten, M. M. S. M., Wagenaar, J. A., and Van Putten, J. P. M. (2004). The FlgS/FlgR two-component signal transduction system regulates the fla regulon in *Campylobacter jejuni*. *J. Biol. Chem.* 279, 16214–16222. doi: 10.1074/jbc.M400357200

Zhang, B., Zhuang, Z., Wang, X., Huang, H., Fu, Q., and Yan, Q. (2019). Dual RNA-Seq reveals the role of a transcriptional regulator gene in pathogen-host interactions between *Pseudomonas* plecoglossicida and Epinephelus coioides. *Fish Shellfish Immunol.* 87, 778–787. doi: 10.1016/j.fsi.2019.02.025

Conflict of Interest: The authors declare that the research was conducted in the absence of any commercial or financial relationships that could be construed as a potential conflict of interest.

frontiers in Microbiology

ORIGINAL RESEARCH
published: 25 March 2020
doi: 10.3389/fmicb.2020.00503

Chlorine Induces Physiological and Morphological Changes on Chicken Meat *Campylobacter* Isolates

*Gayani Kuriyawe Muhandiramlage, Andrea R. McWhorter and Kapil K. Chousalkar**

School of Animal and Veterinary Sciences, University of Adelaide, Adelaide, SA, Australia

Broiler chickens frequently become colonized by *Campylobacter* species. As a consequence, *Campylobacter*, can enter the poultry meat supply chain and represents a significant risk for human public health. A number of on-farm biosecurity and processing measures are used to mitigate the load of *Campylobacter* on chicken meat. In many countries, chlorine is commonly used as a biocide in processing plants to reduce bacterial loads on poultry carcasses but there is limited evidence of its effectiveness on *Campylobacter*. In this study, 116 *Campylobacter* isolates (89 *C. jejuni* and 27 *C. coli*) were isolated from poultry meat carcasses prior to the inside/outside wash step and used in *in vitro* assays exploring the efficacy of chlorine. A high proportion of isolates exhibited MIC and MBC values of 128 ppm but organic material present in the broth likely affected this result. Thus, additional bactericidal assays (time kill and chlorine inactivation) were used to characterize the response of *C. jejuni* isolates to different concentrations of chlorine. At 10^6 CFU, *C. jejuni* was found to be highly sensitive to concentrations of chlorine and was inhibited at low concentrations (0.2–2.0 ppm). At a higher bacterial load (10^8 CFU), variation in the response of different *C. jejuni* isolates was observed. One isolate was growth inhibited at 1.8 ppm while another required 16 ppm. At 10^8 CFU, *C. jejuni* could be resuscitated following exposure to chlorine highlighting a potential limitation of chlorine use. Analysis of UV leakage indicated that high chlorine concentrations resulted in increased 280 nm absorbance values suggesting bacterial membrane damage. Scanning electron and transmission electron microscopy were performed to characterize the morphological effects of chlorine exposure. Some effects of chlorine exposure included changes in shape (coccoid, or elongated), cellular degeneration, and shriveled bacterial cells. Interestingly, *C. jejuni cells* with normal morphology were also observed in the chlorine exposed group and represent a population of cells that could be resuscitated. This study is useful for the chicken meat industry and provides data for future optimization of chlorine use in reducing *Campylobacter* loads.

Keywords: *Campylobacter*, chlorine inactivation, poultry meat, cell damage, bacterial resuscitation

OPEN ACCESS

Edited by:
Ozan Gundogdu,
University of London, United Kingdom

Reviewed by:
Frances Colles,
University of Oxford, United Kingdom
Belchiolina Beatriz Fonseca,
Federal University of Uberlândia, Brazil
Basanta Raj Wagle,
University of Arkansas, United States

****Correspondence:***
Kapil K. Chousalkar
kapil.chousalkar@adelaide.edu.au

Specialty section:
This article was submitted to Food Microbiology, a section of the journal Frontiers in Microbiology

Received: *29 January 2020*
Accepted: *09 March 2020*
Published: *25 March 2020*

Citation:
Muhandiramlage GK, McWhorter AR and Chousalkar KK (2020) Chlorine Induces Physiological and Morphological Changes on Chicken Meat Campylobacter Isolates. Front. Microbiol. 11:503. doi: 10.3389/fmicb.2020.00503

INTRODUCTION

Campylobacter species are the most common cause of bacterial associated foodborne gastrointestinal disease in humans (Havelaar et al., 2015; Kirk et al., 2015). In 2010, of the 600 million global cases of foodborne related disease, 96 million were caused by *Campylobacter* (Havelaar et al., 2015). The number of campylobacteriosis cases are increasing and current

estimations of disease rates in Europe are 30–50 per 100,000 annually, 14–50 per 100,000 in North America, 112 per 100,000 in Australia, and 1512 per 100,000 in Japan (Connerton and Connerton, 2017). There are 26 known *Campylobacter* species and of these, *C. jejuni* and *C. coli*, are among the leading causes of campylobacteriosis (Kirk et al., 2015; Patrick et al., 2018). Humans can be exposed to *Campylobacter* through consumption of contaminated, untreated water and a wide variety of food items. Raw or under-cooked poultry meat and poultry meat products, however, are among the most frequently identified sources of *Campylobacter* (Hoffmann et al., 2017).

At hatch, broiler chicks are generally free from *Campylobacter* but acquire the bacteria in the growing sheds (Herman et al., 2003). Once a few birds become positive, the bacterium spreads horizontally within the flock (Jacobs-Reitsma et al., 1995; Herman et al., 2003) but significant variability in the total *Campylobacter* load has been observed between individuals in a given flock (Hansson et al., 2010). Transport stress from farm to the processing plant has also been linked with higher *Campylobacter* loads being shed in broiler feces (Stern et al., 1995; Whyte et al., 2001). As a consequence, chicken meat can become contaminated during various points of processing (Hermans et al., 2012). High loads of *Campylobacter* entering poultry meat processing plants have been linked with higher increased risk of carcass contamination (Lindblad et al., 2006; Hansson et al., 2007). A recent review revealed that depending on geographical location, between 19–100% of post-production poultry meat products can be contaminated with *Campylobacter* (Suzuki and Yamamoto, 2009). This level of contamination represents a significant public health risk through direct consumption of improperly cooked chicken meat or cross contamination of food preparation environments.

Globally, a number of different methods are used within the poultry meat industry to mitigate the pathogen load on the surface of whole chicken carcasses as well as meat pieces including "generally recognized as safe" (GRAS) chemicals, such as chlorine in the form of sodium hypochlorite, acidified sodium chloride, and peracetic acid (PAA). The use of each of these chemicals, however, varies widely from country to country. The use of PAA in the spin chill wash, for example, has been increasing in the United States (Walsh et al., 2018). The European Union has banned the use of most pathogen reduction chemicals except for water and lactic acid for health and safety reasons (Anonymous, 2004). In Australia and many Asian countries, however, chlorine continues to be the most commonly used poultry meat sanitizer (Anonymous, 2005; Chousalkar et al., 2019). Comparatively, chlorine has a lower cost than other sanitizers and along with ease of use may account for its continued application.

Chlorine is an oxidizing agent that has been shown to cause membrane permeabilization in both Gram negative (*Yersinia enterocolitica* and *Escherichia coli*) and Gram positive (*Listeria monocytogenes* and *Bacillus subtilis*) bacterial species (Virto et al., 2005). Multiple bacterial species, however, are known to have the ability to recover from chemical or environmental stress (Wesche et al., 2009), however, little is known about the resuscitation of *Campylobacter* after sub-lethal exposure to chlorine. The decontamination of poultry carcasses in the processing plant represents a significant challenge because of the constant presence of organic material being added to sanitizing solutions during processing. Increasing concentrations of organic material (such as residual fecal material, blood, skin, or feathers) reduces the total load of free chlorine in solution (LeChevallier et al., 1981; Virto et al., 2005).

Several studies have shown that chlorine wash steps in the poultry meat processing line leads to significant reductions in *Campylobacter* loads (Lu et al., 2019). To date, it has not been demonstrated whether the total *Campylobacter* load has an effect on the efficacy of the sanitizer. The objective of the current study was to isolate *Campylobacter* from poultry meat carcasses and characterize the physiological, morphological and cellular responses of these isolates to chlorine exposure using different concentrations of bacteria. An additional aim was to determine whether there was inherent variability in the chlorine sensitivity of chicken meat *Campylobacter* isolates and their resuscitation potential following exposure to chlorine.

MATERIALS AND METHODS

Isolation of *Campylobacter*

The *Campylobacter* isolates used in this study were isolated during a separate study investigating the efficacy of sanitizers during chicken meat processing (Chousalkar et al., 2019). Briefly, chicken meat carcasses (15 birds from each of eight different broiler production sheds) were collected from two separate processing plants prior to the inside-outside wash step. Bacteria were isolated by massaging chicken carcasses (prior to sanitizer exposure) in buffered peptone water (BPW) (Oxoid, Australia). Two hundred microliters of BPW wash was spread plated onto modified charcoal-cefoperazone deoxycholate agar (mCCDA) (Oxoid, Australia) and incubated at 42°C in 10% CO_2 for 48 h. Putative, *Campylobacter* isolates were sub-cultured once to obtain pure cultures, stored at −80°C in 5% glycerol, and further characterized using PCR. A total of 116 *Campylobacter* isolates were obtained.

In preparation for experiments, bacteria were resuscitated from freezing stocks on to Columbia sheep blood agar (SBA) (Oxoid, Thermo Scientific, Australia) and incubated at 42°C in 10% CO_2 for 48 h. The *Campylobacter jejuni* ATCC 33291 strain was used as a control strain.

Multiplex PCR Identification of *Campylobacter coli* and *Campylobacter jejuni*

Campylobacter isolates were further characterized using a multiplex PCR enabling the distinction of *Campylobacter coli* (*C. coli*) and *Campylobacter jejuni* (*C. jejuni*) strains. Bacterial DNA was extracted using 0.6% Chelex resin (BioRad, United States) according to the manufacturer's instructions. Purified DNA was stored at −20°C until required.

The multiplex PCR method designed by Van et al. (2017) enabled the distinction of *C. coli* and *C. jejuni* strains. To detect *C. jejuni,* primers (Forward: 5′-ACT TCT TTA TTG CTT GCT

GC-3′, Reverse: 5′-GCC ACA ACA AGT AAA GAA GC-3′) designed to the *hipO* gene were used. This reaction generated an amplicon of 323 base pairs. To distinguish *C. coli*, specific primers (Forward: 5′-GCT GCA CTT TTA AAT CCA G-3′, Reverse: 5′-CTT TGG TTT TAC AAT ATG AGC-3′) designed to the *glyA* gene were used. The *C. coli* reaction generated an amplicon of 186 base pairs.

The *C. coli* and *C. jejuni* multiplex PCR reaction was conducted using a total volume of 20 μL. Each reaction contained 100 ng DNA, 1× My Red Taq reaction buffer, 250 nM each *C. jejuni* forward and reverse primer, 500 nM each *C. coli* forward and reverse primer, 0.2 units of My Red Taq polymerase (Bioline, Australia), and nuclease free water. PCR cycling conditions were performed using a Biorad T100 thermocycler. The first step was an initial melt at 98°C for 1 min. The second step included 35 cycles of 98°C for 10 s, 59°C for 30 s, and 72°C for 30 s. A final extension was done at 72°C for 10 min. Products were electrophoresed using a 2% agarose gel.

Determination of Minimum Inhibitory and Minimum Bactericidal Concentrations of Chlorine

The chlorine minimum inhibitory concentration (MIC) was determined for both *C. jejuni* (n = 89) and *C. coli* (n = 27) isolates. The MIC was determined using the broth microdilution method in nutrient broth number 2 (NB2) (Oxoid, Australia) according to the Clinical and Laboratory Standard Institute guidelines (Weinstein, 2018). Chlorine (4% Sodium hypochlorite, Sigma-Aldrich, Australia) concentrations ranging from 2 ppm to 1024 ppm (pH range 7.5–8.0) were prepared using 96 well round bottom microtiter plates (Thermo Scientific, Australia). *Campylobacter* inoculums were prepared using a 0.5 McFarland standard and were confirmed measuring the optical density at 600 nm to obtain 10^8 CFU/mL. Subsequently, 10 μL of the *Campylobacter* inoculum (10^6 CFU) was added into 990 μL of chlorine dilutions. The positive control was comprised of NB2 without chlorine but containing bacteria; the negative control was NB2 only. All isolates were tested in duplicate. *C. jejuni* ATCC 33291 was included as the experimental standard. MIC plates were incubated at 42°C in 10% CO_2 for 20 h. The lowest concentration, which did not give visible bacterial growth was defined as the MIC. Isolates with disparate results in replicate wells were repeated.

After the MIC was determined, wells showing growth inhibition were drop plated on to SBA agar plates to determine the minimum bactericidal concentration (MBC). Briefly, 10 μL of broth from each well in MIC plate was drop plated on to SBA plates and incubated at 42°C in 10% CO_2 for 48 h. The MBC was defined as the lowest bactericidal concentration of chlorine required to kill bacteria after incubation at 42°C in 10% CO_2 for 20 h.

Time Kill Assays

Time-kill assays were used to determine the susceptibility of *Campylobacter* isolates to chlorine. Two *C. jejuni* isolates, with disparate MIC values of 128 ppm (C1) and 16 ppm (C2), were selected for this experiment. To determine the effect of organic load, time-kill experiments were performed using both NB2 and 0.9% saline. Standard chlorine concentrations used in the poultry industry ranges between 8–10 ppm when contacting carcasses (Oyarzabal, 2005), hence, dilutions were prepared at half the standard (4 ppm), standard concentration (8 ppm), and twice the standard (16 ppm). The inoculum was prepared by suspending *Campylobacter* colonies in either NB2 or 0.9% saline and matching the turbidity of an 0.5 McFarland standard. Subsequently, 10 μL of *Campylobacter* inoculum was added to 990 μL of each chlorine dilution for a final bacterial concentration of 10^6 CFU/mL and exposed to chlorine for 24 h at either 5°C and 25°C. Bacterial counts were determined at specific intervals post exposure (2, 20, 60, 90, 120, 240, 480, and 1440 min). Serial 10-fold dilutions in 0.9% saline were immediately prepared and 10 μL was drop plated onto SBA and incubated at 42°C in 10% CO_2. Time kill assays were conducted in triplicate and repeated two times.

Chlorine Inactivation Assay

Microbial resistance to chlorine was evaluated using the chlorine inactivation assay. For these experiments, six *C. jejuni* isolates were randomly selected based on the MIC and MBC results. Low (0.2–2 ppm) and high (2 ppm–256 ppm) chlorine concentrations were prepared in 0.9% saline. To determine whether bacterial load had an effect on the efficacy of chlorine, two inoculum doses, 10^8 CFU/mL and 10^6 CFU/mL, were used. Bacteria were exposed to chlorine for 2 min at 25°C. Bacterial counts were obtained by drop plating 10 μL of serial 10-fold dilutions on to SBA and incubating at 42°C in 10% CO_2 for 48 h. Normal saline without chlorine was used as the bacterial growth control. All isolates were tested in duplicate and each experiment was repeated twice.

Bacterial Resuscitation

After 2 min of exposure to chlorine, 100 μL of all treatment and control groups in the inactivation assay were inoculated into 900 μL of Preston broth (nutrient broth number 2 with *Campylobacter* selective supplement) (Oxoid, Australia) and incubated at 42°C in 10% CO_2 for up to 48 h. After 24 h and 48 h incubation, 10 μL of each treatment was drop plated on to SBA to determine if the *Campylobacter* isolate had recovered from exposure to chlorine. Each resuscitation experiment was performed with two replicates and was repeated twice.

Leakage of UV-Absorbing Material

Quantifying the amount of UV absorbent material is often used as a measure for bacterial membrane damage (Virto et al., 2005; McKenzie et al., 2016). To characterise chlorine induced membrane damage, 300 μL of each treated and untreated samples were collected after the 2-min exposure (inactivation assay) and centrifuged at 6000 × g for 10 min. UV absorbencies were read at 260 nm and 280 nm with a spectrophotometer (ClarioStar, BMG Lab Tech,

Australia). All six isolates were tested in duplicates at 25°C and were repeated.

Preparation of Bacteria for Microscopy

Electron microscopy was performed to characterise the morphological and cellular changes of *C. jejuni* isolates after exposure to 8 ppm chlorine for 2 min. After chlorine exposure, the bacterial pellets of both control and treatment was obtained by centrifuging at 8000 × *g* for 10 min. The pellet was resuspended in normal saline and washed twice to remove excess chlorine. Subsequently, the pelleted cells were fixed in electron microscopy fixative (4% glutaraldehyde in 0.1 M sodium cacodylate buffer (pH 7.2). Sample preparation and microscopy were conducted at Adelaide Microscopy, The University of Adelaide, Adelaide SA, Australia.

Transmission Electronic Microscopy (TEM)

The bacterial pellet was washed twice in PBS with 4% sucrose for 10 min, followed by post-fixation with 1% Osmium tetroxide for 1 h. After washing, bacteria were dehydrated in a graded ethanol series (70, 95, and 100%), substituted with propylene oxide, embedded in LX112 epoxy resin, and placed in a 60°C oven for 24 h to polymerize the resin. Ultrathin (60–80 nm) sections were prepared by cutting resin-fixed pellets with an RMC Power Tome Ultramicrotome and double stained with uranyl acetate and lead citrate. Sections were examined utilizing a TEI Tecnai G2 Spirit Bio TWIN at 20–120 kV and imagining was done via in – column Olympus-SIS Veleta CDD camera.

Scanning Electron Microscopy (SEM)

C. jejuni cultures were filtered through 0.2 μm membrane filters (Whatman, United States), washed with PBS + 4% sucrose and fixed with 2% osmium tetroxide for 45 min. After washing, cells were dehydrated in a graded ethanol series (70, 90, and 100%). The filters were then dried with 1:1 ratio of 100% ethanol: hexamethyldilazane for 30 min followed by 100% hexamethyldilazane for 10 min. Cultures were air dried, mounted on carbon stubs, and sputter coated with platinum. Specimens were examined under FEI DualBeam (FIB/SEM) scan electron microscope, operated at 10 kv.

Statistical Analysis

Experimental data for bacterial counts and UV absorbance data are presented as mean ± standard error. One-way Analysis of Variance (ANOVA) and Two-way ANOVA followed by Tukey's multiple comparison test were used to determine statistical differences of the effects of chlorine on *Campylobacter* bacterial load. Prevalence data were analyzed using Fisher's exact test.

All statistical analyses were performed using either SPSS Version 25 (IBM, United States) or GraphPad Prism Version 8.3.0 (GraphPad Software, Inc., United States). In all cases, a *P*-value of < 0.05 was considered statistically significant.

RESULTS

PCR Typing of *Campylobacter* spp. Isolated From Chicken Meat

Putative *Campylobacter* colonies were collected from positive chicken carcasses and tested using the *C. jejuni* and *C. coli* multiplex PCR. A total of 116 isolates were obtained and of these, 76.7% (89/116) were positive for the *C. jejuni* amplicon while 23.2% (27/116) were positive for the *C. coli* amplicon. The percentage of *C. jejuni* isolates collected from the chicken meat samples was significantly higher ($P < 0.05$) than *C. coli*.

Campylobacter Susceptibility to Chlorine: MIC and MBC Determination

The bactericidal activity of chlorine was tested over a range of concentrations from 2 to 1028 ppm. The MICs and MBCs obtained for both *C. jejuni* and *C. coli* isolates are shown in **Figures 1A,B**, respectively. The majority of both *C. jejuni* (57.3%) and *C. coli* (55.5%) isolates exhibited an MIC of 128 ppm and this result was significant ($P < 0.05$). MBC values were similar for 59.5% of *C. jejuni* and 66.6% of *C. coli* isolates exhibiting an MBC of 128 ppm. No significant difference was observed for MIC or MBC values between *Campylobacter* species.

Chlorine Time Kill Kinetics

Organic material present in the NB2 media used for MIC and MBC tests likely reduced the biocidal effect of chlorine on *Campylobacter*. To confirm this, time kill curves were performed using both NB2 and 0.9% saline. Two *C. jejuni* isolates with disparate chlorine MIC values were selected for this experiment. Isolate C1 had an MIC of 128 ppm while the MIC for C2 was 16 ppm.

Data are presented as mean $\log_{10}$ CFU/mL *C. jejuni*. At 5°C, no significant effect of chlorine was observed on the total *C. jejuni* load over time in NB2 (**Figure 2A**). At 25°C in NB2, the total bacterial load did not vary significantly between 2 min and 8 h of exposure at any of the chlorine concentrations tested (**Figure 2B**). A significant reduction ($P \leq 0.001$) in bacterial loads was observed at 25°C for all treatment groups after 24 h of exposure. A 3-log reduction was observed at 24 h for the C1 treatment groups while a 4-log reduction was observed all C2 treatment groups. Interestingly, the reduction in bacteria observed at 25°C after 24 h of did not occur at 5°C.

In 0.9% saline, the culturability of both *C. jejuni* isolates C1 and C2 was completely inhibited following exposure to chlorine. After 2 min of exposure, no culturable bacteria (either C1 or C2) were obtained from all three chlorine concentrations at either 5 or 25°C (**Figures 2C,D**). No significant difference in the mean bacterial load was observed for the control groups between 2 min and 8 h. After 24 h, however, culturable bacteria were not detected at either temperature.

Inactivation Kinetics of Chlorine on *Campylobacter jejuni*

Based on results from the time kill experiments, two minute inactivation experiments were conducted for the six *C. jejuni*

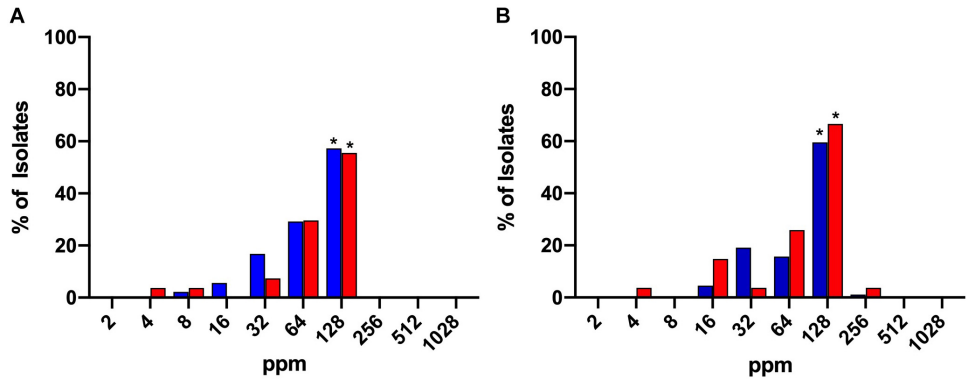

FIGURE 1 | MIC **(A)** and MBC **(B)** values of chlorine (2–1028 ppm) for *C. jejuni* (blue) and *C. coli* (red) strains isolated from chicken meat. A significant majority of both isolates exhibited MIC or MBC values of 128. *Denotes statistical significance ($P < 0.05$).

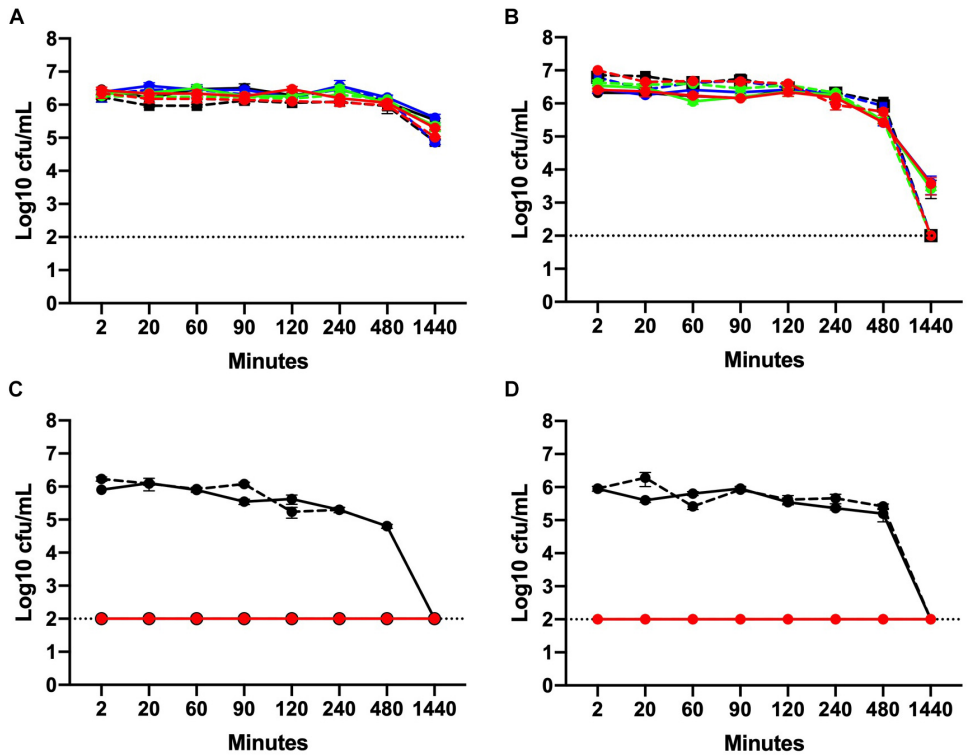

FIGURE 2 | Chlorine time kill curves of two *C. jejuni* isolates with MIC values of 128 ppm (C1) and 16 ppm (C2). Isolates were suspended in either NB2 **(A, B)** or 0.9% saline **(C, D)** at 5°C **(A, C)** or 25°C **(B, D)**. *C. jejuni* isolates were exposed to three different concentrations of chlorine 4 ppm (blue), 8 ppm (green), and 16 ppm (red). Bacteria suspended in either NB2 broth or 0.9% saline were included as control (black). Isolate C1 is designated using solid lines and C2 hashed lines. No significant effect of chlorine was observed for bacteria suspended in NB2 **(A, B)** but a significant effect was observed at all chlorine concentrations for both *C. jejuni* isolates suspended in 0.9% saline ($P \leq 0.001$) **(C, D)**. The dotted line indicates limit detection for culturable bacteria.

isolates using low (0.2 – 2.0 ppm) and high (2 – 256 ppm) concentrations of chlorine (**Figure 3**). At 10^6 CFU/mL, all six isolates were highly sensitive to chlorine at both low and high concentrations and were not culturable following a 2-min exposure (**Figures 3A,B**). Interestingly, at this load, none of the *C. jejuni* isolates were cultured from the lowest chlorine concentration of 0.2 ppm (**Figure 3A**).

At 10^8 CFU/mL, a significant effect of chlorine was observed for both the low ($P < 0.001$) and high ($P < 0.001$) range of concentrations tested. C3, and C4 were the most sensitive *C. jejuni* isolates. At 1.8 and 2.0 ppm of chlorine, culturable C3 bacteria were no longer detected while C4 exhibited a 3 $\log_{10}$ reduction in the total number of culturable bacteria. C3, and C4 exhibited significantly lower ($P < 0.001$) bacterial

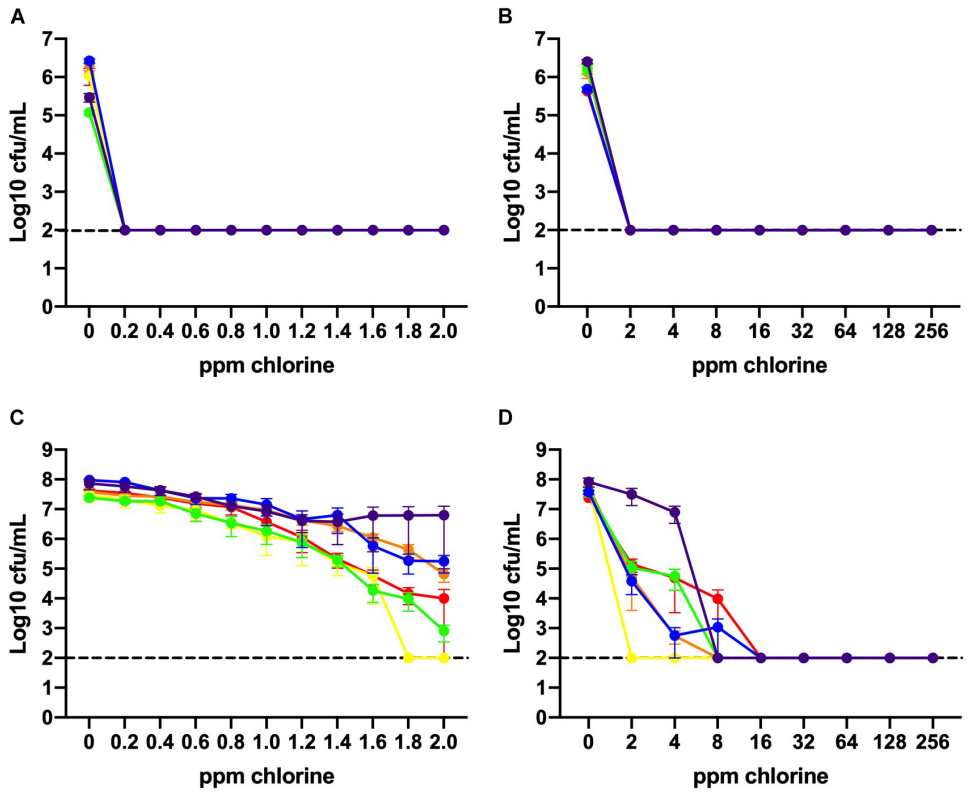

FIGURE 3 | Inactivation kinetics of chlorine on six different *C. jejuni* isolates: C1 (red), C2 (orange), C3 (yellow), C4 (green), C5 (blue), and C6 (purple). 10^6 CFU **(A, B)** and 10^8 CFU **(C, D)** of each isolate were exposed to low **(A, C)** and high **(B, D)** concentrations of chlorine. At 10^6 CFU, all *C. jejuni* isolates were highly sensitive to chlorine at all concentrations **(A, B)**. The higher inoculum, 10^8 CFU, a significant effect of chlorine concentration was observed for both the low **(C)** ($P < 0.001$) and high **(D)** ($P < 0.001$) range. Individual variation between isolates was observed in response to chlorine. Isolate, C3, was the most sensitive to chlorine and was inhibited at the lowest concentration (1.8 ppm). This result was significant ($P < 0.01$).

loads at chlorine concentrations between 1.4–2.0 ppm compared with C2, C5, and C6 isolates. At the low range of chlorine concentration, no significant change in the number of culturable C6 was observed.

A significant effect of chlorine was observed over the high concentration range ($P < 0.001$). Consistent with the low range data, isolate C3 was not culturable at 2 ppm or higher. Significant variability was observed amongst the isolates in their response to chlorine ($P < 0.001$). Isolate C6 retained the highest bacterial loads up to 8 ppm where it was no longer culturable. C1 and C5 remained culturable at 8 ppm but there was no significant difference between the bacterial loads. No isolate was cultured from chlorine suspensions ranging from 16–256 ppm.

Recovery of *Campylobacter* After Chlorine Treatment

After 2 min of exposure to different chlorine concentrations, 100 μL of each *Campylobacter* isolate were added to resuscitation media to determine sub-lethal injury. The number of non-culturable isolates and whether they were resuscitated is shown in **Table 1**. Non-culturable *Campylobacter* from the 10^6 CFU/mL chlorine treatment groups were not resuscitated after either 24 or 48-h incubation in Preston broth.

Bacterial resuscitation in Preston broth was also performed for 10^8 CFU/mL *C. jejuni* treatment groups following exposure to chlorine. At 2 ppm, 1/6 isolate was non-culturable but was resuscitated after both 24 and 48-h incubation in broth. Similarly, at 4 ppm, 2/6 isolates were non-culturable following chlorine exposure and were both resuscitated. All *C. jejuni* isolates were resuscitated in broth after exposure to 8 ppm chlorine. After exposure to both 32 and 64 ppm chlorine, 6/6 isolates were non-culturable but only one isolate was resuscitated at both concentrations. It should be noted that this was the same isolate. None of the *C. jejuni* isolates were culturable after exposure to 128 or 256 ppm and could not be resuscitated.

Leakage of UV-Absorbing Substances Caused by Chlorine Treatment

The values of UV absorbance at 280 nm of the supernatants collected from 10^6 to 10^8 CFU/mL *C. jejuni* suspensions after exposure to low and high chlorine concentrations are shown in **Figure 4**. At 10^6 CFU/mL, membrane damage following exposure to low concentrations of chlorine (0.2–2 ppm) was minimal as UV absorbance values observed were less than 0.150 (**Figure 4A**) and no significant effect of chlorine was observed. Increasing concentration of chlorine resulted in significantly

TABLE 1 | Resuscitation of *C. jejuni* after inactivation at different chlorine levels.

Chlorine (ppm)	Bacterial concentration (10^6 CFU/ml)			Bacterial concentration (10^8 CFU/ml)		
	Unculturable isolates	Resuscitated isolates 24 h	Resuscitated isolates 48 h	Unculturable isolates	Resuscitated isolates 24 h	Resuscitated isolates 48 h
2	6/6	0/6	0/6	1/6	1/1	1/1
4	6/6	0/6	0/6	2/6	2/2	2/2
8	6/6	0/6	0/6	6/6	6/6	6/6
16	6/6	0/6	0/6	6/6	2/6	2/6
32	6/6	0/6	0/6	6/6	1/6	1/6
64	6/6	0/6	0/6	6/6	1/6	1/6
128	6/6	0/6	0/6	6/6	0/6	0/6
256	6/6	0/6	0/6	6/6	0/6	0/6

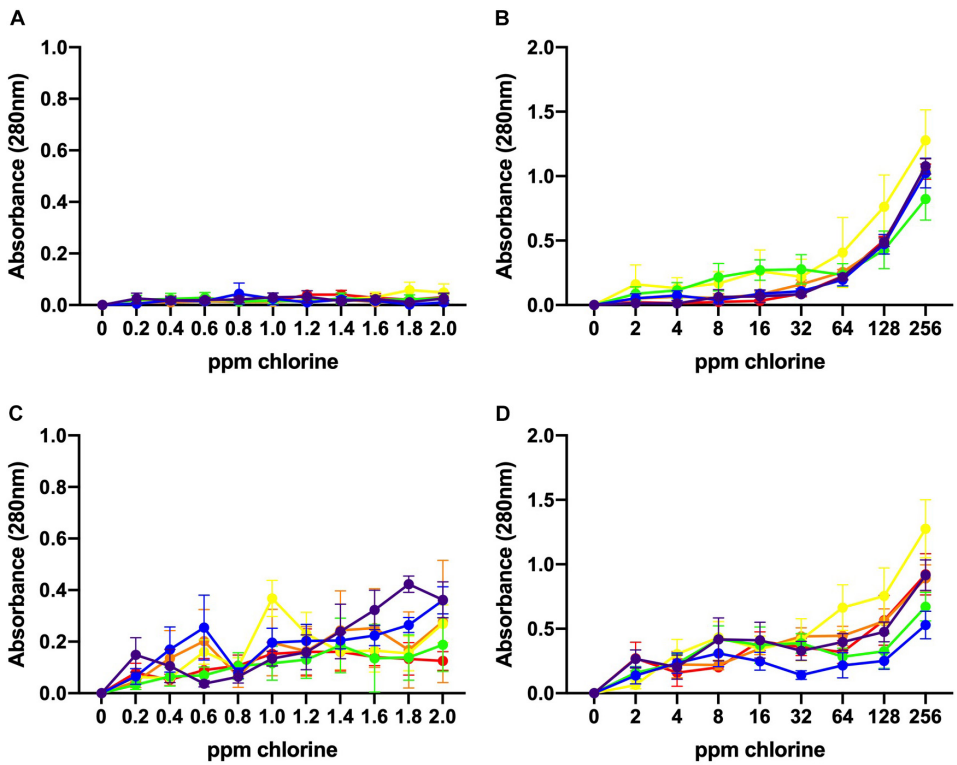

FIGURE 4 | Leakage of UV-absorbing substances caused by chlorine treatment. Absorbance (280 nm) values for six *C. jejuni* isolates: C1 (red), C2 (orange), C3 (yellow), C4 (green), C5 (blue), and C6 (purple) at low, 10^6 CFU/mL **(A, B)**, and high, 10^8 CFU/mL **(C, D)**, loads for over low **(A, C)** and high **(B, D)** chlorine concentrations. At 10^6 CFU/mL, membrane damage following exposure to low concentrations of chlorine was minimal as UV absorbance values observed were <0.150 **(A)**. Increasing concentrations of chlorine resulted in significantly higher ($P < 0.001$) 280 nm absorbance values for the 10^6 CFU/mL *C. jejuni* suspension **(B)**. At low chlorine concentrations, a significant increase in absorbance at 280 nm was also observed for the10^8 CFU/mL suspension ($P < 0.001$) **(C)**. Similar results were observed for the high chlorine range **(D)**. A significant effect of concentration ($P < 0.01$) was detected for the 10^8 CFU/mL suspensions with increasing UV absorbencies observed between 2 – 256 ppm (**Figure 4D**).

higher ($P < 0.001$) 280 nm absorbance values for the 10^6 CFU/mL *C. jejuni* suspension (**Figure 4B**).

Higher absorbencies were observed for the 10^8 CFU/mL *C. jejuni* suspension over the low concentration range as compared with the 10^6 CFU/mL suspension (**Figure 4C**). At low chlorine concentrations, a significant increase in absorbance at 280 nm was observed for the10^8 CFU/mL suspension ($P < 0.001$). Similar results were observed for the high chlorine range. A significant effect of concentration ($P < 0.01$) was detected for the 10^8 CFU/mL suspensions with increasing UV absorbencies observed between 2 – 256 ppm (**Figure 4D**). Variation in UV absorbance values were observed between strains especially when the bacterial load was high but no significant difference between isolates was detected. Of note, isolate C3, which was inactivated at the lowest concentrations exhibited the highest absorbance values at both low (**Figure 4B**)

and high (**Figure 4D**) bacterial concentrations. The results obtained at 260 nm (data not shown) were similar to those obtained at 280 nm.

Morphological Changes Caused by Chlorine Treatment

Based on the UV absorbance data, we investigated the morphological changes in *C. jejuni* after exposure to chlorine using SEM (**Figure 5**) and TEM (**Figure 6**). The cell structure of *C. jejuni* following a 2-min exposure to 8 ppm of chlorine was substantially altered. Under SEM, *C. jejuni* cells appeared either coccoid or exhibited a stretched and shriveled morphology (**Figures 5B–D**). Loss of integrity and complete destruction of the cell membrane was also observed (**Figure 5B**). Unaffected cells exhibiting normal *C. jejuni* morphology were also observed in the chlorine treatment group (**Figure 5D**, white arrow). TEM analysis of *C. jejuni* exposed to chlorine revealed that treated cells were not dense as cells in the control (**Figures 6D–F**). The bacterial cells in various stages of degeneration were also observed. The cytoplasm of some bacterial cells was detached from the cell membrane (**Figure 6D**, white arrow). Cells with severely damaged the cell membranes and extruded cytoplasm were also frequently observed (**Figures 6D,E**).

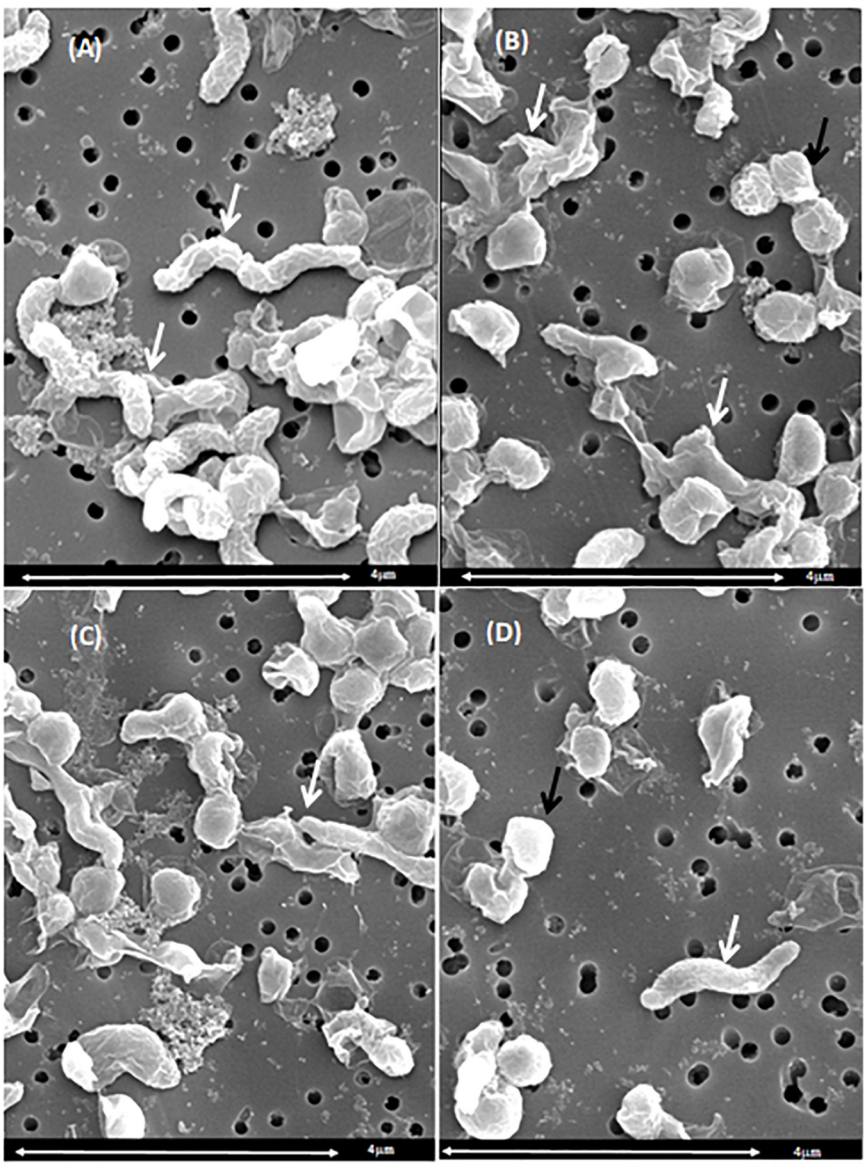

FIGURE 5 | Morphological changes of *C. jejuni* following chlorine exposure: SEM. A *C. jejuni* isolate was exposed to either saline only **(A)** or 8 ppm chlorine **(B–D)** for 2 min. Bacteria with normal spiral morphology can be observed in the saline treatment group **(A**, white arrows). Exposure to chlorine resulted in damaged cell membranes **(B**, white arrow), coccoid morphology **(B–D)**, and stretched morphology **(C**, white arrow). The typical *C. jejuni* spiral morphology was also observed **(D**, white arrow).

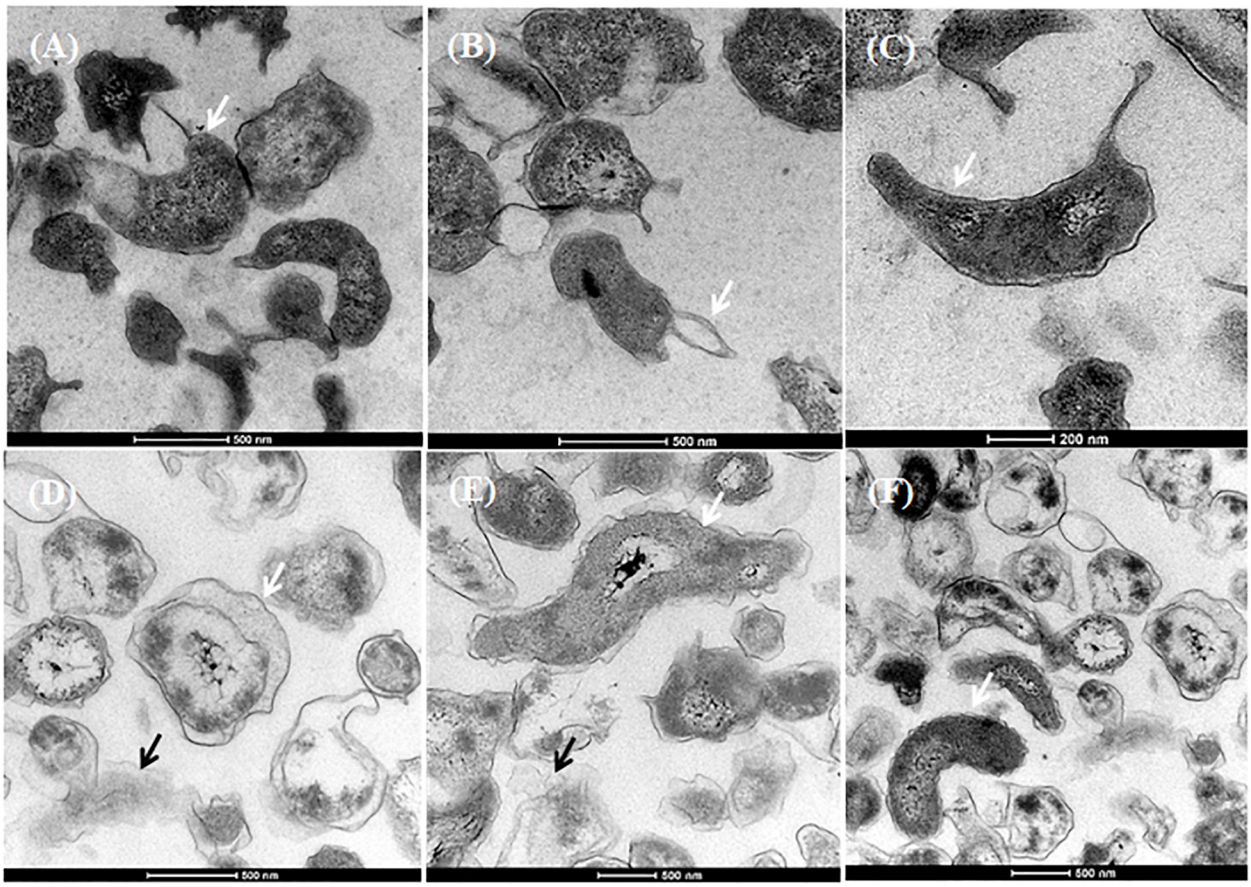

FIGURE 6 | Morphological changes of *C. jejuni* following chlorine exposure. TEM images of *C. jejuni* exposed to either saline only **(A–C)** or 8 ppm chlorine **(D–F)**. Normal morphology was observed in the 0.9% saline treatment group **(A–C**, white arrows). Chlorine exposed bacteria exhibited detached cytoplasm **(D**, black arrow; **E**, white arrow), leakage of cytoplasm **(D**, white arrow; **E**, black arrow). *C. jejuni* cells with normal cytoplasmic morphology were also observed **(F**, white arrow) in the chlorine treated group.

DISCUSSION

In the present study, *Campylobacter* strains were isolated from poultry meat carcasses prior to the inside/outside wash step at the processing plant. Of the 116 *Campylobacter* isolates obtained, 76.7% were identified as *Campylobacter jejuni*. While only a single isolate was collected from each positive carcass, our results are consistent with previous study demonstrating that *C. jejuni* is more common than *C. coli* on chicken meat carcasses (Anonymous, 2010). Another recent Australian report, however, indicated the *C. coli* was more common (Walker et al., 2019). The strains isolated from the present study were then used in experiments designed to characterize their sensitivity to chlorine.

In some countries, chlorine is often used in chicken meat processing plants with the objective to reduce levels of *Campylobacter* and *Salmonella* (Anonymous, 2005; Chousalkar et al., 2019). The MIC experiments revealed that 97.5% of *C. jejuni* and 92.6% *C. coli* isolates required chlorine levels higher than 8 ppm to inhibit their growth completely. Furthermore, MBC results demonstrated that 57.3% of *C. jejuni* and 55.5% of *C. coli* required 128 ppm of chlorine to inhibit the growth completely. The interpretation of these results is limited because due to the presence of chlorine demanding material in the NB2 broth. Furthermore, the free available chlorine is constantly monitored to ensure the consistent bactericidal effects. Therefore, to further explore the response of the *C. jejuni* isolates to chlorine other bactericidal tests were used in the presence and absence of chlorine demanding material.

The time kill experiments conducted here revealed that the effect of chlorine over time was significantly impacted by the presence of organic material in the broth. No significant difference in bacterial loads was observed at any of the chlorine concentrations prepared in NB2. Irrespective of the treatment effect, the bacterial counts of both isolates declined after 24 h incubation at 25°C. This may be due to the fastidious growth requirement of *Campylobacter* and the restriction of growth below 30°C (Park, 2002). In contrast, both C1, C2 isolates exhibited one $\log_{10}$ reduction at 5°C after 24 h. This suggested that regardless of the chlorine effect, *Campylobacter* remained viable when incubated at 5°C. The rapid transformation of *C. jejuni* in to the viable but non-culturable (VBNC) form at 25°C and its viability at low temperatures has been described earlier

(Jang et al., 2007). Further work is necessary to assess the chlorine resistance and survival of *Campylobacter* on chicken carcass under these parameters. Viability of *Campylobacter* at 5°C in presence of chlorine is an important observation for the industry as the chill tanks in processing plants are most often maintained at this temperature. Interestingly, when 0.9% saline was used instead of NB2, both C1, C2 *Campylobacter* isolates were highly sensitive to chlorine at all concentrations. These results could be attributed to the negative effect of chlorine neutralizing substance in the reaction media (NB2). Previous studies have shown that Gram-negative bacteria are resistant to chlorine in the presence of organic matter (Virto et al., 2005). Organic matter reduces the free available chlorine in a solution ultimately providing protection to bacteria (LeChevallier et al., 1981).

Inactivation assays were performed to determine the chemical efficacy bacterial concentrations over a broad range of chlorine concentrations. The low range of concentrations (0.2–2.0 pmm) were used to determine the chlorine sensitivity of the *Campylobacter* isolates used in this study. The high range of concentrations (2.0 ppm to 256 ppm) incorporated the levels of chlorine used globally in poultry processing plants. Chlorine was more effective in reducing *Campylobacter* levels when the bacterial inoculum was low (10^6 CFU/ml). Interestingly, when the bacterial load was 10^8 CFU/ml, reduction in *Campylobacter* level was lower. Our findings suggest that the efficacy of chlorine is highly dependent on a load of *C. jejuni* in the reaction media. This may be due to the reduction of free available chlorine required to inactivate all bacteria. The mechanism behind this difference, however, requires further study. In the present study, strain variation in chlorine sensitivity was also observed among *C. jejuni* isolates. The strain variation in response to chlorine treatment has been previously shown (Blaser et al., 1986). Usually, broiler birds harbor high levels of *Campylobacter* in the fecal material as well as in the crop and cross contaminate carcass during the processing (Newell and Fearnley, 2003). Loads of *Campylobacter* entering processing plants can vary significantly and has been previously reported to range between 5 $\log_{10}$ CFU/mL to 8 $\log_{10}$ CFU/mL of carcass rinse (Bashor et al., 2004).

The resuscitation of *C. jejuni* after exposure to chlorine suggested that it is possible to revive bacteria after a sub-lethal injury caused by chlorine exposure. Notably, resuscitation was observed only, when the *Campylobacter* concentration was 10^8 CFU/mL in the reaction media. About 83.3% of *C. jejuni* isolates were able to resuscitate after exposure to chlorine at 8 ppm. Additionally, 66.6% of isolates were resuscitated at 4 ppm. Isolates were not resuscitated when the bacterial load was low (10^6 CFU/ml) even in the lowest concentration of 0.2 ppm. This may be due to irreversible cell injury caused by chlorine when the bacterial load was high. There was no difference in the resuscitation of bacteria with extended incubation in broth for up to 48 h. This suggested that reversible cellular injury could be repaired within 24 h of enrichment. The bacterial recovery in response to chlorine could also vary from strain to strain. This strain variation of recovery could be due to the genetic variation among the *Campylobacter* strains in order to overcome the chemical stress (Peyrat et al., 2008). Our findings suggested that the bacteria could overcome the sub-lethal injury if provided with sufficient recovery time under appropriate enrichment conditions (Wesche et al., 2009). The recovery of *Campylobacter* in liquid media after exposure to various stressors such as nutrient and heat stress has been previously demonstrated (Bovill and Mackey, 1997) but there is a lack of reports demonstrating *Campylobacter* resuscitation after chlorine exposure.

To demonstrate the extent of bacterial membrane damage due to chlorine treatment, the leakage of the intracellular substances was measured by UV absorbance. When the outer membrane of a Gram-negative bacteria is damaged, the intracellular substances such as lipopolysaccharides, lipids, phospholipids, and periplasmic enzymes leads to leaking out through the membrane and that may disrupt membrane permeability (Wesche et al., 2009). In the present study, the UV absorbance values increased as chlorine concentrations increased. This was, however, also influenced by the number of bacteria (10^6 vs. 10^8 CFU/mL). Our findings can be compared with a previous study where authors reported increasing UV absorbance values from *Escherichia coli* following exposure to increasing concentrations of chlorine (Virto et al., 2005).

The severity of cellular damage after chlorine exposure were further investigated using both TEM and SEM. SEM observations revealed that bacterial cell shape varied markedly after exposure to chlorine. Chlorine stressed bacteria exhibited a loss of their distinct spiral shape. Similar degenerative changes have been previously reported for heat stressed *C. jejuni* (Tangwatcharin et al., 2006). The cell fragmentation and loss of polysaccharide capsule in the present study are evidence of irreversible lethal injury. The SEM confirmed the loss of the typical spiral *C. jejuni* morphology following chlorine stress, with the coccoid form being more dominant in the treated cells. Similar morphological changes have been described for *Campylobacter* cells exposed to antibiotics (Xie et al., 2011). It is important to note that following chlorine exposure, some *C. jejuni* cells exhibited normal morphology under SEM. Therefore, based on the SEM findings and resuscitation assay, it can be concluded that after exposure to chlorine, the non-injured or sub-lethally injured bacterial cells could be repaired if the appropriate enrichment conditions are provided.

CONCLUSION

In conclusion, the results of the present study revealed that, although chlorine is effective in reducing *C. jejuni* contamination, it is unable to eliminate it completely. This study was performed *in vitro*; hence it is essential to perform similar work using chicken meat carcasses. The *Campylobacter* isolates used in this study exhibited varying sensitivities to the chlorine concentrations tested. This could be a result to genetic variation among individual adaptive stress tolerance response mechanisms. Further studies are required to investigate the molecular mechanisms behind the strain variation. If present in high numbers, *Campylobacter* could be resuscitated after chlorine exposure that highlights the limitation of chlorine use. Ultimately, a combined chemical decontamination strategy beneficial for the chicken meat industry but further study is

required. The data obtained in this study is useful for the chicken meat industry for further optimizing the use of chlorine in reducing *Campylobacter* loads.

DATA AVAILABILITY STATEMENT

The data sets generated during this study are available by request from the corresponding author.

AUTHOR CONTRIBUTIONS

GM, AM, and KC designed all the experiments. KC and AM supervised all the experiments. GM performed all the data analyses and *Campylobacter* PCR, MICs, MBCs, SEM and TEM, and prepared the first draft of the manuscript. GM and AM conducted the chlorine inactivation, UV-absorbance assays, and resuscitation experiments. AM and KC provided the assistance with the manuscript preparation and performed the edits.

FUNDING

This study was funded by the School of Animal and Veterinary Sciences, The University of Adelaide. This study was also funded by the AgriFutures Australia project number PRJ-011593.

ACKNOWLEDGMENTS

GM is a recipient of an International Postgraduate Research Scholarship from the University of Adelaide, South Australia. We would like to acknowledge Ruth Williams, Adelaide Microscopy, University of Adelaide, for technical assistance.

REFERENCES

Anonymous (2004). Regulation (EC) No 853/2004 of the European parliament and of the council of 29 april 2004 Laying down specific hygiene rules for food of animal origin. *Official Journal* L 139, 55–205.

Anonymous (2005). *Scientific Assessment of the Public Health and Safety of Poultry Meat in Australia*. New Zealand: Food Standards Australia New Zealand.

Anonymous (2010). Analysis of the baseline survey on the prevalence of *Campylobacter* in broiler batches and of *Campylobacter* and *Salmonella* on broiler carcasses in the EU, 2008-Part A: *Campylobacter* and *Salmonella* prevalence estimates. *Eur. Food Saf. Author. J.* 8:1503.

Bashor, M., Curtis, P., Keener, K., Sheldon, B., Kathariou, S., and Osborne, J. (2004). Effects of carcass washers on *Campylobacter* contamination in large broiler processing plants. *Poult. Sci.* 83, 1232–1239. doi: 10.1093/ps/83.7.1232

Blaser, M. J., Smith, P., Wang, W.-L., and Hoff, J. (1986). Inactivation of *Campylobacter jejuni* by chlorine and monochloramine. *Appl. Environ. Microbiol.* 51, 307–311. doi: 10.1128/aem.51.2.307-311.1986

Bovill, R., and Mackey, D. B. (1997). Resuscitation of 'non-culturable'cells from aged cultures of *Campylobacter jejuni*. *Microbiology* 143, 1575–1581. doi: 10.1099/00221287-143-5-1575

Chousalkar, K., Sims, S., Mcwhorter, A., Khan, S., and Sexton, M. (2019). The effect of sanitizers on microbial levels of chicken meat collected from commercial processing plants. *Int. J. Environ. Res. Public Health* 16:4807. doi: 10.3390/ijerph16234807

Connerton, I., and Connerton, P. (2017). "Campylobacter foodborne disease," in *Foodborne Diseases*, eds C. E. R. Dodd, T. Aldsworth, R. A. Stein, D. O. Cliver, and H. P. Riemann (Amsterdam: Elsevier), 209–221. doi: 10.1016/b978-0-12-385007-2.00008-5

Hansson, I., Forshell, L. P., Gustafsson, P., Boqvist, S., Lindblad, J., Engvall, E. O., et al. (2007). Summary of the Swedish *Campylobacter* program in broilers, 2001 through 2005. *J. Food Protect.* 70, 2008–2014. doi: 10.4315/0362-028x-70.9.2008

Hansson, I., Pudas, N., Harbom, B., and Engvall, E. O. (2010). Within-flock variations of *Campylobacter* loads in caeca and on carcasses from broilers. *Int. J. Food Microbiol.* 141, 51–55. doi: 10.1016/j.ijfoodmicro.2010.04.019

Havelaar, A. H., Kirk, M. D., Torgerson, P. R., Gibb, H. J., Hald, T., Lake, R. J., et al. (2015). World health organization global estimates and regional comparisons of the burden of foodborne disease in 2010. *PLoS Med.* 12:e1001923. doi: 10.1371/journal.pmed.1001923

Herman, L., Heyndrickx, M., Grijspeerdt, K., Vandekerchove, D., Rollier, I., and De Zutter, L. (2003). Routes for *Campylobacter* contamination of poultry meat: epidemiological study from hatchery to slaughterhouse. *Epidemiol. Infect.* 131, 1169–1180. doi: 10.1017/s0950268803001183

Hermans, D., Pasmans, F., Messens, W., Martel, A., Van Immerseel, F., Rasschaert, G., et al. (2012). Poultry as a host for the zoonotic pathogen *Campylobacter jejuni*. *Vector Borne Zoonotic Dis.* 12, 89–98. doi: 10.1089/vbz.2011.0676

Hoffmann, S., Devleesschauwer, B., Aspinall, W., Cooke, R., Corrigan, T., Havelaar, A., et al. (2017). Attribution of global foodborne disease to specific foods: findings from a world health organization structured expert elicitation. *PLoS One* 12:e0183641. doi: 10.1371/journal.pone.0183641

Jacobs-Reitsma, W., Van De Giessen, A., Bolder, N., and Mulder, R. (1995). Epidemiology of *Campylobacter* spp. at two Dutch broiler farms. *Epidemiol. Infect.* 114, 413–421. doi: 10.1017/s0950268800052122

Jang, K., Kim, M., Ha, S., Kim, K., Lee, K., Chung, D., et al. (2007). Morphology and adhesion of *Campylobacter jejuni* to chicken skin under varying conditions. *J. Biotechnol.* 17:202.

Kirk, M. D., Pires, S. M., Black, R. E., Caipo, M., Crump, J. A., Devleesschauwer, B., et al. (2015). World health organization estimates of the global and regional disease burden of 22 foodborne bacterial, protozoal, and viral diseases, 2010: a data synthesis. *PLoS Med.* 12:e1001921. doi: 10.1371/journal.pmed.1001921

LeChevallier, M. W., Evans, T., and Seidler, R. J. (1981). Effect of turbidity on chlorination efficiency and bacterial persistence in drinking water. *Appl. Environ. Microbiol.* 42, 159–167. doi: 10.1128/aem.42.1.159-167.1981

Lindblad, M., Hansson, I., Vågsholm, I., and Lindqvist, R. (2006). Postchill *Campylobacter* prevalence on broiler carcasses in relation to slaughter group colonization level and chilling system. *J. Food Protect.* 69, 495–499. doi: 10.4315/0362-028x-69.3.495

Lu, T., Marmion, M., Ferone, M., Wall, P., and Scannell, A. G. (2019). Processing and retail strategies to minimize *Campylobacter* contamination in retail chicken. *J. Food Process. Preservat.* 43:e14251.

McKenzie, K., Maclean, M., Grant, M. H., Ramakrishnan, P., Macgregor, S. J., and Anderson, J. G. (2016). The effects of 405 nm light on bacterial membrane integrity determined by salt and bile tolerance assays, leakage of UV-absorbing material and SYTOX green labelling. *Microbiology* 162:1680. doi: 10.1099/mic.0.000350

Newell, D., and Fearnley, C. (2003). Sources of *Campylobacter* colonization in broiler chickens. *Appl. Environ. Microbiol.* 69, 4343–4351. doi: 10.1128/aem.69.8.4343-4351.2003

Oyarzabal, O. A. (2005). Reduction of *Campylobacter* spp. by commercial antimicrobials applied during the processing of broiler chickens: a review from the United States perspective. *J. Food Protect.* 68, 1752–1760. doi: 10.4315/0362-028x-68.8.1752

Park, S. F. (2002). The physiology of *Campylobacter* species and its relevance to their role as foodborne pathogens. *Int. J. Food Microbiol.* 74, 177–188. doi: 10.1016/s0168-1605(01)00678-x

Patrick, M., Henao, O., Robinson, T., Geissler, A., Cronquist, A., Hanna, S., et al. (2018). Features of illnesses caused by five species of *Campylobacter*, foodborne

diseases active surveillance network (FoodNet)–2010–2015. *Epidemiol. Infect.* 146, 1–10. doi: 10.1017/S0950268817002370

Peyrat, M.-B., Soumet, C., Maris, P., and Sanders, P. (2008). Phenotypes and genotypes of *Campylobacter* strains isolated after cleaning and disinfection in poultry slaughterhouses. *Vet. Microbiol.* 128, 313–326. doi: 10.1016/j.vetmic.2007.10.021

Stern, N., Clavero, M., Bailey, J., Cox, N., and Robach, M. (1995). Campylobacter spp. in broilers on the farm and after transport. *Poultry Sci.* 74, 937–941. doi: 10.3382/ps.0740937

Suzuki, H., and Yamamoto, S. (2009). *Campylobacter* contamination in retail poultry meats and by-products in the world: a literature survey. *J. Vet. Med. Sci.* 71, 255–261. doi: 10.1292/jvms.71.255

Tangwatcharin, P., Chanthachum, S., Khopaibool, P., and Griffiths, M. W. (2006). Morphological and physiological responses of *Campylobacter jejuni* to stress. *J. Food Protect.* 69, 2747–2753. doi: 10.4315/0362-028x-69.11.2747

Van, T. T. H., Gor, M.-C., Anwar, A., Scott, P. C., and Moore, R. J. (2017). *Campylobacter hepaticus*, the cause of spotty liver disease in chickens, is present throughout the small intestine and caeca of infected birds. *Vet. Microbiol.* 207, 226–230. doi: 10.1016/j.vetmic.2017.06.022

Virto, R., Manas, P., Alvarez, I., Condon, S., and Raso, J. (2005). Membrane damage and microbial inactivation by chlorine in the absence and presence of a chlorine-demanding substrate. *Appl. Environ. Microbiol.* 71, 5022–5028. doi: 10.1128/aem.71.9.5022-5028.2005

Walker, L. J., Wallace, R. L., Smith, J. J., Graham, T., Saputra, T., Symes, S., et al. (2019). Prevalence of *Campylobacter coli* and *Campylobacter jejuni* in retail chicken, beef, lamb, and pork products in three Australian states. *J. Food Protect.* 82, 2126–2134. doi: 10.4315/0362-028X.JFP-19-146

Walsh, R. J., White, B., Hunker, L., Leishman, O., Hilgren, J., and Klein, D. (2018). Peracetic acid and hydrogen peroxide post-dip decay kinetics on red meat and poultry. *Food Protect. Trends* 38, 96–103.

Weinstein, M. P. (2018). *Methods for Dilution Antimicrobial Susceptibility Tests for Bacteria That Grow Aerobically*. Villanova, PA: National Committee for Clinical Laboratory Standards.

Wesche, A. M., Gurtler, J. B., Marks, B. P., and Ryser, E. T. (2009). Stress, sublethal injury, resuscitation, and virulence of bacterial foodborne pathogens. *J. Food Protect. Poult. Sci.* 72, 1121–1138. doi: 10.4315/0362-028x-72.5.1121

Whyte, P., Collins, J., Mcgill, K., Monahan, C., and O'mahony, H. (2001). The effect of transportation stress on excretion rates of campylobacters in market-age broilers. *Poult. Scie.* 80, 817–820. doi: 10.1093/ps/80.6.817

Xie, Y., He, Y., Irwin, P. L., Jin, T., and Shi, X. (2011). Antibacterial activity and mechanism of action of zinc oxide nanoparticles against *Campylobacter jejuni*. *Appl. Environ. Microbiol.* 77, 2325–2331. doi: 10.1128/AEM.02149-10

Conflict of Interest: The authors declare that the research was conducted in the absence of any commercial or financial relationships that could be construed as a potential conflict of interest.

frontiers in Microbiology

ORIGINAL RESEARCH
published: 27 March 2020
doi: 10.3389/fmicb.2020.00523

Differences in the Transcriptomic Response of *Campylobacter coli* and *Campylobacter lari* to Heat Stress

*Carolin Riedel[1], Konrad U. Förstner[2,3,4], Christoph Püning[1], Thomas Alter[1], Cynthia M. Sharma[2] and Greta Gölz[1]**

[1] Institute of Food Safety and Food Hygiene, Freie Universität Berlin, Berlin, Germany, [2] Chair of Molecular Infection Biology II, Institute of Molecular Infection Biology, Julius Maximilian University of Würzburg, Würzburg, Germany, [3] ZB MED - Information Centre for Life Sciences, Köln, Germany, [4] Institute of Information Science, Faculty of Information Science and Communication Studies, TH Köln (University of Applied Sciences), Köln, Germany

OPEN ACCESS

Edited by:
Ozan Gundogdu,
University of London, United Kingdom

Reviewed by:
Craig T. Parker,
Agricultural Research Service (USDA), United States
Xiaonan Lu,
The University of British Columbia, Canada
Bachar Cheaib,
University of Glasgow, United Kingdom

***Correspondence:**
Greta Gölz
greta.goelz@fu-berlin.de

Specialty section:
This article was submitted to Food Microbiology, a section of the journal Frontiers in Microbiology

Received: 16 October 2019
Accepted: 10 March 2020
Published: 27 March 2020

Citation:
Riedel C, Förstner KU, Püning C, Alter T, Sharma CM and Gölz G (2020) Differences in the Transcriptomic Response of Campylobacter coli and Campylobacter lari to Heat Stress. Front. Microbiol. 11:523. doi: 10.3389/fmicb.2020.00523

Campylobacter spp. are one of the most important food-borne pathogens, which are quite susceptible to environmental or technological stressors compared to other zoonotic bacteria. This might be due to the lack of many stress response mechanisms described in other bacteria. Nevertheless, *Campylobacter* is able to survive in the environment and food products. Although some aspects of the heat stress response in *Campylobacter jejuni* are already known, information about the stress response in other *Campylobacter* species are still scarce. In this study, the stress response of *Campylobacter coli* and *Campylobacter lari* to elevated temperatures (46°C) was investigated by survival assays and whole transcriptome analysis. None of the strains survived at 46°C for more than 8 h and approximately 20% of the genes of *C. coli* RM2228 and *C. lari* RM2100 were differentially expressed. The transcriptomic profiles showed enhanced gene expression of several chaperones like *dnaK*, *groES*, *groEL*, and *clpB* in both strains, indicating a general involvement in the heat stress response within the *Campylobacter* species. However, the pronounced differences in the expression pattern between *C. coli* and *C. lari* suggest that stress response mechanisms described for one *Campylobacter* species might be not necessarily transferable to other *Campylobacter* species.

Keywords: *Campylobacter coli*, *Campylobacter lari*, heat stress response, transcriptome sequencing, RNA-seq

INTRODUCTION

Campylobacter is one of the most common causative agents of bacterial food-borne gastroenteritis in humans worldwide. The campylobacteriosis (with clinical symptoms like diarrhea, abdominal cramps, and fever) is mostly self-limiting but sequelae like Guillian–Barré syndrome and reactive arthritis have been described (Poropatich et al., 2010). Handling and consumption of raw or undercooked meat has been identified as a main source for human infections (Alter et al., 2011). *Campylobacter* belongs to the heterogeneous class of *Epsilonproteobacteria* and the species mostly detected in diseased humans are *Campylobacter jejuni* followed by *Campylobacter coli* and to a lesser extent *Campylobacter lari* and *Campylobacter upsaliensis* (Whiley et al., 2013). Whereas

C. jejuni shows high prevalences in poultry and cattle, *C. coli* is usually associated with pigs and *C. lari* is frequently detected in shellfish and shorebirds (Miller et al., 2008; EFSA and ECDC, 2014). However, in these animals, *Campylobacter* belongs to the commensal microbiota. By comprehensive genome comparisons of several strains, it has been shown that *C. jejuni* is more closely related to *C. coli* compared to *C. lari* (Zhou et al., 2013).

Campylobacter spp. possess fastidious growth requirements and are less resistant against environmental and technological stressors compared to other zoonotic pathogens (Park, 2002). This might be explained by the absence of several stress response regulators typically involved in the regulation of stress response to various stressors in other Gram-negative bacteria like *Escherichia coli* or *Salmonella*, e.g., alternative sigma factors like RpoS (σ^{38}) as well as other transcription regulators such as CspA, Lrp, SoxRS, and OxyR (Alter and Scherer, 2006). Unlike *E. coli*, which harbors seven sigma factors, only RpoD (σ^{70}), RpoN (σ^{54}), and RpoF/FliA (σ^{28}) were found in *Campylobacter* spp. (Fouts et al., 2005). However, *Campylobacter* spp. is able to survive in the environment and to overcome the barriers along the food chain. This suggests the existence of alternative regulatory mechanisms or a wider role of known regulatory factors. For example, the transcription of both the peroxide as well as the superoxide defense genes are regulated by PerR in *C. jejuni* while in *E. coli* and *Salmonella* OxyR regulates the expression of the peroxide defense regulon and SoxR of the superoxid defense regulon (Kim et al., 2015).

Several authors have described the response of *C. jejuni* to increased temperatures. Konkel et al. (1998) were able to identify 24 proteins preferentially synthesized following heat stress at 46°C. One of these proteins was identified as the DnaJ chaperon, shown to be necessary for survival at elevated temperatures. Further proteome analyses showed 18 differentially expressed proteins induced by increasing temperature from 37 to 42°C (Zhang et al., 2009). The gene expression profiles associated with these responses have also been investigated by microarray analysis (Stintzi, 2003). This study revealed an increased expression of common genes encoding heat stress proteins like chaperones and proteases (e.g., *groELS*, *grpE*, *dnaK*, *dnaJ*, *clpB*, *lon*) and membrane associated proteins (e.g., *galE*, *gmhA2*). In addition, the chaperon activity of the serine protease HtrA is involved in the heat stress response of *C. jejuni* (Baek et al., 2011). The alternative sigma factor σ^{32} (RpoH) mediating the expression of heat stress related genes in *E. coli* is missing in *Campylobacter* (Parkhill et al., 2000; Yura et al., 2000). So far, RacR, HspR, and HrcA have been identified as regulators of the heat stress response in *C. jejuni* (Holmes et al., 2010; Apel et al., 2012), while RpoN (σ^{54}), known to be involved in various stress responses, is not involved in the heat stress response of *C. jejuni* (Hwang et al., 2011).

Survival strategies of the related species *C. coli* and *C. lari* at high temperatures are largely unexplored. Thus, our study aimed to compare the effects of heat stress (46°C) on the two *Campylobacter* species *C. coli* and *C. lari* by (i) survival studies and (ii) whole transcriptome (RNA-seq) analyses, to identify genes involved in the heat stress response.

MATERIALS AND METHODS

Bacterial Strains, Media, and Growth Conditions

Campylobacter strains were grown on Mueller–Hinton agar containing 5% sheep blood (MHB; OXOID, Wesel, Germany) for 48 h or *Brucella* broth for 24 h (BB; BD, Heidelberg, Germany) at 37°C in microaerobic conditions (6% O_2, 7% CO_2, 7% H_2, 80% N_2) generated by the Mart Anoxomat system (Drachten, Netherlands). The whole genome sequenced strains *C. coli* RM2228 and *C. lari* RM2100 were selected according to their clinical importance. The *C. coli* strain RM2228, isolated from a chicken carcass, belongs to the phylogenetic clade1, which are mainly responsible for human infections (Sheppard et al., 2010). The *C. lari* strain RM2100 was isolated from a child with watery diarrhea (Miller et al., 2008). Two further field strains of each species were included for survival assays. All strains are listed in **Supplementary Table S5**.

Survival Studies

For survival studies, pre-cultures were diluted in BB to an optical density of 0.01 at 600 nm (approximately 7 $\log_{10}$ CFU/ml) and incubated at 46°C in microaerobic conditions in a static cultivation mode. The cell numbers were determined over a 24 h period by plating serial dilutions on MHB. These plates were incubated at 37°C for 48 h and cell counts shown as $\log_{10}$ CFU/ml. Experiments were performed at three individual time points with technical duplicates.

Quantitative Real-Time PCR

The expression of the selected genes *clpB*, *grpE*, *dnaK*, *groEL*, *groES*, *cbpA*, and *dnaJ* of *C. coli* and *C. lari* were analyzed over 60 min stress exposure, induced by increasing temperatures from 37°C to 46°C. RNA extractions of three individual cultures were included for both species. Total RNA was isolated from approximately 9 log CFU using a peqGOLD Bacterial RNA Kit (Peqlab, Erlangen, Germany). Removal of genomic DNA was performed in a total volume of 40 µl containing 4 U DNase I, 40 U Ribolock, 1x DNase buffer (all Fermentas, Leon-Rot, Germany), and 28 µl of RNA. After an incubation for 15 min at 37°C, DNase was inactivated by adding 4 µl 50 mM EDTA and heating at 65°C for 10 min. First-strand cDNA was synthesized of 1 µg RNA using the RevertAid Premium First Strand cDNA synthesis kit and random hexamer primers (all Fermentas) according to manufacturer's instructions.

Primers were designed using the Primer3 web interface[1] based on the *C. coli* RM2228 and *C. lari* RM2100 genome sequences (with primer length 17–25 nt, amplicon size 60–150 nt, and primer Tm 50–62°C). All runs were performed in a 15 µl PCR mixture containing 1 µl of a 1:10 dilution of cDNA, 0.05–0.9 µM of each primer (**Supplementary Table S1**) and a twofold SsoFast EvaGreen Supermix (Bio-Rad, Munich, Germany). The amplification was performed by pre-heating for 30 s at 94°C and 40 cycles of 94°C for 5 s followed by annealing for 10 s

[1] http://frodo.wi.mit.edu/

(annealing temperatures are shown in **Supplementary Table S1**). Quantitative real-time PCR data were processed using the CFX Manager Software (Bio-Rad) with *thiC* and *rpoA* as housekeeping genes. $\Delta\Delta$Cq values of all samples were determined based on two technical replicates. Specificity of the amplification product was confirmed by melting curve analysis.

RNA Isolation for Whole Transcriptome Analysis

As quantitative real-time PCR analysis indicated still enhanced mRNA-level for several genes after 30 min heat stress, this time point was chosen for whole transcriptome analysis. RNA was isolated from two independent cultures for each species. Total RNA was extracted from approximately 9 log CFU of the two species *C. coli* and *C. lari* after 30 min cultivation at 37°C and of heat stress at 46°C using a hot phenol/lysozyme method (Blomberg et al., 1990). Therefore, the bacterial culture was mixed 1:5 with stop-mix (95% v/v ethanol, 5% v/v water saturated phenol, −20°C). Cells were pelleted by centrifugation at 1500 × *g*, supernatant discarded, and samples stored at -80°C. Pellets were resuspended in 600 µl 0.5 mg/ml lysozyme in TE (pH 8.0), 60 µl 10% w/v SDS were added and incubated at 64°C for 2 min. Afterward 66 µl 1 M NaOAc (pH 5.2) and 750 µl Roti-Aqua phenol (Carl Roth, Karlsruhe, Germany) were added. During incubation at 64°C for 6 min, samples were mixed by inversion 6–10 times. Tubes were placed on ice and centrifuged for 15 min at 12,000 × *g* (4°C). Aqueous layer was transferred in a 2 ml Phase Lock Gel-Heavy tube (VWR, Dresden, Germany), 750 µl chloroform (Carl Roth) added and mixed by inversion. After centrifugation for 12 min at 12,000 × *g*, the aqueous layer was transferred, 1.4 ml 30:1 EtOh:3 M NaOAc (pH 6.5) added and incubated overnight at −20°C. Samples were centrifuged at 12,000 × *g* (at 4°C for 30 min), supernatant removed, and pellet washed with 900 µl 75% v/v ethanol (-20°C). Samples were centrifuged as mentioned above, ethanol removed, and the pellet air-dried. The RNA was dissolved by adding 100 µl nuclease-free water (Roth) and shaken for 5 min at 65°C (800–1000 r/min). DNA was removed according to the above-described method. RNA integrity and quantity were determined on an Agilent 2100 Bioanalyzer (Agilent Technologies, Waldbronn, Germany) before cDNA synthesis.

Whole Transcriptome Sequencing

Vertis Biotechnologie AG (Munich, Germany) generated libraries of two independent RNA samples for each condition. The RNA samples were poly(A)-tailed by using poly(A) polymerase. The 5'PPP were removed using tobacco acid pyrophosphatase (TAP) followed by the ligation of the RNA adapter to the 5'-monophosphate of the RNA. First-strand cDNA synthesis was performed with an oligo(dT)-adapter primer and the M-MLV reverse transcriptase. The resulting cDNA was PCR-amplified to reach a concentration of 20–30 ng/µl using a high fidelity DNA polymerase. The cDNA was purified using the Agencourt AMPure XP kit (Beckman Coulter Genomics, Essex, United Kingdom) and was analyzed by capillary electrophoresis. The primers used for PCR amplification were designed for TruSeq sequencing according to the instructions of Illumina (San Diego, CA, United States). The following adapter sequences flank the cDNA inserts: TrueSeq_Sense_primer 5'-AATGATACGGCGACCACCGAGATCTACACTCTTTCCC TACACGACGCTCTTCCGATCT-3' and TrueSeq_Antisense _NNNNNN_primer (NNNNNN = Barcode) 5'-CAAGCA GAAGACGGCATACGAGATNNNNNNGTGACTGG AGTTC AGACGTGTGCTCTTCCGATC(dT25)-3'. The combined length of the flanking sequences is 146 bases. The libraries were sequenced with an Illumina HiSeq machine with 100 cycles in single end mode.

Bioinformatical Analysis

Read Data Analysis

The resulting sequence reads were demultiplexed and the adapter sequences were removed. After that the reads in Fastq format were quality trimmed using fastq_quality_trimmer (from the FastX suite version 0.0.13[2]) with a quality cut-off score of 20 and converted to fasta format using fastq_to_fasta (also from the FastX suite). The read processing [poly(A) removal, size filtering (min 12 nt length), statistics generation, coverage calculation, and normalization] was performed with the RNA-analysis pipeline READemption version 0.3.4 (Forstner et al., 2014; building upon the following libraries Biopython 1.65, pysam 0.8.1, matplotlib 1.4.3, pandas 0.16.0) which used segemehl version 0.1.7 (Hoffmann et al., 2009) for the read alignment. For *C. coli* RM2228, the sequences with the accession number AAFL01000001.1-38.1, DQ518170, DQ518171, as well as DQ518172.1 and for *C. lari* RM2100 the sequences with the accession number NC_012039 as well as NC_01240.1 were used as references (all mapping statistics are shown in **Supplementary Table S2**). Feature wise gene-quantification was performed (also with READemption) and used for differential gene expression analysis. According to the study of Stintzi (2003) genes with $\log_2$ fold changes of expression below -0.58 or above 0.58 and an adjusted (Benjamini–Hochberg corrected) p-value < 0.05 calculated by DESeq2 1.6.3 were defined as regulated (Love et al., 2014).

The RNA-Seq data discussed in this publication have been deposited in NCBI's Gene Expression Omnibus (Edgar et al., 2002) and are accessible through GEO Series accession number GSE67486[3].

Orthologous Mapping

Orthologs were defined, based on the nucleotide sequences, by bidirectional best-BLAST-hit search with max. e-value of 1e-6, word size of 20, and a minimal length of 60% of both query and subject nucleotide sequence. Further some genes were determined as orthologous by similarity of gene name.

Functional Grouping

Functional groups of *C. coli*, *C. lari*, and *C. jejuni* CDS were based on functional categories received by eggNOG4.0 database[4] or by

[2]http://hannonlab.cshl.edu/fastx_toolkit/

[3]www.ncbi.nlm.nih.gov/geo/query/acc.cgi?acc = GSE67486

[4]http://eggnog.embl.de/version_4.0.beta/downloads.v4.html

functional category from orthologs. CDS belonging to two or more different categories were listed in each category. Statistical significance of enrichments of functional groups was calculated with Fisher's exact test using GraphPad Prism version 6.07 for Windows (GraphPad Software, La Jolla, CA, United States[5]).

The bioinformatical analyses represented by Shel and Python scripts as well as their results are deposited at Zenodo[6].

RESULTS

Survival Assays Show High Susceptibility to Heat Stress of *C. lari* and *C. coli*

The two strains *C. coli* RM2228 and *C. lari* RM2100 were heat stressed by cultivation at 46°C under microaerobic conditions and survival of these strains was determined over a period of 24 h. Experiments were started with approximately 7 $\log_{10}$ CFU/ml (**Figure 1A**). Cell counts of *C. coli* and *C. lari* were reduced by one log level after 2 h of incubation at 46°C. *C. lari* cell counts decreased to 3.4 $\log_{10}$ CFU/ml after 4 h and further 1.1 $\log_{10}$ CFU/ml after 6 h of heat stress. The cell counts of *C. coli* were reduced to 4.6 $\log_{10}$ CFU/ml after 4 h and further 1.9 $\log_{10}$ CFU/ml after 6 h of cultivation at 46°C. Already after 8 h of heat stress, no surviving cells were observed for both strains. To verify that the observed heat stress survival ability is not only strain-specific, the experiments were repeated with two more field isolates of each species (**Figure 1B**). Even though variations between the isolates were observed, the overall survival was comparable to the results obtained by the laboratory strains shown in **Figure 1A**.

Gene Expression Profiling of Known Heat Stress Genes Using qRT-PCR

The expression level of selected genes, known to be involved in the heat shock response of *C. jejuni*, was investigated over a time period of 60 min of heat stress at 46°C by quantitative RT-PCR in *C. coli* and *C. lari*. In both strains increased $\log_2$ fold changes of the expression level for the chaperon genes *clpB*, *grpE*, *dnaK*, *groEL*, *groES*, *cbpA* and the negative transcriptional regulator *hrcA* were determined, while expression level of *dnaJ* was only slightly increased in *C. coli* and not regulated in *C. lari* (**Figure 2**). After 15 min of heat stress, the expression level of these genes was highly induced in both strains. While the high expression levels

[5]http://www.graphpad.com

[6]https://doi.org/10.5281/zenodo.3669112

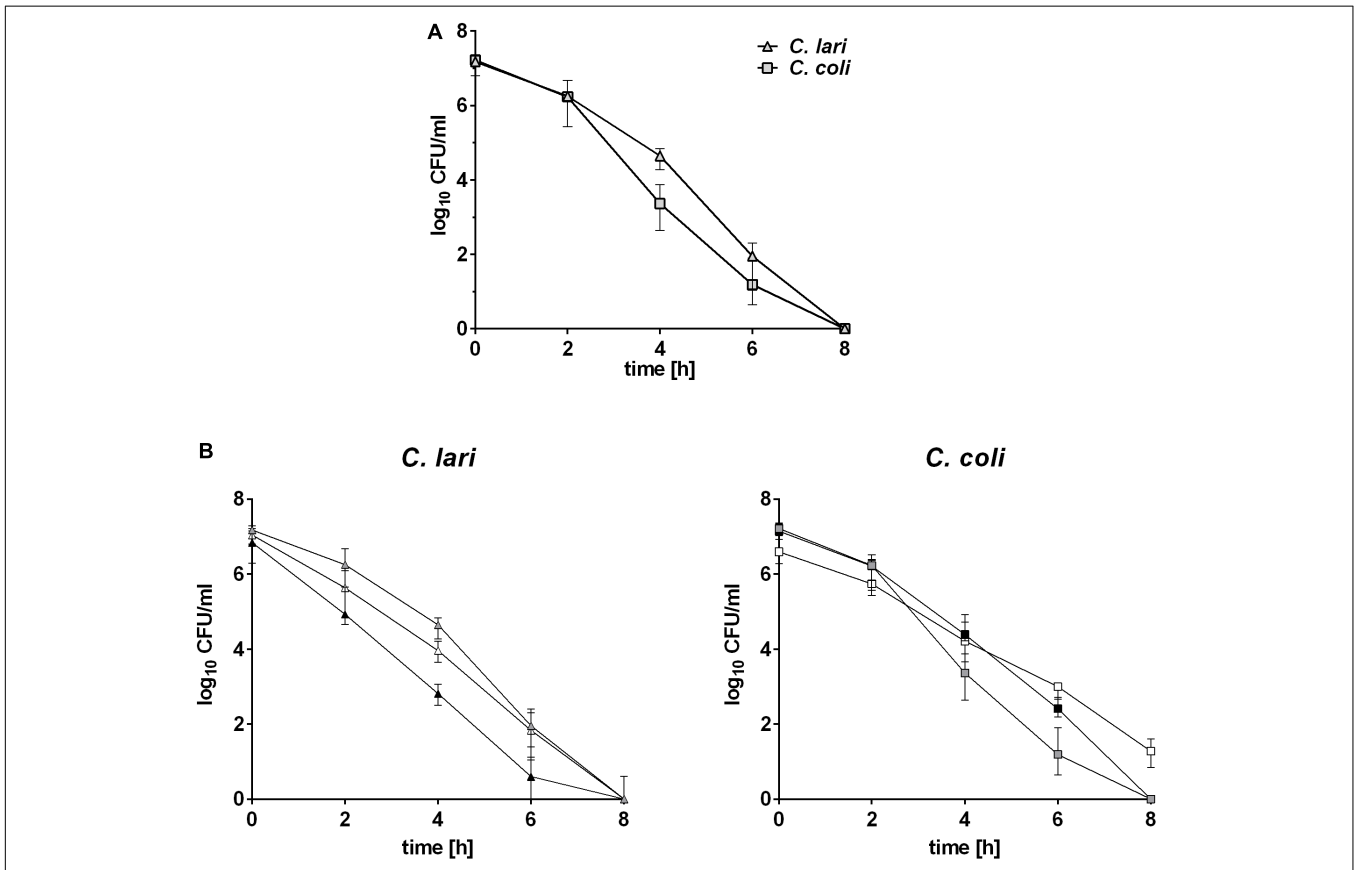

FIGURE 1 | Survival abilities of *C. coli* and *C. lari* at 46°C. Bacterial cultures of approximately 7 $\log_{10}$ CFU/ml were incubated at 46°C and cell counts determined at indicated time points. Data were shown for **(A)** reference strains and **(B)** wild type strains of *C. coli* and *C. lari* as median ± interquartile range of three biological replicates. Gray: sequenced strains, white: first field strain, and black: second field strain.

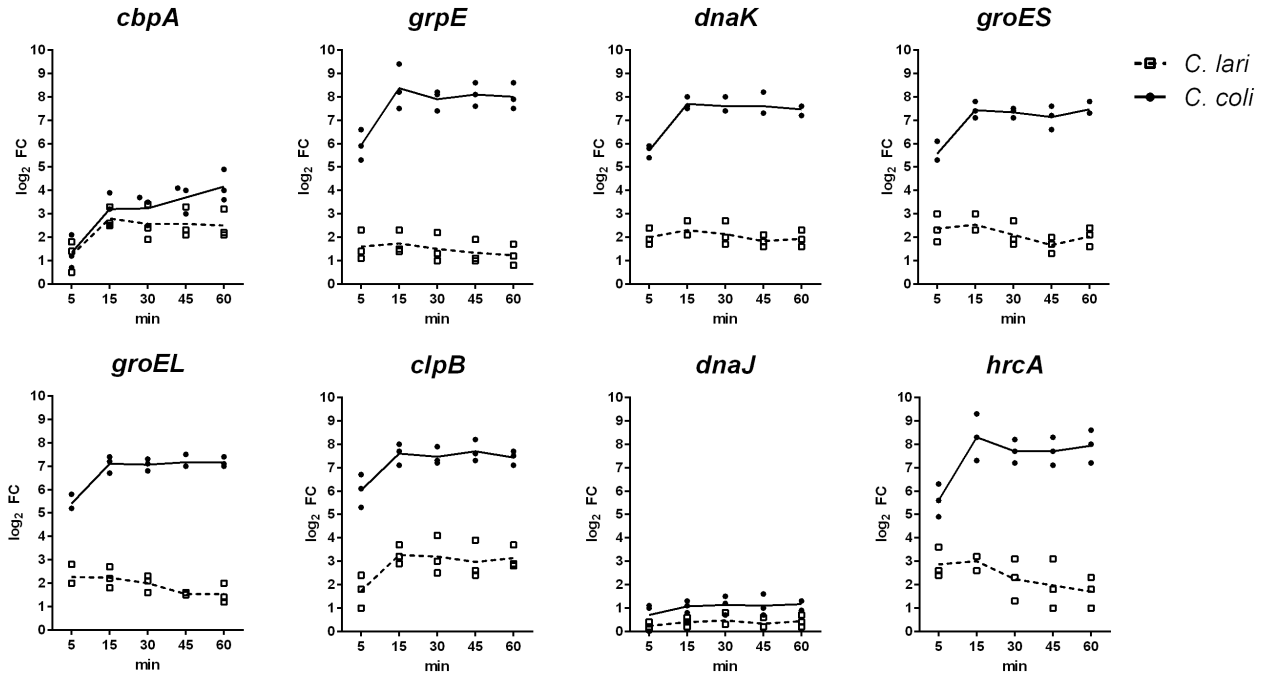

FIGURE 2 | Gene expression of known heat shock genes in *C. coli* RM2228 and *C. lari* RM2100 at 46°C compared to 37°C by qRT-PCR. Gene expression of selected heat shock genes was analyzed by qRT-PCR and normalized to the expression of *rpoA* and *thiC*. Fold changes of expression were calculated by the ΔΔCq method of CFX manager software. Log_2 fold changes for each biological replicate were shown and the means connected by the line.

were stable until the end of the experiments (60 min) in *C. coli*, the levels slightly decreased after 30 min in *C. lari*. Overall, higher fold changes of expression level of these genes were detected in *C. coli* compared to *C. lari*.

Global Transcriptome Analysis Upon Heat Stress Using RNA-Seq

To get further insight into the heat stress response of both species, whole transcriptome analysis of *C. coli* and *C. lari* was performed by RNA sequencing. Therefore, RNA was extracted for each strain after 30 min cultivation at 37 and 46°C of biological duplicates, libraries prepared as described in Section "Materials and Methods" and transcriptome libraries sequenced by Illumina. Log_2 fold changes of expression level were determined by DESeq2 (mapping statistics for all libraries are shown in **Supplementary Table S2** and log_2 fold changes of expression level in **Supplementary Table S3**). The genes already analyzed by qRT-PCR showed similar amplification in the RNA-seq analysis. Expression level of further 18 genes per strain was investigated by qRT-PCR, to correlate the fold changes determined by RNA-seq versus qRT-PCR resulting in a Pearson correlation coefficient R^2 of 0.6644 for *C. coli* and 0.5599 for *C. lari* (**Supplementary Figure S1**).

After 30 min of heat stress 17.2% of the *C. coli* (338/1967) and 19.4% of the *C. lari* genes (300/1545) were shown by RNA-seq analysis to be differentially expressed (**Table 1**). Of these differentially expressed genes, 67.1% were up-regulated in *C. coli*, while only 43.6% were up-regulated in *C. lari* (**Figure 3**).

Enrichment of Regulated Genes After Heat Stress in Several Functional Categories

To analyze if genes with similar function were comparably expressed in both species and if a specific class of genes is significantly enriched upon heat stress, a functional categorization based on orthologous groups according to the eggNOG database was used. Nearly half of the differentially expressed genes (55% for *C. coli* and 49% for *C. lari*) has not been assigned to any category or their functions are only poorly characterized (**Supplementary Table S4**). The other differentially expressed genes are distributed over the 20 functional categories, with significant enrichment in the category T (signal transduction mechanisms) for *C. coli* (27.3%) and significant enrichment in the category I (lipid transport and metabolism) and category Q (secondary metabolites

TABLE 1 | Gene expression profile by RNA sequencing of *C. coli* RM2228 and *C. lari* RM2100 after 30 min heat stress at 46°C compared to 37°C.

	C. coli	*C. lari*
Analyzed genes	1967	1545
Regulated genes	338 (17.2%)	300 (19.4%)
Up-regulated	227 (67.1%)	131 (43.6%)
Down-regulated	111 (32.9%)	169 (56.4%)

The total numbers of analyzed and differentially expressed genes as calculated by DESeq2 1.6.3 are indicated for each strain.

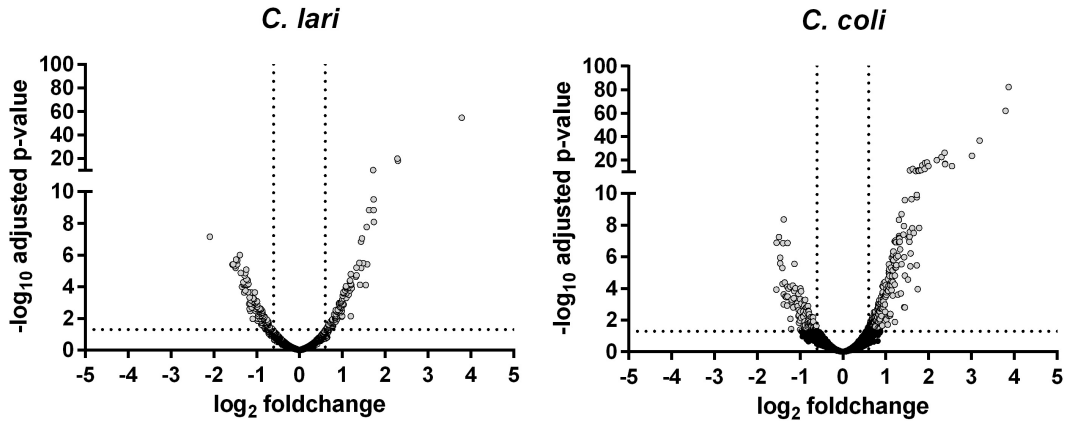

FIGURE 3 | Gene expression profile of the whole transcriptome of *C. coli* RM2228 and *C. lari* RM2100 after 30 min of heat stress. Whole transcriptome was analysis after 30 min incubation at 46°C by RNA sequencing and gene expression shown in volcano plots as $\log_2$ fold change versus $-\log_{10}$ p-values of biological duplicates. Gray: significantly different expressed genes.

biosynthesis, transport, and catabolism) for *C. lari* (33.3 and 40%) (**Figure 4A**).

In both species, the majority of differentially expressed genes in category O (posttranslational modification, protein turn-over, and chaperones) and category H (coenzyme transport and metabolism) were up-regulated, while the majority of differentially expressed genes of category J (translation, ribosomal structure and biogenesis) and U (intracellular trafficking, secretion and vesicular transport) were down-regulated (**Figure 4B**). Expression level of genes belonging to the category of cell wall/membrane/envelop biosynthesis (M), energy production and conversion (C), and amino acid as well as nucleotide transport and metabolism (E, F) were mostly up-regulated in *C. coli* but down-regulated in *C. lari*. In contrast, nearly no genes belonging to category cell cycle control, cell division, chromosome partitioning (D) or defense mechanisms (V) were affected in their expression level in both species (**Supplementary Table S4**).

C. coli and *C. lari* Share a Low Number of Differentially Expressed Orthologs Genes With Each Other After Heat Stress

To compare the heat stress response of both species in more detail, orthologs between the genomes of *C. coli* RM2228 and *C. lari* RM2100 were determined. As the knowledge about gene functionality is more comprehensive for *C. jejuni*, we also included the genome of *C. jejuni* NCTC11168 in the ortholog assignment. Altogether 1372 orthologous groups (consisting of two or three genes) could be assigned in the three combined genomes (**Supplementary Figure S2**) with 759 orthologous genes present in all three genomes. While *C. jejuni* and *C. coli* additionally shared 554 orthologous genes, *C. lari* shared only 18 orthologous genes with *C. coli* and 41 with *C. jejuni*, respectively.

For 70.1% of the 338 regulated genes in *C. coli*, and 57.7% of the 300 regulated genes in *C. lari*, no ortholog could be determined in the other strain. However, the expression of 35 genes, 29 orthologs, and six genes with the same name, but not defined as orthologs at a BLAST e-value of 1e-6 (marked by asterisks in **Table 2**), was similarly regulated in both species, while 2 genes showed oppositional expression between the two strains (**Table 2**).

Orthologous genes with up-regulated expression levels in both species include the heat stress response related genes *hrcA*, *grpE*, *dnaK*, *groEL*, *groES*, *clpB*, *cbpA*, *hspR*, the invasion antigen *ciaB*, flagellar associated genes *flaG* and *pseA*, membrane associated genes (*lolA*, *kefB*, Cla_1506/CCO0311), the threonyl-tRNA-synthetase *thrS* and the exinuclease *uvrB*.

Orthologous genes down-regulated in both species included translation and ribosomal associated genes (*rpmF*, *rpsL*, *dusB*, *aat*, *queA*, an endoribonuclease), the *Campylobacter* transformation system proteins *ctsE* and *ctsD*, the outer membrane efflux protein *cmeD*, and the flagellar P-ring protein *flgI*.

The expression of the genes encoding a histidine triad protein (Cla_0423/CCO0504) and a GTP cyclohydrolase (Cla_0006/CCO0022) were down-regulated in *C. lari* but up-regulated in *C. coli* (**Table 2**).

Genes Affected in Expression After Heat Stress in One Species Only

C. coli

Genes assigned to a functional category and with differential expression after heat stress in *C. coli* only are shown in **Table 3** ($\log_2$ fold changes and *p*-values are shown in **Supplementary Table S3**). The expression of the transcriptional regulators *cmeR*, *furR1* and a regulator belonging to the ArsR-family were also up-regulated in *C. coli*, while expression of CCO1284 (a regulator belonging to the Baf-family) and the transcription termination gene *nusA* were down-regulated. Further, the expression level of several signal transducer or two-component system encoding genes (e.g., *cheV*, the *flgR*-ortholog *rrp-2*, *dccS*) was up-regulated.

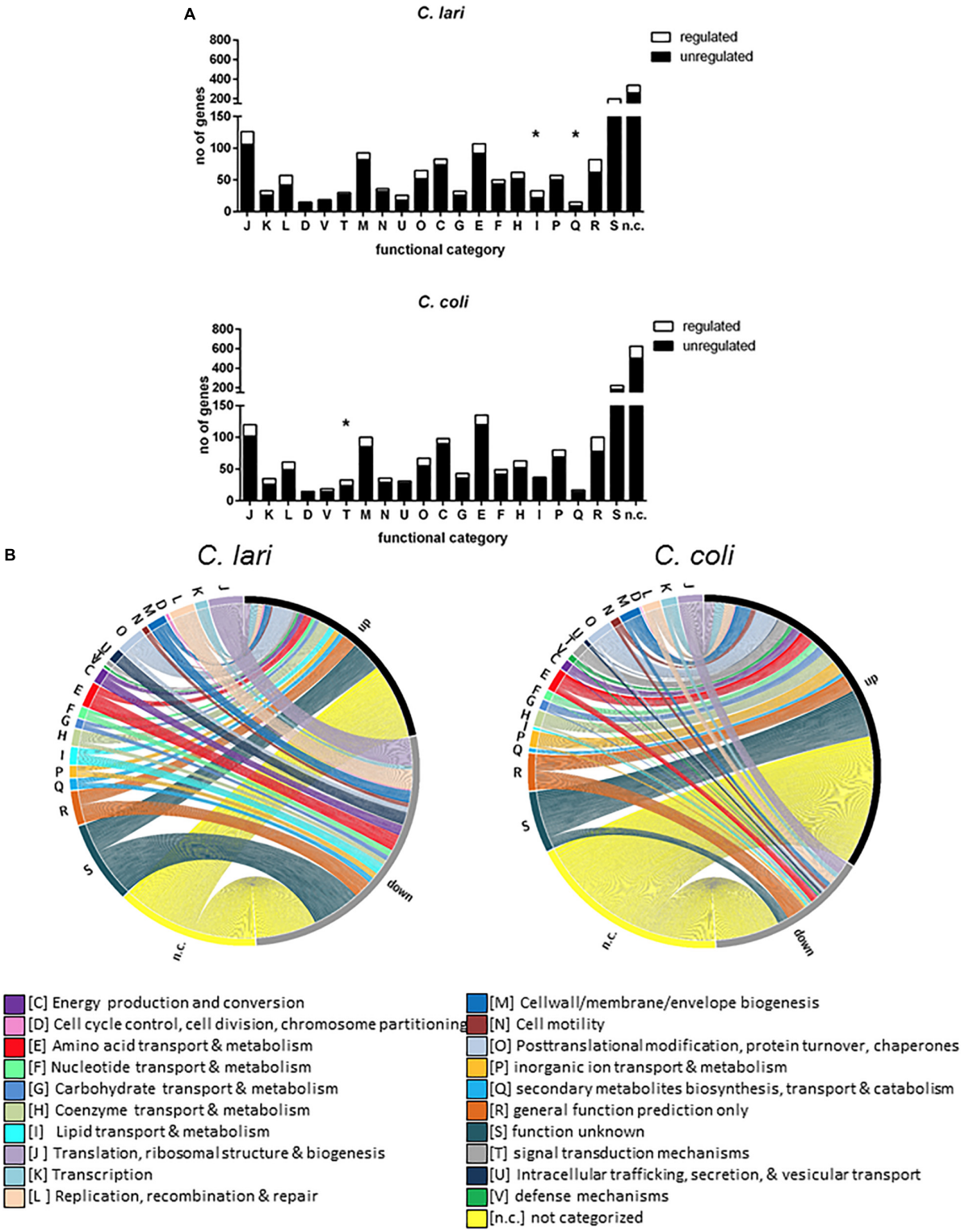

FIGURE 4 | Genes differentially expressed after heat stress according to functional groups. The genes differentially expressed after 30 min of heat stress were shown according to their functional classification (obtained from the evolutionary genealogy of genes: Non-supervised Orthologous Groups http://eggnog.embl.de/version_4.0.beta) for *C. coli* RM2228 and *C. lari* RM2100. **(A)** Total number of regulated and unregulated genes assigned to each functional category were shown for *C. lari* and *C. coli*. Significant enrichment for each category were calculated by Fisher's exact test (*$p < 0.05$). **(B)** The figure was created with the open source tool Circos (http://circos.ca). The thickness of each connection displays the $\log_2$ fold change of gene expression whereas the ending of connection displays if the gene expression is up- or down-regulated.

TABLE 2 | Similar regulated genes after heat stress in *C. coli* RM2228 and *C. lari* RM2100.

Gene	Product	Category	Locus_tag	Log_2 fc	*p*adj	Locus_tag	Log_2 fc	*p*adj
hrcA	Heat-inducible transcription repressor	–	Cla_0937	2.30	0.000	CCO0811	3.87	0.000
pseA	Pseudaminic acid biosynthesis protein PseA	D	Cla_1328	1.08	0.000	CCO1426	0.75	0.006
thyX	FAD-dependent thymidylate synthase	F	Cla_0011	0.87	0.004	CCO0057	0.86	0.003
gapA	Glyceraldehyde-3-phosphate dehydrogenase	G	Cla_0417	0.68	0.024	CCO1511	0.68	0.025
birA	Biotin–protein ligase	H	Cla_0187	0.64	0.044	CCO1782	1.07	0.000
ribB	Bifunctional 3,4-dihydroxy-2-butanone 4-phosphate synthase/GTP cyclohydrolase II protein	H	Cla_0604	1.02	0.001	CCO1384	1.14	0.000
thrS	Threonyl-tRNA synthetase	J	Cla_0028	0.85	0.015	CCO0296	1.07	0.000
hspR	MerR family transcriptional regulator	K	Cla_0777	1.73	0.000	CCO1318	1.73	0.000
uvrB	Excinuclease ABC subunit B	L	Cla_1186	0.69	0.024	CCO0746	1.43	0.000
*lolA**	Outer-membrane lipoprotein carrier protein	M	Cla_0524	1.33	0.000	CCO0952	1.02	0.009
*flaG**	Flagellar protein FlaG	N	Cla_0765	0.85	0.003	CCO0644	0.98	0.000
clpB	Protein disaggregating chaperone ClpB	O	Cla_0711	1.44	0.000	CCO0608	1.92	0.000
grpE	Heat shock protein GrpE	O	Cla_0936	1.72	0.000	CCO0812	2.30	0.000
dnaK	Molecular chaperone DnaK	O	Cla_0935	1.49	0.000	CCO0813	1.78	0.000
groES	Co-chaperonin GroES	O	Cla_1035	1.46	0.000	CCO1296	3.80	0.000
groEL	Molecular chaperone GroEL	O	Cla_1034	1.15	0.000	CCO1297	2.00	0.000
cbpA	Co-chaperone-curved DNA binding protein A	O	Cla_0778	2.28	0.000	CCO1317	2.38	0.000
kefB	Sodium/hydrogen exchanger family protein	P	Cla_0776	1.20	0.000	CCO1319	1.08	0.000
–	Multicopper oxidase	Q	Cla_0353	0.87	0.003	CCO1623	0.83	0.002
–	Hypothetical protein	S	Cla_1506	1.10	0.000	CCO0311	0.93	0.000
–	Hypothetical protein	S	Cla_1010	0.96	0.002	CCO0848	1.14	0.000
ciaB	Invasion antigen B	S	Cla_1268	0.63	0.042	CCO1015	0.71	0.030
plsX	Glycerol-3-phosphate acyltransferase PlsX	I	Cla_1337	−0.97	0.003	CCO0417	−0.62	0.028
dusB	tRNA-dihydrouridine synthase B	J	Cla_0210	−0.71	0.031	CCO1756	−0.83	0.019
rpmF	50S ribosomal protein L32	J	Cla_1336	−1.31	0.000	CCO0418	−1.07	0.001
rpsL	30S ribosomal protein S12	J	Cla_0451	−0.70	0.034	CCO0588	−0.61	0.022
queA	S-adenosylmethionine:tRNA ribosyltransferase-isomerase	J	Cla_0662	−0.73	0.018	CCO1379	−0.71	0.041
–	Endoribonuclease L-PSP	J	Cla_0277	−1.24	0.000	CCO1499	−0.87	0.002
*cmeD**	Outer membrane component of efflux system	M	Cla_0986	−0.81	0.008	CCO1098	−0.66	0.036
flgI	Flagellar basal body P-ring biosynthesis protein FlgI	N	Cla_0400	−0.80	0.012	CCO1569	−0.81	0.001
*aat**	Leucyl/phenylalanyl-tRNA–protein transferase	O	Cla_1064	−1.13	0.001	CCO1187	−0.92	0.006
–	Hypothetical protein	R	Cla_0749	−0.87	0.004	CCO0785	−1.54	0.000
–	Hypothetical protein	S	Cla_1475	−1.25	0.000	CCO1685	−0.69	0.044
*ctsE**	Type II protein secretion system E protein CtsE	U	Cla_0392	−0.83	0.015	CCO1577	−0.81	0.021
*ctsD**	Type II protein secretion system D protein CtsD	U	Cla_0390	−1.12	0.000	CCO1580	−1.20	0.001
–	HIT family hydrolase	FG	Cla_0423	−1.01	0.001	CCO0504	1.24	0.000
–	7-Cyano-7-deazaguanine reductase	R	Cla_0006	−1.28	0.000	CCO0022	1.15	0.000

*The gene locus, log_2 fold change of expression, adjusted p-value, functional category, as well as the putative gene products of orthologous genes regulated in both species are indicated. *Genes included according to same gene name but not defined as orthologs by BLAST e-value of 1e-6.*

Despite the genes of the translational machinery affected in both species, the expression of the 16S rRNA modification protein (*rimM*) and the translation termination factor *prfA* were also down-regulated in *C. coli*. In contrast, the expression of several ribosomal protein encoding genes as well as the translation initiation factor *infC* were up-regulated.

Further, increased expression levels for the genes *ung* and *recA*, both involved in DNA repair, as well as for the chaperone gene *htrA* have been determined.

In addition, the expression levels of several genes involved in amino acid (e.g., *glnA*, *bisZ, glnQ,* CCO1002), carbohydrate (e.g., *fucP*, CCO0582 + 83), nucleotide, and coenzyme transport and metabolism were up-regulated after the heat shock in *C. coli*.

The expression levels of the majority of genes belonging to the cell wall/membrane/envelope biogenesis (e.g., *pseF*, *pseG*) and the multidrug efflux system encoding genes *cmeA* and *cmeB* were significantly up-regulated whereas the expression of *cmeC* was only slightly increased (**Supplementary Table S3**).

The expression level of the flagellar filament structure genes *flaA* and *flaC*, and the chemotaxis gene *cheW* were up-regulated. In contrast, genes belonging to secretory function of the flagella like *fliR* and *fliI* as well as the basal body *flgG_1* and the energy

TABLE 3 | Genes differentially regulated after heat stress in *C. coli* RM2228 only.

Category	Up-regulated	Down-regulated
Energy production and conversion	*aspA*, *cydA*, *hydA2*, *ldh*, CCO0259, CCO0482, CCO1660	*fliI*
Amino acid transport and metabolism	*bisZ*, *dapA*, *glnA*, *hisH*, *potA*, *proB*, *serB*, CCO1002, CCO1668	*ilvE*, *proC*, CCO0338, CCO0845, CCO0846, CCO1354, *glnQ*
Nucleotide transport and metabolism	*carA*, *nrdA*, *panC*, *prsA*, *purC*	*surE*
Carbohydrate transport and metabolism	*fucP*, *pgk*, CCO0581 + CCO0582	CCO1026
Coenzyme transport and metabolism	*folC*, *hemH*, *moeA*-3, *panB*, *pdxJ*, *thiL*, CCO1477	*mobB*, CCO1284
Lipid transport and metabolism	–	CCO1644
Translation, ribosomal structure, and biogenesis	*cca*, *gatC*, *infC*, *rplS*, *rpsU*, CCO0741	*ksgA*, *prfA*, *rimM*, *rpsL*, CCO0191, CCO0716
Transcription	*cmeR*, *furR1*, *rnr*, CCO0384, CCO1673	*nusA*, CCO0483, CCO0137
Replication, recombination, and repair	*dnaB*, *dnaE*, *recA*, *topA*, *ung*, CCO1639	*dnaQ*, *dprA*, *recG*, *rnhB*, CCO0288
Cell wall/membrane/envelope biogenesis	*lepA*, *lgt*, *murF*, *prc*, *pseF*, *pseG*, *rfaF*, *waaV*, CCO0689, CCO0691	*murB2*, *pbpB,* CCO1291
Cell motility	*flaA*, *flaC*, *cheW*, CCO0943	*flgG_1*, *fliR*
Posttranslational modification, protein turnover, chaperones	*htrA*, *hypC*, CCO0150, CCO1189	*msrA*
Inorganic ion transport and metabolism	*cmeB*, *pstC*, *pstS*, CCO0076, CCO0087, CCO0127 + 28, CCO1232	*cysQ*, *feoB*
Secondary metabolites biosynthesis, transport, and catabolism	CCO0052, CCO1043	–
Signal transduction mechanism	*amt*, *arsC*, *cheV*, *dccS*, *rrp-2*, CCO1327, CCO1600	CCO1314
Intracellular trafficking, secretion, and vesicular transport	CCO1188	–
Defense mechanisms	*cmeA*, *hsdR*, *ybjZ*	CCO0655

Summary of genes with up- or down-regulated expression level after heat stress and assignment to a functional category for C. coli RM2228. The log_2 fold changes of expression level for each gene are shown in ***Supplementary Table S3****.*

delivering protein encoded by *fliI* were down-regulated (**Table 3** and **Supplementary Table S3**).

In contrast, the expression level of other genes involved in energy production and conversion were all up-regulated (**Table 3** and **Supplementary Table S3**).

C. lari

Genes assigned to a functional category and with differential expression after heat stress in *C. lari* only are shown in **Table 4** (log_2 fold changes and *p*-values are shown in **Supplementary Table S3**). The expression of the transcriptional regulator genes Cla_1081 and Cla_0872 was up-regulated while *rpoN* and Cla_0784 (transcriptional regulator of the Crp/Fnr-family) was down-regulated in *C. lari* (**Table 4**). Of the two-component system or signal transducer encoding genes, a probable *dccS* (Cla_1102) and Cla_1204 were up-regulated, while Cla_0781 was down-regulated.

Even though decreased expression levels for the majority of genes belonging to the translational machinery were determined, the expression level of *prfB*, involved in termination of translation, and Cla_0258, a ribosomal modification protein, were up-regulated (**Table 4** and **Supplementary Table S3**).

The expression of the chaperon genes *dnaJ*, the DnaJ domain protein encoding gene Cla_0590, as well as *xth* (involved in DNA repair) was up-regulated. However, several other genes also involved in DNA repair and replication were down-regulated (**Table 4** and **Supplementary Table S3**).

A significant enrichment in the category of lipid transport and metabolism has been determined and the majority of the differentially expressed genes were down-regulated.

The expression of genes involved in LOS biosynthesis (*kdsB*), rod shape formation (*mreC*), peptidoglycan biosynthesis (*pbpA*, *murC*), or general cell wall/membrane/envelop biogenesis (*pglF* and Cla_0642) were down-regulated in *C. lari*.

The flagellin modification genes *ptmB* and *pseB* were up-regulated, while the flagellar motor switch protein encoding gene *fliN*, and the basal body rod protein encoding gene *flgG* were down-regulated.

DISCUSSION

It has previously been shown that *Campylobacter* spp. are rather sensitive to elevated temperatures. Baserisalehi et al. (2006) determined similar D-values for *C. coli* and *C. lari* in food matrices at elevated temperatures. Our data showed that *C. coli* and *C. lari* are similarly susceptible to heat stress at 46°C in *Brucella* broth, too. In contrast to *C. jejuni*, studies about the heat shock response of these two *Campylobacter* species on mRNA or protein level were missing so far. Therefore, we analyzed changes in the whole transcriptome of the two strains after heat stress. The overall percentage of differentially expressed genes was comparable between *C. coli* (17.2%) and *C. lari* (19.4%). However, the majority of differentially expressed

TABLE 4 | Genes differentially regulated after heat stress in *C. lari* RM2100 only.

Category	Up-regulated	Down-regulated
Energy production and conversion	*fdxB*, *ndh*	*mez*, *napH*, *oorB*, *petA*, *rdxA*, *torC*
Cell cycle control, cell division, chromosome partitioning	–	*ftsX*
Amino acid transport and metabolism	*pepE*, *selA*, Cla_0593, Cla_0897, Cla_0458	*aroE*, *aspC*, *bioA*, *hisIE*, *livH*, *modC*, *pglE*, *sdaA*, *sdaC*, *selD*
Nucleotide transport and metabolism	*prsA*	*purE*, *pyrE*, Cla_0004
Carbohydrate transport and metabolism	*rpe*, Cla_1277	*tal*, Cla_1361
Coenzyme transport and metabolism	*mobA*, *ribD*, *thiD*, *thiM,* Cla_0686	*dxs*, *folP*, *hemC*
Lipid transport and metabolism	*aas*, *cdsA*, *dxr*, *fabZ*	*fabD*, *fabH3*, *ispE*, *pgpA*, *pgsA*, Cla_1314
Translation, ribosomal structure, and biogenesis	*prfB*, *truB*, Cla_0258	*gltX*, *leuS*, *rbfA*, *rplE*, *rplF*, *rplJ*, *rplX*, *tlyA*, *truA*, Cla_0017, Cla_1325
Transcription	Cla_0872, Cla_1081, Cla_1538	*npdA*, *rpoN*, Cla_0784
Replication, recombination, and repair	*xth*, Cla_0824	*dnaX*, *ligA*, *ligA-2*, *mutS*, *nth*, *rep*, *ruvA*, *uvrC*, Cla_0401, Cla_0671, Cla_0836, Cla_0945
Cell wall/membrane/envelope biogenesis	*pseB*, *ptmB*, Cla_0217	*kdsB*, *murC*, *mreC*, *pbpA*, *pglF*, Cla_0642
Cell motility	–	*flgG*, *fliN*
Posttranslational modification, protein turnover, chaperones	*dnaJ*, Cla_0589 + 90, Cla_1212	*hypA*, Cla_1116
Inorganic ion transport and metabolism	*modB*, *cft*	*cmeF*, Cla_0159, Cla_0643, Cla_0109
Secondary metabolites biosynthesis, transport, and catabolism	Cla_0039, Cla_0565	*iamA*, *iamb*, Cla_0207
Signal transduction mechanism	Cla_1102, Cla_1204	Cla_0781
Intracellular trafficking, secretion, and vesicular transport	–	*ctsG*, *exbD1*, *exbB1*, *secF*, *secY*, Cla_0954
Defense mechanisms	*kpsM*	Cla_1528

Summary of genes with up- or down-regulated expression level after heat stress and assignment to a functional category for C. lari RM2100. The log_2 fold changes of expression level for each gene are shown in ***Supplementary Table S3****.*

genes were up-regulated in *C. coli* (67.1%) but down-regulated in *C. lari* (56.4%), indicating a different heat stress response of the two species.

Of the overall transcriptional changes detected, only 35 genes were similarly expressed indicating a general role in heat stress response of *Campylobacter* spp. This group includes the transcriptional regulators *hspR* and *hrcA* as well as the chaperons *grpE*, *dnaK*, *groEL*, *groES*, *clpB*, and *cbpA*. These genes are included in the 30 genes whose expression has been most highly up-regulated in both species (**Supplementary Table S3**), and are also involved in the heat stress response of *C. jejuni* (Stintzi, 2003; Holmes et al., 2010). Stintzi (2003) described a high and rapid up-regulation of these genes in *C. jejuni* after temperature increase from 37 to 42°C. This up-regulation of gene expression was only transient, as expression levels nearly reached basal levels after 50 min of temperature up-shift indicating that adaptation to the new conditions was achieved (Stintzi, 2003). As we did not observe any growth at 46°C for the strains investigated in our study, we did not expect adaptation to this conditions, and therefore also no transient changes in the gene expression pattern. This was also supported by the observation that known heat shock genes were still highly expressed after 60 min of heat stress in our study (**Figure 2**).

Regarding chaperone DnaJ, Konkel et al. (1998) showed higher protein levels after heat stress for *C. jejuni*. In our study, the expression pattern for *dnaJ* was contradictory. Slightly increased expression of *dnaJ* has been determined by RT-PCR for *C. coli* and by RNA-seq for *C. lari* only. However, Holmes et al. (2010) suggested that CbpA, showing 44% similarity to DnaJ, is the main DnaJ protein in *C. jejuni*. In concordance with that, we observed significantly up-regulated expression of *cbpA* in *C. coli* and *C. lari* in both assays. The only gene belonging to the category of posttranslational modification, protein turnover, chaperons down-regulated in both species was *aat*. The protein Aat might be involved in N-end rule pathway of protein degradation, supposing changes in half-life time of several proteins (Varshavsky, 2011).

The periplasmic chaperone HtrA, which degrades and prevents aggregation of misfolded periplasmic proteins, has been described to be essential for *C. jejuni* growth at 44°C (Baek et al., 2011). Increased expression of *htrA* was also observed in *C. coli* but not in *C. lari*, suggesting that other chaperons or proteases replace the activity of HtrA in *C. lari*. Interestingly, also *racR* was not differentially expressed in *C. coli* and *C. lari*, indicating further regulatory differences compared to the heat shock response of *C. jejuni* (Apel et al., 2012).

Regarding the ribosomal genes, Stintzi (2003) described a transient down-regulated expression in *C. jejuni* after temperature increase from 37 to 42°C. The expression of these genes decreased until 20 min and nearly reached baseline level at 50 min after temperature increase, suggesting that *C. jejuni* transiently reshuffled energy for stress damage repair and adaptation to the new growth condition (Stintzi, 2003). Similarly, the majority of differentially expressed genes assigned to the category of translation and ribosomal structure was also down-regulated in *C. coli* and in *C. lari* at 30 min after heat stress of 46°C. Also comparable to the observations described

for *C. jejuni* (Stintzi, 2003), the majority of all differentially expressed genes was up-regulated in *C. coli*, implying high energy costs of heat stress response. According to this hypothesis, the expression of the majority of genes involved in energy metabolism was also up-regulated in *C. coli*. In contrast, the majority of all differentially expressed genes (including genes assigned to the category of energy metabolism) were down-regulated in *C. lari*, suggesting a divergent energy saving behavior compared to *C. coli* under the heat stress condition investigated in our study. The differences in energy metabolism is further supported by the fact that multiple genes involved in energy metabolism and respiration in *C. jejuni* are missing in *C. lari* (Miller et al., 2008, 2014). Nevertheless, the question which transcriptional changes would be further transferred to protein level remains unanswered.

Additional regulators seem to be involved in the heat stress response in both strains tested. While *C. coli* also up-regulated the expression of the transcriptional regulator *fur1*, the ortholog *perR* was not regulated in *C. lari*. PerR has been shown to regulate the expression of at least 104 genes in *C. jejuni*, most of them involved in oxidative stress response (Palyada et al., 2009). Further, *perR* expression is up-regulated after acid stress (Reid et al., 2008). Our data could indicate a further role of PerR in the heat stress response of *C. coli* but not of *C. lari*.

The two-component system DccRS is required for initial adaptation of *C. jejuni* to the gastrointestinal milieu of chickens and controls a regulon of six genes annotated as putative periplasmic or membrane proteins, and *dccR* itself (Wosten et al., 2010). The expression of the putative sensor *dccS* (CCO1300) was up-regulated after heat stress in *C. coli*. In concordance, six genes defined as orthologs or annotated as probably *C. jejuni* genes of the DccRS regulon (CCO0021, CCO0198, CCO0689, CCO0290, CCO1066, CCO1462) were up-regulated in *C. coli*. For *C. jejuni*, it has been demonstrated that neither temperature of 42°C nor copper but growth phase is responsible for activation of DccRS (Wosten et al., 2010). However, our data suggest that the DccRS system is also involved in the heat stress response of *C. coli* at 46°C.

Likewise to *C. coli,* the expression of further possible transcriptional regulators was regulated in *C. lari*. The highest up-regulated expression in *C. lari* was observed for Cla_0805, encoding a peptidase S24 family protein, predicted as transcriptional repressors of the SOS-response in many bacteria (Butala et al., 2009). Interestingly, many of the SOS-response genes described in other bacteria, including the peptidase S24 LexA, are lacking in *C. jejuni* and no ortholog has been detected in *C. coli* (Zgur-Bertok, 2013). Whether *C. lari* has a complete SOS-response has to be elucidated in further studies.

Further changes observed after heat stress include metabolism pathways. Glutamine is the major nitrogen donor for *C. jejuni* and *C. jejuni* 81-176, mutated in the glutamine ABC-Transporter (Cj0469), was more susceptible to heat stress compared to the wild type (Lin et al., 2009). Further, *C. jejuni* use glutamine as a carbon source (van der Hooft et al., 2018). We determined enhanced gene expression of genes involved in glutamine metabolism for *C. coli*, like the degenerated ammonium transporter (CCO0599), the glutamine synthetase *glnA,* the glutamine transporter ATPase *glnQ*, as well as the adjacent located amino acid transporter permease (CCO1002).

Recently, an energy metabolism pathway involved in the formation of pyruvate and L-lactate from L-fucose has been described for *C. jejuni* (Stahl et al., 2012). These genes are located on a genomic island spanning from Cj0480-89 and determined as ortholog for *C. coli* RM2228 by our comparison (CCO0578-87) (Muraoka and Zhang, 2011; Stahl et al., 2011). As the expression of these genes was up-regulated, we suggest that the activation of nitrogen assimilation and the L-fucose metabolic pathway is part of heat stress response in *C. coli* RM2228.

Many genes assigned to the functional category of cell wall/membrane/envelope biogenesis and hypothetical membrane proteins were differentially expressed in *C. coli* and *C. lari*. However, the expression of the majority of these genes was up-regulated by *C. coli* and down-regulated by *C. lari* suggesting different modifications of cell wall/membrane proteins after heat stress in both species.

CONCLUSION

Despite similar phenotypic survival abilities at 46°C, distinct variations in the transcriptomic response to heat stress could be determined for *C. coli* and *C. lari*. Similar expression changes for chaperone genes after heat stress, which have also been described for *C. jejuni*, indicate a general response mechanism of *Campylobacter* species. However, the differences in expression of transcriptional regulators and metabolism related genes observed between the tested *C. coli* and *C. lari* strains could be explained in part by the phylogenetic distance and therefore the large differences in the genomic content of these two species. Higher similarities have been determined for the heat stress response of *C. coli* with already published data for *C. jejuni*. This is in agreement with the higher amount of orthologous genes determined for *C. jejuni* and *C. coli* compared to *C. lari*.

Overall, the described transcriptomic changes induced after heat stress in *C. coli* and *C. lari* indicate huge differences in the heat stress response between the *Campylobacter* species.

DATA AVAILABILITY STATEMENT

The datasets generated for this study can be found in the GEO Series accession number GSE67486 (www.ncbi.nlm.nih.gov/geo/query/acc.cgi?acc=GSE67486).

AUTHOR CONTRIBUTIONS

GG and TA planned the study. CR and CP performed the experiments in this study. KF and CS performed the RNA sequencing and bioinformatic analyses. CR, TA, and GG analyzed results, formatted the data, and drafted the manuscript.

TA provided funding. All authors read and approved the final manuscript.

FUNDING

This work was funded by the Federal Ministry of Education and Research (BMBF) under project number 01Kl1725A (PAC-Campy) as part of the Research Network Zoonotic Infectious Diseases and project number 01Kl1012 (FBI-Zoo).

SUPPLEMENTARY MATERIAL

The Supplementary Material for this article can be found online at: https://www.frontiersin.org/articles/10.3389/fmicb.2020.00523/full#supplementary-material

FIGURE S1 | Correlation of log_2 fold changes of gene expression by qRT-PCR and RNA-seq. The correlation of the log_2 fold changes of selected gene expression after 30 min of heat stress determined by RNA-seq (*x*-axis) and qRT-PCR (*y*-axis) is depicted with corresponding R^2 values for *C. coli* RM2228 and *C. lari* RM2100.

FIGURE S2 | Orthologous mapping of the complete genomes from *C. coli* RM2228, *C. lari* RM2100, and *C. jejuni* NCzTC11168. Orthologous were defined by bidirectional best BLAST-hit search on nucleotide level with max. e-value of 1e-6, word size of 20, and a minimal length of 60%. The Venn diagram shows orthologous gene shared by the *C. coli* strain RM2228, *C. lari* strain RM2100, and *C. jejuni* strain NCTC11168.

TABLE S1 | Primers used in this study. The target gene, primer sequence and concentration, the amplicon length, and annealing temperature of each primer used for qRT-PCR for both strains are indicated in this table.

TABLE S2 | Mapping statistics for all libraries in the RNA-seq. This table indicates the total number of sequenced cDNA reads considered in the analysis and used for alignment, the total number of aligned and of uniquely aligned reads, the total number of alignments, and the percentage of aligned and uniquely aligned reads for the replicates at 37 and 46°C for both strains.

TABLE S3 | Excel file containing the Orthologs of differentially regulated genes after heat stress in *C. coli* RM2228 and *C. lari* RM2100. All genes for which a significant regulation of expression was calculated by DESeq2 1.6.3 after 30 min heat stress by RNA-seq analysis were indicated in this table. For each gene, the locus_tag, gene name, gene product, log_2 fold change of gene expression with adjusted *p*-value, assignment to functional category by eggnog, and their corresponding ortholog are listed. Gene names in parentheses were transferred from orthologs. -: no gene name, function, or category assigned.

TABLE S4 | Percentage of differentially expressed genes after heat stress according to eggNOG functional categories. The table indicates the percentage of regulated genes for each strain and category. Genes assigned in two categories were listed in each category. Significant enrichment was calculated by Fisher's exact test. $*p < 0.05$.

TABLE S5 | Strains used in this study. The ID, origin, description, and source of each strain used in this study are indicated in this table.

REFERENCES

Alter, T., Bereswill, S., Glunder, G., Haag, L. M., Hanel, I., Heimesaat, M. M., et al. (2011). Campylobacteriosis of man: livestock as reservoir for *Campylobacter* species. *Bundesgesundheitsblatt Gesundheitsforschung Gesundheitsschutz* 54, 728–734. doi: 10.1007/s00103-011-1289-y

Alter, T., and Scherer, K. (2006). Stress response of *Campylobacter* spp. and its role in food processing. *J. Vet. Med. B Infect. Dis. Vet. Public Health* 53, 351–357. doi: 10.1111/j.1439-0450.2006.00983.x

Apel, D., Ellermeier, J., Pryjma, M., Dirita, V. J., and Gaynor, E. C. (2012). Characterization of *Campylobacter jejuni* RacRS reveals roles in the heat shock response, motility, and maintenance of cell length homogeneity. *J. Bacteriol.* 194, 2342–2354. doi: 10.1128/JB.06041-11

Baek, K. T., Vegge, C. S., Skorko-Glonek, J., and Brondsted, L. (2011). Different contributions of HtrA protease and chaperone activities to *Campylobacter jejuni* stress tolerance and physiology. *Appl. Environ. Microbiol.* 77, 57–66. doi: 10.1128/AEM.01603-10

Baserisalehi, M., Bahador, N., and Kapadnis, B. P. (2006). Effect of heat and food preservatives on survival of thermophilic *Campylobacter* isolates in food products. *Res. J. Microbiol.* 1, 512–519. doi: 10.3923/jm.2006.512.519

Blomberg, P., Wagner, E. G., and Nordstrom, K. (1990). Control of replication of plasmid R1: the duplex between the antisense RNA, CopA, and its target, CopT, is processed specifically in vivo and in vitro by RNase III. *EMBO J.* 9, 2331–2340. doi: 10.1002/j.1460-2075.1990.tb07405.x

Butala, M., Zgur-Bertok, D., and Busby, S. J. (2009). The bacterial LexA transcriptional repressor. *Cell Mol. Life. Sci.* 66, 82–93. doi: 10.1007/s00018-008-8378-6

Edgar, R., Domrachev, M., and Lash, A. E. (2002). Gene expression omnibus: NCBI gene expression and hybridization array data repository. *Nucleic Acids Res.* 30, 207–210. doi: 10.1093/nar/30.1.207

EFSA, and ECDC (2014). The European union summary report on trends and sources of zoonoses, zoonotic agents and food-borne outbreaks in 2012. *EFSA J.* 12:312.

Forstner, K. U., Vogel, J., and Sharma, C. M. (2014). READemption-a tool for the computational analysis of deep-sequencing-based transcriptome data. *Bioinformatics* 30, 3421–3423. doi: 10.1093/bioinformatics/btu533

Fouts, D. E., Mongodin, E. F., Mandrell, R. E., Miller, W. G., Rasko, D. A., Ravel, J., et al. (2005). Major structural differences and novel potential virulence mechanisms from the genomes of multiple *Campylobacter* species. *PLoS Biol.* 3:e15. doi: 10.1371/journal.pbio.0030015

Hoffmann, S., Otto, C., Kurtz, S., Sharma, C. M., Khaitovich, P., Vogel, J., et al. (2009). Fast mapping of short sequences with mismatches, insertions and deletions using index structures. *PLoS Comput. Biol.* 5:e1000502. doi: 10.1371/journal.pcbi.1000502

Holmes, C. W., Penn, C. W., and Lund, P. A. (2010). The hrcA and hspR regulons of *Campylobacter jejuni*. *Microbiology* 156, 158–166. doi: 10.1099/mic.0.031708-0

Hwang, S., Jeon, B., Yun, J., and Ryu, S. (2011). Roles of RpoN in the resistance of *Campylobacter jejuni* under various stress conditions. *BMC Microbiol.* 11:207. doi: 10.1186/1471-2180-11-207

Kim, J.-C., Oh, E., Kim, J., and Jeon, B. (2015). Regulation of oxidative stress resistance in *Campylobacter jejuni*, a microaerophilic foodborne pathogen. *Front. Microbiol.* 6:751. doi: 10.3389/fmicb.2015.00751

Konkel, M. E., Kim, B. J., Klena, J. D., Young, C. R., and Ziprin, R. (1998). Characterization of the thermal stress response of *Campylobacter jejuni*. *Infec Immun.* 66, 3666–3672.

Lin, A. E., Krastel, K., Hobb, R. I., Thompson, S. A., Cvitkovitch, D. G., and Gaynor, E. C. (2009). Atypical roles for *Campylobacter jejuni* amino acid ATP binding cassette transporter components PaqP and PaqQ in bacterial stress tolerance and pathogen-host cell dynamics. *Infect. Immun.* 77, 4912–4924. doi: 10.1128/IAI.00571-08

Love, M. I., Huber, W., and Anders, S. (2014). Moderated estimation of fold change and dispersion for RNA-seq data with DESeq2. *Genome Biol.* 15:550.

Miller, W. G., Wang, G., Binnewies, T. T., and Parker, C. T. (2008). The complete genome sequence and analysis of the human pathogen *Campylobacter* lari. *Foodborne Pathog. Dis.* 5, 371–386. doi: 10.1089/fpd.2008.0101

Miller, W. G., Yee, E., Chapman, M. H., Smith, T. P. L., Bono, J. L., Huynh, S., et al. (2014). comparative genomics of the *Campylobacter* lari group. *Genome Biol. Evol.* 6, 3252–3266. doi: 10.1093/gbe/evu249

Muraoka, W. T., and Zhang, Q. (2011). Phenotypic and genotypic evidence for L-fucose utilization by *Campylobacter jejuni*. *J. Bacteriol.* 193, 1065–1075. doi: 10.1128/JB.01252-10

Palyada, K., Sun, Y. Q., Flint, A., Butcher, J., Naikare, H., and Stintzi, A. (2009). Characterization of the oxidative stress stimulon and PerR regulon of *Campylobacter jejuni*. *BMC Genomics* 10:481. doi: 10.1186/1471-2164-10-481

Park, S. F. (2002). The physiology of *Campylobacter* species and its relevance to their role as foodborne pathogens. *Int. J. Food Microbiol.* 74, 177–188. doi: 10.1016/s0168-1605(01)00678-x

Parkhill, J., Wren, B. W., Mungall, K., Ketley, J. M., Churcher, C., Basham, D., et al. (2000). The genome sequence of the food-borne pathogen *Campylobacter jejuni* reveals hypervariable sequences. *Nature* 403, 665–668. doi: 10.1038/35001088

Poropatich, K. O., Walker, C. L., and Black, R. E. (2010). Quantifying the association between *Campylobacter* infection and Guillain-Barre syndrome: a systematic review. *J. Health Popul. Nutr.* 28, 545–552.

Reid, A. N., Pandey, R., Palyada, K., Naikare, H., and Stintzi, A. (2008). Identification of *Campylobacter jejuni* genes involved in the response to acidic pH and stomach transit. *Appl. Environ. Microbiol.* 74, 1583–1597. doi: 10.1128/AEM.01507-07

Sheppard, S. K., Dallas, J. F., Wilson, D. J., Strachan, N. J. C., McCarthy, N. D., Jolley, K. A., et al. (2010). Evolution of an agriculture-associated disease causing *Campylobacter* coli Clade: evidence from national surveillance data in scotland. *PLoS One* 5:e15708. doi: 10.1371/journal.pone.0015708

Stahl, M., Butcher, J., and Stintzi, A. (2012). Nutrient acquisition and metabolism by *Campylobacter jejuni*. *Front. Cell Infect. Microbiol.* 2:5. doi: 10.3389/fcimb.2012.00005

Stahl, M., Friis, L. M., Nothaft, H., Liu, X., Li, J., Szymanski, C. M., et al. (2011). L-fucose utilization provides *Campylobacter jejuni* with a competitive advantage. *Proc. Natl. Acad. Sci. U.S.A.* 108, 7194–7199. doi: 10.1073/pnas.1014125108

Stintzi, A. (2003). Gene expression profile of *Campylobacter jejuni* in response to growth temperature variation. *J. Bacteriol.* 185, 2009–2016. doi: 10.1128/jb.185.6.2009-2016.2003

van der Hooft, J. J. J., Alghefari, W., Watson, E., Everest, P., Morton, F. R., Burgess, K. E. V., et al. (2018). Unexpected differential metabolic responses of *Campylobacter jejuni* to the abundant presence of glutamate and fucose. *Metabolomics* 14:144. doi: 10.1007/s11306-018-1438-5

Varshavsky, A. (2011). The N-end rule pathway and regulation by proteolysis. *Protein Sci* 20, 1298–1345. doi: 10.1002/pro.666

Whiley, H., van den Akker, B., Giglio, S., and Bentham, R. (2013). The role of environmental reservoirs in human campylobacteriosis. *Int. J. Environ. Res. Public Health* 10, 5886–5907. doi: 10.3390/ijerph10115886

Wosten, M. M., van Dijk, L., Parker, C. T., Guilhabert, M. R., van der Meer-Janssen, Y. P., Wagenaar, J. A., et al. (2010). Growth phase-dependent activation of the DccRS regulon of *Campylobacter jejuni*. *J. Bacteriol.* 192, 2729–2736. doi: 10.1128/JB.00024-10

Yura, T., Kanemori, M., and Morita, T. (2000). "The heat shock response: regulation and function," in *Bacterial Stress Responses*, eds G. Storz, and R. Hengge-Aronis, (Washington, D.C: Amercian Society for Microbiology), 3–18.

Zgur-Bertok, D. (2013). DNA damage repair and bacterial pathogens. *PLoS Pathog.* 9:e1003711. doi: 10.1371/journal.ppat.1003711

Zhang, M. J., Xiao, D., Zhao, F., Gu, Y. X., Meng, F. L., He, L. H., et al. (2009). Comparative proteomic analysis of *Campylobacter jejuni* cultured at 37°C and 42°C. *Jpn. J. Infect. Dis.* 62, 356–361.

Zhou, Y., Bu, L., Guo, M., Zhou, C., Wang, Y., Chen, L., et al. (2013). Comprehensive genomic characterization of *Campylobacter* genus reveals some underlying mechanisms for its genomic diversification. *PloS One* 8:e70241. doi: 10.1371/journal.pone.0070241

Conflict of Interest: The authors declare that the research was conducted in the absence of any commercial or financial relationships that could be construed as a potential conflict of interest.

frontiers in Microbiology

REVIEW
published: 09 April 2020
doi: 10.3389/fmicb.2020.00564

Taking Control: *Campylobacter jejuni* Binding to Fibronectin Sets the Stage for Cellular Adherence and Invasion

Michael E. Konkel, Prabhat K. Talukdar, Nicholas M. Negretti and Courtney M. Klappenbach*

School of Molecular Biosciences, College of Veterinary Medicine, Washington State University, Pullman, WA, United States

Campylobacter jejuni, a foodborne pathogen, is one of the most common bacterial causes of gastroenteritis in the world. Undercooked poultry, raw (unpasteurized) dairy products, untreated water, and contaminated produce are the most common sources associated with infection. *C. jejuni* establishes a niche in the gut by adhering to and invading epithelial cells, which results in diarrhea with blood and mucus in the stool. The process of colonization is mediated, in part, by surface-exposed molecules (adhesins) that bind directly to host cell ligands or the extracellular matrix (ECM) surrounding cells. In this review, we introduce the known and putative adhesins of the foodborne pathogen *C. jejuni.* We then focus our discussion on two *C. jejuni* Microbial Surface Components Recognizing Adhesive Matrix Molecule(s) (MSCRAMMs), termed CadF and FlpA, which have been demonstrated to contribute to *C. jejuni* colonization and pathogenesis. *In vitro* studies have determined that these two surface-exposed proteins bind to the ECM glycoprotein fibronectin (FN). *In vivo* studies have shown that *cadF* and *flpA* mutants exhibit impaired colonization of chickens compared to the wild-type strain. Additional studies have revealed that CadF and FlpA stimulate epithelial cell signaling pathways necessary for cell invasion. Interestingly, CadF and FlpA have distinct FN-binding domains, suggesting that the functions of these proteins are non-redundant. In summary, the binding of FN by *C. jejuni* CadF and FlpA adhesins has been demonstrated to contribute to adherence, invasion, and cell signaling.

Keywords: pathogenesis, bacteria-host cell interactions, adhesin, MSCRAMM, fibronectin

OPEN ACCESS

Edited by:
Ozan Gundogdu, University of London, United Kingdom

Reviewed by:
Erin Gaynor, The University of British Columbia, Canada
Abdi Elmi, University of London, United Kingdom

****Correspondence:***
Michael E. Konkel
konkel@wsu.edu

Specialty section:
This article was submitted to Infectious Diseases, a section of the journal Frontiers in Microbiology

Received: *17 November 2019*
Accepted: *16 March 2020*
Published: *09 April 2020*

Citation:
Konkel ME, Talukdar PK, Negretti NM and Klappenbach CM (2020) Taking Control: Campylobacter jejuni Binding to Fibronectin Sets the Stage for Cellular Adherence and Invasion. Front. Microbiol. 11:564. doi: 10.3389/fmicb.2020.00564

RECOGNITION OF *C. jejuni* AS A SIGNIFICANT FOODBORNE PATHOGEN

Campylobacter jejuni has emerged from obscurity to become a leading bacterial cause of diarrheal disease over the course of five decades (Kaakoush et al., 2015). It was not until 1963 that Sebald and Véron proposed the term campylobacter (in Greek, a 'curved rod') to distinguish theses microaerophilic vibrios from the vibrios associated with cholera and other halophiles (Sebald and Véron, 1963). Although veterinarians were the first to recognize that this organism caused mild dysentery in cattle and sheep, a major breakthrough occurred in 1968 when *C. jejuni* was isolated from the diarrheal stool of a young adult using a special filtration technique (Dekeyser et al., 1972). This led to the development of a selective medium for *Campylobacter* isolation from diarrheal

stools of both animals and humans, and a more accurate assessment of the public health burden of *C. jejuni* infections (Butzler and Skirrow, 1979). Presently, there are an estimated 1.3 million illnesses each year from *C. jejuni* in the United States and an estimated 96 million cases worldwide annually (Asuming-Bediako et al., 2019). In high-income countries, acute campylobacteriosis is characterized by fever, severe abdominal cramps, and diarrhea containing blood and leukocytes (Blaser et al., 1979; Karmali and Fleming, 1979; Svedhem and Kaijser, 1980). The most common source of *C. jejuni* infection is the handling or consumption of raw or undercooked poultry products, as chickens are the natural reservoir of this bacterium (Friedman et al., 2004). However, unpasteurized milk, eggs, untreated water, contaminated produce, and contact with animals colonized with *C. jejuni* have also been implicated as sources of infection (Horrocks et al., 2009; Bronowski et al., 2014; Huang et al., 2015). The economic impact of *C. jejuni* infections extends beyond the treatment of acute diarrheal illness, as infection with certain *C. jejuni* strains is correlated with a higher incidence of Guillain-Barré syndrome (GBS). GBS, an autoimmune syndrome, is the leading cause of flaccid paralysis in the post-polio era (Schwerer, 2002). Also, reports of antibiotic-resistant *Campylobacter* have continued to increase over time for multiple classes of antibiotics (Engberg et al., 2001; Coker et al., 2002; Bae et al., 2005; Gibreel and Taylor, 2006; Ruiz-Palacios, 2007). Recently, the Centers for Disease Control and Prevention listed drug-resistant *C. jejuni* as a 'serious threat'[1]. Overall, *C. jejuni* has emerged as a pathogen of significance in human health due to the number of infections worldwide, the emergence of antibiotic-resistant isolates, and the bacterium's association with post-infection sequelae. Given these factors, current efforts to determine the underlying mechanisms by which *C. jejuni* coordinates virulence during its interactions with host tissues should be expanded to develop new intervention strategies to reduce the global impact of campylobacteriosis. Among the most intensely studied *C. jejuni* virulence factors to date are host cell-binding proteins. Here we introduce the *C. jejuni* cell-binding proteins and then focus on the CadF and FlpA proteins, as these are the best-characterized adhesins.

ADHESINS ARE KEY PLAYERS AT THE BACTERIA-HOST CELL INTERFACE: *C. jejuni* ADHESIVE MOLECULES

Bacteria have evolved an abundance of mechanisms to engage and alter the behavior of host cells. Some of these events are facilitated by hydrophobic interactions resulting in non-specific adhesion, while others are highly specific and dependent upon the binding of a bacterial molecule to a host surface receptor and/or component of the extracellular matrix (ECM) (Stones and Krachler, 2016). A common theme shared among pathogenic bacteria is the presentation of surface-exposed molecules known as adhesins. In this review, the term adhesin is defined as a bacterial molecule(s) that facilitates a specific interaction between an individual bacterium and a eukaryotic cell protein, glycoprotein, or glycolipid that is surface-exposed. Adhesins are highly specialized surface adhesive structures, which are comprised of single monomeric proteins as well as intricate multimeric macromolecules, that can play a crucial role in allowing bacteria to colonize and persist in a host (Pizarro-Cerda and Cossart, 2006). The advantage of a gut bacterium adhering to the host cells is that it can aid in establishing intestinal persistence, as the gastric fluids that bathe the surfaces of tissues, combined with the involuntary rhythmic contractions of peristalsis, may wash away bacteria. The specificity of adhesin:receptor interactions can take on many forms and may change over the course of an infection to enable the pathogen to target different host cells and tissues (tissue tropism). An adhesin may target one host cell molecule or may have several domains that permit binding to multiple surface receptors. Alternatively, multiple adhesins may work in an additive or cooperative manner to enable the bacterium to bind to one surface receptor. Adhesins may also be synthesized at different phases during infection in response to physicochemical properties. The colonization of host tissues can affect the gene expression of virulence-specific genes in bacteria as well as alter the bacterium's metabolism and respiration. In several instances, bacterial cellular adherence is also used as a platform for type III, type IV, or type VI contact-dependent secretion systems to deliver effectors (virulence factors) that rewire host cell signaling pathways and behavior in dramatic fashion (Tsang et al., 2010; Stones and Krachler, 2016). Similar to other intensely studied bacteria, such as *Staphylococcus aureus* and *Salmonella* spp. (Vaca et al., 2019), the foodborne pathogen *C. jejuni* synthesizes several adhesins to promote binding to host cells. These adhesins are among the first molecules to make physical contact with a host cell. In addition, the FlpA adhesin, and presumably the CadF adhesin, permit the delivery of effector proteins into the cytosol of a host target cell (Larson et al., 2013).

Campylobacter jejuni binding to the cells lining the intestinal epithelium is dependent on multiple factors, including motility, bacterial cell surface charge, and multiple adhesins. Some 30 years ago, *C. jejuni* was thought not to synthesize specific adhesive proteins or specifically adhere to any tissues, but that host factors such as the O_2/CO_2 concentration and nutrient availability dictated the site of *C. jejuni* colonization in a host. However, in the late 1980's and early 1990's, *Campylobacter* researchers identified several proteins and molecules that could bind to host cells or host cell ligands, providing renewed energy for researchers to search for additional adhesins. While this age of discovery for new virulence determinants was an exciting time for *Campylobacter* researchers, additional studies raised questions regarding whether some of the identified proteins truly act as bacterial adhesins. For example, Cj0268c, Cj0289c (PEB3), Cj0596 (PEB4), Cj0921c (PEB1) are localized in the bacterial periplasmic space, and Cj1349c appears to be localized in the bacterial cytosol (**Supplementary Table S1**). Moreover, a few of these proteins were determined to have other functions (Leon-Kempis Mdel et al., 2006; Min et al., 2009; Kale et al., 2011). These facts highlight the need for more data to clearly demonstrate that an individual protein is surface exposed and

[1]https://www.cdc.gov/drugresistance/biggest_threats.html

binds to a host cell receptor/ligand. Additional research involving the use of a deletion mutant and a complemented isolate is also necessary to determine if a protein facilitates binding to a host cell ligand. The bacterial flagellum, capsular polysaccharide, and lipopolysaccharide have been reported to contribute to *C. jejuni* binding to cells, but the precise role of these bacterial structures in cellular adherence remains to be elucidated (**Supplementary Table S2**). Moreover, generating a deletion of one component of the structure often affects a cellular function (e.g., motility) or influences another bacterial property (e.g., surface charge). For example, deletion in the gene encoding the FlaA filament protein renders the bacteria non-motile. In the past forty years of research on *Campylobacter* virulence factors, a cellular target has been identified for three *C. jejuni* proteins; Cj0983 (JlpA) binds to HSP90, Cj1279c (FlpA) binds to fibronectin (FN), and Cj1478c (CadF) binds to FN (**Supplementary Table S1**). To gain further insight into other *C. jejuni* adhesins and their potential role in colonization and disease, we refer the reader to two previously published review articles (Rubinchik et al., 2012; Lugert et al., 2015).

Microbial Surface Components Recognizing Adhesive Matrix Molecule(s) (MSCRAMMs), which are synthesized by many pathogenic Gram-positive and Gram-negative bacteria, have been demonstrated to contribute to the disease process. Fibronectin-binding proteins (FNBPs) are members of the MSCRAMM family. This article focuses on the *C. jejuni* CadF and FlpA FNBPs, two adhesins that facilitate bacterial colonization and contribute to illness in a disease model (**Figure 1**, and **Table 1**). Continued investigation of the *C. jejuni* FNBPs is needed to fully understand the specificity of the CadF and FlpA proteins in mediating host cell interactions and to better compare these two proteins to the FNBPs of Gram-positive pathogens, Gram-negative pathogens, and commensal organisms.

FIBRONECTIN: A MULTIDOMAIN GLYCOPROTEIN

Many bacterial adhesins target and bind to FN, which is ubiquitously present in the ECM of a variety of human tissues and organs, including intestinal epithelial cells (Frantz et al., 2010). Mature FN is a large glycoprotein (220 kDa) and can exist as two forms. Plasma FN is synthesized by hepatocytes and secreted into the blood plasma, saliva, and other body fluids, where it circulates as a compact dimer (To and Midwood, 2011). In contrast, cellular FN is synthesized and secreted by many cell types, including fibroblasts and endothelial cells, and becomes incorporated into the ECM to form a fibrillar-type (insoluble) matrix (Sottile and Hocking, 2002; To and Midwood, 2011). One of the stages of matrix assembly is FN unfolding, where cryptic binding sites are exposed (Smith et al., 2007; Weinberg et al., 2017). The unfolding of FN molecules enhances its binding to host cells, especially involving the β_1 integrin subunit (Henderson et al., 2011). In mammals, there are 18 α and 8 β integrin subunits that can associate to form 24 integrin heterodimers, which are transmembrane ECM-binding proteins. The binding of FN to the $\alpha_5\beta_1$ integrin heterodimer induces integrin clustering and promotes fibrillar assembly. Moreover, a tripartite linkage is established between FN, the integrins, and the actin cytoskeleton, allowing the cytoplasmic domains of the integrins to trigger intracellular signaling (Singh et al., 2010). FN incorporation into the cellular matrix has been demonstrated to play an important role in cell adhesion, cell migration, cell signaling, ECM remodeling, and tissue regeneration (To and Midwood, 2011).

Plasma (soluble) and cellular (insoluble) FN arise from alternative splicing of a single pre-mRNA (a single gene) (Pankov and Yamada, 2002). While there are variations in the composition of cellular and plasma FN, the proceeding discussion focuses primarily on cellular FN found in the ECM of tissues. The gene encoding cellular FN harbors Extra Domains A and B (EDA and EDB, also termed EIIIA and EIIIB) and a segment connecting two type III repeats (see below) called the type III connecting segment (IIICS, also termed the variable, or V, region). The alternative splicing of the EDA, EDB, and IIICS elements during transcription allows for the expression of different cellular FN isoforms (Schwarzbauer et al., 1983). In contrast to cellular FN, plasma FN does not harbor the EDA and EDB domains, and only one FN subunit possesses a IIICS segment. Typically, both plasma and cellular FN consist of three types of repetitive domains: 12 FN type I repeats (FN I), 2 FN type II repeats (FN II), and 15-18 FN type III repeats (FN III) (Pankov and Yamada, 2002). FN I and FN II are structurally rigid. In contrast, the FN III repeats are flexible due to the absence of disulfide bonds and are required for FN polymerization (Potts and Campbell, 1994). The multimodular structure and intermodular regions of FN provide the molecule with the ability to interact with other host proteins, including collagen, laminin, integrins, and fibrin. Moreover, the complexity of the FN molecule provides multiple targets for FNBPs to bind to this molecule (White et al., 2008).

BACTERIAL BINDING TO FIBRONECTIN

Pathogenic bacteria that have FNBPs can use them to promote tissue adherence and interface with host cell signaling complexes (Stones and Krachler, 2015). More specifically, a three-component bridge is formed between the FNBPs, host cell-associated FN, and transmembrane integrins (Hymes and Klaenhammer, 2016). The linkage between the bacteria and FN stimulates integrin occupancy and clustering, triggering the recruitment of cell signaling molecules and rearrangement of the host cell actin cytoskeleton (Wu, 2007; Zaidel-Bar et al., 2007; Deakin and Turner, 2008). In some instances, it is the intimate binding mediated by FNBPs that enables host cell invasion and intracellular multiplication, resulting in acute disease (Hymes and Klaenhammer, 2016).

In general, FNBPs contain an N-terminal signal sequence, a central binding region, and a C-terminal cell wall anchor (LPXTG motif). The very first observation that a bacterium, *S. aureus*, was capable of binding to FN was reported in 1978 (Kuusela, 1978). More specifically, the FNBPA and FNBPB proteins from *S. aureus* have been reported to bind to the heparin-binding domain of FN (Bae and Schneewind, 2003; Schwarz-Linek et al., 2003) and that the deletion of both genes is required to abolish the organism's

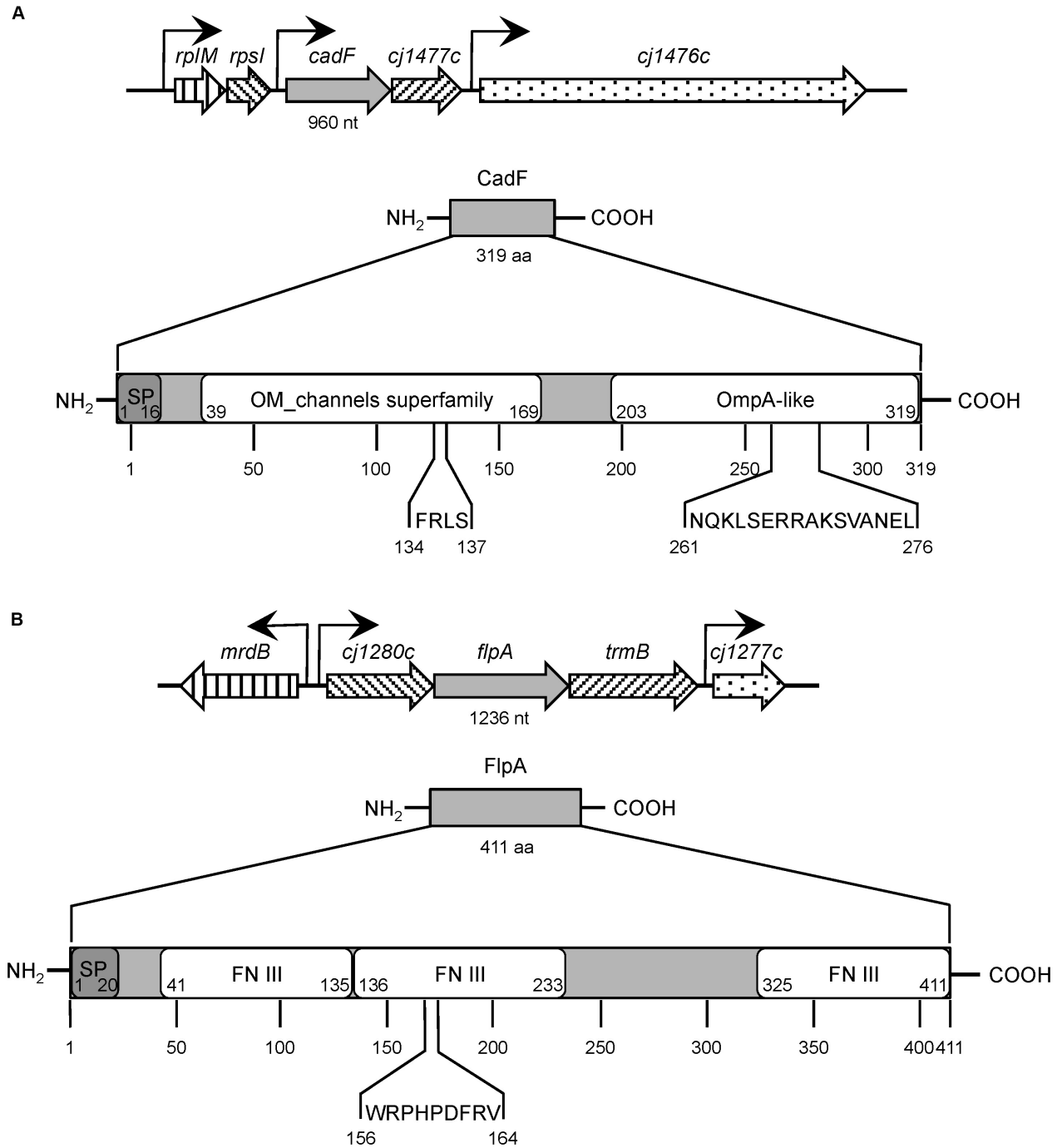

FIGURE 1 | Structural organization of *Campylobacter jejuni* CadF and FlpA fibronectin-binding proteins. Panel **(A)** *C. jejuni* CadF, a 319 amino-acid protein, is encoded by the *cadF* gene, 960 nucleotides in size, expressed as the first gene of a bicistronic operon. CadF has two dominant protein domains: an outer membrane (OM) channel superfamily and an OmpA-like domain. The four amino-acid residues (FRLS) of fibronectin (FN)-binding motif are located in the OM channel superfamily domain at position 134 through 137. The C-terminal region of CadF also contains the 16-residue peptidoglycan-binding motif (NQKLSERRAKSVANEL) located in the OmpA-like domain at position 261 through 276. Panel **(B)** The *C. jejuni* FlpA protein is comprised of 411 amino-acid residues and is encoded by the *flpA* gene. The *flpA* gene is 1,236 nucleotides in size and is expressed as the second gene of a tri-cistronic operon. The FlpA protein has three individual FN type III-like (FN III) domains. The FN-binding motif of FlpA is nine amino-acid residues long (WRPHPDFRV) and located in the second FN III domain at position 156 through 164. The signal peptide sequences, which were identified using SignalP 5.0, are indicated with the 'SP' for both (**A** and **B**). The abbreviations 'nt' and 'aa' refers to nucleotides and amino acids, respectively. The gene information was obtained from the NCBI GenBank database; Accession No: AL111168.1. The protein structure domains were obtained from the UniProt database; CadF UniProtKB Accession No: Q0P8D9, FlpA UniProtKB Accession No: Q0P8X7.

TABLE 1 | *Campylobacter jejuni* CadF and FlpA fibronectin (FN)-binding proteins (FNBPs).

Property or characteristic	CadF (*Campylobacter* adhesion to Fibronectin)	FlpA (Fibronectin-like protein A)
Gene organization	Predicted to be the first gene of a bicistronic operon (*cadF*, *Cj1477c*)	Predicted to be the second gene in an operon containing three genes (*Cj1280c*, *flpA*, and *Cj1278c*)
No. of nucleotides, residues, M_r (strain NCTC 11168)	960 nts, 319 aa, 37 kDa	1,236 nts, 411 aa, 46 kDa
Prominent features	Signal peptide of 16 residues in length (Konkel et al., 1997) and a consensus peptidoglycan-binding motif $NX_2LSX_2RAX_2VX_3I$ (von Heijne, 1985) Fractionates in the outer membrane preparations and has been demonstrated to be surface-exposed using a rabbit CadF-specific serum (Konkel et al., 1997)	Lipoprotein signal sequence of 20 residues comprised of a tripartite structure and an invariant cysteine after the carboxy-terminus of the signal (Konkel et al., 2010) Deduced amino acid sequence contains three FN type III-like domains (Konkel et al., 2010) Fractionates in the outer membrane preparations and has been demonstrated to be surface-exposed using a rabbit FlpA-specific serum (Konkel et al., 2010)
Host cell target	FN	FN
FN-binding domain	Purified CadF displays dose-dependent and saturable FN-binding activity (Konkel et al., 2010) FN-binding domain has been localized to four amino acids [AA 134–137, Phe-Arg-Leu-Ser (FRLS)] (Konkel et al., 2005) FN-binding to an FRLS containing peptide is saturable (Konkel et al., 2005) FRLS domain determined to be surface-exposed using a mouse α-CadF peptide polyclonal antibody (Konkel et al., 2005) A rCadF protein containing the Ala-Ala-Gly-Ser residues at AA 134–137 exhibited a decrease in FN-binding (Konkel et al., 2005)	Purified FlpA protein displays dose-dependent and saturable FN-binding activity (Konkel et al., 2010; Larson et al., 2013) FN-binding domain has been localized to nine amino acids [AA 156–164, Trp-Arg-Pro-His-Pro-Asp-Phe-Arg-Val (WRPHPDFRV)] (Larson et al., 2013)
Site of binding to FN	The site of CadF binding on FN is not known	FlpA exhibits dose-dependent and saturable binding to the 40 kDa gelatin-binding domain of FN (Larson et al., 2013)
Adhesion to cells	A *cadF* mutant demonstrates reduced adhesion to human INT 407 epithelial cells (Monteville et al., 2003) The binding of *C. jejuni* to INT 407 cells is reduced by peptides containing the FRLS residues (Konkel et al., 2005) Competitive inhibition assays revealed that a *cadF* mutant inefficiently competes against the *C. jejuni* wild-type strain for binding to INT 407 cells compared to another wild-type strain (Monteville et al., 2003) Phenotypic changes were initially confirmed by studies performed with a *Cj1477c* mutant (Monteville et al., 2003)	A *flpA* deletion mutant demonstrates reduced adhesion to human INT 407 epithelial cells (Konkel et al., 2010) and chicken LMH hepatocellular carcinoma epithelial cells (Flanagan et al., 2009) Phenotypic changes were confirmed by in *trans* complementation studies (Konkel et al., 2010)

(Continued)

TABLE 1 | Continued

Property or characteristic	CadF (*Campylobacter* adhesion to FN)	FlpA (Fibronectin-like protein A)
Additional cell assays	FN-facilitated invasion of T84 eukaryotic cells by *C. jejuni* occurs preferentially at the basolateral cell surface (Monteville and Konkel, 2002)	A polyclonal serum against FlpA blocks *C. jejuni* adherence to INT 407 cells in a concentration-dependent manner (Konkel et al., 2010)
Host cell signaling pathways	Phosphorylation of paxillin is reduced with a *C. jejuni cadF* insertional mutant (Monteville and Konkel, 2002) Rac1 and Cdc42 GTPase dependent cell-signaling events are blunted with a *C. jejuni cadF* mutant (Krause-Gruszczynska et al., 2007) A *C. jejuni cadF flpA* double mutant is impaired in the activation of the epidermal growth factor receptor and Rho GTPase Rac1 (Larson et al., 2013)	FlpA is required for phosphorylation of Erk1/2 during *C. jejuni* infection (Larson et al., 2013) A *C. jejuni cadF flpA* double mutant is impaired in the activation of epidermal growth factor receptor and Rho GTPase Rac1 (Larson et al., 2013)
Infection of chickens	A *cadF* insertional mutant is impaired in chicken colonization (Ziprin et al., 1999; Flanagan et al., 2009)	A *flpA* deletion mutant is impaired in chicken colonization – 2 of 10 chickens were colonized (Flanagan et al., 2009)
Vaccination of chickens	Vaccination results in a reduction in the median level of *C. jejuni* cecal colonization when compared to the *C. jejuni*-inoculated, non-vaccinated control group (Neal-McKinney et al., 2014)	Vaccination results in a reduction in the median level of *C. jejuni* cecal colonization when compared to the *C. jejuni*-inoculated, non-vaccinated control group (Neal-McKinney et al., 2014)
Human antibody response	Individuals infected with *C. jejuni* generate antibodies against CadF (Konkel et al., 1997)	Not yet tested
Other information related to potential disease	Abiotic IL-$10^{-/-}$ mice show a reduced median pathology score for the *cadF* mutant and lower levels of TNF-α and IFN-γ compared to the wild-type strain (Schmidt et al., 2019) Undergoes post-translational processing to form smaller proteins of 24 kDa ($CadF_{24}$) and 22 kDa ($CadF_{22}$) that retain FN binding but that loses immunogenicity (Scott et al., 2010)	FlpA is required for *C. jejuni* dissemination to the spleen in IL-$10^{-/-}$ germ-free mice (Larson et al., 2013)

ability to bind FN (Greene et al., 1995). Since the initial discovery of an FNBP in *S. aureus*, at least 100 other FNBPs have been identified in both Gram-positive and Gram-negative bacteria (Henderson et al., 2011). Although many of these proteins have been found to possess distinct FN-binding domains, even more interesting is the fact that they bind to different regions within the FN molecule. For example, *S. aureus* FNBPA and FNBPB only bind to the N-terminal five-module region (FN I_{1-5}, heparin-binding domain), whereas the *Streptococcus pyogenes* F1 and Sfb1 bind to the FN I_{1-5} region as well as the FN I_{6-9} gelatin-binding domain (Sela et al., 1993; Bae and Schneewind, 2003; Schwarz-Linek et al., 2003; Schwarz-Linek et al., 2004). Other FNBPs target different FN regions. For example, *Borrelia burgdorferi* BBK32 binds to multiple sites, including FN I_{2-3} of the heparin-binding domain, FN I_{8-9} of the gelatin-binding domain, and FN III_{1-3} (Kim et al., 2004; Harris et al., 2014). The binding of these FNBPs to different sites within the FN molecule likely has different biological consequences.

CadF IS A *C. jejuni* OUTER MEMBRANE PROTEIN CONTAINING FIBRONECTIN-BINDING RESIDUES

In the 1980-90s, studies were conducted to determine if *C. jejuni* were able to bind to various components of the ECM, including FN, collagen, laminin, and vitronectin (Kuusela et al., 1989; Konkel et al., 1997; Moser et al., 1997). Collagen is the most abundant protein found in the ECM and provides structural support to resident cells. Laminin is a major component of the basal lamina, influencing cell differentiation, migration, and adhesion. Vitronectin binds to the $\alpha_5\beta_3$ integrin, promoting cell adhesion and spreading. Kuusela et al. (1989) were the first to report that *C. jejuni* isolates were able to bind to FN, and also reported that some isolates were able to bind to Type I, III, and V collagens. Several years later, the observation was made that *C. jejuni* bound to host cell retraction fibers, which are fingerlike projections enriched in ECM components. This prompted researchers to further investigate *C. jejuni* binding to various ECM components. In contrast to laminin and vitronectin, *C. jejuni* bound to coverslips that were treated with FN (FN-coated coverslips). Radioactive FN ($[^{125}I]$-FN) was then used to probe blots of *C. jejuni* outer membrane protein (OMP) extracts and was found to specifically bind to a 37 kDa OMP (CadF) (Konkel et al., 1997). A rabbit anti-serum was generated against the 37 kDa protein and used to screen *Campylobacter* genomic phage expression libraries. This led to the identification of *Cj1478c,* designated *cadF* for *Campylobacter* adhesion to Fibronectin (Konkel et al., 1997). The *cadF* gene encodes a protein of 326 amino acids, with a calculated molecular mass of 36,872 Da (**Figure 1**).

The *C. jejuni* CadF protein is a surface-exposed OMP that binds to soluble and insoluble FN (**Table 1**). Key features of the deduced amino acid sequence included a signal peptide of 16 residues (von Heijne, 1985) and a consensus peptidoglycan-binding motif, $NX_2LSX_2RAX_2VX_3l$. Sequence analysis showed that the protein consists of an N-terminal transmembrane domain that forms a β-barrel pore and a C-terminal domain forming a mixed α/β fold. Additional evidence confirmed that the 37 kDa protein bound to FN. First, biotinylated FN bound to a protein with an apparent molecular mass of 37 kDa (CadF) in the *C. jejuni* OMP extracts as judged by ligand-binding blots (Konkel et al., 1997). Second, the FN-binding domain within CadF was localized to four amino acids [AA 134–137, Phe-Arg-Leu-Ser (FRLS)] using overlapping 30-mer and 16-mer peptides coupled with enzyme-linked immunosorbent assays (ELISA) (Konkel et al., 2005). Third, *C. jejuni* mutants containing insertions in *cadF*, which disrupted the coding sequence, demonstrated a significant reduction in binding to FN. Moreover, the FRLS domain of CadF was determined to be surface-exposed using a mouse polyclonal α-CadF peptide antibody coupled with laser scanning confocal microscopy (Konkel et al., 2005). Finally, a recombinant CadF protein containing mutated FRLS residues (AA 134-137, FRLS > AAGS) exhibited a 91% decrease in FN-binding activity compared to the unmodified/native CadF protein. Although the FN-binding residues within CadF have been identified, researchers have yet to identify the CadF-binding site in FN.

FlpA IS A *C. jejuni* OUTER MEMBRANE LIPOPROTEIN CONTAINING FIBRONECTIN-BINDING RESIDUES

A second FNBP was identified in 2009 and was designated FlpA for Fibronectin-like protein A (Flanagan et al., 2009). The *C. jejuni flpA* gene is 1,236 nucleotides (411 residues) and is capable of encoding a protein with a calculated molecular mass of 46,124 Da (**Figure 1**, **Table 1**). The *flpA* gene is located in an operon containing three genes (*Cj1280c*, *flpA*, and *Cj1278c*). Sequence analysis of FlpA revealed the presence of three domains with similarity to the FN type III domain. Based on the presence of the FN type III domains, assays were performed to determine if FlpA binds to FN and the FN-binding phenotype of a *C. jejuni flpA* mutant. Purified FlpA protein displays dose-dependent and saturable FN-binding activity, as judged by ELISA using purified FlpA-GST protein (Konkel et al., 2010). The FN-binding site within FlpA was localized to a span of nine amino acids: Trp-Arg-Pro-His-Pro-Asp-Phe-Arg-Val (Larson et al., 2013). Assays were also performed to determine where FlpA binds within the FN molecule; proteolysis of FN with thermolysin (protease, type X) is a well-documented method for generating fragments of 29, 40–45, 65, and 130 kDa. Interestingly, thermolysin-digested FN fragments retain their biological activity. FlpA was determined to bind to the 40–45 kDa fragment (gelatin-binding domain) composed of four FN I repeats (FN I_{6-9}) and two FN II repeats (FN $II_{1,2}$). FlpA is likely a surface-exposed lipoprotein based on the data obtained from analysis using SignalP 5.0 (Almagro Armenteros et al., 2019) coupled with the application of indirect immunofluorescence microscopy of *C. jejuni* incubated with the FlpA-specific serum (Konkel et al., 2010).

ROLE OF CadF AND FlpA IN *C. jejuni* COLONIZATION OF CHICKENS

Campylobacteriosis often results from the handling and consumption of foods cross-contaminated with raw poultry products. The linkage between human infection and the handling of fresh poultry is mainly due to the fact that *C. jejuni* endemically colonizes commercial chicken flocks. Given that the antibodies passed from hens to chicks are partially protective against *Campylobacter* colonization, research has been performed to identify *C. jejuni* membrane-associated proteins recognized by maternal antibodies (Sahin et al., 2003). Immunoblots coupled with tandem mass spectrometry revealed a list of *C. jejuni* proteins recognized by maternal antibodies that included CadF and FlpA (Shoaf-Sweeney et al., 2008). This finding is consistent with previous findings that a *C. jejuni cadF* mutant and a *C. jejuni flpA* mutant are impaired in colonizing chickens (Ziprin et al., 1999; Flanagan et al., 2009). Based on the premise that specific adhesins are pivotal to colonization, disruption of *C. jejuni* adherence by anti-adhesin antibodies seems to be an obvious way to incapacitate the bacterium. In this regard, vaccination of chickens with a combination of CadF and FlpA peptides together with the full-length CadF and FlpA proteins resulted in an antibody response and a reduction in the median level of *C. jejuni* cecal colonization when compared to the *C. jejuni*-inoculated, non-vaccinated control group (Neal-McKinney et al., 2014). These results support the proposal that CadF and FlpA significantly contribute to *C. jejuni* chicken colonization.

Additional work is required to understand the interaction of *C. jejuni* within the gut of chickens and the biological consequences of *C. jejuni* infection in poultry (Awad et al., 2018). For decades, *C. jejuni* has been considered a commensal organism of poultry, as chickens, in contrast to humans, do not develop disease symptoms. More specifically, *C. jejuni*, which are principally found in the ceca (mucosal crypts) of chickens at very high CFUs, have been reported to stimulate a poor or inefficient inflammatory response, leading to tolerance and persistent cecal colonization (Hermans et al., 2012). In contrast, it has also been reported that certain *Campylobacter* strains can adversely affect the health and welfare of chickens and that the clinical signs of *C. jejuni* infection of poultry are not obvious (Humphrey et al., 2014). As our understanding of the bacteria and host cell factors that influence *C. jejuni* infection in chickens results in a better understanding of disease outcome, studies are warranted to determine if CadF and FlpA contribute to steps beyond the colonization of chickens.

CadF AND FlpA REGULATION IN RESPONSE TO INTESTINAL CONDITIONS

The intestinal life cycle of *C. jejuni* requires transition to an animal's gut, where it responds to changes in physiological conditions. The abundance of the CadF and FlpA proteins has been demonstrated to be responsive to host conditions, including temperature, oxygen levels, oxidative stress, and mucin (Tu et al., 2008; Hong et al., 2014; Koolman et al., 2016; Guccione et al., 2017; de Oliveira et al., 2019). For example, Hong and colleagues reported that culturing *C. jejuni* with porcine mucin resulted in an increase in 32 proteins and a decrease in 20 proteins compared to bacteria grown in the absence of mucin for 24 h using a label-free LC-MS/MS technique (Hong et al., 2014). In this study, more than a 3-fold increase was detected in CadF abundance after growth in medium supplemented with porcine mucin. In contrast, Tu et al. (2008) reported a 1.9-fold decrease in the expression of *cadF* when *C. jejuni* were cultured in medium with a component of human mucin (MUC2) for 12 h using quantitative RT-PCR. Based on this finding, the investigators concluded that the CadF protein is not required for the bacteria to penetrate the mucus barrier. Although the two investigations used different methodologies (Tu et al., 2008; Hong et al., 2014), it is possible that CadF levels change over the course of an infection. Furthermore, in a study conducted by Guccione et al., a 2.4-fold increase in CadF abundance and a 1.7-fold increase in FlpA abundance was reported following an oxygen-tension downshift (from high to low oxygen tension), as determined by label-free proteomic analysis (Guccione et al., 2017). Noteworthy is that the abundance of the Peb1A protein was also reduced in response to the shift from high to low oxygen-tension. The investigators rationalized their findings based on the primary functions of the proteins. Peb1A, originally proposed to be an adhesin, was subsequently found to be an ABC-transporter involved in aspartate and glutamate uptake whereas CadF and FlpA are dedicated adhesins. Although much work needs to be done to determine how *C. jejuni* responds to the host environment, the studies conducted to date suggest that this bacterium responds to the gut, in part, by increasing CadF and FlpA protein levels.

IN VITRO EVIDENCE OF FIBRONECTIN RECOGNITION BY *C. jejuni* IN PROMOTING HOST CELL ADHERENCE

Molecular biologists have utilized mutational studies to assess the function of a particular gene product. Likewise, a genetic approach has been taken to assess the individual role of CadF and FlpA in *C. jejuni*-host cell interactions by generating single-gene mutations. A *cadF* mutant was created by disrupting the *cadF* gene by homologous recombination via a single crossover event between the *cadF* gene on the chromosome and an internal fragment of the *cadF* gene on a suicide vector (Konkel et al., 1997). As mentioned above, the *C. jejuni cadF* knockouts were deficient in FN-binding. At the time, one of the obstacles facing *Campylobacter* researchers for the generation of a *cadF* complemented isolate was the fact that repeated attempts to clone the entire *cadF* gene and its endogenous promoter in *E. coli* failed, perhaps due to toxicity (Monteville et al., 2003; Mamelli et al., 2006). Because *cadF* and *Cj1477c* are the first and second genes of a bicistronic operon, the possibility was raised that *Cj1477c*, which encodes a putative hydrolase, might contribute to the observed reduction in host cell adherence.

To address this concern, a knockout was generated in *Cj1477c*. While the *C. jejuni cadF* mutant was found to be deficient in binding to INT 407 cells (Monteville et al., 2003), no reduction was noted in the binding of the *Cj1477c* knockout to INT 407 cells when compared to a *C. jejuni* wild-type isolate. To address the contribution of the CadF adhesin in *C. jejuni*-host cell attachment in the context of other adhesive proteins, competitive inhibition adherence assays were performed with a *C. jejuni cadF* mutant and a *C. jejuni* wild-type strain and compared with a competition between two different *C. jejuni* wild-type strains. The adherence assay performed with the two wild-type strains revealed a dose-dependent decrease in the adherence of one strain when the inoculum of the competing wild-type strain was increased (Monteville et al., 2003). However, the *C. jejuni cadF* mutant was unable to competitively inhibit the binding of a *C. jejuni* wild-type strain to INT 407 cells (Monteville et al., 2003). The application of a polarized cell model revealed that *C. jejuni* translocate a cell monolayer via a paracellular route, and then bind to FN localized on the basolateral surface of cells via CadF (Monteville and Konkel, 2002). These findings were in accordance with earlier studies, indicating that CadF binds to host cell-associated FN and promotes *C. jejuni*-host cell adherence.

The generation of a *flpA* knockout and complemented isolate was more straightforward than for *cadF*, as *flpA* containing its endogenous promoter can readily be cloned in *E. coli*. The *flpA* deletion mutant was generated using standard molecular techniques, and the mutant isolate was complemented by the introduction of a shuttle vector harboring *flpA* driven by a constitutive promoter (in *trans* complementation). Adherence assays revealed that the binding of the *C. jejuni flpA* mutant to INT 407 epithelial cells was significantly reduced compared with that of a wild-type strain. The reduction in binding of the *C. jejuni flpA* mutant was judged to be specific since complementation of the mutant in *trans* with a wild-type copy of the gene restored the organism's binding to INT 407 cells (Konkel et al., 2010; Larson et al., 2013). Moreover, rabbit polyclonal serum generated against FlpA blocked *C. jejuni* adherence to INT 407 cells in a concentration-dependent manner.

C. jejuni CadF AND FlpA STIMULATE HOST CELL SIGNALING PATHWAYS ASSOCIATED WITH HOST CELL INVASION

A model of the *C. jejuni*-host cell interface is presented in **Figure 2**. This figure shows the interaction of the CadF and FlpA proteins with host cell-associated FN and $\alpha_5\beta_1$ integrins, and the cell signaling pathways activated upon *C. jejuni* binding FN. *C. jejuni* manipulates focal adhesions (FAs) to stimulate host cell signaling and promote cell invasion (Eucker and Konkel, 2012; Konkel et al., 2013; Larson et al., 2013; Samuelson and Konkel, 2013). FAs are dynamic cellular structures that link ECM components, including FN, to intracellular cytoskeletal structures. They are comprised of integrin receptors, adaptor proteins, signaling proteins, and actin. Central to signaling through the FA is paxillin, which serves to integrate and disseminate signals from integrins to associated kinases that regulate membrane trafficking and cytoskeletal rearrangement (Schaller, 2001; Zaidel-Bar et al., 2007; Deakin and Turner, 2008). Although paxillin does not exhibit enzymatic activity, when phosphorylated, it serves as a central hub for other proteins. More specifically, phosphorylated paxillin acts as a scaffold for both signaling [kinases such as focal adhesion kinase (FAK) and Src] and adaptor proteins (vinculin and p130Cas). It is the establishment of the mature FA that ultimately results in signals being transduced from the integrins to the actin cytoskeleton (outside-in signaling).

CadF and FlpA appear to set the stage for cell invasion by promoting *C. jejuni* binding to the FN present on the basolateral surfaces of cells (i.e., *C. jejuni* bound to FN bound to the $\alpha_5\beta_1$ integrin) and by initiating host cell signaling events. More specifically, *C. jejuni* infection of INT 407 epithelial cells results in the phosphorylation of paxillin, and the phosphorylation is partially dependent on CadF (Monteville et al., 2003). This is based on the findings that a lower Multiplicity of Infection (MOI) of the *C. jejuni cadF* mutant (100 to 1) did not induce phosphorylation of paxillin. However, paxillin phosphorylation was observed in cells infected with a higher MOI of the *C. jejuni cadF* mutant (2000 to 1). This implies that CadF is not solely responsible for the host cell signaling. Consistent with paxillin activation playing a role in *C. jejuni* invasion, treatment of epithelial cells with TAE 226 and PP2, selective inhibitors of FAK and Src kinase activity, results in a significant decrease in *C. jejuni* internalization as judged by the gentamicin-protection assay (Eucker and Konkel, 2012). *C. jejuni* internalization is also significantly reduced in the presence of both PD168393 and erlotinib, which are specific inhibitors of epidermal growth factor (EGF) receptor tyrosine phosphorylation (Eucker and Konkel, 2012). This is relevant because the EGF receptor can be stimulated in the absence of an extracellular ligand via integrin signaling, and the activation of this receptor can alter components of the cytoskeleton involved with actin organization, FA formation and resolution, and cell-cell adhesion (Thelemann et al., 2005). Researchers have reported that *C. jejuni* induces EGF receptor activation in a CadF and FlpA dependent manner; however, whether one or both proteins are required for EGF receptor activation is currently not known (Eucker and Konkel, 2012).

β_1 integrins, FAK, Src, and paxillin also contribute to the activation of the MAP kinase Erk1/2 in *C. jejuni* infected cells (Eucker et al., 2014). Moreover, the phosphorylation of Erk1/2 is associated with FlpA-mediated activation of β_1 integrins and EGF receptor signaling (Larson et al., 2013). Consistent with this finding, inhibition of Erk1/2 activation with PD98059 results in a significant reduction in *C. jejuni* internalization (Zaidel-Bar et al., 2007; Deakin and Turner, 2008). Finally, FAs can also activate the Rac1 and Cdc42 Rho GTPases, thereby stimulating the formation of actin-based membrane protrusions and bacterial invasion (von Heijne, 1985; Mitra et al., 2005; Hu et al., 2006; Krause-Gruszczynska et al., 2007; Eucker and Konkel, 2012; Neal-McKinney and Konkel, 2012; Samuelson and Konkel, 2013;

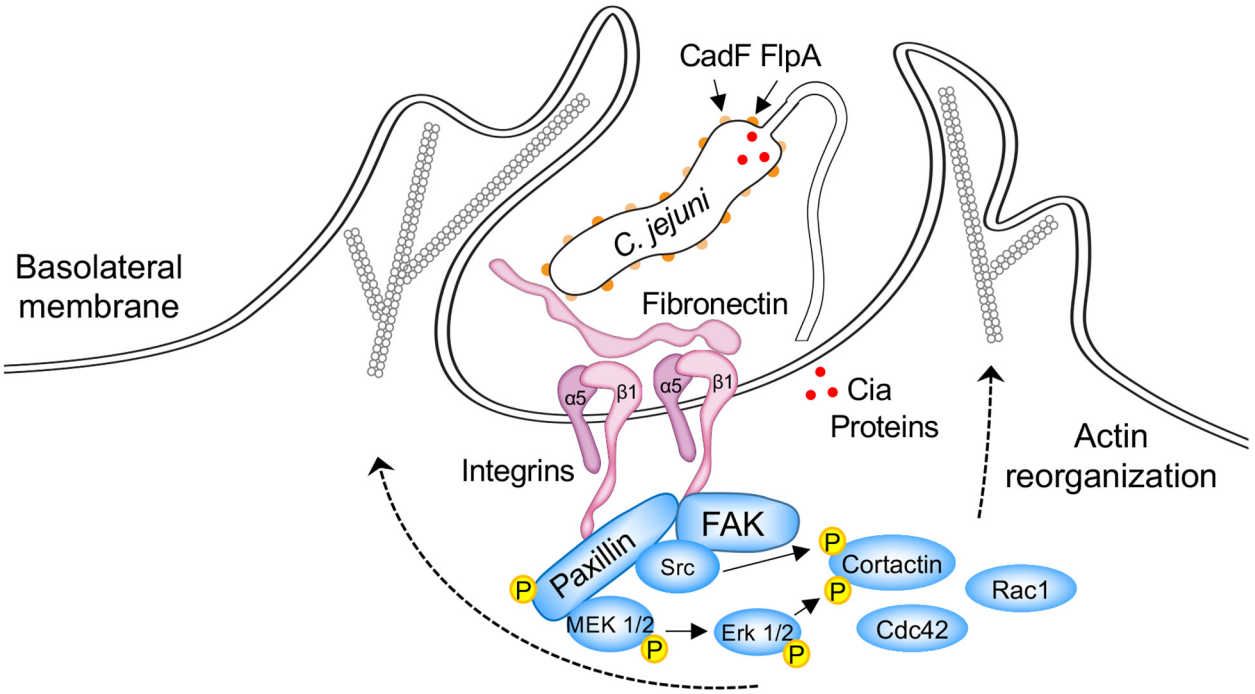

FIGURE 2 | Schematic overview of host cell signaling events triggered by *C. jejuni* CadF and FlpA binding to fibronectin and engagement of the $\alpha_5\beta_1$ integrin heterodimer. Focal adhesions (FAs) are dynamic protein complexes that connect the extracellular matrix to intracellular actin bundles. FAs contain over 100 proteins, including paxillin, focal adhesion kinase (FAK), and Src. Paxillin is a multi-domain adaptor protein that localizes to FAs. During FA assembly, paxillin becomes indirectly associated with the tails of β integrin subunits, is phosphorylated on multiple tyrosine, serine, and threonine residues, and serves as a central hub for other proteins. In particular, the phosphorylation of paxillin provides a binding platform for FAK and Src. The FAK-Src dual-activated signaling complex is responsible for the recruitment and activation of additional signaling and adaptor proteins that result in the activation of the Cdc42 and Rac1 Rho GTPases. Cortactin is a monomeric cytoplasmic protein that is also involved in polymerization and rearrangement of the actin cytoskeleton. The coordinated effort of key signaling proteins, scaffold proteins, and cytoskeletal components stimulate the formation of actin-based membrane protrusions and bacterial invasion. *C. jejuni cadF flpA* mutants are impaired in the ability to stimulate the activation of paxillin, Erk1/2, and Cdc42/Rac1 Rho GTPases (see the text for additional detail). The delivery of the Cia effector proteins (red dots) to the cytosol of host cells is impaired in a *C. jejuni flpA* mutant. Not known is whether CadF participates in the delivery of the effector proteins to host cells. The reader is referred to other papers for detailed models of *C. jejuni*-host cell interactions (Krause-Gruszczynska et al., 2007, 2011; Boehm et al., 2011; Eucker and Konkel, 2012; Konkel et al., 2013; Samuelson and Konkel, 2013).

Figure 2). Noteworthy is that GTPase dependent cell-signaling events are blunted with a *C. jejuni cadF* mutant compared to a wild-type strain (Krause-Gruszczynska et al., 2011; Boehm et al., 2012). Collectively, these findings demonstrate that *C. jejuni* binding to host cell-associated FN, via CadF and FlpA, is necessary to stimulate signaling pathways associated with cellular invasion. A potential caveat to these findings is that the binding of the *C. jejuni cadF* and *flpA* mutants to cells is reduced when compared to a wild-type strain, which could disrupt the delivery of secreted effector proteins.

DELIVERY OF *C. jejuni* EFFECTOR PROTEINS TO CELLS

Researchers have reported that the treatment of *C. jejuni* with chloramphenicol, a specific inhibitor of bacterial protein synthesis, significantly reduced host cell internalization, as compared to untreated controls (Konkel and Cieplak, 1992; Negretti et al., 2019). However, chloramphenicol treatment has little effect on *C. jejuni* adherence to host cells. Together, these data demonstrate that *C. jejuni* binding to host cell ligands is facilitated by adhesins, which are not sufficient to promote host cell internalization, but rather that internalization requires a second signal to stimulate host cell signaling pathways. The simplest view is that the *C. jejuni* FNBPs promote the bacterium's binding to host cells, whereas *C. jejuni* invasion of epithelial cells requires *de novo* bacterial protein synthesis (McSweegan and Walker, 1986; Karlyshev and Wren, 2005). The question then arises of whether the *C. jejuni* CadF or FlpA proteins set the stage for cell invasion by merely binding to FN or whether they prime/stimulate host cell signaling pathways (albeit not to the level that would promote cell invasion).

The translocation of bacterial Type III secretion effectors to the cytosol of a host cell has been demonstrated using the adenylate cyclase domain (ACD) of *Bordetella pertussis* CyaA as a reporter (Sory and Cornelis, 1994; Desvaux et al., 2006; Ono et al., 2006; Schechter et al., 2006; Neal-McKinney and Konkel, 2012). The basis of the ACD assay is that adenylate cyclase (adenylyl cyclase) only catalyzes the production of cAMP when bound by calmodulin in the eukaryotic cell cytosol (Ladant and Ullmann, 1999; Dautin et al., 2002). *C. jejuni* was first reported to

secrete proteins in 1999 (Konkel et al., 1999b) and later found to export proteins via the flagellar Type III Secretion System (T3SS) (Konkel et al., 2004). These secreted proteins were termed the *Campylobacter* invasion antigens (Cia), as they were found to contribute to cell invasion (Konkel et al., 1999b).

The delivery of most Type III secreted effectors requires the bacteria to contact the host cells (Schlumberger et al., 2005; Winnen et al., 2008). Different Cia proteins have been studied in several different *C. jejuni* strain backgrounds, including 81-176, NCTC 11168, and F38011. The Cia proteins have been found to play a role in *C. jejuni* cell invasion and survival but not in cell adherence (Christensen et al., 2009; Novik et al., 2010; Buelow et al., 2011; Samuelson et al., 2013; Naz, 2014). The most studied Cia proteins to date are CiaC and CiaD, which are necessary for maximal *C. jejuni* cellular invasion (Christensen et al., 2009; Neal-McKinney and Konkel, 2012; Samuelson and Konkel, 2013; Samuelson et al., 2013). *Cj1242* (*ciaC*) and *Cj0788* (*ciaD*) were initially identified to harbor a T3SS export signal using a genetic screen in a heterologous system, and *Cj0788* (*ciaD*) was also identified to play a role in *C. jejuni* cell invasion using a non-targeted transposon screen (Christensen et al., 2009; Novik et al., 2010). Relevant to the role of *C. jejuni* adhesins in Cia delivery to host cells was the discovery that the CiaC effector protein was delivered to the cytosol of host target cells using the ACD assay (Neal-McKinney and Konkel, 2012). Two additional experiments support the proposal that CiaC delivery requires bacteria-host cell contact. First, no increase was observed in intracellular cAMP levels when a bacterial supernatant containing the CiaC-ACD fusion protein was added to INT 407 cells versus non-infected cells. Second, no cAMP production was observed when a 0.2 μm pore filter was used to block the physical contact of *C. jejuni* with host cells (a two-chamber system: the apical chamber contained a *C. jejuni* strain harboring a *ciaC-ACD* construct and the bottom chamber contained the epithelial cells) (Neal-McKinney and Konkel, 2012). Similar methods were then used to test whether CiaC could be delivered to the host cell cytosol using a *C. jejuni flpA* mutant (Larson et al., 2013). The assay was performed in parallel with a *C. jejuni* wild-type strain transformed with the *ciaC-ACD* construct. Significantly less cAMP was detected in the cytosol of host cells infected with the *C. jejuni flpA* mutant when compared to cells inoculated with the *C. jejuni* wild-type strain transformed with the *ciaC-ACD* construct. Experiments have yet to be performed to determine if a Cia effector can be delivered to host cells from a *C. jejuni cadF* mutant. Taken together, it seems reasonable that the *C. jejuni* adhesins work in conjunction with the effector proteins to alter host cell behavior, including promoting host cell internalization.

POTENTIAL ROLE OF CadF AND FlpA IN HUMAN DISEASE

Presumably, the ability of *C. jejuni* to bind to the cells lining the human gastrointestinal tract is necessary for disease. In one study, *C. jejuni* isolates recovered from individuals with fever and diarrhea were found to adhere to cultured cells at a greater efficiency than those strains isolated from individuals without diarrhea or fever (Fauchere et al., 1989). Whether the adherence capacity and disease severity are correlated for *C. jejuni* isolates needs to be further studied. Based on the data generated with *C. jejuni* infection of cultured human intestinal cells, it is probable that CadF and FlpA mediate *C. jejuni* binding to the epithelial cells lining the human intestinal tract. This binding is likely to set the stage for host cell invasion and intracellular multiplication, resulting in acute disease (van Spreeuwel et al., 1985; Black et al., 1988). Several options exist for how *C. jejuni* may gain access to FN as a substrate; three possibilities are discussed below. Each possibility is predicated on the belief that the bacteria must be able to penetrate the mucus overlying the intestinal epithelial cells and that FN is primarily found at the basolateral (internal) surface or between cells within the gut epithelium. First, *C. jejuni* could target sites where the host intestinal cells are shed by extrusion (at the tips of the intestinal villi), similar to that proposed for *Listeria monocytogenes* (Pentecost et al., 2006). Data supporting this possibility has been observed in *C. jejuni*-infected piglets, where the infection site is evident from villus blunting and cell necrosis (Babakhani et al., 1993). Piglets infected with different strains of *C. jejuni* develop a range of clinical symptoms similar to humans, ranging from watery stools to bloody diarrhea. The dysenteric-like illness (blood in the stool) is a severe form of the disease and is illustrative of cell adherence/invasion. Second, *C. jejuni* could reach the basolateral surfaces of the intestinal cells by cellular translocation. Laboratory studies with polarized intestinal cells have demonstrated that *C. jejuni* can translocate across an intact cell barrier by migrating between cells (i.e., a paracellular route of translocation) (Monteville and Konkel, 2002; Boehm et al., 2012). Third, *C. jejuni* may breach the intestinal barrier by transcytosis across Microfold (M) cells in Peyer's patches of the intestine (Walker et al., 1988). Together, it is possible for the bacteria to either initially colonize at sites where the epithelium is disrupted and FN is readily accessible and/or bind to FN on the basolateral surface of epithelial cells following cellular translocation or via passage across Peyer's patches.

Two animal studies have been done to date in order to specifically address the role of CadF and FlpA in disease (Larson et al., 2013; Schmidt et al., 2019). Recently, the contribution of CadF in clinical disease was assessed using an abiotic (gnotobiotic) IL-$10^{-/-}$ mouse model (Schmidt et al., 2019). In this model, the mice were inoculated with 10^9 CFU of a *C. jejuni* wild-type isolate and *cadF* mutant, on two consecutive days, and disease parameters were assessed daily for six days. While the authors concluded that CadF is not required for campylobacteriosis in mice, the pro-inflammatory responses, such as TNF-α and IFN-γ, were lower for the *cadF* mutant compared to the wild-type isolate. In addition, the median pathology score for the *cadF* mutant was approximately 8 at day six, whereas a median pathology score of 12 was recorded for the mice infected with the wild-type strain. Disease severity was determined based on the presence of blood in the stool, diarrhea, and animal behavior. Thus, the mice inoculated with the *cadF* mutant develop less severe disease symptoms when compared to mice inoculated with the wild-type strain. These data demonstrate that CadF, while not being essential for disease, contributes to the severity of disease in a mouse model. Because

C. jejuni-cell adherence is multifactorial, we speculate that it is possible to overcome the involvement of CadF and FlpA in a disease model by using high or repeated doses of mutant bacteria. Regarding the role of the FlpA protein in disease, a study with IL-$10^{-/-}$ germ-free mice reported a reduced number of the *C. jejuni flpA* mutant in spleen when compared to mice inoculated with the *C. jejuni* wild-type strain (Larson et al., 2013). Studies are required to determine whether CadF and FlpA are necessary for human disease.

Although CadF is highly immunogenic, Scott and colleagues published an article revealing the possibility that CadF could retain its adhesive property and escape immune recognition in a host by post-translational processing (Scott et al., 2010). More specifically, the investigators demonstrated that CadF undergoes post-translational processing (proteolytic cleavage) to form smaller proteins of 24 kDa ($CadF_{24}$) and 22 kDa ($CadF_{22}$). Interestingly, the $CadF_{24}$ and $CadF_{22}$ variant forms were fully capable of binding to FN but were not recognized by patient sera. In addition, the processing of CadF appeared to be less abundant in the NCTC 11168 laboratory-adapted or avirulent strain ("GS" genome sequenced strain) when compared to the NCTC 11168 virulent strain ("O" original strain). The investigators concluded that the processing of CadF to the $CadF_{24}$ and $CadF_{22}$ variants provided antigenic variation that enabled evasion from the host immune response while enabling the protein to retain its adhesin-like function. Based on these findings, studies are warranted to determine whether the post-translational processing of CadF is common in other *C. jejuni* strains. Taken together, the data support the proposal that CadF may play a role in *C. jejuni* pathogenesis in a human host.

PRESENCE OF CadF AND FlpA IN *C. jejuni* ISOLATES

Previous survey studies have suggested that the *cadF* and *flpA* genes are conserved amongst *C. jejuni* isolates (Konkel et al., 1999a; Ripabelli et al., 2010; Ghorbanalizadgan et al., 2014; Levican et al., 2019; Wei et al., 2019). To explore this proposition, we assessed 20,218 full *C. jejuni* genome sequences that were available on the GenBank FTP server as of August 1st, 2019. After the removal of misidentified isolates (*Campylobacter coli, Campylobacter upsaliensis,* and *Campylobacter lari*), the remaining 20,166 sequences were searched for the presence of the *cadF* or *flpA* genes using the blastn command line tool with the default parameters. The *cadF* gene was absent in the genomes deposited for eight *C. jejuni* isolates, and the *flpA* gene was absent in the genomes for another seven isolates (**Supplementary Figure S1**). No genomes were identified in which both the *cadF* and *flpA* genes were absent. The caveat of this analysis is that the genomes reported for these 15 isolates may not be complete; it is not possible to determine the accuracy/completeness of the deposited sequences. At the very least, this analysis indicates that at a minimum, 99.93% of the sequenced *C. jejuni* isolates have both *cadF* and *flpA*. Based on this bioinformatic analysis, we conclude that *cadF* and *flpA* are ubiquitous and highly conserved amongst *C. jejuni* isolates.

Molecular-based diagnostics are being used more and more frequently in epidemiological studies. As opposed to conventional diagnostic methods utilizing a combination of culture and biochemical testing, molecular methods (e.g., polymerase chain reaction, PCR) offer the advantage of being fast. Relevant to this review is that *cadF* is a common target gene for the testing of both human and animal samples for *Campylobacter* spp. More specifically, epidemiologists have utilized *cadF* as a *C. jejuni*/*C. coli*-specific diagnostic marker. In contrast to other potential virulence-associated genes [e.g., the CDT subunit genes (*cdtA, cdtB,* and *cdtC*), *iamA*, *iamB*, and *vir*B11], *cadF* is present in nearly 100% of *C. jejuni* and *C. coli* isolates (**Supplementary Figure S1**) (Ghorbanalizadgan et al., 2014; Levican et al., 2019; Wei et al., 2019). The *cadF* and *flpA* genes do not appear to be present in other pathogenic bacteria. Given that molecular diagnostics is becoming a more common approach, we have cited only a few articles where researchers have used PCR amplification of the *cadF* gene for diagnostic purposes (Ghorbanalizadgan et al., 2014; Francois et al., 2018; Levican et al., 2019; Wei et al., 2019).

PERSPECTIVE (SUMMARY AND FUTURE DIRECTIONS)

MSCRAMMs are fascinating in that they help establish an infection for many Gram-positive and Gram-negative bacteria. While many pathogenic bacteria harbor MSCRAMMs, it is evident from several decades of research that *C. jejuni* is a unique pathogen. The identification of CadF and FlpA in *C. jejuni*, two distinctive MSCRAMMs, is a perfect illustration of this fact, as the FN-binding domains within CadF and FlpA are unique among FNBPs. Moreover, CadF and FlpA are two proteins that have drawn the attention of researchers due to their adhesive properties, as well as their potential role in stimulating host cell signaling pathways and cytoskeletal rearrangement (via a mechanism that is either direct or indirect).

The CadF and FlpA FNBPs from *C. jejuni* are currently recognized as important virulence factors, as they are involved in the early interactions occurring at the bacteria-host cell interface. Both CadF and FlpA bind to FN, facilitate *C. jejuni* adherence to host cells, and enable *C. jejuni* colonization of chickens at a high level. Also known are the FN-binding domains within both the CadF and FlpA proteins, as well as the FN fragment to which the FlpA protein binds. Experimental evidence suggests that *C. jejuni* binding to FN allows the microorganism to communicate with the cell cytoskeleton via outside-in signaling through integrins, leading to bacterial internalization into a host cell. Internalization by an intestinal cell allows the bacterium to avoid the powerful killing mechanisms of a phagocyte. Several studies suggest that *C. jejuni* invasion of the cells lining the intestinal tract is a primary mechanism of colonic damage (van Spreeuwel et al., 1985; Babakhani et al., 1993; Russell et al., 1993). While CadF and FlpA are required for maximal host cell invasion (Eucker and Konkel, 2012), the contribution of these two proteins to invasion is, in part, due to their role in triggering host cell signaling pathways, possibly by aiding the delivery of effector proteins. Relevant to

this point is that CadF and FlpA are involved in the activation of Cdc42 and Rac1 in human cells (Krause-Gruszczynska et al., 2011; Boehm et al., 2012; Eucker and Konkel, 2012; Larson et al., 2013); these are the two primary host cell Rho GTPases involved in *C. jejuni* invasion. These findings are likely due to the fact that *C. jejuni* adhesion mutants, including a *flpA* mutant, are impaired in the delivery of effector proteins to host cells (Larson et al., 2013). In addition, we propose that CadF and FlpA are both involved in the activation of the β_1 integrin, which is required for *C. jejuni* invasion (Krause-Gruszczynska et al., 2011; Konkel et al., 2013). Studies are needed to address outstanding questions (e.g., Where does CadF bind within the FN molecule?; Do CadF and FlpA bind to FN simultaneously or is binding sequential?; Do CadF and FlpA bind to other substrates or ECM components?; What role do CadF and FlpA play individually in binding to FN and initiating downstream host cell signaling events?; Do other *C. jejuni* adhesins work cooperatively with CadF and FlpA?; Are CadF and/or FlpA necessary for biofilm formation?, etc.).

In spite of CadF and FlpA having unique FN-binding domains, the mechanistic basis for how they modify FN function will likely have broader implications given the number of pathogenic microbes that have FNBPs. As mentioned earlier, the FN molecule is a complex glycoprotein composed of multiple repeating domains. The different domains in FN allow this glycoprotein to bind to cells and to molecules within the surrounding matrix simultaneously. Moreover, pathogen binding to specific domains may afford different functional outcomes (e.g., cell binding, cell invasion, etc.). While many FNBPs target the 29 kDa N-terminal fragment of FN that is composed of five FN I repeats (FN I_{1-5}), other FNBPs bind to the 40–45 kDa FN fragment that is comprised of four FN I and two FN II repeats (FN I_6 - FN II_{1-2} - FN I_{7-9}). While FlpA has been determined to bind to the 40–45 kDa fragment, it is not known where CadF binds to the FN molecule. It is possible that the binding of a pathogen to a distinct FN domain can alter various FN functions, including the modulation of integrin function. It will be of interest to compare the functional attributes of the CadF and FlpA proteins from *C. jejuni* with the FNBPs from other more intensely studied bacterial pathogens, as this additional information may provide further insight into pathogenic mechanisms. Finally, continued investigation of FNBPs is necessary to provide a greater understanding of their diversity and specificity in mediating bacteria-host cell interactions. Please note that following the submission of this article, we submitted a research article on the cooperative interaction of CadF and FlpA in binding to FN and host cells that has been published (Talukdar et al., 2020).

AUTHOR CONTRIBUTIONS

MK worked on the original draft preparation, **Table 1** preparation, project design and management. PT reviewed the manuscript, prepared **Figure 1** and **Supplementary Tables S1, S2**. NN reviewed the manuscript, prepared **Figure 2** and **Supplementary Figure S1**. CK reviewed the manuscript and prepared **Figure 2**.

FUNDING

Research in the Konkel Lab is supported, in part, by a grant from the National Institutes of Health to MK (Award Number R01AI125356). The content is solely the responsibility of the authors and does not necessarily represent the official views of the NIH.

ACKNOWLEDGMENTS

We thank Dr. Kerry Cooper (University of Arizona), Dr. Christopher R. Gourley, and Kyrah L. Turner for proofreading this manuscript.

SUPPLEMENTARY MATERIAL

The Supplementary Material for this article can be found online at: https://www.frontiersin.org/articles/10.3389/fmicb.2020.00564/full#supplementary-material

REFERENCES

Almagro Armenteros, J. J., Tsirigos, K. D., Sonderby, C. K., Petersen, T. N., Winther, O., Brunak, S., et al. (2019). SignalP 5.0 improves signal peptide predictions using deep neural networks. *Nat. Biotechnol.* 37, 420–423. doi: 10.1038/s41587-019-0036-z

Asuming-Bediako, N., Parry-Hanson Kunadu, A., Abraham, S., and Habib, I. (2019). *Campylobacter* at the human-food interface: the African perspective. *Pathogens* 8:E87. doi: 10.3390/pathogens8020087

Awad, W. A., Hess, C., and Hess, M. (2018). Re-thinking the chicken-*Campylobacter jejuni* interaction: a review. *Avian Pathol.* 47, 352–363. doi: 10.1080/03079457.2018.1475724

Babakhani, F. K., Bradley, G. A., and Joens, L. A. (1993). Newborn piglet model for campylobacteriosis. *Infect. Immun.* 61, 3466–3475.

Bae, T., and Schneewind, O. (2003). The YSIRK-G/S motif of staphylococcal protein A and its role in efficiency of signal peptide processing. *J. Bacteriol.* 185, 2910–2919.

Bae, W., Kaya, K. N., Hancock, D. D., Call, D. R., Park, Y. H., and Besser, T. E. (2005). Prevalence and antimicrobial resistance of thermophilic *Campylobacter* spp. from cattle farms in Washington State. *Appl. Environ. Microbiol.* 71, 169–174.

Black, R. E., Levine, M. M., Clements, M. L., Hughes, T. P., and Blaser, M. J. (1988). Experimental *Campylobacter jejuni* infection in humans. *J. Infect. Dis.* 157, 472–479.

Blaser, M. J., Berkowitz, I. D., Laforce, F. M., Cravens, J., Reller, L. B., and Wang, W. L. (1979). *Campylobacter* enteritis: clinical and epidemiologic features. *Ann. Intern. Med.* 91, 179–185.

Boehm, M., Hoy, B., Rohde, M., Tegtmeyer, N., Baek, K. T., Oyarzabal, O. A., et al. (2012). Rapid paracellular transmigration of *Campylobacter jejuni* across polarized epithelial cells without affecting TER: role of proteolytic-active HtrA cleaving E-cadherin but not fibronectin. *Gut Pathog.* 4:3. doi: 10.1186/1757-4749-4-3

Boehm, M., Krause-Gruszczynska, M., Rohde, M., Tegtmeyer, N., Takahashi, S., Oyarzabal, O. A., et al. (2011). Major host factors involved in epithelial cell

invasion of *Campylobacter jejuni*: role of fibronectin, integrin beta1, FAK, Tiam-1, and DOCK180 in activating Rho GTPase Rac1. *Front. Cell. Infect. Microbiol.* 1:17. doi: 10.3389/fcimb.2011.00017

Bronowski, C., James, C. E., and Winstanley, C. (2014). Role of environmental survival in transmission of *Campylobacter jejuni*. *FEMS Microbiol. Lett.* 356, 8–19. doi: 10.1111/1574-6968.12488

Buelow, D. R., Christensen, J. E., Neal-McKinney, J. M., and Konkel, M. E. (2011). *Campylobacter jejuni* survival within human epithelial cells is enhanced by the secreted protein CiaI. *Mol. Microbiol.* 80, 1296–1312. doi: 10.1111/j.1365-2958.2011.07645.x

Butzler, J. P., and Skirrow, M. B. (1979). *Campylobacter* enteritis. *Clin. Gastroenterol.* 8, 737–765.

Christensen, J. E., Pacheco, S. A., and Konkel, M. E. (2009). Identification of a *Campylobacter jejuni*-secreted protein required for maximal invasion of host cells. *Mol. Microbiol.* 73, 650–662. doi: 10.1111/j.1365-2958.2009.06797.x

Coker, A. O., Isokpehi, R. D., Thomas, B. N., Amisu, K. O., and Obi, C. L. (2002). Human campylobacteriosis in developing countries. *Emerg. Infect. Dis.* 8, 237–244.

Dautin, N., Karimova, G., and Ladant, D. (2002). *Bordetella pertussis* adenylate cyclase toxin: a versatile screening tool. *Toxicon* 40, 1383–1387.

de Oliveira, M. G., Rizzi, C., Galli, V., Lopes, G. V., Haubert, L., Dellagostin, O. A., et al. (2019). Presence of genes associated with adhesion, invasion, and toxin production in *Campylobacter jejuni* isolates and effect of temperature on their expression. *Can. J. Microbiol.* 65, 253–260. doi: 10.1139/cjm-2018-0539

Deakin, N. O., and Turner, C. E. (2008). Paxillin comes of age. *J. Cell Sci.* 121, 2435–2444. doi: 10.1242/jcs.018044

Dekeyser, P., Gossuin-Detrain, M., Butzler, J. P., and Sternon, J. (1972). Acute enteritis due to related vibrio: first positive stool cultures. *J. Infect. Dis.* 125, 390–392.

Desvaux, M., Hebraud, M., Henderson, I. R., and Pallen, M. J. (2006). Type III secretion: what's in a name? *Trends Microbiol.* 14, 157–160.

Engberg, J., Aarestrup, F. M., Taylor, D. E., Gerner-Smidt, P., and Nachamkin, I. (2001). Quinolone and macrolide resistance in *Campylobacter jejuni* and *C. coli*: resistance mechanisms and trends in human isolates. *Emerg. Infect. Dis.* 7, 24–34.

Eucker, T. P., and Konkel, M. E. (2012). The cooperative action of bacterial fibronectin-binding proteins and secreted proteins promote maximal *Campylobacter jejuni* invasion of host cells by stimulating membrane ruffling. *Cell Microbiol.* 14, 226–238. doi: 10.1111/j.1462-5822.2011.01714.x

Eucker, T. P., Samuelson, D. R., Hunzicker-Dunn, M., and Konkel, M. E. (2014). The focal complex of epithelial cells provides a signalling platform for interleukin-8 induction in response to bacterial pathogens. *Cell Microbiol.* 16, 1441–1455. doi: 10.1111/cmi.12305

Fauchere, J. L., Kervella, M., Rosenau, A., Mohanna, K., and Veron, M. (1989). Adhesion to HeLa cells of *Campylobacter jejuni* and *C. coli* outer membrane components. *Res. Microbiol.* 140, 379–392.

Flanagan, R. C., Neal-McKinney, J. M., Dhillon, A. S., Miller, W. G., and Konkel, M. E. (2009). Examination of *Campylobacter jejuni* putative adhesins leads to the identification of a new protein, designated FlpA, required for chicken colonization. *Infect. Immun.* 77, 2399–2407. doi: 10.1128/IAI.01266-08

Francois, R., Yori, P. P., Rouhani, S., Siguas Salas, M., Paredes Olortegui, M., Rengifo Trigoso, D., et al. (2018). The other *Campylobacters*: not innocent bystanders in endemic diarrhea and dysentery in children in low-income settings. *PLoS Negl. Trop. Dis.* 12:e0006200. doi: 10.1371/journal.pntd.0006200

Frantz, C., Stewart, K. M., and Weaver, V. M. (2010). The extracellular matrix at a glance. *J. Cell Sci.* 123, 4195–4200.

Friedman, C. R., Hoekstra, R. M., Samuel, M., Marcus, R., Bender, J., Shiferaw, B., et al. (2004). Risk factors for sporadic *Campylobacter* infection in the United States: a case-control study in FoodNet sites. *Clin. Infect. Dis.* 38(Suppl. 3), S285–S296.

Ghorbanalizadgan, M., Bakhshi, B., Kazemnejad Lili, A., Najar-Peerayeh, S., and Nikmanesh, B. (2014). A molecular survey of *Campylobacter jejuni* and *Campylobacter coli* virulence and diversity. *Iran Biomed. J.* 18, 158–164.

Gibreel, A., and Taylor, D. E. (2006). Macrolide resistance in *Campylobacter jejuni* and *Campylobacter coli*. *J. Antimicrob. Chemother.* 58, 243–255.

Greene, C., Mcdevitt, D., Francois, P., Vaudaux, P. E., Lew, D. P., and Foster, T. J. (1995). Adhesion properties of mutants of *Staphylococcus aureus* defective in fibronectin-binding proteins and studies on the expression of *fnb* genes. *Mol. Microbiol.* 17, 1143–1152.

Guccione, E. J., Kendall, J. J., Hitchcock, A., Garg, N., White, M. A., Mulholland, F., et al. (2017). Transcriptome and proteome dynamics in chemostat culture reveal how *Campylobacter jejuni* modulates metabolism, stress responses and virulence factors upon changes in oxygen availability. *Environ. Microbiol.* 19, 4326–4348. doi: 10.1111/1462-2920.13930

Harris, G., Ma, W., Maurer, L. M., Potts, J. R., and Mosher, D. F. (2014). *Borrelia burgdorferi* protein BBK32 binds to soluble fibronectin via the N-terminal 70-kDa region, causing fibronectin to undergo conformational extension. *J. Biol. Chem.* 289, 22490–22499. doi: 10.1074/jbc.M114.578419

Henderson, B., Nair, S., Pallas, J., and Williams, M. A. (2011). Fibronectin: a multidomain host adhesin targeted by bacterial fibronectin-binding proteins. *FEMS Microbiol. Rev.* 35, 147–200. doi: 10.1111/j.1574-6976.2010.00243.x

Hermans, D., Pasmans, F., Heyndrickx, M., Van Immerseel, F., Martel, A., Van Deun, K., et al. (2012). A tolerogenic mucosal immune response leads to persistent *Campylobacter jejuni* colonization in the chicken gut. *Crit. Rev. Microbiol.* 38, 17–29. doi: 10.3109/1040841X.2011.615298

Hong, S., Cha, I., Kim, N. O., Seo, J. B., Kim, S. Y., Kim, J. H., et al. (2014). Comparative proteomic label-free analysis of *Campylobacter jejuni* NCTC 11168 cultured with porcine mucin. *Foodborne Pathog. Dis.* 11, 240–247. doi: 10.1089/fpd.2013.1596

Horrocks, S. M., Anderson, R. C., Nisbet, D. J., and Ricke, S. C. (2009). Incidence and ecology of *Campylobacter jejuni* and *coli* in animals. *Anaerobe* 15, 18–25. doi: 10.1016/j.anaerobe.2008.09.001

Hu, L., Mcdaniel, J. P., and Kopecko, D. J. (2006). Signal transduction events involved in human epithelial cell invasion by *Campylobacter jejuni* 81-176. *Microb. Pathog.* 40, 91–100.

Huang, H., Brooks, B. W., Lowman, R., and Carrillo, C. D. (2015). *Campylobacter* species in animal, food, and environmental sources, and relevant testing programs in Canada. *Can. J. Microbiol.* 61, 701–721. doi: 10.1139/cjm-2014-0770

Humphrey, S., Chaloner, G., Kemmett, K., Davidson, N., Williams, N., Kipar, A., et al. (2014). *Campylobacter jejuni* is not merely a commensal in commercial broiler chickens and affects bird welfare. *mBio* 5:e01364-14. doi: 10.1128/mBio.01364-14

Hymes, J. P., and Klaenhammer, T. R. (2016). Stuck in the Middle: fibronectin-binding proteins in Gram-positive bacteria. *Front. Microbiol.* 7:1504. doi: 10.3389/fmicb.2016.01504

Kaakoush, N. O., Castano-Rodriguez, N., Mitchell, H. M., and Man, S. M. (2015). Global epidemiology of *Campylobacter* infection. *Clin. Microbiol. Rev.* 28, 687–720. doi: 10.1128/CMR.00006-15

Kale, A., Phansopa, C., Suwannachart, C., Craven, C. J., Rafferty, J. B., and Kelly, D. J. (2011). The virulence factor PEB4 (Cj0596) and the periplasmic protein Cj1289 are two structurally related SurA-like chaperones in the human pathogen *Campylobacter jejuni*. *J. Biol. Chem.* 286, 21254–21265. doi: 10.1074/jbc.M111.220442

Karlyshev, A. V., and Wren, B. W. (2005). Development and application of an insertional system for gene delivery and expression in *Campylobacter jejuni*. *Appl. Environ. Microbiol.* 71, 4004–4013.

Karmali, M. A., and Fleming, P. C. (1979). *Campylobacter* enteritis in children. *J. Pediatr.* 94, 527–533.

Kim, J. H., Singvall, J., Schwarz-Linek, U., Johnson, B. J., Potts, J. R., and Hook, M. (2004). BBK32, a fibronectin binding MSCRAMM from *Borrelia burgdorferi*, contains a disordered region that undergoes a conformational change on ligand binding. *J. Biol. Chem.* 279, 41706–41714.

Konkel, M. E., Christensen, J. E., Keech, A. M., Monteville, M. R., Klena, J. D., and Garvis, S. G. (2005). Identification of a fibronectin-binding domain within the *Campylobacter jejuni* CadF protein. *Mol. Microbiol.* 57, 1022–1035.

Konkel, M. E., and Cieplak, W. Jr. (1992). Altered synthetic response of *Campylobacter jejuni* to cocultivation with human epithelial cells is associated with enhanced internalization. *Infect. Immun.* 60, 4945–4949.

Konkel, M. E., Garvis, S. G., Tipton, S. L., Anderson, D. E. Jr., and Cieplak, W. Jr. (1997). Identification and molecular cloning of a gene encoding a fibronectin-binding protein (CadF) from *Campylobacter jejuni*. *Mol. Microbiol.* 24, 953–963.

Konkel, M. E., Gray, S. A., Kim, B. J., Garvis, S. G., and Yoon, J. (1999a). Identification of the enteropathogens *Campylobacter jejuni* and *Campylobacter*

coli based on the *cadF* virulence gene and its product. *J. Clin. Microbiol.* 37, 510–517.

Konkel, M. E., Kim, B. J., Rivera-Amill, V., and Garvis, S. G. (1999b). Bacterial secreted proteins are required for the internaliztion of *Campylobacter jejuni* into cultured mammalian cells. *Mol. Microbiol.* 32, 691–701.

Konkel, M. E., Klena, J. D., Rivera-Amill, V., Monteville, M. R., Biswas, D., Raphael, B., et al. (2004). Secretion of virulence proteins from *Campylobacter jejuni* is dependent on a functional flagellar export apparatus. *J. Bacteriol.* 186, 3296–3303.

Konkel, M. E., Larson, C. L., and Flanagan, R. C. (2010). *Campylobacter jejuni* FlpA binds fibronectin and is required for maximal host cell adherence. *J. Bacteriol.* 192, 68–76. doi: 10.1128/JB.00969-09

Konkel, M. E., Samuelson, D. R., Eucker, T. P., Shelden, E. A., and O'loughlin, J. L. (2013). Invasion of epithelial cells by *Campylobacter jejuni* is independent of caveolae. *Cell Commun. Signal.* 11:100. doi: 10.1186/1478-811X-11-100

Koolman, L., Whyte, P., Burgess, C., and Bolton, D. (2016). Virulence gene expression, adhesion and invasion of *Campylobacter jejuni* exposed to oxidative stress (H_2O_2). *Int. J. Food Microbiol.* 220, 33–38. doi: 10.1016/j.ijfoodmicro.2016.01.002

Krause-Gruszczynska, M., Boehm, M., Rohde, M., Tegtmeyer, N., Takahashi, S., Buday, L., et al. (2011). The signaling pathway of *Campylobacter jejuni*-induced Cdc42 activation: role of fibronectin, integrin beta1, tyrosine kinases and guanine exchange factor Vav2. *Cell Commun. Signal.* 9:32. doi: 10.1186/1478-811X-9-32

Krause-Gruszczynska, M., Rohde, M., Hartig, R., Genth, H., Schmidt, G., Keo, T., et al. (2007). Role of the small Rho GTPases Rac1 and Cdc42 in host cell invasion of *Campylobacter jejuni*. *Cell Microbiol.* 9, 2431–2444.

Kuusela, P. (1978). Fibronectin binds to *Staphylococcus aureus*. *Nature* 276, 718–720.

Kuusela, P., Moran, A. P., Vartio, T., and Kosunen, T. U. (1989). Interaction of *Campylobacter jejuni* with extracellular matrix components. *Biochim. Biophys. Acta* 993, 297–300.

Ladant, D., and Ullmann, A. (1999). *Bordatella pertussis* adenylate cyclase: a toxin with multiple talents. *Trends Microbiol.* 7, 172–176.

Larson, C. L., Samuelson, D. R., Eucker, T. P., O'loughlin, J. L., and Konkel, M. E. (2013). The fibronectin-binding motif within FlpA facilitates *Campylobacter jejuni* adherence to host cell and activation of host cell signaling. *Emerg. Microbes Infect.* 2:e65. doi: 10.1038/emi.2013.65

Leon-Kempis Mdel, R., Guccione, E., Mulholland, F., Williamson, M. P., and Kelly, D. J. (2006). The *Campylobacter jejuni* PEB1a adhesin is an aspartate/glutamate-binding protein of an ABC transporter essential for microaerobic growth on dicarboxylic amino acids. *Mol. Microbiol.* 60, 1262–1275.

Levican, A., Ramos-Tapia, I., Briceno, I., Guerra, F., Mena, B., Varela, C., et al. (2019). Genomic analysis of Chilean strains of *Campylobacter jejuni* from human faeces. *Biomed. Res. Int.* 2019:1902732. doi: 10.1155/2019/1902732

Lugert, R., Gross, U., and Zautner, A. E. (2015). *Campylobacter jejuni*: components for adherence to and invasion of eukaryotic cells. *Berl. Munch. Tierarztl. Wochenschr.* 128, 90–97.

Mamelli, L., Pages, J. M., Konkel, M. E., and Bolla, J. M. (2006). Expression and purification of native and truncated forms of CadF, an outer membrane protein of *Campylobacter*. *Int. J. Biol. Macromol.* 39, 135–140.

McSweegan, E., and Walker, R. I. (1986). Identification and characterization of two *Campylobacter jejuni* adhesins for cellular and mucous substrates. *Infect. Immun.* 53, 141–148.

Min, T., Vedadi, M., Watson, D. C., Wasney, G. A., Munger, C., Cygler, M., et al. (2009). Specificity of *Campylobacter jejuni* adhesin PEB3 for phosphates and structural differences among its ligand complexes. *Biochemistry* 48, 3057–3067. doi: 10.1021/bi802195d

Mitra, S. K., Hanson, D. A., and Schlaepfer, D. D. (2005). Focal adhesion kinase: in command and control of cell motility. *Nat. Rev. Mol. Cell Biol.* 6, 56–68.

Monteville, M. R., and Konkel, M. E. (2002). Fibronectin-facilitated invasion of T84 eukaryotic cells by *Campylobacter jejuni* occurs preferentially at the basolateral cell surface. *Infect. Immun.* 70, 6665–6671.

Monteville, M. R., Yoon, J. E., and Konkel, M. E. (2003). Maximal adherence and invasion of INT 407 cells by *Campylobacter jejuni* requires the CadF outer-membrane protein and microfilament reorganization. *Microbiology* 149, 153–165.

Moser, I., Schroeder, W., and Salnikow, J. (1997). *Campylobacter jejuni* major outer membrane protein and a 59-kDa protein are involved in binding to fibronectin and INT 407 cell membranes. *FEMS Microbiol. Lett.* 157, 233–238.

Naz, N. (2014). *Reinvestigation into the Mechanism of Campylobacter jejuni Invasion of Intestinal Epithelial Cells*. Doctoral Dissertation, London School of Hygiene and Tropical Medicine, London.

Neal-McKinney, J. M., and Konkel, M. E. (2012). The *Campylobacter jejuni* CiaC virulence protein is secreted from the flagellum and delivered to the cytosol of host cells. *Front. Cell Infect. Microbiol.* 2:31. doi: 10.3389/fcimb.2012.00031

Neal-McKinney, J. M., Samuelson, D. R., Eucker, T. P., Nissen, M. S., Crespo, R., and Konkel, M. E. (2014). Reducing *Campylobacter jejuni* colonization of poultry via vaccination. *PLoS One* 9:e114254. doi: 10.1371/journal.pone.0114254

Negretti, N. M., Clair, G., Talukdar, P. K., Gourley, C. R., Huynh, S., Adkins, J. N., et al. (2019). *Campylobacter jejuni* demonstrates conserved proteomic and transcriptomic responses when co-cultured with human INT 407 and Caco-2 epithelial cells. *Front. Microbiol.* 10:755. doi: 10.3389/fmicb.2019.00755

Novik, V., Hofreuter, D., and Galan, J. E. (2010). Identification of *Campylobacter jejuni* genes involved in its interaction with epithelial cells. *Infect. Immun.* 78, 3540–3553.

Ono, T., Park, K. S., Ueta, M., Iida, T., and Honda, T. (2006). Identification of proteins secreted via *Vibrio parahaemolyticus* type III secretion system 1. *Infect. Immun.* 74, 1032–1042.

Pankov, R., and Yamada, K. M. (2002). Fibronectin at a glance. *J. Cell Sci.* 115, 3861–3863.

Pentecost, M., Otto, G., Theriot, J. A., and Amieva, M. R. (2006). *Listeria monocytogenes* invades the epithelial junctions at sites of cell extrusion. *PLoS Pathog.* 2:e3.

Pizarro-Cerda, J., and Cossart, P. (2006). Bacterial adhesion and entry into host cells. *Cell* 124, 715–727.

Potts, J. R., and Campbell, I. D. (1994). Fibronectin structure and assembly. *Curr. Opin. Cell Biol.* 6, 648–655.

Ripabelli, G., Tamburro, M., Minelli, F., Leone, A., and Sammarco, M. L. (2010). Prevalence of virulence-associated genes and cytolethal distending toxin production in *Campylobacter* spp. isolated in Italy. *Comp. Immunol. Microbiol. Infect. Dis.* 33, 355–364. doi: 10.1016/j.cimid.2008.12.001

Rubinchik, S., Seddon, A., and Karlyshev, A. V. (2012). Molecular mechanisms and biological role of *Campylobacter jejuni* attachment to host cells. *Eur. J. Microbiol. Immunol. (Bp)* 2, 32–40. doi: 10.1556/EuJMI.2.2012.1.6

Ruiz-Palacios, G. M. (2007). The health burden of *Campylobacter* infection and the impact of antimicrobial resistance: playing chicken. *Clin. Infect. Dis.* 44, 701–703.

Russell, R. G., O'donnoghue, M., Blake, D. C. Jr., Zulty, J., and Detolla, L. J. (1993). Early colonic damage and invasion of *Campylobacter jejuni* in experimentally challenged infant *Macaca mulatta*. *J. Infect. Dis.* 168, 210–215.

Sahin, O., Luo, N., Huang, S., and Zhang, Q. (2003). Effect of *Campylobacter*-specific maternal antibodies on *Campylobacter jejuni* colonization in young chickens. *Appl. Environ. Microbiol.* 69, 5372–5379.

Samuelson, D. R., Eucker, T. P., Bell, J. A., Dybas, L., Mansfield, L. S., and Konkel, M. E. (2013). The *Campylobacter jejuni* CiaD effector protein activates MAP kinase signaling pathways and is required for the development of disease. *Cell Commun. Signal.* 11:79. doi: 10.1186/1478-811X-11-79

Samuelson, D. R., and Konkel, M. E. (2013). Serine phosphorylation of cortactin is required for maximal host cell invasion by *Campylobacter jejuni*. *Cell Commun. Signal.* 11:82. doi: 10.1186/1478-811X-11-82

Schaller, M. D. (2001). Paxillin: a focal adhesion-associated adaptor protein. *Oncogene* 20, 6459–6472.

Schechter, L. M., Vencato, M., Jordan, K. L., Schneider, S. E., Schneider, D. J., and Collmer, A. (2006). Multiple approaches to a complete inventory of *Pseudomonas syringae* pv. tomato DC3000 type III secretion system effector proteins. *Mol. Plant Microbe Interact.* 19, 1180–1192.

Schlumberger, M. C., Muller, A. J., Ehrbar, K., Winnen, B., Duss, I., Stecher, B., et al. (2005). Real-time imaging of type III secretion: *Salmonella* SipA injection into host cells. *Proc. Natl. Acad. Sci. U.S.A.* 102, 12548–12553.

Schmidt, A. M., Escher, U., Mousavi, S., Tegtmeyer, N., Boehm, M., Backert, S., et al. (2019). Immunopathological properties of the *Campylobacter jejuni* flagellins

and the adhesin CadF as assessed in a clinical murine infection model. *Gut Pathog.* 11:24. doi: 10.1186/s13099-019-0306-9

Schwarzbauer, J. E., Tamkun, J. W., Lemischka, I. R., and Hynes, R. O. (1983). Three different fibronectin mRNAs arise by alternative splicing within the coding region. *Cell* 35, 421–431.

Schwarz-Linek, U., Pilka, E. S., Pickford, A. R., Kim, J. H., Hook, M., Campbell, I. D., et al. (2004). High affinity streptococcal binding to human fibronectin requires specific recognition of sequential F1 modules. *J. Biol. Chem.* 279, 39017–39025.

Schwarz-Linek, U., Werner, J. M., Pickford, A. R., Gurusiddappa, S., Kim, J. H., Pilka, E. S., et al. (2003). Pathogenic bacteria attach to human fibronectin through a tandem beta-zipper. *Nature* 423, 177–181.

Schwerer, B. (2002). Antibodies against gangliosides: a link between preceding infection and immunopathogenesis of Guillain-Barré syndrome. *Microbes Infect.* 4, 373–384.

Scott, N. E., Marzook, N. B., Deutscher, A., Falconer, L., Crossett, B., Djordjevic, S. P., et al. (2010). Mass spectrometric characterization of the *Campylobacter jejuni* adherence factor CadF reveals post-translational processing that removes immunogenicity while retaining fibronectin binding. *Proteomics* 10, 277–288. doi: 10.1002/pmic.200900440

Sebald, M., and Véron, M. (1963). Base DNA content and classification of vibrios. *Ann. Inst. Pasteur (Paris)* 105, 897–910.

Sela, S., Aviv, A., Tovi, A., Burstein, I., Caparon, M. G., and Hanski, E. (1993). Protein F: an adhesin of *Streptococcus pyogenes* binds fibronectin via two distinct domains. *Mol. Microbiol.* 10, 1049–1055.

Shoaf-Sweeney, K. D., Larson, C. L., Tang, X., and Konkel, M. E. (2008). Identification of *Campylobacter jejuni* proteins recognized by maternal antibodies of chickens. *Appl. Environ. Microbiol.* 74, 6867–6875. doi: 10.1128/AEM.01097-08

Singh, P., Carraher, C., and Schwarzbauer, J. E. (2010). Assembly of fibronectin extracellular matrix. *Annu. Rev. Cell Dev. Biol.* 26, 397–419. doi: 10.1146/annurev-cellbio-100109-104020

Smith, M. L., Gourdon, D., Little, W. C., Kubow, K. E., Eguiluz, R. A., Luna-Morris, S., et al. (2007). Force-induced unfolding of fibronectin in the extracellular matrix of living cells. *PLoS Biol.* 5:e268.

Sory, M. P., and Cornelis, G. R. (1994). Translocation of a hybrid YopE-adenylate cyclase from *Yersinia enterocolitica* into HeLa cells. *Mol. Microbiol.* 14, 583–594.

Sottile, J., and Hocking, D. C. (2002). Fibronectin polymerization regulates the composition and stability of extracellular matrix fibrils and cell-matrix adhesions. *Mol. Biol. Cell* 13, 3546–3559.

Stones, D. H., and Krachler, A. M. (2015). Fatal attraction: how bacterial adhesins affect host signaling and what we can learn from them. *Int. J. Mol. Sci.* 16, 2626–2640. doi: 10.3390/ijms16022626

Stones, D. H., and Krachler, A. M. (2016). Against the tide: the role of bacterial adhesion in host colonization. *Biochem. Soc. Trans.* 44, 1571–1580.

Svedhem, A., and Kaijser, B. (1980). *Campylobacter fetus* subspecies *jejuni*: a common cause of diarrhea in Sweden. *J. Infect. Dis.* 142, 353–359.

Talukdar, P. K., Negretti, N. M., Turner, K. L., and Konkel, M. E. (2020). Molecular dissection of the *Campylobacter jejuni* CadF and FlpA virulence proteins in binding to host cell fibronectin. *Microorganisms* 8:389. doi: 10.3390/microorganisms8030389

Thelemann, A., Petti, F., Griffin, G., Iwata, K., Hunt, T., Settinari, T., et al. (2005). Phosphotyrosine signaling networks in epidermal growth factor receptor overexpressing squamous carcinoma cells. *Mol. Cell. Proteomics* 4, 356–376.

To, W. S., and Midwood, K. S. (2011). Plasma and cellular fibronectin: distinct and independent functions during tissue repair. *Fibrogenesis Tissue Repair* 4:21. doi: 10.1186/1755-1536-4-21

Tsang, T. M., Felek, S., and Krukonis, E. S. (2010). Ail binding to fibronectin facilitates *Yersinia pestis* binding to host cells and Yop delivery. *Infect. Immun.* 78, 3358–3368. doi: 10.1128/IAI.00238-10

Tu, Q. V., Mcguckin, M. A., and Mendz, G. L. (2008). *Campylobacter jejuni* response to human mucin MUC2: modulation of colonization and pathogenicity determinants. *J. Med. Microbiol.* 57, 795–802. doi: 10.1099/jmm.0.47752-0

Vaca, D. J., Thibau, A., Schutz, M., Kraiczy, P., Happonen, L., Malmstrom, J., et al. (2019). Interaction with the host: the role of fibronectin and extracellular matrix proteins in the adhesion of Gram-negative bacteria. *Med. Microbiol. Immunol.* doi: 10.1007/s00430-019-00644-3

van Spreeuwel, J. P., Duursma, G. C., Meijer, C. J., Bax, R., Rosekrans, P. C., and Lindeman, J. (1985). *Campylobacter* colitis: histological immunohistochemical and ultrastructural findings. *Gut* 26, 945–951.

von Heijne, G. (1985). Signal sequences. The limits of variation. *J. Mol. Biol.* 184, 99–105.

Walker, R. I., Schmauder-Chock, E. A., Parker, J. L., and Burr, D. (1988). Selective association and transport of *Campylobacter jejuni* through M cells of rabbit Peyer's patches. *Can. J. Microbiol.* 34, 1142–1147.

Wei, B., Kang, M., and Jang, H. K. (2019). Genetic characterization and epidemiological implications of *Campylobacter* isolates from wild birds in South Korea. *Transbound. Emerg. Dis.* 66, 56–65. doi: 10.1111/tbed.12931

Weinberg, S. H., Mair, D. B., and Lemmon, C. A. (2017). Mechanotransduction dynamics at the cell-matrix interface. *Biophys. J.* 112, 1962–1974. doi: 10.1016/j.bpj.2017.02.027

White, E. S., Baralle, F. E., and Muro, A. F. (2008). New insights into form and function of fibronectin splice variants. *J. Pathol.* 216, 1–14. doi: 10.1002/path.2388

Winnen, B., Schlumberger, M. C., Sturm, A., Schupbach, K., Siebenmann, S., Jenny, P., et al. (2008). Hierarchical effector protein transport by the *Salmonella* Typhimurium SPI-1 type III secretion system. *PLoS One* 3:e2178. doi: 10.1371/journal.pone.0002178

Wu, C. (2007). Focal adhesion: a focal point in current cell biology and molecular medicine. *Cell Adh. Migr.* 1, 13–18.

Zaidel-Bar, R., Milo, R., Kam, Z., and Geiger, B. (2007). A paxillin tyrosine phosphorylation switch regulates the assembly and form of cell-matrix adhesions. *J. Cell Sci.* 120, 137–148.

Ziprin, R. L., Young, C. R., Stanker, L. H., Hume, M. E., and Konkel, M. E. (1999). The absence of cecal colonization of chicks by a mutant of *Campylobacter jejuni* not expressing bacterial fibronectin-binding protein. *Avian Dis.* 43, 586–589.

Conflict of Interest: The authors declare that the research was conducted in the absence of any commercial or financial relationships that could be construed as a potential conflict of interest.

frontiers in Microbiology

ORIGINAL RESEARCH
published: 09 April 2020
doi: 10.3389/fmicb.2020.00541

"These Aren't the Strains You're Looking for": Recovery Bias of Common *Campylobacter jejuni* Subtypes in Mixed Cultures

Benjamin M. Hetman[1,2†], Steven K. Mutschall[3], Catherine D. Carrillo[4], James E. Thomas[1], Victor P. J. Gannon[2], G. Douglas Inglis[5] and Eduardo N. Taboada[6]*

[1] Department of Biological Sciences, University of Lethbridge, Lethbridge, AB, Canada, [2] National Microbiology Laboratory at Lethbridge, Public Health Agency of Canada, Lethbridge, AB, Canada, [3] National Centre for Animal Diseases, Canadian Food Inspection Agency, Lethbridge, AB, Canada, [4] Canadian Food Inspection Agency, Ottawa Laboratory (Carling), Ottawa, ON, Canada, [5] Lethbridge Research and Development Centre, Agriculture and Agri-Food Canada, Lethbridge, AB, Canada, [6] National Microbiology Laboratory, Public Health Agency of Canada, Winnipeg, MB, Canada

Microbiological surveillance of the food chain plays a critical role in improving our understanding of the distribution and circulation of food-borne pathogens along the farm to fork continuum toward the development of interventions to reduce the burden of illness. The application of molecular subtyping to bacterial isolates collected through surveillance has led to the identification of strains posing the greatest risk to public health. Past evidence suggests that enrichment methods for *Campylobacter jejuni*, a leading bacterial foodborne pathogen worldwide, may lead to the differential recovery of subtypes, obscuring our ability to infer the composition of a mixed-strain sample and potentially biasing prevalence estimates in surveillance data. To assess the extent of potential selection bias resulting from enrichment-based isolation methods, we compared enrichment and non-enrichment isolation of mixed subtype cultures of *C. jejuni*, followed by subtype-specific enumeration using both colony plate-counts and digital droplet PCR. Results differed from the null hypothesis that similar proportions of *C. jejuni* subtypes are recovered from both methods. Our results also indicated a significant effect of subtype prevalence on isolation frequency post-recovery, with the recovery of more common subtypes being consistently favored. This bias was exacerbated when an enrichment step was included in the isolation procedure. Taken together, our results emphasize the importance of selecting multiple colonies per sample, and where possible, the use of both enrichment and non-enrichment isolation procedures to maximize the likelihood of recovering multiple subtypes present in a sample. Moreover, the effects of subtype-specific recovery bias should be considered in the interpretation of strain prevalence data toward improved risk assessment from microbiological surveillance data.

Keywords: *Campylobacter jejuni*, microbiological surveillance, culture methods, enrichment, molecular subtyping

OPEN ACCESS

Edited by:
Ozan Gundogdu, University of London, United Kingdom

Reviewed by:
Komala Arsi, University of Arkansas, United States
Ben Pascoe, University of Bath, United Kingdom
Abdi Elmi, University of London, United Kingdom

****Correspondence:***
Eduardo N. Taboada
eduardo.taboada@canada.ca

†Present address:
Benjamin M. Hetman, Canadian Field Epidemiology Program, Center for Emergency Preparedness and Response, Public Health Agency of Canada, Ottawa, ON, Canada

Specialty section:
This article was submitted to Food Microbiology, a section of the journal Frontiers in Microbiology

Received: *25 November 2019*
Accepted: *12 March 2020*
Published: *09 April 2020*

Citation:
Hetman BM, Mutschall SK, Carrillo CD, Thomas JE, Gannon VPJ, Inglis GD and Taboada EN (2020) "These Aren't the Strains You're Looking for": Recovery Bias of Common Campylobacter jejuni Subtypes in Mixed Cultures. Front. Microbiol. 11:541. doi: 10.3389/fmicb.2020.00541

INTRODUCTION

Campylobacteriosis is among the leading bacterial foodborne infections worldwide, commonly manifesting as an inflammatory disease of the intestine, and sometimes results in bloody diarrheal syndrome, or more serious auto-immune sequelae (Acheson and Allos, 2001). The causative agents include several species from the genus *Campylobacter*, with the majority of infections attributed to *C. jejuni*. When adjusted for significant under-reporting, the per capita rate of campylobacteriosis cases in Canada was recently estimated to be 447 cases per 100,000 (Thomas et al., 2013), and it is among the most prevalent bacterial foodborne illnesses worldwide (Kaakoush et al., 2015). The epidemiology of *C. jejuni* is complex, with the majority of cases of human illness thought to be sporadic (Silva et al., 2011). Although it is generally accepted that consumption and handling of contaminated poultry products is the primary source of exposure leading to human infection, *C. jejuni* is found in a wide range of animal and environmental reservoirs (Williams and Oyarzabal, 2012; Whiley et al., 2013), providing additional routes for the introduction of *C. jejuni* into the food chain as well as non-food-related pathways of exposure (Pintar et al., 2016). Molecular subtyping of *C. jejuni* isolates recovered from samples throughout the food chain and the environment has helped to shed light on routes of transmission from various reservoirs to the human population, while providing important insights on the distribution and prevalence of *C. jejuni* subtypes that pose an increased risk to human health (Wilson et al., 2008; Müllner et al., 2009; Sheppard et al., 2009).

A significant challenge to any microbial surveillance program is ensuring that isolates obtained through sampling of the targeted reservoirs are representative of the population in circulation. To date, several studies have noted the potential for biased recovery in the isolation of foodborne pathogens such as *Listeria monocytogenes*, *Salmonella*, and *Campylobacter* (Gorski, 2012; Williams et al., 2012; Zilelidou et al., 2016). The use of different isolation protocols and media has been shown to influence the frequency of detection and can affect the diversity of *C. jejuni* subtypes observed in mixed-strain populations (Williams et al., 2012; Ugarte-Ruiz et al., 2013). A recovery step in enrichment broth was originally suggested for cases where low numbers of cells may be present (Hutchinson and Bolton, 1984), where cells may be under physiological stress (Bovill and Mackey, 1997), or to help resuscitate cells in the viable but non-culturable state (Jones et al., 1991). Subsequent culturing using antimicrobial supplements and incubation under microaerobic conditions is then used to enhance recovery of *Campylobacter* cells when competing background microflora may be present in the sample. Currently, enrichment media are widely adopted in *Campylobacter* isolation protocols from matrices such as meat, animal feces, and water, including standard methods recommended by the International Standard Organization (International Organization for Standardization, 2006) and the U.S. Food and Drug Administration (Hunt et al., 1998).

Several studies have compared non-enrichment and enrichment-based recovery methods and found that sample pre-enrichment could improve *Campylobacter* recovery over non-enrichment methods (Habib et al., 2011), as has been suggested for isolation from cattle feces (Garcia et al., 1985; Atabay et al., 1998; Stanley et al., 1998; Gharst et al., 2006). However, there is significant evidence suggesting that isolation methods employing a pre-enrichment step may favor certain subtypes and thus bias the subtype representation obtained (Devane et al., 2013; Ugarte-Ruiz et al., 2013). It is not known, however, to what extent different isolation methods affect the distribution of subtypes recovered from animal or environmental samples. If some subtypes are preferentially suited to growth under particular isolation conditions, this may affect downstream assessment of their relative prevalence. This outcome would obscure our understanding of the population circulating in various reservoirs and distort the assessment of their epidemiological significance and, ultimately, the public health risk that they present.

The objective of the current study was to examine the effects of culture conditions on the recovery of *C. jejuni* subtypes from multi-strain (i.e. mixed) samples. A significant challenge in assessing the effect of culture methods on the recovery of subtypes from naturally contaminated matrices is the inherent uncertainty in the composition and proportions of subtypes present in the original sample. To mitigate this uncertainty, we developed a controlled recovery experiment using normalized mixtures comprising defined *C. jejuni* subtypes in broth culture. Cells in these mixtures were re-isolated using enrichment and non-enrichment culture methods and the relative recoveries of each subtype were then measured by subtype-specific enumeration. This experimental set-up was used to test the hypothesis that enrichment-based culture methods differentially affect recovery in a subtype-dependent manner. It was also used to test the hypothesis that enrichment conditions preferentially select for *C. jejuni* strains representing common subtypes that are historically prevalent in Canadian surveillance data. Finally, to address uncertainty in the relative abundance of cells from each subtype at the start and throughout the progression of the experiment, we performed additional parallel overnight recovery on one of the strain mixtures and measured the relative amounts of DNA from each subtype in the total mixture using digital-droplet PCR.

MATERIALS AND METHODS

Identification of *Campylobacter* Subtypes for Recovery Experiments

Subtypes from the Canadian *Campylobacter* Comparative Genomic Fingerprinting database (C3GFdb) were ranked by frequency and assessed for sources of isolation. Data for non-human sample sources were aggregated into six major groups consisting of: "Cattle," "Poultry," "Environmental," "Other Bird," "Other Animal," and "Other Food" in order to compare the source distributions of the ten most common subtypes from each database. *Campylobacter* isolate data from the C3GFdb was examined to identify three "common" or prevalent subtypes; an additional set of nine "uncommon" or rare subtypes was also identified. Three multi-strain

mixtures comprising four strains from distinct CGF subtypes were designed for controlled recovery experiments, which allowed for subtype-specific enumeration. Each mixture was chosen to be representative of a variety of sampling sources (**Table 1**) and designed to contain one common and three uncommon subtypes in order to test the hypothesis that subtypes exhibit different rates of recovery. Relative subtype prevalence was confirmed using data from the international *Campylobacter* pubMLST database (Jolley and Maiden, 2010) where possible.

Preparation of Pooled Spike-in Mixtures for Recovery Experiments

Pure cultures of the 12 selected *C. jejuni* strains were revived from frozen glycerol stocks stored at −80°C by sub-culturing a 20 μl loop of frozen culture into brain heart infusion broth (BHIB; Fisher Oxoid CM1135), and incubating for 24 h in a tri-gas (85% N_2, 10% CO_2, 5% O_2) microaerobic atmosphere (MAA) incubator at 42°C. A 100 μl aliquot was then spread onto blood agar (BD 211037, BBL infusion agar base supplemented with 7% sheep blood) and grown overnight in MAA for subsequent culture harvesting and DNA extraction for CGF analysis to verify the subtype as described below. Following CGF verification, a 20 μl loop of the remaining culture was harvested and re-cultured into BHIB for 24 h and growth was assessed spectrophotometrically by measuring the optical density at 600 nm (OD_{600}). Cultures selected for each sample mixture were normalized to a consistent optical density using sterile BHIB, and 1 ml volumes from each of the normalized broth cultures were co-inoculated into 10 ml of phosphate-buffered saline (1 × PBS, pH 7.5) to create the multi-strain spike-in mixture. This procedure was repeated in duplicate for each of the three strain mixtures. Pooled samples were then vortexed, and ten-fold serial dilutions from 10^{-1} to 10^{-5} were prepared in BHIB.

Recovery of Isolates From Spike-in Experiments

Non-enrichment Method

For each of the three pooled sample mixtures, 100 μl from each dilution was spread onto five petri dishes containing Charcoal-Cefoperazone Deoxycholate Agar (CCDA) (Fisher Oxoid CM0739) without antibiotic supplement, and incubated in MAA at 42°C. After 24–48 h, dishes were assessed for suitable growth (e.g. containing approximately 20 to 50 well-formed, separate colonies per dish) and the dilution series that best matched suitable growth was selected for subsequent steps. Culture dishes were shuffled into random order, and a total of 100 colonies were arbitrarily chosen by selecting every isolate from the first and subsequent dishes until a total of 100 colonies were selected. Each of these colonies were then individually streaked to a petri dish containing CCDA. Following 24–48 h of incubation on CCDA in MAA at 42°C, cells originating from single isolated colonies were sub-cultured onto BBL blood agar and grown in MAA at 42°C for 24–48 h for subsequent DNA extraction.

Enrichment Method

To test the effects of including an enrichment step on subtype recovery from the pooled sample mixtures, 100 μl from each dilution of the spike-in mixture was first transferred to 20 ml of Bolton Broth (BB) (Fisher Oxoid CM983) with modified BB supplement (Fisher Oxoid SR0208E) and incubated for 24 h in a MAA at 42°C. Following enrichment, 100 μl of liquid BB culture was then processed in the same manner as described above.

DNA Extraction and Subtype Verification by PCR

Cell biomass was harvested from BBL blood agar using a 20 μl loop and genomic DNA was extracted using a modified protocol of the Epicenter Masterpure DNA Extraction kit (Epicenter MC85200). Briefly, biomass was suspended into 300 μl of Cell and Tissue Lysis Solution (MTC096H) containing RNAaseA (1 μl, 5 mg/ml) and proteinase K (5 μl, 50 mg/ml) and heated at 65°C for up to 60 min to allow lysates to clear. Samples were then cooled on ice and 175 μl of chilled MPC protein precipitation solution (MMP095H) was added to each sample, followed by vortexing and centrifugation to remove cellular debris. Ethanol precipitation was used to recover the DNA from the resulting supernatant. The DNA pellets were suspended in buffer containing 1 × Tris-EDTA (pH 8.0) and stored at −20°C until verification by Comparative Genomic Fingerprinting (CGF) (Taboada et al., 2012). To determine the frequency of recovery for each of the four subtypes an abbreviated version of the 40-loci CGF assay, based on a subset of two of the eight five-plex PCRs required for the assay, was used to partially subtype each isolate to facilitate subtype-specific enumeration.

Investigating Growth Dynamics in Mixed Culture Using Digital Droplet PCR (ddPCR)

Primer Design

The growth dynamics of mixture "C", containing *C. jejuni* strains 07_1875, CI_4820, CE_R_11_0073, and CE_R_11_0249 were investigated using ddPCR. Diagnostic loci for each *C. jejuni* strain were identified by comparison of their CGF subtypes and identifying loci unique to each subtype within the four-strain mixture. Primers and probes were then designed for these sequences using the online version of Primer3[1]. The sequence of a single-copy conserved core gene (*cj0102*) was identified from draft whole-genome sequence analysis (unpublished work) and used as a control in the ddPCR experiment. Primer and probe sequences for each marker are listed in **Table 2**.

Growth Dynamics Experiments

Pure broth cultures for each strain were prepared and normalized using the same methods as described above. Ten milliliters from each normalized culture were then combined and vortexed to create the spike-in inoculum, and 1 ml from the mixture was added to each of 18 tubes containing 25 ml BB (i.e. "enrichment) and 18 tubes containing 25 ml BHI (i.e. "non-enrichment").

[1]https://primer3.org/

TABLE 1 | Strains of *C. jejuni* used in this study and colony counts from repeated microbiological recovery experiments.

Mixture[†]	Strain	Source[‡]	CGF Subtype	C3GFdb frequency and rank[¥]	MLST[§]	Non-enrichment Recovery		Enrichment Recovery	
						Trial 1 (*n* = 100)	Trial 2 (*n* = 88)	Trial 1 (*n* = 100)	Trial 2 (*n* = 83)
A	CI_5178	W	957.1.1	274 (1)	ST-45	42	52	90	73
A	CI_4685	W	844.3.1	13 (2)	ST-692	12	11	6	10
A	CI_5043	W	540.1.3	3 (3)	ST-1224	31	18	2	0
A	CI_5039	W	540.1.4	1 (4)	ST-4029	15	7	2	0
						Trial 1 (*n* = 99)	Trial 2 (*n* = 100)	Trial 1 (*n* = 99)	Trial 2 (*n* = 100)
B	CE_M_10_4053	P	169.1.2	593 (1)	ST-982	32	26	45	49
B	CI_2669	W	782.4.2	27 (2)	ST-2524	20	28	16	17
B	07_2680	H	83.7.1	38 (3)	ST-918	18	16	8	5
B	CGY_HR_241	H	27.1.3	24 (4)	ST-452	29	30	30	29
						Trial 1 (*n* = 98)	Trial 2 (*n* = 98)	Trial 1 (*n* = 99)	Trial 2 (*n* = 99)
C	07_1875	H	735.5.1	217 (1)	ST-42	34	18	52	53
C	CI_4820	W	812.2.1	51 (2)	ST-42	23	46	21	29
C	CE_R_11_0073	P	18.1.2	71 (3)	ST-1698	13	12	0	1
C	CE_R_11_0249	P	123.1.2	67 (4)	ST-51	28	22	26	16

[†]*Mixture indicates the pooled strain mixtures used in recovery experiments.* [‡]*Source: W – Water; P – Poultry; H – Human.* [¥]*Subtype frequency indicates the number of isolates of matching subtype in the Canadian Campylobacter Comparative Genomic Fingerprinting database (C3GFdb). Rank number in parentheses indicates rank given to each subtype within its mixture, corresponding to the respective frequency of its subtype cluster in the C3GFdb.* [§] *MLST Sequence Type.*

TABLE 2 | Sequences and modifications of primers and probes designed for digital droplet PCR assay.

Strain	Target	Product	Sequence	Modification
CE_R_11_0249	cj0033-F	Primer	TGGGATAAAAGGGGTGAGAA	
	cj0033-R	Primer	CGTGAAGCCAAGTAAAACCAA	
	cj0033-Hyb	Probe	TGTTTCGAGAATTCGGGATTTTATGG	FAM
All (Control)	Cj0102-F	Primer	CAAAGCACAAAAAGTGAGATTT	
	Cj0102-R	Primer	CAACATTGTGAATAAGCTCCAT	
	Cj0102-Hyb	Probe	TGCTCCTTATGCAAAAGGTGGT	HEX
CI_4820	cj0569-F	Primer	TTGGTTTGGACATTTAGCATC	
	cj0569-R	Primer	GCTAGTGTTTGTCTATGTTGTC	
	cj0569-Hyb	Probe	TGATTGGTGTGGATCTAGTGGAGG	FAM
CE_R_11_0073	cj1431c-F	Primer	AATTGCAGGAAGGGATGATG	
	cj1431c-R	Primer	CAAATTTGCCCAAGGAATCA	
	cj1431c-Hyb	Probe	TGGTTTTAAATTCGGTTTTGTATGGAGA	FAM
07_1875	cj1550c-F	Primer	GGAAAGATGGTTGAATGGAAAG	
	cj1550c-R	Primer	TCTAAGGCTAACAAAGCATCG	
	cj1550c-Hyb	Probe	AGCAAGTAATGTGAATATGCCTAGCGT	FAM

Tubes were then vortexed and incubated in MAA at 42°C. At 4-h intervals, three tubes of each BB and BHI were removed for ddPCR analysis. Tubes were centrifuged at 9000RPM for 10 min and after discarding of the supernatant, DNA was extracted from the remaining cell pellet as described above.

Quantification by ddPCR

Genomic DNA from each of the samples in the overnight trial was quantified using the Quant-iT broad-range DNA quantification kit (Thermo Fisher Scientific Q33130) following manufacturer's specifications. The DNA was then diluted to 10 ng/ul in water and digested using NciI for approximately 120 min at 37°C. Digested DNA was then diluted to 0.002 ng/ul for use in the generation of droplets following the manufacturer's recommendations (Bio-Rad Qx100), then used in a 40-cycle PCR with the following settings: pre-denature (95°C) 10 min; denature (94°C) 30 s; annealing (60°C) 30 s; extension (60°C) 1 min; inactivation (98°C) 10 min. The final PCR product

was then loaded and read using the ddPCR droplet reader (Bio-Rad QX100).

Statistical Analyses

Statistical analyses were performed using the R language for statistical computing (version 3.3.1) (R Core Team, 2016). Unless otherwise indicated, all tests were performed using a Type I error rate of $\alpha = 0.05$. Figures were generated from results using the R package ggplot2 (Wickham and Winston, 2015).

Analysis of Effect of Isolation Method

The Chi-square goodness of fit test ("chisq.test") was used to assess the hypothesis that isolates from each subtype would be recovered in equal proportions under both enrichment and non-enrichment isolation methods. Analysis of variance ("aov") was performed to test the null hypothesis that isolation protocol had no effect on the distribution of recovered isolates from each mixture across each of two independent trials. The dependent variable assessed was the recovered frequency of each subtype, and the effects of "subtype" and "isolation method" were assessed as independent variables.

Analysis of Effect of Cluster Size

To assess the relationship of historic subtype prevalence (i.e. cluster size) on the frequency of subtypes recovered post-isolation, the strains within each mixture were assigned a descending rank based on the size of the CGF subtype cluster from which they were derived (e.g. ranked one to four, with "Rank 1" corresponding to the CGF cluster containing the greatest number of isolates) (**Table 1**). Analysis of variance was then used to assess the difference between the frequency of isolates recovered from each rank, and whether there was a significant effect of isolation method on this recovery.

Comparison of Mean Cell Counts From ddPCR

Copy number results from the ddPCR analysis for each diagnostic marker were compared against those from the control marker (cj0102) to establish relative amounts of DNA in the total mixture corresponding to each strain. These ratios were then corrected so that each strain accounted for 25% of the total mixture at initiation of the recovery experiment (time = 0h). For each subsequent measurement, the ratio of marker to control was divided by the total abundance of the four strains in the mixture to establish the amount of DNA relative to each strain in the mixture at each time point. These results were then averaged across the triplicate trials, and the mean relative abundance for each strain was compared between enrichment and non-enrichment recovery methods at each time point using the Student's *t*-test in R ("*t*.test") to identify significant differences in relative strain abundance.

Analysis of Probability of Recovering Multiple Subtypes From a Mixed Sample

Experimental frequencies from each subtype rank were averaged to establish the mean probability of successfully selecting each subtype based on picking one colony from a mixed plate post recovery using both enrichment and non-enrichment methods. These probabilities were then combined to compare posterior binomial probabilities of selecting at least one of each subtype from a mixed plate after each recovery method as a function of the total number of colonies sampled.

RESULTS

Analysis of Subtype Prevalence in *Campylobacter* Databases

At the time of writing (Oct. 2019), the C3GFdb contained information on a pan-Canadian collection of 23,142 isolates comprising 5,037 distinct CGF subtypes from a wide range of sources including animal, human, and environmental origin. Similarly, the *Campylobacter* pubMLST database contained information on 72,806 *Campylobacter* isolates with 9,778 distinct Sequence Types (STs), also from a diverse range of international sources. Examination of the distribution of subtype frequencies observed within these databases revealed that a small number of subtypes have contributed disproportionately toward the overall number of entries in each database (**Figure 1**). For example, the ten most common subtypes accounted for 22% (n = 5099/23142) of the total isolates in the C3GFdb, with 73% (n = 3685/5037) of CGF subtypes observed in only single isolates ("singletons"), and over 92% of subtypes (n = 4648/5037) representing small clusters of five or fewer isolates. A similar trend was observed in the pubMLST database, whereby the ten most common subtypes represented nearly 27% (n = 19542/72806) of the total isolates in the collection. Meanwhile, nearly 66% of subtypes in this database (n = 6445/9778) had only been observed as singletons, and over 91% of subtypes (n = 8952/9778) representing small clusters of five or fewer isolates. To explore whether the subtype distribution observed in both the C3GFdb and pubMLST was associated with single-source sampling, we assessed the source distributions of the ten most prevalent subtypes in each database, in order to identify any subtypes with very narrow source range. No evidence of source restriction was observed among prevalent subtypes, as each one represented isolates derived from human and multiple non-human sources (**Figure 2**).

Microbiological Competitive Recovery Experiments

In each of the pooled mixtures, the mean number of isolates from a single dominant subtype increased following an enrichment step, compared to isolates from the remaining three subtypes, which collectively decreased in relative frequency of recovery (**Table 1** and **Figure 3A**). Chi-square goodness of fit test showed a significant deviation from the null hypothesis that equal or similar proportions of isolates from each of the 12 strains tested would be recovered after both non-enrichment (χ^2 = 99.23, df = 11, $p < 0.0001$) and enrichment (χ^2 = 572.37, df = 11, $p < 0.0001$) isolation procedures. Analysis of variance indicated that a significant difference ($p < 0.0001$) existed between the total number of recovered isolates for each subtype within each of mixtures A-C, and an interaction was observed between subtype and isolation method ($p < 0.0001$), suggesting that

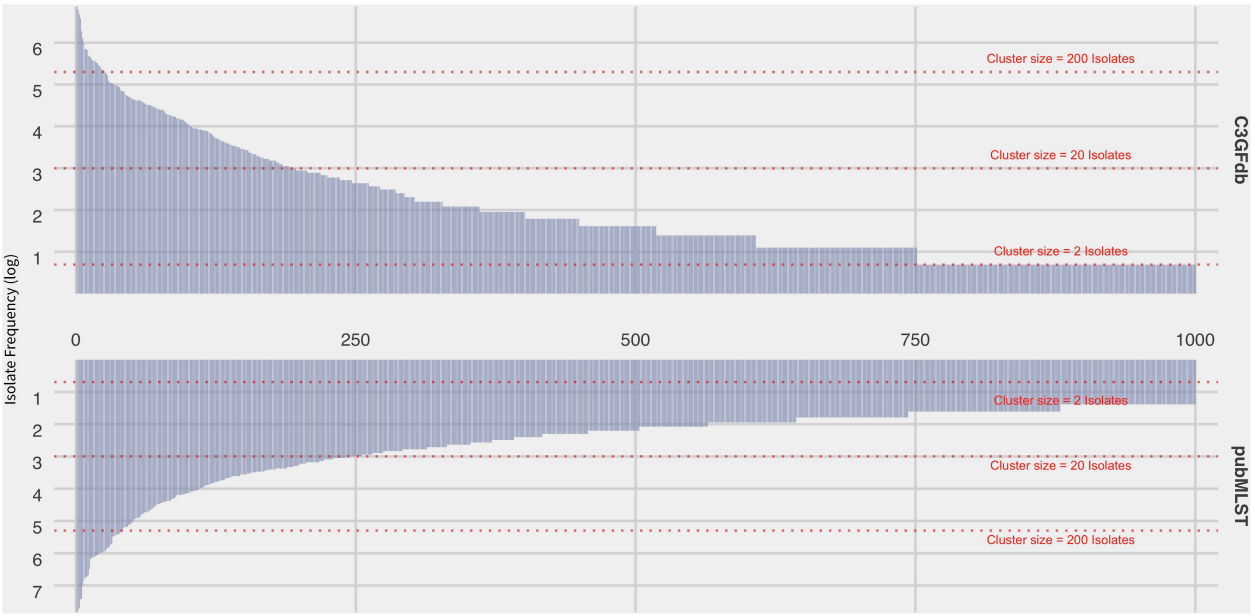

FIGURE 1 | Frequency distribution of subtype clusters from the Canadian *Campylobacter* Comparative Genomic Fingerprinting database (C3GFdb) and the *C. jejuni* Multilocus Sequence Type database (pubMLST). Each bar along the horizontal axis represents a unique C3GFdb Comparative Genomic Fingerprint subtype or MLST Sequence Type. The top 1000 subtypes, in descending order by overall frequency, are shown. Visual guides are provided to indicate various cluster size ranges. A log scale is used.

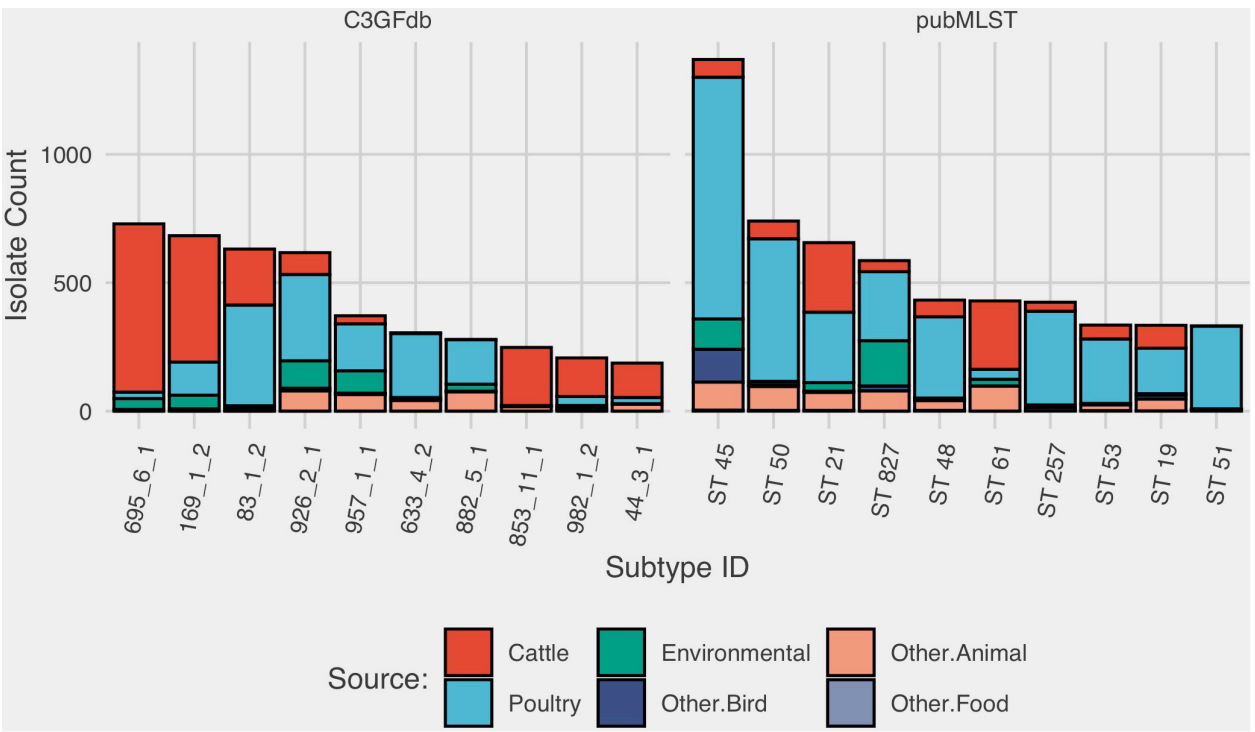

FIGURE 2 | Source-distribution bias among common subtypes in the Canadian *Campylobacter* Comparative Genomic Fingerprinting and the *C. jejuni* Multilocus Sequence Type databases. Each bar along the horizontal axis represents a unique Comparative Genomic Fingerprint subtype or MLST Sequence Type. The top 10 subtypes, in descending order by overall frequency, are shown.

the mean frequency of recovered subtypes differed based on the isolation method used (**Table 1** and **Figure 3A**). Follow-up pairwise analyses indicated that the recovery of strains CI_5178 (mixture A) and 07_1875 (mixture C) differed significantly based on isolation method used ($p = 0.0012$ and $p = 0.0265$, respectively). The frequency of strain CI_5043 (mixture B) did not differ significantly at a 95% significance level ($p = 0.0762$), but this result still suggested that isolation method may affect the recovery frequency of this strain.

When ranked as a function of subtype cluster frequency from the C3GFdb, the mean number of isolates from subtypes designated "Rank 1" increased from 34.00 (95% CI: 21.5–46.5) following non-enrichment recovery to 60.3 (95% CI: 42.0–78.7) following enrichment (**Figure 3B**). A significant effect for the recovery of isolates was found for "Subtype Rank" ($p < 0.0001$), and follow-up analyses revealed that subtypes selected from "Rank 1" in each experimental mixture were recovered in higher amounts than any of the three remaining subtypes ($p < 0.0001$) while no differences were found between the recovery of isolates from subtypes ranked two to four. Furthermore, when including the effect of "Isolation Method" in the model (i.e. enrichment vs. non-enrichment), an interaction with "Subtype Rank" was found ($p = 0.0002$), suggesting that the recovery of isolates based on subtype ranking significantly differed based on the isolation method used. Post hoc follow-up indicated that only the recovery of subtypes from the largest subtype clusters ("Rank 1") differed significantly as a function of isolation method ($p = 0.0048$), suggesting that isolates from the largest clusters were recovered at a significantly higher frequency when an enrichment step was used in the isolation procedure (**Figure 3B**).

Quantification of Strain-Specific DNA in Mixed Culture Using Digital Droplet PCR

After 4 h in non-enrichment recovery, moderate differences were observed between the growth rates of the four strains in mixture C, with final relative abundances ranging from 13.3 to 35.3% after 24 h (**Figure 4**). Under enrichment conditions in BB, the differences in relative abundances of the four strains were much more pronounced. After 8 h of incubation in BB, the relative amounts of strain 07_1875 increased disproportionately to the other strains in mixture C. At the final measurement of 24 h, *C. jejuni* strain 07_1875 comprised almost 67% of the total DNA in the mixture. This is in contrast to the other three strains in the mixture, with each experiencing a decline in relative abundance after the 8-h incubation measurement. Several significant differences in measurements were observed when comparing the relative abundances for each strain between enrichment and non-enrichment recovery methods. In particular, the growth of strain 07_1875 significantly increased under enrichment starting at the 12-h mark when compared to the growth of the same strain under non-enrichment. By contrast, strains CI_4820, CE_R_11_0073, and CE_R_11_0249 demonstrated significantly lower relative abundances in the enrichment recovery compared to non-enrichment, beginning at the eight, 16 and 24-h time-points, respectively (**Figure 4**).

Predicted Probability of Recovering Multiple Subtypes From Mixed Samples

A binomial probability distribution was constructed based on the results of ranked recoveries to assess the posterior probability of recovering colonies from all four subtypes present in a sample mixture by either enrichment or non-enrichment isolation methods. Under non-enrichment isolation, we found that a selection of a minimum of 18 isolates was required to recover at least one colony from each of four subtypes present with 95% probability. By contrast, when performing isolation following a pre-enrichment step, the selection of 109 colonies was required to recover at least one colony from each subtype with 95% probability (**Figure 5**).

DISCUSSION

Studies assessing the prevalence of *C. jejuni* subtypes from animal, food and environmental sources have shown that a select number of subtypes are commonly found; globally, the most consistent of these lineages have been characterized as belonging to MLST sequence types ST-45 and ST-21 (Dingle et al., 2002; Kwan et al., 2008; Sheppard et al., 2009; Müllner et al., 2010; Gripp et al., 2011). These subtypes are often characterized by their diverse host association and high prevalence worldwide and have thus been termed "generalists" due to their pervasive nature across ecologic niches and apparent adaptability to diverse conditions (Sheppard et al., 2011, 2013). Although high frequency of isolation of certain subtypes may be truly reflective of their prevalence throughout the sampled environments, it is also possible that augmented rates of recovery observed for some subtypes may at least be partly due to the selective advantage conferred by the isolation method used. Anecdotally, we have previously observed limited genotypic diversity among isolates recovered from water samples potentially impacted by agricultural activities and thus expected to reflect these inputs. To experimentally address the possibility of subtype-specific recovery bias, we empirically assessed the effects of a commonly used enrichment-based culture method on the recovery of *C. jejuni* subtypes *in-vitro* from multi-strain samples using select isolates from Canadian surveillance (i.e. C3GFdb).

Recovery experiments were performed under controlled laboratory conditions using sterile Bolton's enrichment broth (BB) spiked with normalized quantities of broth culture from four *C. jejuni* strains of known subtype. While previous studies have documented differences in genotype diversity when comparing isolation procedures (Devane et al., 2013; Ugarte-Ruiz et al., 2013), our experimental design included several features selected to avoid confounding factors related to the analysis of field-collected samples. These included: (a) the use of mixtures composed of known *Campylobacter* subtypes, which avoided complications related with the analysis of samples comprising unknown subtype composition; (b) the use of controlled culture conditions, which avoided issues related to different sample matrices or background organisms present in samples collected from the field; (c) the use of BB, which was selected for this study because it was used in the original

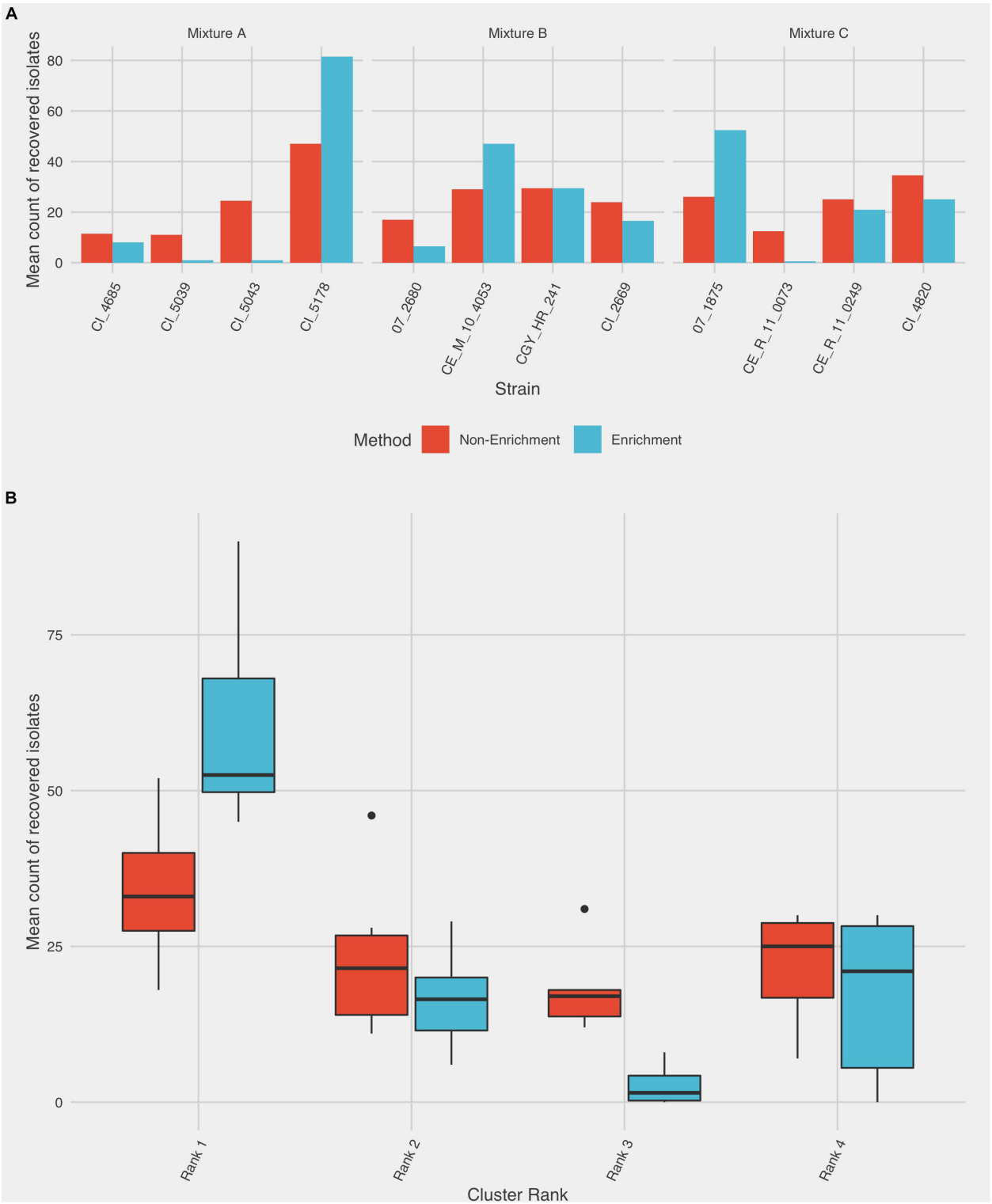

FIGURE 3 | Summary of *C. jejuni* subtype recovery using enrichment and non-enrichment. Colonies were recovered from three different mixtures comprising strains from four distinct CGF subtypes using enrichment and non-enrichment methods and subjected to subtype-specific enumeration to assess relative rates of recovery. Each mixture was tested in duplicate; the frequency of isolation is based on 100 colonies selected per replicate. **(A)** The average frequency of recovery between the two trials is shown for each strain. **(B)** Frequency of recovery by subtype ranking, which was derived from prevalence in the Canadian *Campylobacter* Comparative Genomic Fingerprinting database (C3GFdb). Boxes represent the first and third quartiles and are split by a line representing the median; whiskers extend to 1.5x the interquartile range of the data. Outliers outside of this range are denoted individually as points.

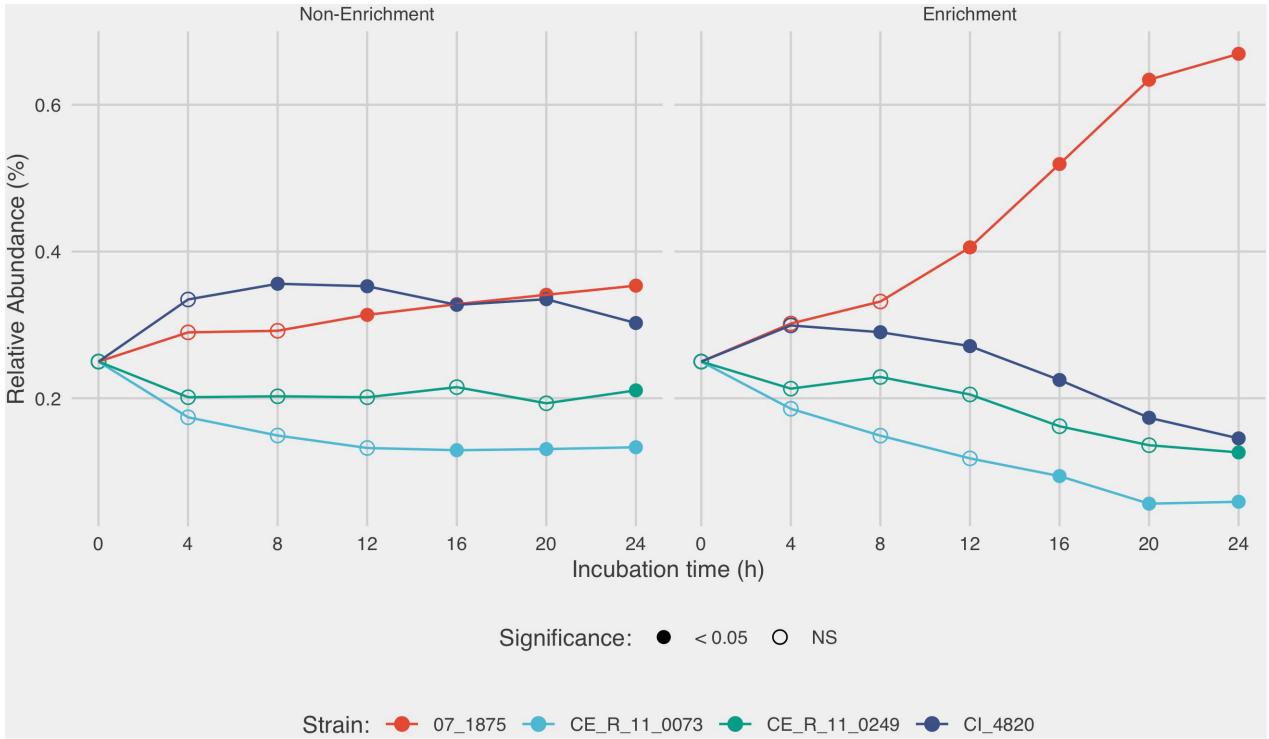

FIGURE 4 | Analysis of growth dynamics of a mixed culture under enrichment and non-enrichment conditions via digital droplet PCR (ddPCR). Strain mixture "C" was grown in enrichment and non-enrichment broth with DNA extracted at 4-h intervals over a 24-h incubation period. For each time point, strain specific-DNA was quantified using ddPCR to estimate mean relative abundance of each strain in the mixture. After 4 h in non-enrichment recovery, moderate differences were observed between the growth rates of the four strains, with final relative abundances ranging from 13.3 to 35.3% after 24 h. The mean of three replicates is shown. Filled circles denote time points in which there is significant difference ($p < 0.05$) in relative abundance between enrichment and non-enrichment recovery methods.

culturing of isolates used in our experiments; BB is one of the most widely used enrichment mediums for the culturing of *Campylobacter* species and it is recommended for use by the International Standard Organization (International Organization for Standardization, 2006) and the U.S. Food and Drug Administration (Hunt et al., 1998).

Under the null hypothesis that no recovery bias exists for either the enrichment or non-enrichment isolation method, the recovery of similar proportions of each of the four subtypes within each cohort was expected. While we anticipated that recovery using enrichment may bias the growth of particular *C. jejuni* strains, surprisingly, we observed significant variation in the recovery of the four strains present after non-enrichment recovery as well. This variation was likely in part due to limitations in the experimental set-up (e.g. normalization of bacterial inoculum using OD_{600}, inherent differences in growth rate between the individual strains, stochastic variation, etc.). However, similar co-culturing experiments have shown biased growth competition between strains independent of growth rate or initial inoculum, illustrating complex inter-strain dynamics (Mellefont et al., 2008; Zilelidou et al., 2015). Importantly, the results from the non-enrichment isolation experiments in this study served as a useful baseline for assessing results from the enrichment-based recovery experiments. In all enrichment recovery experiments conducted, we observed a statistically significant deviation from the null hypothesis, and the extent of this bias was much more pronounced compared to that observed when using the non-enrichment isolation procedure. This suggests that employing an enrichment step may preferentially enhance the recovery of particular subtypes either by directly favoring their growth or by hampering the growth of others.

The experimental design of the recovery experiments only included measurement by spectrophotometer (OD_{600}) to provide estimates for normalizing strain concentrations prior to pooling the starting inoculum. To deliver more quantifiable evidence for the differences in strain growth dynamics under enrichment and non-enrichment, we designed an additional experiment for one of the strain mixtures using a digital droplet PCR system (ddPCR). Using a similar experimental design, including normalization of broth inoculum via OD_{600}, we again noticed variation in copy number estimates of each strain at $t = 0$; these initial estimates ranged from 18-31% of the total abundance of the original inoculum. These results indicated that, as expected, OD_{600} alone provided an insufficient means of normalizing concentrations of the broth cultures. However, one of the advantages of the ddPCR approach was the ability to control for these discrepancies in the analysis stage, thereby providing estimates of relative strain growth unaffected by the differences in the original inoculum. After applying analytical input controls, we still observed trends in the growth of the

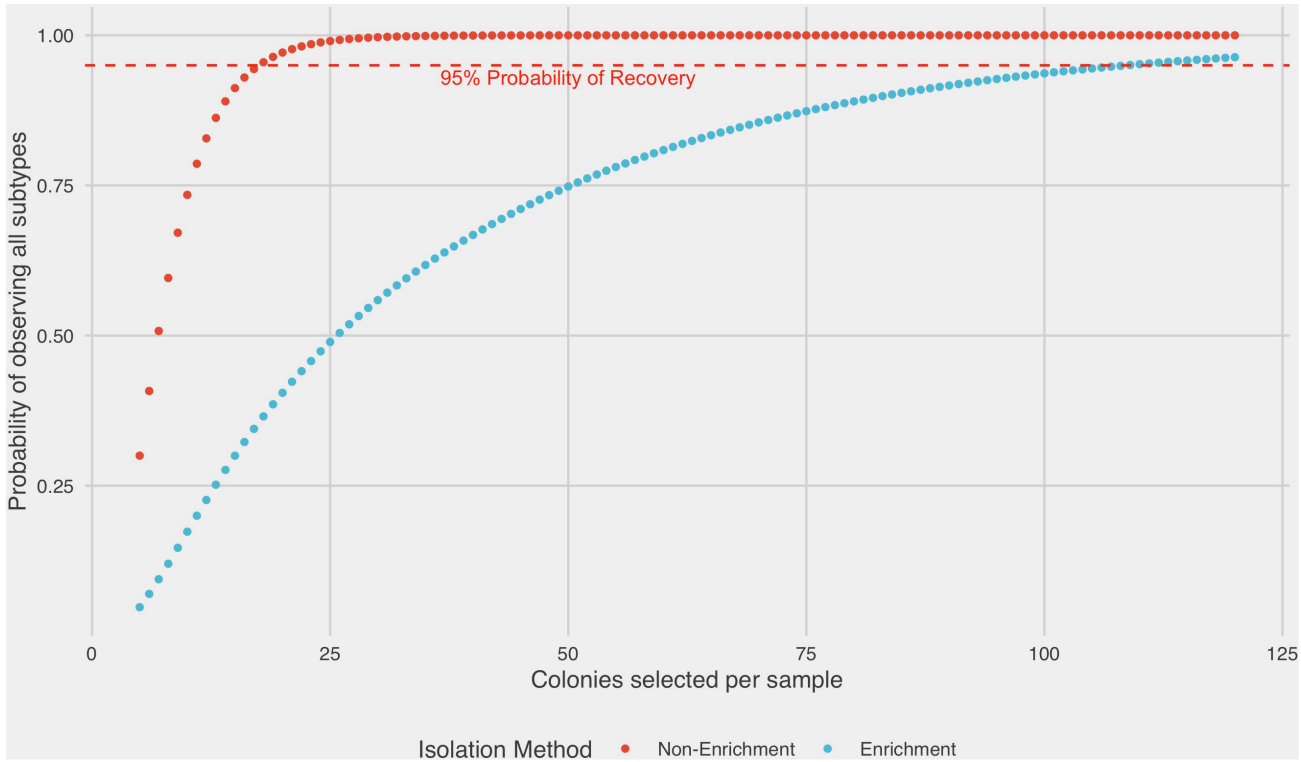

FIGURE 5 | Binomial probability distribution of selecting all subtypes present in a mixed sample as a function of isolation protocol. A minimum of 18 colonies would need to be selected in order to recover at least one colony from each subtype in a four-strain mixed sample by non-enrichment isolation (95% probability level). In contrast, 109 colonies would be required to recover at least one colony from each subtype by enrichment.

four strains in mixture similar to that seen in the culturing experiments, suggesting that overall, the results from the original microbiological culturing methods were likely sound, although the exact estimates should be interpreted with caution. As observed in the original experiments, we observed significant differences in the growth profiles of the four strains measured using ddPCR that were exacerbated by the use of enrichment media. The clinical strain 07_1875 performed significantly better under enrichment conditions compared to the remaining strains, whose growth by comparison seemed to suffer under enrichment. Interestingly, at $t = 24$ h, the order of relative abundance for each strain remained constant under both recovery methods, though magnitudes differed significantly, suggesting that each of these four strains may have inherently different growth rates under the laboratory conditions used.

To test the hypothesis that high subtype frequency in surveillance data may at least in part reflect selection bias under laboratory conditions, overall recovery frequencies from all microbiological recovery experiments were compared by assigning the subtypes in each mixture a rank in descending order from "1" to "4" corresponding to the relative frequency of each subtype in the C3GFdb. We observed a substantial difference in recovery frequency when comparing the results from non-enrichment isolation versus enrichment noting that the "Rank 1" subtypes increased in frequency from 40.5% of recovered isolates using non-enrichment recovery to 62.4% under enrichment. This is in contrast to the frequency of recovery observed for the remaining subtypes (Ranks 2, 3 and 4), which collectively decreased from 59.5% of the population recovered by non-enrichment isolation to 37.6% of isolates by enrichment. These results are consistent with studies by Williams et al. (2012) and Ugarte-Ruiz et al. (2013) in which they assessed the genotype diversity of *C. jejuni* isolated from poultry samples using a variety of isolation protocols and found method-specific differences in the genotypes and numbers of isolates observed. They concluded that enrichment methods, in particular, limit the "genotypic richness" of the population recovered (Williams et al., 2012; Ugarte-Ruiz et al., 2013). In contrast to using natural samples for experimentation, our controlled experimental set-up allowed us to examine the nature of these findings more directly owing to the removal of potential confounders when dealing with recovery of isolates from samples of unknown strain composition.

A primary concern was that the physiology of isolates sampled from different ecologies may impact their performance in the laboratory, e.g. isolates recovered from river water may not perform well at laboratory temperatures that more closely reflect those of avian or human intestinal tracts. Thus, in designing each of the experimental strain mixtures, we attempted to mitigate effects related to the original source of sampling by creating mixtures that contained isolates sampled from environmental, food-animal, and human clinical sources. As such, when selecting isolates from highly prevalent subtypes, we attempted to ensure

that mixtures represented isolates from subtypes of both single and mixed origins. Our results did not appear to indicate systematic bias related to the original sampling source of isolates used in our experiments, though a separate analysis would be required to fully assess this.

While it may not be surprising that certain subtypes could be better adapted to laboratory conditions, leading to higher isolation frequencies in microbiological surveillance, the more significant implication is the much-reduced chance of recovery of other subtypes as a result of being out-competed under standard isolation conditions. The international standard ISO 10272:2006 recommends up to 5 well-formed colonies be selected for subtyping analysis (International Organization for Standardization, 2006; Habib et al., 2011). We have recently shown that specialized isolation methods resulted in a greater than 2-fold increase in culture-positive diarrheic stools in samples submitted for diagnostic testing in Southwestern Alberta when compared to conventional diagnostic methods used across Canada (Inglis et al., 2019). Anecdotally, many laboratories operate under a resource-constrained environment that may preclude implementing this recommendation. Based on the frequencies of each subtype rank from our experimental results, we found that selecting only five colonies resulted in a 70% chance of missing at least one of the subtypes present in a mixed-strain sample when performing recovery without BB enrichment, and this rose to 95% when using enrichment with BB. Our model suggests that in order to increase the likelihood of identifying less common subtypes recovery protocols should include: (1) employing culturing methods that do not contain an enrichment step or performing parallel enrichment- and a non-enrichment-based methodologies, and (2) increasing the number of colonies selected for subtyping. However, the results derived here should be interpreted with caution, given practical limitations surrounding laboratory procedures in these experiments and the need for more comprehensive examination of the kind of dynamics described here using a wider selection of strains and additional culture conditions, which should be performed to determine the extent of potential bias in surveillance data.

CONCLUSION

Findings from the current study demonstrate that culture methods for the isolation of *C. jejuni* can bias the recovery frequency of isolates from mixed strain samples by obscuring the presence of less common subtypes while over-representing others, an effect that can be exacerbated by the use of enrichment-based protocols. Importantly, this bias may compromise our ability to identify subtypes of high public health significance but low adaptation to laboratory conditions. Although this is not likely to have a direct impact on patient treatment given the lack of routine *C. jejuni* subtyping to inform diagnosis or epidemiological follow-up in most jurisdictions, microbiological surveillance can play an essential role in the development of mitigation strategies to reduce the incidence of campylobacteriosis through the identification of potential sources of exposure, transmission vehicles, and reservoirs. Our findings underscore the need for further research to help minimize bias from findings based on culture-based microbiological surveillance.

DATA AVAILABILITY STATEMENT

The raw data supporting the conclusions of this article will be made available by the authors, without undue reservation, to any qualified researcher.

AUTHOR CONTRIBUTIONS

BH participated in all aspects of laboratory and downstream analyses and drafted the manuscript. SM participated in laboratory work and drafting the manuscript. CC, JT, GI, VG, and ET contributed to study design, funding and/or writing the manuscript.

FUNDING

Financial support for this work was provided through the Alberta Livestock and Meat Agency (project 2012F034R) and through the Government of Canada's Genomics Research and Development Initiative.

ACKNOWLEDGMENTS

The authors would like to thank Carole Beaudry and Lyz Boyd for technical assistance. The authors also would like to thank the many contributors to the Canadian *Campylobacter* Comparative Genomic Fingerprinting Database (C3GFdb), without whom this work would not have been possible.

REFERENCES

Acheson, D., and Allos, B. M. (2001). *Campylobacter jejuni* Infections: update on emerging issues and trends. *Clin. Infect. Dis.* 32, 1201–1206. doi: 10.1086/319760

Atabay, H. I., Corry, J. E. L., and On, S. L. W. (1998). Identification of unusual *Campylobacter*-like isolates from poultry products as *Helicobacter* pullorum. *J. Appl. Microbiol.* 84, 1017–1024. doi: 10.1046/j.1365-2672.1998.00438.x

Bovill, R. A., and Mackey, B. M. (1997). Resuscitation of "non-culturable" cells from aged cultures of *Campylobacter jejuni*. *Microbiology* 143, 1575–1581. doi: 10.1099/00221287-143-5-1575

Devane, M., Gilpin, B., Robson, B., Klena, J., Savill, M., and H udson, J. (2013). Identification of multiple subtypes of *Campylobacter jejuni* in chicken meat and the impact on source attribution. *Agriculture* 3, 579–595. doi: 10.3390/agriculture3030579

Dingle, K. E., Colles, F. M., Ure, R., Wagenaar, J. A., Duim, B., Bolton, F. J., et al. (2002). Molecular characterization of *Campylobacter jejuni* clones: a basis

for epidemiologic investigation. *Emerg. Infect. Dis.* 8, 949–955. doi: 10.3201/eid0809.02-0122

Garcia, M. M., Lior, H., Stewart, R. B., Ruckerbauer, G. M., Trudel, J. R., and Skljarevski, A. (1985). Isolation, characterization, and serotyping of *Campylobacter jejuni* and *Campylobacter coli* from slaughter cattle. *Appl. Environ. Microbiol.* 49, 667–672. doi: 10.1128/aem.49.3.667-672.1985

Gharst, G., Hanson, D., and Kathariou, S. (2006). Effect of direct culture versus selective enrichment on the isolation of thermophilic *Campylobacter* from feces of mature cattle at harvest. *J. Food Prot.* 69, 1024–1027. doi: 10.4315/0362-028x-69.5.1024

Gorski, L. (2012). Selective enrichment media bias the types of *Salmonella enterica* strains isolated from mixed strain cultures and complex enrichment broths. *PLoS One* 7:e034722. doi: 10.1371/journal.pone.0034722

Gripp, E., Hlahla, D., Didelot, X., Kops, F., Maurischat, S., Tedin, K., et al. (2011). Closely related *Campylobacter jejuni* strains from different sources reveal a generalist rather than a specialist lifestyle. *BMC Genomics* 12:584. doi: 10.1186/1471-2164-12-584

Habib, I., Uyttendaele, M., and De Zutter, L. (2011). Evaluation of ISO 10272:2006 standard versus alternative enrichment and plating combinations for enumeration and detection of *Campylobacter* in chicken meat. *Food Microbiol.* 28, 1117–1123. doi: 10.1016/j.fm.2011.03.001

Hunt, J., Abeyta, C., and Tran, T. (1998). "Isolation of *Campylobacter* species from food and water," in *Bacteriological Analytical Manual*, (Rockville, MA: Association of Official Analytical Chemists).

Hutchinson, D., and Bolton, F. (1984). Improved blood free selective medium for isolating *Campylobacter jejuni* from faecal specimens. *J. Clin. Pathol.* 37, 956–957. doi: 10.1136/jcp.41.6.704-b

Inglis, G. D., Boras, V. F., Webb, A. L., Suttorp, V. V., Hodgkinson, P., and Taboada, E. N. (2019). Enhanced microbiological surveillance reveals that temporal case clusters contribute to the high rates of campylobacteriosis in a model agroecosystem. *Int. J. Med. Microbiol.* 309, 232–244. doi: 10.1016/j.ijmm.2019.04.003

International Organization for Standardization (2006). *ISO 10272-1:2006. Microbiology of Food and Animal Feeding Stuffs. Horizontal Method for Detection and Enumeration of Campylobacter spp. Part* 1*: Detection Method*. London: International Organization for Standardization, 1–16.

Jolley, K. A., and Maiden, M. C. J. (2010). BIGSdb: scalable analysis of bacterial genome variation at the population level. *BMC Bioinformatics* 11:595. doi: 10.1186/1471-2105-11-595

Jones, D. M., Sutcliffe, E. M., and Curry, A. (1991). Recovery of viable but non-culturable *Campylobacter jejuni*. *J. Gen. Microbiol.* 137, 2477–2482. doi: 10.1099/00221287-137-10-2477

Kaakoush, N. O., Castaño-Rodríguez, N., Mitchell, H. M., and Man, S. M. (2015). Global epidemiology of *Campylobacter* infection. *Clin. Microbiol. Rev.* 28, 687–720. doi: 10.1128/CMR.00006-15

Kwan, P. S. L., Birtles, A., Bolton, F. J., French, N. P., Robinson, S. E., Newbold, L. S., et al. (2008). Longitudinal study of the molecular epidemiology of *Campylobacter jejuni* in cattle on dairy farms. *Appl. Environ. Microbiol.* 74, 3626–3633. doi: 10.1128/AEM.01669-1667

Mellefont, L. A., McMeekin, T. A., and Ross, T. (2008). Effect of relative inoculum concentration on *Listeria monocytogenes* growth in co-culture. *Int. J. Food Microbiol.* 121, 157–168. doi: 10.1016/j.ijfoodmicro.2007.10.010

Müllner, P., Collins-Emerson, J. M., Midwinter, A. C., Carter, P., Spencer, S. E. F., Van Der Logt, P., et al. (2010). Molecular epidemiology of *Campylobacter jejuni* in a geographically isolated country with a uniquely structured poultry industry. *Appl. Environ. Microbiol.* 76, 2145–2154. doi: 10.1128/AEM.00862-869

Müllner, P., Spencer, S. E. F., Wilson, D. J., Jones, G., Noble, A. D., Midwinter, A. C., et al. (2009). Assigning the source of human campylobacteriosis in New Zealand: a comparative genetic and epidemiological approach. *Infect. Genet. Evol.* 9, 1311–1319. doi: 10.1016/j.meegid.2009.09.003

Pintar, K. D. M., Thomas, K. M., Christidis, T., Otten, A., Nesbitt, A., Marshall, B., et al. (2016). A Comparative Exposure Assessment of *Campylobacter* in Ontario. *Canada* 37, 677–715. doi: 10.1111/risa.12653

R Core Team (2016). *R: A Language and Environment for Statistical Computing*. Vienna: Foundation for Statistical Computing.

Sheppard, S. K., Colles, F. M., McCarthy, N. D., Strachan, N. J. C., Ogden, I. D., Forbes, K. J., et al. (2011). Niche segregation and genetic structure of *Campylobacter jejuni* populations from wild and agricultural host species. *Mol. Ecol.* 20, 3484–3490. doi: 10.1111/j.1365-294X.2011.05179.x

Sheppard, S. K., Dallas, J. F., Strachan, N. J. C., MacRae, M., McCarthy, N. D., Wilson, D. J., et al. (2009). *Campylobacter* genotyping to determine the source of human infection. *Clin. Infect. Dis.* 48, 1072–1078. doi: 10.1086/597402

Sheppard, S. K., Didelot, X., Jolley, K. A., Darling, A. E., Pascoe, B., Meric, G., et al. (2013). Progressive genome-wide introgression in agricultural *Campylobacter coli*. *Mol. Ecol.* 22, 1051–1064. doi: 10.1111/mec.12162

Silva, J., Leite, D., Fernandes, M., Mena, C., Gibbs, P. A., and Teixeira, P. (2011). *Campylobacter* spp. as a foodborne pathogen: a review. *Front. Microbiol.* 2:200. doi: 10.3389/fmicb.2011.00200

Stanley, K. N., Wallace, J. S., Currie, J. E., Diggle, P. J., and Jones, K. (1998). The seasonal variation of thermophilic campylobacters in beef cattle, dairy cattle and calves. *J. Appl. Microbiol.* 85, 472–480. doi: 10.1046/j.1365-2672.1998.853511.x

Taboada, E. N., Ross, S. L., Mutschall, S. K., MacKinnon, J. M., Roberts, M. J., Buchanan, C. J., et al. (2012). Development and validation of a comparative genomic fingerprinting method for high-resolution genotyping of *Campylobacter jejuni*. *J. Clin. Microbiol.* 50, 788–797. doi: 10.1128/JCM.00669-611

Thomas, M. K., Murray, R., Flockhart, L., Pintar, K., Pollari, F., Fazil, A., et al. (2013). Estimates of the burden of foodborne illness in Canada for 30 specified pathogens and unspecified agents, circa 2006. *Foodborne Pathog. Dis.* 10, 639–648. doi: 10.1089/fpd.2012.1389

Ugarte-Ruiz, M., Wassenaar, T. M., Gómez-Barrero, S., Porrero, M. C., Navarro-Gonzalez, N., and Domínguez, L. (2013). The effect of different isolation protocols on detection and molecular characterization of *Campylobacter* from poultry. *Lett. Appl. Microbiol.* 57, 427–435. doi: 10.1111/lam.12130

Whiley, H., van den Akker, B., Giglio, S., and Bentham, R. (2013). The role of environmental reservoirs in human campylobacteriosis. *Int. J. Environ. Res. Public Health* 10, 5886–5907. doi: 10.3390/ijerph10115886

Wickham, H., and Winston, C. (2015*). Ggplot2: an implementation of the grammar of graphics. *Compr. R Arch. Netw*

Williams, A., and Oyarzabal, O. A. (2012). Prevalence of *Campylobacter* spp. in skinless, boneless retail broiler meat from 2005 through 2011 in Alabama. USA. *BMC Microbiol.* 12:184. doi: 10.1186/1471-2180-12-184

Williams, L. K., Sait, L. C., Cogan, T. A., Jørgensen, F., Grogono-Thomas, R., and Humphrey, T. J. (2012). Enrichment culture can bias the isolation of *Campylobacter* subtypes. *Epidemiol. Infect.* 140, 1227–1235. doi: 10.1017/S0950268811001877

Wilson, D. J., Gabriel, E., Leatherbarrow, A. J. H., Cheesbrough, J., Gee, S., Bolton, E., et al. (2008). Tracing the source of campylobacteriosis. *PLoS Genet.* 4:e1000203. doi: 10.1371/journal.pgen.1000203

Zilelidou, E., Manthou, E., and Skandamis, P. (2016). Growth differences and competition between *Listeria monocytogenes* strains determine their predominance on ham slices and lead to bias during selective enrichment with the ISO protocol. *Int. J. Food Microbiol.* 235, 60–70. doi: 10.1016/j.ijfoodmicro.2016.07.016

Zilelidou, E. A., Rychli, K., Manthou, E., Ciolacu, L., Wagner, M., and Skandamis, P. N. (2015). Highly invasive *Listeria monocytogenes* strains have growth and invasion advantages in strain competition. *PLoS One* 10:e0141617. doi: 10.1371/journal.pone.0141617

Conflict of Interest: The authors declare that the research was conducted in the absence of any commercial or financial relationships that could be construed as a potential conflict of interest.

frontiers in Public Health

ORIGINAL RESEARCH
published: 15 April 2020
doi: 10.3389/fpubh.2020.00099

Co-occurrence of *Campylobacter* Species in Children From Eastern Ethiopia, and Their Association With Environmental Enteric Dysfunction, Diarrhea, and Host Microbiome

Yitagele Terefe[1,2,3†], Loïc Deblais[1,3†], Mostafa Ghanem[1,3†‡], Yosra A. Helmy[1], Bahar Mummed[2], Dehao Chen[4], Nitya Singh[5], Vida Ahyong[6], Katrina Kalantar[7], Getnet Yimer[1,3], Jemal Yousuf Hassen[8], Abdulmuen Mohammed[2], Sarah L. McKune[4], Mark J. Manary[9], Maria Isabel Ordiz[9], Wondwossen Gebreyes[1,3], Arie H. Havelaar[5] and Gireesh Rajashekara[1,3]*

[1] The Ohio State University, Columbus, OH, United States, [2] Veterinary Medicine, Haramaya University, Dire Dawa, Ethiopia, [3] Global One Health Initiative, The Ohio State University, Addis Ababa, Ethiopia, [4] Department of Environmental and Global Health, University of Florida, Gainesville, FL, United States, [5] Emerging Pathogens Institute, University of Florida, Gainesville, FL, United States, [6] Chan Zuckerberg Biohub, San Francisco, CA, United States, [7] Chan Zuckerberg Initiative, Redwood City, CA, United States, [8] Department of Rural Development and Agricultural Extension, Haramaya University, Dire Dawa, Ethiopia, [9] Department of Pediatrics, Washington University, St. Louis, MI, United States

High *Campylobacter* prevalence during early childhood has been associated with stunting and environmental enteric dysfunction (EED), especially in low resource settings. This study assessed the prevalence, diversity, abundance, and co-occurrence of *Campylobacter* spp. in stools from children in a rural area of eastern Ethiopia and their association with microbiome, diarrhea, and EED in children. Stool samples ($n = 100$) were collected from randomly selected children (age range: 360–498 days) in five kebeles in Haramaya District, Ethiopia. Diarrhea, compromised gut permeability, and gut inflammation were observed in 48, 45, and 57% of children, respectively. *Campylobacter* prevalence and species diversity were assessed using PCR and meta-total RNA sequencing (MeTRS). The prevalence of *Campylobacter* spp. in the children's stools was 50% (41–60%) by PCR and 88% (80–93.6%) by MeTRS ($P < 0.01$). Further, seven *Campylobacter* species (*Campylobacter jejuni*, *Campylobacter upsaliensis, Campylobacter hyointestinalis, Campylobacter coli, Campylobacter* sp. RM6137, uncultured *Campylobacter* sp., and *Campylobacter* sp. RM12175) were detected by MeTRS in at least 40% of children stools in high abundance (>1.76-log read per million per positive stool sample). Four clusters of *Campylobacter* species (5–12 species per cluster) co-occurred in the stool samples, suggesting that *Campylobacter* colonization of children may have occurred through multiple reservoirs or from a reservoir in which several *Campylobacter* species may co-inhabit. No associations between *Campylobacter* spp., EED, and diarrhea were detected in this cross-sectional study; however, characteristic microbiome profiles were identified based on the prevalence of *Campylobacter* spp., EED severity, and diarrhea. Forty-seven bacterial species were correlated with *Campylobacter*, and 13 of them also correlated with gut permeability, gut inflammation and/or EED severity. Forty-nine species not correlated with *Campylobacter*

OPEN ACCESS

Edited by:
Nicolae Corcionivoschi, Agri-Food and Biosciences Institute (AFBI), United Kingdom

Reviewed by:
Brendan Wren, University of London, United Kingdom
Christine M. Szymanski, University of Alberta, Canada

***Correspondence:**
Gireesh Rajashekara
rajashekara.2@osu.edu

[†] These authors have contributed equally to this work

[‡] Present address:
Mostafa Ghanem, Department of Veterinary Medicine, Virginia-Maryland College of Veterinary Medicine, University of Maryland, College Park, MD, United States

Specialty section:
This article was submitted to Infectious Diseases - Surveillance, Prevention and Treatment, a section of the journal Frontiers in Public Health

Received: 05 December 2019
Accepted: 12 March 2020
Published: 15 April 2020

Citation:
Terefe Y, Deblais L, Ghanem M, Helmy YA, Mummed B, Chen D, Singh N, Ahyong V, Kalantar K, Yimer G, Yousuf Hassen J, Mohammed A, McKune SL, Manary MJ, Ordiz MI, Gebreyes W, Havelaar AH and Rajashekara G (2020) Co-occurrence of Campylobacter Species in Children From Eastern Ethiopia, and Their Association With Environmental Enteric Dysfunction, Diarrhea, and Host Microbiome. Front. Public Health 8:99. doi: 10.3389/fpubh.2020.00099

were correlated with gut permeability, gut inflammation, EED severity and/or diarrhea. This study demonstrated that (1) in addition to *C. jejuni* and *C. coli*, multiple non-thermophilic *Campylobacter* spp. (i.e., *Campylobacter hyointestinalis, Campylobacter fetus,* and *Campylobacter concisus*) were frequently detected in the children's stools and (2) the *Campylobacter*, gut permeability, gut inflammation, EED severity, and diarrhea were associated with characteristic microbiome composition. Additional spatial and longitudinal studies are needed to identify environmental reservoirs and sources of infection of children with disparate *Campylobacter* species and to better define their associations with EED in low-income countries.

Keywords: *Campylobacter*, non-thermotolerant *Campylobacter*, EED, diarrhea, malnutrition, stunting, livestock reservoirs, MeTRS

INTRODUCTION

Campylobacter species are the most common zoonotic pathogens and the most frequent bacterial cause of foodborne disease worldwide (1). *Campylobacter* infection is frequently asymptomatic, and clinical cases may present with symptoms ranging from diarrhea, abdominal pain, and fever to severe consequences like reactive arthritis and, although rarely occurring, Guillain–Barré syndrome (2). Among the cases of diarrhea in children <5 years old, 15% was caused by *Campylobacter* infections (3). Warm-blooded animals, and particularly avian species, are common reservoir hosts for *Campylobacter* and infection in animals in most cases is asymptomatic. *Campylobacter* transmission from animal reservoirs to humans may occur through multiple routes, including contaminated food (especially poultry meat) and water, the environment, and contact with infected animals (4, 5). Children can be exposed to *Campylobacter* spp. directly or indirectly through exposure to animal feces (6).

Recent studies have also shown association of both symptomatic and asymptomatic *Campylobacter* infections with growth faltering in children from developing countries (7, 8). Approximately 24 million (35.2%) children under five, from East Africa were stunted, 4.1 million (6%) were wasted, and 2.9 million (4.3%) were overweight in 2018 (9). High exposure to enteric pathogens may result in environmental enteric dysfunction (EED), a subclinical disorder of the small intestine characterized by villous atrophy, crypt elongation, inflammatory cells infiltration of the crypts and a loss of barrier function or increased permeability (10). EED is considered to be involved in the causal pathway from pathogen exposure to stunting (11, 12). A study in multi-country settings, *Campylobacter* spp. were isolated in both diarrheic and non-diarrheic children in their first and second year of life (13). In addition to these, the MAL-ED project revealed a high *Campylobacter* infection in children in eight low-resource settings and this was associated with growth shortfalls, increased intestinal permeability, and intestinal and systemic inflammation at 24 months of age (7).

In Ethiopia, the rate of stunting among children under five is alarmingly high (38% in 2016); and a recent study indicated that the average height-for-age Z-score (HAZ) in a large sample of Ethiopian children decreased from −0.7 to −2.0 standard deviations between 6 and 18 months of age (14). In previous studies, high prevalence of thermophilic *Campylobacter* spp. in humans and domestic animals have been documented (15–18). Studies from Gondar, Hawassa and Jimma, Ethiopia indicated that *Campylobacter* was a major cause of diarrhea in children <5 years (15, 16) with high prevalence of *Campylobacter* in children who had exposure to domestic animals mainly chicken (15). Evidence are still lacking in Ethiopia concerning the association between *Campylobacter* spp. and EED in children. Thermotolerant *Campylobacter* spp. (i.e., *Campylobacter jejuni*, *Campylobacter coli, Campylobacter lari,* and *Campylobacter upsaliensis*) are frequent causal agents of campylobacterioisis. However, infection of children with non-thermophilic *Campylobacter* spp. (e.g., *Campylobacter hyointestinalis*, *Campylobacter fetus*, *Campylobacter showae*, and *Campylobacter concisus*) is largely underestimated due to unsuitable culturing methods and their public health risks specifically in EED pathogenesis is not known (19, 20).

Improving gut health in children can improve growth and cognitive development and the efficacy of oral vaccines (21). The fight against stunting and wasting is the prioritized agenda of several regional, national and international interventions in low and middle-income countries (22). Understanding the causes of EED and specifically characterizing the associated pathogens provide opportunities to design effective interventions to improve the health and well-being of children. Therefore, the current study is aimed at estimating the prevalence, abundance, diversity, and co-occurrence of *Campylobacter* spp. in children stools collected in the Haramaya District/Woreda, East Hararghe zone, Oromia region, in rural eastern Ethiopia, and to assess their association with EED, diarrhea, and host microbiome. This study is a part of the cross-sectional formative research of the *Campylobacter* Genomics and Environmental Enteric Dysfunction (CAGED) project, which included an epidemiological investigation of *Campylobacter* exposure, EED, stunting, and their associated risk factors. Results provided by this cross-sectional study will provide a strong baseline for examining the role of *Campylobacter* in EED.

MATERIALS AND METHODS

Study Area

The study was conducted in five rural kebeles (Biftu Geda, Damota, Finkile, Gobe Chala, and Negeya;

smallest administrative unit in Ethiopia) in the Haramaya District/Woreda, East Hararghe zone of Oromia Regional state, Eastern Ethiopia (**Figure 1**). Haramaya District is located about 525 km from Addis Ababa (capital city of Ethiopia). The altitude of Haramaya District ranges from 1,400 to 2,340 meters above sea level. Haramaya District has 36 rural kebeles and three urban kebeles. The national census of 2007 reported a total population of 271,018 (138,282 men and 132,736 women) (23) for this District. A survey of the land in Haramaya District shows that 36.1% is arable or cultivable, 2.3% pasture, 1.5% forest, and the remaining 60.1% is considered built-up, degraded, or otherwise unusable. The livestock population of the Haramaya District was estimated as; 111,528 cattle, 69,950 sheep, 106,145 goats, 137,545 chickens, 529 camels, and 31,385 donkeys. Khat, vegetables, and fruits represent major cash crops of this district (Haramaya District Agriculture and Livestock office; unpublished data).

Study Design and Sample Size Calculation

A cross-sectional study was conducted on children between October 2018 to December 2018 (age range: 360–498 days). For the prevalence estimation, sample size was calculated based on a binomial distribution. A sample of 100 children allows estimation of 50% prevalence with a precision of 10% at 95% confidence interval, and a power of 80%. The target number of 100 children was distributed over the five kebeles (between 9 and 32 children per kebeles) based on the number of children in the sampling frame but rounded to the nearest multiple of 10. Full details of the enrollment process are described in Chen et al. (under review).

Sample Collection and Transportation

Stool samples were collected weekly from 10 children in one of the selected kebeles over 3 month period until the desired sample size ($n = 100$) was achieved. Child caretakers were invited to bring the children to the local health post for stool sampling. The samples were collected in a clean plastic sheet and then immediately transferred into four FluidX™ 2D-Barcoded 2.0 mL sample storage tubes (Thermo Scientific™, Waltham, MA, USA) and kept in an ice box and transferred to the laboratory at Haramaya University on the same day. Sample ID, date, and time of collection were verified, and samples were stored at −80°C

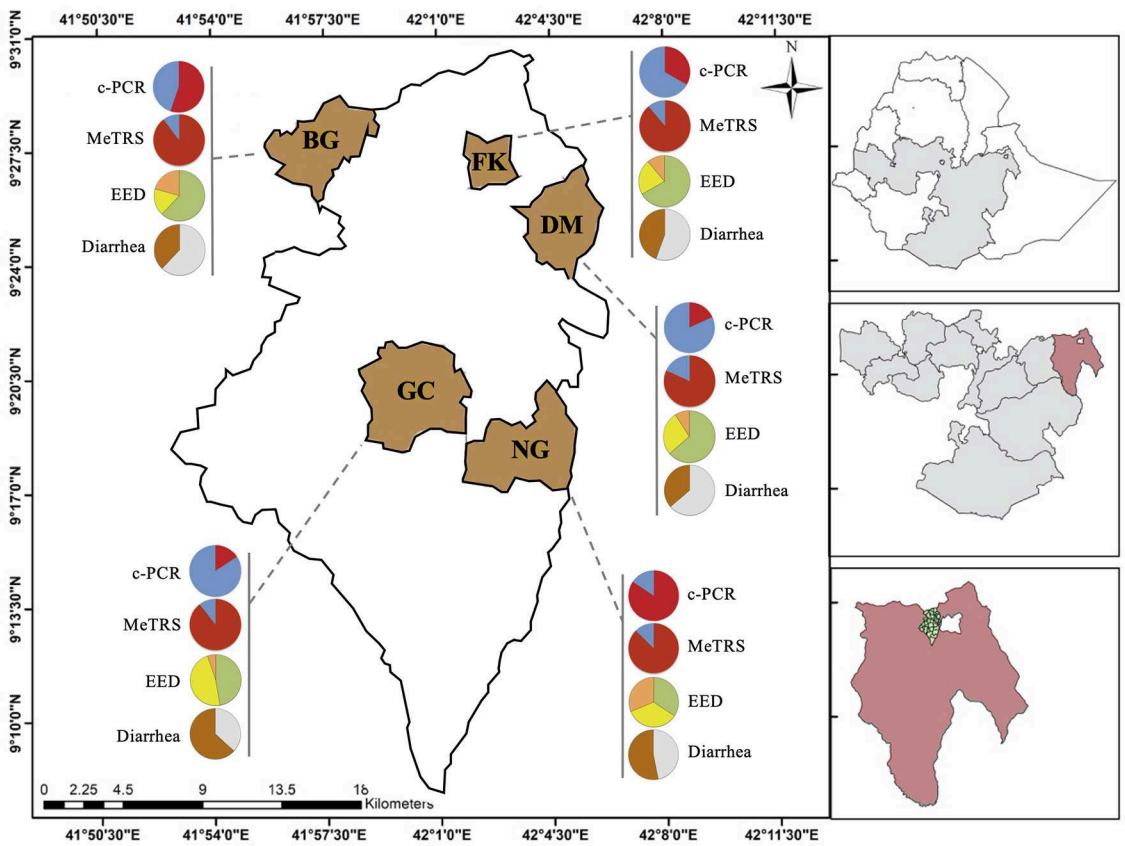

FIGURE 1 | Prevalence of *Campylobacter*, environmental enteric dysfunction (EED) and diarrhea in children in the five kebeles from Haramaya District (East Ethiopia). Pie graphs in red (positive for *Campylobacter*) and blue (negative for *Campylobacter*) represent the *Campylobacter* prevalence in stool samples ($n = 100$) collected from the designated kebele. Prevalence was determined using conventional PCR (c-PCR) or MeTRS (meta-total RNA sequencing). Pie graphs in green ("normal"), yellow ("moderate" EED), and orange ("severe" EED) represent the prevalence and severity of the EED for the designated kebele. Additional details concerning the EED severity determination are presented in **Table S1**. Pie graphs in brown (child currently having or had diarrhea in the past 15 days), gray (child had no diarrhea in the past 15 days) represent the diarrheal status of the children. GC, Gobe Chala; NG, Negaya; FK, Finkle; DM, Damota; BG: Biftu Geda.

until further use for DNA extraction. The child caretaker was asked whether the child had diarrhea during the 15 days before collection. Additional details concerning the diarrhea scoring are described in Chen et al. (under review).

Prevalence and Measurement of EED

Prevalence of EED and its measurements are described in detail in Chen et al. (under review). EED was determined by assessing both gut permeability and inflammation. The lactulose absorption (L%) was measured via sugar absorption test, as previously described (24), and was used as a maker to assess the gut permeability of the children. Classification of EED severity was performed as previously described (25). The child was considered "normal" if the L% was lower than 0.2; "moderate" if the L% was between 0.2 and 0.45, and "severe" if the L% was above 0.45. Myeloperoxidase (MPO) in the stool samples was measured using a commercially available enzyme linked immunosorbent assay (MPO RUO, Alpco, Salem, NH) to assess the gut inflammation. The child was considered having "normal" gut integrity if the [MPO] was lower than 2,000 ng/ml, "moderate" gut inflammation if the [MPO] was in between 2,000 and 11,000 ng/ml, and "severe" gut inflammation if the [MPO] was above 11,000 ng/ml. Due to the lack of correlation between the abundance of *Campylobacter* in stool and lactulose absorption and MPO data ($r^2 < 0.2$; $P > 0.05$), the EED severity in the children was estimated by cross-tabulating the classifications generated for both L% and [MPO] (**Figure S1**).

Extraction of Genomic DNA

Extraction of the genomic DNA from stool samples was performed by using Purelink™ Microbiome DNA purification kit (Invitrogen, Carlsbad, CA, USA). Traces of RNA were removed using RNAse treatment (Thermo Scientific™, Waltham, MA, USA) as previously described (26, 27). Genomic DNA was resuspended in 50 μl of nuclease free water (Qiagen, CA, USA) and stored at −20°C for further use. Quality and quantity of the extracted DNA was assessed using 1.5% agarose gel electrophoresis and Nanodrop 2000C Spectrophotometer (Thermo Scientific™, Waltham, MA, USA).

Detection of *Campylobacter* spp. in child Stool Samples Using Conventional PCR

Detection of *Campylobacter* spp. in DNA from stool samples was performed using multiplex conventional PCR with the GoTaq Green Master Mix kit (Promega Life Sciences, Madison, WI, USA). *C. jejuni* 81–176, *C. coli* ATCC33559, and sterile water were used as controls. *Campylobacter* genus-specific PCR was performed using 16S RNA primers and *Campylobacter* species-specific PCR was performed using *ceuE* primers for the detection of *C. coli* and *mapA* primers for the detection of *C. jejuni* (28). The primers used and the expected PCR product sizes are described in **Table S1**. The PCR was performed as described in Denis et al. (28) in a Mastercycler nexus gradient PCR system (Eppendorf, Hamburg, Germany). PCR products were visualized using 1.5% agarose gel (VWR International, Radnor, PA, USA) under UV light.

RNA Extraction, Library Preparation and Sequencing

RNA extraction was performed using approximately 0.25 g of stool sample with the Quick-RNA Fecal/Soil Microbe Microprep Kit (Zymo Research, CA, USA) according to the manufacturer's protocol. Four water samples were used as controls during extraction and library preparation. RNA concentration was measured using Qubit (Invitrogen, Carlsbad, CA, USA). Meta-total RNA sequencing (MeTRS) was used to analyze the microbiome composition of the children stools based on previously published work (29). The library generation was performed with NEBNext® Ultra™ II RNA Library Prep (New England Biolabs, MA, USA). Sequencing was performed to obtain ∼400M reads using the Illumina NextSeq (Illumina, Inc., San Diego, CA, USA) across the 100 stool samples. For each sample, 25 pg of External RNA Controls Consortium (ERCC) RNA Spike-In Mix (Life Technologies, Carlsbad, CA, USA) was added prior to library preparation to determine the limit of detection for each sample. The average lower limit of detection was 49 attomoles. The average RNA input per samples was calculated using the following equation (total input RNA = ercc_pg/ercc_reads * total_reads) where "ercc_reads" is the number of reads generated from the water control and "total_reads" is the number of reads generated from test RNA including the water control. The average input was ∼66 ng/sample.

Bioinformatic Analysis of the MeTRS Data

MeTRS data analysis was performed using IDseq pipeline version 3.7 available at https://github.com/chanzuckerberg/idseq-web/wiki (30). The details of the IDseq pipeline used for MeTRS data analysis is included in the **Supplemental Material 1**. Only identified organisms with at least 10 reads, an alignment length above 50 bp, and a Z-score above 1 were considered for the statistical analyses.

Statistical Analysis

MeTRS abundance data (reads per million; rpm) were log transformed. Statistical analyses were performed using JMP PRO 14 software (SAS Institute, Cary, NC, USA). The homogeneity of the MeTRS data for each child was analyzed using a principal component analysis (PCA) combined with restricted maximum likelihood (REML) estimation and T^2 statistic test (square of the Mahalanobis distance). Similarity in the *Campylobacter* spp. profiles between children obtained with the MeTRS data was determined using hierarchical clustering. Discriminant analyses were performed to identify specific members of the microbial species responsible for the variability observed in the PCA and clustering data based on the designated nominal parameter used (kebeles, presence/absence of *Campylobacter,* EED severity, and diarrhea status). The percentage of stool samples clustering within their own group (confidence interval of 95%; CI 95%) was used to determine whether the designated nominal parameters explained the variability observed between stool samples. A Wilcoxon test was performed to identify rpm abundance differences for a given member of the microbial species based on a specific nominal parameter. Correlations

TABLE 1 | Prevalence of *Campylobacter*, *Campylobacter jejuni,* and *Campylobacter coli* in child stools using conventional PCR and MeTRS approaches.

Taxonomic group	Conventional PCR		MeTRS*	
	Positive samples	Prevalence (%)	Positive samples	Prevalence (%)
Campylobacter genus	51	50 (40-61)	88	88 (80–93.6)
C. jejuni	13	13 (7-21)	37	37 (27-46)
C. coli	2	2 (0.2–7)	24	24 (17-32)

*samples were considered positive for Campylobacter spp. if at least 10 reads per sample of at least 50 bp long were mapped to reference genome with a Z-score higher than 1.

between the MeTRS, EED severity, and diarrhea data were performed using a multivariate analysis combined with Pearson product-moment correlation coefficient. The co-occurrence of the *Campylobacter* spp. was studied using Cluster and Factoextra R packages (SAS Institute, Cary, NC, USA) on the K-means clustering data extracted from the multivariate analysis data (r^2) obtained with the *Campylopbacter* spp. prevalence data. The optimization of the number of clusters for the PCA was performed using the Silhouette method. The abundance of each bacteria in the stool samples was estimated using MeTRS approach, which is based on RNA read quantification; therefore, we do not exclude the possibility that this approach over or under estimates the quantitative data (reads per million) described in this study.

Data Accession

MeTRS raw reads have been deposited in the IDseq platform (https://idseq.net) in accordance with the Chan Zuckerberg Biohub and Chan Zuckerberg Initiative (CZI).

RESULTS

Prevalence of *Campylobacter* spp. in child Stool Using Conventional PCR

The genus-specific PCR analysis showed that 50% (40–60%, 95% CI) of the child stools ($n = 100$) were positive for the *Campylobacter* genus across the five kebeles (**Table 1**); however, the *Campylobacter* prevalence significantly differed between kebeles ($P < 0.05$; **Figure 1** and **Figure S2A**). The prevalence was higher in Negeya (84.4%) compared to Biftu Geda (55.2%), followed by Finkile (33.3%), Damota (18.2%) and Gobe Chala (15.8%; **Figure 1** and **Figure S2A**).

The species-specific PCR analysis showed that 13% (7–21%) of children were colonized with *C. jejuni* and only 2% (0.2–7%) with *C. coli* (**Table 1**). The prevalence of children positive for *C. jejuni* and *C. coli* did not differ between kebeles (**Figure S2A**). These results suggested that large proportion of *Campylobacter* in children stools likely represent other *Campylobacter* species, possibly including non-thermotolerant *Campylobacter*.

Prevalence of *Campylobacter* spp. in child Stools Using Meta-Total RNA Sequencing

In order to identify the full spectrum of *Campylobacter* species present in the stool samples, MeTRS was performed on 100 children stool samples. The MeTRS analysis showed that *Campylobacter* was detected in 88% (95% CI: 80–94%) of the children's stools (**Table 1**). A total of 27 classified *Campylobacter* species and 12 unclassified *Campylobacter* species were detected among the 88 *Campylobacter* positive stools based on the annotation in the NCBI database with average sequence identity of 97% for each species (https://www.ncbi.nlm.nih.gov/Taxonomy/Browser/wwwtax.cgi; **Figure 2**). An average of 11 *Campylobacter* spp. was detected per *Campylobacter* positive stool. Seven *Campylobacter* spp. (from highest to lowest prevalence; *Campylobacter* sp. RM12175, *C. hyointestinalis, C. jejuni*, *Campylobacter* sp. RM6137, uncultured *Campylobacter* sp., *C. upsaliensis,* and *C. coli*) were detected in at least 40% of the stools at high abundance (at least 1.76-log rpm per positive stool; **Figure 2**); and seven other *Campylobacter* spp. (*Campylobacter* sp. NCTC 13003*, Campylobacter helveticus, Campylobacter lanienae, C. concisus, C. fetus, Campylobacter pinnipediorum,* and *C. showae*) were detected in at least 40% of the stools but at lower abundance (between 0.95-log and 1.76-log rpm per positive stool; **Figure 2**).

Further, based on the prevalence data (**Figure 2**), it was also observed that specific *Campylobacter* spp. often co-occurred in the children stools (**Figure 3** and **Figure S3**). A total of four clusters of co-occurrences ($n = 5$–12 *Campylobacter* spp. per cluster) were detected. The green cluster (*C. coli*, *C. jejuni*, *C. helveticus*, *C. upsaliensis C. iguaniorum,* and *C. lari)* and the red cluster (*C. gracillis*, *C.* sp. RM12175, *C. sputorum*, and *C. ureolyticus*, *C. hyointestinalis*, *C. curvus*, *C. fetus*, *C. lanienae*, *C. pinnipediorum*, *Campylobacter* sp. RM6137, *Campylobacter* sp. RM12175, *C. showae,* and uncultured *Campylobacter* sp.) displayed higher co-occurrence similarities compared to the blue cluster (*C. rectus*, *C. subantarcticus, C. hepaticus, C. hominis, C. concisus, C. canadensis, and C. pelondis)* and the violet cluster (*C. avium*, *C. cuniculorum, C. insulaenigrae, C. volucris,* and *C. troglodytis*), respectively based on dimension 1, which explained 44.4% variability between the cluster. Interestingly, the green cluster was mostly composed of the five most commonly reported thermotolerant *Campylobacter* species (*C. coli*, *C. jejuni*, *C. helveticus*, *C. upsaliensis,* and *C. lari*), while the red cluster consisted of non-thermotolerant *Campylobacter* species (*C. hyointestinalis*, *C. fetus*, and *C. showae*).

Unlike the PCR data, the distribution of the *Campylobacter* positive children stools (at the genus and species level), and the prevalence of the *Campylobacter* species in the stools were overall independent of the kebeles ($P > 0.05$; **Figure 2**, **Figures S4A,B**). Approximately 65% (45–84%) of the stool samples clustered within their own kebeles based on the abundance of the *Campylobacter* spp. detected in the stool samples (**Figure S4C**). Therefore, due to the high variability observed within most of the kebeles (4/5), the five kebeles were pooled into one ($n = 100$) to enhance the veracity of the MeTRS data described below. Only the abundance (read per

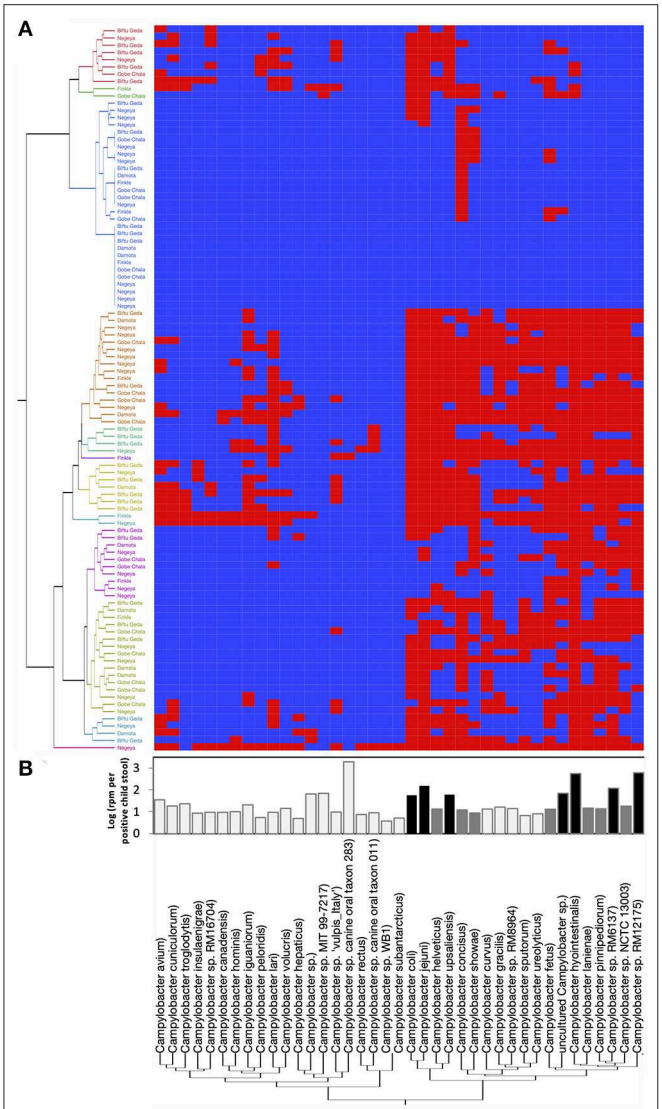

FIGURE 2 | *Campylobacter* spp. prevalence, diversity, and abundance in children stools. A total of 27 classified *Campylobacter* spp. and 12 unclassified *Campylobacter* spp. were detected in the 100 child stool samples collected from children in the five kebeles using MeTRS. **(A)** *Campylobacter* spp. prevalence and diversity in the stool samples. Blue and red cells represent the absence or presence of *Campylobacter* spp. in the designated stool samples (cut-off; contigs number ≥ 10; Read length ≥ 50; Z-score ≥ 1). Kebeles with the same color code belong to the same cluster and therefore harbored equivalent *Campylobacter* sp. diversity. **(B)** Abundance of *Campylobacter* spp. in the positive stools. White bar represents *Campylobacter* spp. with a prevalence lower than 40% and an abundance lower than 0.95-log rpm per stool sample. Gray bar represents *Campylobacter* spp. with a prevalence higher than 40% and an abundance lower than 1.76-log rpm per stool sample. Black bar represents *Campylobacter* spp. with a prevalence higher than 40% and an abundance higher than 1.76-log rpm per stool sample. rpm: read per million.

million) of *C. hyointestinalis* and *Campylobacter* sp. RM12175 significantly differed between kebeles ($P < 0.01$; **Figure S5**). Finkle harbored significantly higher level of *C. hyointestinalis* in the stools compared to Gobe Chala, Negeya, and Biftu Geda (**Figure S5A**); and Damota harbored significantly higher level of *Campylobacter* sp. RM12175 in the stools compared to the other four kebeles (**Figure S5B**).

Overall, the percentage of *Campylobacter* positive stools was significantly higher using the MeTRS approach compared to the conventional PCR approach ($P < 0.01$; **Figures S2A,S2B).** Further, some discrepancies were observed between the two methods used (**Figure S2C**). Out of the 88 stools positive for *Campylobacter* via MeTRS, 42 of them (48%) were also identified positive via conventional PCR (16S genus-specific primers); however, five of the 50 (10%) stools positive for the *Campylobacter* genus via conventional PCR were not positive for the *Campylobacter* via MeTRS analysis (**Figure S2C**). Similarly, based on the species-specific PCR (*ceuE* and *mapA* primers), six of 13 (46%) and two of two (100%) stools were positive for *C. jejuni* and *C. coli,* respectively only by PCR but not with MeTRS (**Figure S2C**).

The *Campylobacter* in the Stools Was Not Associated With Diarrhea and EED Severity

To determine the role of *Campylobacter* in EED, the levels of lactulose and MPO were measured as indicators of EED (24, 25). Additional details concerning the prevalence of EED and stunting among children in this study are described in Chen et al. (under review).

Out of the 100 children studied, 55 children possessed "normal" gut permeability (L% below 0.2), 29 children possessed "moderate" defect in gut permeability (L% between 0.2 and 0.45), and 16 children possessed "severe" defect in gut permeability (L% ratio above 0.45). No correlations were identified when a multivariate analysis was performed between L% and the prevalence or the abundance of *Campylobacter* detected in the children stools ($P > 0.05$). On the other hand, the discriminant analysis showed that the overall *Campylobacter* spp. composition in the stool differed between the L% status ("normal," "moderate," and "severe"; $r^2 = 0.37$; **Figure S6A**). Eighty two percent (45/55) of the children identified as "normal" clustered together based on the *Campylobacter* composition in the stool. Besides, only 66% (19/29) and 44% (7/16) of the child identified as with "moderate" and "severe" permeability defect, respectively clustered within their own group based on the *Campylobacter* composition in the stool (**Figure S6B**). Further, 28% (8/29) and 41% (7/17) of the children identified as with "moderate" and "severe" permeability defect clustered with the children identified as "normal." Overall, the *Campylobacter* composition in the stool samples was associated with 58% of the children with "moderate" and "severe" gut permeability defect based on the L% data.

Similarly, based on the MPO levels, out of the 100 children studied, 43 children possessed "normal" gut ([MPO] below 2,000 ng/ml), 32 children possessed "moderate" gut inflammation ([MPO] between 2,000 and 11,000), and 25 children possessed "severe" gut inflammation ([MPO] above 11,000). No correlations were identified when a multivariate analysis was performed between [MPO] and the prevalence or the abundance of *Campylobacter* detected in the children stools ($P > 0.05$); however, the *Campylobacter* spp. composition

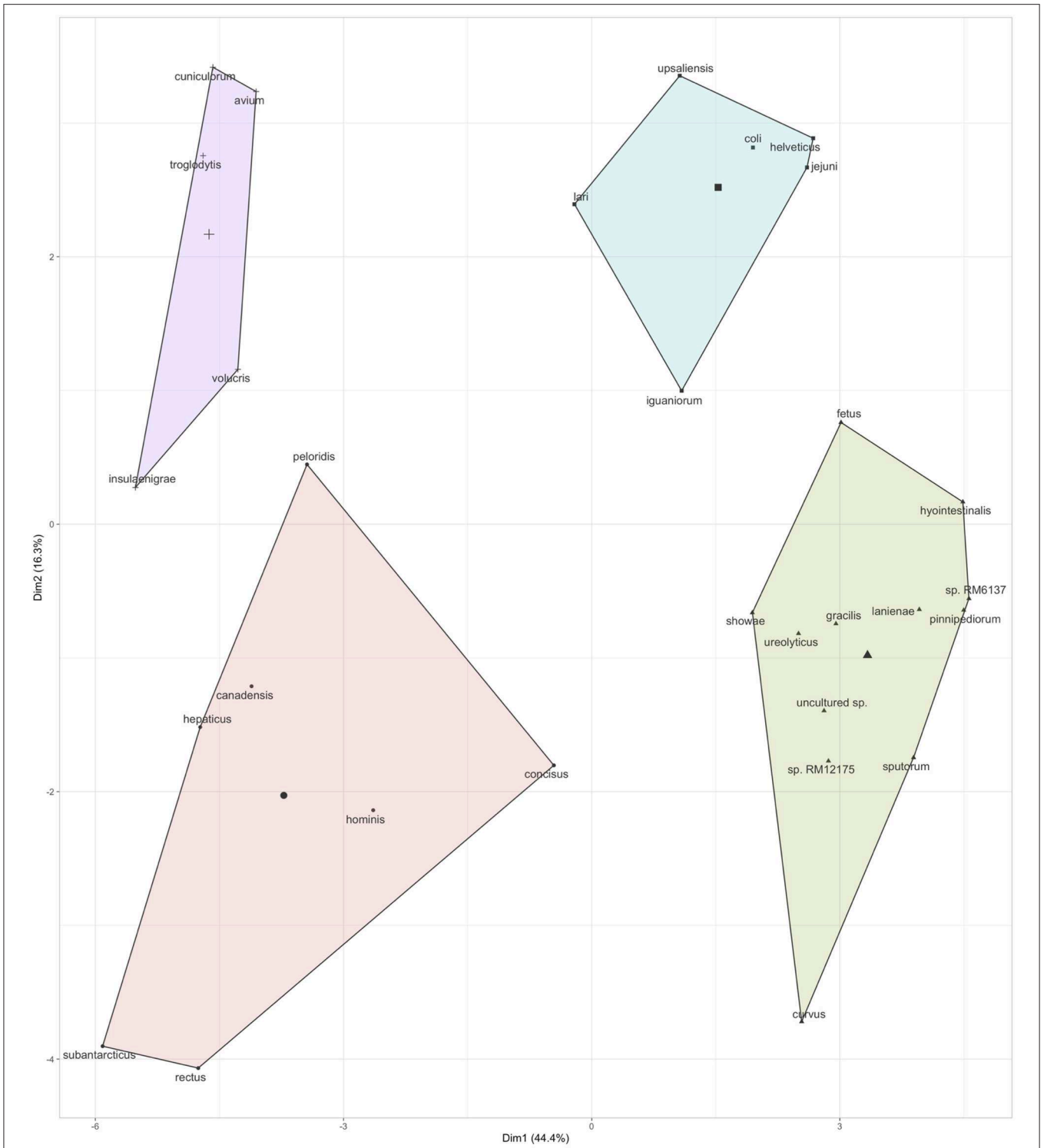

FIGURE 3 | Co-occurrence of *Campylobacter* spp. in the children stool samples. Co-occurrence profiles were created using K-means clustering data extracted from the multivariate analysis data (r^2) based on the prevalence of *Campylobacter* spp. in the stool samples (see **Figure 2**). Additional details regarding the multivariate data are displayed in **Figure S3**.

in the stool differed between the inflammation status (r^2 = 0.37; **Figure S6C**). Fifty eight percent (25/43), 88% (28/32) and 48% (12/25) of the children with inflammation status "normal," "moderate," and "severe," respectively clustered within their own group based on the *Campylobacter* composition in the stool (**Figure S6D**). Only 9% (3/32) and 8% (2/25) of the children

identified as having "moderate" and "severe" gut inflammation clustered with the children identified as "normal." Overall, the *Campylobacter* composition in the stool was associated with 70% of the children with "moderate" and "severe" gut inflammation based on the MPO data.

Because of the lack of correlation between the *Campylobacter* and the L% and MPO, both parameters were combined together to build an index estimating the EED (**Figure S1**). Out of the 100 children studied, 50 children were classified as "normal," 33 children having "moderate" EED, and 25 children having "severe" EED (**Figure 1**). As observed above, the *Campylobacter* spp. composition in the stool differed between the EED status ($r^2 = 0.38$; **Figure S6E**). Ninety percent (45/50), 61% (20/33), and 53% (9/17) of the children identified as "normal," "moderate," and "severe," respectively clustered within their own group based on the *Campylobacter* composition in the stool (**Figure S6F**). Overall, the *Campylobacter* composition in the stool was associated with 58% of the children with "moderate" and "severe" EED based on the EED status data.

In addition, the prevalence of child with diarrhea was recorded to determine the associations with *Campylobacter* spp. prevalence and abundance in the stool samples. Additional details concerning the diarrhea data are described in Chen et al. (under review). Out of the 100 children studied, 48% of the children had diarrhea on the day of the stool collection or 15 days before stool collection (**Figure 1**). No correlations were identified when a multivariate analysis was performed between the diarrhea data and the prevalence or abundance of *Campylobacter* spp. in the stool samples ($P > 0.05$). However, the discriminant analysis showed that overall the *Campylobacter* spp. composition in the stool differed based on the diarrhea status of the children ($r^2 = 0.32$; **Figure S6G**). Eighty-one percent (39/48) of the children with diarrhea clustered together based on the *Campylobacter* composition in the stool samples, while 58% (30/52) of the children without diarrhea clustered together as a separate cluster based on the *Campylobacter* composition in stool (**Figure S6H**).

Specific Bacteria of the Stool Microbiome Correlated With the *Campylobacter* Prevalence and EED Severity

Post-filtering, the MeTRS identified a total of 2,353 bacteria, 642 Archaea, 17 virus/viroid, and 249 eukaryotes at the species level among the 100 children stool samples studied. The global analysis of the fecal microbiota revealed that the majority of children ($n = 89$) harbored similar microbiota profile ($P < 0.01$; **Figure S7A**). Between 68% and 84% of the stool samples clustered by kebeles based on the microbiota composition (**Figure S7B)**. None of the stool samples from Damota and Biftu Geda displayed microbiome composition similarities to Finkle stool samples (**Figures S7B,S7C**), despite the fact that Finkle is geographically closer to Damota and Biftu Geda compared to the other kebeles (**Figure 1**). Further, 19 stools samples displayed higher microbiome composition similarities with Biftu Geda or Negeya stool samples compared to the original kebeles (**Figures S7B,S7C)**, independently of the distance between the kebeles (**Figure 1**). Given the discriminant analysis showed that the ellipses (CI 95%) of most kebeles (4/5) were overlapping, the MeTRS data were analyzed as one population ($n = 100$). No distinct correlation was detected between the *Campylobacter* species and the virus/viroid and eukaryotes ($P > 0.05$, $r^2 < 0.25$); by consequence, the majority of the results described below focused on the interconnections between *Campylobacter* spp. and stool bacterial community.

Our analysis showed that the bacterial composition in the stool samples was related to the overall presence of *Campylobacter* spp. (**Figure S8A**). Ninety-four percent (83/94) of the children stools positive for *Campylobacter* spp. clustered together based on their microbiome composition (**Figure S8B**). Only 58% (7/12) of the child stools negative for *Campylobacter* spp. clustered together in a separate cluster based on their microbiome composition. Approximately 16.9% of the bacteria identified in stool samples ($n = 387/2{,}353$) were positively or negatively correlated with the prevalence or abundance of *Campylobacter* in the stool samples ($r^2 > 0.2$ or $r^2 < -0.20$; $P < 0.05$). Among the bacteria correlated with *Campylobacter*, several of them belonged to *Arcobacter*, *Bacillus*, *Bacteroides*, *Bifidobacterium*, *Capnocytophaga*, *Clostridium*, *Collinsella*, *Corynebacterium*, *Enterobacter*, *Enterococcus*, *Helicobacter*, *Lactobacillus*, *Olsenella*, *Paenibacillus*, *Pantoea*, *Prevotella*, *Serratia*, *Streptococcus*, and *Veilonella*.

However, out of the 387 species mentioned above only 47 were correlated (25 negatively and 22 positively) with the prevalence or abundance of *Campylobacter* in the stool samples ($r^2 > 0.2$ or $r^2 < -0.2$; $P < 0.05$) and detected in at least 25 children stool samples (average of 60 children; **Figure 4**). *Olsenella*, *Clostridium*, and *Streptococcus* were the most represented genus in this subset. *Anaerotignum propionicum* ($r^2 = 0.53$), *Clostridium butyricum* ($r^2 = 0.47$), *Hydrogenophilus islandicus* ($r^2 = 0.46$) displayed the highest positive correlation with *Campylobacter* abundance in the stool samples; while *Burkholderiales* bacterium GJ-E10 ($r^2 = -0.36$), *Pasteurellaceae* bacterium NI1060 ($r^2 = -0.35$), and *Clostridium baratii* ($r^2 = -0.38$), displayed the highest negative correlation with *Campylobacter* abundance and/or prevalence in the stool samples.

Only *Prevotella dentallis* (2.63-log rpm per positive stool sample) was negatively correlated with both the *Campylobacter* abundance and/or prevalence in the stool samples ($r^2 = -0.2$) and the [MPO] ($r^2 = -0.22$). On the other hand, Butyrate-producing bacterium SS3/4, [*Clostridium*] *clostridioforme*, and *Streptococcus australis* were positively correlated with both the *Campylobacter* abundance and/or prevalence in the stool ($r^2 > 0.2$) and at least with one of the following parameters ([MPO], lactulose%, and/or EED severity; $r^2 > 0.21$). *Anaerobiospirillum succiniciproducens*, *Coriobacterium glomerans*, *Escherichia coli*, *Megamonas hypermegale*, *Olsenella* sp. oral taxon 807, *Olsenella umbonata*, and *Pediococcus pentosaceus* were negatively correlated with the *Campylobacter* abundance and/or prevalence in the stool ($r^2 < -0.2$) but positively correlated with at least one of the following parameters ([MPO], lactulose%, and/or EED severity; $r^2 > 0.23$). Only *Bifidobacterium kashiwanohense* was positively correlated with the *Campylobacter* abundance and/or

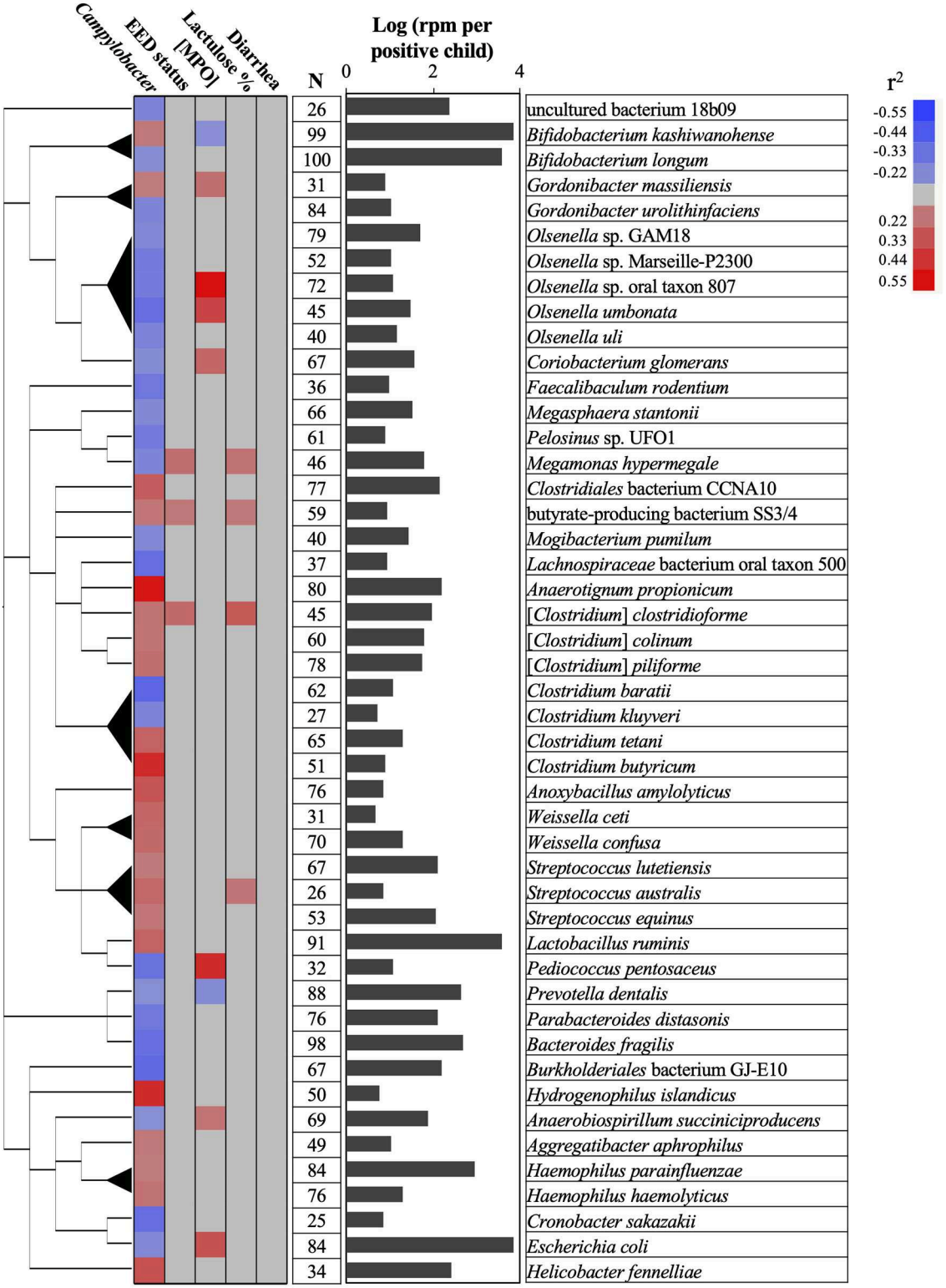

FIGURE 4 | Associations between *Campylobacter*, gut permeability, gut inflammation, environmental enteric dysfunction (EED), diarrhea, and child stool microbiome. A total of 47 bacterial species positively or negatively correlated (red or blue cells, respectively) with *Campylobacter* prevalence and abundance (reads per million, rpm; $r^2 > 0.20$ or $r^2 < -0.20$; $P < 0.05$), gut permeability (lactulose %), [MPO] in ng/ml, EED status ("normal," "moderate" EED, "severe" EED), and/or the diarrhea prevalence data. Additional details concerning the EED severity determination are presented in **Table S1**. The phylogenetic tree was built using NCBI website (https://www.ncbi.nlm.nih.gov/Taxonomy/CommonTree/wwwcmt.cgi). N: number of stools positive for the designated bacterial species. The bar graph represents the average abundance (log rpm per positive stool sample) for the selected bacterial species. rpm, read per million; MPO, myeloperoxidase.

prevalence in the stool ($r^2 > 0.21$) and negatively correlated with [MPO] ($r^2 < -0.2$).

No bacteria correlated with *Campylobacter* spp. were correlated with the presence or absence of diarrhea.

Specific Bacteria of the Stool Microbiome Correlated With the Gut Permeability, Gut Inflammation, EED Severity, and Diarrhea in Children

The microbiome composition was related to the gut permeability (L%), gut inflammation (MPO), and EED status (**Figure S9B**), as observed with the *Campylobacter* composition in the stool samples (**Figure S6**); however, higher correlations between the L%, EED status and the microbiome composition were observed compared to the correlation obtained with *Campylobacter*. Out of the 100 children studied, 80% (44/55), 79% (23/29), and 81% (13/16) of the children identified as "normal," "moderate," and "severe" based on the L%, respectively, clustered within their own group based on the microbiome composition (**Figures S9A,S9B**). Eighty one percent (35/43), 72% (23/32), and 68% (17/25) of the children identified as "normal," "moderate," and "severe" based on MPO levels, respectively, clustered within their own group based on the microbiome composition in the stool (**Figures S9C,S9D**). Eighty percent (40/50), 79% (26/33), and 76% (13/17) of the children identified as "normal," "moderate," and "severe" based on the EED status (both L% and MPO combined; **Table S1**), respectively, clustered within their own group based on the microbiome composition in the stool (**Figures S9E,S9F**). Overall, the microbiome composition was associated with 80% of the gut permeability data, 70% of the gut inflammation data, and 78% of the EED severity data observed in the children with "moderate" and "severe" status. Similarly, children with diarrhea displayed different microbiome composition compared to children with no diarrhea (**Figure S9G**). Out of the 100 children, 81% (42/52) of the stools from children with no diarrhea and 85% (41/48) of the stools from children with diarrhea clustered to their respective groups based on the microbiome composition (**Figure S9H**).

A total of 49 bacteria not-associated with *Campylobacter* were correlated (30 positively [$r^2 > 0.21$; $P < 0.05$] and 19 negatively [$r^2 < -0.20$; $P < 0.05$]) with the L%, MPO levels, and/or the EED severity and detected in at least 25 children stool samples (**Figure S9I**). Only *Neisseria elongata* was positively correlated with the EED severity ($r^2 = 0.31$; 2.2-fold increased between the "normal" children and the children with "severe" EED) and also L% (lactulose%; $r^2 = 0.21$; 1.7-fold increased between the children with "normal" and "severe" gut permeability). Eight bacteria (*Lachnoclostridium* sp. YL32, [*Clostridium*] *bolteae, Bifidobacterium bifidum*, *Mordavella* sp. Marseille-P3756, *Bacteroides thetaiotaomicron, Streptococcus salivarius*, and *Libanicoccus massiliensis*) highly prevalent (>71%) and abundant (>2.0-log rpm per stool sample in children with "severe" status) in the stools were positively correlated (r^2 between 0.24 and 0.36) with L% or MPO levels. On the other hand, *Lactobacillus mucosae* and *Pasteurella multocida* were less prevalent (39 and 60%, respectively) and less abundant (below 1.0 and 1.5-log rpm per stool, respectively) in the stools, but they were higher (2.5- and 2-fold, respectively) in the children with "severe" gut inflammation compared to the "normal" children.

Five bacteria (*Mogibacterium diversum, Ethanoligenens harbinense, Roseburia hominis, Ruminococcus* sp. SR1/5, and *Bacteroides dorei*) were negatively correlated with the EED severity (r^2 between −0.21 and −0.27) and detected in at least 40% of the children stools (**Figure S9I**). Interestingly, only *M. diversum* was negatively correlated with all the parameters studied (EED severity [$r^2 = -0.27$], L% [$r^2 = -0.20$], MPO [$r^2 = -0.26$], and diarrhea prevalence [$r^2 = -0.25$]). Further, *M. diversum* abundance in stools was higher in the "normal" children compared to the children with "severe" EED (2.7-fold), with "severe" L% (4-fold), and with diarrhea (2-fold). Similarly, *E. harbinense* was higher (2.3-fold) in the stools of "normal" children compared to the children with "severe" EED. Four bacteria (*Clostridium taeniosporum*, *Hungatella hathewayi*, *Selenomonas ruminantium*, and *Cryotobacterium curtum*) were less prevalent (between 40% and 58%) and abundant (<1.3-log rpm per stool) in the stools, but they were detected at higher level (2.2-, 2-, 2.6-, and 2-fold, respectively) in the stools of "normal" children compared to the children with "severe" MPO. Further, *Selenomonas ruminantium* was also detected at higher level (2-fold) in children with no diarrhea compared to the ones with diarrhea.

Three additional bacteria (*Prevotella scopos, S. ruminantium,* and *Measphaera els*) highly prevalent (>79%) and abundant (>2.1-log rpm per stool) in the stools and not-associated with *Campylobacter* were negatively correlated (r^2 between −0.2 and −0.22) with the diarrhea data (**Figure S9I**).

DISCUSSION

The purpose of this study was to estimate the prevalence, diversity, abundance and co-occurrence of *Campylobacter* in the stool of young children from Eastern Ethiopia and assess potential associations between *Campylobacter* and diarrhea and EED (31). To accomplish this task, the use of traditional microbiology approaches to isolate thermophilic *Campylobacter* spp. was attempted; however, due to technical and logistical challenges faced in Ethiopia, the results generated were deemed unreliable (data not shown). The fastidious nature of *Campylobacter* and difficulty of isolation, rendered culture and isolation unreliable for estimation of prevalence (32). By consequence, other studies utilized different approaches to estimate the prevalence of *Campylobacter* in stool samples, including enzyme immunoassay (EIA), PCR, and shotgun metagenomics (7, 33, 34). Two different culture independent approaches (conventional PCR and MeTRS) were used in this study to estimate the prevalence of *Campylobacter* in the child stool samples.

The number of child stools detected positive for the *Campylobacter* genus was significantly higher using the MeTRS approach (88% [80–93.6%]) compared to the genus-specific PCR approach (50% [40–61%]; 16S RNA primer). Several studies

showed that shotgun metagenomics and MeTRS had at least equal sensitivity to real-time PCR based approach for different pathogens (29, 35–37). Further, discrepancies between the two detection methods was observed, especially with the species-specific PCR approach (*ceuE* primer for *C. coli* and *mapA* primer for *C. jejuni*). However, the reason for this discrepancy is unknown and needs further investigation. Many factors could affect the sensitivity of both PCR and MeTRS approaches, including the type of the sample, the quality and quantity of the extracted DNA, the agreement between the method used, the type of the organism under investigation, and the tools used to analyze the data. A recent study suggested that shotgun metagenomics might overestimate the prevalence of microbial population due to the presence of plasmid sequences within the assembled genome and the high sequences similarities between bacterial species (38). In our study, by taking an approach of sequencing the total RNA component, we are able to better identify species rather than by sequencing DNA alone. However, the genome coverage obtained with the MeTRS approach was not high enough to provide information about strain relatedness within the same species. Therefore, metagenomic studies using long read technologies or whole genome sequencing of pure isolates are still needed for source attribution purposes.

It is commonly known that *C. jejuni* and *C. coli* are leading causes of campylobacteriosis in the western world (39); however, our study revealed that most of the children stools positive for *Campylobacter* (94%) harbored more than one *Campylobacter* species. This finding suggests that *Campylobacter* colonization of children may have occurred through multiple reservoirs or from a reservoir in which several *Campylobacter* species may co-inhabit. This hypothesis is supported by the existing literature which describes colonization of multiple hosts by a given *Campylobacter* species; for example, *C. hyointestinalis* is commonly found in swine, sheep, dog, and in cattle (40). Further, twelve *Campylobacter* spp. (*Campylobacter* sp. RM12175, *C. hyointestinalis*, *Campylobacter* sp. RM6137, uncultured *Campylobacter* sp., *C. upsaliensis, Campylobacter* sp. NCTC 13003, *C. helveticus, C. lanienae, C. concisus, C. fetus, C. pinnipediorum,* and *C. showae*) in addition to *C. jejuni* and *C. coli* were detected in at least 40% of the stool samples at relatively high abundance. Our study also showed that several *Campylobacter* species were commonly co-occurring within the same stool samples, while others had opposite trends. However, none of the clusters representing different *Campylobacter* species (**Figure 3**) were correlated with the gut permeability, gut inflammation, EED severity, and diarrhea (data not shown). These facts raise many questions about the mechanisms underlying the *Campylobacter* species diversity observed and their potential effect on gut health and children's growth. A possible contributor to this diversity could be the diverse environment surrounding these children. A previous study demonstrated significant associations between *Campylobacter* isolated from children (under 5 years of age) and the exposure to domestic animal (pets, chickens, and pigeons) in Gondar, North Western Ethiopia (15). It was estimated that approximately 83% of the rural households in Ethiopia possess livestock (cattle, goat, and sheep and chicken) (23). Further, most of these *Campylobacter* species mentioned above (except *Campylobacter* sp. RM6137) were reported in livestock such as cattle, sheep, and goat (41). Therefore, livestock most likely plays a major role as reservoir and in the horizontal transmission of *Campylobacter* to children in Ethiopia. Hence, concurrently studying the prevalence and diversity of *Campylobacter* in livestock and children would provide key information concerning the horizontal transmission of *Campylobacter* between livestock and children. It is also important to notice that four of the most prevalent *Campylobacter* species (*C. hyointestinalis, C. helveticus, C. fetus,* and *C. upsaliensis*) detected in the children stools in this study have not been commonly reported in previous studies, compared to other species such as *C. jejuni*, *C. coli*, *C. fetus, C. showae,* and *C. concisus,* which have been associated with human disease (41, 42). The reservoirs of non-thermotolerant *Campylobacters* are very diverse and not well-understood especially in low to middle income countries.

Among all the *Campylobacter* species detected in our study (27 classified species and 12 unclassified species), the non-thermotolerant *C. hyointestinalis* was the second most abundant and the third most prevalent *Campylobacter* species in the children stools. *C. hyointestinalis* was previously isolated from numerous livestock species such as swine (43), cattle (43–48), sheep (43). However, its implication in human diseases is rare and sporadic (49–53). *C. hyointestinalis* has also been reported in developed countries, more precisely in feces collected from dairy farms in Canada (19.3%), in Finland (10.8%) and from dairy goat farms in New Zealand (2%), and in 3.2% milk samples collected from dairy farms in Italy (45, 47, 48, 54). *C. hyointestinalis*, as well as, other *Campylobacter* species were also isolated from wild boar in Japan and dogs in Canada (55, 56). By consequence, studying the prevalence, diversity, and abundance of *Campylobacter* species in livestock, also in domestic- and wild animals that have a high likelihood of interacting with livestock or humans is essential to understand the transmission dynamics of *Campylobacter* to children.

Overall, the MeTRS data showed that the microbial population in the stools in different kebeles was homogeneous between the children. No correlations between *Campylobacter* spp. and gut permeability, gut inflammation, EED severity, or diarrhea status were observed in our study; however, characteristic stool microbiome composition profiles were detected based on the prevalence and abundance of *Campylobacter* spp. in the stools, gut permeability, gut inflammation, EED severity, and diarrhea status. Up to 0.9% ($n = 22$ bacterial species) of the microbiome was positively correlated ($r^2 > 0.20$) and 1.1% ($n = 25$ bacterial species) was negatively correlated ($r^2 < -0.21$) with the prevalence and/or abundance of *Campylobacter* spp. in the stools. Among them, only *Prevotella dentalis* was highly prevalent (88%) and abundant (2.63-log rpm per stool) in the stools, and negatively correlated with both *Campylobacter* prevalence ($r^2 = -0.2$) and the gut inflammation ($r^2 = -0.21$). *Prevotella* is associated with plant-rich diets and also promotes chronic inflammation (57, 58). *Prevotella* is known to provide key nutrients to other bacteria of the human microbiota and may act on the pathogenicity of specific pathobionts (59–63); however, no studies demonstrated

yet potential antagonistic interactions between *P. dentalis* and *Campylobacter*.

Bifidobacterium kashiwanohense was highly prevalent (99%) and abundant (3.84-log rpm per stool) in the stools and was also negatively correlated with gut inflammation ($r^2 = -0.2$). This bacterium possesses high iron sequestration properties and might produce indole-3-lactic acids, which was shown to be a successful strategy to inhibit and compete with enteric pathogens (i.e., *Salmonella* and *E. coli*) (64, 65). However, *B. kashiwanohense* was also positively correlated ($r^2 = 0.21$) with *Campylobacter* in our study, suggesting that the modulation of *B. kashiwanohense* may reduce the impact of pathobiont on the intestinal homeostasis but facilitates the persistence of *Campylobacter* in the child intestinal tract. On the other hand, *Bifidobacterium longum* was negatively correlated with *Campylobacter* in our study, which concords with previous published studies (66). Similarly, other bacteria (*Gordonibacter urolithinfaciens, Mogibacterium pumilum, Megasphaera stantonii, E. coli, Clostridium* spp., *Olsenella* spp., and *Bacteroides fragilis*) were negatively correlated with *Campylobacter* in the stools. Several studies showed that *Bacteroides, Gordonibacter,* and *Escherichia* produce molecules with antimicrobial and anti-inflammatory properties (lactic acids, short chain fatty acids, enterocins, and urolithins), which could modulate the microbiome quality, intestinal homeostasis, and host immune responses and could be effective against *Campylobacter* (67–74). Interestingly, several *Olsenella* spp. ($n = 5$) were frequently detected in the stool samples and were negatively correlated with *Campylobacter* prevalence. *Olsenella* was previously identified as a part of the microbiome associated with the infant health status (stunting, autism spectrum disorder, and chronic malnutrition) in China and Bangladesh (75–77). Therefore, the anti-*Campylobacter* properties of several species identified in this study and their potential application as dietary supplement to control *Campylobacter* in developing countries needs further investigation.

Interestingly, *M. diversum* was the only bacteria of the stool microbiome with a distinct positive effect on the child gut permeability ($r^2 = -0.2$), gut inflammation ($r^2 = -0.26$), EED severity ($r^2 = -0.27$), and diarrhea prevalence ($r^2 = -0.24$), but no association with *Campylobacter*. No information is available concerning this bacterium. Therefore, further investigations are required to support the beneficial properties of *M. diversum* against EED and their potential application as dietary supplement in developing countries to improve intestinal homeostasis. On the other hand, the abundance of four bacterial species (butyrate-producing bacterium SS3/4, *Megamonas hypermegale*, *Streptococcus australis*, and *Gordonibacter massiliensis*) were positively correlated with the abundance of *Campylobacter* in the stools and with the severity of the gut inflammation, gut permeability and/or EED severity; Therefore, these bacteria might have an important impact on the gut microbiome quality, the persistence of *Campylobacter* in the gut, and the children's health.

In conclusion, we report in this study high prevalence and diversity of *Campylobacter* spp. in children in eastern Ethiopia, including the non-thermophilic *Campylobacter* spp. (i.e., *C. hyointestinalis* and *C. fetus*-like species). The MeTRS revealed co-occurrence of several *Campylobacter* spp. More studies are needed to better understand the prevalence, sources, and transmission dynamics of *Campylobacter* to children as well as to establish a clear link between *Campylobacter* infection (including non-thermotolerant species) in children with EED and stunting. Furthermore, even though no direct correlation was identified between *Campylobacter* prevalence and abundance, and the EED severity or the diarrhea, the metagenomic analysis highlighted the association between stool microbiome and the prevalence and abundance of *Campylobacter* spp., EED severity, and diarrhea in children. The unique changes in microbiome may serve as biomarkers for disease status and can help to elucidate the complex interactions between *Campylobacter*, the gut microbiome, EED and stunting in the context of the socio-economic environment of children in rural Ethiopia.

DATA AVAILABILITY STATEMENT

The datasets generated for this study can be found in the BioProject ID: PRJNA608948 https://www.ncbi.nlm.nih.gov/sra/?term=SRR11194563.

ETHICS STATEMENT

All the study procedures were performed in accordance with the Declaration of Helsinki (78) and approvals from the HU Institutional Health Ethics Research Review Committee (Ref. No. IHRERC/152/2018), the Ethiopia National Research Ethics Review Committee (Ref. No. MoST/3-10/168/2018), the Institutional Review Board at the University of Florida (UF) (Ref. No. 201703252) and Washington University School of Medicine (Protocol No. 201806021). Additionally, the operational district officers and local village chiefs were informed about the objectives of the study and the future impacts and their consent was obtained. Written and oral consents were also obtained from child's mother/caregiver and father. Material and Data Transfer Agreements (MDTA) were signed between Haramaya University and all US-based partners. Export permits to ship biological specimens from Ethiopia to the U.S.A were approved by the Ministry of Science and Higher Education (Ref. No. SHE/SSM/19.1/008/11/19). Written informed consent to participate in this study was provided by the participants' legal guardian/next of kin.

AUTHOR CONTRIBUTIONS

GR, SM, JY, WG, MM, AH, and LD conceived and designed the experiment. YT, AM, and GY collected samples. YT, LD, MG, YH, BM, VA, MO, and KK processed the samples for PCR and MeTRS analyses. YT, LD, AH, YH, GR, NS, MG, VA, KK, and DC analyzed the PCR and MeTRS data. YT, LD, MG, AH, and GR wrote the manuscript.

FUNDING

The CAGED project was funded by the Bill & Melinda Gates Foundation to address food insecurity issues in Ethiopia and Burkina Faso through the project Equip - Strengthening Smallholder Livestock Systems for the Future (grant number OPP11755487). These funds are administered by the Feed the Future Innovation Lab for Livestock Systems, which was established by funding from the United States Agency for International Development (USAID) and is co-led by the University of Florida's Institute of Food and Agricultural Sciences and the International Livestock Research Institute. Support for the Feed the Future Innovation Lab for Livestock Systems is made possible by the generous support of the American people through USAID. The contents are the responsibility of the authors and do not necessarily reflect the views of USAID or the United States Government. REDCap is hosted at the University of Florida Clinical and Translational Science Institute (CTSI), supported by NIH National Center for Advancing Translational Sciences grant UL1 TR000064. The CAGED is a collaborative project between University of Florida, The Ohio State University, Washington University, and Haramaya University (Ethiopia). The CAGED project was supported by a Technical Advisory Group consisting of Eric Fèvre (University of Liverpool and International Livestock Research Institute), Nigel French (Massey University), Aulo Gelli (International Food Policy Research Institute), Andrew Jones (University of Michigan), Vivek Kapur (Penn State University), Nick Juleff and Supriya Kumar (Bill & Melinda Gates Foundation) and James Platts-Mills (University of Virginia).

ACKNOWLEDGMENTS

We thank Chan Zuckerberg Biohub, San Francisco, CA, USA and Chan Zuckerberg Initiative, Redwood City, CA, USA for their support with sequencing of total RNA and the bioinformatics analysis of the MeTRS data. We thank Drs. Volker Mai and Nigel French for their critical reading of the manuscript. We also thank Ame Yousuf, Beyan Abdullahi, Yehararework Abebaw, Yenenesh Elias Ahmed, Ibsa Ahmed, Jafer Amin, Seyum Tezera, Dr. Nigussie Bussa, and Ibsa Usmane at Haramaya University, and Jenna Daniels and Anna Rabil at University of Florida for their contributions to the project. We thank Srevi Devaraj (Clinical Chemistry and POCT, Texas Children's Hospital, Baylor College of Medicine, Houston, TX) for analysis of sugars in the dual sugar absorption test. The study would not have been possible without cooperation of study communities and local administration of the study kebeles. We would like to express our appreciation for the study households and all who supported the study directly or otherwise.

SUPPLEMENTARY MATERIAL

The Supplementary Material for this article can be found online at: https://www.frontiersin.org/articles/10.3389/fpubh.2020.00099/full#supplementary-material

Pipeline used for the processing of the MeTRS data.

Figure S1 | Estimation of environmental enteric dysfunction severity based on gut permeability and gut inflammation data. The gut permeability was assessed using the percentage of lactulose in the urine. The gut inflammation was assessed based on the concentration in MPO (ng/ml) in the urine. Both parameters were used to estimate the environmental enteric dysfunction (EED) severity for each infant. The gut inflammation was considered normal if [MPO] was lower than 2,000 ng/ml, moderated if [MPO] was between 2,000 and 11,000 ng/ml, and severe if [MPO] was higher than 11,000 ng/ml. The gut permeability was considered normal if the lactulose value was lower than 0.2%, moderated if the lactulose value was between 0.2 and 0.45%, and severe if the lactulose value was higher than 0.45%; MPO, myeloperoxidase.

Figure S2 | *Campylobacter* spp. prevalence in the children stools ($n = 100$) collected from five kebeles using conventional PCR **(A)** and MeTRS **(B)** data. Orange and blue bars represent the percentage of the stools positive or negative, respectively for *Campylobacter* for a given kebele. C) Comparison of the *Campylobacter* prevalence using conventional PCR (c-PCR) and meta-total RNA sequencing (MeTRS). In red and blue are the stools positive or negative, respectively for *Campylobacter*. The heat map is composed of 100 columns (one column per child). Genus-specific PCR was performed using 16S RNA primers and species-specific PCR for *C. coli* and *C. jeju*ni were performed using *ceuE* and *mapA* primers, respectively (**Table S1**).

Figure S3 | Co-occurrence of *Campylobacter* spp. in the children stool samples. Co-occurrence Heatmap profile was created using the multivariate analysis data (r^2) based on the prevalence of *Campylobacter* spp. in the stool samples (see **Figure 2**).

Figure S4 | *Campylobacter* spp. profile between children stool samples based on the meta-total RNA sequencing (MeTRS). **(A)** Principal component analysis of the *Campylobacter* spp. diversity and abundance in the stools. Each colored dot represents one child stool sample ($n = 100$). Black dot represents the average profile for a given kebele ($n = 5$). **(B)** Discriminant analysis of the *Campylobacter* spp. diversity and abundance in the stools based on kebeles. The outside ellipse contains ∼50% of the observations. The inside ellipse represents 95% confidence level (Cut-off for MeTRS data; contigs number ≥ 10; Read length ≥ 50; Z-score ≥ 1. **(C)**. Clusterization profile of the stools based on the *Campylobacter* spp. diversity, prevalence, and abundance data.

Figure S5 | Differences in abundance of *Campylobacter hyointestinalis and Campylobacter* RM12175 between kebeles. Letters **(A,B)** indicates different statistical groups ($P < 0.01$). Star: read per million (rpm) are significantly higher in the designated kebele compared to the other kebeles.

Figure S6 | *Campylobacter* spp. profiles between children stool samples based EED severity and diarrhea. Discriminant analysis of the *Campylobacter* spp. abundance in the children stools based on **(A)** the gut permeability (lactulose%), **(C)** gut inflammation ([myeloperoxidase] in ng/ml), **(E)** EED severity, and **(G)** diarrhea prevalence data. The outside ellipse contains approximately 50% of the observations. The inside ellipse represents 95% confidence level. Clusterization profile of the *Campylobacter* spp. abundance in the stools based on **(B)** the gut permeability (lactulose%), **(D)** gut inflammation ([myeloperoxidase] in ng/ml), **(F)** EED severity, and **(H)** diarrhea prevalence data. Additional details concerning the EED severity determination are presented in **Table S1**.

Figure S7 | Microbiome profiles between children stool samples based on kebeles. **(A)** Principal component analysis of the children stool samples based on kebeles. Each colored dot represents one stool sample ($n = 100$). Kebeles with the same color code belong to the same cluster and therefore harbored equivalent microbiota diversity and abundance. A T^2 test revealed a total of 11 outliers (stools with significantly different microbiota profile compared to the rest of the population; outside the red oval). **(B)** Discriminant analysis of the stool microbiome based on kebeles. The outside ellipse contains ∼50% of the observations. The inside ellipse represents 95% confidence level. **(C)** Clusterization profile of the stool microbiome based on kebeles.

Figure S8 | Microbiome profile based on *Campylobacter* prevalence. **(A)** Discriminant analysis of the children stool microbiome based on *Campylobacter* prevalence. The outside ellipse contains ∼50% of the observations. The inside ellipse represents 95% confidence level. **(B)** Clusterization profile of the stool's microbiome based on *Campylobacter* prevalence.

Figure S9 | Microbiome profile based on environmental enteric dysfunction (EED). Discriminant analysis of the children stool microbiome composition based on **(A)** the gut permeability (lactulose%), **(C)** gut inflammation ([MPO] in ng/ml), **(E)** EED severity, and **(G)** diarrhea prevalence data. The outside ellipse contains ∼50% of the observations. The inside ellipse represents 95% confidence level. Clusterization profile of the *Campylobacter* spp. abundance in the stools based on **(B)** the gut permeability (lactulose%), **(D)** gut inflammation ([MPO] in ng/ml), **(F)** EED severity, and **(H)** diarrhea prevalence data. Additional details concerning the EED severity determination are presented in **Table S1**. **(I)** Correlation between the specific bacterial species of the children stool microbiome and the gut permeability (lactulose%), gut inflammation ([MPO] in ng/ml), EED severity, and diarrhea prevalence data. N, number of stools positive for the designated bacterium. Values in the table represent the mean (log [read per million]) ± standard error for the designated bacterial species for a given status. Stars represent bacterial species harboring at least 2-fold difference in abundance between the "normal" and "severe" status for at least one of the parameters studied. MPO: myeloperoxidase.

Table S1 | Primers used in the study. Source: Adapted from Deals et al. (28).

REFERENCES

1. Havelaar AH, Kirk MD, Torgerson PR, Gibb HJ, Hald T, Lake RJ, et al. World Health Organization global estimates and regional comparisons of the burden of foodborne disease in 2010. *PLoS Med.* (2015) 12:e1001923. doi: 10.1371/journal.pmed.1001923
2. Janssen R, Krogfelt KA, Cawthraw SA, van Pelt W, Wagenaar JA, Owen RJ. Host-pathogen interactions in *Campylobacter* infections: the host perspective. *Clin Microbiol Rev.* (2008) 21:505–18. doi: 10.1128/CMR.00055-07
3. GBD 2015 Mortality and Causes of Death Collaborators. Global, regional, and national life expectancy, all-cause mortality, and cause-specific mortality for 249 causes of death, 1980-2015: a systematic analysis for the Global Burden of Disease Study 2015. *Lancet.* (2016) 388:1459–544. doi: 10.1016/S0140-6736(16)31012-1
4. Coker AO, Isokpehi RD, Thomas BN, Amisu KO, Obi CL. Human campylobacteriosis in developing countries. *Emerg Infect Dis.* (2002) 8:237–44. doi: 10.3201/eid0803.010233
5. Lee G, Pan W, Peñataro Yori P, Paredes Olortegui M, Tilley D, Gregory M, et al. Symptomatic and asymptomatic *Campylobacter* infections associated with reduced growth in Peruvian children. *PLoS Negl Trop Dis.* (2013) 7:e2036. doi: 10.1371/journal.pntd.0002036
6. Ngure F, Gelli A, Becquey E, Ganaba R, Headey D, Huybregts L, et al. Exposure to livestock feces and water quality, sanitation, and hygiene (WASH) conditions among caregivers and young children: formative research in Rural Burkina Faso. *Am J Trop Med Hyg.* (2019) 100:998–1004. doi: 10.4269/ajtmh.18-0333
7. Amour C, Gratz J, Mduma E, Svensen E, Rogawski ET, McGrath M, et al. Epidemiology and impact of *Campylobacter* infection in children in 8 low-resource settings: results from the MAL-ED study. *Clin Infect Dis.* (2016) 63:1171–9. doi: 10.1093/cid/ciw542
8. Rogawski ET, Liu J, Platts-Mills JA, Kabir F, Lertsethtakarn P, Siguas M, et al. Use of quantitative molecular diagnostic methods to investigate the effect of enteropathogen infections on linear growth in children in low-resource settings: longitudinal analysis of results from the MAL-ED cohort study. *Lancet Glob Health.* (2018) 6:e1319-28. doi: 10.1016/S2214-109X(18)30351-6
9. World Health Organization. *WHO | Joint Child Malnutrition Estimates - Levels and Trends,* 2019 ed. WHO (2018). Available at: http://www.who.int/nutgrowthdb/estimates2018/en/ (accessed October 16, 2019).
10. Keusch GT, Denno DM, Black RE, Duggan C, Guerrant RL, Lavery JV, et al. Environmental enteric dysfunction: pathogenesis, diagnosis, and clinical consequences. *Clin Infect Dis.* (2014) 59(Suppl. 4):S207–12. doi: 10.1093/cid/ciu485
11. Guerrant RL, DeBoer MD, Moore SR, Scharf RJ, Lima AAM. The impoverished gut—a triple burden of diarrhoea, stunting and chronic disease. *Nat Rev Gastroenterol Hepatol.* (2013) 10:220–9. doi: 10.1038/nrgastro.2012.239
12. Richard SA, McCormick BJJ, Murray-Kolb LE, Lee GO, Seidman JC, Mahfuz M, et al. Enteric dysfunction and other factors associated with attained size at 5 years: MAL-ED birth cohort study findings. *Am J Clin Nutr.* (2019) 110:131–8. doi: 10.1093/ajcn/nqz004
13. Platts-Mills JA, Babji S, Bodhidatta L, Gratz J, Haque R, Havt A, et al. Pathogen-specific burdens of community diarrhoea in developing countries: a multisite birth cohort study (MAL-ED). *Lancet Glob Health.* (2015) 3:e564–75. doi: 10.1016/S2214-109X(15)00151-5
14. Headey D, Hirvonen K. Is exposure to poultry harmful to child nutrition? An observational analysis for rural Ethiopia. *PloS ONE.* (2016) 11:e0160590. doi: 10.1371/journal.pone.0160590
15. Lengerh A, Moges F, Unakal C, Anagaw B. Prevalence, associated risk factors and antimicrobial susceptibility pattern of *Campylobacter* species among under five diarrheic children at Gondar University Hospital, Northwest Ethiopia. *BMC Pediatr.* (2013) 13:82. doi: 10.1186/1471-2431-13-82
16. Mulatu G, Beyene G, Zeynudin A. Prevalence of *Shigella*, *Salmonella* and *Campylobacter* species and their susceptibility patters among under five children with diarrhea in Hawassa town, south Ethiopia. *Ethiop J Health Sci.* (2014) 24:101–8. doi: 10.4314/ejhs.v24i2.1
17. Abamecha A, Assebe G, Tafa B, Beyene W. Prevalence of thermophilic campylobacter and their antimicrobial resistance profile in food animals in Lare District, Nuer Zone, Gambella, Ethiopia. *J Drug Res Dev.* (2015) 1:2470–1009. doi: 10.16966/2470-1009.108
18. Thomas KM, de Glanville WA, Barker GC, Benschop J, Buza JJ, Cleaveland S, et al. Prevalence of *Campylobacter* and *Salmonella* in African food animals and meat: A systematic review and meta-analysis. *Int J Food Microbiol.* (2019) 315:108382. doi: 10.1016/j.ijfoodmicro.2019.108382
19. Forsythe SJ. *The Microbiology of Safe Food*. Nottingham, UK: John Wiley and Sons; Nottingham Trent University (2011).
20. Wilkinson DA, O'Donnell AJ, Akhter RN, Fayaz A, Mack HJ, Rogers LE, et al. Updating the genomic taxonomy and epidemiology of *Campylobacter hyointestinalis*. *Sci Rep.* (2018) 8:1–12. doi: 10.1038/s41598-018-20889-x
21. Owino V, Ahmed T, Freemark M, Kelly P, Loy A, Manary M, et al. Environmental enteric dysfunction and growth failure/stunting in Global child health. *Pediatrics.* (2016) 138:1–10. doi: 10.1542/peds.2016-0641
22. Bado AR, Susuman AS, Nebie EI. Trends and risk factors for childhood diarrhea in sub-Saharan countries (1990-2013): assessing the neighborhood inequalities. *Glob Health Action.* (2016) 9:30166. doi: 10.3402/gha.v9.30166
23. Central Statistical Agency (CSA). *Demographic and Health Survey, Ethiopia, 2016*. (2016). Available online at: https://microdata.worldbank.org/index.php/catalog/2886 (accessed September 22, 2019).
24. Faubion WA, Camilleri M, Murray JA, Kelly P, Amadi B, Kosek MN, et al. Improving the detection of environmental enteric dysfunction: a lactulose, rhamnose assay of intestinal permeability in children aged under 5 years exposed to poor sanitation and hygiene. *BMJ Glob Health.* (2016) 1:66. doi: 10.1136/bmjgh-2016-000066
25. Ordiz MI, Davitt C, Stephenson K, Agapova S, Divala O, Shaikh N, et al. EB 2017 article: interpretation of the lactulose:mannitol test in rural Malawian children at risk for perturbations in intestinal permeability. *Exp Biol Med.* (2018) 243:677–83. doi: 10.1177/1535370218768508
26. Deblais L, Helmy YA, Kathayat D, Huang H, Miller SA, Rajashekara G. Novel imidazole and methoxybenzylamine growth inhibitors affecting *Salmonella* cell envelope integrity and its persistence in chickens. *Sci Rep.* (2018) 8:1–17. doi: 10.1038/s41598-018-31249-0
27. Kumar A, Vlasova AN, Deblais L, Huang H-C, Wijeratne A, Kandasamy S, et al. Impact of nutrition and rotavirus infection on the infant gut microbiota in a humanized pig model. *BMC Gastroenterol.* (2018) 18:93. doi: 10.1186/s12876-018-0810-2
28. Denis M, Soumet C, Rivoal K, Ermel G, Blivet D, Salvat G, et al. Development of a m-PCR assay for simultaneous identification of *Campylobacter jejuni* and *C. coli*. *Lett Appl Microbiol.* (1999) 29:406–10. doi: 10.1046/j.1472-765X.1999.00658.x

29. Cottier F, Srinivasan KG, Yurieva M, Liao W, Poidinger M, Zolezzi F, et al. Advantages of meta-total RNA sequencing (MeTRS) over shotgun metagenomics and amplicon-based sequencing in the profiling of complex microbial communities. *NPJ Biofilms Microbiomes.* (2018) 4:1–7. doi: 10.1038/s41522-017-0046-x
30. Saha S, Ramesh A, Kalantar K, Malaker R, Hasanuzzaman M, Khan LM, et al. Unbiased metagenomic sequencing for pediatric meningitis in Bangladesh reveals neuroinvasive Chikungunya virus outbreak and other unrealized pathogens. *bioRxiv.* (2019) 10:579532. doi: 10.1128/mBio.02877-19
31. Schnee AE, Petri WA. *Campylobacter jejuni* and associated immune mechanisms: short-term effects and long-term implications for infants in low-income countries. *Curr Opin Infect Dis.* (2017) 30:322–8. doi: 10.1097/QCO.0000000000000364
32. Rodgers JD, Simpkin E, Lee R, Clifton-Hadley FA, Vidal AB. Sensitivity of direct culture, enrichment and PCR for Detection of *Campylobacter jejuni* and *C. coli* in Broiler Flocks at Slaughter. *Zoonoses Public Health.* (2017) 64:262–71. doi: 10.1111/zph.12306
33. Platts-Mills JA, Liu J, Gratz J, Mduma E, Amour C, Swai N, et al. Detection of *Campylobacter* in stool and determination of significance by culture, enzyme immunoassay, and PCR in developing countries. *J Clin Microbiol.* (2014) 52:1074–80. doi: 10.1128/JCM.02935-13
34. Ricke SC, Feye KM, Chaney WE, Shi Z, Pavlidis H, Yang Y. Developments in rapid detection methods for the detection of foodborne *Campylobacter* in the United States. *Front Microbiol.* (2018) 9:3280. doi: 10.3389/fmicb.2018.03280
35. Lewandowska DW, Zagordi O, Geissberger F-D, Kufner V, Schmutz S, Böni J, et al. Optimization and validation of sample preparation for metagenomic sequencing of viruses in clinical samples. *Microbiome.* (2017) 5:94. doi: 10.1186/s40168-017-0317-z
36. Plaire D, Puaud S, Marsolier-Kergoat M-C, Elalouf J-M. Comparative analysis of the sensitivity of metagenomic sequencing and PCR to detect a biowarfare simulant (*Bacillus atrophaeus*) in soil samples. *PloS ONE.* (2017) 12:e0177112. doi: 10.1371/journal.pone.0177112
37. Gigliucci F, von Meijenfeldt FAB, Knijn A, Michelacci V, Scavia G, Minelli F, et al. Metagenomic characterization of the human intestinal microbiota in fecal samples from STEC-infected patients. *Front Cell Infect Microbiol.* (2018) 8:25. doi: 10.3389/fcimb.2018.00025
38. Doster E, Rovira P, Noyes NR, Burgess BA, Yang X, Weinroth MD, et al. A cautionary report for pathogen identification using shotgun metagenomics; a comparison to aerobic culture and polymerase chain reaction for *Salmonella enterica* identification. *Front Microbiol.* (2019) 10:2499. doi: 10.3389/fmicb.2019.02499
39. Kaakoush NO, Castaño-Rodríguez N, Mitchell HM, Man SM. Global epidemiology of *Campylobacter* infection. *Clin Microbiol Rev.* (2015) 28:687–720. doi: 10.1128/CMR.00006-15
40. Costa D, Iraola G. Pathogenomics of emerging *Campylobacter* species. *Clin Microbiol Rev.* (2019) 32:1–24. doi: 10.1128/CMR.00072-18
41. Spickler AR, Leedom Larson K. *Campylobacteriosis* (2013). Retrieved from: http://www.cfsph.iastate.edu/DiseaseInfo/factsheets.php
42. Liu F, Ma R, Wang Y, Zhang L. The Clinical Importance of Campylobacter concisus and Other Human Hosted Campylobacter Species. *Front Cell Infect Microbiol.* (2018) 8:243. doi: 10.3389/fcimb.2018.00243
43. Oporto B, Hurtado A. Emerging thermotolerant *Campylobacter* species in healthy ruminants and swine. *Foodborne Pathog Dis.* (2011) 8:807–13. doi: 10.1089/fpd.2010.0803
44. Inglis GD, Kalischuk LD, Busz HW. Chronic shedding of *Campylobacter* species in beef cattle. *J Appl Microbiol.* (2004) 97:410–20. doi: 10.1111/j.1365-2672.2004.02313.x
45. Hakkinen M, Heiska H, Hänninen M-L. Prevalence of *Campylobacter* spp. in cattle in Finland and antimicrobial susceptibilities of bovine *Campylobacter jejuni* strains. *Appl Environ Microbiol.* (2007) 73:3232–8. doi: 10.1128/AEM.02579-06
46. Salihu MD, Abdulkadir JU, Oboegbulem SI, Egwu GO, Magaji AA, Lawal M, et al. Isolation and prevalence of *Campylobacter* species in cattle from Sokoto state, Nigeria. *Vet Ital.* (2009) 45:501–5.
47. Serraino A, Florio D, Giacometti F, Piva S, Mion D, Zanoni RG. Presence of *Campylobacter* and *Arcobacter* species in in-line milk filters of farms authorized to produce and sell raw milk and of a water buffalo dairy farm in Italy. *J Dairy Sci.* (2013) 96:2801–7. doi: 10.3168/jds.2012-6249
48. Guévremont E, Lamoureux L, Loubier CB, Villeneuve S, Dubuc J. Detection and characterization of *Campylobacter* spp. from 40 dairy cattle herds in Quebec, Canada. *Foodborne Pathog Dis.* (2014) 11:388–94. doi: 10.1089/fpd.2013.1706
49. Gorkiewicz G, Feierl G, Zechner R, Zechner EL. Transmission of *Campylobacter hyointestinalis* from a pig to a human. *J Clin Microbiol.* (2002) 40:2601–5. doi: 10.1128/JCM.40.7.2601-2605.2002
50. Miller WG, Chapman MH, Yee E, On SLW, McNulty DK, Lastovica AJ, et al. Multilocus sequence typing methods for the emerging *Campylobacter* species, *C. hyointestinalis, C lanienae, C sputorum, C concisus, and C curvus, Front Cell Infect Microbiol.* (2012) 2:45. doi: 10.3389/fcimb.2012.00045
51. Patrick ME, Gilbert MJ, Blaser MJ, Tauxe RV, Wagenaar JA, Fitzgerald C. Human infections with new subspecies of *Campylobacter fetus*. *Emerg Infect Dis.* (2013) 19:1678–80. doi: 10.3201/eid1910.130883
52. Kim DK, Hong SK, Kim M, Ahn JY, Yong D, Lee K. *Campylobacter hyointestinalis* isolated from a human stool specimen. *Ann Lab Med.* (2015) 35:657–9. doi: 10.3343/alm.2015.35.6.657
53. Samosornsuk W, Asakura M, Yoshida E, Taguchi T, Eampokalap B, Chaicumpa W, et al. Isolation and characterization of *Campylobacter* strains from diarrheal patients in central and Suburban Bangkok, Thailand. *Jpn J Infect Dis.* (2015) 68:209–15. doi: 10.7883/yoken.JJID.2014.229
54. Rapp D, Ross CM. Prevalence of six *Campylobacter* species in a New Zealand dairy goat herd. *N Z J Agric Res.* (2012) 55:235–40. doi: 10.1080/00288233.2012.672427
55. Chaban B, Ngeleka M, Hill JE. Detection and quantification of 14 *Campylobacter* species in pet dogs reveals an increase in species richness in feces of diarrheic animals. *BMC Microbiol.* (2010) 10:73. doi: 10.1186/1471-2180-10-73
56. Sasaki Y, Goshima T, Mori T, Murakami M, Haruna M, Ito K, et al. Prevalence and antimicrobial susceptibility of foodborne bacteria in wild boars (Sus scrofa) and wild deer (Cervus nippon) in Japan. *Foodborne Pathog Dis.* (2013) 10:985–91. doi: 10.1089/fpd.2013.1548
57. Ley RE. Gut microbiota in 2015: *Prevotella* in the gut: choose carefully. *Nat Rev Gastroenterol Hepatol.* (2016) 13:69–70. doi: 10.1038/nrgastro.2016.4
58. Larsen JM. The immune response to *Prevotella* bacteria in chronic inflammatory disease. *Immunology.* (2017) 151:363–74. doi: 10.1111/imm.12760
59. Pybus V, Onderdonk AB. Evidence for a commensal, symbiotic relationship between *Gardnerella vaginalis* and *Prevotella bivia* Involving ammonia: potential significance for bacterial vaginosis. *J Infect Dis.* (1997) 175:406–13. doi: 10.1093/infdis/175.2.406
60. Pybus V, Onderdonk AB. A commensal symbiosis between *Prevotella bivia* and *Peptostreptococcus anaerobius* involves amino acids: potential significance to the pathogenesis of bacterial vaginosis. *FEMS Immunol Med Microbiol.* (1998) 22:317–27. doi: 10.1111/j.1574-695X.1998.tb01221.x
61. Margolis E, Fredricks DN. Chapter 83 - bacterial vaginosis-associated bacteria. In: Tang YW, Sussman M, Liu D, Poxton I, Schwartzman J, editors. *Molecular Medical Microbiology*, 2nd ed. Boston, MA: Academic Press (2015). p. 1487–96.
62. Pedersen HK, Gudmundsdottir V, Nielsen HB, Hyotylainen T, Nielsen T, Jensen BAH, et al. Human gut microbes impact host serum metabolome and insulin sensitivity. *Nature.* (2016) 535:376–81. doi: 10.1038/nature18646
63. Giri S, Mangalam A. Chapter 34 - the gut microbiome and metabolome in multiple sclerosis. In: Faintuch J, Faintuch S, editors. Academic Press (2019). p. 333–40.
64. Vazquez-Gutierrez P, de Wouters T, Werder J, Chassard C, Lacroix C. High Iron-sequestrating bifidobacteria inhibit enteropathogen growth and adhesion to intestinal epithelial cells *in vitro*. *Front Microbiol.* (2016) 7:1480. doi: 10.3389/fmicb.2016.01480
65. Sakurai T, Odamaki T, Xiao J-Z. Production of indole-3-lactic acid by bifidobacterium strains isolated fromhuman infants. *Microorganisms.* (2019) 7:340. doi: 10.3390/microorganisms7090340
66. Mundi A, Delcenserie V, Amiri-Jami M, Moorhead S, Griffiths MW. Cell-free preparations of *Lactobacillus acidophilus* strain La-5 and Bifidobacterium longum strain NCC2705 affect virulence gene expression in Campylobacter jejuni. *J Food Prot.* (2013) 76:1740–6. doi: 10.4315/0362-028X.JFP-13-084

67. Hashizume K, Tsukahara T, Yamada K, Koyama H, Ushida K. *Megasphaera elsdenii* JCM1772T normalizes hyperlactate production in the large intestine of fructooligosaccharide-fed rats by stimulating butyrate production. *J Nutr.* (2003) 133:3187–90. doi: 10.1093/jn/133.10.3187
68. Wexler HM. Bacteroides: the good, the bad, and the nitty-gritty. *Clin Microbiol Rev.* (2007) 20:593–621. doi: 10.1128/CMR.00008-07
69. Spanogiannopoulos P, Bess EN, Carmody RN, Turnbaugh PJ. The microbial pharmacists within us: a metagenomic view of xenobiotic metabolism. *Nat Rev Microbiol.* (2016) 14:273–87. doi: 10.1038/nrmicro.2016.17
70. Ščerbová J, Lauková A. Sensitivity to enterocins of thermophilic *Campylobacter spp*. from different poultry species. *Foodborne Pathog Dis.* (2016) 13:668–73. doi: 10.1089/fpd.2016.2158
71. Helmy YA, Kassem II, Kumar A, Rajashekara G. *In vitro* evaluation of the impact of the probiotic *E. coli* nissle 1917 on *Campylobacter jejuni*'s invasion and intracellular survival in human colonic cells. *Front. Microbiol.* (2017) 8:1588. doi: 10.3389/fmicb.2017.01588
72. Johnson TJ, Shank JM, Johnson JG. Current and potential treatments for reducing *Campylobacter* colonization in animal hosts and disease in HUMANS. *Front Microbiol.* (2017) 8:487. doi: 10.3389/fmicb.2017.00487
73. Maki JJ, Looft T. Complete genome sequence of megasphaera stantonii ajh120t, isolated from a chicken cecum. *Microbiol Resour Announc.* (2018) 7:e01148-18. doi: 10.1128/MRA.01148-18
74. Ueda A, Kobayashi A, Tsuchida S, Yamada T, Murata K, Nakamura H, et al. Cecal microbiome analyses on wild Japanese Rock Ptarmigans (Lagopus muta japonica) reveals high level of coexistence of lactic acid bacteria and lactate-utilizing bacteria. *Microorganisms.* (2018) 6:77. doi: 10.3390/microorganisms 6030077
75. Gough EK, Stephens DA, Moodie EEM, Prendergast AJ, Stoltzfus RJ, Humphrey JH, et al. Linear growth faltering in infants is associated with *Acidaminococcus* sp. *and* community-level changes in the gut microbiota. *Microbiome.* (2015) 3:24. doi: 10.1186/s40168-015-0089-2
76. Dinh DM, Ramadass B, Kattula D, Sarkar R, Braunstein P, Tai A, et al. Longitudinal analysis of the intestinal microbiota in persistently stunted young children in South India. *PloS ONE.* (2016) 11:e0155405. doi: 10.1371/journal.pone.0155405
77. Liu S, Li E, Sun Z, Fu D, Duan G, Jiang M, et al. Altered gut microbiota and short chain fatty acids in Chinese children with autism spectrum disorder. *Sci Rep.* (2019) 9:1–9. doi: 10.1038/s41598-018-36430-z
78. World Medical Association. World Medical Association Declaration of Helsinki: ethical principles for medical research involving human subjects. *JAMA.* (2013) 310:2191–4. doi: 10.1001/jama.2013.281053

Conflict of Interest: The authors declare that the research was conducted in the absence of any commercial or financial relationships that could be construed as a potential conflict of interest.

frontiers in Microbiology

ORIGINAL RESEARCH
published: 27 April 2020
doi: 10.3389/fmicb.2020.00632

Bacteriophages to Control *Campylobacter* in Commercially Farmed Broiler Chickens, in Australia

Helene N. Chinivasagam[1], Wiyada Estella[1], Lance Maddock[1], David G. Mayer[1], Caitlin Weyand[1], Phillippa L. Connerton[2] and Ian F. Connerton[2]**

[1] EcoSciences Precinct, Department of Agriculture and Fisheries, Queensland Government, Brisbane, QLD, Australia, [2] Division of Microbiology, Brewing and Biotechnology, School of Biosciences, University of Nottingham, Nottingham, United Kingdom

This study describes the development and use of bacteriophage cocktails to control *Campylobacter* in broiler chickens, in a commercial setting, in Queensland Australia, following the birds from farm to the processing plant. The components of the bacteriophage cocktails were selected to be effective against the maximum number of *Campylobacter jejuni* and *Campylobacter coli* isolates encountered on SE Queensland farms. Farms were identified that had suitable *Campylobacter* target populations and phage were undetectable 1 week prior to the intended treatment. Cocktails of phages were administered at 47 days of age. Groups of study birds were slaughtered the following day, on-farm, at the end of flock transport to the plant, and at processing (approximately 28 h post-treatment). On Farm A, the phage treatment significantly reduced *Campylobacter* levels in the ceca at the farm in the range of 1–3 $\log_{10}$ CFU/g ($p = 0.007$), compared to mock treated controls. However, individual birds sampled on farm (1/10) or following transport (2/10) exhibited high cecal *Campylobacter* counts with low phage titers, suggesting that treatment periods > 24 h may be required to ensure phage replication for effective biocontrol *in vivo*. At the time of the trial the control birds in Farm B were phage positive despite having been negative one week earlier. There was no significant difference in the cecal *Campylobacter* counts between the treatment and control groups following treatment but a fall of 1.7 $\log_{10}$ CFU/g was observed from that determined from birds collected the previous week ($p = 0.0004$). *Campylobacter* isolates from both farms retained sensitivity to the treatment phages. These trials demonstrated bacteriophages sourced from Queensland farms have the potential to reduce intestinal *Campylobacter* levels in market ready broiler chickens.

Keywords: bacteriophage, *Campylobacter*, broiler chicken, Queensland (Australia), poultry

OPEN ACCESS

Edited by:
Nicolae Corcionivoschi, Agri-Food and Biosciences Institute (AFBI), United Kingdom

Reviewed by:
Manan Sharma, United States Department of Agriculture (USDA), United States
Mariana Carmen Chifiriuc, University of Bucharest, Romania

****Correspondence:***
Helene N. Chinivasagam
nalini.chinivasagam@daf.qld.gov.au
Ian F. Connerton
ian.connerton@nottingham.ac.uk

Specialty section:
This article was submitted to Food Microbiology, a section of the journal Frontiers in Microbiology

Received: *26 September 2019*
Accepted: *20 March 2020*
Published: *27 April 2020*

Citation:
Chinivasagam HN, Estella W, Maddock L, Mayer DG, Weyand C, Connerton PL and Connerton IF (2020) Bacteriophages to Control Campylobacter in Commercially Farmed Broiler Chickens, in Australia. Front. Microbiol. 11:632. doi: 10.3389/fmicb.2020.00632

INTRODUCTION

Campylobacter infection is one of the most frequently reported causes of food-borne enteritis in Australia and worldwide (Kaakoush et al., 2015). Australia began a National Notifiable Diseases Surveillance System in 1991 and since then, the number of cases of human infection has steadily risen to 137.5/100,000, in 2018[1]. This incidence rate is higher than many other parts of the world

[1] http://www9.health.gov.au/cda/source/rpt_4.cfm

(Kaakoush et al., 2015) and it is estimated that only around 10% of *Campylobacter* infection cases are recorded (Hall et al., 2008). Thus, *Campylobacter* has a significant impact on the health and economic prosperity of the Australia population.

Consumption of poultry meat has been identified as an important risk factor for human infection from source attribution studies (Mughini Gras et al., 2012; Ravel et al., 2017). *Campylobacter* spp., particularly *Campylobacter jejuni* and to a lesser extent *Campylobacter coli* are ubiquitous in the intestinal contents of broiler chickens (European Food Safety Authority [EFSA] and European Centre for Disease Prevention and Control [ECDC], 2018). During slaughter and processing, poultry carcasses frequently become contaminated with *Campylobacter* from the intestinal contents, providing a reservoir for human infection (European Food Safety Authority [EFSA], 2010). Consequently, managing *Campylobacter* numbers in poultry hosts, on-farm, is a promising strategy to reduce disease burden. A 3 $\log_{10}$ reduction in *Campylobacter* numbers in the intestines of infected birds at slaughter, could potentially contribute to a 90% reduction in public health risks (Crotta et al., 2017). European studies indicate that on-farm interventions can be very effective with a 1.0 $\log_{10}$ reduction in fecal count supported by a 1.0 $\log_{10}$ reduction in contamination of the exterior of chickens (during processing) could result in a 90% reduction of human infections (Havelaar et al., 2007). Biocontrol using bacteriophages has the potential to control *Campylobacter* numbers in highly contaminated flocks (Crotta et al., 2017).

Biocontrol using bacteriophages has been exploited for controlling other food-borne pathogens such as *Salmonella*, *Escherichia coli* O157:H7 and *Listeria monocytogenes* (Goodridge and Bisha, 2011). Bacteriophages have been shown to be naturally present in poultry environments in the United Kingdom and Australia along with their host campylobacters (Connerton et al., 2004; Loc Carrillo et al., 2007; Owens et al., 2013). Poultry farms are a natural source of phages from which to develop appropriate on-farm treatments as their use will not introduce any agent that is not already frequently encountered (Atterbury et al., 2005; El-Shibiny et al., 2005). These considerations are of commercial importance against a background of consumer anxiety regarding the adoption of intervention strategies against campylobacters from poultry (MacRitchie et al., 2014). Experimental studies have demonstrated the potential to use phages to reduce *C. jejuni* in broiler chicken ceca (Loc Carrillo et al., 2005; El-Shibiny et al., 2009) and the surface of chicken skin (Atterbury et al., 2003; Goode et al., 2003). Bacteriophages can be used to reduce *Campylobacter* either on-farm or on the processed product (Connerton et al., 2011). A one $\log_{10}$ reduction in the numbers of *C. jejuni* and *C. coli* in feces has been reported (Carvalho et al., 2010). The use of phages on-farm is a welfare friendly option for the biological control of *Campylobacter* that can be adopted from a logistic perspective for use with commercial poultry.

Phage selection, method, and timing of application on commercial farms are important criteria to achieve meaningful reductions in terms of the risk to the consumer. Wagenaar et al. (2005) have demonstrated 1–3 $\log_{10}$ reductions in *Campylobacter* counts at various points in the rearing cycle. Loc Carrillo et al. (2005) have also demonstrated log reductions (0.5 and 5 $\log_{10}$ CFU/g) over an extended treatment period (5 days) on experimentally infected birds (25 days old). Similarly, *Campylobacter* reductions in ceca have been demonstrated over a shorter period (i.e., 2 $\log_{10}$ CFU/g reduction over 48 h) in experimentally inoculated broilers (El-Shibiny et al., 2009). Treatment of naturally colonized commercial birds has been demonstrated to produce significant reductions in *Campylobacter* levels of 3.2 $\log_{10}$ CFU/g of ceca from one of the three commercial broiler houses involved in the trial (Kittler et al., 2013).

The present study was designed to provide a better understanding of the application of phages for typical Australian commercial farm settings. *Campylobacter* counts were assessed at the end of rearing on the farm, after transport, and on carcasses post processing.

METHODOLOGY

Campylobacter Strains

Campylobacter strains used as bacteriophage hosts were as follows: *C. jejuni* NCTC 12662, *C. jejuni* NC3142 (Farm C isolate sourced from re-use litter in 2011), and *C. coli* NC2934 (Farm C isolate sourced from non-reused litter in 2011). These were grown on Blood agar No 2 (Oxoid CM0271) with 5% (v/v) lyzed horse blood added (LHB; Oxoid Australia), for 24 h at 42°C, under microaerobic conditions, produced by using Campygen gas packs (Oxoid, CN0025A; Basingstoke, United Kingdom). Isolates used for resistance testing were sourced from chicken ceca and carcasses pre- and post-initiation of the study.

Bacteriophage Isolation, Characterization, and Selection

Bacteriophages used in this study were isolated between 2012 and 2015, from samples of: cecal contents, litter, carcass rinses, and soil from Queensland broiler chicken farms and pig effluent. For direct isolation from cecal contents, a 10% suspension in SM buffer (100 mM NaCl; 8 mM $MgSO_4.7H_2O$; 0.01% gelatin; 50 mM Tris-HCl, pH7.5), incubated over-night at 4°C, centrifuged at 15,000 *g* for 10 min at 4°C, filtered through 0.2 μm filters (Minisart; Sartorius) then 100 μl added containing 200 μl of *Campylobacter* host strains (10^8 CFU/ml) and incubated at 42°C for 30 min to allow phage to bind to host. The proportion of sample to broth was as follows: cecal contents and pig effluent 1:4; litter 1:6; soil 1:3, and carcass rinse 1:2. The suspension was the added to 5 ml of molten 0.6% NZCYM (Difco, Beckton Dickinson, United States) soft agar overlay at 48°C, poured onto 1% NZCYM plates and allowed to set. The plates were then dried with lids partially open and then incubated at 42°C for 24 h, under microaerobic conditions (Connerton et al., 2004). Isolated plaques were collected using a pipette tip and suspended in 100 μl of SM buffer. Each single plaque was propagated three times to ensure that the isolates represented a single clone. In addition, an enrichment technique using modified Preston broth (Bolton et al., 1983) was used. The base Preston broth was prepared from Nutrient Broth Number 2 (NB2; Oxoid CM0067), 5% (v/v) LHB (Oxoid), with *Campylobacter* growth supplement (Oxoid,

SR0232) and Preston *Campylobacter* selective supplement (Oxoid SR0117). This was modified for phage enrichment by addition of 10 mM $MgSO_4 7H_2O$ and 1 mM $CaCl_2$ to stabilize phage capsids (Adams, 1959). Fifty microliters of overnight cultures of *C. jejuni* 12662, *C. jejuni* NC3142, and *C. coli* NC2934 (that had been grown in NB2 with 5% LHB (v/v) and incubated overnight at 42°C) were added to the diluted samples. The enrichment broth containing sample and host bacteria were incubated at 42°C for 24 h under microaerobic conditions. After incubation, centrifugation, and filtration, phages were isolated using the soft agar technique as described above for direct isolation, using all three hosts on separate plates. Approximately 600 bacteriophages were isolated using these methods from using either direct isolation or enrichment. A total of 128 (from the 600) phages were screened (described below) against 486 *Campylobacter* isolates using multiple combinations to narrow down representation to a 17-member phage panel. A further two phages from Queensland pig farm effluent were also included based on their lytic activity to arrive at a 19-member cocktail candidate panel. The *Campylobacter* isolates used, represented a mix of *C. jejuni* and *C. coli*, sourced from 17 South East Queensland farms across 36 farm samplings that occurred from 2009 to 2013.

Screening of Farm *Campylobacter* Isolates Against Phage Cocktail Candidates

The lytic activities of 19 phage cocktail candidates were tested against 241 representative *Campylobacter* isolates sourced between 2012 and 2016 from nine different Queensland farms. The 19 phage cocktail candidates, diluted to contain 10^6 PFU/ml were dispensed as 10 μl droplets, onto test bacterial lawns prepared as above. Following incubation, strains were scored as sensitive to a bacteriophage, if clear lysis or semi-clear lysis was observed following incubation.

Pre-screening of Birds to Enable Farm Selection

Six farms all having birds of roughly the same age were pre-screened approximately 1 week before the end of the growth cycle. Three chickens were randomly picked from two to four sheds. The criteria for final selection was that the farm should have a high-level resident *Campylobacter* population that was sensitive to more than one of the 19 selected phage candidates, and that the digesta samples were negative for indigenous phage. The absence of indigenous phage was considered a prerequisite because a previous survey demonstrated that such phage can effect mean *Campylobacter* populations (Atterbury et al., 2005). Birds were euthanized at the farm and the ceca were removed before transport on ice to the laboratory within 3–4 h. For *Campylobacter* enumeration, serial dilutions of cecal contents were prepared in MRD then 100 μl of each dilution was spread in triplicate, onto mCCDA (Oxoid CM0739) plates, containing selective supplement (Oxoid SR0155), and then incubated at 37°C for 48 h under microaerobic conditions as above. Ten well-separated *Campylobacter* colonies per shed were randomly picked across the three samples and re-streaked for purity. Their lysis profiles were then assessed against the 19 phage cocktail candidates (described above). Two farms which fulfilled the three criteria were selected (Farm A and Farm B) and the most appropriate phages selected to form a cocktail to administer to the test birds on these farms. These were PH5, PH8, PH11, and PH13 for Farm A and PH18 and PH19 for Farm B.

TABLE 1 | Description of trial farms and conditions relevant to trial.

Farm situation	Farm A	Farm B
Shed dimensions	153 × 15.2 m	122 × 13.7 m
Shed area	2325 m^2	1670 m^2
Pen sizes	6 m (L) × 1.5 (W) = 9 m^2	4 m (L) × 2.5 (W) = 10 m^2
Distance between treatment and control	5.5 m	4.5 m
Birds remaining at dosing	16,800	12,750
Bird density	7.22/m^2	7.63/m^2
Bird age at pick-up	48 days	48 days
Litter practice	Australian partial re-use	Australian partial re-use
Other commercial practices relevant to the trial birds		
Feed withdrawal	8 h prior pick-up (as others)	
Water withdrawal	1 h prior pick-up (as others)	
Transport	Placed in designated transport module and transport in truck with other commercial birds	
Processing	Moved along process chain along with other non-trial birds and removed prior chlorination	

Farm Trials

Descriptions of the two test farms and conditions employed during the trial are presented in **Table 1**. For each of the two selected farms, two groups of randomly picked 30 birds (phage treated and placebo groups) were segregated into two pens, within the chicken barn using wire mesh, but all other farming conditions remained same as the rest of barn. All the birds were 47 days of age at this point. Phage or placebo were administered by oral gavage, 1 day prior to transport to the processing plant. The placebo group of chickens received 3 ml of sterile tap water while the phage treatment group were given 3 ml of 10^7 PFU/ml of each phage combined in sterile tap water. Food and water were withdrawn 8 h prior to collection according to normal farm practice. The following day, when the main cohort were collected for transport to the processing plant, 10 birds from each group were euthanized at the farm. A further 10 birds were euthanized following transport (which took approximately 4 h) and the carcasses of the final group were processed by the plant and collected before the chlorine rinse stage.

Sample Preparation and Enumeration of *Campylobacter*

Chicken ceca were removed aseptically and transported to the laboratory on ice. The ceca were chopped into fine material, from which 10 g samples were aseptically blended using a homogenizer for 1 min, with a diluent consisting of NB2 with

LHB 5% (v/v). A 10 cm length of the ileum was measured from the ileal–cecal junction similarly transported on ice to laboratory. The total ileum contents were weighed, and appropriate 10-fold dilutions prepared. Carcasses were removed prior to chlorination and spin-chilling and placed in a sterile bag with 200 ml of 0.1% peptone (Oxoid LP0037) and shaken for 2 min in a shaker designed for the purpose. Ten-fold dilutions were prepared using Preston broth, and *Campylobacter* enumerated using a three tube, MPN technique for Farm B (Chinivasagam et al., 2009). Briefly the dilution tubes were incubated at 42°C for 48 h under microaerobic conditions, then sub-cultured on mCCDA and further incubated at 42°C for 48 h under microaerobic conditions, and finally scored as positive or negative. The MPN was calculated using tables with correction for dilution.

Enumeration of Phage in Ceca, Ileum and on Carcasses

Bacteriophages were enumerated from cecal and ileum contents by decimal dilution in SM buffer as described above. For carcass rinses, the suspension used for *Campylobacter* enumeration was diluted 1:1 in SM buffer and then treated as for the ceca and ileum samples.

Statistical Analysis

Data were analyzed using Prism8 (GraphPad Software, San Diego, CA, United States). The Shapiro–Wilks test of normality was employed on all $\log_{10}$-transformed bacterial counts or phage titers. Non-parametric tests were used as indicated when the data did not conform to normality at a significance level of 0.05. Spearman's rank correlation coefficients were calculated using Prism8 to assess rank correlations between two variables from non-parametric data.

RESULTS

Diversity of the 19-Phage Panel Against a Selection of Farm *Campylobacter* Isolates

The selected cocktail candidates demonstrated diversity in their lytic activity against farm *Campylobacter* isolates. Among the 241 farm *Campylobacter* isolates compared, 200 were identified as *C. jejuni*, 39 were *C. coli*, and two were not speciated. One hundred and eighty-eight of the *Campylobacter* strains (78%) were sensitive to at least one member of the bacteriophage panel. The results for each bacteriophage are shown in **Table 2**.

This analysis revealed that bacteriophages PH18 and PH19 had the broadest lytic activity, and although effective against most *C. jejuni* strains appeared to be more efficacious against *C. coli*. In contrast, some bacteriophages, for example, bacteriophages PH1, PH7, PH19, and PH17, were active against multiple *C. jejuni* strains, but did not lyze any of the *C. coli* isolates tested.

Selection of Suitable Locations for On-Farm Treatment Trials

Table 3 presents the *Campylobacter* and phage counts and *Campylobacter* species identity for 18 sheds screened across six potential farms. The lytic profiles for each of the 10 isolates tested were similar indicating that a single *Campylobacter* type was dominant at that point in the rearing cycle. All isolates tested from these six farms represented both *C. jejuni* and *C. coli*, with *C. jejuni* being dominant (**Table 3**) Rejected farms Farm D and F had a phage presence (though those farms met the other phage candidate selection criteria). The criteria for *Campylobacter* were met across all six farms which ranged from $\log_{10}$ 7.00 to 9.00 CFU/g. For Farm A, all 10 isolates were sensitive to 13 out of the 19 candidate phages with only one phage having no activity (presented in **Supplementary Table S1**). Phages PH5, PH8, PH11, and PH13 were selected from the 13 candidates for the Farm A trial. For Farm B, Phages PH1–PH17 showed no activity against any of the 10 test isolates, but all the isolates were sensitive to PH18 and PH19 (**Supplementary Table S1**), which were therefore selected for Farm B trial.

Enumeration of *Campylobacter* and Phages From Intestinal Contents of Birds On-Farm and at the Plant

Campylobacter and phages were enumerated from cecal and ileal samples of the birds before transport and after transport, but only phages were enumerated from the processed carcasses of Farm B, due to high levels of competitive flora overgrowing the *Campylobacter* selective medium. Unlike the control $\log_{10}$

TABLE 2 | The panel of 19 bacteriophages were tested for sensitivity to 241 *Campylobacter* hosts.

Phage	Number of sensitive *Campylobacter* hosts	Sensitive *C. jejuni* (% of total number tested)	Sensitive *C. coli* (% of total number tested)
PH 1	53	26	0
PH 2	65	30	13
PH 3	60	27	13
PH 4	55	27	3
PH 5	89	43	5
PH 6	77	35	18
PH 7	28	14	0
PH 8	83	38	15
PH 9	66	30	13
PH 10	69	34	0
PH 11	72	34	8
PH 12	64	29	13
PH 13	37	18	3
PH 14	31	15	3
PH 15	46	22	3
PH 16	76	36	8
PH 17	54	27	0
PH 18	128	48	82
PH 19	153	61	79

TABLE 3 | Pre-screening the cecal contents from 40 days birds to select test farms.

Farm	Shed	*Campylobacter* $\log_{10}$ CFU/g[1]	Species	Phage $\log_{10}$ PFU/g[1]
A	1	8.56	all *C. jejuni*	<2
	2	8.35	all *C. jejuni*	<2
	7	**8.59**[2]	all *C. jejuni*	**<2**
B	1	7.00	all *C. jejuni*	<2
	2	6.97	all *C. jejuni*	<2
	3	**7.84**[2]	all *C. jejuni*	**<2**
	B	7.2	all *C. jejuni*	<2
C	7	7.53	all *C. jejuni*	<2
	8	7.89	all *C. jejuni*	<2
D	1	7.12	all *C. jejuni*	5.30
	3	8.16	all *C. jejuni*	5.70
	5	7.37	all *C. jejuni*	ND[3]
E	1	8.98	all *C. jejuni*	<2
	2	8.78	all *C. jejuni*	<2
	3	8.7	all *C. jejuni*	<2
F	1	7.00	all *C. coli*	<2
	2	9.08	all *C. coli*	<2
	3	9.08	all *C. coli*	3.66

[1]*Value represents the mean Campylobacter count or mean phage titer from the cecal contents of three randomly sampled birds, where the limit of detection was 2 $\log_{10}$ PFU/g1.* [2]*Farm/shed selected for trial.* [3]*ND, not determined.*

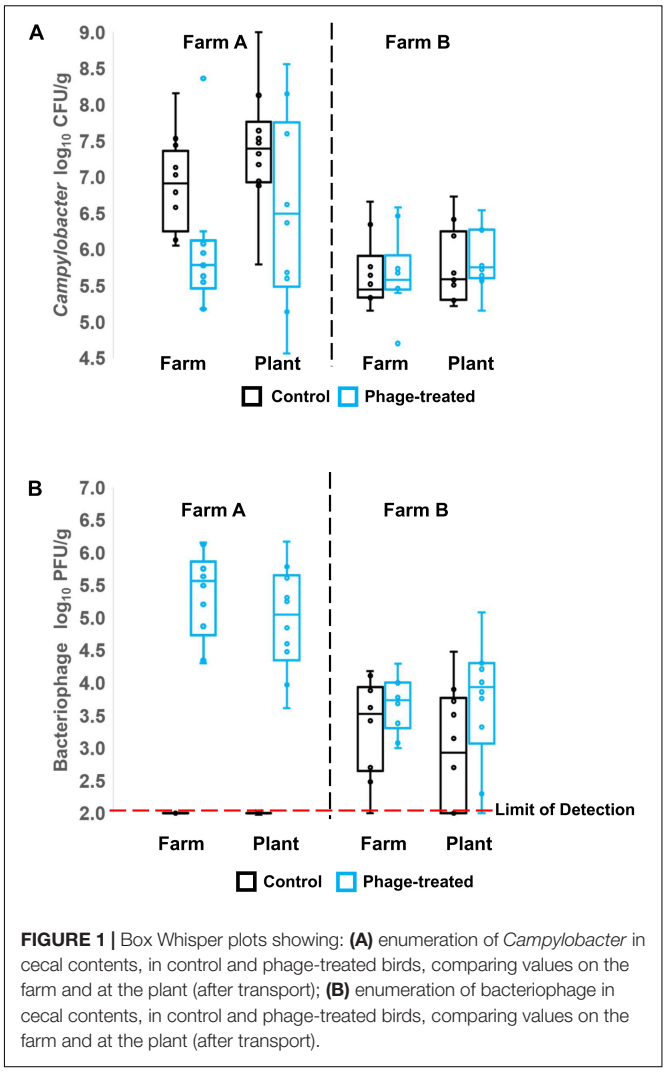

FIGURE 1 | Box Whisper plots showing: **(A)** enumeration of *Campylobacter* in cecal contents, in control and phage-treated birds, comparing values on the farm and at the plant (after transport); **(B)** enumeration of bacteriophage in cecal contents, in control and phage-treated birds, comparing values on the farm and at the plant (after transport).

CFU/g *Campylobacter* counts from the ceca, the counts for the phage-treated birds were not normally distributed from Farm A (Shapiro–Wilk test). The median for the control was 6.91 $\log_{10}$ CFU/g compared to 5.79 $\log_{10}$ CFU/g for the phage treated birds (**Figure 1A**, Farm A). Non-parametric analysis indicates the phage treated cecal *Campylobacter* counts were significantly lower than controls (p = 0.007; Mann–Whitney U-test). The data feature an outlier of 8.36 $\log_{10}$ CFU/g that was investigated by reference to repeat enumeration data at 24 h and the phage titer recorded for the bird. The cecal *Campylobacter* count was confirmed and included in the analysis, but it was noted that the phage titer for the sample was the lowest recorded and may represent a situation where the phages have not efficiently replicated throughout the digesta in the treatment period. Following transport to the plant, no significant difference (p = 0.242; Mann–Whitney U-test) was observed between the *Campylobacter* counts in phage-treated and control birds (**Figure 1A**; Farm A), although the median for the control was greater at 7.39 $\log_{10}$ CFU/g compared to 6.49 $\log_{10}$ CFU/g for the phage treated birds. The *Campylobacter* counts for the phage-treated data also contained two high cecal counts > 8.0 $\log_{10}$ CFU/g that correspond with low phage titers. Analysis of the data using the Spearman's rank correlation coefficient indicates a strong negative correlation is evident between the *Campylobacter* count and the phage titer in the treatment birds (r_s = −0.746; p = 0.02). **Figure 1B** shows the titers of bacteriophages recovered on-farm and at the plant for Farm A (left panel). As expected, for the control birds from Farm A, bacteriophages were not detected (below limit of detection). There was no significant difference between farm and plant for those birds that had been treated with bacteriophage with median values of 5.6 and 5.0 $\log_{10}$ PFU/g cecal contents, respectively.

Figure 1A (right panel) shows the *Campylobacter* enumeration data for the cecal contents of birds from Farm B, on-farm and after transport to the plant. *Campylobacter* counts in the control and phage-treated birds either on farm (p = 0.373; Mann–Whitney U-test) or after transport (p = 0.384; Mann–Whitney U-test) were not significantly different. Enumeration of *Campylobacter* from the ileum did not show any significant difference at either farm or plant (data not shown). However, the phage titer data for farm B were unexpected in that control birds were colonized by phage despite having been administered a placebo and had been selected as phage-negative at pre-screen 1 week earlier (**Figure 1B**, right panel). The difference in the mean *Campylobacter* counts from Farm B at pre-screen and the experimental values of the control birds recorded on-farm represents a significant reduction of 1.7 $\log_{10}$ CFU/g (p = 0.006; Mann–Whitney U-test).

Enumeration of *Campylobacter* on Carcasses

The *Campylobacter* numbers recovered from carcasses comparing treated and control birds from Farm B were not significantly different (p = 0.406; Mann–Whitney U-test), although six carcasses were below detection limit of <6000 organisms per carcass. Bacteriophage were detected at low titer (<100 PFU/carcass) from four carcasses of Farm B, but not detected on any carcasses from Farm A.

Continued Sensitivity to Isolates to Cocktail Before and After Phage-Treatment

The lytic profile of the cocktail phages to *Campylobacter* strains isolated after phage treatment, from both farms were unchanged compared to those isolated before treatment (**Table 4**). Development of resistance to the treatment phages was therefore not detected.

DISCUSSION

One of the reasons that phage therapy was superseded by antibiotic therapies is that utilizing a biological agent requires care in selection of the appropriate agent and in application. However, the subtlety of being able to target pathogenic species within a complex microbiota, without causing dysbiosis represents a major advantage. Campylobacters are not overt pathogens of chickens so the ability to target the zoonotic component of the microbiota is a key advantage to the welfare of the bird and the quality of the product (Richards et al., 2019). However, for success the bacteriophages must be virulent against the target bacteria, and able to reach the target in sufficient quantities to affect a change in the host bacterial population. Exposure time is also a key consideration for a self-amplifying antimicrobial. Phages must have enough time to achieve a titer that will enable their access to all host-rich environments within the gut to kill the target bacteria. Intestinal transit will limit the exposure time to high titers, which will limit the development of resistance in the target populations. Experiments in the laboratory have gone a long way to understanding what is required for successful reduction of *Campylobacter* in chickens but studies are required to assess operation in commercial settings where the birds are subjected to feed withdrawal and the stress of transportation.

Selecting of the optimum phages from a panel that are active against this dominant *Campylobacter* is key to a successful intervention. Data from *Campylobacter* and non-*Campylobacter* studies suggest that the optimal number of phages in a cocktail is between two and four (for examples, see Carvalho et al., 2010; Fischer et al., 2013; Manohar et al., 2019). For Farm A, where 17 phages were active against the host bacteria, using four as the maximum was a logical choice. However, for Farm B, only two of the candidate phages had activity to the *Campylobacter* host, so only two phages were used in the cocktail. The use of the four-phage cocktail on Farm A brought about a significant decline in the *Campylobacter* count compared to control birds within the ceca that represents the major reservoir of intestinal contamination.

Once the birds had been transported to the processing plant, it is possible that the increases in the mean *Campylobacter* counts for both phage-treated and control birds were due to transport stress. Increases in *Campylobacter* count following transport have been noted previously for cecal content and fecal matter, which have been postulated to arise as a result of the effects of transport on peristaltic movements of the chicken gut (Stern et al., 1995; Whyte et al., 2001). This was not manifest as a consistent increase in all birds, but it appeared that some birds were more affected than others, illustrated by the wide range of counts in the phage-treated birds including some that were very high at approximately 8 $\log_{10}$ CFU/g and some that were below 6 $\log_{10}$ CFU/g. The data do, however, demonstrate a strong negative correlation between the *Campylobacter* count and the phage titer. The high *Campylobacter* counts in some of the phage-treated birds may therefore represent birds where the phages have not attained a great enough titer in the ceca to affect a reduction in the population. All birds were treated similarly so the failure is likely due to low host concentrations encountered in the amplification phase, for example, in the intestinal tract prior to reaching the ceca. Success under these circumstances would then be reliant on titer amplification and dissemination in the ceca, which is subject to regular cecal evacuation. The treatment period to affect the *Campylobacter* reductions in as many birds as possible needs to be increased from 24 h as the phage may not have sufficient time to achieve the titer and/or the required dispersion within the intestine. However, in the majority of the phage treated birds of Farm A, the phage did replicate and were effective at reducing *Campylobacter* numbers in the cecal contents.

The main difference from experimental models is that birds become naturally infected with *Campylobacter* strains that provoke competition with each other. Although dominant types can emerge that predominate in surveys (El-Shibiny et al., 2005). Similarly, biosecurity measures applied on a commercial farm may not prevent the incursion of native phages from the environment. Phage isolation studies report variable frequencies of between 20 and 50% recovery from chicken sources, which suggests phages are not always present in *Campylobacter* infected flocks (Atterbury et al., 2005; El-Shibiny et al., 2005; Owens et al., 2013). Campylobacters exposed to phage can become resistant to the infecting phage; however, there is frequently an associated cost in competitive fitness (Connerton et al., 2004; Scott et al., 2007). Thus, selection favors phage-sensitive hosts when phages are not present or are at low titers. Commercial farms are challenged by multiple campylobacters that undergo succession, and one facet of the competition is the evasion of phage. A longitudinal study across successive flocks of a *Campylobacter* and phage infected barn resulted in the elimination of the phage when a new phage insensitive

TABLE 4 | Lytic profiles of *Campylobacter* isolates from Farm A and Farm B, to the candidate bacteriophage pre-and post-treatment, and after transport to the plant.

Lytic profile	Candidate bacteriophages																		
	PH1	PH2	PH3	PH4	PH5	PH6	PH7	PH8	PH9	PH10	PH11	PH12	PH13	PH14	PH15	PH16	PH17	PH18	PH19
Farm A Pre-treatment	S	S	S	S	**S**	S	S	S	I	S	S	I	S	S	S	I	S	S	S
	I	S	S	S	**S**	I	S	S	I	I	S	I	S	S	S	S	S	S	S
	S	S	S	S	**S**	I	S	S	I	I	S	S	S	S	S	S	S	S	S
Farm A Post-treatment	S	S	S	S	S	S	S	S	I	S	S	I	S	S	S	I	S	S	S
	S	S	S	S	S	S	S	S	I	I	S	I	S	S	S	I	S	S	S
	S	S	S	S	S	S	S	S	I	I	S	S	S	S	S	S	S	S	S
Farm A Plant	I	I	I	S	S	S	I	S	I	S	S	I	S	I	I	I	S	S	S
	S	S	S	S	S	S	S	S	I	I	S	I	S	S	S	I	S	S	S
	S	S	S	S	S	S	S	S	I	I	S	S	S	S	S	S	S	S	S
Farm B Pre-treatment	I	I	I	I	I	I	I	I	I	I	I	I	I	I	I	I	I	S	S
	I	I	I	I	I	I	I	I	I	I	I	I	I	I	I	I	I	S	S
	I	I	I	I	I	I	I	I	I	I	I	I	I	I	I	I	I	S	S
Farm B post-treatment	I	I	I	I	I	I	I	I	I	I	I	I	I	I	I	I	I	S	S
	I	I	I	I	I	I	I	I	I	I	I	I	I	I	I	I	I	S	S
	I	I	I	I	I	I	I	I	I	I	I	I	I	I	I	I	I	S	S
Farm B plant	I	I	I	I	I	I	I	I	I	I	I	I	I	I	I	I	I	S	S
	I	I	I	I	I	I	I	I	I	I	I	I	I	I	I	I	I	S	S
	I	I	I	I	I	I	I	I	I	I	I	I	I	I	I	I	I	S	S

S = sensitive to phage; I = insensitive to phage. The bacteriophages used in the treatment cocktails are indicated by the darkest shading.

strain entered the environment to dominate (Connerton et al., 2004). This scenario is consistent with evidence from Farm B that became colonized by a previously undetectable phage that proliferated on sensitive *Campylobacter* populations in the final week of rearing after the pre-screen. However, we also acknowledge that the presence of an indigenous phage, albeit not detected at pre-screen, may also have affected the narrow choice of treatment phage able to lyse campylobacters from Farm B. A similar situation was also reported by Kittler et al. (2013), in one of three sites investigated. The infiltrating phages clearly spread rapidly throughout the flock and it seems likely that they reduced the numbers of *Campylobacter* in cecal contents of both control and test birds, either before or concurrently, with the phage intervention. At the time of sampling, the average *Campylobacter* number in the cecal contents was 5.6 $\log_{10}$ CFU/g in contrast to 7.8 $\log_{10}$ CFU/g, when pre-screened, 1 week earlier, with no phages detected. While this makes the results difficult to interpret with respect to the treatment phage, it sheds light on the process of concurrent phage infection that are part of the natural *Campylobacter*–phage interactions occurring in the intestinal tracts of farm chickens, and confirms earlier reports that the presence of phage in broiler flocks can reduce cecal *Campylobacter* population levels (Atterbury et al., 2005). Reduced concentrations of the target bacteria below the phage proliferation threshold will also diminish the likelihood of *in situ* amplification of the treatment phage and the effectiveness of the intervention (Cairns et al., 2009). These observations suggest that the selection of the treatment phage should also take in to account the action of concurrent phage infections, which may make phage intervention more effective if optimized correctly.

The development of resistance to phage treatment is often cited as a negative aspect of phage intervention but resistance to the phage cocktails selected was not detected on either farm. This may have been partly because the time between intervention and slaughter was less than 24 h, which reduces the time for resistant strains to emerge although this was also minimized by using cocktails of phages rather than just one. Increasing the time between treatment and slaughter from 24 to 2–4 days may increase the effectiveness of treatment (Loc Carrillo et al., 2005; Wagenaar et al., 2005; El-Shibiny et al., 2009; Kittler et al., 2013) but may also lead to the emergence of resistance. The short exposure of the birds to the phage cocktail treatment may have contributed to low phage titers observed and the strong correlation with the *Campylobacter* counts observed on Farm A in the absence of emerging phage resistant populations. Phage resistant mutants were also absent amongst the campylobacters recovered from birds of Farm B that had been pre-exposed to indigenous phage. A combination of competition and exposure to new virulent phage may have eliminated any resistant types in the treatment group. However, phage insensitive isolates were also not evident from the control group *Campylobacter* isolates. The residual population surviving intestinal colonization by the indigenous phage may not have been exposed to the phage to become resistant, and similarly were either not exposed to the treatment phage or not exposed to sufficient phage titer to affect a further reduction in the colonization level. This study highlights a general need to understand system specific phage–host interactions that are likely critical for successful treatment outcomes.

DATA AVAILABILITY STATEMENT

The datasets generated for this study are available on request to the corresponding author.

ETHICS STATEMENT

The experimental design was approved by the Animal Ethics Committee of the Department of Agriculture and Fisheries Queensland before commencing farm screening and experimental intervention trials. Broiler chickens were reared in accordance with the National Animal Welfare Standards for the Chicken Meat Industry (available at: chicken.org.au/wp-content/uploads/2017/09/ME-083-Chicken-Standards-The-Standards-3.pdf) and the National Farm Biosecurity Manual for chicken growers (available at: chicken.org.au/wp-content/uploads/2017/09/National-Farm-Biosecurity-Manual-for-Chicken-Growers-Feb-2010-web.pdf).

AUTHOR CONTRIBUTIONS

HC and IC designed the experiments. LM executed the farm trials, WE, LM, CW, and HC executed the lab experiments. HC, PC, IC, and DM analyzed the data. HC, PC, and IC prepared the manuscript.

FUNDING

This study received funding from Poultry CRC. The funder was not involved in the study design, collection, analysis, interpretation of data, the writing of this article or the decision to submit it for publication.

ACKNOWLEDGMENTS

We are grateful to Margaret MacKenzie and Kelly McTavish from the integrator company for providing industry access to enable the performance of these trials and logistical support with planning and executing these trials on farm and the plant. We acknowledge the support of Katherine McGlasshan for lab experiments during both farm trials. We acknowledge the contributions of the farmers for providing access and support to maintain the trial conditions.

SUPPLEMENTARY MATERIAL

The Supplementary Material for this article can be found online at: https://www.frontiersin.org/articles/10.3389/fmicb.2020.00632/full#supplementary-material

REFERENCES

Adams, M. H. (1959). *Bacteriophages*. New York, NY: Interscience Publishers Inc.

Atterbury, R. J., Connerton, P. L., Dodd, C. E., Rees, C. E., and Connerton, I. F. (2003). Application of host-specific bacteriophages to the surface of chicken skin leads to a reduction in recovery of *Campylobacter jejuni*. *Appl. Environ. Microbiol.* 69, 6302–6306. doi: 10.1128/aem.69.10.6302-6306.2003

Atterbury, R. J., Dillon, E., Swift, C., Connerton, P. L., Frost, J. A., Dodd, C. E., et al. (2005). Correlation of *Campylobacter* bacteriophage with reduced presence of hosts in broiler chicken ceca. *Appl. Environ. Microbiol.* 71, 4885–4887. doi: 10.1128/aem.71.8.4885-4887.2005

Bolton, F. J., Coates, D., Hinchliffe, P. M., and Robertson, L. (1983). Comparison of selective media for isolation of *Campylobacter jejuni/coli*. *J. Clin. Pathol.* 36, 78–83. doi: 10.1136/jcp.36.1.78

Cairns, B. J., Timms, A. R., Jansen, V. A., Connerton, I. F., and Payne, R. J. (2009). Quantitative models of *in vitro* bacteriophage-host dynamics and their application to phage therapy. *PLoS Pathog.* 5:e1000253. doi: 10.1371/journal.ppat.1000253

Carvalho, C., Susano, M., Fernandes, E., Santos, S., Gannon, B., Nicolau, A., et al. (2010). Method for bacteriophage isolation against target *Campylobacter* strains. *Lett. Appl. Microbiol.* 50, 192–197.

Chinivasagam, H. N., Tran, T., Maddock, L., Gale, A., and Blackall, P. J. (2009). Mechanically ventilated broiler sheds: a possible source of aerosolized *Salmonella*, *Campylobacter*, and *Escherichia coli*. *Appl. Environ. Microbiol.* 75, 7417–7425. doi: 10.1128/aem.01380-09

Connerton, P. L., Loc Carrillo, C. M., Swift, C., Dillon, E., Scott, A., Rees, C. E., et al. (2004). Longitudinal study of *Campylobacter jejuni* bacteriophages and their hosts from broiler chickens. *Appl. Environ. Microbiol.* 70, 3877–3883. doi: 10.1128/aem.70.7.3877-3883.2004

Connerton, P. L., Timms, A. R., and Connerton, I. F. (2011). *Campylobacter* bacteriophages and bacteriophage therapy. *J. Appl. Microbiol.* 111, 255–265. doi: 10.1111/j.1365-2672.2011.05012.x

Crotta, M., Georgiev, M., and Guitian, J. (2017). Quantitative risk assessment of *Campylobacter* in broiler chickens – Assessing interventions to reduce the level of contamination at the end of the rearing period. *Food Control* 75, 29–39. doi: 10.1016/j.foodcont.2016.12.024

El-Shibiny, A., Connerton, P. L., and Connerton, I. F. (2005). Enumeration and diversity of campylobacters and bacteriophages isolated during the rearing cycles of free-range and organic chickens. *Appl. Environ. Microbiol.* 71, 1259–1266. doi: 10.1128/aem.71.3.1259-1266.2005

El-Shibiny, A., Scott, A., Timms, A., Metawea, Y., Connerton, P., and Connerton, I. (2009). Application of a group II Campylobacter bacteriophage to reduce strains of *Campylobacter jejuni* and *Campylobacter coli* colonizing broiler chickens. *J. Food Prot.* 72, 733–740. doi: 10.4315/0362-028x-72.4.733

European Food Safety Authority [EFSA] (2010). Scientific Opinion on Quantification of the risk posed by broiler meat to human campylobacteriosis in the EU. *EFSA J.* 8:1437. doi: 10.2903/j.efsa.2010.1437

European Food Safety Authority [EFSA], and European Centre for Disease Prevention and Control [ECDC] (2018). The European Union summary report on trends and sources of zoonoses, zoonotic agents and food-borne outbreaks in 2017. *EFSA J.* 16:5500. doi: 10.2903/j.efsa.2018.5500

Fischer, S., Kittler, S., Klein, G., and Glünder, G. (2013). Impact of a single phage and a phage cocktail application in broilers on reduction of *Campylobacter jejuni* and development of resistance. *PLoS One* 8:e78543. doi: 10.1371/journal.pone.0078543

Goode, D., Allen, V. M., and Barrow, P. A. (2003). Reduction of experimental *Salmonella* and *Campylobacter* contamination of chicken skin by application of lytic bacteriophages. *Appl. Environ. Microbiol.* 69, 5032–5036. doi: 10.1128/aem.69.8.5032-5036.2003

Goodridge, L. D., and Bisha, B. (2011). Phage-based biocontrol strategies to reduce foodborne pathogens in foods. *Bacteriophage* 1, 130–137. doi: 10.4161/bact.1.3.17629

Hall, G., Yohannes, K., Raupach, J., Becker, N., and Kirk, M. (2008). Estimating community incidence of *Salmonella*, *Campylobacter,* and Shiga

toxin-producing *Escherichia coli* infections, Australia. *Emerg. Infect. Dis.* 14, 1601–1609.

Havelaar, A. H., Mangen, M. J., de Koeijer, A. A., Bogaardt, M. J., Evers, E. G., Jacobs-Reitsma, W. F., et al. (2007). Effectiveness and efficiency of controlling *Campylobacter* on broiler chicken meat. *Risk Anal.* 27, 831–844. doi: 10.1111/j.1539-6924.2007.00926.x

Kaakoush, N. O., Castaño-Rodríguez, N., Mitchell, H. M., and Man, S. M. (2015). Global epidemiology of *Campylobacter* infection. *Clin. Microbiol. Rev.* 28, 687–720. doi: 10.1128/cmr.00006-15

Kittler, S., Fischer, S., Abdulmawjood, A., Glünder, G., and Klein, G. (2013). Effect of bacteriophage application on *Campylobacter jejuni* loads in commercial broiler flocks. *Appl. Environ. Microbiol.* 79, 7525–7533. doi: 10.1128/aem.02703-13

Loc Carrillo, C., Atterbury, R. J., El-Shibiny, A., Connerton, P. L., Dillon, E., Scott, A., et al. (2005). Bacteriophage therapy to reduce *Campylobacter jejuni* colonization of broiler chickens. *Appl. Environ. Microbiol.* 71, 6554–6563. doi: 10.1128/aem.71.11.6554-6563.2005

Loc Carrillo, C. M., Connerton, P. L., Pearson, T., and Connerton, I. F. (2007). Free-range layer chickens as a source of *Campylobacter* bacteriophage. *Antonie Van Leeuwenhoek* 92, 275–284. doi: 10.1007/s10482-007-9156-4

MacRitchie, L. A., Hunter, C. J., and Strachan, N. J. C. (2014). Consumer acceptability of interventions to reduce *Campylobacter* in the poultry food chain. *Food Control* 35, 260–266. doi: 10.1016/j.foodcont.2013.06.005

Manohar, P., Tamhankar, A. J., Lundborg, C. S., and Nachimuthu, R. (2019). Therapeutic characterization and efficacy of bacteriophage cocktails infecting *Escherichia coli*, *Klebsiella pneumoniae*, and *Enterobacter* species. *Front. Microbiol.* 10:574. doi: 10.3389/fmicb.2019.00574

Mughini Gras, L., Smid, J. H., Wagenaar, J. A., de Boer, A. G., Havelaar, A. H., Friesema, I. H., et al. (2012). Risk factors for campylobacteriosis of chicken, ruminant, and environmental origin: a combined case-control and source attribution analysis. *PLoS One* 7:e42599. doi: 10.1371/journal.pone.0042599

Owens, J., Barton, M. D., and Heuzenroeder, M. W. (2013). The isolation and characterization of *Campylobacter jejuni* bacteriophages from free range and indoor poultry. *Vet. Microbiol.* 162, 144–150. doi: 10.1016/j.vetmic.2012.08.017

Ravel, A., Hurst, M., Petrica, N., David, J., Mutschall, S. K., Pintar, K., et al. (2017). Source attribution of human campylobacteriosis at the point of exposure by combining comparative exposure assessment and subtype comparison based on comparative genomic fingerprinting. *PLoS One* 12:e0183790. doi: 10.1371/journal.pone.0183790

Richards, P. J., Connerton, P. L., and Connerton, I. F. (2019). Phage biocontrol of *Campylobacter* jejuni in chickens does not produce collateral effects on the gut microbiota. *Front. Microbiol.* 10:476. doi: 10.3389/fmicb.2019.00476

Scott, A. E., Timms, A. R., Connerton, P. L., El-Shibiny, A., and Connerton, I. F. (2007). Bacteriophage influence *Campylobacter jejuni* types populating broiler chickens. *Environ. Microbiol.* 9, 2341–2353. doi: 10.1111/j.1462-2920.2007.01351.x

Stern, N. J., Clavero, M. R., Bailey, J. S., Cox, N. A., and Robach, M. C. (1995). *Campylobacter* spp. In broilers on the farm and after transport. *Poult. Sci.* 74, 937–941. doi: 10.3382/ps.0740937

Wagenaar, J. A., Van Bergen, M. A., Mueller, M. A., Wassenaar, T. M., and Carlton, R. M. (2005). Phage therapy reduces *Campylobacter jejuni* colonization in broilers. *Vet. Microbiol.* 109, 275–283. doi: 10.1016/j.vetmic.2005.06.002

Whyte, P., Collins, J. D., McGill, K., Monahan, C., and O'Mahony, H. (2001). The effect of transportation stress on excretion rates of campylobacters in market-age broilers. *Poult. Sci.* 80, 817–820. doi: 10.1093/ps/80.6.817

Conflict of Interest: The authors declare that the research was conducted in the absence of any commercial or financial relationships that could be construed as a potential conflict of interest.

frontiers in Microbiology

ORIGINAL RESEARCH
published: 17 June 2020
doi: 10.3389/fmicb.2020.01191

Influence of Protein Glycosylation on *Campylobacter fetus* Physiology

Justin Duma[1,2†], Harald Nothaft[3†], Danielle Weaver[4], Christopher Fodor[3], Bernadette Beadle[3], Dennis Linton[4], Stéphane L. Benoit[1], Nichollas E. Scott[5], Robert J. Maier[1] and Christine M. Szymanski[1,2]**

[1] Department of Microbiology, University of Georgia, Athens, GA, United States, [2] Complex Carbohydrate Research Center, University of Georgia, Athens, GA, United States, [3] Department of Biological Sciences, University of Alberta, Edmonton, AB, Canada, [4] School of Biological Sciences, Faculty of Biology, Medicine and Health, The University of Manchester, Manchester, United Kingdom, [5] Department of Microbiology and Immunology, The Peter Doherty Institute, The University of Melbourne, Melbourne, VIC, Australia

OPEN ACCESS

Edited by:
Ozan Gundogdu,
University of London, United Kingdom

Reviewed by:
Derrick Richard Samuelson,
University of Nebraska Medical Center, United States
Abdi Elmi,
University of London, United Kingdom

***Correspondence:**
Robert J. Maier
rmaier@uga.edu
Christine M. Szymanski
cszymans@uga.edu;
cszymans@ualberta.ca

† These authors have contributed equally to this work

Specialty section:
This article was submitted to Food Microbiology, a section of the journal Frontiers in Microbiology

Received: 31 January 2020
Accepted: 11 May 2020
Published: 17 June 2020

Citation:
Duma J, Nothaft H, Weaver D, Fodor C, Beadle B, Linton D, Benoit SL, Scott NE, Maier RJ and Szymanski CM (2020) Influence of Protein Glycosylation on Campylobacter fetus Physiology. Front. Microbiol. 11:1191. doi: 10.3389/fmicb.2020.01191

Campylobacter fetus is commonly associated with venereal disease and abortions in cattle and sheep, and can also cause intestinal or systemic infections in humans that are immunocompromised, elderly, or exposed to infected livestock. It is also believed that *C. fetus* infection can result from the consumption or handling of contaminated food products, but *C. fetus* is rarely detected in food since isolation methods are not suited for its detection and the physiology of the organism makes culturing difficult. In the related species, *Campylobacter jejuni*, the ability to colonize the host has been linked to N-linked protein glycosylation with quantitative proteomics demonstrating that glycosylation is interconnected with cell physiology. Using label-free quantitative (LFQ) proteomics, we found more than 100 proteins significantly altered in expression in two *C. fetus* subsp. *fetus* protein glycosylation (*pgl*) mutants (*pglX* and *pglJ*) compared to the wild-type. Significant increases in the expression of the (NiFe)-hydrogenase HynABC, catalyzing H_2-oxidation for energy harvesting, correlated with significantly increased levels of cellular nickel, improved growth in H_2 and increased hydrogenase activity, suggesting that N-glycosylation in *C. fetus* is involved in regulating the HynABC hydrogenase and nickel homeostasis. To further elucidate the function of the *C. fetus pgl* pathway and its enzymes, heterologous expression in *Escherichia coli* followed by mutational and functional analyses revealed that PglX and PglY are novel glycosyltransferases involved in extending the *C. fetus* hexasaccharide beyond the conserved core, while PglJ and PglA have similar activities to their homologs in *C. jejuni*. In addition, the *pgl* mutants displayed decreased motility and ethidium bromide efflux and showed an increased sensitivity to antibiotics. This work not only provides insight into the unique protein N-glycosylation pathway of *C. fetus*, but also expands our knowledge on the influence of protein N-glycosylation on *Campylobacter* cell physiology.

Keywords: *Campylobacter fetus*, N-linked protein glycosylation, glycosyltransferase, proteomics, metal regulation, hydrogenase

INTRODUCTION

Asparagine-linked protein glycosylation is a post-translational modification present in species from all three domains of life. The prototypical bacterial protein N-glycosylation system (referred to as *pgl*) was first identified in *Campylobacter jejuni* over two decades ago (Szymanski et al., 1999). This system utilizes five glycosyltransferases (*pglA*, *pglC*, *pglH*, *pglI*, *pglJ*) to produce the heptasaccharide GalNAc-α1,4-GalNAc-α1,4-(Glc-β1,3-)GalNAc-α1,4-GalNAc-α1,4-GalNAc-α1,3-diNAcBac-β1,N-Asn (diNAcBac is 2,4-diacetamido-2,4,6-trideoxyglucopyranose) which is attached to protein (**Figure 1**; Glover et al., 2005, 2006; Linton et al., 2005). The assembly of the full-length glycan occurs on the cytoplasmic side of the inner membrane through the sequential transfer of nucleotide-activated sugars onto the lipid carrier undecaprenyl-phosphate. The lipid-linked heptasaccharide is then flipped into the periplasm by the flippase PglK (Alaimo et al., 2006; Kelly et al., 2006) and transferred to the asparagine residue within the consensus sequon D/E-X_1-N-X_2-S/T (where X_1, X_2 can be any amino acid except proline) by the oligosaccharyltransferase PglB (Kowarik et al., 2006; Chen et al., 2007; Scott et al., 2011), or is released as free oligosaccharide (Nothaft et al., 2009), a process that is conserved among *Campylobacter* species (Nothaft et al., 2012). In *C. jejuni*, the conserved heptasaccharide has been found on more than 80 periplasmic and membrane-bound proteins (Scott et al., 2011; Cain et al., 2019). Mutagenesis of the *pgl* genes indicates that this glycosylation system impacts multiple cell functions including: (i) colonization of chickens and mice; (ii) adherence and invasion of epithelial cells; (iii) functionality of the multidrug efflux complex CmeABC; (iv) stability of the type IV secretion system; and (v) interactions with the immune system (Nothaft and Szymanski, 2013; Dubb et al., 2020). More specifically, two recent proteomics studies of *C. jejuni pglB* mutants have revealed multiple physiological functions associated with N-glycosylation (Abouelhadid et al., 2019; Cain et al., 2019). These include increased expression of stress response proteins, decreased survival in high temperature and osmolarity, altered metabolic activities, decreased chemotaxis, impaired efflux, and decreased nitrate reductase activity (Abouelhadid et al., 2019; Cain et al., 2019).

Orthologs of the *pgl* pathway have been found in all *Campylobacter* spp., select *Helicobacter* spp., *Desulfovibrio desulfuricans*, *Wolinella succinogenes*, *Deferribacter desulfuricans*, *Sulfurovum* sp., *Nitratiruptor* sp., and some less characterized δ- and ε-Proteobacteria (Nakagawa et al., 2007; Jervis et al., 2010; Ielmini and Feldman, 2011; Nothaft et al., 2012; Mills et al., 2016). Despite the conservation of the *pgl* pathway *per se*, different *Campylobacter* species produce N-glycans that vary in structure and composition (Jervis et al., 2012; Nothaft et al., 2012). This is particularly evident among the non-thermotolerant *Campylobacter* species which produce multiple N-linked glycoforms (Jervis et al., 2012; Nothaft et al., 2012). For instance, *Campylobacter fetus* synthesizes two distinct N-linked hexasaccharides: the major GlcNAc-α1-6-(GlcNAc-β1-3)-GlcNAc-α1-4-GalNAc-α1-4-GalNAc-α1-3-diNAcBac-β1,N-Asn and the minor GlcNAc-α1-6-(Glc-β1-3)-GlcNAc-α1-4-GalNAc-α1-4-GalNAc-α1-3-diNAcBac-β1,N-Asn at a 4:1 ratio, respectively (Nothaft et al., 2012).

Campylobacter fetus grows best between 25 and 37°C and consists of three subspecies: *C. fetus* subsp. *fetus* (*Cff*), *C. fetus* subsp. *venerealis* (*Cfv*), and the more recently described subspecies *C. fetus* subsp. *testudinum* (*Cft*) thought to originate from reptiles, but also associated with human infections (Patrick et al., 2013; Fitzgerald et al., 2014). *Cff* has the broadest host range and is found in cattle, sheep, reptiles, and humans (Tu et al., 2004; Wagenaar et al., 2014). In livestock, both *Cfv* and *Cff* are known to cause reproductive failure and infertility (Duncan et al., 2014), and although *Cfv* has been isolated from humans, it only causes disease in cattle (Holst et al., 1987). The majorities of human *C. fetus* infections are attributed to *Cff* and are associated with meningitis, acute diarrhea, and most commonly bacteremia (Wagenaar et al., 2014). Human infections are generally sporadic, with only a few reported outbreaks (Klein et al., 1986; Marchand-Senecal et al., 2017). Recent metagenomic analysis found *C. fetus* in 8% of feces from healthy humans, suggesting it is a possible pathobiont (Iraola et al., 2017).

In this study, we examined the role of several *C. fetus* *pgl*-encoded glycosyltransferases through mutagenesis and functional transfer into *Escherichia coli*. We demonstrate that the *Cff*-PglA and *Cff*-PglJ homologs have the same function as their counterparts in *C. jejuni* building the conserved GalNAc-α1,4-GalNAc-α1,3-diNAcBac reducing-end core. PglX (previously annotated as PglH1) and PglY (previously annotated as PglH2) are associated with the biosynthesis of the structurally variable region at the non-reducing end of the *Cff*-hexasaccharides. To assess the potential impact of the N-glycan truncations on other cellular functions, a label-free quantitative proteomics approach was used to examine the *Cff-pglJ* and *pglX* mutants. Proteomics demonstrated widespread changes in protein abundance with a notable impact on metal transport proteins, several (NiFe) hydrogenase subunits, and oxidative response proteins compared to the wild-type (WT). The results presented in this study provide new insights into the assembly and roles of N-linked glycoproteins in *C. fetus*.

Nomenclature: *Cf*, *Campylobacter fetus*; *Cff*, *Campylobacter fetus* subsp. *fetus*; *Cft*, *Campylobacter fetus* subsp. *testudinum*; *Cfv*, *Campylobacter fetus* subsp. *venerealis*; *Cj*, *Campylobacter jejuni*; diNAcBac, 2,4-diacetamido-2,4,6-trideoxyglucopyranose; fOS, free oligosaccharides; GalNAc, N-acetyl-galactosamine; Glc, glucose; GlcNAc, N-acetyl-glucosamine; GTase, Glycosyltransferase; Hex, hexose; HexNAc, N-acetyl-hexosamine; LLO, lipid-linked oligosaccharide; MS, mass spectrometry.

RESULTS

Characterization of *Cff pgl* Cluster

The *C. fetus* (*Cf*) *pgl* cluster is syntenic with the *C. jejuni* (*Cj*) *pgl* gene cluster (Jervis et al., 2012; Nothaft et al., 2012) apart from lacking *pglI* and possessing two homologs of *pglH* (**Figure 1**). The similarities between the two loci are reflected in their N-glycan structures, with both sharing the same three reducing end sugars. In *C. jejuni, pglC*, *pglA,* and *pglJ* are responsible for the formation of this initial diNAcBac-$GalNAc_2$

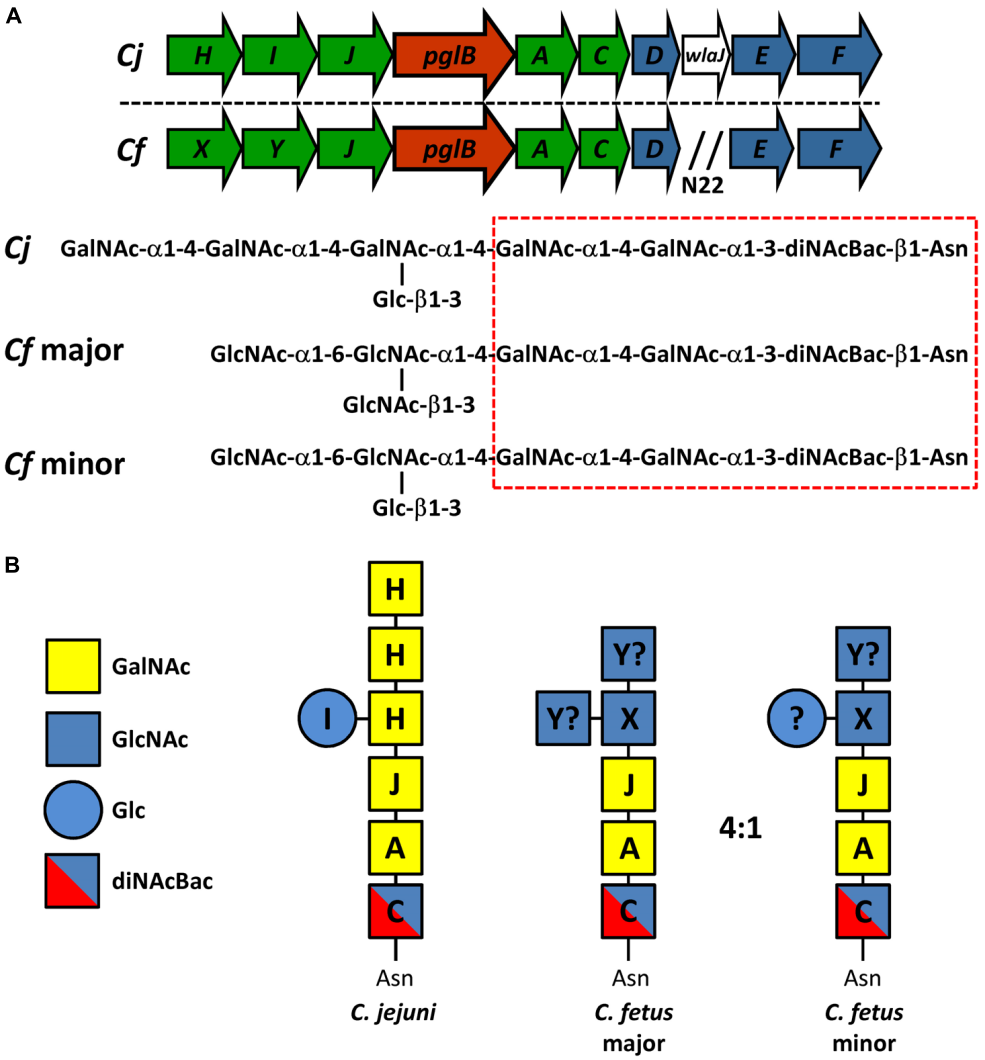

FIGURE 1 | Comparison of the N-linked protein glycosylation (*pgl*) pathway in *C. jejuni* and *C. fetus*. **(A)** The N-linked glycan structures and the genetic organization of the *pgl* locus for *C. jejuni* 11168 (*Cj*) and *C. fetus fetus* ATCC 27374 (*Cf*) (according to Nothaft et al., 2012) are shown. Genes encoding glycosyltransferases are in green, the oligosaccharyltransferase gene is in red, and genes for the biosynthesis of diNAcBac are in blue. N_{22} indicates an insertion of 22 genes (between *pglD* and *pglE*) in the *Cff-pgl* operon. The hatched red box indicates the conserved group of sugars at the reducing end. **(B)** Similar to *Cj*, we propose that *Cf*-PglC transfers diNAcBAc which is synthesized by *Cj/Cf* PglDEF (not shown) to undecaprenyl-phosphate (Nothaft and Szymanski, 2010). Subsequently, we show that *Cf*-PglA transfers the first α1–3 linked GalNAc followed by the second α1–4 linked GalNAc residue added by *Cf*-PglJ, comparable to the *Cj* homologs. To this trisaccharide, *Cj*-PglH transfers three α1–4 linked GalNAc residues and *Cj*-PglI subsequently transfers the β1–3 linked Glc branch (Kelly et al., 2006). For *Cf*, PglX most likely transfers the first HexNAc (α1–4 linked GlcNAc), but it remains to be determined if PglY can transfer the β1–3 linked Glc or the remaining two GlcNAc residues in the major and the minor glycan forms. The question mark indicates that another enzyme outside the gene cluster could be responsible for the addition of those sugar residues.

trisaccharide that is conserved across nearly all *Campylobacter* species (Jervis et al., 2012; Nothaft et al., 2012). Previously, *Cf* was annotated to possess two *pglH* homologs; however, compositional and structural analyses of the *Cf-pgl* pathway products showed that it does not contain the three GalNAc residues added by the *Cj-pglH* gene product (Nothaft et al., 2012). Since it is the non-reducing end of the *C. jejuni* and *C. fetus* N-glycans that varies in structure, the *pgl* genes in the "variable" glycosyltransferase (GTase) region upstream of *pglB* most likely differ in function. We therefore named the two *pglH* homologs, *pglX* and *pglY* (**Figure 1**). Interestingly, both proteins contain the catalytic EX_7E motif previously annotated in PglH (Cid et al., 2000; Troutman and Imperiali, 2009; **Figure 2**). In addition to this catalytic EX_7E, PglY and PglX contain one and two additional EX_7E motifs, respectively. K68 of *Cj*-PglH, which is believed to be involved in lipid-linked oligosaccharide (LLO) association, is altered to N67 and T70 in PglX and PglY, respectively. In addition, the binding site of the *Cj*-PglH catalytic EX_7E motif that involves L269 and P270 was found to be altered in PglX and PglY. Both enzymes possess a G instead

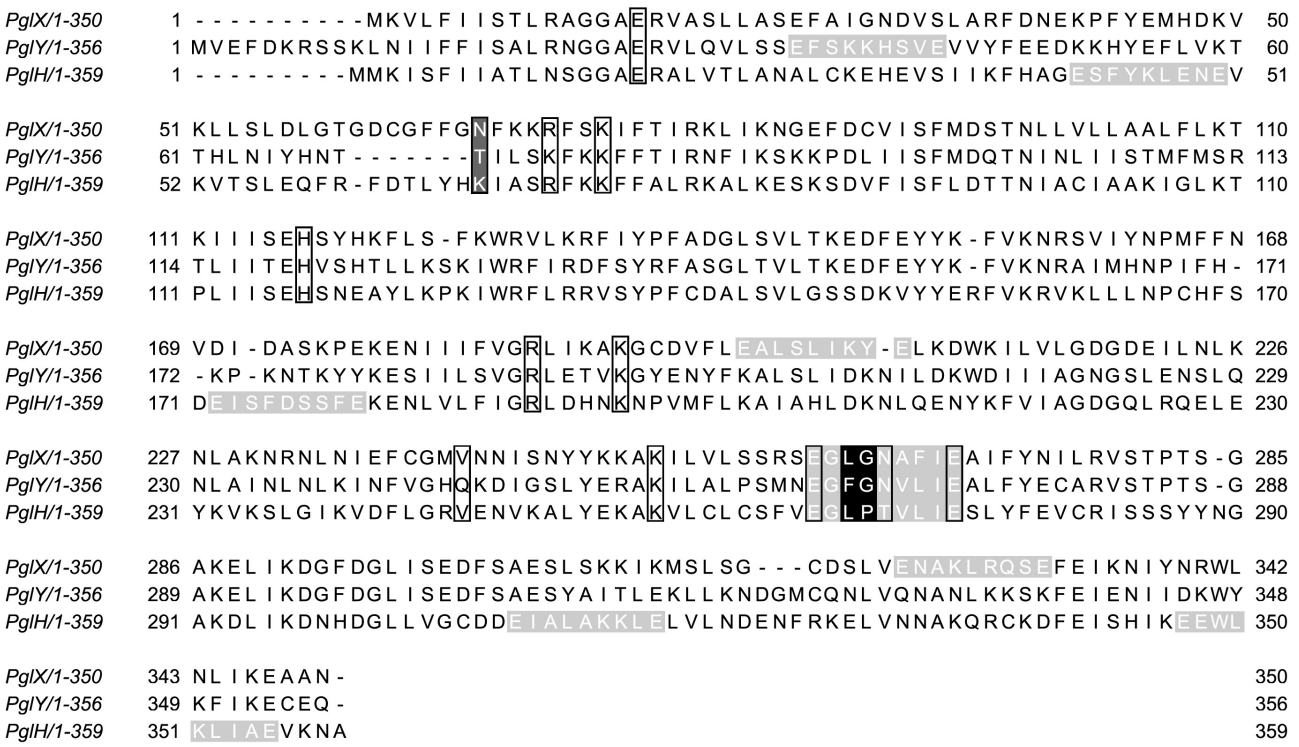

FIGURE 2 | Sequence alignment of *C. fetus* (*Cf*) PglX, PglY, and *C. jejuni* (*Cj*) PglH. Black boxes indicate specific amino acids associated with activity in PglH (Troutman and Imperiali, 2009; Ramirez et al., 2018). Black and dark gray amino acids represent functional residues that show non-conserved substitutions in PglX and PglY. Light gray highlighted sequences indicate EX_7E motifs commonly found in glycosyltransferases (Cid et al., 2000; Coutinho et al., 2003; Troutman and Imperiali, 2009). The catalytic EX_7E motif of *Cj*-PglH is located at residues E266 to E274. *Cf*-PglX CFF8240_1386, *Cf*-PglY CFF8240_1385, and *Cj* DDV78_00080 sequences were analyzed by Jalview (Waterhouse et al., 2009).

of a P at position P270; however, only PglY possesses an F at position 267 that corresponds to L269 in *C. jejuni*. These minor changes in the amino acid residues may explain the differences in enzyme specificity and the formation of the shorter glycans when compared to *C. jejuni*.

N-Glycan Analysis of *Cff-pgl* Mutants

To assess the functions of the "variable" GTases, we constructed mutants by insertion of a kanamycin resistance cassette (referred to as "kan") into the respective gene loci. Both *pglX* (*pglX:kan*, further referred to as *pglX*-) and *pglJ* (*pglJ:kan*, further referred to as *pglJ*-) were constructed in the *Cff* strain ATCC 27374 (**Supplementary Figure S1**), however multiple attempts at generating mutants in *pglY* were unsuccessful.

Insertion of the *kan* cassette in the *pglJ* and *pglX* genes was verified by PCR with oligonucleotides hybridizing outside of the recombination event (**Supplementary Figure S1**). When compared to the PCR product size obtained with chromosomal DNA isolated from *Cff*-WT, an increase in size by approximately 1.8 kb was observed when the *kan* cassette was present on the respective PCR product, clearly indicating insertion at the correct position within the *Cff* chromosome. To further investigate the effect of the mutations on N-glycan biosynthesis, western blot analysis of whole cell lysates probed with *Cff*-N-glycan specific serum was performed. Complete loss of serum reactivity in *pglX*- and *pglJ*- was observed when compared to the WT (**Figure 3A** and **Supplementary Figure S6A**). Lectin blotting with WGA confirmed those results, i.e., loss of reactivity in whole cell lysates of the *pglJ* mutant and strongly reduced reactivity (with only one signal present) in lysates of the *pglX* mutant (**Figure 3B** and **Supplementary Figure S6B**). Similarly, no free oligosaccharides (fOS) could be detected in the two *pgl* mutants when analyzed by thin layer chromatography (TLC) (**Figure 3C**). Here, two spots for the *Cff*-fOS variants could be seen when a fOS preparation of the WT was applied, confirming previous observations (Dwivedi et al., 2013), and these spots were absent in similar preparations from the *pglX*- and *pglJ*- strains.

To investigate the N-glycan in the two *Cff-pgl* mutants in more detail, proteomics analysis of *Cff*-WT and the *pgl* mutants was performed. As the disruption of *Cff-pgl* was predicted to truncate the N-linked glycan, we examined whole cell lysates to avoid potential biases in the detection of glycoforms that can result from glycopeptide enrichment (Alagesan et al., 2019). Consistent with our previous work (Nothaft et al., 2012), we observed both GlcNAc-α1-6-(GlcNAc-β1-3)-GlcNAc-α1-4-GalNAc-α1-4-GalNAc-α1-3-diNAcBac and GlcNAc-α1-6-(Glc-β1-3)-GlcNAc-α1-4-GalNAc-α1-4-GalNAc-α1-3-diNAcBac glycans on multiple protein substrates within the WT (**Figures 4A,B**), which were absent within *pglX- and pglJ-* (**Supplementary MS Data 1**).

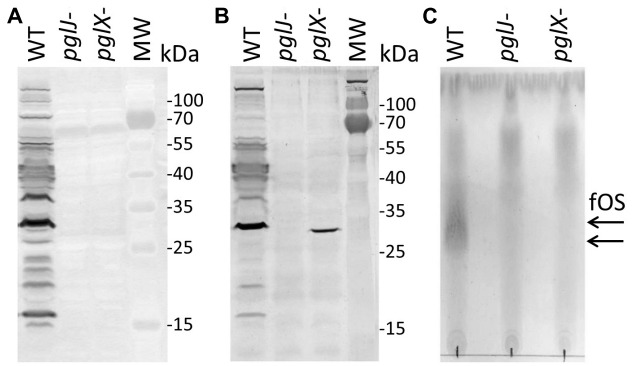

FIGURE 3 | Product analysis of *Cf* WT, *pglX*- and *pglJ*- strains. **(A)** Western blot of whole-cell lysates with *Cff*-N-glycan-specific antiserum, and **(B)** wheat germ agglutinin reactivity of whole cell lysates of the WT, *pglJ*-, and *pglX*- strains. **(C)** Thin-layer chromatography (TLC)-free oligosaccharide (fOS) analysis of WT, *pglJ*-, and *pglX*- strains. Molecular weight (MW) markers for the western blots (in kDa) are indicated on the right; arrows indicate the migration of WT fOS on the TLC plate.

Consistent with our western and lectin blotting assays, multiple truncated N-linked glycans were observed within *pglX*- and *pglJ*- including diNAcBac-$HexNAc_2$ glycans, diNAcBac-HexNAc glycans (**Figures 4C,D**) as well as diNAcBac alone. Within *pglX*-, the diNAcBac-$HexNAc_2$ glycan was the predominant glycoform (**Supplementary MS Data 1**) and is consistent with the *Cff* N-glycan core structure, diNAcBac-$GalNAc_2$ (Nothaft et al., 2012). In contrast, multiple glycoforms were identified in *pglJ*- including diNAcBac-$HexNAc_2$-, diNAcBac-HexNAc, and diNAcBac glycans (**Supplementary MS Data 1**). Taken together these results confirm the involvement of PglJ in the formation of the conserved reducing end trisaccharide and that PglX functions in extension of the non-conserved N-linked glycan structure.

Mutations in *pglX* and *pglJ* Have No Effect on Growth and the Expression of Downstream Genes but Reduces Motility

Growth curves were performed to investigate a potential influence of the *pgl* mutations. Although the *pgl* mutants reached a slightly higher optical density in the late logarithmic phase when compared to the WT, the final optical densities, as well as the growth rates in the early and mid-exponential phases, were similar among the three strains (**Supplementary Figure S2**). In addition, we did not observe a significant difference in *pgl* gene transcript levels after the insertion of the *kan* cassette in either *pglX* or *pglJ* (**Supplementary Figure S3**). This indicates that expression of the antibiotic cassette has no effect or that other transcriptional start sites in the *Cff-pgl* operon are compensating, as observed in the *C. jejuni pgl* operon (Szymanski et al., 1999; Dwivedi et al., personal communication). A downstream effect would influence expression of *pglB* but we see similar abundance of the PglB protein in WT when compared to either mutant (**Supplementary Table S1**). In addition, we still observe different forms of glycans on each mutant whereas in the absence of PglB we would not expect any glycans at all. However, we observed a significantly reduced swimming behavior in *pglX*- and *pglJ*- when compared to *Cff*-WT (**Supplementary Figure S4**) indicating that N-glycosylation either directly or indirectly affects motility.

Characterization of PglJ and PglA in *E. coli*

Since the N-glycan phenotype observed in the *pglJ* mutant was somewhat unexpected, the function of *Cff*-PglJ and *Cff*-PglA was further investigated by using a modified heterologous *E. coli Cj*/*Cff* hybrid glycosylation system (Wacker et al., 2002). Within this system, *Cff*-Pgl proteins are expressed in the presence of a mutant *Cj-pgl* operon (lacking select *Cj-pgl* genes). The glycans produced are then transferred to *Cj*-CmeA-His_6 (N-glycosylation acceptor protein) via *Cj*-PglB. Western blotting of whole cell lysates of *E. coli* CLM24 prepared after co-expression of *Cj*-CmeA-His_6 and *Cj-pglA* or *Cj-pglJ* in the presence of p*pgl* operon derivatives lacking either *pglA* or *pglJ* were probed with anti-His_6 and anti-*Cj*-N-glycan antibodies (**Figure 5A** and **Supplementary Figure S7A**). The three *Cj*-Cme-His_6-specific signals with anti-His (**Figure 5A** and **Supplementary Figure S7A** upper panel) and two N-glycans specific signals with the *Cj*-N-glycan specific R1 antiserum (**Figure 5A** and **Supplementary Figure S7A** lower panel) clearly identified the bands as non-(0N), mono-(1N), and di-(2N) glycosylated CmeA-His_6. A similar *Cj*-CmeA-His_6 pattern was produced in cells harboring the native *Cj-pgl* operon (from p*pgl*) and upon expression of *Cff-pglA* or *Cff-pglJ* (although with lower glycosylation efficiency) only when the *Cj*-homologous gene was knocked-out. In addition, no cross-complementation could be observed when *Cj* or *Cff-pglA* or *pglJ* were expressed in the presence of the p*pgl* plasmid lacking *pglJ* or *pglA*, respectively. These results confirm that *Cff*-PglA and *Cff*-PglJ fulfill the same functions as the homologous *Cj*-Pgl proteins, i.e., the addition of the second and third monosaccharide building blocks, respectively, to Und-diNAcBac, to form the diNAcBac-$GalNAc_2$- trisaccharide. As expected, no *Cj*-CmeA-His_6 glycosylation was observed in the absence of p*pgl* resulting in only non-glycosylated (0N) acceptor protein represented by a single band in the anti-His_6 western blot and further confirmed by the absence of the N-glycan-specific signals in the anti-N-glycan (R1) blot (**Figure 5A** and **Supplementary Figure S7A** lower panel). Mass spectrometric analysis of isolated *Cj*-CmeA confirmed the modification of CmeA glycopeptides with the expected glycoforms supporting these western blot results (**Supplementary Material** and **Supplementary MS Data 2**). Here, the full length *Cj*-heptasaccharide was produced only when the *Cj-pgl* operon plasmids with mutations in *pglA* or *pglJ* were co-expressed with plasmids containing the corresponding *pglA* or *pglJ* from *Cj* or *Cff*.

Characterization of *Cff-pglX* and *pglY* Using the *E. coli* Heterologous Glycosylation System

Since we could not obtain a mutant in *Cff-pglY* and therefore could not assign the functions of the two remaining GTases in the "variable" *pgl* region, we decided to analyze PglX and PglY using the heterologous *E. coli* glycosylation system (Wacker

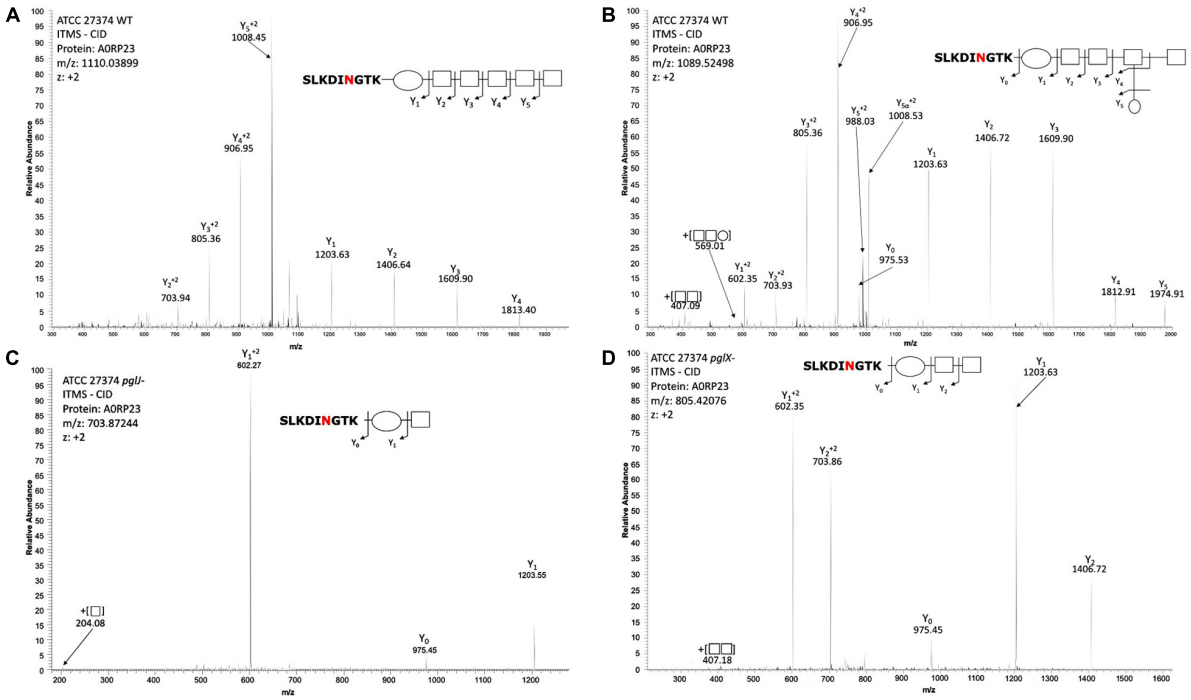

FIGURE 4 | Mass-spectrometric analysis of *Cff* WT, *pglJ-*, and *pglX-* glycopeptides. Fragmentation of characteristic ions obtained by precursor ion scanning of digested *Cff* lysate samples using liquid chromatography-mass spectrometry. Red lettering indicates possible glycosylation site. Spectra of WT *Cff* have two glycans: **(A)** $HexNAc_5$-diNAcBac and **(B)** HexNAc-[Hex]-$HexNAc_3$-diNAcBac. **(C)** The peptide from the *pglJ-* mutant only shows the presence of a mass consistent with HexNAc-diNAcBac. **(D)** The peptide from the *pglX-* mutant indicates that it is modified with HexNAc-HexNac-diNAcBac.

et al., 2002). In this case we employed the *Cj-pgl* operon lacking *pglH* that produces a trisaccharide (diNABacGalNAc$_2$) identical to that found in *Cff,* potentially providing a substrate for PglX or PglY activity. In addition, we constructed and analyzed the complementation of a p*pgl-pglHI*:*kan* mutant plasmid (lacking *Cj-pglH* and *Cj-pglI*) to rule out the possibility of the *Cj*-PglI GTase adding or competing with the potential addition of a glucose residue to the N-glycan chain by either *Cff*-PglX or *Cff*-PglY. To do so, plasmid pCE111/28 derivatives expressing *Cj-pglH* (positive control), *Cff-pglX*, *Cff-pglY,* or *Cff-pglXY* served as complementation vectors. Western blots of whole cell lysates probed with anti-His$_6$ antibodies were performed to investigate the *Cj*-CmeA-His$_6$ glycosylation pattern in the underlying strains (**Figure 5B** and **Supplementary Figure S7B**). Expression of p*pgl* in combination with CmeA-His$_6$ and CmeA-His$_6$ alone served as positive and negative glycosylation controls, respectively. First, we demonstrated that expression of *Cj-pglH* in combination with the *pgl* operon lacking *pglH* resulted in a glycosylation pattern similar to the strain co-expressing CmeA-His$_6$ and the *Cj*-WT *pgl* operon (on p*pgl*), i.e., production of non-(0N), mono-(1N), and di-(2N) glycosylated CmeA-His$_6$, whereas in the absence the complementation plasmid, glycobands were migrating slightly faster due to the addition of only the trisaccharide N-glycan (missing the GalNAc$_3$-Glc that is added by PglH and PglI in the full length *Cj*-heptasaccharide). Expression of *Cff-pglY* with p*pgl-pglH*:*kan* did not alter the migration behavior of the glycobands when compared to p*pgl-pglH*:*kan* alone, whereas transformation of *Cff-pglX* resulted in a slight mass increase compared to p*pgl-pglH*:*kan/Cff-pglY*, indicating that PglX, but not PglY, might be responsible for the addition of a sugar residue to the p*pgl-pglH*:*kan* glycan (**Figure 5B**). A slight increase in mass of the *Cj*-CmeA-His$_6$ glycoprotein was also observed upon expression of *Cff-pglXY* (*pglXY* cloned as one PCR product), however a difference in the running behavior compared to p*pgl-pglH*:*kan/Cff-pglY* could not be resolved by SDS-PAGE and western blotting analysis alone (**Figure 5B** and **Supplementary Figure S7B**).

Similar results were obtained upon introduction of *Cj-pglH* and *Cff pglX*, *Cff-pglY* and *Cff-pglXY* into CLM24 expressing p*pgl-pglHI:kan* and *Cj*-CmeA-His$_6$. Here, the glycobands in the *Cj-pglH* complements were expected to display a slightly faster running behavior when compared to the full length heptasaccharide due to the loss of the Glc residue; however, similar to the complementation analysis of the p*pglH:kan* strains, an obvious difference in the running behavior of the CmeA-His$_6$ glycobands upon introduction of *Cff-pglX*, and *Cff-pglXY* could not be resolved (**Figure 5B**).

To further investigate the N-glycans produced upon expression of the different *Cj-pgl* operon mutants in combination with the *Cff-pglX* and *pglY* complementation plasmids, mass-spectrometric analyses of trypsinized CmeA was undertaken. While N-glycan structures observed upon complementation with the *Cj*-control (p*pgl-pglH* mutant expressing *Cj-pglH*) resulted in the formation of the expected full length *Cj*-N-glycan, only one

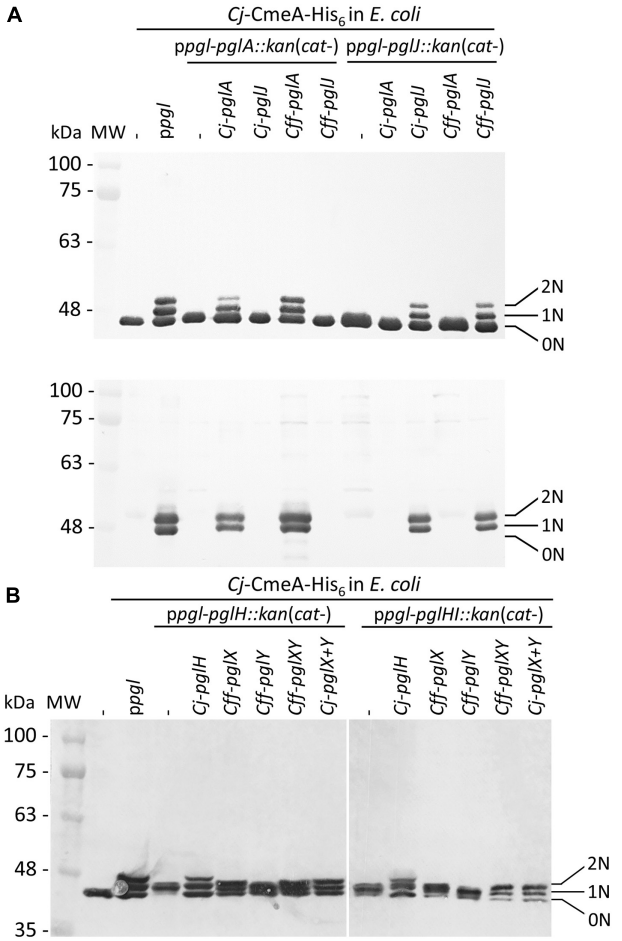

FIGURE 5 | Functional analysis of *Cff*-Pgl pathway glycosyltransferases (GTases) in the heterologous *E. coli* glycosylation system. The GTase-activities of **(A)** PglA and PglJ were analyzed in western blots of *Cj*-CmeA-His_6 with His_6-tag antibodies (upper panel) and *Cj*-N-glycan specific (R1) antibodies (lower panel). **(B)** PglX and PglY activities were analyzed with His_6-tag specific antibodies in western blots of CmeA-His_6 used as the glycan acceptor to determine N-glycosylation activities. Whole cell extracts (5 μg) of *E. coli* CLM24 expressing the indicated gene/plasmid combinations are indicated above each lane. Non-, mono-, and di-glycosylated CmeA-His_6 proteins are labeled as 0N, 1N, and 2N, respectively. Molecular weight markers (MW) in kDa are indicated on the left.

plasmid combination, the expression of *Cff-pglXY* in the p*pgl-pglH* mutant background resulted in the formation of a structure that was similar in composition and sequence to the minor form of the native *Cff*-N-glycan, diNAcBac-$HexNAc_4$-Hex (**Supplementary Material** and **Supplementary MS Data 2**).

Mutations in *pglX* and *pglJ* Have an Impact on Multiple Cellular Functions in *Cff*

To further understand the role of N-glycosylation in *Cff*, label-free quantitative (LFQ) proteomics analysis of whole cell lysates of *Cff*-WT, and the *pglX*- and *pglJ*- was done. Across five biological replicates of each sample type (**Supplementary Figure S5**), 914 proteins were identified representing ∼77% of the *Cff* ATCC 27374 predicted proteome of 1,190 proteins (**Supplementary Table S1**). Quantitative proteome analyses revealed more than 100 proteins with significantly different abundance across various biological groups as shown in heat maps of the most prominent differences in abundance comparing WT to *pglX*- and *pglJ*- strains (**Figures 6A,B**). These results indicate that mutating glycosyltransferases involved in assembly of the N-linked glycan has a significant effect on abundance of numerous cellular proteins.

Expression of the H_2-Uptake Hydrogenase Complex HynABC Is Significantly Induced in Both *pglJ* and *pglX* N-Glycosylation Mutants

Among the proteins with increased abundance in both the *pglJ* and *pglX* mutants (compared to WT) were the three subunits (HynABC) of a putative nickel-iron (NiFe) H_2-uptake hydrogenase complex (Benoit et al., 2020). In both *pgl* mutants, the expression levels of all three hydrogenase subunits, HynA, HynB, and HynC, were significantly higher compared to the WT (means of 29.3-fold, 21.5-fold, and 7.8-fold, respectively) (**Figure 7A** and **Supplementary Table S1**). This complex, found in a number of bacterial pathogens, enables the microbes to use the electron donor H_2 as an energy source, thus providing an alternative respiratory pathway that is important for *in vivo* survival (Olson and Maier, 2002; Benoit and Maier, 2018). HynABC-associated proteins, such as hydrogenase accessory/maturation proteins (e.g., HypABCDEF) or the nickel specific transcriptional regulator (NikR) also showed moderate increases in protein levels in both mutants compared to WT (**Figure 7A**).

Since H_2 increases growth of various ε-Proteobacteria species, including *Helicobacter pylori* and *Campylobacter concisus* (Kuhns et al., 2016; Benoit and Maier, 2018), we determined whether higher hydrogenase expression in the *C. fetus* N-glycosylation mutants correlates with elevated H_2-supported microaerobic growth. To do so, the cell yield (CFU/mL) of the WT and the *pglJ* and *pglX* mutants was assessed after 48 h of growth under microaerobic conditions in the presence or absence of 20% H_2 (**Figure 7B**). We only determined the end point of growth due to the extended lag phase of *Cff* cultures grown under these conditions. With no added H_2, *Cff* WT had a significantly higher growth yield compared to both mutants. However, in H_2-enriched conditions, WT cells showed growth levels comparable to both *pgl* mutants. Although the addition of H_2 was originally predicted to be beneficial for WT growth, we observed decreased growth in H_2 for other *Cf* strains, *Cft* 03-427 and *Cff* 82-40 (data not shown). In contrast, we observed a significant increase in *pglJ*- growth compared to the other strains in the presence of H_2. A slight increase in *pglX*- growth was also observed in the presence of H_2, but it was not significant compared to WT. These results indicate that the *pgl* mutants have increased growth yield in H_2 opposed to WT where H_2 is deleterious.

H_2-uptake in whole cells was examined to determine whether increased HynABC levels in the mutants correlate with

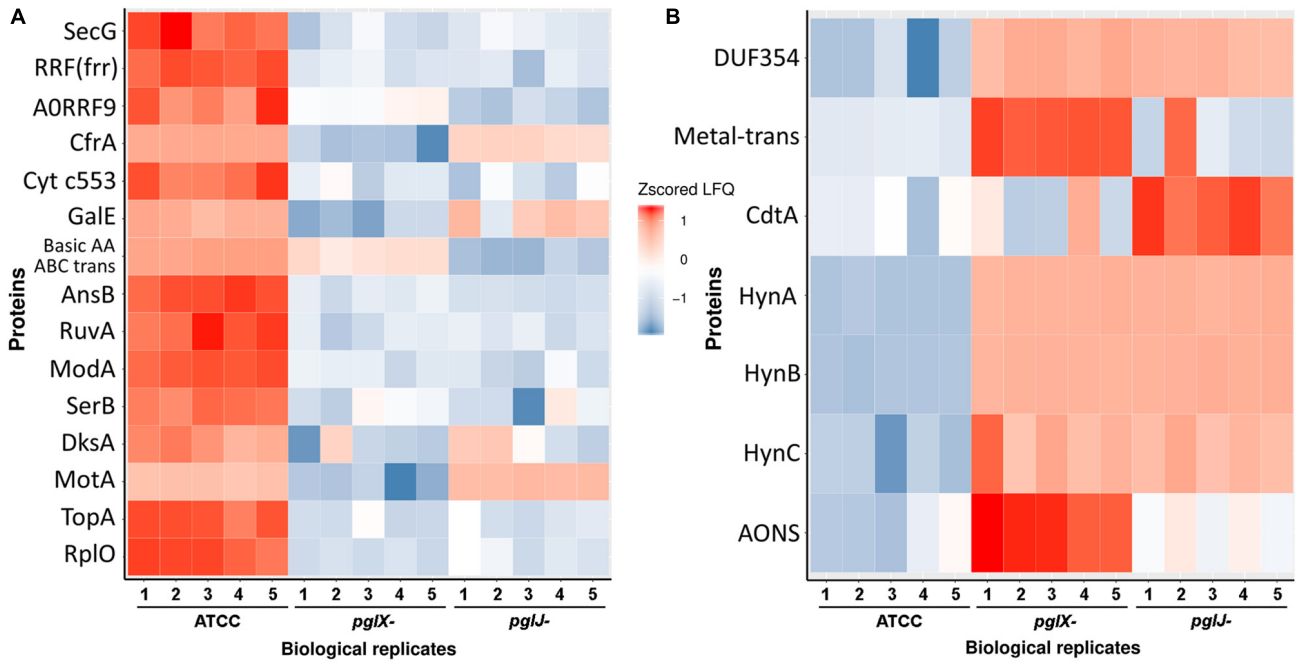

FIGURE 6 | Label-free quantification of proteins in *Cff-pglJ-* and *pglX-* strains compared to WT. **(A,B)** Heat maps of specific proteins with statistically significant decreases **(A)** or increases **(B)** in *pglJ-* and *pglX-* mutants compared to WT (labeled ATCC). Values are gray where MS did not identify fragments. This data represents samples from five biological replicates (B1–B5). The complete dataset is included in **Supplementary Table S1**.

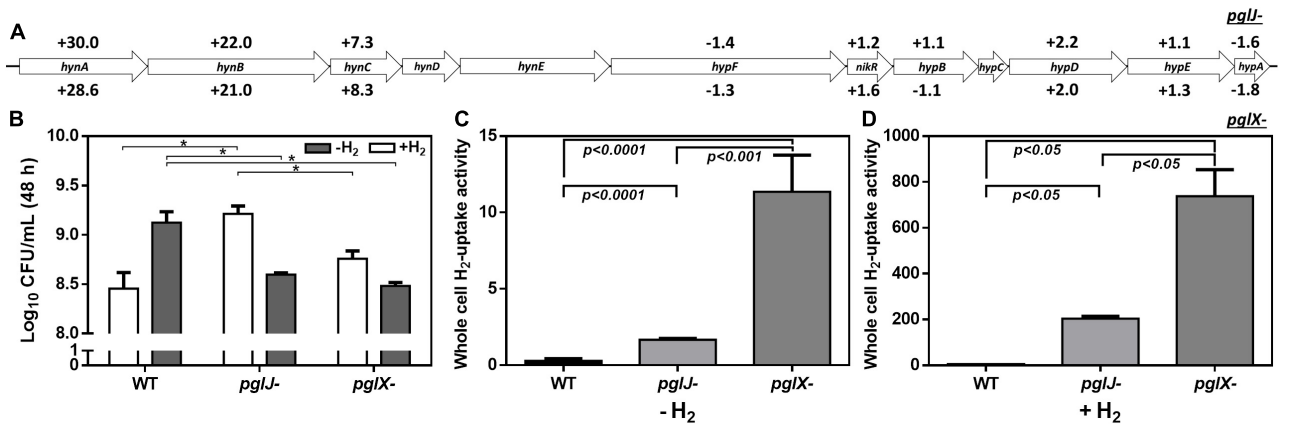

FIGURE 7 | Elevated hydrogenase levels in *Cff-pgl* mutants correlate with increased H_2 uptake. **(A)** Gene arrangements of *hyn* and *hyp* clusters in *Cff* ATCC 27374 with LFQ proteomic protein abundance in *pgl* mutants vs WT are shown. Protein fold changes of *pglJ-* and *pglX-* with respect to WT are indicated above and below each gene respectively. Genes with no values associated had no coverage in our proteomics data analyses. Only HynABC showed significant protein level increases when compared to WT. **(B)** Effect of H_2 on microaerobic growth of *Cff* WT, *pglJ-*, and *pglX-* strains. The data set is derived from three biological replicates (with two technical replicates each) of cells grown under the indicated condition. Number of cells obtained after 48 h of growth is represented by Log_{10} colony forming units per mL (CFU/mL). The error bars represent the standard error within each group. **(C,D)** Whole cell H_2-uptake of *Cff* WT, *pglX-*, and *pglJ-* strains. *Cff* was grown on BHI agar in microaerophilic conditions for 24 h at 37°C in 10% H_2 (+H_2) or absence of hydrogen (–H_2). Whole cell H_2-uptake activity is expressed as nanomoles of H_2 used per min per 10^9 cells. Results in **(C)** represent the mean ± SD of four independent assays; results in **(D)** represent the mean ± SD of two independent assays. *p*-values as analyzed by a two-tailed t-test are either indicated by an asterisk (*p-value ≤ 0.05 in **B**) or are directly included in the figure (for **C,D**).

increased H_2-uptake activity. Cells were grown in microaerobic conditions in the presence or absence of supplemental H_2 and hydrogenase activity was determined using a previously described amperometric method (Maier et al., 1996). The hydrogenase activity (expressed in nmoles of H_2 oxidized per min per 10^9 cells) was 0.3 ± 0.07, 1.7 ± 0.04, and 11.4 ± 1.2 for WT *pglJ-*, and *pglX*, respectively, when cells where grown under microaerobic conditions in the absence of supplemental H_2 (**Figure 7C**). This represented almost a 6-fold (for *pglJ-*) to 39-fold (for *pglX-*) increase in activity compared to WT. When

cells were grown in the presence of 10% H_2, we observed a 122- and 65-fold increase in hydrogenase activity in *pglJ*- and *pglX*-, respectively, and a 20-fold increase in WT (**Figure 7D**). The remarkable H_2-uptake levels measured for *pglJ*- (204 ± 7 nmoles H_2/min/10^9 cells) and *pglX*- (738 ± 82 nmoles H_2/min/10^9 cells) mutants grown with H_2 were the highest recorded values to date for a bacterial pathogen. Taken together, these results indicate an inverse correlation between N-glycosylation and H_2 usage (i.e., hydrogenase synthesis and activity) in *Cff*.

N-Glycosylation Influences Transition Metal Profiles

Proteomics data indicate that multiple proteins associated with transition metals were significantly altered in both *pgl* mutants. These include ModA, involved in molybdenum transport (−49.9-fold in *pglX*- and −71.8-fold in *pglJ*-); the ZinT/AdcA family protein involved in zinc binding (−12.2-fold in *pglX*- and −6.5-fold in *pglJ*-); CfrA, a ferric receptor (−118.4-fold and −3.3-fold); and an iron ABC transporter (−5.1-fold and −7.6-fold) (**Supplementary Table S1**). Also, a copper/cadmium-translocating P-type ATPase protein was found to be significantly increased (51.9-fold) in *pglX*-; however, the increase was not significant (1.4-fold) in *pglJ*-.

The increased levels, especially of the HynABC (Ni-Fe) hydrogenase observed in both *pgl* mutants, led us to further investigate nickel and iron levels in these strains. Using atomic absorption spectrometry (AAS) of lysed cells, we found that iron levels were dramatically decreased in *pglX*- (125.1 ng/mg protein), that is almost sixfold lower when compared to WT (683.2 ng/mg protein) whereas iron levels in *pglJ*- were modestly, but statistically significantly, decreased (**Figure 8A**). In addition, the *pgl* mutants had significantly higher levels of cellular nickel content compared to WT (**Figure 8B**); *pglX*- had a nickel content of 33.2 ng/mg protein that was almost 10-times higher than in the WT (3.5 ng/mg protein). Although still significantly higher when compared to the WT, *pglJ*- (5.2 ng/mg protein) had almost sixfold less nickel than *pglX*-. These results indicate that N-glycosylation might be vital in regulation of nickel homeostasis, iron, or both.

Antibiotic Sensitivity and Increased Membrane Efflux

Our previous study showed that *C. jejuni* N-glycosylation was required for optimal activity of the CmeABC multidrug efflux pump necessary for antibiotic resistance (Dubb et al., 2020). In *Cff*, albeit not statistically significant, we found increased levels of CmeA, CmeB, and CmeC in *pglX*- and *pglJ*- (mean of both mutants: 2.0-fold CmeA, 1.9-fold CmeB, and 2.0-fold CmeC). Therefore, we examined the antibiotic sensitivity profiles of both *Cff* N-glycosylation mutants. As shown in **Supplementary Table S2**, the *pglX*- and *pglJ*- strains showed twofold increase in sensitivities to chloramphenicol, gentamicin, azithromycin, and sulfisoxazole, and a fourfold increase in sensitivity to ampicillin suggesting a correlation between N-glycosylation and antibiotic resistance in *C. fetus*, similar to previously observed in *C. jejuni* (Abouelhadid et al., 2019; Dubb et al., 2020). To explore this further, we used ethidium bromide (EtBr), a DNA intercalating agent, to quantitatively assess efflux pump activity over time. Both *pglJ* and *pglX* mutant strains showed significantly higher levels of EtBr accumulation compared to WT (**Figure 9**); however, accumulation was less pronounced in the *pglX* mutant. Taken together, these results suggest that N-glycosylation in *C. fetus* may be important for efflux pump activity and antibiotic sensitivity.

DISCUSSION

N-glycosylation is a conserved mechanism in all domains of life. The prototypical *pgl* N-glycosylation system, originally characterized in *C. jejuni* (*Cj*), has orthologs in many δ- and ε-Proteobacteria (Nakagawa et al., 2007; Jervis et al., 2010; Ielmini and Feldman, 2011; Nothaft et al., 2012; Mills et al., 2016). Non-thermotolerant *Campylobacter* species, like *C. fetus* (*Cf*), including *C. fetus fetus* (*Cff*) and *C. fetus venerealis* (*Cfv*), have been found to produce more than one N-glycan, unlike *Cj* which expresses one distinct heptasaccharide (Scott et al., 2011; Nothaft et al., 2012; Cain et al., 2019).

In our study, we generated mutants in PglX and PglJ in *Cff* strain ATCC 27374. Glycopeptides from the *pglX*- mutant

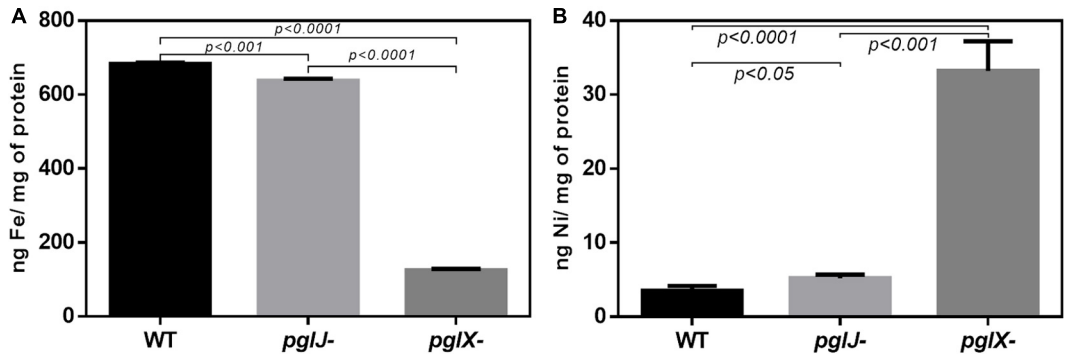

FIGURE 8 | Cellular iron and nickel content of *Cff* WT, *pglX*-, and *pglJ*- strains. Atomic absorption spectroscopy (AAS) was employed for the detection of **(A)** iron (Fe) and **(B)** nickel (Ni) in lysed cells of the indicated strain. Data are presented as the mean of at least three replicates, error bars depict the standard deviations. Statistically significant differences determined by a two-tailed *t*-test are indicated.

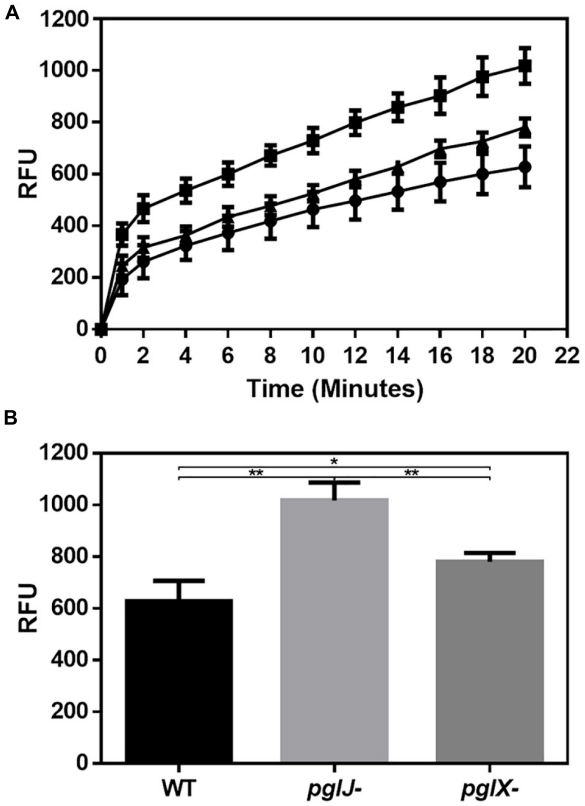

FIGURE 9 | Mutations in N-linked protein glycosylation decreased efflux in *pglX*- and *pglJ*- strains. **(A)** Accumulation of ethidium bromide in cultures of *Cff* WT (circle), *pglJ*- (square), and *pglX*- (triangle) over a time frame of 20 min. Relative fluorescent units (RFU) are indicated on the *y*-axis. **(B)** Bar graph depicting the relative fluorescence at $t = 20$ min. The error bars represent the standard error for each data set consisting of four biological replicates with three technical replicates each. $^{**}p$-value ≤ 0.001, $^{*}p$-value ≤ 0.05 as determined by a two-tailed *t*-test.

showed fragmentation patterns consistent with the conserved diNAcBac-GalNAc$_2$ (Nothaft et al., 2012), suggesting that PglX is responsible for the addition of the first GlcNAc residue to the *Cf* N-glycan structure (**Figure 1**). The loss of *Cf* N-glycan-specific serum reactivity and WGA lectin binding to lysates from the *pglX*- strain support this claim. Proteomics of the *pglJ*- strain resulted in a mixture of glycopeptides, primarily consisting of diNAcBac and a few fragments of diNAcBac-HexNAc, typically more characteristic of a *Cj* PglA mutant. To investigate this further, we used an *E. coli* expression system followed by MS-analyses and were able to show that the *Cff*-PglJ and *Cff*-PglA had similar transferase activities onto recombinantly expressed *Cj*-CmeA as the *Cj* homologs. However, we did not see reactivity with WGA or the *Cff*-N-glycan specific antiserum in the *Cff-pgl* mutants, except for a single band for *pglX*- in the WGA blot. These results suggest possible WGA interaction with another glycan, such as LPS, however the reason behind the absence of specific binding in the *pglJ* mutant strain has yet to be explained. Nevertheless our results suggest that the formation of the diNAcBac-GalNAc$_2$ trisaccharide is conserved between *Cj* and *Cff* and that the observed differences in antigenicity (Jervis et al., 2010; Nothaft et al., 2012) stem from the non-reducing end.

Expression of *Cff*-PglX in *E. coli* showed a CmeA mass shift and with transfer of an additional sugar, consistent with transfer of an additional sugar and with our MS-analysis of glycopeptides from the native host (i.e., diNAcBac-GalNAc$_2$-GlcNAc). Since we were unable to generate a pglY mutant in *Cff*, we also used the *E. coli* system to investigate *Cff*-PglY activity and detected a major glycoform with an additional sugar only when both PglX and PglY were co-expressed, suggesting that PglY's activity is dependent on the initial modification by PglX. Based on our MS results, an N-linked glycan with a composition resembling the minor *Cff* N-glycan [i.e., GlcNAc-α1-6-(Glc-β1-3)-GlcNAc-α1-4-GalNAc-α1-4-GalNAc-α1-3-diNAcBac] was also observed in *E. coli* p*pgl-pglH*:*kan* expressing *pglX* in combination with *pglY*, although the addition of the Glc residue by *Cj*-PglI could not be ruled out since we observed less peptides containing the minor *Cff*-N-glycan in the p*pgl-pglHI* background, and also observed Glc addition in a p*pgl-pglHI*:*kan* mutant demonstrating that an *E. coli* enzyme could be contributing this residue. Thus, the GlcTF reaction requires further investigation either in *Cff* or *in vitro*. No N-glycan that resembles the major form of the *Cff* N-glycan could be detected with any *Cj-pgl* mutant/*Cff-pgl* gene combinations. Nevertheless, these data suggest that *pglX* and *pglY* can mediate the construction of a partial *C. fetus* N-linked glycan using the *C. jejuni* diNAcBac-GalNAc$_2$ trisaccharide as a substrate. *C. jejuni* PglB does not have strict substrate specificity and can transfer full-length and truncated N-glycans and diverse O-antigen structures in *E. coli* and to a lesser extent, in the native host (Feldman et al., 2005; Linton et al., 2005). Therefore, we did not expect preferential transfer of certain *Cj-Cff* hybrid N-glycans to CmeA. However, since we only generated one potential variant of the *Cff*-N-glycan, this suggests that the GTase involved in the formation of the second *Cff*-N-glycan structure is either not fully functional in *E. coli* or is not part of the *pgl* locus, similar to the lack of *pgl* gene clustering in *Helicobacter* species and *D. desulfuricans* (Jervis et al., 2010; Nothaft and Szymanski, 2010).

To better understand the role of N-glycosylation in *Cff*, we utilized LFQ proteomics comparing *Cff* ATCC 27374 with two isogenic *pgl* mutants, *pglX*- and *pglJ*-. Through this approach, we were able to detect almost 77% of the (genome-inferred) total proteins. Analysis of proteins that were significantly up- or down-regulated indicated that more than 100 proteins were altered in the *Cff pgl* mutants in comparison to WT. It is worth noting that differences between *pgl* mutants may be due to differences in glycan length (diNAcBac-GalNAc in *pglJ*- and diNAcBac-GalNAc$_2$ in *pglX*-) or differential feedback regulation in these two backgrounds. Although N-glycosylation was not completely eliminated, we observed a decrease in NapB (−6.7-fold in *pglX*- and −8.4-fold in *pglJ*-, **Supplementary Table S1**), similar to that previously seen in a *Cj-pglB* mutant (Cain et al., 2019). In *C. jejuni*, the nitrate reductase NapAB has been shown to be a two-subunit enzyme, with both subunits being N-glycosylated (Scott et al., 2011; Mintmier et al., 2018; Abouelhadid et al., 2019; Cain et al., 2019). In contrast, in *Cff* ATCC 27374, NapA lacks an N-glycosylation sequon, while at the same time NapB has

two potential sequons. This may explain why we only observed a decrease in NapB (see above), while the difference in NapA protein levels was not significant (1.1-fold in both *pgl* mutants).

No effect on growth or on the expression of downstream genes was observed, but the *pgl* mutants were impaired in motility. Similarly, loss of *pglB* (and therefore complete loss of N-glycosylation) in *C. jejuni* JHH1 and *C. jejuni* 11168 also resulted in decreased motility when compared to WT cells (Scott et al., 2012; Cain et al., 2019). In addition, Cain et al. (2019) demonstrated that levels of specific proteins required for motility were expressed at significantly lower levels in the *C. jejuni* 11168 *pglB* mutant; among them MotA, MotB, and FlgP. We also observed lower levels of MotA and MotB (significantly lower in *pglX*-; 94- and 8.6-fold, respectively), but not in *pglJ*- (**Supplementary Table S1**); FliG [significantly lower in *pglX*- (5.7-fold) and *pglJ*- (4.7-fold) (**Supplementary Table S1**)], as well as the *Cj*-FlaA homolog flagellin protein [significantly lower in *pglX*- (9.7-fold) and *pglJ*- (7.1-fold) (**Supplementary Table S1**)]. This could imply that motility may be correlated with N-glycosylation changes in some Campylobacters. However, *pglB, pglE*, *pglF,* and *pglH* mutants in *C. jejuni* 81–178 were described to display WT levels of motility (Szymanski et al., 1999; Hendrixson and DiRita, 2004), therefore it seems that this regulatory network varies even among strains.

We did not observe a reduction in CmeABC in either the *Cff pglX* or *pglY* mutant. In contrast, we observed a slight, but not statistically significant, increase in these efflux proteins in both mutants. Despite that discrepancy, our *pgl* mutants still displayed decreased EtBr efflux activity compared to WT when cells were grown under the same conditions that were used to prepare whole cell lysates for proteomic analysis. This suggests that *Cf* N-glycosylation directly influences the activity of the efflux pump, an effect that has previously been described for *C. jejuni* (Abouelhadid et al., 2019; Dubb et al., 2020). However, the increased sensitivity to various classes of antibiotics observed in both *Cff-pgl* mutants is most likely indirect since not all of those antibiotics are substrates for the efflux pump in other *Campylobacter* species; however, variations in CmeABC substrate specificities have been observed even between strains (Lin et al., 2002; Akiba et al., 2006; Guo et al., 2010). One might speculate that membrane permeability increases due to lower abundance of certain periplasmic and/or membrane proteins or that loss of periplasmic fOS could result in a higher influx of those antibiotics and therefore lead to the observed decrease in MICs. It is worth noting that the observed effects were less pronounced in *pglX*- compared to *pglJ*-. This could be due to the fact that glycoproteins contain a longer N-glycan chain in *pglX*- compared to *pglJ*. Together these results indicate that N-glycosylation in *Cf* plays a role in efflux, although the mechanism is currently unknown.

Our proteomics data indicate that all three components (HynABC) of the (NiFe)-containing H_2-uptake hydrogenase were significantly upregulated in both *pgl* mutants, suggesting that protein glycosylation plays a role in H_2 utilization. Based on homology with hydrogenase complexes found in related ε-Proteobacteria, such as *H. pylori*, *C. jejuni,* and *C. concisus* (Olson and Maier, 2002; Weerakoon et al., 2009; Benoit and Maier, 2018), the *Cff* HynABC complex is likely to be involved in H_2 oxidation. Consistent with the proteomics data, higher H_2-mediated growth rates were observed in both *pgl* mutants compared to WT, with the highest growth rate seen in the *pglJ*- strain grown under H_2 rich conditions. Surprisingly, H_2-enriched conditions seemed to have a deleterious effect on WT growth. Nevertheless, we infer from these results that the improved growth observed in the mutants could be due to enhanced utilization of H_2 from the drastically increased expression levels of the HynABC complex. In correlation with higher HynABC protein levels, H_2-uptake activities were higher in both *pglJ*- and *pglX* mutants compared to WT in the absence and in the presence of H_2. The increased (NiFe) hydrogenase synthesis (and activity) observed in the mutants might be linked to changes in metal homeostasis, particularly that pertaining to Fe and Ni. Studies conducted in the related organism *H. pylori* can provide insight into the respective roles of Fe and Ni with respect to transcriptional regulation of hydrogenase genes, through Fur and NikR regulators, respectively. For instance, *H. pylori* apo-Fur has been shown to repress *hynABC* (Ernst et al., 2005). Furthermore, addition of Ni to the medium leads to decreased *hynABC* expression; however, this repression was not observed in a *nikR* mutant background (Ernst et al., 2005) suggesting that either Ni-bound NikR represses or apo-NikR activates hydrogenase expression in *H. pylori*; in addition Ni-NikR has been shown to repress *fur* (Dosanjh et al., 2009). Taken together, these sets of results suggest the possible following mechanism in *Cff*: if Ni-bound NikR represses *fur* and (apo-) Fur represses *hynABC*, then elevated Ni levels (as observed in both *pgl* mutants) would be expected to de-repress Fur-controlled *hynABC*. The final outcome would be increased HynABC levels and increased hydrogenase activity, and indeed protein activities correlated well in cells and whole cell lysates grown under the same conditions. Obviously, the mechanism at play in *Cff* has yet to be elucidated. Nevertheless, taken together, our results indicate a clear link between N-glycosylation (or the lack thereof) and (NiFe) HynABC hydrogenase expression and/or enzymatic activity.

It is worth noting that *Cff* contains two additional hydrogenase complexes: a (FeFe) hydrogenase (HydA), hypothesized to be a H_2-uptake type, and a (NiFe) H_2-evolving complex (HycBCDEFG) predicted to be part of a formate hydrogen lyase (FHL) complex that links formate oxidation to hydrogen production (Benoit et al., 2020). Based on our proteomic study, neither HydA nor HycBCDEFG hydrogenase subunits were found to be expressed at different levels between WT and the N-glycosylation mutants.

The increase in (NiFe) HynABC and decrease in certain metal-related proteins prompted us to quantify Ni and Fe levels. In both *pgl* mutants we saw a significant decrease in iron; however, the decrease in iron for *pglX*- was fivefold lower than *pglJ*- and sixfold lower than WT. This may be because *pglX*- has a 118.4-fold decrease, and only 3.3-fold decrease in *pglJ*-, in the CfrA ferric enterobactin receptor present in *Cj*, which is responsible for high-affinity iron acquisition (Miller et al., 2009).

Although nickel is essential for both nickel containing hydrogenases in *Cf*, it is also toxic in excessive amounts,

potentially causing oxidative stress and perturbing enzyme activities (Macomber and Hausinger, 2011). One mechanism of modulating nickel levels that was previously identified in *E. coli* is the nickel defense system (RcnA), which utilizes a proton gradient to translocate nickel to the periplasm where it can either be bound by sequestering proteins or effluxed from the cell (Macomber and Hausinger, 2011). We observed a 50-fold increase in a metal P-type ATPase in *pglX*- (A0RQS6), annotated as copper/cadmium-translocating P-type ATPase with similarly predicted activities. These metal P-type ATPase translocators are involved in detoxification of metals by transporting metals across the inner membrane (Ma et al., 2009). It is possible that this P-type metal translocator may be deficient at translocating; however, there is no clear link to N-glycosylation. These data are consistent with the cellular nickel levels of the *pglX*- strain, which were 6-times higher than the *pglJ*- strain. These increased nickel levels may be responsible for the higher hydrogenase activity levels measured in *pglX*- compared to the other two strains, while nickel toxicity could explain the decreased growth in H_2 growth assays. Our data indicate that N-glycosylation regulates (NiFe)-hydrogenases HynABC, correlating with cellular nickel levels. Taken together, this suggests a possible link between our findings; however, their specific interaction with N-glycosylation is still unknown.

Our research connects N-glycosylation to HynABC hydrogenase regulation and nickel/iron homeostasis, two cellular processes which have been associated with pathogenicity in other bacteria (Palyada et al., 2004; Maier and Benoit, 2019; Benoit et al., 2020). The presented results deepen our understanding of the role of N-glycosylation in *C. fetus* cell physiology. In addition, the *Cf*-N-glycosylation system provides glycan diversity through PglX and PglY, which may further impact the biology of the microbe and warrants further investigation.

MATERIALS AND METHODS

Bacterial Strains, Plasmids, Oligonucleotides and Growth Conditions

Oligonucleotides used in this study are listed in **Supplementary Table S3**. Bacterial strains and plasmids are listed in **Supplementary Table S4**. *C. fetus* was grown using Brain-Heart Infusion (BHI) medium (BHI-Hardy Diagnostics) and Columbia agar (CBA-Hardy Diagnostics) with 5% defibrinated horse blood (Hemostat, Dixon, CA, United States) under microaerobic conditions (10% CO_2, 5% O_2, 85% N_2) at 37°C. *E. coli* was grown on 2xYT at 37°C or as indicated. If required, antibiotics were added to the following working concentrations: 100 μg/mL ampicillin, 25 μg/mL chloramphenicol, 50 μg/mL kanamycin, and 100 μg/mL spectinomycin.

Preparation of Whole Cell Lysates and Western Blotting

Whole cell lysates of bacterial cells were prepared as described previously (Liu et al., 2006). Protein concentrations were determined using either the NanoVue Plus Spectrophotometer (GE) at A_{280} or by the BioRad DC Bradford assay kit with bovine serum albumin as a protein standard. Samples were either analyzed immediately or were frozen at −20°C until further use. Western blot analyzes was carried out as described (Nothaft et al., 2010) with anti-His (1:2000) (Rockland), anti-*Cff*-N-glycan (1:5000) (Nothaft et al., 2012), anti-*Cj*-N-glycan (R1, 1:7500) (Nothaft et al., 2012) or anti-CmeA (1:5000) (Wacker et al., 2002) as the primary, and anti-rabbit IgG (1:2000) (Santa Cruz Biotechnology) as the secondary antibody or with alkaline phosphatase labeled wheat germ agglutinin (WGA, 1:500) (EY Labs). Antibody and WGA-lectin reactive bands were visualized directly on the membrane with nitro-blue tetrazolium chloride (NBT) and 5-bromo-4-chloro-3′-indolyphosphate p-toluidine salt (BCIP) alkaline phosphatase substrate solution (Roche) according to the protocol of the manufacturer.

Free Oligosaccharides Preparation and Analysis

Free oligosaccharides were obtained by ethanol extraction as described previously (Dwivedi et al., 2013) from 1 g of wet cell pellets. Free oligosaccharides (fOS) preparations were further purified using porous graphite carbon (PGC) columns as described (Liu et al., 2006). After elution and lyophilization fOS were dissolved in 100 μl of milliQ water and either stored at −20°C or directly analyzed by TLC as described (Dwivedi et al., 2013).

Generation of *Cff pgl* Gene Mutant Constructs

First, a PCR product containing *Cff-pglKXYJ* (4868 nt) was generated with oligo CS469 and CS470 using chromosomal DNA from *Cff* as a template and inserted into the *Eco*RV site of plasmid pPCR-Script Amp SK(+). After transforming *E. coli* DH5α, plasmid-containing cells were isolated on plates supplemented with Amp and X-gal (40 μg/ml) and plasmids isolated from white colonies were analyzed by restriction digestion. One positive candidate (pPCR-Script-*Cffpgl*) that had the PCR product with the *Cff pgl* genes inserted in opposite direction to the *lacZ* gene was processed further. Next, plasmid pPCR-Script-*Cffpgl* was digested with either *Eco*RV (1 site within *pglX*), *Acc*I (1 site within *pglY*), or *Spe*I (1 site within *pglJ*). The linearized plasmid backbones were isolated and in the case of the *Acc*I and *Spe*I digests, T4 DNA polymerase was used to generate blunt ends before the DNA fragments were purified by agarose gel extraction. The kanamycin (*kan*) resistance cassette obtained and isolated after *Sma*I digestion of plasmid pMW2 was ligated with each vector backbone preparation. Amp and Kan resistant colonies obtained after ligation and transformation were screened and verified by restriction analyzes. One positive clone in which the *kan* cassette is transcribed in the same orientation as the corresponding reading frame (*pgl* gene) was used to generate the gene-specific insertions by double homologous recombination into the chromosome of *Cff*.

Transformation and Insertion Mutagenesis of *Cff*

Natural transformation (on a BHI agar surface) (Wang and Taylor, 1990) and electroporation (Baillon et al., 1999) protocols were employed to introduce *Cff-pgl* gene:*kan* plasmid DNA for double homologous integration of the *kan* cassette into *Cff*. To do so, the corresponding suicide plasmids (pPCR-Script-*CffpglX:kan*, pPCR-Script-*CffpglY:kan,* and pPCR-Script-*CffpglJ:kan*) were isolated from either *E. coli* DH5α or *E. coli* JM110. The latter strain was used to generate non-methylated DNA to circumvent the *Campylobacter* restriction modification system. Transformants were selected on BHI plates for kanamycin resistance and individual colonies were isolated, streaked on fresh agar plates, and used to isolate chromosomal DNA. Candidate colonies were analyzed and verified by PCR with oligonucleotides hybridizing outside of the recombination event (**Supplementary Figure S1**) to confirm integration of the *kan* cassette at the correct position on the chromosome. One positive candidate (for *pglX*- and *pglJ*-) was used for further phenotypical analyzes, whereas (even after multiple attempts) no positive candidate could be obtained for the integration of the *kan* cassette into the *Cff-pglY* gene locus.

Growth Curves and Motility Assays

Growth comparison was performed in BHI broth and growth curves were recorded as described (Dubb et al., 2020). Motility assays were carried out as outlined previously (Golden and Acheson, 2002) with slight modifications. Briefly, *Cff*-WT and *pgl* mutant strains were grown for 18 h on BHI agar. Cells were harvested from the plates with 2 ml of BHI broth and cell suspensions were diluted to an OD_{600} of 0.05. Then, 1 μl of each cell suspension was spotted onto a BHI 0.3% agar plate and after 24 h of incubation, images were taken and the diameter of the motility zone was measured horizontally and vertically.

Reverse Transcriptase PCR

Reverse transcriptase (RT) PCR was performed according to Muraoka and Zhang (2011) with RNA extracted from cells grown on BHI agar for 18 h using the RNeasy Kit following the instructions of the manufacturer (Qiagen). PCR conditions after the RT-step were identical for each primer pair and were carried out as follows: 35 cycles with 30 s, 95°C; 30 s, 52°C and 20 s, 72°C followed by a 72°C finalizing step for 3 min. Samples were stored at 4°C before 15 μl of each 50 μl reaction were analyzed by 0.8% agarose gel electrophoresis.

Pgl Gene Expressing Plasmids

Gene-specific oligonucleotides (**Supplementary Table S3**) were used to amplify *Cj-pglH, Cj-pglA*, *Cj-pglJ*, *Cff-pglA*, *Cff-pglJ*, *Cff-pglX,* and *Cff-pglY* as well as *Cff-pglXY* for expression in *E. coli*. To do so, PCR products obtained with specific template DNA (plasmid p*pgl* for the *C. jejuni pgl* genes or chromosomal DNA from *Cff*) were purified, treated with restriction enzymes (see **Supplementary Table S3**), and inserted into plasmid pCE111/28 digested with the same enzymes. To generate the *Cff-pglXY* expression plasmid, a PCR product encompassing both open reading frames was generated; in addition, a second plasmid was generated by inserting the *Cff-pglY* PCR product into the pCE111/28 (*Cff-pglX*) product via *Pst*I (introduced by PCR during the cloning of *pglX*) and *Xho*I simultaneously introducing an optimized RBS site upstream of the *Cff-pglY* start codon, as was done for all the other *pgl* genes. After ligation, transformation, and screening on selective (Cm) plates, plasmids isolated from candidate colonies were analyzed by restriction analyzes and verified by DNA sequencing. One positive candidate for each construct was used for further analysis.

Pgl Operon Expression Plasmids

To generate p*pgl* operon mutant plasmids that are compatible with the generated *Cj* and *Cff-pgl* gene expression plasmids (pCE111/28-derivatives, Cm^R), the *cat* cassette from all *pgl* operon plasmids with a *kan* cassette insertion in the various *pgl* genes (**Supplementary Table S4**; Linton et al., 2005) was deleted. To do so, plasmids p*pgl-pglH:kan,* p*pgl-pglI:kan*, p*pgl-pglJ:kan,* and p*pgl-pglA:kan* were treated with *Bsa*AI excising the *cat* gene but leaving the rest of the plasmid intact. The complete DNA digest reactions were purified and directly re-ligated. To generate the *pgl* operon plasmid lacking *pglH* and *pglI* (p*pgl-pglHI:kan*), two PCR products were generated: the first reaction was performed with plasmid p*pgl-pglH:kan* as a template and with oligonucleotides pglHI-kan-R and pglHI-pACYC-F amplifying the 5-prime half of the *kan* cassette in *pglH* and the upstream part of the *Cj-pgl* operon. The second reaction was performed with plasmid p*pgl-pglI:kan* as template and with oligonucleotides pglHI-aph-FR and pglHI-pACYC-R amplifying the 3-prime half of the *kan* cassette in *pglI*, the *pglI* downstream region of the *pgl* operon, as well as the origin of replication. The obtained PCR products were purified and ligated without further treatment.

After transformation of DH5α candidate colonies for each ligation reaction were pre-screened on LB agar for Kan^R and Cm^S. The loss of the *cat* cassette and the correct gene organization on plasmids isolated form those colonies were further verified by restriction digest analyzes and DNA sequencing. One positive candidate for each construct (p*pgl*op *pgl*-gene:*kan*, cat-derivative) was used for further analyzes.

Expression of CmeA-His_6 in Glycosylation Competent *E. coli* Cells

Functional analysis of certain *Cff-pgl* proteins was performed in the heterologous *E. coli* glycosylation system. *E. coli* CLM24 was sequentially transformed with the individual *pgl* gene expression plasmids (pCE11/28 derivatives), the CmeA-His_6 expression plasmid (pIH18, pEXT21-derivative), and either the plasmid carrying the WT *Cj-pgl* operon on p*pgl* or the compatible *pgl* operon mutant plasmids (*cat*- derivatives) with a *kan* cassette inserted into *pglA*, *pglJ*, *pglH,* and *pglHI* (double mutant). Cells stably maintaining the plasmid combinations were grown as 4 ml cultures overnight before inoculating 100 ml of fresh medium to a starting OD_{600} of 0.1. Cells were further grown until an OD_{600} of 0.5–0.7 was reached and CmeA-His_6 expression (constitutively

low expressed from the tetracycline promoter on pIH18) was further induced by the addition of IPTG to a final concentration of 0.5 mM. After growth for an additional 4 h, cells were cooled on ice for 10–15 min, pelleted by centrifugation (10 min, 12,000 rpm, 4°C), and washed twice with ice-cold 1 × PBS buffer. Then, 1/10 of the pellet (corresponding to 10 ml of culture volume) was used to produce whole cell lysates using Bacterial Protein Extraction Reagent B-PER (Thermo Fisher Scientific) according to the instructions of the manufacturer and the remainder of cells was used to generate whole cell lysates (as described in Liu et al., 2006) for the purification of the corresponding CmeA-His_6 proteins by Ni-NTA affinity chromatography. To do so, whole cell extracts were filtered (0.22 μm) and loaded onto a 10 ml gravity-flow cartridge (Amersham Pharmacia Biosciences) pre-loaded with 0.5 ml Ni-NTA agarose and pre-equilibrated with 1 column volume 1 × PBS. The column was subsequently washed with at least 5 column volumes of 1 × PBS containing 20 mM imidazole and bound CmeA-His_6 protein was eluted with 0.5–1.5 ml of PBS containing 0.5 M imidazole. Purified proteins were stored at 4°C until further use or immediately analyzed by 12.5% PAGE/mass spectrometry and/or western blotting.

Hydrogen Growth Conditions

Growth of *Cff* under hydrogen was performed as previously described (Benoit and Maier, 2018) with the following changes. *Cff* cells were grown for 48 h then streaked on BHI plates and further incubated for 12 h at 37°C under microaerobic conditions. Cells were resuspended in BHI broth and standardized to the same optical density at 600 nm (OD_{600}), 3.0–4.0. Sealed 165 mL bottles containing 10 mL BHI were flushed with N_2 gas for 10 min, then CO_2 (10% headspace partial pressure, h.p.p.) and O_2 (5% h.p.p.) were injected in every bottle. H_2 (20% h.p.p.) was added as indicated. Cells were inoculated (1:100) and grown at 37°C while shaking at 200 rpm. Growth yields from three biological replicates (each performed in duplicate) were determined after 48 h by serially diluting in BHI and plating on CBA. Plates were incubated at 37°C in microaerobic conditions for three days before being counted.

Whole-Cell H_2-Uptake Hydrogenase Assays

H_2-uptake was performed as previously described (Maier et al., 1996). *Cff* cells were grown at 37°C for 24 h on BHI plates under microaerobic conditions either with 10% H_2 or without. Cells were harvested and resuspended in phosphate buffered saline (PBS) to an optical density (OD_{600}) of 1 which corresponds to ∼2.3 × 10^9 cells/mL. A 2 mL chamber was filled with cells followed by an injection with PBS saturated with H_2. H_2-uptake was monitored as previously described (Maier et al., 1996). Values are reported as nanomoles of H_2 used per min per 10^9 cells and represent four independent measurements for cells grown in microaerobic conditions (and no H_2) and two measurements for cells grown in microaerobic conditions with the addition of 10% H_2.

Determination of Iron and Nickel Content

Campylobacter fetus subsp. *fetus* cells were grown at 37°C for 24 h on two BHI plates under microaerobic conditions and harvested with a loop in 1 mL metal-free double distilled water. Samples were centrifuged at 10,000 *g* for 5 min, washed once with water, resuspended and lyzed by sonication. A portion of lyzed sample was used to determine the protein concentration using the bicinchoninic acid (BCA, Thermo Scientific Pierce) assay. Samples were centrifuged at 15,000 × *g* for 5 min and the supernatant was analyzed for iron and nickel. The remaining sample portion was used for metal (Fe or Ni) content analysis. Briefly, Fe and Ni concentrations were measured by atomic absorption, using a Shimadzu AA-6701F spectrophotometer. All samples were diluted (in 1% HNO_3) to be in the range of the standard curve (0 to 0.4 μM of either Fe or Ni) generated using atomic absorption-grade standard Fe or Ni solutions (Sigma). Results shown are means and standard deviations for 3–5 measurements.

Ethidium Bromide Accumulation Assay

Accumulation of EtBr was performed as previously described (Lin et al., 2002) with the following changes. *Cff* strains were grown overnight on BHI agar at 37°C in microaerobic conditions and harvested with MEM (Gibco). Cultures were adjusted to OD_{600} of 0.2 and then incubated at 37°C for 30 min in microaerobic conditions. EtBr was added to a final concentration of 2 μg/mL. Fluorescence was measured, with an excitation of 530 nm and emission of 600 nm, every 2 min over a 20 min time using a Bio Tek Synergy H1 plate reader. This was performed in three biological replicates, which included three technical replicates. Background fluorescence of MEM with EtBr was subtracted from these values.

Antibiotic MIC Assay

Campylobacter fetus subsp. *fetus* cells were grown for 24 h at 37°C in microaerobic conditions on CBA plates. Antibiotic MIC was assessed using the Sensititre (Trek Diagnostic Systems) platform. Sensititre plate EQUIN1F was used, following manufacturer's instructions.

Preparation of Bacterial Whole Cell Proteome Samples

Campylobacter fetus subsp. *fetus* cells were grown for 24 h at 37°C under microaerobic conditions on BHI agar. Cells were harvested with ice-cold PBS and inactivated with PBS, 10% sodium azide for 30 min at 4°C. Cell pellets obtained after centrifugation (4000 × *g* for 15 min) were lyophilized and stored at −20°C until further use. Cell lysates for proteomic analyses were prepared as follows: cells were solubilized in 4% SDS, 100 mM Tris pH 8.0, and 20 mM DTT and boiled at 95°C with shaking at 2000 rpm for 10 min. Insoluble material was removed by centrifugation at 17,000 × *g* for 10 min at room temperature and the supernatant was collected. Protein concentrations were determined using the bicinchoninic acid assay (Thermo Scientific Pierce) and 200 μg of protein from each sample was acetone-precipitated overnight at −20°C by mixing

volumes of ice-cold acetone with one volume of sample. Samples were then spun down at 16,000 × *g* for 10 min at 4°C. The precipitated protein pellets were resuspended with 80% ice-cold acetone and precipitated for an additional 4 h at −20°C. Samples were spun down at 17,000 × *g* for 10 min at 4°C to collect the precipitated protein.

Digestion of Complex Protein Lysates

Dried protein pellets were resuspended in 6 M urea, 2 M thiourea, 40 mM NH_4HCO_3 and reduced/alkylated prior to digestion with Lys-C (1/200 w/w) and then trypsin (1/50 w/w) overnight as previously described (Scott et al., 2011). Digested samples were acidified to a final concentration of 0.5% formic acid and desalted with home-made high-capacity StageTips composed on 5 mg Empore™ C18 material (3M, Maplewood, Minnesota) and 5 mg of OLIGO R3 reverse phase resin (Thermo Fisher Scientific) according to the protocol of Ishihama and Rappsilber (Ishihama et al., 2006; Rappsilber et al., 2007). Bound peptides were eluted with buffer B, dried and stored at −20°C.

Reversed Phase Liquid Chromatography-Mass Spectrometry

Purified peptides were resuspended in Buffer A* and separated using a two-column chromatography set up comprising a PepMap100 C18 20 mm × 75 μm trap and a PepMap C18 500 mm × 75 μm analytical column (Thermo Fisher Scientific). Samples were concentrated onto the trap column at 5 μl/min for 5 min and infused into an Orbitrap Elite™ Mass Spectrometer (Thermo Fisher Scientific) at 300 nl/min via the analytical column using a Dionex Ultimate 3000 UPLC (Thermo Fisher Scientific). Then, 180 min gradients were run altering the buffer composition from 3% buffer B to 28% B over 150 min, then from 28% B to 40% B over 10 min, then from 40% B to 100% B over 2 min, followed by the composition held at 100% B for 3 min, and then dropped to 3% B over 5 min and held at 3% B for another 10 min. The Orbitrap Mass Spectrometer was operated in a data-dependent mode automatically switching between the acquisition of a single Orbitrap MS scan (60,000 resolution) followed by one data-dependent HCD (resolution 15 k AGC target of 4×10^5 with a maximum injection time of 250 ms, NCE 40) and CID (ion trap, AGC target of 5×10^4 with a maximum injection time of 100 ms, NCE 35) event for each precursor (total of five precursors per cycle with 45 s dynamic exclusion enabled).

Proteome Data Analyses

Proteome analysis to assess the expression of proteins within *Cff* strains was undertaken with MaxQuant [v1.5.3.30 (Cox and Mann, 2008)]. Database searching was carried out against the *C. fetus* subsp. *fetus* strain ATCC 27374 proteome (generated from a Maxquant generated six frame translation of the in-house sequenced strain). Searches were undertaken with the following search parameters: carbamidomethylation of cysteine as a fixed modification; oxidation of methionine, acetylation of protein N-terminal trypsin/P cleavage with a maximum of two missed cleavages. To enhance the identification of peptides between samples, the Match between Runs option was enabled with a precursor match window set to 2 min and an alignment window of 10 min. For label free quantitation, the MaxLFQ option within Maxquant was enabled in addition to the re-quantification module (Cox et al., 2014). The resulting outputs were processed within the Perseus (v1.5.0.9) analysis environment to remove reverse matches and common proteins contaminations prior to further analysis (Tyanova et al., 2016). Statistical analysis was undertaken in Perseus by grouping biological replicates, imputing missing values based on observed values (downshifted by 2.5 standard deviations with a width of 0.3 standard deviations) and then comparing groups using a student *t*-test. To define an appropriate *p*-value threshold, multiple hypothesis correction was undertaken using a Benjamini-Hochberg correction with a FDR of 0.05. All statistical outputs are provided within **Supplementary Table S1**. All mass spectrometry proteomics data have been deposited to the ProteomeXchange Consortium via the PRIDE partner repository (Vizcaino et al., 2016) with the dataset identifier PXD014538 [LFQ experiments of *C. fetus fetus* mutants (**Supplementary MS Data 1**) accessible using the **username:** reviewer71456@ebi.ac.uk, **password:** B5YuYNx8) and PXD017832 [analysis of *C. fetus fetus pgl* enzymes in the heterologous *E. coli* glycosylation system (**Supplementary MS Data 2**) accessible using the **username:** reviewer23740@ebi.ac.uk **password:** PHKlhnSp].

Glycopeptide Data Analysis

Glycopeptides were identified by manually interrogating possible glycopeptide scans based on the presence of the diagnostic oxonium ion (204.09 m/z) of HexNAc. To facilitate glycopeptide assignments from HCD scans, the ions below the mass of the predicted deglycosylated peptides were extracted with Xcalibur v2.2 using the Spectrum list function. Ions with a deconvoluted mass above that of the deglycosylated peptide and ions corresponding to known carbohydrate oxoniums were removed in a similar approach to post-spectral processing of ETD data and then searched with Mascot[1]. Searches were carried out using semi-trypsin specificity, carbamidomethylation of cysteine as a fixed modification, and oxidation (M) as a variable modification. A precursor and product tolerance of 20 ppm was used, and the taxonomy restricted to "Other Proteobacteria." All spectra were searched with the decoy option enabled with all peptides passing a 1% FDR. Identified glycopeptide spectra were manually inspected and spectra annotated according to the nomenclature of Roepstorff and Fohlman (1984) for peptides as well as Domon and Costello (1988) for glycans.

DATA AVAILABILITY STATEMENT

The mass spectrometry proteomics data have been deposited to the ProteomeXchange Consortium via the PRIDE (1) partner repository with the dataset identifiers PXD014538 and PXD017832.

[1]http://www.matrixscience.com/, v2.5

AUTHOR CONTRIBUTIONS

JD, HN, and CS designed the experiments, interpreted the results, and wrote the manuscript. BB and CF constructed expression plasmids and *Cf-pgl* mutants. SB and RM performed the hydrogenase activity and assisted with analysis and interpretation of hydrogenase and AAS data. NS performed all mass spectrometry and LFQ analysis. DW and DL made *pgl* expression constructs for *E. coli* and assisted in data analysis and interpretation. All authors read and approved of the final manuscript.

FUNDING

JD was previously supported by the Alberta Glycomics Centre and subsequently the National Institute of General Medical Sciences Training Grant Award Number T32GM107004. NS was supported by the National Health and Medical Research Council of Australia (NHMRC) project grant (APP1100164) and by an Overseas (Biomedical) Fellowship (APP1037373). SB and RM received support from the University of Georgia Foundation. CS was an Alberta Innovates Strategic Chair in Bacterial Glycomics. DW was supported by a Society for Applied Microbiology Studentship.

ACKNOWLEDGMENTS

We thank the Melbourne Mass Spectrometry and Proteomics Facility of the Bio21 Molecular Science and Biotechnology Institute at The University of Melbourne for mass spectrometry analysis. We also thank Susan Sanchez and the Athens Veterinary Diagnostic Laboratory for help with the antibiotic sensitivity assay.

SUPPLEMENTARY MATERIAL

The Supplementary Material for this article can be found online at: https://www.frontiersin.org/articles/10.3389/fmicb.2020.01191/full#supplementary-material

REFERENCES

Abouelhadid, S., North, S. J., Hitchen, P., Vohra, P., Chintoan-Uta, C., Stevens, M., et al. (2019). Quantitative analyses reveal novel roles for N-glycosylation in a major enteric bacterial pathogen. *mBio* 10:e00297-19. doi: 10.1128/mBio.00297-19

Akiba, M., Lin, J., Barton, Y. W., and Zhang, Q. (2006). Interaction of CmeABC and CmeDEF in conferring antimicrobial resistance and maintaining cell viability in *Campylobacter jejuni*. *J. Antimicrob. Chemother.* 57, 52–60. doi: 10.1093/jac/dki419

Alagesan, K., Hinneburg, H., Seeberger, P. H., Silva, D. V., and Kolarich, D. (2019). Glycan size and attachment site location affect electron transfer dissociation (ETD) fragmentation and automated glycopeptide identification. *Glycoconj J.* 36, 487–493. doi: 10.1007/s10719-019-09888-w

Alaimo, C., Catrein, I., Morf, L., Marolda, C. L., Callewaert, N., Valvano, M. A., et al. (2006). Two distinct but interchangeable mechanisms for flipping of lipid-linked oligosaccharides. *EMBO J.* 25, 967–976. doi: 10.1038/sj.emboj.7601024

Baillon, M. L., Van Vliet, A. H., Ketley, J. M., Constantinidou, C., and Penn, C. W. (1999). An iron-regulated alkyl hydroperoxide reductase (AhpC) confers aerotolerance and oxidative stress resistance to the microaerophilic pathogen *Campylobacter jejuni*. *J. Bacteriol.* 181, 4798–4804. doi: 10.1128/jb.181.16.4798-4804.1999

Benoit, S. L., and Maier, R. J. (2018). Site-directed mutagenesis of *Campylobacter concisus* respiratory genes provides insight into the pathogen's growth requirements. *Sci. Rep.* 8:14203. doi: 10.1038/s41598-018-32509-9

Benoit, S. L., Maier, R. J., Sawers, R. G., and Greening, C. (2020). Molecular hydrogen metabolism: a widespread trait of pathogenic bacteria and protists. *Microbiol. Mol. Biol. Rev.* 84:e00092-19. doi: 10.1128/MMBR.00092-19

Cain, J. A., Dale, A. L., Niewold, P., Klare, W. P., Man, L., White, M. Y., et al. (2019). Proteomics reveals multiple phenotypes associated with N-linked glycosylation in *Campylobacter jejuni*. *Mol. Cell. Proteomics* 18, 715–734. doi: 10.1074/mcp.RA118.001199

Chen, M. M., Glover, K. J., and Imperiali, B. (2007). From peptide to protein: comparative analysis of the substrate specificity of N-linked glycosylation in *C. jejuni*. *Biochemistry* 46, 5579–5585. doi: 10.1021/bi602633n

Cid, E., Gomis, R. R., Geremia, R. A., Guinovart, J. J., and Ferrer, J. C. (2000). Identification of two essential glutamic acid residues in glycogen synthase. *J. Biol. Chem.* 275, 33614–33621. doi: 10.1074/jbc.M005358200

Coutinho, P. M., Deleury, E., Davies, G. J., and Henrissat, B. (2003). An evolving hierarchical family classification for glycosyltransferases. *J. Mol. Biol.* 328, 307–317. doi: 10.1016/s0022-2836(03)00307-3

Cox, J., Hein, M. Y., Luber, C. A., Paron, I., Nagaraj, N., and Mann, M. (2014). Accurate proteome-wide label-free quantification by delayed normalization and maximal peptide ratio extraction, termed MaxLFQ. *Mol. Cell. Proteomics* 13, 2513–2526. doi: 10.1074/mcp.M113.031591

Cox, J., and Mann, M. (2008). MaxQuant enables high peptide identification rates, individualized p.p.b.-range mass accuracies and proteome-wide protein quantification. *Nat. Biotechnol.* 26, 1367–1372. doi: 10.1038/nbt.1511

Domon, B., and Costello, C. E. (1988). A systematic nomenclature for carbohydrate fragmentations in FAB-MS/MS spectra of glycoconjugates. *Glycoconjugate J.* 5, 397–409. doi: 10.1007/BF01049915

Dosanjh, N. S., West, A. L., and Michel, S. L. (2009). *Helicobacter pylori* NikR's interaction with DNA: a two-tiered mode of recognition. *Biochemistry* 48, 527–536. doi: 10.1021/bi801481j

Dubb, R. K., Nothaft, H., Beadle, B., Richards, M. R., and Szymanski, C. M. (2020). N-glycosylation of the CmeABC multidrug efflux pump is needed for optimal function in *Campylobacter jejuni*. *Glycobiology* 30, 105–119. doi: 10.1093/glycob/cwz082

Duncan, J. S., Leatherbarrow, A. J., French, N. P., and Grove-White, D. H. (2014). Temporal and farm-management-associated variation in faecal-pat prevalence of *Campylobacter fetus* in sheep and cattle. *Epidemiol. Infect.* 142, 1196–1204. doi: 10.1017/S0950268813002379

Dwivedi, R., Nothaft, H., Reiz, B., Whittal, R. M., and Szymanski, C. M. (2013). Generation of free oligosaccharides from bacterial protein N-linked glycosylation systems. *Biopolymers* 99, 772–783. doi: 10.1002/bip.22296

Ernst, F. D., Kuipers, E. J., Heijens, A., Sarwari, R., Stoof, J., Penn, C. W., et al. (2005). The nickel-responsive regulator NikR controls activation and repression of gene transcription in *Helicobacter pylori*. *Infect. Immun.* 73, 7252–7258. doi: 10.1128/IAI.73.11.7252-7258.2005

Feldman, M. F., Wacker, M., Hernandez, M., Hitchen, P. G., Marolda, C. L., Kowarik, M., et al. (2005). Engineering N-linked protein glycosylation with diverse O antigen lipopolysaccharide structures in *Escherichia coli*. *Proc. Natl. Acad. Sci. U.S.A.* 102, 3016–3021. doi: 10.1073/pnas.0500044102

Fitzgerald, C., Tu, Z. C., Patrick, M., Stiles, T., Lawson, A. J., Santovenia, M., et al. (2014). *Campylobacter fetus* subsp. testudinum subsp. nov., isolated from humans and reptiles. *Int. J. Syst. Evol. Microbiol.* 64, 2944–2948. doi: 10.1099/ijs.0.057778-0

Glover, K. J., Weerapana, E., Chen, M. M., and Imperiali, B. (2006). Direct biochemical evidence for the utilization of UDP-bacillosamine by PglC, an essential glycosyl-1-phosphate transferase in the *Campylobacter jejuni* N-linked glycosylation pathway. *Biochemistry* 45, 5343–5350. doi: 10.1021/bi0602056

Glover, K. J., Weerapana, E., and Imperiali, B. (2005). *In vitro* assembly of the undecaprenylpyrophosphate-linked heptasaccharide for prokaryotic N-linked glycosylation. *Proc. Natl. Acad. Sci. U.S.A.* 102, 14255–14259. doi: 10.1073/pnas.0507311102

Golden, N. J., and Acheson, D. W. (2002). Identification of motility and autoagglutination *Campylobacter jejuni* mutants by random transposon mutagenesis. *Infect. Immun.* 70, 1761–1771. doi: 10.1128/iai.70.4.1761-1771.2002

Guo, B., Lin, J., Reynolds, D. L., and Zhang, Q. (2010). Contribution of the multidrug efflux transporter CmeABC to antibiotic resistance in different *Campylobacter* species. *Foodborne Pathog. Dis.* 7, 77–83. doi: 10.1089/fpd.2009.0354

Hendrixson, D. R., and DiRita, V. J. (2004). Identification of *Campylobacter jejuni* genes involved in commensal colonization of the chick gastrointestinal tract. *Mol. Microbiol.* 52, 471–484. doi: 10.1111/j.1365-2958.2004.03988.x

Holst, E., Wathne, B., Hovelius, B., and Mardh, P. A. (1987). Bacterial vaginosis: microbiological and clinical findings. *Eur. J. Clin. Microbiol.* 6, 536–541. doi: 10.1007/bf02014242

Ielmini, M. V., and Feldman, M. F. (2011). *Desulfovibrio desulfuricans* PglB homolog possesses oligosaccharyltransferase activity with relaxed glycan specificity and distinct protein acceptor sequence requirements. *Glycobiology* 21, 734–742. doi: 10.1093/glycob/cwq192

Iraola, G., Forster, S. C., Kumar, N., Lehours, P., Bekal, S., Garcia-Pena, F. J., et al. (2017). Distinct *Campylobacter fetus* lineages adapted as livestock pathogens and human pathobionts in the intestinal microbiota. *Nat. Commun.* 8:1367. doi: 10.1038/s41467-017-01449-9

Ishihama, Y., Rappsilber, J., and Mann, M. (2006). Modular stop and go extraction tips with stacked disks for parallel and multidimensional Peptide fractionation in proteomics. *J. Proteome Res.* 5, 988–994. doi: 10.1021/pr050385q

Jervis, A. J., Butler, J. A., Lawson, A. J., Langdon, R., Wren, B. W., and Linton, D. (2012). Characterization of the structurally diverse N-linked glycans of *Campylobacter* species. *J. Bacteriol.* 194, 2355–2362. doi: 10.1128/JB.00042-12

Jervis, A. J., Langdon, R., Hitchen, P., Lawson, A. J., Wood, A., Fothergill, J. L., et al. (2010). Characterization of N-linked protein glycosylation in *Helicobacter pullorum*. *J. Bacteriol.* 192, 5228–5236. doi: 10.1128/JB.00211-10

Kelly, J., Jarrell, H., Millar, L., Tessier, L., Fiori, L. M., Lau, P. C., et al. (2006). Biosynthesis of the N-linked glycan in *Campylobacter jejuni* and addition onto protein through block transfer. *J. Bacteriol.* 188, 2427–2434. doi: 10.1128/JB.188.7.2427-2434.2006

Klein, B. S., Vergeront, J. M., Blaser, M. J., Edmonds, P., Brenner, D. J., Janssen, D., et al. (1986). *Campylobacter* infection associated with raw milk. An outbreak of gastroenteritis due to Campylobacter jejuni and thermotolerant Campylobacter fetus subsp fetus. *JAMA* 255, 361–364. doi: 10.1001/jama.255.3.361

Kowarik, M., Young, N. M., Numao, S., Schulz, B. L., Hug, I., Callewaert, N., et al. (2006). Definition of the bacterial N-glycosylation site consensus sequence. *EMBO J.* 25, 1957–1966. doi: 10.1038/sj.emboj.7601087

Kuhns, L. G., Benoit, S. L., Bayyareddy, K., Johnson, D., Orlando, R., Evans, A. L., et al. (2016). Carbon fixation driven by molecular hydrogen results in chemolithoautotrophically enhanced growth of *Helicobacter pylori*. *J. Bacteriol.* 198, 1423–1428. doi: 10.1128/JB.00041-16

Lin, J., Michel, L. O., and Zhang, Q. (2002). CmeABC functions as a multidrug efflux system in *Campylobacter jejuni*. *Antimicrob. Agents Chemother.* 46, 2124–2131. doi: 10.1128/aac.46.7.2124-2131.2002

Linton, D., Dorrell, N., Hitchen, P. G., Amber, S., Karlyshev, A. V., Morris, H. R., et al. (2005). Functional analysis of the *Campylobacter jejuni* N-linked protein glycosylation pathway. *Mol. Microbiol.* 55, 1695–1703. doi: 10.1111/j.1365-2958.2005.04519.x

Liu, X., Mcnally, D. J., Nothaft, H., Szymanski, C. M., Brisson, J. R., and Li, J. (2006). Mass spectrometry-based glycomics strategy for exploring N-linked glycosylation in eukaryotes and bacteria. *Anal. Chem.* 78, 6081–6087. doi: 10.1021/ac060516m

Ma, Z., Jacobsen, F. E., and Giedroc, D. P. (2009). Coordination chemistry of bacterial metal transport and sensing. *Chem. Rev.* 109, 4644–4681. doi: 10.1021/cr900077w

Macomber, L., and Hausinger, R. P. (2011). Mechanisms of nickel toxicity in microorganisms. *Metallomics* 3, 1153–1162. doi: 10.1039/c1mt00063b

Maier, R. J., and Benoit, S. L. (2019). Role of nickel in microbial pathogenesis. *Inorganics* 7:80. doi: 10.3390/inorganics7070080

Maier, R. J., Fu, C., Gilbert, J., Moshiri, F., Olson, J., and Plaut, A. G. (1996). Hydrogen uptake hydrogenase in *Helicobacter pylori*. *FEMS Microbiol. Lett.* 141, 71–76. doi: 10.1111/j.1574-6968.1996.tb08365.x

Marchand-Senecal, X., Bekal, S., Pilon, P. A., Sylvestre, J. L., and Gaudreau, C. (2017). *Campylobacter fetus* cluster among men who have sex with men, montreal, quebec, Canada, 2014-2016. *Clin. Infect. Dis.* 65, 1751–1753. doi: 10.1093/cid/cix610

Miller, C. E., Williams, P. H., and Ketley, J. M. (2009). Pumping iron: mechanisms for iron uptake by *Campylobacter*. *Microbiology* 155, 3157–3165. doi: 10.1099/mic.0.032425-0

Mills, D. C., Jervis, A. J., Abouelhadid, S., Yates, L. E., Cuccui, J., Linton, D., et al. (2016). Functional analysis of N-linking oligosaccharyl transferase enzymes encoded by deep-sea vent *Proteobacteria*. *Glycobiology* 26, 398–409. doi: 10.1093/glycob/cwv111

Mintmier, B., Mcgarry, J. M., Sparacino-Watkins, C. E., Sallmen, J., Fischer-Schrader, K., Magalon, A., et al. (2018). Molecular cloning, expression and biochemical characterization of periplasmic nitrate reductase from *Campylobacter jejuni*. *FEMS Microbiol. Lett.* 365:fny151. doi: 10.1093/femsle/fny151

Muraoka, W. T., and Zhang, Q. (2011). Phenotypic and genotypic evidence for L-fucose utilization by *Campylobacter jejuni*. *J. Bacteriol.* 193, 1065–1075. doi: 10.1128/JB.01252-10

Nakagawa, S., Takaki, Y., Shimamura, S., Reysenbach, A. L., Takai, K., and Horikoshi, K. (2007). Deep-sea vent epsilon-*Proteobacteria*l genomes provide insights into emergence of pathogens. *Proc. Natl. Acad. Sci. U.S.A.* 104, 12146–12150. doi: 10.1073/pnas.0700687104

Nothaft, H., Liu, X., Mcnally, D. J., Li, J., and Szymanski, C. M. (2009). Study of free oligosaccharides derived from the bacterial N-glycosylation pathway. *Proc. Natl. Acad. Sci. U.S.A.* 106, 15019–15024. doi: 10.1073/pnas.0903078106

Nothaft, H., Liu, X., Mcnally, D. J., and Szymanski, C. M. (2010). N-linked protein glycosylation in a bacterial system. *Methods Mol. Biol.* 600, 227–243. doi: 10.1007/978-1-60761-454-8_16

Nothaft, H., Scott, N. E., Vinogradov, E., Liu, X., Hu, R., Beadle, B., et al. (2012). Diversity in the protein N-glycosylation pathways among *Campylobacter* species. *Mol. Cell Proteomics* 11, 1203–1219. doi: 10.1074/mcp.M112.021519

Nothaft, H., and Szymanski, C. M. (2010). Protein glycosylation in bacteria: sweeter than ever. *Nat. Rev. Microbiol.* 8, 765–778. doi: 10.1038/nrmicro2383

Nothaft, H., and Szymanski, C. M. (2013). Bacterial protein N-glycosylation: new perspectives and applications. *J. Biol. Chem.* 288, 6912–6920. doi: 10.1074/jbc.R112.417857

Olson, J. W., and Maier, R. J. (2002). Molecular hydrogen as an energy source for *Helicobacter pylori*. *Science* 298, 1788–1790. doi: 10.1126/science.1077123

Palyada, K., Threadgill, D., and Stintzi, A. (2004). Iron acquisition and regulation in *Campylobacter jejuni*. *J. Bacteriol.* 186, 4714–4729. doi: 10.1128/JB.186.14.4714-4729.2004

Patrick, M. E., Gilbert, M. J., Blaser, M. J., Tauxe, R. V., Wagenaar, J. A., and Fitzgerald, C. (2013). Human infections with new subspecies of *Campylobacter fetus*. *Emerg. Infect. Dis.* 19, 1678–1680. doi: 10.3201/eid1910.130883

Ramirez, A. S., Boilevin, J., Mehdipour, A. R., Hummer, G., Darbre, T., Reymond, J. L., et al. (2018). Structural basis of the molecular ruler mechanism of a bacterial glycosyltransferase. *Nat. Commun.* 9:445. doi: 10.1038/s41467-018-02880-2

Rappsilber, J., Mann, M., and Ishihama, Y. (2007). Protocol for micro-purification, enrichment, pre-fractionation and storage of peptides for proteomics using StageTips. *Nat. Protoc.* 2, 1896–1906. doi: 10.1038/nprot.2007.261

Roepstorff, P., and Fohlman, J. (1984). Proposal for a common nomenclature for sequence ions in mass spectra of peptides. *Biomed. Mass Spectrom.* 11:601. doi: 10.1002/bms.1200111109

Scott, N. E., Nothaft, H., Edwards, A. V., Labbate, M., Djordjevic, S. P., Larsen, M. R., et al. (2012). Modification of the *Campylobacter jejuni* N-linked glycan by EptC protein-mediated addition of phosphoethanolamine. *J. Biol. Chem.* 287, 29384–29396. doi: 10.1074/jbc.m112.380212

Scott, N. E., Parker, B. L., Connolly, A. M., Paulech, J., Edwards, A. V., Crossett, B., et al. (2011). Simultaneous glycan-peptide characterization using hydrophilic interaction chromatography and parallel fragmentation by CID, higher energy collisional dissociation, and electron transfer dissociation MS applied to the N-linked glycoproteome of *Campylobacter jejuni*. *Mol. Cell. Proteomics* 10:M000031-MCP201. doi: 10.1074/mcp.M000031-MCP201

Szymanski, C. M., Yao, R., Ewing, C. P., Trust, T. J., and Guerry, P. (1999). Evidence for a system of general protein glycosylation in *Campylobacter jejuni*. *Mol. Microbiol.* 32, 1022–1030. doi: 10.1046/j.1365-2958.1999.01415.x

Troutman, J. M., and Imperiali, B. (2009). *Campylobacter jejuni* PglH is a single active site processive polymerase that utilizes product inhibition to limit sequential glycosyl transfer reactions. *Biochemistry* 48, 2807–2816. doi: 10.1021/bi802284d

Tu, Z. C., Zeitlin, G., Gagner, J. P., Keo, T., Hanna, B. A., and Blaser, M. J. (2004). *Campylobacter fetus* of reptile origin as a human pathogen. *J. Clin. Microbiol.* 42, 4405–4407. doi: 10.1128/JCM.42.9.4405-4407.2004

Tyanova, S., Temu, T., Sinitcyn, P., Carlson, A., Hein, M. Y., Geiger, T., et al. (2016). The Perseus computational platform for comprehensive analysis of (prote)omics data. *Nat. Methods* 13, 731–740. doi: 10.1038/nmeth.3901

Vizcaino, J. A., Csordas, A., Del-Toro, N., Dianes, J. A., Griss, J., Lavidas, I., et al. (2016). 2016 update of the PRIDE database and its related tools. *Nucleic Acids Res.* 44:11033. doi: 10.1093/nar/gkw880

Wacker, M., Linton, D., Hitchen, P. G., Nita-Lazar, M., Haslam, S. M., North, S. J., et al. (2002). N-linked glycosylation in *Campylobacter jejuni* and its functional transfer into *E. coli*. *Science* 298, 1790–1793. doi: 10.1126/science.298.5599.1790

Wagenaar, J. A., Van Bergen, M. A., Blaser, M. J., Tauxe, R. V., Newell, D. G., and Van Putten, J. P. (2014). *Campylobacter fetus* infections in humans: exposure and disease. *Clin. Infect. Dis.* 58, 1579–1586. doi: 10.1093/cid/ciu085

Wang, Y., and Taylor, D. E. (1990). Natural transformation in *Campylobacter* species. *J. Bacteriol.* 172, 949–955. doi: 10.1128/jb.172.2.949-955.1990

Waterhouse, A. M., Procter, J. B., Martin, D. M., Clamp, M., and Barton, G. J. (2009). Jalview Version 2–a multiple sequence alignment editor and analysis workbench. *Bioinformatics* 25, 1189–1191. doi: 10.1093/bioinformatics/btp033

Weerakoon, D. R., Borden, N. J., Goodson, C. M., Grimes, J., and Olson, J. W. (2009). The role of respiratory donor enzymes in *Campylobacter jejuni* host colonization and physiology. *Microb. Pathog.* 47, 8–15. doi: 10.1016/j.micpath.2009.04.009

Conflict of Interest: The authors declare that the research was conducted in the absence of any commercial or financial relationships that could be construed as a potential conflict of interest.

frontiers in Microbiology

ORIGINAL RESEARCH
published: 19 June 2020
doi: 10.3389/fmicb.2020.01072

Genome-Scale Metabolic Model Driven Design of a Defined Medium for *Campylobacter jejuni* M1cam

Noemi Tejera[1], Lisa Crossman[1,2,3], Bruce Pearson[1], Emily Stoakes[4], Fauzy Nasher[5], Bilal Djeghout[1], Mark Poolman[6], John Wain[1] and Dipali Singh[1]*

[1] Microbes in Food Chain, Quadram Institute Biosciences, Norwich Research Park, Norwich, United Kingdom, [2] SequenceAnalysis.co.uk, NRP Innovation Centre, Norwich, United Kingdom, [3] University of East Anglia, Norwich, United Kingdom, [4] Department of Veterinary Medicine, University of Cambridge, Cambridge, United Kingdom, [5] London School of Hygiene and Tropical Medicine, University of London, London, United Kingdom, [6] Cell Systems Modelling Group, Oxford Brookes University, Oxford, United Kingdom

Campylobacter jejuni, the most frequent cause of food-borne bacterial gastroenteritis, is a fastidious organism when grown in the laboratory. Oxygen is required for growth, despite the presence of the metabolic mechanism for anaerobic respiration. Amino acid auxotrophies are variably reported and energy metabolism can occur through several electron donor/acceptor combinations. Overall, the picture is one of a flexible, but vulnerable metabolism. To understand *Campylobacter* metabolism, we have constructed a fully curated, metabolic model for the reference organism M1 (our variant is M1cam) and validated it through laboratory experiments. Our results show that M1cam is auxotrophic for methionine, niacinamide, and pantothenate. There are complete biosynthesis pathways for all amino acids except methionine and it can produce energy, but not biomass, in the absence of oxygen. M1cam will grow in DMEM/F-12 defined media but not in the previously published *Campylobacter* specific defined media tested. Using the model, we identified potential auxotrophies and substrates that may improve growth. With this information, we designed simple defined media containing inorganic salts, the auxotrophic substrates, L-methionine, niacinamide, and pantothenate, pyruvate and additional amino acids L-cysteine, L-serine, and L-glutamine for growth enhancement. Our defined media supports a 1.75-fold higher growth rate than Brucella broth after 48 h at 37°C and sustains the growth of other *Campylobacter jejuni* strains. This media can be used to design reproducible assays that can help in better understanding the adaptation, stress resistance, and the virulence mechanisms of this pathogen. We have shown that with a well-curated metabolic model it is possible to design a media to grow this fastidious organism. This has implications for the investigation of new *Campylobacter* species defined through metagenomics, such as *C. infans*.

Keywords: *Campylobacter jejuni*, genome-scale metabolic model, linear programming, defined growth media, metabolism, auxotrophy, metabolic network

OPEN ACCESS

Edited by:
Nicolae Corcionivoschi, Agri-Food and Biosciences Institute (AFBI), United Kingdom

Reviewed by:
Monique Zagorec, INRA Centre Angers-Nantes Pays de la Loire, France
Odile Tresse, INRA Centre Angers-Nantes Pays de la Loire, France

***Correspondence:**
John Wain
john.wain@quadram.ac.uk

Specialty section:
This article was submitted to Food Microbiology, a section of the journal Frontiers in Microbiology

Received: *31 January 2020*
Accepted: *29 April 2020*
Published: *19 June 2020*

Citation:
Tejera N, Crossman L, Pearson B, Stoakes E, Nasher F, Djeghout B, Poolman M, Wain J and Singh D (2020) Genome-Scale Metabolic Model Driven Design of a Defined Medium for Campylobacter jejuni M1cam. Front. Microbiol. 11:1072. doi: 10.3389/fmicb.2020.01072

1. INTRODUCTION

1.1. Background

Campylobacter, the leading cause of acute bacterial gastroenteritis, is Gram-negative, microaerophilic, spiral-shaped, highly motile bacteria (Debruyne et al., 2008; Lastovica et al., 2014). The epidemiology in low to middle income countries is poorly studied but appears to be different from that in high-income countries (Platts-Mills and Kosek, 2014). Acquisition in high

income countries is mainly through ingestion of contaminated poultry, milk, or water (Altekruse et al., 1998; Butzler, 2004; Ruiz-Palacios, 2007; Westrell et al., 2009). The genus *Campylobacter* can be divided into 28 species (Wilkinson et al., 2018) (and further into sub-species), that may vary in their temperature, oxygen, and nutrient requirements for growth. The most common species associated with campylobacteriosis is *Campylobacter jejuni*, with *Campylobacter coli* reported in 10–25% of cases. The disease is economically important, with an estimated cost to the UK economy at around £50 million (Tam and O'Brien, 2016). Under reporting of cases (Gibbons et al., 2014) and failure to consider sequelae (Mangen et al., 2016), however, makes this an underestimate. Disease symptoms in humans may vary, but in the UK, they include diarrhea, fever, and abdominal pain. The sequelae however include colitis, reactive arthritis, and Miller-Fisher and Guillain-Barré syndromes (Jacobs et al., 1996; Blaser and Engberg, 2008). Along with an increase in reported incidence, and improving diagnosis, resistance to antibiotics is becoming a concern (Châtre et al., 2010; Deckert et al., 2010; Gormley et al., 2010). The diagnosis of campylobacteriosis has depended, until recently, on culture-based methods, but these methods may not grow all *Campylobacter* spp. causing human infections (Buss et al., 2019; Bian et al., 2020). An understanding of how to grow these "non-culturable" *Campylobacter* spp. may change our understanding of campylobacterosis, particularly in low income countries where the burden is high and predominantly occurs in children (Platts-Mills and Kosek, 2014). The conditions used in diagnostic laboratories vary, but commonly include a gas mix of 5–10% O_2, 5–10% CO_2 and 80–85% N_2 (with some mixes also containing H_2), a temperature of 37°C or 42°C, with complex media containing blood, peptone, meat, or yeast extract (Hsieh et al., 2018). These media are not chemically defined, and may vary from batch to batch, making comparisons between strains and the growth conditions used for isolation difficult. The use of recently developed commercial PCR assays have improved diagnosis, but new variants would not be detected. As metagenomic methods are not yet freely available, a more permissive culture media is required for comprehensive burden studies and pathogen discovery.

1.1.1. Growth Culture

Until the introduction of selective agars (Skirrow, 1977; Lauwers et al., 1978), filtration techniques were used to isolate *Campylobacter* (Dekeyser et al., 1972; Butzler et al., 1973). An understanding of the microaerophilic nature of *Campylobacter* (Hoffman et al., 1979) improved the culture still further. The development of *Campylobacter* specific culture media (Corry et al., 1995; Davis and DiRita, 2008; Kim et al., 2016) now represents the state of the art, however, the availability of a permissive defined media for *Campylobacter* spp. remains elusive. Although defined media have been described (Dickgiesser and Czylwik, 1985; Tenover et al., 1985; Guccione et al., 2010; Alazzam et al., 2011), the use of complex, undefined media (Wright et al., 2009; Liu et al., 2012) persists, because of the need to culture a wide range of *Campylobacter* strains that demonstrate different auxotrophies (Dickgiesser and Czylwik, 1985; Tenover and Patton, 1987; Alazzam et al., 2011; Vorwerk et al., 2014). A method to investigate the ingredients required for a permissive media is clearly needed. One way to do this is to look at the metabolic requirements of campylobacter cells in terms of nutrient sources, biomass, and energy production.

1.1.2. Campylobacter Metabolism

Campylobacter spp. have considerable flexibility for energy production in terms of electron acceptors and donors that can be used in the electron transport chain (ETC); in addition to the ability to utilize O_2 as an electron acceptor, nitrate, nitrite, and fumarate have also been described as alternatives. *Campylobacter* spp. would therefore appear to have the potential to carry out anaerobic respiration (Sellars et al., 2002; Kelly, 2008), however, many strains do not grow in the absence of oxygen, even in the presence of alternative electron acceptors (Sellars et al., 2002). The reason for this oxygen dependency is not absolutely certain but is likely to be related to oxygen dependent DNA synthesis enzymes (Jordan and Reichard, 1998; Kelly, 2008). The ETC also has a high degree of flexibility in terms of electron donors, with pyruvate, H_2, formate, and succinate having been reported to fulfil this role (Sellars et al., 2002; Kelly, 2008). In contrast to the ETC, other areas of central metabolism are quite limited, when compared with that of most other gut bacteria. In particular, they lack transporters for many small carbohydrates, with two essential enzymes in the upper limb of the Embden–Meyerhof–Parnas pathway (glucokinase and phosphofructokinase) being absent. Most strains lack the Entner-Doudoroff pathway, and the oxidative steps of the oxidative pentose phosphate pathway are also absent (although the non-oxidative branch is present Velayudhan and Kelly, 2002; Line et al., 2010). The absence of carbohydrate utilization pathways suggests that amino acids and tricarboxylic acid (TCA) cycle intermediates act as the primary nutrient sources for *C. jejuni* (Westfall et al., 1986; Velayudhan et al., 2004; Del Rocio Leon-Kempis et al., 2006; Stahl et al., 2012; Hofreuter, 2014), but detailed knowledge as to how such substrates may be utilized, remains limited. Furthermore, the ability of this organism to survive right through the food chain, suggests it can utilize a variety of metabolic strategies. Our understanding of *Campylobacter* physiology, thus, remains limited, with most descriptions of *Campylobacter* physiology being based on a single isolate of *C. jejuni* NCTC11168 (Carrillo et al., 2004; Alazzam et al., 2011; Metris et al., 2011; Xu et al., 2015; van der Hooft et al., 2018).

1.2. Metabolic Modeling

Genome-scale metabolic models (GSMs) describe the metabolic interactions of an organism with its environment, based on a reaction network ultimately inferred from enzymes encoded by the genome. Their analyses enable an investigation of metabolic behavior of the whole system, rather than individual reactions and pathways, and can be used to identify mechanistic links between cellular genotype and metabolic phenotype.

Genome-scale metabolic models overview

Over the last two decades, GSMs have become a valuable tool to analyze cellular behavior under different biological conditions, to design drug targets, to investigate metabolic interactions in microbial communities, and to design defined growth media (reviewed in Liu et al., 2010; Zhang and Hua, 2016; Kim et al., 2017; Gu et al., 2019). GSMs can now be used to inform experimental design and to provide a rationale for experimental observations (Zampieri and Sauer, 2016; Villanova et al., 2017; van der Ark et al., 2018).

Construction of GSMs starts with the identification of enzymes and transport proteins from an annotated genome. Reactions catalyzed by enzymes thus identified, are further characterized by their stoichiometry and assumed (ir)reversibility. Such information can usually be obtained from a number of on-line databases including databases such as BioCyc (Caspi et al., 2015; Karp et al., 2017), MetaCyc (Caspi et al., 2013, 2017), KEGG (Ogata et al., 1999; Kanehisa and Goto, 2000; Kanehisa et al., 2006), BIGG (Schellenberger et al., 2009), SEED (DeJongh et al., 2007), and BRENDA (Barthelmes et al., 2007).

In addition to defining the properties of internal reactions, it is, for all practical purposes, necessary to identify the properties of transport processes, representing the consumption and production of compounds in the assumed environment. Compounds present in the environment are referred to as *external* (or sometimes *boundary*) metabolites, otherwise they are referred to as *internal* metabolites. Reactions that only involve internal metabolites are therefore internal reactions, while those which involve internal and external metabolites are transport reactions. Although gene annotation with regard to enzymes is usually well-defined, annotation of transporters tends to be less comprehensive. Experimental investigations involving growth on defined media thus proves a useful independent method to infer the presence of transport processes, as well as providing useful data for subsequent analyses of the model.

Despite the fundamental importance of online databases, any reconstruction based solely upon these is likely to exhibit a number of problems, the most common of which are: missing gene-protein-reaction (GPR) associations, inconsistent naming of metabolites, and reaction identifiers, incorrect reaction stoichiometries, and reversibility, which propagates to the draft model. Thus, in order to represent a realistic representation of a given organism, an initial draft model will require refinement and curation by the user. The curation process usually begins with correcting reaction stoichiometries and reversibility to ensure that the model follows the law of mass and energy conservation, followed by checking consistency of identifiers, and identifying missing reactions by "gap-filling." Such gap-filling may often lead to an updated gene annotation. One area of metabolism that requires special attention is the electron transport chain, to ensure that translocated protons are correctly assigned to their location in the cell or the environment.

Usually, large-scale metabolic models such as GSMs, are analyzed using constraint based linear programming (LP) approaches (Fell and Small, 1986; Varma and Palsson, 1993, 1994), an optimization technique that assigns fluxes to reactions, assuming that the system is at steady state, according to some objective function, and subject to one or more defined constraints. Typical objective functions are either maximization of growth rate, or minimization of total flux in the system, and constraints are used to apply upper or lower limits on reactions, and commonly to specify the export of one or more product as defined.

1.2.1. Aims of the Current Study

The aim of this study is to explore *Campylobacter* spp. nutrient requirements through the analysis of a newly created genome scale model of *C. jejuni* (M1Cam) with experimental validation. In doing so we define new, chemically defined, media compositions that will serve as a basis for further modeling and experimental studies of this organism.

2. MATERIALS AND METHODS

2.1. Model Construction

The model was developed in an iterative manner, as illustrated in **Figure 1**, from the available gene sequence of *C. jejuni* M1cam (https://www.ncbi.nlm.nih.gov/nuccore/CP012149). Genes were predicted and annotated, and used to construct a strain specific Pathway/Genome database (PGDB) for *C. jejuni* M1cam. This was used as the basis for the model which was structured in a modular fashion as described by Poolman et al. (2009), Poolman et al. (2013), Hartman et al. (2014), and Ahmad et al. (2017). It consists of:

1. A "top-level" module defining some basic properties and importing the other modules as described;
2. A "PGDB reactions" module with a set of reactions directly imported from the strain-specific PGDB which was subjected to revision as described in 2.1.3.
3. "Media transporter" module describing the import and export of substrates to/from the medium.
4. "Biomass transporter" module describing the export of biomass precursors and metabolites produced as side products of biomass synthesis for which there are no known degradation pathways, also called "sink transporters."
5. The ETC module describing stoichiometries of all ETC reactions.
6. Additional reactions required for the generation of biomass precursors, not reported in the PGDB.

2.1.1. Draft Reconstruction

Gene prediction and annotation was carried out using Prodigal (Hyatt et al., 2010) version 2.6.31 and Prokka (Seemann, 2014) version 1.142 respectively, with default cutoff scores.

The "Pathologic component" of Pathway Tools (Karp et al., 2002, 2015) version 23.0 and MetaCyc (Caspi et al., 2017) version 23.0 was used to generate the strain-specific Pathway/Genome databases (PGDB), from the annotated genome sequence. The pathway hole filler component (Green and Karp, 2004) of Pathway Tools was used to automatically fill pathway holes in PGDB. Pathways were inferred using the pathway prediction algorithm (Karp et al., 2011) with a default cutoff score of 0.15. Missing genes and GPR associations (see sections 3.1.1), were curated manually with reference to BLAST (Camacho et al., 2009) and the online databases KEGG (Ogata et al., 1999), Gene Ontology terms (Ashburner et al., 2000), BRENDA (Jeske et al., 2018), Pfam (El-Gebali et al., 2018), RHEA (Morgat et al., 2019), and String v11 accessed 2019 (Szklarczyk et al., 2018).

All the reactions from PGDB were extracted, using the ScrumPy (Poolman, 2006), metabolic modeling package, version 1254, to populate the "PGDB reactions" module described above, and to generate the initial draft model.

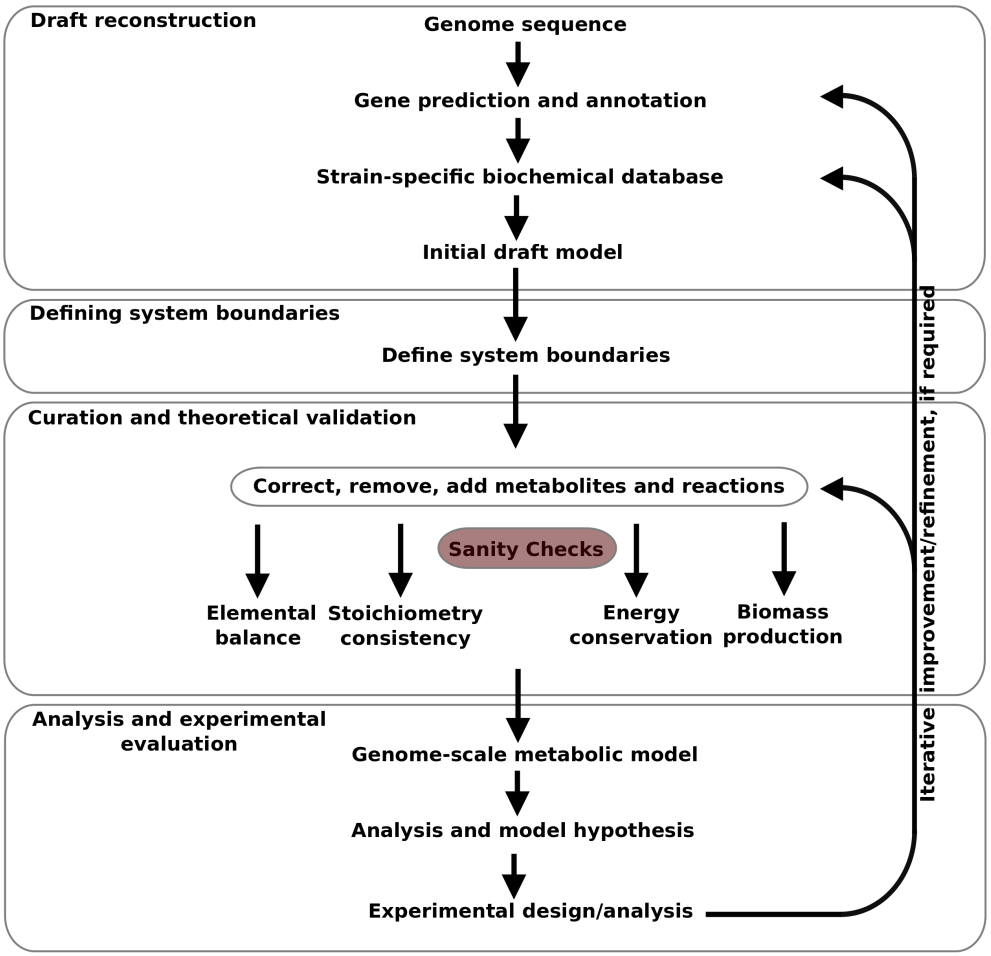

FIGURE 1 | Pipeline for genome-scale metabolic model construction used in this study.

2.1.2. Defining System Boundaries

Media transporters were assigned for import of 33 organic substrates, out of 38 organic substrates in the DMEM/F-12 medium (**Table S1**). Transporters for the remaining five organic substrates, choline chloride, folic acid, lipoic acid, thymidine, and vitamin B12 (cobalamine) were not included because metabolic routes were not present for these metabolites in the PGDB. Transporters were assigned for exchange of the gases O_2, CO_2, H_2, NH_4 and H_2S between the environment and the system and for the export of metabolic by-products, such as acetate, lactate, and succinate.

Biomass transporters were defined for the export of biomass components as individual components (amino acids, lipopolysacharides, peptidoglycan, nucleotides, vitamins, etc.), as described by Thiele et al. (2005) and Metris et al. (2011). Note that in contrast to these authors who represented biomass as a single lumped reaction, we assigned biomass transporters to individual biomass components, and subsequently set their relative fluxes to represent the observed biomass composition. There are five sink transporters added to the model for export of by-products from biomass synthesis [eg. adenosyl-4-methylthio-2-oxobutanoate produced during biotin synthesis (Metris et al., 2011)].

2.1.3. Curation and Theoretical Validation

The atomic balance of individual reactions were determined and all the reactions in the model were balanced with respect to carbon (C), nitrogen (N), phosphorus (P), and sulfur (S), iron (Fe), sodium (Na), oxygen (O), proton (H), and charge. Metabolites with unknown atomic compositions or generic compounds and reactions involved with such metabolites were replaced, where possible, by balanced reactions with known atomic composition of metabolites. For example, reactions involved with generic compounds (e.g., Alcohols) were replaced with specific metabolites and the stoichiometric coefficient balanced on both sides of the reaction. Reactions involved with non-metabolic species (e.g., tRNA, RNA) were excluded from the model. Similarly, reactions were corrected for reversibility so that the model is not able to generate energy (in the form of ATP and NAD(P)H) in absence of a mass flux through the system. Thus, the model is ensured to follow the laws of mass and energy

conservation, and is free from stoichiometric inconsistencies (Gevorgyan et al., 2008).

2.2. Model Analysis

2.2.1. Linear Programming Formulation

Except where noted otherwise, model analysis was undertaken using appropriate variants of the linear program defined as:

$$\text{minimise}: \sum |\mathbf{v}|$$

$$\text{subject to:} \begin{cases} \mathbf{N} \cdot \mathbf{v} = \mathbf{0} \\ v_{i..j} = b_{i..j} \\ v_{k..l} \geq 0 \text{ (see below)} \\ v_{ATPase} = A \\ v_{Otx} \leq Otx_{max} \end{cases} \quad (1)$$

Where $\mathbf{v}$ is the vector of all reaction fluxes and $\mathbf{N}$ is the stoichiometry matrix; the objective is to minimize the sum of all (absolute) flux values (including transporters), subject to the constraints: $\mathbf{Nv} = \mathbf{0}$ (steady-state assumption), $v_{i..j} = b_{i..j}$ defines flux in biomass transporters, as described in section 2.1.2, $v_{k..l}$ defines fluxes in the reactions importing media components, as described in section 2.1.2, $v_{ATPase} = A$ defines flux in a hypothetical ATPase reaction in order to account for a growth and non-growth associated maintenance cost and $v_{Otx} \leq Otx_{max}$ defines a maximum microaerophilic O_2 consumption rate. A was assigned a value of 16 mmol/g DW/hr (Varma and Palsson, 1994), and Otx_{max} (= 5 mmol/g DW/hr) (Metris et al., 2011).

2.2.2. Identification of Substrate Auxotrophies

Substrate auxotrophies were determined, using the model, by repeatedly attempting to solve Equation (1) with individual media transporters ($v_{k..l}$) set to zero, one at a time. Failure to obtain a solution was taken as demonstrating auxotrophy with respect to the component whose transporter was thus constrained.

2.3. Model Curation and Refinement From Experimental Observation

Although *Campylobacter* spp. was successfully cultured in the DMEM/F-12 medium (section 2.4), the initial model could not account for the production of all biomass components from these nutrients. These components were identified by modifying Equation (1) to account for the production of a single biomass component, sequentially. Additional reactions were then identified by their presence in other *Campylobacter* spp. specific biochemical databases in Biocyc and KEGG, literature surveys, and with reference to BLAST (Camacho et al., 2009). Once identified, these reactions were used to populate the "Additional Reactions" module described above.

Initial model analysis suggested that biotin and asparagine were essential nutrients, although this was found not to be the case in the experimental investigation. This discrepancy was due to gaps in the biosynthesis pathways of biotin and asparagine. Gap-filling reactions were identified, based on a literature study on biotin synthesis (Stok and Voss, 2000; Manandhar and Cronan, 2017) and BlastP analysis, and were added to the "Additional Reactions" module as above.

Conversely, initial model analysis suggested that niacinamide was not an essential nutrient, although subsequent experimental investigation showed that this was not the case. In order to identify spurious reactions in the model responsible for this heterotrophy, Equation (1) was modified to represent *production* of niacinamide, utilizing the other media components. Reactions in the resulting solution for which no GPR could be identified were removed, thus bringing model behavior into alignment with our experimentally observed behavior.

2.4. Experimental Conditions

2.4.1. Materials

Brucella broth was purchased from Sigma-Aldrich (Sigma-Aldrich, Poole, UK) and Brucella agar from BD (Becton, Dickinson U.K. Limited). Gibco Dulbecco's Modified Eagle Medium/Nutrient Mixture F-12 (DMEM/F-12) media with no added phenol red, was purchased from Thermo Fisher Scientific (Thermo Fisher Scientific, Darmstadt, Germany). All chemicals were of commercial analytical grade and obtained from Sigma-Aldrich. All solutions, except amino acids and vitamins, were made every week, sterile filtered (0.22 μM, Fisher-Scientific, UK), and kept at −4°C until needed. Amino acids and vitamins were prepared immediately before use.

2.4.2. Bacterial Strains Used

C. jejuni M1 has a published genome sequence (Friis et al., 2010) and is a well-studied laboratory model organism from a well-documented case of direct transmission between poultry and humans. The M1 used in this study was obtained from the Department of Veterinary Medicine, Cambridge University, and annotated as M1cam (de Vries et al., 2015), an "M1" strain which differs from the M1 reference strain (published by Friis et al., 2010) by 50 SNPs (insertions/deletions and true SNPs) (de Vries et al., 2015).

The other 7 strains, selected from different clades, according to Champion et al. (2005) and Stabler et al. (2013), were tested for their ability to grow in the final defined medium. These were: 81116 (NCTC11828), Calf 3, 11168H, 81-176, 12912, RM1221, and M1, obtained from the London School of Hygiene and Tropical Medicine. Strains were stored at −80°C using Protect - Multipurpose Microorganism Preservation System vials (Technical Service Consultants Ltd, Lancashire, UK) or Microbank^{TM} cryotubes (Pro-Lab Diagnostics, Merseyside, UK).

2.4.3. Culture Conditions

All strains were grown under microaerophilic conditions (10% O_2 [v/v], 5% CO_2 [v/v], 85% N_2 [v/v]), using an anaerobic cabinet and gas supply (BOC Ltd, Surrey, UK), on Brucella broth agar plates, for 48 h at 37°C, except those tested in the Department of Veterinary Medicine, Cambridge University, which were grown at 42°C using a gas mix of hydrogen (5% O_2 [v/v], 5% H_2 [v/v], 5% CO_2 [v/v], 85% N_2 [v/v]), also using an anaerobic cabinet and gas supply (BOC Ltd, Surrey, UK).

All *C. jejuni* strains were harvested from agar plates and inoculated with a starting optical density (OD) OD600 of

approximately 0.004 in Brucella broth, incubated with shaking (180 rpm) using the same temperature and gas supply indicated previously, to an OD600nm of 0.6 (approximately 2.8×10^9 CFU/ml). Cultures with OD600 different to 0.6 were standardized to that value using sterile PBS. After 20 h, 1.7 mL of this culture was collected, washed twice and resuspended in 1.7 mL of sterile PBS. Each one of the media tested in our study was inoculated in triplicate at 1% (100 μL in 10 mL of media), using *C. jejuni* washed cells. Cultures were then incubated microaerobically for 48 h with shaking (180 rpm), under the same temperature and gas conditions stated above, and growth was assessed daily, measuring OD600 in triplicate of each of the technical replicates, using a plate reader (FLUOstar® Omega, BMG Labtech Ltd, Aylesbury, UK). For this purpose, cultures were sampled in a class II cabinet and returned immediately to the anaerobic cabinet. All experiments performed in this study were repeated three times, each time using a new starting culture, prepared from glycerol stock, and with freshly made simple defined media.

2.4.4. Checks for Contamination

To confirm the identity of the experimental organisms, typical cellular morphology was checked using x1000 bright field microscopy of carbol fuchsin stained cultures and whole genome sequencing (WGS) was performed on selected isolates. *C. jejuni* M1cam genomic DNA for WGS was extracted using Maxwell® RSC Cultured Cells DNA Kit. DNA extracts were converted into a Nextera library for sequencing on an Illumina NextSeq 500 platform and genomes were assembled using Velvet *de-novo* genomic assembler and then subjected to multi-locus sequence typing (MLST).

2.4.5. Media Design and Confirmation of Auxotrophies

A modification of DMEM/F-12, not including glucose, was used as the starting point to develop our defined media for *C. jejuni* M1cam (**Table S1**). The inorganic substrates in our media were kept in the same concentrations present in the original DMEM/F-12 media formulation. To achieve a simple defined media, non-essential substrates identified by the model analysis, were gradually removed from the media, and growth, measured as OD, was compared to that of growth in Brucella broth (0.58 ± 0.06 at 24 h) and synthetic DMEM/F-12 media (0.38 ± 0.01 at 24 h). Removal of substrates in media design were compensated for the net amount of N and S, by increasing the concentration of remaining substrates proportionally to ensure that the total N and S was equal or higher than the original formulation.

Substrate auxotrophy was confirmed when removal of substrate could not support growth of M1cam. Growth was monitored over longer incubation times (up to 144 h) to confirm auxotrophy of the compounds tested. If no growth was obtained, experiments were repeated, to confirm results.

2.4.6. Media Testing

The media to be tested was made fresh on the day of the inoculation. After addition of all components and before adjusting the final volume to 100 mL using purified water, the pH of each of the minimal media tested in this study was measured using a pH meter [LAQUAtwin pH Meter PH-22 (HORIBA Advanced Techno Co., Ltd., Kyoto, Japan)] and adjusted to pH 7 using 1M NaOH or 1M HCl solutions. To maintain sterility, work was carried out in a class II microbiological safety cabinet, and 10 mL of media was filtered into each of the four 50 mL sterile cell culture flasks (Sigma-Aldrich, Poole, UK), closed with their filter caps and kept at 37°C until inoculation. Maintaining media at 37°C until inoculation proved to be very important to obtain reproducible results. Finally, in order to compare our results with previously published defined media, we also tested growth of *C. jejuni* M1cam in the defined media given by Guccione et al. (2010) and Alazzam et al. (2011).

3. RESULTS

3.1. Model Building and Analysis

3.1.1. Pathway/Genome Databases

The automatically generated *C. jejuni* M1cam PGDB comprised of 228 pathways with a total 1,366 reactions, including 22 transport reactions, and 1,009 compounds. There were 291 reactions without any assigned gene and were inferred from pathway prediction algorithm. This also included reactions that were essential for biomass productions in the model. There were also genes that encoded metabolic enzymes but were not associated with reactions. The reason for the missing GPR association was mainly: (i) information necessary to attribute a particular reaction to specific gene was missing in the annotated file (ii) though the gene product had been annotated it was not detected by the Pathologic software. Reactions, particularly those inferred as essential for biomass production, without any gene association were revisited to establish GPR relation (see 2.1.1) where possible. **Table S2** lists GPR relationships that have been curated in the PGDB. Curated PGDB, after being re-inferred using pathway prediction algorithm, comprises a total 262 pathways, 1,581 reactions, and 1,104 compounds (summarized in **Table 1** along with other prokaryotic PGDBs) and is available from Pathway Tools Registry and https://data.quadram.ac.uk/dipali.singh/CJM1cam_DB/.

TABLE 1 | Main content of *C. jejuni* M1cam Pathway/Genome database along with other prokaryotic databases.

Content/ Strains	*C. jejuni* M1cam	*C. jejuni* M1	*H. pylori* 26695	*P. aeruginosa* PAO1	*Escherichia coli* K-12 (MG1655)
PGDB curation level	Tier 2	Tier 3	Tier 2	Tier 3	Tier 1
Total genes	1,679	1,675	1,610	5,677	4,501
Total pathways	262	228	152	405	433
Total reactions	1,581	1,005	970	1,833	2,852
Total compounds	1,104	746	708	1,285	2,965

3.1.2. Model Properties

The curated model consists of 994 reactions. The number is less than that of the initial draft model generated from the PGDB due to removal of reactions involved with non-metabolic species and those of unknown atomic composition, as described in 2.1.3. 76% of reactions in the model have gene associations, 6% are spontaneous, while the remainder are inferred by the gap filling algorithm or added after careful curation. The model includes 115 transporters, 968 internal metabolites and 93 external metabolites, summarized in **Table 2**.

3.1.3. Model Analysis—Biomass Production

The solution to Equation (1), with DMEM/F-12 media, has a total of 326 reactions, including transporters. There are 165 essential for biomass production: removal of any one of these results in Equation (1) having no feasible solution. The solution has no net import flux of amino acids, leucine, arginine, histidine, valine, asparagine, phenylalanine, alanine, threonine, tyrosine, tryptophan, and lysine (i.e., flux in these amino acid media transporters were equal to flux in their respective biomass transporters). There was, however, notable net import of pyruvate, as a carbon source, and the amino acids, aspartate, serine, glutamine, and proline; Acetate, succinate, NH_4 and CO_2 were among the excreted by-products. The model is able to account for ATP generation under anaerobic conditions through oxidative phosphorylation, using nitrate or fumarate electron acceptors. However, it is not able to generate biomass in the absence of O_2.

3.1.4. Model Analysis—Identification of Substrate Auxotrophy

Out of the 33 organic substrates tested in the model, 30 substrates were identified as non-essential. The remaining three substrates, *methionine*, *pantothenate* and *niacinamide* (after the curation based on experimental observation in 2.3) were identified as auxotrophic. The pathways for the *de-novo* biosynthesis of these metabolites were absent in the PGDB and thus the model. These included homoserine O-succinyltransferase and methionine synthase from the methionine biosynthesis pathway, 3-methyl-2-oxobutanoate hydroxymethyltrasferase, pantothenate synthetase, and 2-oxopantoate reductase from the pantothenate biosynthesis pathway, and nicotinate-nucleotide diphosphorylase and quinolinate synthetase from the niacinamide biosynthesis pathway.

3.1.5. Model Analysis—Specification of Minimal Nutrient Requirements

The model analysis suggests that growth can be supported with a medium containing only pyruvate, methionine, pantothenate, and niacinamide (in addition to inorganic salts). Furthermore, the fact that aspartate, serine, glutamine, and proline were imported in excess, relative to that required by the biomass composition, suggests that the presence of these compounds in the media would enhance growth.

3.2. Experimental Analysis

3.2.1. Media Design and Confirmation of Auxotrophies

A simplified defined media containing pyruvate, four amino acids (methionine, cysteine, serine and glutamine or glutamate), pantothenate, and niacinamide (along with inorganic salts) supported growth of *C. jejuni* M1cam. The removal of *methionine*, *pantothenate* and *niacinamide* from the DMEM/F-12 media (**Table S1**) resulted in no growth of M1cam, thus, confirming auxotrophies predicted by the model analysis.

As part of the media development, the concentration of sodium pyruvate, as a carbon source, was increased from 0.5 to 10 mM. In addition, the concentrations of auxotrophic substrates, niacinamide and pantothenate, were optimized to 33.1 and 9.4 μM, respectively (**Table 3**). The inorganic substrates were kept identical to those in DMEM/F-12 media. Amino acids cysteine, serine and glutamine or glutamate, although not essential for

TABLE 2 | Summary of genome-scale metabolic model of *C. jejuni* M1cam.

Total no. of reactions		994
Total no. of transporters		115
Total no. of metabolites		1,061
Reactions	Spontaneous reactions	56
	With gene association	761
	Without gene association	170
	Added reactions	7
Transporters	media	41
	Exchange and by-products	18
	Biomass	51
	Sink	5
Metabolites	Internal metabolites	968
	External metabolites	93

TABLE 3 | Defined media composition designed in this study.

Substrates	DMEM/F-12*	MM1	MM2	MM3	MM4
Auxotropic					
Methionine	115.7 μM	4 mM	4mM	8 mM	6.8 mM
Pantothenate	4.7 μM	9.4 μM	9.4 μM	9.4μM	9.4 μM
Niacinamide	16.6 μM	33.1 μM	33.1 μM	33.1 μM	33.1 μM
Carbon source					
Pyruvate	0.5 mM	10 mM	10 mM	10 mM	10 mM
Growth-improving					
Cysteine·HCl	100 μM	4 mM	4 mM	–	4 mM
Serine	250 μM	10 mM	10 mM	10 mM	–
Glutamine	2.5 mM	10 mM	–	10 mM	13.6
Glutamate	50 μM	–	20 mM	–	–
Inorganic salts	same as DMEM/F-12 (**Table S1**)				
Growth (OD 600)					
24 h	0.38 ± 0.01	0.31 ± 0.05	0.14 ± 0.03	0.02 ± 0.01	0.15 ± 0.01
48 h	0.34 ± 0.04	1.05 ± 0.06	1.07 ± 0.09	0.41 ± 0.04	0.57 ± 0.01

OD results expressed as mean ± stdev (n = 3).
**Table S1 for all the components of DMEM/F-12.*

growth, had a significant growth promoting effect i.e., removal of any of these substrates from the media decreased the growth compared to DMEM/F-12 media. In contrast, removal of any other amino acids or vitamins did not have any significant effect on growth as compared to DMEM/F-12 media.

Thus, four simple defined media compositions were defined, where all four included the auxotrophic substrates, methionine, pantothenate, and niacinamide along with pyruvate as a carbon source, and with different combinations of non-essential but growth-improving organic substrates, presented in **Table 3**.

The best results, in terms of growth, were obtained when cysteine, serine, and glutamine or glutamate where present (MM1 and MM2 in **Table 3**). Individual removal of cysteine and serine from the media decreased growth to 0.41 ± 0.04 and 0.57 ± 0.01 at 48 h, respectively (MM3 and MM4 in **Table 3**). Glutamate and glutamine were exchangeable, having similar effects on growth (MM1 and MM2 in **Table 3**). However, removal of both substrates at the same time resulted in around 4.5 times lower OD (0.24±0.03 at 48 h, data not shown) when compared to MM1 and MM2. Providing only the essential auxotrophic substrates, i.e., methionine, pantothenate, and niacinamide, together with pyruvate as a carbon source and inorganic compounds, did not support growth (0.05 ± 0.02, data not shown). This confirmed the impact of each of the growth promoting amino acids in culturing *C. jejuni* M1cam. Although each of MM1 and MM2 had a similar effect on growth of *C. jejuni* M1cam, MM1 was selected as final defined media, as it had a higher starting pH and required less NaOH to reach pH 7.

Therefore, this media was tested for growth of 7 additional *C. jejuni* strains, with the experiments being performed in two different laboratories, the Department of Veterinary Medicine, Cambridge University and the London School of Hygiene and Tropical Medicine. All isolates tested in this study grew in the designed defined media MM1 by 48 h, using the conditions of growth as defined by each laboratory, resulting in a range of OD600 from 0.23 to 1.05 (**Table 4**). By 48 h, all strains had reached a plateau and the replicates were stable. The variation in growth was probably caused by different growth conditions and the genetics of the strains.

TABLE 4 | Growth of different *C. jejuni* strains in the defined media MM1, designed in this study.

Labs and Culture conditions	Strains	Standardized Inoculum (cfu/ml)	OD600 24 h	OD600 48 h
QIB[a]				
Temperature: 37°C	M1cam (ST 137)	1.73e+09	0.31 ± 0.05	1.05 ± 0.06
Gas mix: 10% O_2, 5% CO_2, 85% N_2	81116 (ST 283)	1.57e+09	0.17 ± 0.10	0.86 ± 0.11
Cambridge[b]				
Temperature: 42°C	M1cam (ST 137)	7.63e+07	0.09 ± 0.04	0.75 ± 0.04
Gas mix: 5% O_2, 5% CO_2, 5% H_2,85% N_2	calf 3 (ST 514)	4.28e+07	1.01 ± 0.05	1.11 ± 0.10
London[c]				
	11168H (ST 43)	1.07e+09	0.18 ± 0.12	0.23 ± 0.09
Temperature: 37°	81–176 (ST 604)	2.05e+09	0.13 ± 0.02	0.65 ± 0.10
Gas mix: 10% O_2, 5% CO_2, 85% N_2	12912 (HS 50)	8.47e+07	0.34 ± 0.02	0.84 ± 0.12
	M1 (ST 137)	6.67e+08	0.07 ± 0.01	0.53 ± 0.12
	RM1221 (ST 354)	1.24e+08	0.36 ± 0.04	0.50 ± 0.07

Standardized inoculum (OD = 0.6) colonies formation units/mL (cfu/mL) is expressed as average of replicates (n = 9). OD results expressed as mean ± stdev (n = 9). ST: sequence type. [a]Quadram Institute Biosciences, UK. [b]Department of Veterinary Medicine, University of Cambridge, UK. [c]London School of Hygiene and Tropical Medicine, University of London, UK.

3.2.2. Testing Previously Published *Campylobacter* Specific Growth Media

We tested growth of M1cam on the previously published defined media by Guccione et al. (2010) and Alazzam et al. (2011) (MCLMAN media). Both formulations did not support growth of M1cam. MCLMAN media could support growth only after the addition of pantothenate, which was confirmed as an auxotrophic substrate for M1cam in our study. The OD at 600 nm of this culture (0.33 ± 0.03, data not shown) after 48 h of incubation, however, was still lower than the growth observed in our defined media (1.05 ± 0.06).

4. DISCUSSION AND CONCLUSION

In this study, we have constructed, a well-curated, strain-specific GSM of *C. jejuni* M1cam. We have examined the GSM to investigate the *de-novo* biosynthesis ability and substrate auxotrophy of the strain. We have experimentally validated the model results and curated the GSM for missing GPR associations or over-predicted reactions. A metabolic model guided the design of a simple defined media for the growth of *C. jejuni*. Additionally, we have shown that 8 diverse strains of *C. jejuni* are able to grow in the defined simple media.

4.1. Model Analysis

Our analysis showed that when all amino acids are available, leucine, arginine, histidine, valine, asparagine, phenylalanine, alanine, threonine, tyrosine, tryptophan, and lysine were imported at a rate equal to their demand for protein synthesis. However, the network described by the model has the ability for the *de novo* synthesis of these amino acids, as a solution to Equation 1 could still be found when their respective uptake transporters were blocked.

In contrast, aspartate, proline, serine, and glutamine were all taken up at a rate above that required for protein synthesis. It is worth noting that, without any constraint on media uptake, the model prefers uptake of aspartate, proline, serine, and glutamine, which are preferred by *C. jejuni* and are the most common amino acids found in chicken excreta (Parsons, 1984). In addition,

the metabolic profile of *C. jejuni* liquid cultures' supernatant has shown significant depletion of these four amino acids from nutrient rich medium, reviewed in Hofreuter (2014).

Among all amino acids, serine has been most widely reported to be preferred by *C. jejuni* (Guccione et al., 2008; Wright et al., 2009; Gao et al., 2017). Glutamine utilization in *C. jejuni* is known to vary between strains: *C. jejuni* NCTC11168 has been reported not to utilize it (Hofreuter et al., 2008), while strains such as 81116 and 81-176 readily do (Hofreuter et al., 2006). Aspartate has been shown to be growth promoting under oxygen limitation (Guccione et al., 2008). Proline utilization has also been described at the stationary phase of *C. jejuni* growth, after the preferred nutrients become exhausted (Wright et al., 2009). These reports suggest that amino acid utilization varies between different strains of *C. jejuni*. It would therefore be necessary to build a model which represented that variation.

Whilst specific amino acids uptake from media remains to be tested experimentally for M1cam, similar experimental observations have been reported by Gao et al. (2017) where *C. jejuni* exhibits uptake capacity for amino acids such as arginine, cysteine, histidine, lysine, phenylalanine, or threonine that are directly incorporated into synthesized proteins rather than being catalyzed for energy or conversion to other intermediates.

Model analysis also reveals that *C. jejuni* M1cam has the ability for anaerobic respiration, however, it requires O_2 for biomass. Although model observation is consistent with previous reports from Sellars et al. (2002), Kelly (2008), van der Stel et al. (2017), and van der Stel and Wösten (2019), this is a vast research topic in itself and details remain to be addressed experimentally.

4.2. Auxotrophic Substrates

The modeling and experimental results presented here, indicate that *C. jejuni* M1cam is auxotrophic for methionine, pantothenate, and niacinamide. In this study, we established that *C. jejuni* M1cam presents auxotrophy for methionine but not for cysteine. It can utilize methionine as a S source for cysteine biosynthesis as also reported in *Helicobacter pylorii*. The results presented here suggest that cysteine auxotrophy is strain dependent and not a conserved metabolic property in all *C. jejuni* strains as suggested by Vorwerk et al. (2014). On the contrary, we found that methionine auxotrophy is maintained in M1cam even under increased cysteine concentration. Cysteine, although not auxotrophic, is one of the growth improving components possibly because of its role in the *de novo* synthesis of proteins associated with FeS clusters, such as the serine dehydratase, pyruvate pyruvate:acceptor and oxoglutarate:acceptor oxidoreductases. Moreover, most *C. jejuni*, as a common feature of host associated epsilonproteobacteria, are unable to assimilate sulfate as the S source (Alazzam et al., 2011; Vorwerk et al., 2014) and to compensate for this limited anabolic capacity, it is reasonable to suggest that *Campylobacter* spp. retain auxotrophy (or prefer) S containing amino acids, methionine, and cysteine.

Auxotrophy for pantothenate, a precursor for CoA synthesis, is related to host specificity. The pantothenate biosynthesis gene (panB, panC, and panD) cluster lies in the hypervariable region (Pearson et al., 2003) and has been shown to be more frequently present in isolates from cattle compared to isolates from chickens (Sheppard et al., 2013). *C. jejuni* M1cam is the derivative of the human isolate *C. jejuni* M1 and is epidemiologically related to poultry strains (Friis et al., 2010; de Vries et al., 2015); thus, it retains pantothenate auxotrophy. There is notable differences in *C. jejuni* M1cam auxotrophy from that of the more commonly studied strain, *C. jejuni* NCTC 11168. The latter presents auxotrophy for methionine and cysteine; niacinamide, although being growth improving, is not essential and removal of pantothenate had no effect on growth in this strain (Alazzam et al., 2011). *C. jejuni* isolates 81176, on the other hand, present auxotrophy for cysteine but not methionine Vorwerk et al. (2014). Differences in substrate auxotrophy seems to be common among *Campylobacter* spp.. Tenover and Patton (1987), based on 439 *C. jejuni* isolates and 46 *C. coli* isolates, have reported *Cambylobacter* auxotrophy for cysteine, cystine, arginine, proline, and methionine. The Dickgiesser and Czylwik (1985) study, based on 52 *C. jejuni* strains, reported methionine, cysteine, cystine, panthothenate, thiamine, and NAD as important substrates for auxotyping of strains.

4.3. Media Design

We have designed simple defined media specifically for *C. jejuni* M1cam which can support growth of 7 other *C. jejuni* strains tested in this study. The fact that previously reported MCLMAN media was designed based on *C. jejuni* NCTC11168 (Alazzam et al., 2011), which presents a different auxotrophy than *C. jejuni* M1cam, and did not include panthothenate, explains why *C. jejuni* M1cam growth was not supported in this media.

Our media, apart from *C. jejuni* M1cam specific auxotrophic substrates (methionine, pantothenate, niacinamide) and pyruvate as the carbon source, contains amino acids cysteine, serine, and glutamate/glutamine. The latter amino acids, though not essential for growth, had a significant growth promoting effect on *C. jejuni* M1cam under our experimental condition. Similar, reports have been shown for strains 81176 and NCTC11168 where substrates, though not essential, had to be added to improve growth (Alazzam et al., 2011; Vorwerk et al., 2014), although preference of these growth improving substance seems to vary between strains and culture conditions. This varying amino acid preference suggests their potential metabolic roles beyond nitrogen and the carbon source (Bièche et al., 2012). Thus, a detailed study on amino acid utilization is needed to increase our knowledge in nutrient acquisition and metabolism of *Campylobacter*. Although pyruvate transporters have not been identified, pyruvate has been shown to be used as an exogenous carbon source when present in growth medium (Mendz et al., 1997; Velayudhan and Kelly, 2002; Stahl et al., 2012; Wagley et al., 2014) and have a protective role in the presence of oxidative stress (Bolton et al., 1984; Hodge and Krieg, 1994). In our study, increasing the pyruvate concentration improved growth rate in *C. jejuni* M1cam. It should be noted that the media designed in this study was optimized to maximize the growth of *C. jejuni* M1cam. Further tests will be needed to optimize the growth of other strains, however it is clear that the designed media

MM1 can support the growth of a variety of strains under different conditions.

4.4. Conclusion

By adopting a systems-biology approach and using a newly annotated genome of *C. jejuni* M1Cam, we have built and analyzed a strain specific genome-scale model of this organism. The analysis allowed us to identify specific auxotrophies, as well as compounds which are preferentially consumed, and this allowed us to develop a new media suitable for the study of M1Cam and other *Campylobacter* spp. strains. The model analysis also replicated the apparently paradoxical, but widely reported observation, that although *Campylobacter* spp. can operate the electron transport chain in the absence of oxygen, oxygen is nonetheless essential for growth. Experimentally confirming all aspects of our model results, in particular the generation of metabolic by-products in the media, was beyond the scope of the current contribution. However, we believe the experimental and modeling results we have presented here, when taken together, provide a solid foundation upon which to build further investigations of *C. jejuni* M1cam and related organisms.

DATA AVAILABILITY STATEMENT

The datasets generated for this study can be found in the https://data.quadram.ac.uk/dipali.singh/CJM1cam_MM/, https://data.quadram.ac.uk/dipali.singh/CJM1cam_DB/. Additionally, Pathway/Genome database generated in this study is available from Pathway Tool Registry.

AUTHOR CONTRIBUTIONS

NT and DS designed and supervised research plans with input from JW. DS constructed the biochemical database and genome-scale metabolic model. NT performed experiments for minimal media design with input from BP. LC performed gene predictions and annotations. ES and FN tested minimal media designed in this work in other strains. BD performed sequence analysis. MP and DS analyzed GSM and together with NT wrote the paper with revision from JW. All authors contributed to the article and approved the submitted version.

FUNDING

NT, LC, BP, ES, FN, MP, JW, and DS gratefully acknowledge the support of the Biotechnology and Biological Sciences Research Council (BBSRC); this research was funded by the BBSRC Institute Strategic Programme Microbes in the Food Chain BB/R012504/1 and its constituent project BBS/E/F/000PR10349 (Theme 2, Microbial Survival in the Food Chain). BD was funded by the Bill and Melinda Gates Foundation.

ACKNOWLEDGMENTS

Special thanks to Andrew Grant, from the Department of Veterinary Medicine, University of Cambridge, for donating the main strain used in this study, *C. jejuni* M1cam. We also deeply thank Ozan Gundogdu and Brendan Wren, from the London School of Hygiene and Tropical Medicine, for donating the other 7 strains to test final defined media in this study. From the Quadram Institute Biosciences Core Sequencing facility, we thank David Baker and Stephen Rudder, for the whole-genome sequence analysis of the genomic DNA of *C. jejuni* M1cam. And last, but not least, the authors would like to thank Zahra Omole for her technical assistance in the experiments performed in the London School of Hygiene and Tropical Medicine.

SUPPLEMENTARY MATERIAL

The Supplementary Material for this article can be found online at: https://www.frontiersin.org/articles/10.3389/fmicb.2020.01072/full#supplementary-material

Table S1 | Composition of modified DMEM/F-12 media used in this study.

Table S2 | List of Gene-Protein-Reaction relationships curated in the *C. jejuni* M1cam PGDB.

REFERENCES

Ahmad, A., Hartman, H., Krishnakumar, S., Fell, D., Poolman, M., and Srivastava, S. (2017). A genome scale model of *Geobacillus thermoglucosidasius* (C56-YS93) reveals its biotechnological potential on rice straw hydrolysate. *J. Biotechnol.* 251, 30–37. doi: 10.1016/j.jbiotec.2017.03.031

Alazzam, B., Bonnassie-Rouxin, S., Dufour, V., and Ermel, G. (2011). MCLMAN, a new minimal medium for *Campylobacter jejuni* NCTC 11168. *Res. Microbiol.* 162, 173–179. doi: 10.1016/j.resmic.2010.09.024

Altekruse, S. F., Swerdlow, D. L., and Stern, N. J. (1998). *Campylobacter Jejuni. Vet. Clin. N. Am. Food Anim. Pract.* 14, 31–40. doi: 10.1016/S0749-0720(15)30277-2

Ashburner, M., Ball, C., Blake, J., Botstein, D., Butler, H., Cherry, J., et al. (2000). Gene ontology: tool for the unification of biology. The gene ontology consortium. *Nat. Genet.* 25, 25–29. doi: 10.1038/75556

Barthelmes, J., Ebeling, C., Chang, A., Schomburg, I., and Schomburg, D. (2007). BRENDA, AMENDA and FRENDA: the enzyme information system in 2007. *Nucleic Acids Res.* 35(Suppl_1):D511–D514. doi: 10.1093/nar/gkl972

Bian, X., Garber, J. M., Cooper, K. K., Huynh, S., Jones, J., Mills, M. K., et al. (2020). Campylobacter abundance in breastfed infants and identification of a new species in the global enterics multicenter study. *mSphere* 5, e00735-19. doi: 10.1128/mSphere.00735-19

Bièche, C., de Lamballerie, M., Chevret, D., Federighi, M., and Tresse, O. (2012). Dynamic proteome changes in *Campylobacter jejuni* 81-176 after high pressure shock and subsequent recovery. *J. Proteomics* 75, 1144–1156. doi: 10.1016/j.jprot.2011.10.028

Blaser, M. J., and Engberg, J. (2008). "Clinical aspects of *Campylobacter jejuni* and *Campylobacter coli* infections," in *Campylobacter, 3rd Edn*, eds I. Nachamkin, C. Szymanski, and M. Blaser (Washington, DC: American Society of Microbiology), 99–121. doi: 10.1128/9781555815554.ch6

Bolton, F., Coates, D., and Hutchinson, D. (1984). The ability of Campylobacter media supplements to neutralize photochemically induced toxicity and hydrogen peroxide. *J. Appl. Bacteriol.* 56, 151–157. doi: 10.1111/j.1365-2672.1984.tb04707.x

Buss, J., Cresse, M., Doyle, S., Buchan, B., Craft, D., and Young, S. (2019). Campylobacter culture fails to correctly detect Campylobacter in 30% of positive patient stool specimens compared to non-cultural methods. *Eur. J. Clin. Microbiol. Infect. Dis* 38, 1087–1093. doi: 10.1007/s10096-019-03499-x

Butzler, J., Dekeyser, P., Detrain, M., and Dehaen, F. (1973). Related vibrio in stools. *J. Pediatr*. 82, 493–495. doi: 10.1016/S0022-3476(73)80131-3

Butzler, J.-P. (2004). Campylobacter, from obscurity to celebrity. *Clin. Microbiol. Infect*. 10, 868–876. doi: 10.1111/j.1469-0691.2004.00983.x

Camacho, C., Coulouris, G., Avagyan, V., Ma, N., Papadopoulos, J., Bealer, K., et al. (2009). Blast+: architecture and applications. *BMC Bioinform*. 10:421. doi: 10.1186/1471-2105-10-421

Carrillo, C. D., Taboada, E., Nash, J. H. E., Lanthier, P., Kelly, J., Lau, P. C., et al. (2004). Genome-wide expression analyses of *Campylobacter jejuni* NCTC11168 reveals coordinate regulation of motility and virulence by flhA. *J. Biol. Chem*. 279, 20327–20338. doi: 10.1074/jbc.M401134200

Caspi, R., Billington, R., Ferrer, L., Foerster, H., Fulcher, C. A., Keseler, I. M., et al. (2015). The MetaCyc database of metabolic pathways and enzymes and the BioCyc collection of pathway/genome databases. *Nucleic Acids Res*. 44, D471–D480. doi: 10.1093/nar/gkv1164

Caspi, R., Billington, R., Fulcher, C. A., Keseler, I. M., Kothari, A., Krummenacker, M., et al. (2017). The MetaCyc database of metabolic pathways and enzymes. *Nucleic Acids Res*. 46, D633–D639. doi: 10.1093/nar/gkx935

Caspi, R., Dreher, K., and Karp, P. (2013). The challenge of constructing, classifying, and representing metabolic pathways. *FEMS Microbiol. Lett*. 345. doi: 10.1111/1574-6968.12194

Châtre, P., Haenni, M., Meunier, D., Botrel, M.-A., Calavas, D., and Madec, J.-Y. (2010). Prevalence and antimicrobial resistance of *Campylobacter jejuni* and *Campylobacter coli* isolated from cattle between 2002 and 2006 in France. *J. Food Protect*. 73, 825–831. doi: 10.4315/0362-028X-73.5.825

Champion, O. L., Gaunt, M. W., Gundogdu, O., Elmi, A., Witney, A. A., Hinds, J., et al. (2005). Comparative phylogenomics of the food-borne pathogen *Campylobacter jejuni* reveals genetic markers predictive of infection source. *Proc. Natl. Acad. Sci. U.S.A*. 102, 16043–16048. doi: 10.1073/pnas.0503252102

Corry, J. E., Post, D., Colin, P., and Laisney, M. (1995). Culture media for the isolation of campylobacters. *Int. J. Food Microbiol*. 26, 43–76. doi: 10.1016/0168-1605(95)00044-K

Davis, L., and DiRita, V. (2008). Growth and laboratory maintenance of *Campylobacter jejuni*. *Curr. Protoc. Microbiol*. Chapter 8:Unit 8A.1.1-8A.1.7. doi: 10.1002/9780471729259.mc08a01s10

de Vries, S., Gupta, S., Baig, A., L'Heureux, J., Pont, E., Wolanska, D., et al. (2015). Motility defects in *Campylobacter jejuni* defined gene deletion mutants caused by second-site mutations. *Microbiology* 161, 2316–2327. doi: 10.1099/mic.0.000184

Debruyne, L., Gevers, D., and Vandamme, P. (2008). "Taxonomy of the family Campylobacteraceae," in *Campylobacter, 3rd Edn*, eds I. Nachamkin, C. Szymanski, and M. Blaser (Washington, DC: American Society of Microbiology), 3–25. doi: 10.1128/9781555815554.ch1

Deckert, A., Valdivieso Garcia, A., Reid Smith, R., Tamblyn, S., Seliske, P., Irwin, R., et al. (2010). Prevalence and antimicrobial resistance in *Campylobacter* spp. isolated from retail chicken in two health units in Ontario. *J. Food Protect*. 73, 1317–1324. doi: 10.4315/0362-028X-73.7.1317

DeJongh, M., Formsma, K., Boillot, P., Gould, J., Rycenga, M., and Best, A. (2007). Toward the automated generation of genome-scale metabolic networks in the seed. *BMC Bioinform*. 8:139. doi: 10.1186/1471-2105-8-139

Dekeyser, P., Gossuin-Detrain, M., Butzler, J. P., and Sternon, J. (1972). Acute enteritis due to related vibrio: first positive stool cultures. *J. Infect. Dis*. 125, 390–392. doi: 10.1093/infdis/125.4.390

Del Rocio Leon-Kempis, M., Guccione, E., Mulholland, F., Williamson, M. P., and Kelly, D. J. (2006). The *Campylobacter jejuni* PEB1a adhesin is an aspartate/glutamate-binding protein of an ABC transporter essential for microaerobic growth on dicarboxylic amino acids. *Mol. Microbiol*. 60, 1262–1275. doi: 10.1111/j.1365-2958.2006.05168.x

Dickgiesser, N., and Czylwik, D. (1985). Chemically defined media for auxotyping of *Campylobacter jejuni*. *Z. Bakteriol. Mikrobiol. Hyg. Ser. A Med. Microbiol. Infect. Dis. Virol. Parasitol*. 260, 57–64. doi: 10.1016/S0176-6724(85)80098-5

El-Gebali, S., Mistry, J., Bateman, A., Eddy, S., Luciani, A., Potter, S., et al. (2018). The PFAM protein families database in 2019. *Nucleic Acids Res*. 47, D427–D432. doi: 10.1093/nar/gky995

Fell, D. A., and Small, R. J. (1986). Fat synthesis in adipose tissue. An examination of stoichiometric constraints. *Biochem. J*. 238, 781–6. doi: 10.1042/bj2380781

Friis, C., Wassenaar, T. M., Javed, M. A., Snipen, L., Lagesen, K., Hallin, P. F., et al. (2010). Genomic Characterization of *Campylobacter jejuni* Strain M1. *PLoS ONE* 5:e12253. doi: 10.1371/journal.pone.0012253

Gao, B., Vorwerk, H., Huber, C., Lara-Tejero, M., Mohr, J., Goodman, A. L., et al. (2017). Metabolic and fitness determinants for *in vitro* growth and intestinal colonization of the bacterial pathogen *Campylobacter jejuni*. *PLoS Biol*. 15:e2001390. doi: 10.1371/journal.pbio.2001390

Gevorgyan, A., Poolman, M. G., and Fell, D. A. (2008). Detection of stoichiometric inconsistencies in biomolecular models. *Bioinformatics* 24, 2245–2251. doi: 10.1093/bioinformatics/btn425

Gibbons, C., Mangen, M.-J., Plass, D., Havelaar, A., Brooke, R., Kramarz, P., et al. (2014). Measuring underreporting and under-ascertainment in infectious disease datasets: a comparison of methods. *BMC Public Health* 14:147. doi: 10.1186/1471-2458-14-147

Gormley, F. J., Strachan, N. J., Reay, K., MacKenzie, F. M., Ogden, I. D., Dallas, J. F., et al. (2010). Antimicrobial resistance profiles of Campylobacter from humans, retail chicken meat, and cattle feces. *Foodborne Pathog. Dis*. 7, 1129–1131. doi: 10.1089/fpd.2009.0532

Green, M. L., and Karp, P. D. (2004). A Bayesian method for identifying missing enzymes in predicted metabolic pathway databases. *BMC Bioinform*. 5, 76–76. doi: 10.1186/1471-2105-5-76

Gu, C., Kim, G., Kim, W., Kim, T. Y., and Lee, S. Y. (2019). Current status and applications of genome-scale metabolic models. *Genome Biol*. 20:121. doi: 10.1186/s13059-019-1730-3

Guccione, E., Del Rocio Leon-Kempis, M., Pearson, B. M., Hitchin, E., Mulholland, F., Van Diemen, P. M., et al. (2008). Amino acid-dependent growth of *Campylobacter jejuni*: key roles for aspartase (ASPA) under microaerobic and oxygen-limited conditions and identification of ASPB (CJ0762), essential for growth on glutamate. *Mol. Microbiol*. 69, 77–93. doi: 10.1111/j.1365-2958.2008.06263.x

Guccione, E., Hitchcock, A., Hall, S. J., Mulholland, F., Shearer, N., Van Vliet, A. H. M., et al. (2010). Reduction of fumarate, mesaconate and crotonate by MFR, a novel oxygen-regulated periplasmic reductase in *Campylobacter jejuni*. *Environ. Microbiol*. 12, 576–591. doi: 10.1111/j.1462-2920.2009.02096.x

Hartman, H. B., Fell, D. A., Rossell, S., Jensen, P. R., Woodward, M. J., Thorndahl, L., et al. (2014). Identification of potential drug targets in *Salmonella enterica* sv. Typhimurium using metabolic modelling and experimental validation. *Microbiology* 160, 1252–1266. doi: 10.1099/mic.0.076091-0

Hodge, J., and Krieg, N. (1994). Oxygen tolerance estimates in campylobacter species depend on the testing medium. *J. Appl. Bacteriol*. 77, 666–673. doi: 10.1111/j.1365-2672.1994.tb02817.x

Hoffman, P. S., Krieg, N. R., and Smibert, R. M. (1979). Studies of the microaerophilic nature of *Campylobacter fetus* subsp. jejuni. I. Physiological aspects of enhanced aerotolerance. *Can. J. Microbiol*. 25, 1–7. doi: 10.1139/m79-001

Hofreuter, D. (2014). Defining the metabolic requirements for the growth and colonization capacity of *Campylobacter jejuni*. *Front. Cell. Infect. Microbiol*. 4:137. doi: 10.3389/fcimb.2014.00137

Hofreuter, D., Novik, V., and Galan, J. E. (2008). Metabolic diversity in *Campylobacter jejuni* enhances specific tissue colonization. *Cell Host Microbe* 4, 425–433. doi: 10.1016/j.chom.2008.10.002

Hofreuter, D., Tsai, J., Watson, R. O., Novik, V., Altman, B., Benitez, M., et al. (2006). Unique features of a highly pathogenic *Campylobacter jejuni* strain. *Infect. Immunity* 74, 4694–4707. doi: 10.1128/IAI.00210-06

Hsieh, Y.-H., Simpson, S., Kerdahi, K., and Sulaiman, I. M. (2018). A comparative evaluation study of growth conditions for culturing the isolates of *Campylobacter* spp. *Curr. Microbiol*. 75, 71–78. doi: 10.1007/s00284-017-1351-6

Hyatt, D., Chen, G.-L., LoCascio, P. F., Land, M. L., Larimer, F. W., and Hauser, L. J. (2010). Prodigal: prokaryotic gene recognition and translation initiation site identification. *BMC Bioinform*. 8:119. doi: 10.1186/1471-2105-11-119

Jacobs, B. C., van Doorn, P. A., TioGillen, A. P., Visser, L. H., van der Meché, F. G. A., et al. (1996). *Campylobacter jejuni* infections and anti-GM1 antibodies in GuillainBarré syndrome. *Ann. Neurol*. 40, 181–187. doi: 10.1002/ana.410400209

Jeske, L., Placzek, S., Schomburg, I., Chang, A., and Schomburg, D. (2018). Brenda in 2019: a European elixir core data resource. *Nucleic acids Res*. 47, D542–D549. doi: 10.1093/nar/gky1048

Jordan, A., and Reichard, P. (1998). Ribonucleotide reductases. *Annu. Rev. Biochem*. 67, 71–98. doi: 10.1146/annurev.biochem.67.1.71

Kanehisa, M., and Goto, S. (2000). KEGG: Kyoto encyclopedia of genes and genomes. *Nucleic Acids Res*. 28, 27–30. doi: 10.1093/nar/28.1.27

Kanehisa, M., Goto, S., Hattori, M., Aoki-Kinoshita, K. F., Itoh, M., Kawashima, S., et al. (2006). From genomics to chemical genomics: new developments in KEGG. *Nucleic Acids Res*/ 34(Suppl_1):D354–D357. doi: 10.1093/nar/gkj102

Karp, P. D., Billington, R., Caspi, R., Fulcher, C. A., Latendresse, M., Kothari, A., et al. (2017). The BioCyc collection of microbial genomes and metabolic pathways. *Brief. Bioinform*. 20, 1085–1093. doi: 10.1093/bib/bbx085

Karp, P. D., Latendresse, M., and Caspi, R. (2011). The pathway tools pathway prediction algorithm. *Stand Genomic Sci*. 5, 424–429. doi: 10.4056/sigs.1794338

Karp, P. D., Latendresse, M., Paley, S. M., Ong, M. K. Q., Billington, R., Kothari, A., et al. (2015). Pathway tools version 19.0: integrated software for pathway/genome informatics and systems biology. *Brief. Bioinform*. 17, 877–890. doi: 10.1093/bib/bbv079

Karp, P. D., Paley, S., and Romero, P. (2002). The pathway tools software. *Bioinformatics* 18(Suppl_1):S225–S232. doi: 10.1093/bioinformatics/18.suppl_1.S225

Kelly, D. J. (2008). "Complexity and versatility in the physiology and metabolism of *Campylobacter jejuni*," in *Campylobacter, 3rd Edn*, eds I. Nachamkin, C. Szymanski, and M. Blaser (Washington, DC: American Society of Microbiology), 41–61. doi: 10.1128/9781555815554.ch3

Kim, J., Oh, E., Banting, G. S., Braithwaite, S., Chui, L., Ashbolt, N. J., et al. (2016). An improved culture method for selective isolation of *Campylobacter jejuni* from wastewater. *Front. Microbiol*. 7:1345. doi: 10.3389/fmicb.2016.01345

Kim, W. J., Kim, H. U., and Lee, S. Y. (2017). Current state and applications of microbial genome-scale metabolic models. *Curr. Opin. Syst. Biol*. 2, 10–18. doi: 10.1016/j.coisb.2017.03.001

Lastovica, A. J., On, S. L. W., and Zhang, L. (2014). *The Family Campylobacteraceae*. Berlin; Heidelberg: Springer. doi: 10.1007/978-3-642-39044-9_274

Lauwers, S., Boeck, M. D., and Butzler, J. (1978). Campylobacter enteritis in Brussels. *Lancet* 311, 604–605. Originally published as Volume 1, Issue 8064. doi: 10.1016/S0140-6736(78)91045-0

Line, J., Hiett, K., Guard-Bouldin, J., and Seal, B. (2010). Differential carbon source utilization by *Campylobacter jejuni* 11168 in response to growth temperature variation. *J. Microbiol. Methods* 80, 198–202. doi: 10.1016/j.mimet.2009.12.011

Liu, L., Agren, R., Bordel, S., and Nielsen, J. (2010). Use of genome-scale metabolic models for understanding microbial physiology. *FEBS Lett*. 584, 2556–2564. doi: 10.1016/j.febslet.2010.04.052

Liu, X., Gao, B., Novik, V., and Galán, J. (2012). Quantitative proteomics of intracellular *Campylobacter jejuni* reveals metabolic reprogramming. *PLoS Pathog*. 8:e1002562. doi: 10.1371/journal.ppat.1002562

Manandhar, M., and Cronan, J. (2017). Pimelic acid, the first precursor of the *Bacillus subtilis* biotin synthesis pathway, exists as the free acid and is assembled by fatty acid synthesis: *Bacillus subtilis* biotin synthesis. *Mol. Microbiol*. 104, 595–607. doi: 10.1111/mmi.13648

Mangen, M.-J., Havelaar, A., Haagsma, J., and Kretzschmar, M. (2016). The burden of campylobacter-associated disease in six European countries. *Microb. Risk Anal*. 2–3:48–52. doi: 10.1016/j.mran.2016.04.001

Mendz, G. L., Ball, G. E., and Meek, D. J. (1997). Pyruvate metabolism in *Campylobacter* spp. *Biochim. Biophys. Acta Gen. Subj*. 1334, 291–302. doi: 10.1016/S0304-4165(96)00107-9

Metris, A., Reuter, M., Gaskin, D., Baranyi, J., and van Vliet, A. (2011). *In vivo* and *in silico* determination of essential genes of *Campylobacter jejuni*. *BMC Genomics* 12:535. doi: 10.1186/1471-2164-12-535

Morgat, A., Lombardot, T., Coudert, E., Axelsen, K., Neto, T. B., Gehant, S., et al. (2019). Enzyme annotation in UniProtKB using Rhea. *Bioinformatics*. 36, 1896–1901. doi: 10.1093/bioinformatics/btz817

Ogata, H., Goto, S., Sato, K., Fujibuchi, W., Bono, H., and Kanehisa, M. (1999). KEGG: Kyoto encyclopedia of genes and genomes. *Nucleic Acids Res*. 27, 29–34. doi: 10.1093/nar/27.1.29

Parsons, C. M. (1984). Influence of caecectomy and source of dietary fibre or starch on excretion of endogenous amino acids by laying hens. *Brit. J. Nutr*. 51, 541–548. doi: 10.1079/BJN19840059

Pearson, B., Pin, C., Wright, J., I'Anson, K., Humphrey, T., and Wells, J. (2003). Comparative genome analysis of *Campylobacter jejuni* using whole genome DNA microarrays. *FEBS Lett*. 554, 224–230. doi: 10.1016/S0014-5793(03)01164-5

Platts-Mills, J., and Kosek, M. (2014). Update on the burden of Campylobacter in developing countries. *Curr. Opin. Infect. Dis* 27, 444–450. doi: 10.1097/QCO.0000000000000091

Poolman, M. G. (2006). ScrumPy: metabolic modelling with Python. *IEE Proc. Syst. Biol*. 153, 375–378. doi: 10.1049/ip-syb:20060010

Poolman, M. G., Kundu, S., Shaw, R., and Fell, D. A. (2013). Responses to light intensity in a genome-scale model of rice metabolism. *Plant Physiol*. 162, 1060–1072. doi: 10.1104/pp.113.216762

Poolman, M. G., Miguet, L., Sweetlove, L. J., and Fell, D. A. (2009). A genome-scale metabolic model of Arabidopsis and some of its properties. *Plant Physiol*. 151, 1570–1581. doi: 10.1104/pp.109.141267

Ruiz-Palacios, G. M. (2007). The health burden of Campylobacter infection and the impact of antimicrobial resistance: playing chicken. *Clin. Infect. Dis*. 44, 701–703. doi: 10.1086/509936

Schellenberger, J., Park, J. O., Conrad, T. M., and Palsson, B. O. (2009). BIGG: a biochemical genetic and genomic knowledgebase of large scale metabolic reconstructions. *BMC Bioinform*. 11:213. doi: 10.1186/1471-2105-11-213

Seemann, T. (2014). PROKKA: rapid prokaryotic genome annotation. *Bioinformatics* 30, 2068–2069. doi: 10.1093/bioinformatics/btu153

Sellars, M. J., Hall, S. J., and Kelly, D. J. (2002). Growth of *Campylobacter jejuni* supported by respiration of fumarate, nitrate, nitrite, trimethylamine-n-oxide, or dimethyl sulfoxide requires oxygen. *J. Bacteriol*. 184, 4187–4196. doi: 10.1128/JB.184.15.4187-4196.2002

Sheppard, S. K., Didelot, X., Meric, G., Torralbo, A., Jolley, K. A., Kelly, D. J., et al. (2013). Genome-wide association study identifies vitamin b5 biosynthesis as a host specificity factor in Campylobacter. *Proc. Natl. Acad. Sci. U.S.A*. 110, 11923–11927. doi: 10.1073/pnas.1305559110

Skirrow, M. B. (1977). Campylobacter enteritis: a "new" disease. *British Med. J*. 6078, 9–11. doi: 10.1136/bmj.2.6078.9

Stabler, R. A., Larsson, J. T., Al-Jaberi, S., Nielsen, E. M., Kay, E., Tam, C. C., et al. (2013). Characterization of water and wildlife strains as a subgroup of *Campylobacter jejuni* using DNA microarrays. *Environ. Microbiol*. 15, 2371–2383. doi: 10.1111/1462-2920.12111

Stahl, M., Butcher, J., and Stintzi, A. (2012). Nutrient acquisition and metabolism by *Campylobacter jejuni*. *Front. Cell. Infect. Microbiol*. 2:5. doi: 10.3389/fcimb.2012.00005

Stok, J. E., and Voss, J. J. D. (2000). Expression, purification, and characterization of biol: a carbon-carbon bond cleaving cytochrome p450 involved in biotin biosynthesis in *Bacillus subtilis*. *Arch. Biochem. Biophys*. 384, 351–360. doi: 10.1006/abbi.2000.2067

Szklarczyk, D., Gable, A., Lyon, D., Junge, A., Wyder, S., Huerta-Cepas, J., et al. (2018). String v11: protein-protein association networks with increased coverage, supporting functional discovery in genome-wide experimental datasets. *Nucleic Acids Res*. 47, D607–D613. doi: 10.1093/nar/gky1131

Tam, C., and O'Brien, S. (2016). Economic cost of Campylobacter, norovirus and rotavirus disease in the United Kingdom. *PLoS ONE* 11:e0138526. doi: 10.1371/journal.pone.0138526

Tenover, F. C., Knapp, J. S., Patton, C., and Plorde, J. J. (1985). Use of auxotyping for epidemiological studies of *Campylobacter jejuni* and *Campylobacter coli* infections. *Infect. Immunity* 48, 384–388. doi: 10.1128/IAI.48.2.384-388.1985

Tenover, F. C., and Patton, C. M. (1987). Naturally occurring auxotrophs of *Campylobacter jejuni* and *Campylobacter coli*. *J. Clin. Microbiol*. 25, 1659–1661. doi: 10.1128/JCM.25.9.1659-1661.1987

Thiele, I., Vo, T. D., Price, N. D., and Palsson, B. Ø. (2005). Expanded metabolic reconstruction of *Helicobacter pylori* (IIT341 GSM/GPR): an *in silico* genome-scale characterization of single- and double-deletion mutants. *J. Bacteriol*. 187, 5818–5830. doi: 10.1128/JB.187.16.5818-5830.2005

van der Ark, K. C. H., Aalvink, S., Suarez-Diez, M., Schaap, P. J., de Vos, W. M., and Belzer, C. (2018). Model-driven design of a minimal medium for

Akkermansia muciniphila confirms mucus adaptation. *Microb. Biotechnol.* 11, 476–485. doi: 10.1111/1751-7915.13033

van der Hooft, J. J., Alghefari, W., Watson, E., Everest, P., Morton, F. R., Burgess, K. E., et al. (2018). Unexpected differential metabolic responses of *Campylobacter jejuni* to the abundant presence of glutamate and fucose. *Metabolomics* 14:144. doi: 10.1007/s11306-018-1438-5

van der Stel, A.-X., Boogerd, F. C., Huynh, S., Parker, C. T., van Dijk, L., van Putten, J. P. M., et al. (2017). Generation of the membrane potential and its impact on the motility, ATP production and growth in *Campylobacter jejuni*. *Molecular Microbiol.* 105, 637–651. doi: 10.1111/mmi.13723

van der Stel, A.-X., and Wösten, M. M. S. M. (2019). Regulation of respiratory pathways in campylobacterota: a review. *Front. Microbiol.* 10:1719. doi: 10.3389/fmicb.2019.01719

Varma, A., and Palsson, B. O. (1993). Metabolic capabilities of *Escherichia coli*: I. synthesis of biosynthetic precursors and cofactors. *J. Theor. Biol.* 165, 477–502. doi: 10.1006/jtbi.1993.1202

Varma, A., and Palsson, B. O. (1994). Stoichiometric flux balance models quantitatively predict growth and metabolic by-product secretion in wild-type *Escherichia coli* W3110. *Appl. Environ. Microbiol.* 60, 3724–31. doi: 10.1128/AEM.60.10.3724-3731.1994

Velayudhan, J., Jones, M. A., Barrow, P., and Kelly, D. J. (2004). L-serine catabolism via an oxygen-labile l-serine dehydratase is essential for colonization of the avian gut by *Campylobacter jejuni*. *Infect. Immun.* 72, 260-268. doi: 10.1128/IAI.72.1.260-268.2004

Velayudhan, J., and Kelly, D. J. (2002). Analysis of gluconeogenic and anaplerotic enzymes in *Campylobacter jejuni*: an essential role for phosphoenolpyruvate carboxykinase. *Microbiology* 148, 685–694. doi: 10.1099/00221287-148-3-685

Villanova, V., Fortunato, A. E., Singh, D., Bo, D. D., Conte, M., Obata, T., et al. (2017). Investigating mixotrophic metabolism in the model diatom *Phaeodactylum tricornutum*. *Philos. Trans. R. Soc. B* 372:1728. doi: 10.1098/rstb.2016.0404

Vorwerk, H., Mohr, J., Huber, C., Wensel, O., Schmidt-Hohagen, K., Gripp, E., et al. (2014). Utilization of host-derived cysteine-containing peptides overcomes the restricted sulphur metabolism of *Campylobacter jejuni*. *Mol. Microbiol.* 93, 1224–1245. doi: 10.1111/mmi.12732

Wagley, S., Newcombe, J., Laing, E., Yusuf, E., Sambles, C., Studholme, D., et al. (2014). Differences in carbon source utilisation distinguish *Campylobacter jejuni* from *Campylobacter coli*. *BMC Microbiol.* 14:262. doi: 10.1186/s12866-014-0262-y

Westfall, H. N., Rollins, D. M., and Weiss, E. (1986). Substrate utilization by *Campylobacter jejuni* and *Campylobacter coli*. *Appl. Environ. Microbiol.* 52, 700–705. doi: 10.1128/AEM.52.4.700-705.1986

Westrell, T., Ciampa, N., Boelaert, F., Helwigh, B., Korsgaard, H., Chrael, M., et al. (2009). Zoonotic infections in Europe in 2007: a summary of the EFSA-ECDC annual report. *Eurosurveillance* 14:19100.

Wilkinson, D., O'Donnell, A., Akhter, R., Fayaz, A., Mack, H., Rogers, L., et al. (2018). Updating the genomic taxonomy and epidemiology of *Campylobacter hyointestinalis*. *Sci. Rep.* 8:2393. doi: 10.1038/s41598-018-20889-x

Wright, J. A., Grant, A. J., Hurd, D., Harrison, M., Guccione, E. J., Kelly, D. J., et al. (2009). Metabolite and transcriptome analysis of *Campylobacter jejuni in vitro* growth reveals a stationary-phase physiological switch. *Microbiology* 155, 80–94. doi: 10.1099/mic.0.021790-0

Xu, F., Wu, C., Guo, F., Cui, G., Zeng, X., Yang, B., et al. (2015). Transcriptomic analysis of *Campylobacter jejuni* nctc 11168 in response to epinephrine and norepinephrine. *Front. Microbiol.* 6:452. doi: 10.3389/fmicb.2015.00452

Zampieri, M., and Sauer, U. (2016). Model-based media selection to minimize the cost of metabolic cooperation in microbial ecosystems. *Bioinformatics* 32, 1733–1739. doi: 10.1093/bioinformatics/btw062

Zhang, C., and Hua, Q. (2016). Applications of genome-scale metabolic models in biotechnology and systems medicine. *Front. Physiol.* 6:413. doi: 10.3389/fphys.2015.00413

Conflict of Interest: LC is the director of SequenceAnalysis.co.uk and was paid to perform this work.

The remaining authors declare that the research was conducted in the absence of any commercial or financial relationships that could be construed as a potential conflict of interest.

frontiers in Microbiology

ORIGINAL RESEARCH
published: 19 November 2020
doi: 10.3389/fmicb.2020.530906

Membrane Proteocomplexome of *Campylobacter jejuni* Using 2-D Blue Native/SDS-PAGE Combined to Bioinformatics Analysis

*Alizée Guérin[1], Sheiam Sulaeman[1], Laurent Coquet[2,3], Armelle Ménard[4], Frédérique Barloy-Hubler[5], Emmanuelle Dé[2] and Odile Tresse[1]**

[1] UMR 1014 Sacelim, INRAE, Oniris, Nantes, France, [2] UMR 6270 Laboratoire Polymères Biopolymères Surfaces, UNIROUEN, INSA Rouen, CNRS, Normandie Université, Rouen, France, [3] UNIROUEN, Plateforme PISSARO, IRIB, Normandie Université, Mont-Saint-Aignan, France, [4] INSERM, UMR 1053 Bordeaux Research in Translational Oncology, BaRITOn, Bordeaux, France, [5] UMR 6290, CNRS, Institut de Génétique et Développement de Rennes, University of Rennes, Rennes, France

OPEN ACCESS

Edited by:
Ozan Gundogdu, University of London, United Kingdom

Reviewed by:
David Smith, Heriot-Watt University, United Kingdom
Harald Nothaft, University of Alberta, Canada
Nicolae Corcionivoschi, Agri-Food and Biosciences Institute (AFBI), United Kingdom

***Correspondence:**
Odile Tresse
odile.tresse@inrae.fr

Specialty section:
This article was submitted to Food Microbiology, a section of the journal Frontiers in Microbiology

Received: *30 January 2020*
Accepted: *14 October 2020*
Published: *19 November 2020*

Citation:
Guérin A, Sulaeman S, Coquet L, Ménard A, Barloy-Hubler F, Dé E and Tresse O (2020) Membrane Proteocomplexome of Campylobacter jejuni Using 2-D Blue Native/SDS-PAGE Combined to Bioinformatics Analysis. Front. Microbiol. 11:530906. doi: 10.3389/fmicb.2020.530906

Campylobacter is the leading cause of the human bacterial foodborne infections in the developed countries. The perception cues from biotic or abiotic environments by the bacteria are often related to bacterial surface and membrane proteins that mediate the cellular response for the adaptation of *Campylobacter jejuni* to the environment. These proteins function rarely as a unique entity, they are often organized in functional complexes. In *C. jejuni*, these complexes are not fully identified and some of them remain unknown. To identify putative functional multi-subunit entities at the membrane subproteome level of *C. jejuni*, a holistic non *a priori* method was addressed using two-dimensional blue native/Sodium dodecyl sulfate (SDS) polyacrylamide gel electrophoresis (PAGE) in strain *C. jejuni* 81–176. Couples of acrylamide gradient/migration-time, membrane detergent concentration and hand-made strips were optimized to obtain reproducible extraction and separation of intact membrane protein complexes (MPCs). The MPCs were subsequently denatured using SDS-PAGE and each spot from each MPCs was identified by mass spectrometry. Altogether, 21 MPCs could be detected including multi homo-oligomeric and multi hetero-oligomeric complexes distributed in both inner and outer membranes. The function, the conservation and the regulation of the MPCs across *C. jejuni* strains were inspected by functional and genomic comparison analyses. In this study, relatedness between subunits of two efflux pumps, CmeABC and MacABputC was observed. In addition, a consensus sequence CosR-binding box in promoter regions of MacABputC was present in *C. jejuni* but not in *Campylobacter coli*. The MPCs identified in *C. jejuni* 81–176 membrane are involved in protein folding, molecule trafficking, oxidative phosphorylation, membrane structuration, peptidoglycan biosynthesis, motility and chemotaxis, stress signaling, efflux pumps and virulence.

Keywords: foodborne pathogen, proteomics, functional genomics, complexes, membrane proteins, efflux pumps, regulation, blue native electrophoresis

INTRODUCTION

Campylobacter is a Gram-negative spiral-shaped bacterium. It has emerged as the leading cause of foodborne bacterial gastroenteritis in humans (Epps et al., 2013; Kaakoush et al., 2015; EFSA and ECDC, 2018). The number of campylobacteriosis cases has been increasing in Europe since 2005 and has reached an incidence of 65 per 100,000 people with 246–158 confirmed cases in 2018 (EFSA and ECDC, 2018). Most cases were attributed to *Campylobacter jejuni*, an invasive microorganism causing gastroenteritis associated with fever and frequent watery bloody diarrhea, abdominal pains and occasionally nausea (Moore et al., 2005; Silva et al., 2011; Epps et al., 2013). It is also associated with post-infection complications including the immune-mediated neurological disease Guillain-Barré Syndrome (Nachamkin, 2002; Alshekhlee et al., 2008), its variant Miller Fisher Syndrome (Ang et al., 2001) or reactive arthritis (Altekruse et al., 1999). Notably, the infectious dose is considered to be lower than the one for other foodborne pathogens as only 500–800 bacteria trigger human infection (Robinson, 1981; Black et al., 1988; Boyanova et al., 2004; Castano-Rodriguez et al., 2015). *Campylobacter* cost of illness was estimated at 2.4 billion euros per year in Europe (EFSA, 2016). *C. jejuni* infections are mainly associated with consumption of poultry and cross-contamination from poultry products (Hue et al., 2010; Guyard-Nicodeme et al., 2013; Hald et al., 2016). For the first time, the European Commission regulation has amended the regulation (EC) No 2073/2005 in 2017 on the hygiene of foodstuffs as regards *Campylobacter* on broiler carcasses stating a limit of 1000 CFU/g applied from January 2018. This microaerophilic, capnophilic and thermophilic microorganism requires fastidious growth conditions and it growth is rapidly hampered by several environmental stress conditions. Optimal growth is obtained using a modified atmosphere limited in dioxygen and enriched in carbon dioxide, a temperature between 37 and 45 C and a pH between 6.5 and 7.5 (Mace et al., 2015). Nonetheless, *C. jejuni* is able to survive harmful conditions by developing adaptation mechanisms in response to stress conditions throughout the food chain (Atack and Kelly, 2009; Rodrigues et al., 2016). Living as biofilms is also a phenotypical feature that was demonstrated for *C. jejuni,* indicating multiple surviving ways outside hosts (Turonova et al., 2015).

Proteomic techniques have been applied to *Campylobacter* to better understand how changes in genetic expression, bacterial state, nutrient limitation, food plant processing and environmental conditions could affect *C. jejuni* at the protein level (Tresse, 2017). Natural compartmentalization has facilitated subfraction proteome analyses of *Campylobacter* such as the cytosolic proteome (Kalmokoff et al., 2006; Bieche et al., 2012; Asakura et al., 2016), the membrane proteome (Seal et al., 2007; Cordwell et al., 2008; Scott et al., 2014; Watson et al., 2014), the inner or outer membrane proteome (Sulaeman et al., 2012) and the exoproteome (Kaakoush et al., 2010). In addition, the genomic and computational era have brought exciting and challenging prospects for proteomics like assigning a function to each protein and subsequently its relationship to other proteins in the cell. Functional genomics and protein structural modeling approaches can predict protein-protein interactions (PPIs), which constitutes the theoretical protein interactome of an organism. Predicted interactomes, including potential stable or transient PPIs, are limited to databases content but PPIs already demonstrated to be biologically functional, specific genetic organizations (operons, gene clusters and regulons) or structural features (domains and loops) (Planas-Iglesias et al., 2013; Wetie et al., 2013). Genomic analyses of the main pathogenic species of *Campylobacter*, revealed a lack of some of the well-described organizations into operons or gene clusters in Gram-negative bacteria (Parkhill et al., 2000). For instance, genes involved in the amino-acid biosynthesis are scattered in distinct loci across the genome of *C. jejuni* whereas they are organized into operons in other bacteria. In *H. pylori*, the closest specie relative to *Campylobacter,* the presence of some genetic elements organized into operons, gene clusters or islands could have contributed to the specialization of this pathogen (Sohn and Lee, 2011; You et al., 2012). In *C. jejuni*, the virulence variation among strains could not be assigned to any specific genetic organization other than point mutations in the virulence-associated genes or indels in individual loci (Bell et al., 2013). A reduced genetic organization has probably participated to the idiosyncrasy of *C. jejuni*.

The alternative method to identify PPIs, which does not result necessary from a specific genetic organization, is to detect complexes of proteins using non-hypothesis driven methods. When these complexes are composed of only protein subunits, the global approach is called proteocomplexomic. This is the case of the two-dimensional (2-D) blue native (BN)/SDS-PAGE which aims at highlighting intact protein complexes using mild non-ionic and non-denaturing detergents (Dresler et al., 2011; Lasserre and Menard, 2012; Wohlbrand et al., 2016). This method consists in separating native protein complexes according to their molecular mass during the first dimension and subsequently in separating protein subunits of each complex in SDS-denaturated conditions in an orthogonal second dimension. It has been applied with success to monitor oligomeric state, stoichiometry and protein subunit composition of protein complexes.

This study aimed at exploring protein machineries of *C. jejuni* at the membrane level. The bacterial membrane as a hydrophobic lipid structure is a suitable site for protein complex organization. Numerous well-characterized proteins embedded in the membrane are organized into functional units involved in various cellular processes. These membrane protein complexes (MPCs) could be also influenced by the membrane structural integrity and their molecular environment (Sachs and Engelman, 2006). In *didermata* such as *C. jejuni*, MPCs could be either organized throughout both membranes and the periplasmic space or specifically in the inner or in the outer membrane. The first objective was to apply and to optimize 2-D BN/SDS-PAGE technique on the *C. jejuni* membrane proteins to obtain reproducible gels. The second goal was to identify MPCs present in *C. jejuni* during optimal growth. As this analysis was conducted on the membrane compartment, it was called membrane proteocomplexomic analysis.

MATERIALS AND METHODS

Bacterial Cell Cultures and Sample Preparation

The virulent *C. jejuni* strain 81–176 (NC_008787), whose whole genome is available in Genoscope Platform (MicroScope Vallenet et al., 2017), was selected for the experiments. A loopful of frozen 81–176 cells culture, conserved at −80°C in Brain-Heart Infusion (BHI) broth (Biokar, Beauvais, France) containing 20% sterile glycerol, was cultured on fresh Karmali agar plates (Oxoid, Dardilly, France) (Air Liquid, Paris, France) at 42°C for 48 h in microaerobic conditions (MAC) generated using gas replacement jars operated by MACSmics gassing system (BioMérieux, France) with a gas blend composed of 5% O_2, 10% CO_2, and 85% N_2 (Air Liquid, Paris, France) and 4 filled/flushed cycles at −50 kPa as described in Mace et al. (2015). Cultures were obtained by inoculating 500 mL of BHI broth in a 1-L flask and incubating them for 16 h under MAC at 42°C in a rotary shaker.

Membrane Protein Complex (MPC) Extraction

The cells were harvested by centrifugation for 20 min at 4°C at 6,000 × *g*. The supernatant was discarded and about 3 g of dry pellet was obtained. The cells were washed twice with lysis buffer containing 50 mM Tris, 750 mM 6-amino-n-caproic acid as a zwitterionic salt, with each wash followed by centrifugation at 6,000 × *g* for 20 min at 4°C. The cells were then resuspended in 5.5 mL of lysis buffer supplemented with 60 μL phenylmethylsulfonyl fluoride (PMSF) and sonicated at 50 kHz for 6 × 30 s with 5 min intervals on ice (Vibracell 72434, Bioblock Scientific, Illkirch, France) as previously described by Bieche et al. (2012). The proteins present in the supernatant were then collected and centrifuged twice at 10,000 × *g* for 30 min at 4°C in order to remove the cellular debris. The whole protein lysate was treated with 0.2 mg/ml DNase I for 1 h at 25°C and then ultra centrifuged at 100,000 × *g* for 1 h at 4°C. The pellet containing membrane complexes was resuspended in 10 mL of lysis buffer with 50 μL PMSF supplemented with the mild detergent Dodecyl-β-D-Maltoside (DDM) (Sigma, France) at concentrations ranging from 1 to 5% (w/v) to maintain the integrity of protein complexes and limiting dissociation or denaturation as previously recommended by Bernarde et al. (2010). After 15 min on ice, each sample solubilized with DDM was directly ultra-centrifuged at 100,000 × *g* for 1 h at 4°C. The MPC extraction was performed in triplicate from three independent cultures. Aliquots of the supernatant containing the membrane protein complexes were stored at −80°C. The protein concentration of membrane complexes was determined using the Micro BCA™ Protein Assay Kit (Perbio Science, Brebieres, France) according to the manufacturer protocol.

MPC Separation Using 2-D BN/SDS-PAGE

First Dimension in Native Conditions (BN-PAGE)

The first dimension was performed in a blue native polyacrylamide gel (BN-PAGE) according to Schagger (Schagger and von Jagow, 1991) with the following modifications. The MCP separation using BN-PAGE gels (15 cm × 16 cm × 0.1 cm) was assayed on linear acrylamide gradients: 4–14% (w/v), 4–18% (w/v), 8–18% (w/v) or 10–20% (w/v) using a gradient forming unit and Protean II cell (Bio-Rad, Hercules, CA, United States). Each separating gel was overlaid with a 3% stacking BN-PAGE. Both anode and cathode buffers contained 50 mM Tris and 75 mM Glycine. Only the cathode buffer was supplemented with 0.002% (w/v) Coomassie Blue G250 (Serva Biochemicals, Heidelberg, Germany). The assembly of gels were embedded with anode and cathode buffers and maintained at 4°C for 3 h before loading the protein sample. A volume of 1–5 μL of sample buffer (500 mM 6-amino-*n*-caproic acid and 5% Serva blue G) was added to DDM-solubilized membrane protein complex samples. Thyroglobulin (669 kDa), ferritin (440 kDa), catalase (232 kDa), lactate dehydrogenase (140 kDa) and BSA (67 kDa) were used as high molecular weight native protein marker mixture (GE Healthcare, Buckinghamshire, United Kingdom). The migration was run at 4°C with 1 W per gel and limited at 150 V and 90 mA during 4 to 48 h according to the assays.

To check the optimal solubilization of the protein complexes using DDM, migration through BN-PAGE was performed as described above with 3% stacking gel. Samples of 10 or 20 μg of protein complexes solubilized in 1, 2 or 5% (w/v) DDM were prepared as described above and loaded for each lane of the BN-PAGE. For protein complex analyses, gels were silver stained and scanned with a GS-800 densitometer (Bio-Rad) operated with the Quantity One® software (Bio-Rad) at the resolution of 42.3 microns as described previously by Sulaeman et al. (2012). For the protein identification, the gels were loaded with 50 μg of protein complexes. Following the 1-D migration, the protein complexes in the BN-PAGE were fixed using the kit Bio Safe™ Coomassie G-250 Stain (Bio-Rad) according to the manufacturer's instructions.

Second-Dimension SDS-PAGE

The second dimension was performed under denaturing conditions using 10% (w/v) acrylamide SDS-PAGE (15 cm × 16 cm × 0.15 cm). An individual lane was cut off from the first dimension BN-PAGE using a glass plate. Gel lane was equilibrated for 5 min in a buffer containing 1% (w/v) SDS and 125 mM Tris. Then, the proteins were reduced for 15 min into equilibrating buffer supplemented with 50 mM dithiothreitol (DTT) (Sigma, France), and subsequently alkylated for 15 min in equilibrating buffer supplemented with 125 mM iodoacetamide (Bio-Rad). An ultimate washing step lasting 5 min was performed in the equilibrating buffer without supplement. After polymerization of the separating SDS-PAGE and equilibration, the gel lane was laid on a plastic support and introduced between the gel glass plates over the separation gel and embedded with low-melting agarose. Migration was carried out for 4 h at 16°C at 300 V maximum and 10 mA/gel for the first 45 min and then at 20 mA/gel. After migration, proteins were silver stained and scanned as described above.

In-Gel Trypsin Digestion

The silver-stained spots separated by SDS-PAGE were excised manually. At first, the spots were discolored, then washed and reduced/alkylated using an automated system (MultiProbe II, Perkin Elmer, France) as following: each spot was washed several times in water, once in 25 mM ammonium carbonate and dehydrated with acetonitrile (ACN). After drying the gel pieces, the reduction was achieved by incubation for 1 h with 10 mM DTT at 55°C. The alkylation was achieved by incubation the samples with 25 mM iodoacetamide for 1 h at room temperature. Finally, the gel spots were washed three times in water for 10 min, again alternating between ammonium carbonate and ACN. The gel pieces were completely dried before trypsin digestion and rehydrated by trypsin addition. The digestion was carried out overnight at 37°C. The gel fragments were subsequently incubated twice for 15 min in a H_2O/ACN solution and in ACN to allow extraction of peptides from the gel pieces. The peptide extracts were then pooled, dried and dissolved in 10 μL starting buffer for chromatographic elution, consisting of 3% (v/v) ACN and 0.1% (v/v) formic acid in water.

Protein Identification by LC MS/MS

The peptides were enriched and separated using a lab-on-a-chip technology (Agilent, Massy, France) and fragmented using an on-line XCT mass spectrometer (Agilent). The fragmentation data were interpreted using the Data Analysis program (version 3.4, Bruker Daltonic, Billerica, MA, United States). For the protein identification, the MS/MS peak lists were extracted, converted into mgf-format files and compared to the *C. jejuni*, strain 81–176 protein database (UniprotKB, CP000538 for the chromosome, CP000549 for plasmid pTet and CP000550 for plasmid pVir) with the MASCOT Daemon search engine (version 2.6.0; Matrix Science, London, United Kingdom). The following search parameters were used: trypsin was used as the cutting enzyme, the mass tolerance for monoisotopic peptide window was set to ±1.0 Da and the MS/MS tolerance window was set to ±0.5 Da. Two missed cleavages were allowed. Carbamidomethylation, oxidized methionine, acetylation and pyroglutamate in Nt and amidation in Ct were chosen as variable modifications. Generally, the peptides with individual ions scores higher than the score indicated for $p < 0.05$ were selected. The proteins with two or more unique peptides matching the protein sequence were automatically considered as a positive identification. The main raw data are presented in **Supplementary Data Sheet S1**. Other raw data are available upon request.

Western Blotting

The western blots of 2-D BN/SDS PAGE were performed according to Sulaeman et al. (2012). Briefly, prior to transfer, the 2-D SDS gels were cut into two horizontal sections and each section was soaked for 15 min in transfer buffer. Then, the proteins of each gel section were transferred to a nitrocellulose membrane by electrophoresis using Mini Trans Blot (Bio-Rad). The transferred proteins were then probed with a 1/2000 dilution of antibody anti-PorA or antibody anti-CadF. The immunoreactive proteins were detected using a 1/2000 dilution goat-anti-rabbit alkaline phosphatase antibody [Anti-Rabbit IgG, F(avb)2 fragment-Alkaline Phosphatase, Sigma, Saint-Quentin-Fallavier, France], followed by BCIP/NBT staining (Bio-Rad). Gels were scanned using the GS-800 Imaging densitometer (Bio-Rad).

Bioinformatic Analyses

In silico Determination of Complex Function

The presence and organization of genes encoded protein subunits of identified complexes in 81–176 and other *Campylobacter* complete genomes was explored using the Platform MicroScope described in Vallenet et al., 2017. The biological function of these proteins and complexes were inferred using KEGG and Microcyc (Kanehisa et al., 2016). The conformation analyses of the proteins alone or in a complex were performed using UniProt (Zommiti et al., 2016), RCSB (Stephen et al., 2018), RCSB PDB (Young et al., 2018), Swiss-model (Biasini et al., 2014) and OPM (Lomize et al., 2012). The functional links between partners of complex was explored using STRING (Szklarczyk et al., 2017). If the complex protein subunits were not identified in *Campylobacter*, homologous genes were searched using conventional gene alignment tools (BlatN).

Phylogenetic Tree of Efflux Pumps

The protein sequences of CmeA, CmeB, CmeC and MacA, MacB, putMacC (for putative MacC) on fourteen complete genomes of *C. jejuni* strains and six complete genomes of *Campylobacter coli* strains were recovered (**Supplementary Data Sheet S1**). MAFFT alignments (reference) and Fast Tree (reference) phylogenetic trees were performed using Geneious R9 and visualized using FigTree V1.4.3 software[1]. The proteins structures predictions were determined using Philus transmembrane prediction server (reference,)[2].

Distribution of Efflux Pumps CmeABC and MacABputC in Bacteria

BlastP analyses were performed for each protein sequence of the components of these efflux pumps in *C. jejuni* 81–176 against domain bacteria in RefSeq (NCBI Reference Sequence Database) protein database. The general parameters applied for similarity validation were Max target sequences at 20000, automatically adjust parameters for short input sequences, expect threshold at 10, word size at 6 and max matches in a query range at 0. Scoring parameters were obtained from the blosum62 matrix, gap costs with existence at 11 and extension at one with a conditional compositional score matrix adjustment.

Identification of CosR DNA-Binding Box

The sequence logo of CosR-binding box previously defined by Turonova et al. (2017) was used to check the presence of cosR-binding box in the promoter regions of the operons encoding the efflux pumps *cme*ABC and *mac*ABputC among the complete genomes of *C. jejuni* and *C. coli* (**Supplementary Data Sheet S1**). For that, a sequence length of maximum 120 pb in the

[1] http://tree.bio.ed.ac.uk/software/figtree/

[2] www.yeastrc.org/philius/pages/philius/runPhilius.jsp

intergenic regions upstream to *cmeA* and *macA* was recovered. Based on these sequences, a new sequence logo of CosR DNA-binding box with sequences was drawn using WebLogo platform[3] (Crooks et al., 2004).

RESULTS

Optimization of Protein Complex Solubilization and Separation

The BN-PAGE was applied first to check the solubilization efficiency of the extracted MPCs. In order to approach a useful detergent concentration for protein complex solubilization for BN-PAGE, Dodecyl-β-D-Maltoside (DDM) has turned out to be suitable (Schägger, 2002). The solubilization of the membrane was tested in a concentration of 1, 2, or 5% of DDM. The loading quantities of 10 μg or 20 μg of MPCs on BN-PAGE were found appropriate to determine the reliable concentration of DDM detergent for *C. jejuni* (**Figure 1**). In native conditions, MPCs migrate according to their mass and their form in space (steric hindrance). The bands detected in BN-PAGE in the range of 20 kDa to 670 kDa indicate that MCPs were stable after membrane solubilization and during the separation. All tested concentrations of DDM (1, 2, and 5%) seem to be suitable to solubilize MPCs from *C. jejuni*. However, over the three independent extractions, less reproducibility was obtained with 5% DDM for the lower molecular mass complexes (not shown). Consequently, only 2% DDM were selected to explore MPCs of *C. jejuni* 81–176. In addition, the better separation of MPCs was obtained by extending the migration time until 40 h (**Supplementary Figure S1**). Acrylamide gradients of BN-PAGE were also optimized by testing different couples of lower concentrations (ranging from 4 to 10%) and higher concentration (ranging from 14 to 20%). Even though some protein complexes were more distinct on some gradients, the linear gradient which gives more detectable complexes was 4 to 18% of acrylamide. In general, a lack of reproducibility of the 2-D gels and vertical smearing altering the resolution of MPCs subunits on SDS-PAGE were frequently reported. To circumvent these biases, many gels were run in previous studies until obtaining at least three similar replicates. In the present study, obtaining gel repeatability in a consecutive manner was the first goal. This goal was reached by decreasing vertical smearing, adjusting the thickness of the gels, fixing the supports and isolating the homemade strip from glass using a five-step protocol (**Supplementary Figure S1**). All these optimization steps resulted in performing consecutive reproducible gels. The reproducibility was validated once three consecutive profiles could be aligned with the same number of detected spots. The results of optimization steps during the first and second dimensions are presented in **Supplementary Figure S2**.

Analysis of 2D-BN/SDS-PAGE Data

Using the criteria mentioned by Reisinger and Eichacker (2006), all protein spots that are located vertically below each other with a similar shape on the 2-D were considered as subunits of one MPC. Consequently, the complexes were numbered from the left side to the right side of the 2-D gel and the detected subunits for each complex with a second number starting from the top of the gel (**Figure 2**). The spots, which were located side by side in a horizontal row, could potentially be an identical subunit in protein complexes of different molecular masses. If we assume that the molecular mass of a protein complex is increased during assembly of its structural subunits, the analysis of the protein pattern allows to determine the stepwise subunit assembly. The lower toward the higher molecular mass should correspond to complexes located from the right side of the gel toward its left side (Reisinger and Eichacker, 2008). When a complex

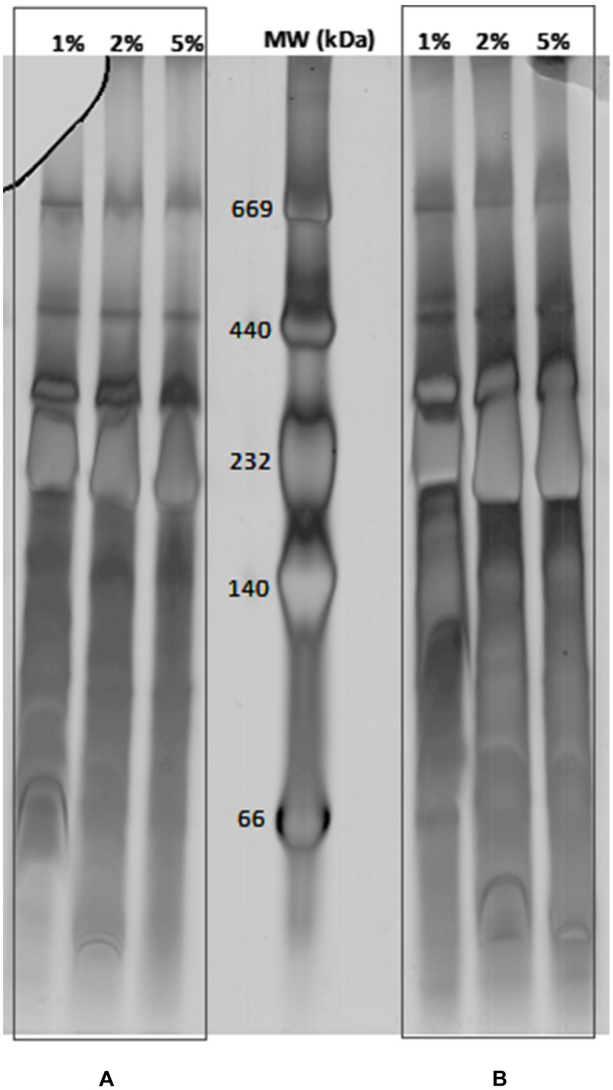

FIGURE 1 | Separation of membrane protein complexes from *C. jejuni* Strain 81–176 by BN-PAGE. 10 μg **(A)** and 20 μg **(B)** of membrane protein complexes were solubilized with DDM at concentrations ranging from 1, 2, and 5% (w/v). Mass marker are indicated in the central lane (MW in kDa).

[3]http://weblogo.threeplusone.com

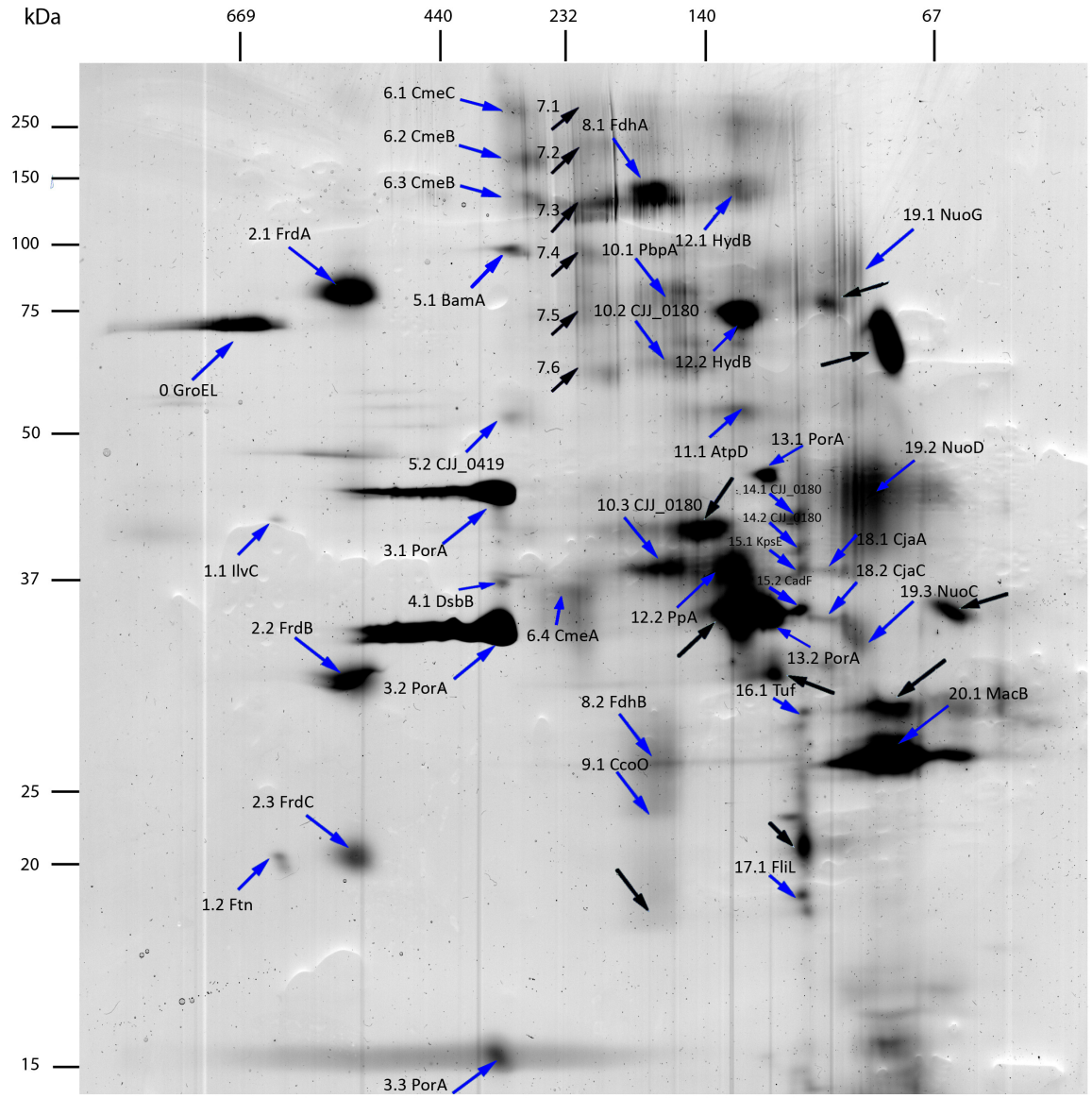

FIGURE 2 | 2D-BN/SDS-PAGE separation of membrane protein complexes of *C. jejuni* 81–176. Acrylamide gradient was 4–18% for BN-PAGE and acrylamide concentration was 10% for SDS-PAGE. Mass markers for BN-PAGE and SDS-PAGE are respectively, indicated at the top left side of the gel. Proteins identified by LC-MS/MS are indicated by blue arrows. Proteins that do not reach identification criteria after LC-MS/MS analysis are indicated with black arrows. First numbers correspond to complexes and second numbers to subunits of these complexes.

was composed of subunits from the same gene product, they were called multihomooligomeric complexes and when they were composed of different subunits, they were named multi hetero-oligomeric complexes as described before (Bernarde et al., 2010). Some complexes could not be detected due to a relatively low abundance in the membrane, solubilization parameters or separation parameters. In addition, depending on the solubilization and separation parameters more than one protein complex could run at the same molecular mass during BN-PAGE. This was observed more frequently for smaller protein complexes. In this case, the spot identification helps to separate different complexes when the biological function was previously described. The solubilization, the migration parameters, the interaction between subunits and the subunit organization in or associated with the membrane could also result in partial identification of complexes.

The identification of the spots was achieved by nanoLC MS/MS and validated using Mascot score (**Table 1** and **Supplementary Data Sheet S1**). The western blots using polyclonal antibodies anti-PorA and anti-CadF were used to target specific outer membrane proteins (**Supplementary Figure S3**). Three spots of PorA and one spot of CadF could be identified using Western-blot confirming the identification performed by LC MS/MS. In addition,

TABLE 1 | Description of membrane protein complexes identified in *C. jejuni* strain 81–176 using two-dimensional BN/SDS-PAGE.

Complex function	Complex ID	Spot ID	Access No. (NCBI)	Protein ID	Gene name	Mascot score (a)	NPM/PC (%) (b)	pI/MW (kDa) (theoretical)
Oxidative phosphory-lation	2	2.1	EAQ73056.1			413	12/20	6.36/74
		2.2	EAQ73378.1	Fumarate reductase iron-sulfur subunit	*frdB*	153	4/22	5.37/27
		2.3	EAQ73136.1	Fumarate reductase cytochrome b-556 subunit	*frdC*	38	2*/5	9.37/30
	9	9.1	EAQ72593.1	Cytochrome c oxidase, cbb3-type, subunit II	*ccoO*	136	4/23	5.86/25
	11	11.1	EAQ71910.1	F0F1 ATP synthase subunit beta	*atpD*	102	2/5	4.97/51
	19	19.1	EAQ72569.1	NADH dehydrogenase subunit G	*nuoG*	205	6/9	5.49/93
		19.2	EAQ72908.1	NADH dehydrogenase subunit D	*nuoD*	121	3/7	5.51/47
		19.3	EAQ72659.1	NADH dehydrogenase subunit C	*nuoC*	131	2/10	7.77/31
Respiration	8	8.1	EAQ72956.1	Formate dehydrogenase, alpha unit, selenocysteine-containing	*fdhA*	401	12/19	6.09/83
		8.2	EAQ72781.1	Formate dehydrogenase, iron-sulfur subunit	*fdhB*	65	2*/9	5.99/24
	12	12.1	EAQ72716.1	Quinone-reactive Ni/Fe-hydrogenase, large subunit	*hydB*	98	2/6	6.26/64
		12.2	EAQ72716.1	Quinone-reactive Ni/Fe-hydrogenase, large subunit	*hydB*	164	6/14	6.26/64
	0	0	EAQ72817.1	Chaperonin GroEL	*groEL*	698	16/39	5.02/58
Protein	4	4.1	EAQ71919.1	DsbB family disulfide bond formation protein	*dsbB*	139	3/7	8.57/57
biosynthesis and	10	10.1	EAQ73315.1	Penicillin-binding protein 1A	*pbpA*	81	3/5	8.35/73
folding		10.2	EAQ73158.1	Methyl-accepting chemotaxis protein	*CJJ_0180*	101	3/5	4.94/73
		10.3	EAQ73158.1	Methyl-accepting chemotaxis protein	*CJJ_0180*	132	4/6	4.94/73
	3	3.1	EAQ72728.1	Major outer membrane protein	*porA***	2004	14/49	4.72/46
Efflux pumps,		3.2	EAQ72728.1	Major outer membrane protein	*porA***	1989	14/48	4.72/46
virulence and		3.3	EAQ72728.1	Major outer membrane protein	*porA***	1133	8/30	4.72/46
molecules	5	5.1	EAQ73202.1	Outer membrane protein	*bamA*	70	2*/4	5.57/83
trafficking		5.2	EAQ72997.1	Conserved hypothetical protein (putative lipoprotein)	*CJJ_0419*	196	5/17	8.48/37
	6	6.1	EAQ73082.1	RND efflux system, outer membrane lipoprotein CmeC	*cmeC*	129	7/10	5.14/55
		6.2	EAQ73146.1	RND efflux system, inner membrane transporter CmeB	*cmeB*	101	2/2	6.48/114
		6.3	EAQ73146.1	RND efflux system, inner membrane transporter CmeB	*cmeB*	121	2/2	6.48/114
		6.4	EAQ72976.1	RND efflux system, membrane fusion protein CmeA	*cmeA*	102	3/10	8.29/40
	13	13.1	EAQ72728.1	Major outer membrane protein	*porA***	231	4/11	4.72/46
		13.2	EAQ72728.1	Major outer membrane protein	*porA***	419	10/30	4.72/46
	15	15.1	EAQ72952.1	Capsular polysaccharide ABC transporter	*kpsE*	136	3/8	6.22/43
		15.2	EAQ72738.1	Outer membrane fibronectin-binding protein	*cadF***	55	2/8	5.89/36
	20	20.1	EAQ73027.1	Macrolide-specific efflux protein macB	*CJJ_0636*	35	2*/1	9.25/70
	18	18.1	EAQ72087.1	CjaA protein	*cjaA*	21	1/4	5.69/31
		18.2	EAQ72374.1	CjaC protein	*cjaC*	250	6/25	6.48/28
Mobility	17	17.1	EAQ72823.1	Flagellar basal body-associated protein FliL	*fliL*	47	1/15	4.93/20
Unknown	1	1.1	EAQ73148.1	Ketol acid reductoisomerase	*ilvC*	365	8/27	6.1/37
		1.2	EAQ72988.1	Non-heme iron-containing ferritin	*ftn*	73	2/16	5.34/20
	14	14.1	EAQ73158.1	Methyl-accepting chemotaxis protein	*CJJ_0180*	94	2/4	4.94/73
		14.2	EAQ73158.1	Methyl-accepting chemotaxis protein	*CJJ_0180*	111	4/6	4.94/73
Other	16	16.1	EAQ73030.1	Elongation factor Tu	*tuf*	60	2/8	5.11/44

*None of the proteins from the complex no. 7 have been identified. (a) From all identified peptides (b) Peptides with only a significant individual ion score were considered for NPM (Number of Peptide Match) and PC (Protein Coverage). *One peptide with a non-significant score but mainly identified from y and b ions (see MS/MS fragmentation in Supplementary Data) are included to validate the identification. **Proteins verified by western blot.*

the LC MS/MS identified two supplementary spots of PorA indicating that it has a probable higher sensitivity than Western-blot according to the protein abundance. As expected, PorA, also named major outer membrane protein (MOMP) is among the predominant proteins. It was previously reported that PorA could account for 45% of the total visible membrane proteins of *C. jejuni* (Cordwell et al., 2008).

Protein Complex Identification by Two-Dimensional (2-D) Blue Native (BN)/SDS-PAGE

Overall, 55 spots were submitted to LC-MS/MS analysis (**Figure 2** and **Table 1**). Among them, nine isolated spots and all spots of complex 7 could not be identified, although attempts using different MS technologies were performed. No contamination

with exogenous protein, like keratin, was detected. The spectrograms seem to show noise-to-signal trouble shootings. Two proteins identified with a low scoring (Mascot score <30) were discarded from the analysis. The remaining spots could be grouped into 20 complexes according to their location in the gel, identification and biological functions when available. Overall, 39 proteins predicted as membrane proteins or membrane associated proteins were identified indicating the efficiency of the extraction of the protein complexes from *C. jejuni* 81–176. These complexes were grouped according to biological functions of KEGG classification (**Table 1**). Four complexes are involved in oxidative phosphorylation, two in the respiration process, seven in molecules trafficking, three in protein biosynthesis and folding, one in motility and three with unknown functions in the membrane. Altogether, 6 multi hetero-oligomeric and fourteen multihomooligomeric complexes were identified (**Table 1**). Certain identified complexes were already described in *C. jejuni* such as efflux pump CmeABC (Gibreel et al., 2007), validating this technique to identify MPC in this bacteria. However, novel complexes are presented, such as complexes 2 and 8 comprised of FrdABC and FdhAB, respectively. These complexes were already described in *Helicobacter pylori* by Bernarde et al. (2010) and *Eubacterium acidaminophilum* (Graentzdoerffer et al., 2003), respectively.

In silico Analysis of Efflux Pumps CmeABC and MacAB

Among the 20 identified complexes, subunits belonging to two efflux pumps were detected in complex 6 with CmeA, CmeB and CmeC and complex 20 with MacB (**Figure 2** and **Table 1**). The subunits of these two pumps were further investigated in this study. CmeABC is a multridrug efflux system in *Campylobacter* working as an RND efflux pump (Lin et al., 2002; Akiba et al., 2006; Grinnage-Pulley and Zhang, 2015). It contributes to the resistance acquisition of *Campylobacter* to various antimicrobials including macrolides and fluoroquinolones (Yan et al., 2006; Gibreel et al., 2007; Jeon and Zhang, 2009). This efflux pump has also an important role in the resistance to bile (Lin et al., 2003). It includes the inner membrane drug transporter CmeB, the periplasmic membrane fusion protein CmeA and the outer membrane channel CmeC. These proteins can be glycosylated at various sites (Scott et al., 2011) which could explain two CmeB proteins identified with a different molecular weight (**Figure 2**). The bioinformatics analysis confirmed the organization in operon of the two efflux pumps amongst both *C. jejuni* and *C. coli*. For the other efflux pump, the subunit MacB, previously identified to be associated with MacA, was detected in the multihomooligomeric complex 20 which belongs to the efflux pump specific to macrolides (Yum et al., 2009; Bogomolnaya et al., 2013). Using Platform MicroScope, STRING, blastp and blastn, both DNA and protein sequences of these efflux pump partners were analyzed across *C. jejuni* and *C. coli*. Genes *cmeA* and *macA* are homologous and *cmeC* is homologous to a gene encoding a putative outer membrane protein (CJJ81176_0637) located downstream to *macB*. This putative outer membrane protein contains the same functional domain TolC as the one described in CmeC suggesting that this putative protein is probably the third partner of MacAB efflux pump. Further experimental assays will be required to validate the biological function of this putative protein for macrolide efflux pump operation. The phylogenetic and functional analyses confirm the similarities between proteins sequences of subunits of these two efflux pumps across *Campylobacter* strains (**Figure 3** and **Supplementary Table S1**). CmeA and MacA belong to the HlyD superfamily showing a structure composed of the signal peptide and the non-cytoplasmic domain. The phylogenic analysis of the putative outer membrane protein CJJ81176_0637 confirmed it similarly to CmeC which likely is the third subunit of the efflux pump MacAB (**Figure 3**). Considering this data, this putative outer membrane protein was named putative MacC (putMacC) and the system MacABputC. In contrast to the similarly between sequences and structural functions of CmeC and putMacC in one hand and CmeA and MacA in the other hand, differences observed between CmeB and MacB is probably at the origin of the restriction of MacB to macrolides efflux.

Analysis of the Potential Regulation of MacABC

The efflux pump CmeABC was previously shown to be regulated by CmeR and CosR (Lin et al., 2005; Hwang et al., 2012; Grinnage-Pulley et al., 2016) while no regulation was identified for MacABC. Using the CosR binding box sequence (5′-wdnnhdwnwhwwTTwnhhTTd- 3′) previously described by Turonova et al. (2017), *in silico* analysis revealed the presence of a CosR-like DNA-binding box upstream to *macA* in *C. jejuni* 81–176. Screening for the presence of the CosR binding box in the promoter region of *mac*A in the complete genomes of *C. jejuni* and *C. coli,* this consensus sequence was found in *C. jejuni* but not in *C. coli*. All the binding box DNA sequences of CosR in the *cme*A promoter region of both *C. jejuni* and *C. coli* strains and the *mac*A promoter region of *C. jejuni* strains were compared so as to propose a consensus sequence logo refined for CosR-binding box (**Figure 4**).

Distribution of Gene Subunit Encoding CmeABC and MacABputC Across Bacteria Domain

Analyses of genes encoding proteins belonging to these two efflux pumps using across Bacteria domain Blastp analysis indicates that they are mainly observed in proteobacteria (**Figure 5** and **Supplementary Table S2**). CmeA, CmeB, and CmeC were mainly found in the delta/epsilon proteobacteria groups while MacABputC also highly more represented in beta and gamma proteobacteria. Proteins of MacABputC were also found in the fusobacteriaceae family belonging to the fusobacterial phylum (**Figure 5** and **Supplementary Table S2**). The presence of this third subunit in outer membrane (putMaC and CmeC) is probably crucial for the functionality of these complexes.

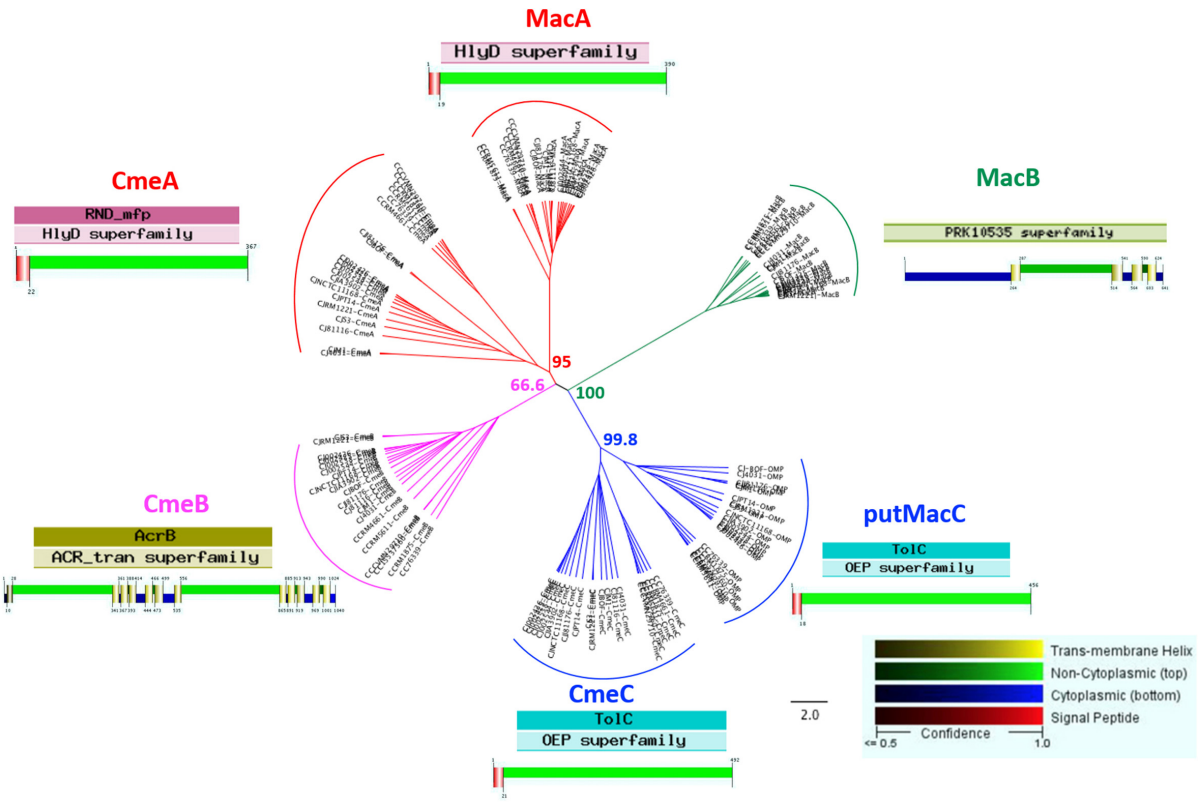

FIGURE 3 | Phylogenetic tree of proteins belonging to efflux pumps CmeABC and MacABputC. Alignment was performed using MAFFT (Geneious R9) with functional domain and protein structure (Philus) in 14 *C. jejuni* strains and 6 *C. coli* strains. Bootstraps percentages were added to internal branches for 1000 replicates. Strains used in this study are listed in **Supplementary Table S1**.

DISCUSSION

Beyond the protein mapping at the organism or a biological compartment scale using holistic approaches, identifying functional multi-subunit entities at the proteome level is a real challenge. Many cellular processes are carried out by sophisticated multi-subunit protein machineries, i.e., different protein complexes maintained by stable protein interactions. These functional entities could be defined as protein complexes composed of a minimal biologically structure of assembled protein subunits necessary for a specific cellular process (Reisinger and Eichacker, 2007). Membrane proteocomplexome of *C. jejuni* 81–176 cultivated in optimal growth conditions was explored using 2-D BN/SDS PAGE. The prerequisite goal was to obtain reproducible profiles after optimizing and stabilizing homemade strips. The objective was reached when three consecutive gels with resolved spots could be performed. Twenty-one MPCs were found with this method in *C. jejuni* 81–176 (**Figure 6**). We found incomplete complexes suggesting that subunits were probably lost during MPC extraction or unidentified by LC MS/MS.

Oxidative Phosphorylation

Oxidative phosphorylation is the metabolic pathway in which bacteria use enzymatic complexes to re-oxidize cofactors and produce ATP. It ensures the electron transfer between electron donors and the final electron acceptor which is oxygen for aerobic and microaerobic bacteria such as *C. jejuni*. The redox reactions are carried out by a series of four protein complexes (I, II, III, and IV) located in the inner membrane. Membrane proteocomplexomic profiling revealed the presence of complexes involved in oxidative phosphorylation. Complex 19 corresponds to the NADH ubiquinone oxidoreductase, the first complex of the oxidative phosphorylation chain. This complex catalyzes the transfer of two electrons from NADH to quinone with the translocation of four protons across the inner membrane: $NADH + H^+ + Q + 4H^+_{in} \rightarrow NAD^+ + QH_2 + 4H^+_{out}$ (Baranova et al., 2007; Weerakoon and Olson, 2008; Efremov and Sazanov, 2011; Baradaran et al., 2013). Genomic analysis revealed fourteen genes *nuo* organized in operon in *C. jejuni* and *C. coli* genomes with a highly conserved synteny. NuoFEGDCBI are involved in the hydrophilic domain of the NADH dehydrogenase complex while NuoAHJKLMN is localized into the membrane (Baradaran et al., 2013). The partners of this complex NuoC, NuoD and NuoG detected from our MPC fingerprinting are predicted to be localized on the basal part of the hydrophilic domain, close to the inner membrane. In *Escherichia coli*, NuoC and NuoD are fused and NuoG is close to them (Baranova et al., 2007; Baradaran et al., 2013). If these subunits are similarly organized in *C. jejuni*, this would indicate that 2%

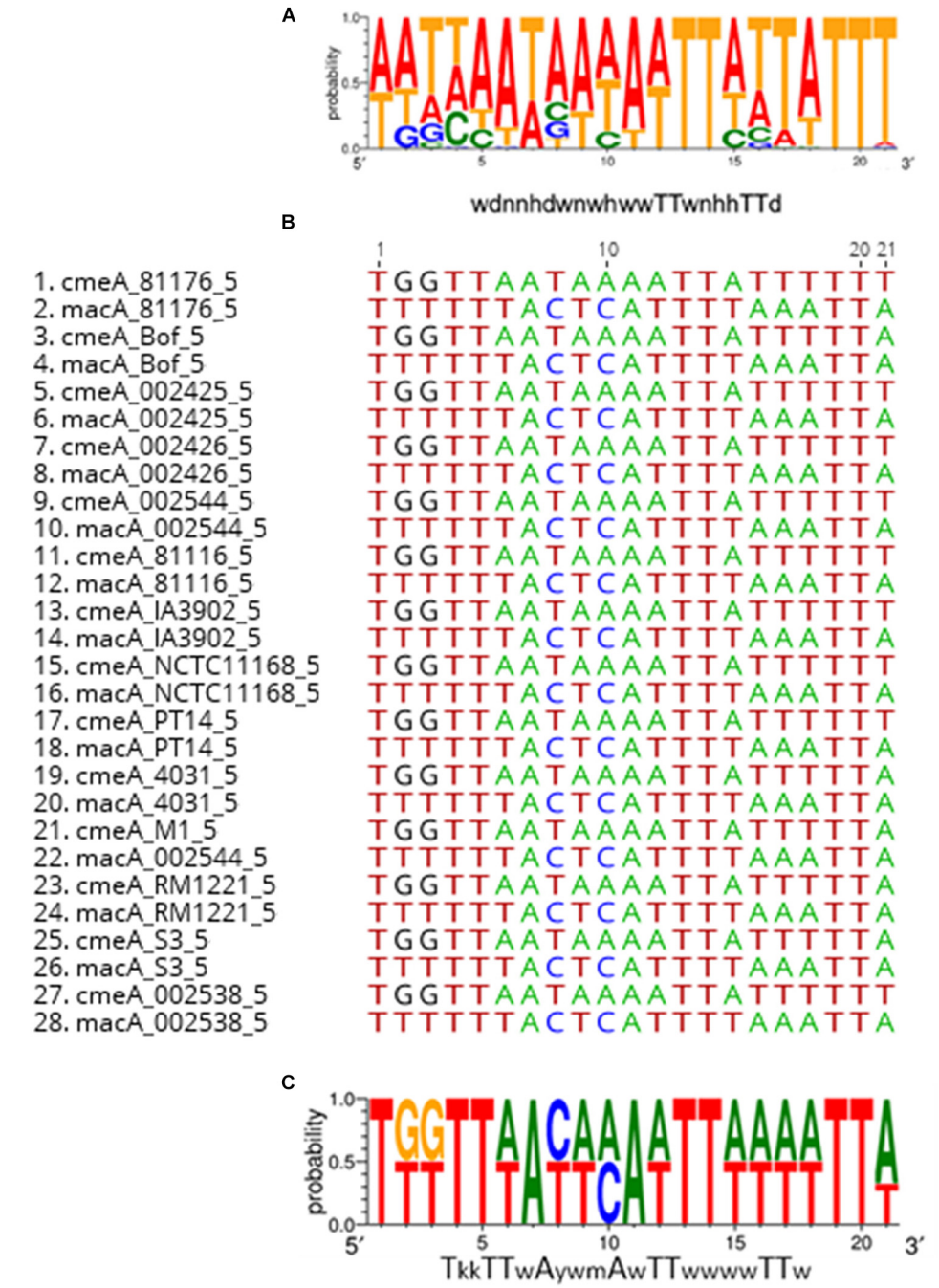

FIGURE 4 | Consensus sequence logo of CosR-binding box of the upstream sequences of genes with CosR-binding capacity (*cme*A and *mac*A). Consensus sequence logo of CosR-binding box defined by Turonova et al. (2017) **(A)** alignment of upstream sequences of cmeA and macA by Geneious 9.1.8 **(B)** Consensus sequence logo of CosR-binding box redefined **(C)**. w-A or T; y-C or T; m-A or C and k-G or T.

DMM MPC extraction, detection and subunit identification mainly selected this part of NADH dehydrogenase complex. The complex 2 corresponds to complex II of the oxidative phosphorylation chain. The fumarate reductase complex is generally composed of FrdA, FrdB and FrdC (Weingarten et al., 2009; Guccione et al., 2010; Jardim-Messeder et al., 2017). All three subunits were detected and identified on all the proteocomplexomic finger printings performed in the present study. In *C. jejuni*, this inner membrane system is bifunctional being able to catalyze both succinate oxidation and fumarate reduction (Guccione et al., 2010; Hofreuter, 2014). The succinate oxidation is favored under microaerobic conditions

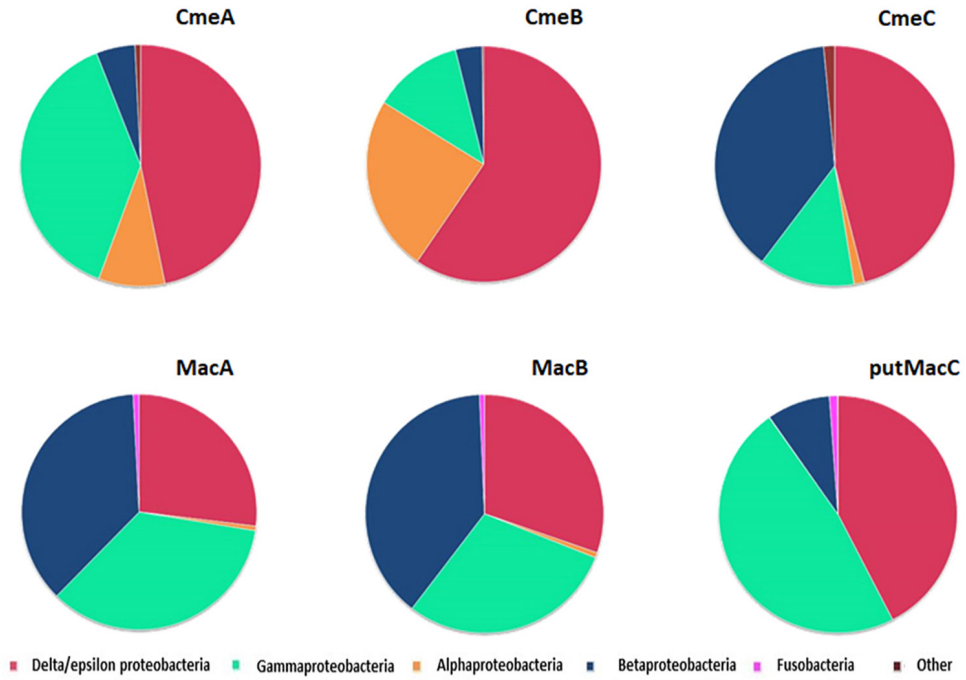

FIGURE 5 | Distribution of CmeABC and MacABputC subunits in bacteria using Blastp with *C. jejuni* 81–176 protein sequences of each subunit as queries in RefSeq_protein database. The data are based on the hits presented in **Supplementary Table S2**.

while the fumarate reduction is operated under oxygen-limited conditions. All three genes are close located on the genome of both *C. jejuni* and *C. coli*. FrdA is the fumarate reductase flavoprotein, FrdB is the iron-sulfur subunit and FrdC is the cytochrome B-556 subunit. This fumarate reductase complex FrdABC was also described in *H. pylori* (Pyndiah et al., 2007). A fourth partner, FrdD is described in *E. coli* (Rothery et al., 2005). However, the bioinformatic analyses did not reveal any homologous gene to FrdD in *C. jejuni* and *C. coli* genomes. This would indicate that complex 2 does exist and might be functional in *C. jejuni* and *H. pylori* without FrdD subunit. Any subunit of the ubiquinol-cytochrome c reductase, complex III of the oxidative phosphorylation, was not detected in this study. However, predicted functional partners of this proton pump were detected in *C. jejuni* genome: *petA* encoding the iron sulfur subunit, *petB* encoding the cytochrome b subunit and *petC* encoding the cytochrome c1 subunit which indicates the absence of this complex in optimal growth conditions or DMM limitations to extract all MPCs. Partners, function and pathways of cytochrome c oxidase (complex IV) in *Campylobacter* remain elusive. It is encoded by *ccoNOPQ*. The protein CcoO (Complex 9) was detected in our study. It corresponds to the subunit II of cytochrome c oxidase complex with a high affinity for O_2 (Cosseau and Batut, 2004; Hofreuter, 2014). In complex V, the ATP synthase is usually composed of nine subunits, AtpABCDEFFGH often identified as subunit α, A, ε, β, C, B, B', γ and δ (Rastogi and Girvin, 1999; Altendorf et al., 2000; Cingolani and Duncan, 2011; Okuno et al., 2011). The bioinformatics analyses revealed that genes *atpF, atpF', atpH, atpA, atpG, atpD* and *atpC* are close located in *C. jejuni* and *C. coli* genomes while genes *atpB* and *atpE* are present in different loci. The proteocomplexomic analysis identified AptD (also called subunit β in complex 11). The membrane-bound ATP synthase is a key energy carrier in bacteria using the energy of an electrochemical ion gradient and the synthesis of ATP from ADP with inorganic phosphate (Rastogi and Girvin, 1999; Altendorf et al., 2000; Cingolani and Duncan, 2011; Okuno et al., 2011).

Respiration

The complex formate dehydrogenase (complex 8) contributes to the respiration process by producing CO_2 from formate oxidation (Hofreuter, 2014). This complex is composed of two FdhA and FdhB, two subunits detected on complexomic fingerprinting. As an asaccharolytic microorganism, carbon supply in *Campylobacter* is ensured from amino and organic acids and formate is one of the preferred substrate when hosted in poultry. The second detected complex involved the respiration process is hydrogenase complex HydAB complex 12. Two HydB with different weights (around 75 kDa and 130 kDa) were identified in complex 12 indicating the possible presence of a dimeric form of HydB (spot 12.1) in *C. jejuni* membrane. For these two complexes, single conserved copies of the encoding genes were observed in all analyzed genomes except for *C. jejuni* 4031 where a second copy of *FdhA* was found. Two other subunits for each complex (FdhC/FdhD and HydC/HydD) were previously identified in *C. jejuni* (Andreesen and Makdessi, 2008; Smart et al., 2009; Weerakoon et al.,

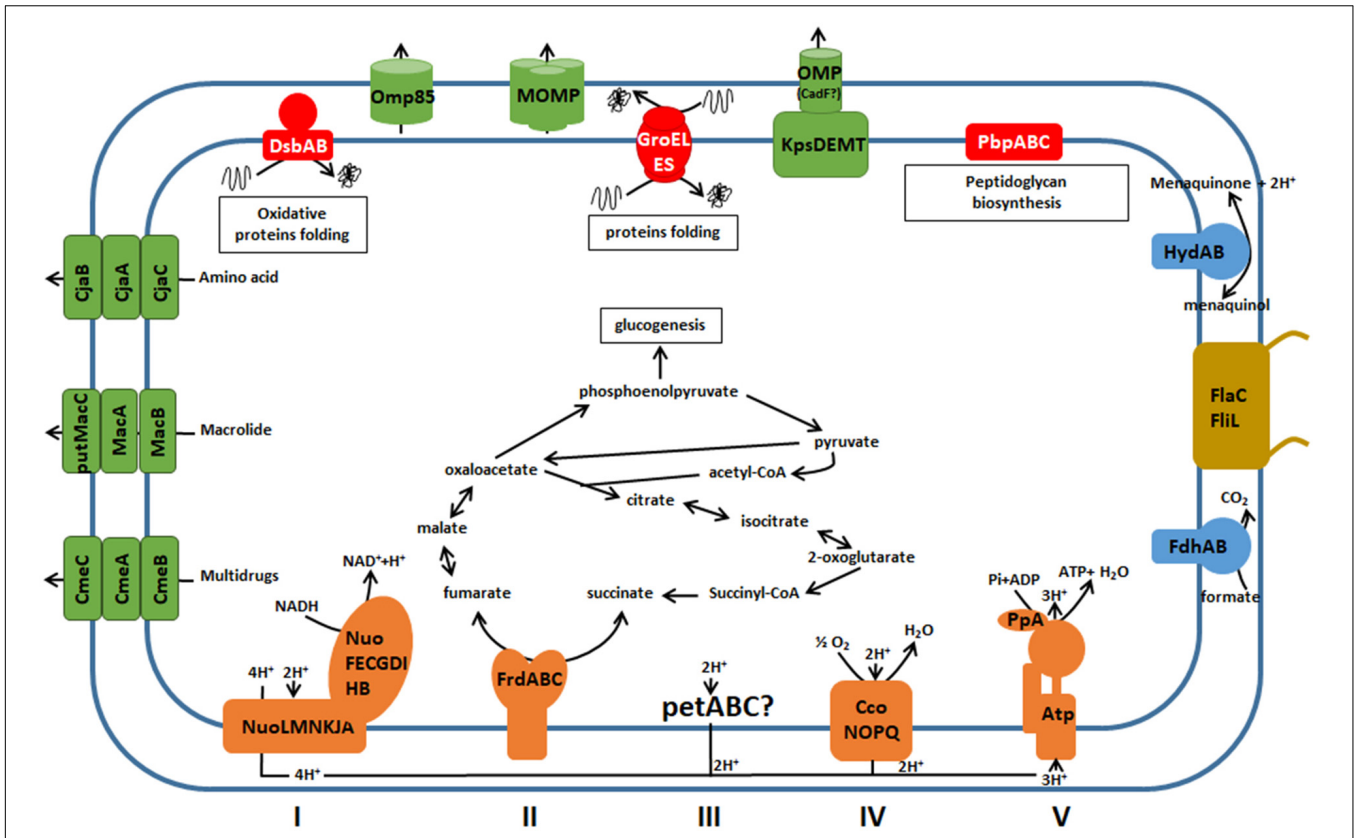

FIGURE 6 | Membrane protein complexes identified by 2-D BN/SDS-PAGE in *C. jejuni* 81–176. Color of complexes corresponds to their function in cell: Green for molecules trafficking, Red for protein biosynthesis and folding, Blue for respiration, Yellow for motility, and Orange for the oxidative phosphorylation.

2009; Pryjma et al., 2012; Shaw et al., 2012; Hofreuter, 2014). These two other partners interact with the main ones only under environmental stress conditions. The genes encoding these environment dependent conditions are present on *C. jejuni* and *C. coli* genomes. As MPCs of *C. jejuni* 81–176 were explored under optimal growth in our study, it is not a surprise not having detected them.

Biosynthesis and Folding of Proteins

Several proteins are biosynthesized and folded by different complexes localized in membrane. Different membrane protein complexes were extracted and identified in this study.

The chaperonin GroEL (complex 0) is a cylindrical complex with two stacked heptameric rings with ATPase activity that binds non-native substrate protein (SP). GroEL is associated with cofactor GroES and form a nano-cage where SP can be folded up (Klancnik et al., 2006; Chi et al., 2015; Haldar et al., 2015; Motojima and Yoshida, 2015; Hayer-Hartl et al., 2016). As its cofactor GroES has a too small molecular weight (10 kDa), it could not be detected on our profiling fingerprinting. Another complex (complex 4) playing a role in protein folding was detected. DsbB-DsbA is a disulfide bond generation system operating in the oxidative pathway (Inaba et al., 2006; Inaba and Ito, 2008; Ito and Inaba, 2008; Grabowska et al., 2011; Sperling et al., 2013). In this study, only DsbB subunit was identified although two *dsb*A genes with 51% homology were present in *C. jejuni* 81–176 genome. DsbB localized in inner-membrane interacts with the periplasmic dithiol oxidase DsbA (Inaba et al., 2006; Inaba and Ito, 2008).

Molecules Trafficking in Membrane

Several membrane protein complexes identified in this study have a function in molecule trafficking through the *C. jejuni* 81–176 membrane. These complexes play an important role in adaptation and virulence capabilities. For instance, the major *Campylobacter* porin PorA was extracted and identified in the complexes 3 and 13. This porin corresponding to MOMP, involved in the adaptation of *Campylobacter* to host environments (De et al., 2000; Zhang et al., 2000; Clark et al., 2007; Ferrara et al., 2016), is a multihomooligomeric porin with three PorA subunits (Zhang et al., 2000; Ferrara et al., 2016). This porin can be identified in three conformational forms including the folded monomer (35 kDa), the denatured monomer (40 to 48 kDa), and the native trimer (120 to 140 kDa) (Huyer et al., 1986; Zhang et al., 2000). In our gel, two complexes corresponding to native trimer MOMP at two different weights were identified. The complex 13 was estimated between 120–140 kDa and after subunit separation proteins corresponding to the folded monomer at 35 kDa and the denatured monomer between

40 and 48 kDa could be detected as previously described by Zhang et al. (2000). In the complex 3, the spot with apparent weight between 350 kDa and 400 kDa could correspond to the fusion of two trimeric MOMPs. The associated forms of MOMP in the complex 3 with likely a folded monomer, denatured monomer and a truncated form at 16 kDa was not previously described.

Antibiotic Efflux Pumps

In this work, units of complexes corresponding to two efflux pumps CmeABC and MacAB were detected (complex 6 and 20). These two efflux pumps were known to play a role in antimicrobials resistance. The multidrug efflux pump CmeABC was more studied compared to the macrolide efflux pump MacABputC in *Campylobacter* (Lin et al., 2002, 2003; Akiba et al., 2006; Yan et al., 2006; Gibreel et al., 2007; Jeon and Zhang, 2009; Grinnage-Pulley and Zhang, 2015). In our study, the genetic and proteomic similarities between the constitutive proteins of these efflux pumps were highlighted by bioinformatics analyses. We were able to identify a potential third partner of the macrolide efflux pump, putMacC with a functional domain TolC similarly to CmeC. Subunits composing these two efflux pumps were mainly found in the proteobacteria phylum. Furthermore, the presence of CosR-binding box of the upstream sequences of *macA* was found in *C. jejuni* strains. However, this CosR-binding box could not be detected upstream *macA* in *C. coli* strains. Further biological analyses are required to explore the potential rule of CosR to regulate expression of transcripts of this macrolide efflux pump and to state its presumptive species specificity.

New Membrane Protein Complexes

Two complexes (complex 1 and 14) were extracted and their subunits could be identified. The subunits of the complex 1, IlvC a ketol-acid reductoisomerase and Ftn a non-heme iron-containing ferritin were detected on the same horizontal line. IlvC is involved in L-isoleucine and L-valine biosynthesis (Pyndiah et al., 2007; Wu et al., 2016) while Ftn has a role in storing available cytosolic iron and to reduce cellular toxicity under conditions of intermittent or constant iron excess during infection (Wai et al., 1996). There are few information concerning these two proteins in *Campylobacter* and no interactions were reported. Complexes 10 and 14 are made of two isoforms of the methyl accepting chemotaxis protein CJJ_0180. This protein plays a role in chemotaxis and colonization of the gastrointestinal tract (Gonzalez et al., 1998; Zautner et al., 2012; Li et al., 2014; Chandrashekhar et al., 2015). However, weight of complexes 10 and 14 are different, indicating that these multihomooligomeric complex might be composed of different forms of the subunit as it was described for MOMP complex.

To conclude, this study is the first 2-D BN/SDS-PAGE method applied to identify membrane proteocomplexome of *Campylobacter jejuni*. Although not all the subunits of functional complexes in the membrane of *C. jejuni* could be detected, functional genomics analyses assisted us in reconstituting probable functional complexes. For instance, we were able to pinpoint a potential third partner in the macrolide efflux pump and raised hypothesis concerning its regulation by CosR. The 2-D BN/SDS-PAGE raised also limitations for studying bacterial proteocomplexomes. Assignment of spots to independent membrane protein complexes in low molecular weight areas is less easy. In certain cases, protein complexes were probably too weakly expressed as compared to others, or absent in optimal conditions. The tune up of DDM concentration, the conformation of complexes and their location, as full or part of the membrane, might contribute to the extraction of entire and stable complexes. Altogether, this study has allowed to better described the membrane proteocomplexome of *C. jejuni* providing new focus for further studies of protein complexes previously annotated with unknown functions.

DATA AVAILABILITY STATEMENT

The raw data supporting the conclusions of this article will be made available by the authors, without undue reservation, to any qualified researcher.

AUTHOR CONTRIBUTIONS

OT conceived the work and contributed to finishing the manuscript writing and preparing the figures. SS, LC, and AG performed the experiments. AG prepared the manuscript and the figures. OT, ED, LC, FB-H, and AM revised the manuscript. All authors contributed to the article and approved the submitted version.

FUNDING

AG was financed by INRAE through the program RFI "Food for Tomorrow" in region Pays de la Loire. This study was supported by Comp*Camp* project. This work was presented in part at the 19th International Workshop on Campylobacter, Helicobacter and Related Organisms: CHRO, 2017.

ACKNOWLEDGMENTS

The authors are grateful to Pr Mégraud (University of Bordeaux, INSERM, UMR1053 Bordeaux Research in Translational Oncology, BaRITOn, Bordeaux) for helping us to develop complexomic analyses. Thank you to Lucile Bougro for her technical assistance.

SUPPLEMENTARY MATERIAL

The Supplementary Material for this article can be found online at: https://www.frontiersin.org/articles/10.3389/fmicb.2020.530906/full#supplementary-material

Supplementary Figure 1 | Homemade strips in 5 steps to separate the subunits of protein complexes in a reproducing manner. **(A)** Cut the strip with a clean glass plate following the well where the sample was deposited, equilibrate the gel lane in DTT and iodoacetamide buffers as indicated in materials and methods; **(B)** lay the gel strip on the wet plastic support using clean forceps; **(C)** Stick the plastic face of the strip on the glass behind; **(D)** Slide the strip until touching the precast polyacrylamide gel; **(E)** Fill the gap and overlaid the strip with low melting agarose using a sterile syringe.

Supplementary Figure 2 | 2D-BN-SDS-PAGE profiling before **(A)** and after optimization **(B)** of protein complexes and their subunit separation. The first dimension for complex separation was performed on 4 to 18% acrylamide gradient gels with 2% Dodecyl-β-D-Maltoside (DDM).

Supplementary Figure 3 | 2D-BN/SDS-PAGE western blot, using antibody anti-MOMP **(A)** and antibody anti-CadF **(B)**. The image in the middle corresponds to the identified proteins complexes before the Western-blot the black arrow indicate the identified proteins with anti-PorA antibody and the white arrow the identify protein with anti-CadF antibody on the 2D-BN/SDS-PAGE.

Supplementary Table 1 | *Campylobacter* strains with complete genome sequencing used in this study.

Supplementary Table 2 | Number of hits corresponding to the protein sequence of each three subunits of efflux pumps Cme and Mac of *C. jejuni* 81–176 in RefSeq_protein database. One hit is the result of sequence similarity using comparison tool Blastp with the parameters indicated in materials and methods section. The number of the different occurrences is defined by the threshold of word size.

REFERENCES

Akiba, M., Lin, J., Barton, Y. W., and Zhang, Q. J. (2006). Interaction of CmeABC and CmeDEF in conferring antimicrobial resistance and maintaining cell viability in *Campylobacter jejuni*. *J. Antimicrob. Chemother.* 57, 52–60. doi: 10.1093/jac/dki419

Alshekhlee, A., Hussain, Z., Sultan, B., and Katirji, B. (2008). Guillain-Barre syndrome - Incidence and mortality rates in US hospitals. *Neurology* 70, 1608–1613. doi: 10.1212/01.wnl.0000310983.38724.d4

Altekruse, S. F., Stern, N. J., Fields, P. I., and Swerdlow, D. L. (1999). *Campylobacter jejuni* - An emerging foodborne pathogen. *Emerg. Infect. Dis* 5, 28–35. doi: 10.3201/eid0501.990104

Altendorf, K., Stalz, W. D., Greie, J. C., and Deckers-Hebestreit, G. (2000). Structure and function of the F-o complex of the ATP synthase from *Escherichia coli*. *J. Exp. Biol.* 203, 19–28.

Andreesen, J. R., and Makdessi, K. (2008). "Tungsten, the surprisingly positively acting heavy metal element for prokaryotes," in *Incredible Anaerobes: From Physiology to Genomics to Fuels*, eds J. Wiegel, R. J. Maier, and M. W. W. Adams (Oxford: Blackwell Publishing), 215–229. doi: 10.1196/annals.1419.003

Ang, C. W., De Klerk, M. A., Endtz, H. P., Jacobs, B. C., Laman, J. D., Van Der Meche, F. G. A., et al. (2001). Guillain-Barre syndrome- and Miller Fisher syndrome-associated *Campylobacter jejuni* lipopolysaccharides induce anti-GM(1) and anti-GQ(1b) antibodies in rabbits. *Infect. Immun.* 69, 2462–2469. doi: 10.1128/iai.69.4.2462-2469.2001

Asakura, H., Kawamoto, K., Murakami, S., Tachibana, M., Kurazono, H., Makino, S., et al. (2016). Ex vivo proteomics of *Campylobacter jejuni* 81-176 reveal that FabG affects fatty acid composition to alter bacterial growth fitness in the chicken gut. *Res. Microbiol.* 167, 63–71. doi: 10.1016/j.resmic.2015.10.001

Atack, J. M., and Kelly, D. J. (2009). Oxidative stress in *Campylobacter jejuni*: responses, resistance and regulation. *Future Microbiol.* 4, 677–690. doi: 10.2217/fmb.09.44

Baradaran, R., Berrisford, J. M., Minhas, G. S., and Sazanov, L. A. (2013). Crystal structure of the entire respiratory complex I. *Nature* 494, 443–448. doi: 10.1038/nature11871

Baranova, E. A., Holt, P. J., and Sazanov, L. A. (2007). Projection structure of the membrane domain of *Escherichia coli* respiratory complex I at 8 angstrom resolution. *J. Mol. Biol.* 366, 140–154. doi: 10.1016/j.jmb.2006.11.026

Bell, J., Jerome, J., Plovanich-Jones, A., Smith, E., Gettings, J., Kim, H., et al. (2013). Outcome of infection of C57BL/6 IL-10(-/-) mice with *Campylobacter jejuni* strains is correlated with genome content of open reading frames up- and down-regulated in vivo. *Microb. Pathog.* 54, 1–19. doi: 10.1016/j.micpath.2012.08.001

Bernarde, C., Lehours, P., Lasserre, J. P., Castroviejo, M., Bonneu, M., Megraud, F., et al. (2010). Complexomics study of two *Helicobacter* pylori strains of two pathological origins: potential targets for vaccine development and new insight in bacteria metabolism. *Mol. Cell. Proteomics* 9, 2796–2826. doi: 10.1074/mcp.m110.001065

Biasini, M., Bienert, S., Waterhouse, A., Arnold, K., Studer, G., Schmidt, T., et al. (2014). SWISS-MODEL: modelling protein tertiary and quaternary structure using evolutionary information. *Nucleic Acids Res.* 42, W252–W258.

Bieche, C., De Lamballerie, M., Chevret, D., Federighi, M., and Tresse, O. (2012). Dynamic proteome changes in *Campylobacter jejuni* 81-176 after high pressure shock and subsequent recovery. *J. Proteom.* 75, 1144–1156. doi: 10.1016/j.jprot.2011.10.028

Black, R. E., Levine, M. M., Clements, M. L., Hughes, T. P., and Blaser, M. J. (1988). Experimental *Campylobacter jejuni* Infection in Humans. *J. Infect. Dis.* 157, 472–479. doi: 10.1093/infdis/157.3.472

Bogomolnaya, L. M., Andrews, K. D., Talamantes, M., Maple, A., Ragoza, Y., Vazquez-Torres, A., et al. (2013). The ABC-Type Efflux Pump MacAB Protects *Salmonella enterica* serovar Typhimurium from Oxidative Stress. *mBio* 4:11.

Boyanova, L., Gergova, G., Spassova, Z., Koumanova, R., Yaneva, P., Mitov, I., et al. (2004). Campylobacter infection in 682 Bulgarian patients with acute enterocolitis, inflammatory bowel disease, and other chronic intestinal diseases. *Diagn. Microbiol. Infect. Dis* 49, 71–74. doi: 10.1016/j.diagmicrobio.2003.12.004

Castano-Rodriguez, N., Kaakoush, N. O., Lee, W. S., and Mitchell, H. M. (2015). Dual role of *Helicobacter* and *Campylobacter* species in IBD: a systematic review and meta-analysis. *Gut* 66, 235–249.

Chandrashekhar, K., Gangaiah, D., Pina-Mimbela, R., Kassem, I. I., Jeon, B. H., and Rajashekara, G. (2015). Transducer like proteins of *Campylobacter jejuni* 81-176: role in chemotaxis and colonization of the chicken gastrointestinal tract. *Front. Cell. Infect. Microbiol.* 5:46. doi: 10.3389/fcimb.2015.00046

Chi, H. X., Wang, X. Q., Li, J. Q., Ren, H., and Huang, F. (2015). Folding of newly translated membrane protein CCR5 is assisted by the chaperonin GroEL-GroES. *Sci. Rep.* 5:11.

Cingolani, G., and Duncan, T. M. (2011). Structure of the ATP synthase catalytic complex (F-1) from *Escherichia coli* in an autoinhibited conformation. *Nat. Struct. Mol. Biol.* 18, 701–U100.

Clark, C. G., Beeston, A., Bryden, L., Wang, G. H., Barton, C., Cuff, W., et al. (2007). Phylogenetic relationships of *Campylobacter jejuni* based on porA sequences. *Can. J. Microbiol.* 53, 27–38.

Cordwell, S. J., Alice, C. L. L., Touma, R. G., Scott, N. E., Falconer, L., Jones, D., et al. (2008). Identification of membrane-associated proteins from *Campylobacter jejuni* strains using complementary proteomics technologies. *Proteomics* 8, 122–139. doi: 10.1002/pmic.200700561

Cosseau, C., and Batut, J. (2004). Genomics of the ccoNOQP-encoded cbb(3) oxidase complex in bacteria. *Arch. Microbiol.* 181, 89–96. doi: 10.1007/s00203-003-0641-5

Crooks, G. E., Hon, G., Chandonia, J. M., and Brenner, S. E. (2004). WebLogo: a sequence logo generator. *Genome Res.* 14, 1188–1190. doi: 10.1101/gr.849004

De, E., Jullien, M., Labesse, G., Pages, J. M., Molle, G., and Bolla, J. M. (2000). MOMP (major outer membrane protein) of *Campylobacter jejuni*; a versatile pore-forming protein. *FEBS Lett.* 469, 93–97. doi: 10.1016/s0014-5793(00)01244-8

Dresler, J., Klimentova, J., and Stulik, J. (2011). Bacterial protein complexes investigation using blue native PAGE. *Microbiol. Res.* 166, 47–62. doi: 10.1016/j.micres.2010.01.005

Efremov, R. G., and Sazanov, L. A. (2011). Structure of the membrane domain of respiratory complex I. *Nature* 476, 414–U462.

EFSA (2016). Scientific report of EFSA and ECDC - The European Union summary report on trends and sources of zoonoses, zoonotic agents and food-borne outbreaks in 2014. *EFSA J.* 13:4329.

EFSA, and ECDC (2018). European Food Safety Authority, European Centre for Disease Prevention and Control: The European Union Summary Report on Trends and Sources of Zoonoses, Zoonotic Agents and Food-borne Outbreaks in 2017. *EFSA J.* 16:5500.

Epps, S. V. R., Harvey, R. B., Hume, M. E., Phillips, T. D., Anderson, R. C., and Nisbet, D. J. (2013). Foodborne campylobacter: infections, metabolism, pathogenesis and reservoirs. *Int. J. Environ. Res. Public Health* 10, 6292–6304. doi: 10.3390/ijerph10126292

Ferrara, L. G. M., Wallat, G. D., Moynié, L., Dhanasekar, N. N., Aliouane, S., Acosta-Gutiérrez, S., et al. (2016). MOMP from *Campylobacter jejuni* Is a Trimer of 18-Stranded β-Barrel Monomers with a Ca2 + Ion Bound at the Constriction Zone. *J. Mol. Biol.* 428, 4528–4543. doi: 10.1016/j.jmb.2016.09.021

Gibreel, A., Wetsch, N. M., and Taylor, D. E. (2007). Contribution of the CmeABC efflux pump to macrolide and tetracycline resistance in *Campylobacter jejuni*. *Antimicrob. Agents Chemother.* 51, 3212–3216. doi: 10.1128/aac.01592-06

Gonzalez, I., Richardson, P. T., Collins, M. D., and Park, S. F. (1998). Identification of a gene encoding a methyl-accepting chemotaxis-like protein from Campylobacter coli and its use in a molecular typing scheme for campylobacters. *J. Appl. Microbiol.* 85, 317–326. doi: 10.1046/j.1365-2672.1998.00510.x

Grabowska, A. D., Wandel, M. P., Lasica, A. M., Nesteruk, M., Roszczenko, P., Wyszynska, A., et al. (2011). *Campylobacter jejuni* dsb gene expression is regulated by iron in a Fur-dependent manner and by a translational coupling mechanism. *BMC Microbiol.* 11:16. doi: 10.1186/1471-2180-11-166

Graentzdoerffer, A., Rauh, D., Pich, A., and Andreesen, J. R. (2003). Molecular and biochemical characterization of two tungsten- and selenium-containing formate dehydrogenases from Eubacterium acidaminophilum that are associated with components of an iron-only hydrogenase. *Arch. Microbiol.* 179, 116–130. doi: 10.1007/s00203-002-0508-1

Grinnage-Pulley, T., Mu, Y., Dai, L., and Zhang, Q. J. (2016). Dual Repression of the Multidrug Efflux Pump CmeABC by CosR and Cmer in *Campylobacter jejuni*. *Front. Microbiol.* 7:1097. doi: 10.3389/fmicb.2016.01097

Grinnage-Pulley, T., and Zhang, Q. J. (2015). Genetic basis and functional consequences of differential expression of the CmeABC Efflux Pump in *Campylobacter jejuni* Isolates. *PLoS One* 10:e131534. doi: 10.1371/journal.pone.0131534

Guccione, E., Hitchcock, A., Hall, S. J., Mulholland, F., Shearer, N., Van Vliet, A. H. M., et al. (2010). Reduction of fumarate, mesaconate and crotonate by Mfr, a novel oxygen-regulated periplasmic reductase in *Campylobacter jejuni*. *Environ. Microbiol.* 12, 576–591. doi: 10.1111/j.1462-2920.2009.02096.x

Guyard-Nicodeme, M., Tresse, O., Houard, E., Jugiau, F., Courtillon, C., El Manaa, K., et al. (2013). Characterization of *Campylobacter* spp. transferred from naturally contaminated chicken legs to cooked chicken slices via a cutting board. *Int. J. Food Microbiol.* 164, 7–14. doi: 10.1016/j.ijfoodmicro.2013.03.009

Hald, B., Skov, M. N., Nielsen, E. M., Rahbek, C., Madsen, J. J., Waino, M., et al. (2016). *Campylobacter jejuni* and Campylobacter coli in wild birds on Danish livestock farms. *Acta Vet. Scand.* 58:11.

Haldar, S., Gupta, A. J., Yan, X., Miličiæ, G., Hartl, F. U., and Hayer-Hartl, M. (2015). Chaperonin-assisted protein folding: relative population of asymmetric and symmetric GroEL:GroES Complexes. *J. Mol. Biol.* 427, 2244–2255. doi: 10.1016/j.jmb.2015.04.009

Hayer-Hartl, M., Bracher, A., and Hartl, F. U. (2016). The GroEL-GroES Chaperonin Machine: a Nano-Cage for Protein Folding. *Trends Biochem. Sci.* 41, 62–76. doi: 10.1016/j.tibs.2015.07.009

Hofreuter, D. (2014). Defining the metabolic requirements for the growth and colonization capacity of *Campylobacter jejuni*. *Front. Cell. Infect. Microbiol.* 4:137. doi: 10.3389/fcimb.2014.00137

Hue, O., Le Bouquin, S., Laisney, M.-J., Allain, V., Lalande, F., Petetin, I., et al. (2010). Prevalence of and risk factors for *Campylobacter* spp. contamination of broiler chicken carcasses at the slaughterhouse. *Food Microbiol.* 27, 992–999. doi: 10.1016/j.fm.2010.06.004

Huyer, M., Parr, T. R., Hancock, R. E. W., and Page, W. J. (1986). Outer-membrane porin protein of *Campylobacter-jejuni*. *FEMS Microbiol. Lett.* 37, 247–250. doi: 10.1111/j.1574-6968.1986.tb01803.x

Hwang, S., Zhang, Q. J., Ryu, S., and Jeon, B. (2012). Transcriptional Regulation of the CmeABC Multidrug Efflux Pump and the KatA Catalase by CosR in *Campylobacter jejuni*. *J. Bacteriol.* 194, 6883–6891. doi: 10.1128/jb.01636-12

Inaba, K., and Ito, K. (2008). Structure and mechanisms of the DsbB-DsbA disulfide bond generation machine. *Biochim. Biophys. Acta* 1783, 520–529. doi: 10.1016/j.bbamcr.2007.11.006

Inaba, K., Murakami, S., Suzuki, M., Nakagawa, A., Yamashita, E., Okada, K., et al. (2006). Crystal structure of the DsbB-DsbA complex reveals a mechanism of disulfide bond generation. *Cell* 127, 789–801. doi: 10.1016/j.cell.2006.10.034

Ito, K., and Inaba, K. (2008). The disulfide bond formation (Dsb) system. *Curr. Opin. Struct. Biol.* 18, 450–458. doi: 10.1016/j.sbi.2008.02.002

Jardim-Messeder, D., Cabreira-Cagliari, C., Rauber, R., Turchetto-Zolet, A. C., Margis, R., and Margis-Pinheiro, M. (2017). Fumarate reductase superfamily: a diverse group of enzymes whose evolution is correlated to the establishment of different metabolic pathways. *Mitochondrion* 34, 56–66. doi: 10.1016/j.mito.2017.01.002

Jeon, B., and Zhang, Q. J. (2009). Sensitization of *Campylobacter jejuni* to fluoroquinolone and macrolide antibiotics by antisense inhibition of the CmeABC multidrug efflux transporter. *J. Antimicrob. Chemother.* 63, 946–948. doi: 10.1093/jac/dkp067

Kaakoush, N. O., Castano-Rodriguez, N., Mitchell, H. M., and Man, S. M. (2015). Global Epidemiology of Campylobacter Infection. *Clin. Microbiol. Rev.* 28, 687–720. doi: 10.1128/cmr.00006-15

Kaakoush, N. O., Man, S. M., Lamb, S., Raftery, M. J., Wilkins, M. R., Kovach, Z., et al. (2010). The secretome of Campylobacter concisus. *FEBS J.* 277, 1606–1617. doi: 10.1111/j.1742-4658.2010.07587.x

Kalmokoff, M., Lanthier, P., Tremblay, T. L., Foss, M., Lau, P. C., Sanders, G., et al. (2006). Proteomic analysis of *Campylobacter jejuni* 11168 biofilms reveals a role for the motility complex in biofilm formation. *J. Bacteriol.* 188, 4312–4320. doi: 10.1128/jb.01975-05

Kanehisa, M., Sato, Y., Kawashima, M., Furumichi, M., and Tanabe, M. (2016). KEGG as a reference resource for gene and protein annotation. *Nucleic Acids Res.* 44, D457–D462.

Klancnik, A., Botteldoorn, N., Herman, L., and Mozina, S. S. (2006). Survival and stress induced expression of groEL and rpoD of *Campylobacter jejuni* from different growth phases. *Int. J. Food Microbiol.* 112, 200–207. doi: 10.1016/j.ijfoodmicro.2006.03.015

Lasserre, J. P., and Menard, A. (2012). Two-dimensional blue native/SDS gel electrophoresis of multiprotein complexes. *Methods Mol. Biol.* 869, 317–337. doi: 10.1007/978-1-61779-821-4_27

Li, Z. F., Lou, H. Q., Ojcius, D. M., Sun, A. H., Sun, D., Zhao, J. F., et al. (2014). Methyl-accepting chemotaxis proteins 3 and 4 are responsible for *Campylobacter jejuni* chemotaxis and jejuna colonization in mice in response to sodium deoxycholate. *J. Med. Microbiol.* 63, 343–354. doi: 10.1099/jmm.0.068023-0

Lin, J., Akiba, M., Sahin, O., and Zhang, Q. J. (2005). CmeR functions as a transcriptional repressor for the multidrug efflux pump CmeABC in *Campylobacter jejuni*. *Antimicrob. Agents Chemother.* 49, 1067–1075. doi: 10.1128/aac.49.3.1067-1075.2005

Lin, J., Michel, L. O., and Zhang, Q. J. (2002). CmeABC functions as a multidrug efflux system in *Campylobacter jejuni*. *Antimicrob. Agents Chemother.* 46, 2124–2131. doi: 10.1128/aac.46.7.2124-2131.2002

Lin, J., Sahin, O., Michel, L. O., and Zhang, O. J. (2003). Critical role of multidrug efflux pump CmeABC in bile resistance and in vivo colonization of *Campylobacter jejuni*. *Infect. Immun.* 71, 4250–4259. doi: 10.1128/iai.71.8.4250-4259.2003

Lomize, M. A., Pogozheva, I. D., Joo, H., Mosberg, H. I., and Lomize, A. L. (2012). OPM database and PPM web server: resources for positioning of proteins in membranes. *Nucleic Acids Res.* 40, D370–D376.

Mace, S., Haddad, N., Zagorec, M., and Tresse, O. (2015). Influence of measurement and control of microaerobic gaseous atmospheres in methods for Campylobacter growth studies. *Food Microbiol.* 52, 169–176. doi: 10.1016/j.fm.2015.07.014

Moore, J. E., Corcoran, D., Dooley, J. S. G., Fanning, S., Lucey, B., Matsuda, M., et al. (2005). Campylobacter. *Vet. Res.* 36, 351–382.

Motojima, F., and Yoshida, M. (2015). Productive folding of a tethered protein in the chaperonin GroEL–GroES cage. *Biochem. Biophys. Res. Commun.* 466, 72–75. doi: 10.1016/j.bbrc.2015.08.108

Nachamkin, I. (2002). Chronic effects of Campylobacter infection. *Microbes Infect.* 4, 399–403. doi: 10.1016/s1286-4579(02)01553-8

Okuno, D., Iino, R., and Noji, H. (2011). Rotation and structure of FoF1-ATP synthase. *J. Biochem.* 149, 655–664. doi: 10.1093/jb/mvr049

Parkhill, J., Wren, B. W., Mungall, K., Ketley, J. M., Churcher, C., Basham, D., et al. (2000). The genome sequence of the food-borne pathogen *Campylobacter jejuni* reveals hypervariable sequences. *Nature* 403, 665–668. doi: 10.1038/35001088

Planas-Iglesias, J., Bonet, J., Garcia-Garcia, J., Marin-Lopez, M. A., Feliu, E., and Oliva, B. (2013). Understanding protein-protein interactions using local structural features. *J. Mol. Biol.* 425, 1210–1224. doi: 10.1016/j.jmb.2013.01.014

Pryjma, M., Apel, D., Huynh, S., Parker, C. T., and Gaynor, E. C. (2012). FdhTU-modulated formate dehydrogenase expression and electron donor availability enhance recovery of *Campylobacter jejuni* following host cell infection. *J. Bacteriol.* 194, 3803–3813. doi: 10.1128/jb.06665-11

Pyndiah, S., Lasserre, J. P., Menard, A., Claverol, S., Prouzet-Mauleon, V., Megraud, F., et al. (2007). Two-dimensional blue native/SDS gel electrophoresis of multiprotein complexes from *Helicobacter pylori*. *Mol. Cell. Proteom.* 6, 193–206. doi: 10.1074/mcp.m600363-mcp200

Rastogi, V. K., and Girvin, M. E. (1999). Structural changes linked to proton translocation by subunit c of the ATP synthase. *Nature* 402, 263–268. doi: 10.1038/46224

Reisinger, V., and Eichacker, L. A. (2006). Analysis of membrane protein complexes by blue native PAGE. *Proteomics* 6, 6–15. doi: 10.1002/pmic.200600553

Reisinger, V., and Eichacker, L. A. (2007). How to analyze protein complexes by 2D blue native SDS-PAGE. *Proteomics* 7(Suppl. 1), 6–16. doi: 10.1002/pmic.200700205

Reisinger, V., and Eichacker, L. A. (2008). Solubilization of membrane protein complexes for blue native PAGE. *J. Proteom.* 71, 277–283. doi: 10.1016/j.jprot.2008.05.004

Robinson, D. A. (1981). Infective dose of *Campylobacter jejuni* in milk. *Br. Med. J.* 282, 1584–1584. doi: 10.1136/bmj.282.6276.1584

Rodrigues, R. C., Haddad, N., Chevret, D., Cappelier, J. M., and Tresse, O. (2016). Comparison of Proteomics Profiles of *Campylobacter jejuni* Strain Bf under microaerobic and aerobic conditions. *Front. Microbiol.* 7:1596. doi: 10.3389/fmicb.2016.01596

Rothery, R. A., Seime, A. M., Spiers, A. M. C., Maklashina, E., Schroder, I., Gunsalus, R. P., et al. (2005). Defining the Q(P)-site of *Escherichia coli* fumarate reductase by site-directed mutagenesis, fluorescence quench titrations and EPR spectroscopy. *FEBS J.* 272, 313–326. doi: 10.1111/j.1742-4658.2004.04469.x

Sachs, J. N., and Engelman, D. M. (2006). "Introduction to the membrane protein reviews: the interplay of structure, dynamics, and environment in membrane protein function," in *Annual Review of Biochemistry*, ed. R. D. Kornberg (Palo Alto, CA: Annual Reviews), 707–712. doi: 10.1146/annurev.biochem.75.110105.142336

Schägger, H. (2002). Respiratory chain supercomplexes of mitochondria and bacteria. *Biochim. Biophys. Acta* 1555, 154–159. doi: 10.1016/s0005-2728(02)00271-2

Schagger, H., and von Jagow, G. (1991). Blue native electrophoresis for isolation of membrane protein complexes in enzymatically active form. *Anal. Biochem.* 199, 223–231. doi: 10.1016/0003-2697(91)90094-a

Scott, N. E., Marzook, N. B., Cain, J. A., Solis, N., Thaysen-Andersen, M., Djordjevic, S. P., et al. (2014). Comparative Proteomics and Glycoproteomics Reveal Increased N-Linked Glycosylation and Relaxed Sequon Specificity in *Campylobacter jejuni* NCTC11168 O. *J. Proteome Res.* 13, 5136–5150. doi: 10.1021/pr5005554

Scott, N. E., Parker, B. L., Connolly, A. M., Paulech, J., Edwards, A. V. G., Crossett, B., et al. (2011). Simultaneous Glycan-Peptide Characterization Using Hydrophilic Interaction Chromatography and Parallel Fragmentation by CID, Higher Energy Collisional Dissociation, and Electron Transfer Dissociation MS Applied to the N-Linked Glycoproteome of *Campylobacter jejuni*. *Mol. Cell. Proteom.* 10,

Seal, B. S., Hiett, K. L., Kuntz, R. L., Woolsey, R., Schegg, K. M., Ard, M., et al. (2007). Proteomic analyses of a robust versus a poor chicken gastrointestinal colonizing isolate of *Campylobacter jejuni*. *J. Proteome Res.* 6, 4582–4591. doi: 10.1021/pr070356a

Shaw, F. L., Mulholland, F., Le Gall, G., Porcelli, I., Hart, D. J., Pearson, B. M., et al. (2012). Selenium-Dependent Biogenesis of Formate Dehydrogenase in *Campylobacter jejuni* is controlled by the fdhTU accessory genes. *J. Bacteriol.* 194, 3814–3823. doi: 10.1128/jb.06586-11

Silva, J., Leite, D., Fernandes, M., Mena, C., Gibbs, P. A., and Teixeira, P. (2011). *Campylobacter* spp. as a foodborne pathogen: a review. *Front. Microbiol.* 2:200. doi: 10.3389/fmicb.2011.00200

Smart, J. P., Cliff, M. J., and Kelly, D. J. (2009). A role for tungsten in the biology of *Campylobacter jejuni*: tungstate stimulates formate dehydrogenase activity and is transported via an ultra-high affinity ABC system distinct from the molybdate transporter. *Mol. Microbiol.* 74, 742–757. doi: 10.1111/j.1365-2958.2009.06902.x

Sohn, S. H., and Lee, Y. C. (2011). The genome-wide expression profile of gastric epithelial cells infected by naturally occurring cagA isogenic strains of *Helicobacter pylori*. *Environ. Toxicol. Pharmacol.* 32, 382–389. doi: 10.1016/j.etap.2011.08.006

Sperling, L. J., Tang, M., Berthold, D. A., Nesbitt, A. E., Gennis, R. B., and Rienstra, C. M. (2013). Solid-State NMR Study of a 41 kDa Membrane Protein Complex DsbA/DsbB. *J. Phys. Chem. B* 117, 6052–6060. doi: 10.1021/jp400795d

Stephen, K. B., Helen, M. B., Cole, C., Jose, M. D., Zukang, F., John, W., et al. (2018). RCSB Protein Data Bank: sustaining a living digital data resource that enables breakthroughs in scientific research and biomedical education. *Protein Sci.* 27, 316–330. doi: 10.1002/pro.3331

Sulaeman, S., Hernould, M., Schaumann, A., Coquet, L., Bolla, J. M., De, E., et al. (2012). Enhanced adhesion of *Campylobacter jejuni* to abiotic surfaces is mediated by membrane proteins in oxygen-enriched conditions. *PLoS One* 7:e46402. doi: 10.1371/journal.pone.0046402

Szklarczyk, D., Morris, J. H., Cook, H., Kuhn, M., Wyder, S., Simonovic, M., et al. (2017). The STRING database in 2017: quality-controlled protein-protein association networks, made broadly accessible. *Nucleic Acids Res.* 45, D362–D368.

Tresse, O. (2017). Proteomics Analyses Applied to the Human Foodborne Bacterial Pathogen Campylobacter spp.

Turonova, H., Briandet, R., Rodrigues, R., Hernould, M., Hayek, N., Stintzi, A., et al. (2015). Biofilm spatial organization by the emerging pathogen *Campylobacter jejuni*: comparison between NCTC 11168 and 81-176 strains under microaerobic and oxygen-enriched conditions. *Front. Microbiol.* 6:709. doi: 10.3389/fmicb.2015.00709

Turonova, H., Haddad, N., Hernould, M., Chevret, D., Pazlarova, J., and Tresse, O. (2017). Profiling of *Campylobacter jejuni* proteome in exponential and stationary phase of growth. *Front. Microbiol.* 8:913. doi: 10.3389/fmicb.2017.00913

Vallenet, D., Calteau, A., Cruveiller, S., Gachet, M., Lajus, A., Josso, A., et al. (2017). MicroScope in 2017: an expanding and evolving integrated resource for community expertise of microbial genomes. *Nucleic Acids Res.* 45, D517–D528.

Wai, S. N., Nakayama, K., Umene, K., Moriya, T., and Amako, K. (1996). Construction of a ferritin-deficient mutant of *Campylobacter jejuni*: contribution of ferritin to iron storage and protection against oxidative stress. *Mol. Microbiol.* 20, 1127–1134. doi: 10.1111/j.1365-2958.1996.tb02633.x

Watson, E., Sherry, A., Inglis, N. F., Lainson, A., Jyothi, D., Yaga, R., et al. (2014). Proteomic and genomic analysis reveals novel *Campylobacter jejuni* outer membrane proteins and potential heterogeneity. *EuPA Open Proteom.* 4, 184–194. doi: 10.1016/j.euprot.2014.06.003

Weerakoon, D. R., Borden, N. J., Goodson, C. M., Grimes, J., and Olson, J. W. (2009). The role of respiratory donor enzymes in *Campylobacter jejuni* host colonization and physiology. *Microb. Pathog.* 47, 8–15. doi: 10.1016/j.micpath.2009.04.009

Weerakoon, D. R., and Olson, J. W. (2008). The *Campylobacter jejuni* NADH : Ubiquinone oxidoreductase (complex I) utilizes flavodoxin rather than NADH. *J. Bacteriol.* 190, 915–925. doi: 10.1128/jb.01647-07

Weingarten, R. A., Taveirne, M. E., and Olson, J. W. (2009). The dual-functioning fumarate reductase is the sole succinate: quinone reductase in *Campylobacter jejuni* and is required for full host colonization. *J. Bacteriol.* 191, 5293–5300. doi: 10.1128/jb.00166-09

Wetie, A., Sokolowska, I., Woods, A., Roy, U., Loo, J., and Darie, C. (2013). Investigation of stable and transient protein-protein interactions: past, present, and future. *Proteomics* 13, 538–557. doi: 10.1002/pmic.201200328

Wohlbrand, L., Ruppersberg, H. S., Feenders, C., Blasius, B., Braun, H. P., and Rabus, R. (2016). Analysis of membrane-protein complexes of the marine sulfate reducer Desulfobacula toluolica Tol2 by 1D blue native-PAGE complexome profiling and 2D blue native-/SDS-PAGE. *Proteomics* 16, 973–988. doi: 10.1002/pmic.201500360

Wu, W. H., Tran-Gyamfi, M. B., Jaryenneh, J. D., and Davis, R. W. (2016). Cofactor engineering of ketol-acid reductoisomerase (IlvC) and alcohol dehydrogenase (YqhD) improves the fusel alcohol yield in algal protein anaerobic fermentation. *Algal Res.-Biomass Biofuels Bioproducts* 19, 162–167. doi: 10.1016/j.algal.2016.08.013

Yan, M. G., Sahin, O., Lin, J., and Zhang, Q. J. (2006). Role of the CmeABC efflux pump in the emergence of fluoroquinolone-resistant Campylobacter under selection pressure. *J. Antimicrob. Chemother.* 58, 1154–1159. doi: 10.1093/jac/dkl412

You, Y., He, L., Zhang, M., Fu, J., Gu, Y., Zhang, B., et al. (2012). Comparative genomics of *Helicobacter* pylori strains of China associated with different clinical outcome. *PLoS One* 7:e38528. doi: 10.1371/journal.pone.0038528

Young, J. Y., Westbrook, J. D., Feng, Z. K., Peisach, E., Persikova, I., Sala, R., et al. (2018). Worldwide Protein Data Bank biocuration supporting open access to high-quality 3D structural biology data. *Database J. Biol. Databases Curation*

Yum, S., Xu, Y., Piao, S., Sim, S., Kim, H., Jo, W., et al. (2009). Crystal structure of the periplasmic component of a tripartite macrolide-specific efflux pump. *J. Mol. Biol.* 387, 1286–1297. doi: 10.1016/j.jmb.2009.02.048

Zautner, A. E., Tareen, A. M., Groß, U., and Lugert, R. (2012). Chemotaxis in *Campylobacter jejuni*. *Eur. J. Microbiol. Immunol.* 2, 24–31.

Zhang, Q. J., Meitzler, J. C., Huang, S. X., and Morishita, T. (2000). Sequence polymorphism, predicted secondary structures, and surface-exposed conformational epitopes of *Campylobacter major* outer membrane protein. *Infect. Immun.* 68, 5679–5689. doi: 10.1128/iai.68.10.5679-5689.2000

Zommiti, M., Almohammed, H., and Ferchichi, M. (2016). Purification and characterization of a novel anti-campylobacter bacteriocin produced by *Lactobacillus curvatus* DN317. *Probiot. Antimicrob. Proteins* 8, 191–201. doi: 10.1007/s12602-016-9237-7

Conflict of Interest: The authors declare that the research was conducted in the absence of any commercial or financial relationships that could be construed as a potential conflict of interest.

Advantages of publishing in Frontiers

OPEN ACCESS
Articles are free to read for greatest visibility and readership

FAST PUBLICATION
Around 90 days from submission to decision

HIGH QUALITY PEER-REVIEW
Rigorous, collaborative, and constructive peer-review

TRANSPARENT PEER-REVIEW
Editors and reviewers acknowledged by name on published articles

Frontiers
Avenue du Tribunal-Fédéral 34
1005 Lausanne | Switzerland

Visit us: www.frontiersin.org
Contact us: frontiersin.org/about/contact

REPRODUCIBILITY OF RESEARCH
Support open data and methods to enhance research reproducibility

DIGITAL PUBLISHING
Articles designed for optimal readership across devices

FOLLOW US
@frontiersin

IMPACT METRICS
Advanced article metrics track visibility across digital media

EXTENSIVE PROMOTION
Marketing and promotion of impactful research

LOOP RESEARCH NETWORK
Our network increases your article's readership